A CRYSTALLOGRAPHIC INVESTIGATION OF MULTIDENTATE LIGAND HAFNIUM(IV) HALIDO COMPLEXES

by

JOHANNES AUGUSTINUS VILJOEN

A thesis submitted to meet the requirements for the degree of

PHILOSOPHIAE DOCTOR

In the

DEPARTMENT OF CHEMISTRY

FACULTY OF NATURAL- AND AGRICULTURAL SCIENCES

at the

UNIVERSITY OF THE FREE STATE

SUPERVISOR: PROF. ANDREAS ROODT
CO-SUPERVISOR: PROF. HENDRIK G. VISSER

NOVEMBER 2021

Acknowledgements

Professor Andreas Roodt, thank you for your guidance, support and motivation. Prof believed in me over all these years when most others had written me off. The advice that you have given me both personally and professionally will always be appreciated. I'm truly honoured to be associated with a man such as you. It will always be a privilege to have had you as a promoter.

To Prof. Deon Visser, thank you for your guidance throughout this project. The value of the advice and support that you've given me over time cannot be quantified.

To my 'assistant', Dr. Maryke Steyn, thank you again for always being there with me in the lab and bearing with me throughout this project!!

To my father, Theuns Viljoen, who passed away in the first year of this study. Thank you for shaping me into the man I am today.

To my mother, Magda Viljoen, thank you for putting up with all my nonsense over the years. I would not have come this far without your never-ending support and love and could not ask for a better role model.

To my close friends, thank you for all the fun, the jokes and the occasional drink that made life and going to work worthwhile. There are too many to personally thank but to all, thank you for sharing knowledge and always being there to listen and give advice.

Financial assistance from the Advanced Metals Initiative (AMI) and the Department of Science and Technology (DST) of South Africa as well as The New Metals Development Network (NMDN) and the South African Nuclear Energy Corporation Limited (Necsa) and the University of the Free State are gratefully acknowledged.

“IT ALWAYS
SEEMS
IMPOSSIBLE
UNTIL
IT’S DONE”

-NELSON MANDELA-

Table of Contents

Chapter 3

Synthesis of Hafnium(IV) and Zirconium(IV) Complexes – Experimental Techniques and Preliminary Characterisation

Chapter 4

X-Ray Diffraction Studies of Hafnium(IV) Complexes Containing Non- and Substituted 8-Hydroxyquinoline Ligands

Chapter 5

X-Ray Diffraction Studies of Hafnium(IV) Complexes Containing Di-halogen Substituted 8-Hydroxyquinoline Ligands

Chapter 6

X-Ray Diffraction Studies of Hafnium(IV) Complexes Containing Substituted Acetylacetone Ligands

Chapter 7

X-Ray Diffraction Studies of Hafnium and Zirconium Complexes Containing Tetradentate N,O- and N,N'- donor ligands.

Chapter 8

Evaluation and Structural Correlation of Hafnium(IV) Bi- and Multidentate Ligand Complexes

Chapter 9

Evaluation and Structural Correlation of Hafnium(IV)- and Zirconium(IV) Bi- and Multidentate Ligand Complexes

Chapter 10

Preliminary Solvent Extraction and Attempted Separation of Tetrakis(oxine-type) Hafnium(IV) and -Zirconium(IV) Complexes

Chapter 11

Evaluation of Study and Future Aims

List of Abbreviations

Symbol / Abbreviation	Meaning
(*L,L'*)	Bidentate ligand
OxH	8-hydroxyquinoline / oxine / quinolinols
5Cl-OxH	5-chloro-8-hydroxyquinoline
7Br-OxH	7-bromo-8-hydroxyquinoline
diMeOxH	5,7-dimethyl-8-hydroxyquinoline
diClOxH	5,7-dichloro-8-hydroxyquinoline
diBrOxH	5,7-dibromo-8-hydroxyquinoline
diIOxH	5,7-diiodo-8-hydroxyquinoline
acacH	Acetylacetone / 2,4-Pentanedione
tfaaH	1,1,1-trifluoroacetylacetone
hfaaH	1,1,1,5,5,5-hexafluoroacetylacetone
dbmH	Dibenzoylmethane
tfbaH	4,4,4-Trifluoro-1-phenyl-1,3-butanedione
pbpH	*N,N'*-(1,2-phenylene)bis(pyridine-2-carboxamide)
salophen	*N,N'*-bis(salicylidene)-1,2-phenylene-diamine
Lig	Ligand
Lig #	Specific numbered ligand, with # = ligand number as coordinated
NMR	Nuclear Magnetic Resonance Spectroscopy
ppm	(Unit of chemical shift) parts per million
IR	Infrared spectroscopy
UV/Vis	Ultraviolet/Visible
XRD	X-Ray diffractometry
Z	Number of molecules in a unit cell
Å	Angstrom
υ	Stretching frequency on IR
π	Pi
σ	Sigma

α	Alpha
β	Beta
γ	Gamma
σ*	Sigma anti-bonding
λ	Wavelength
θ	Sigma
º	Degrees
ºC	Degrees Celsius
cm	Centimetre
g	Gram
mg	Milligram
M	(mol/dm^{-3})
mmol	Millimol
CO	Carbonyl
F_{hkl}	Structure factor
k_{obs}	Observed pseudo-first-order rate constant
DMF	*N,N*-dimethylformamide
Tol	Toluene

SUMMARY

Hafnium, the chemical element with atomic number 72 in the titanium-triad on the periodic table, was first discovered by Dirk Coster and George von Hevesy in 1923 by analysing X-Ray spectra of Norwegian zircon samples (sea sand). Hafnium is considered relatively abundant and comprises about three parts per million by weight of the earth's crust. Unfortunately, hafnium only occurs naturally in zirconium ores at an approximate ratio of 1:50 and has almost identical general chemical properties to that of zirconium. Zirconium has a very desirable application in the nuclear industry as a cladding material for nuclear fuel rods due to its low affinity for thermal neutrons. However, for zirconium to be used as a cladding material in nuclear reactors, it must be virtually hafnium free since hafnium has a 600 times larger affinity for thermal neutrons than that of zirconium, turning it into a "*poison*" in zirconium *cladding* materials. However, this high affinity for thermal neutrons is exactly why pure Hf makes an excellent *shielding* material. Therefore, for hafnium and zirconium to be utilised in the nuclear industry, it is apparent why the effective and economically viable separation of these metals to their pure chemical state is vital.

The principle aim of this study is focused on studying the solid-state and solution behaviour of hafnium(IV), with various *N*- and *O*-donating multidentate ligand systems, in order to obtain valuable new data that could potentially be used to compare to zirconium(IV) to evaluate if metal separation is feasible for industrial applications.

Therefore, in this study, the solid-state and solution behaviour of novel hafnium(IV) and zirconium(IV) coordination compounds, obtained from a systematic range of *N*- and *O*- bi- and multidentate ligands, is investigated. A detailed description of the synthesis of the hafnium(IV) and zirconium(IV) complexes containing different *N,O*- and *O,O'*-bidentate ligand systems as well as *N,O,O,N*- and *N,N',N',N*-tetradentate ligands are reported and characterised by means of IR, UV/Vis and NMR (^{1}H and ^{13}C) spectroscopies.

Moreover, it is clearly illustrated by this study that it is possible to synthesise hafnium(IV) and zirconium(IV) complexes under simple bench-top aerobic conditions. Furthermore, the solid-state structural characterisation by means of single crystal X-Ray Diffraction studies of ten of these synthesised complexes is described in detail.

Thus, six novel hafnium(IV)-oxinato complexes containing a systematic range of substituents on the outer periphery of the ligand are firstly presented: **(1)** $[Hf(Ox)_4]\cdot 2(C_7H_8)$, **(2)** $[Hf(5\text{-}ClOx)_4]\cdot 2(C_7H_8)$, **(3)** $[Hf(diMeOx)_4]\cdot 2(DMF)$, **(4)** $[Hf(diClOx)_4]\cdot 3DMF$, **(5)** $[Hf(diBrOx)_4]\cdot 3DMF$ and **(6)** $[Hf(diIOx)_4]\cdot DMF$ and described. The complexes contain non- and substituted 8-hydroxyquinoline (OxH) ligands [*with (5-ClOxH) = 5-chloro-8-hydroxyquinoline, (diMeOxH) = 5,7-dimethyl-8-hydroxy-quinoline, (diClOxH) = 5,7-dichloro-8-hydroxyquinoline, (diBrOxH = 5,7-dibromo-8-hydroxyquinoline, (diIOxH) = 5,7-diiodo-8-hydroxyquinoline*], and are discussed and compared with regard to the intimate geometric environment around the hafnium(IV) metal centre. It is clearly illustrated by this study that *tetrakis*-(oxinato)hafnium(IV) complexes prefer the square-antiprismatic coordination geometry in the *D_2-corner* clipped isomer form. It is further shown that all the hafnium(IV) -and zirconium(IV) oxine complexes are very similar with relation to bond lengths, angles and packing modes.

Secondly, two new hafnium(IV)-*β*-diketonato complexes – **(7)** $[Hf(dbm)_4]$ and **(8)** $[Hf(OH)(tfba)_3]_2\cdot 2DMF$ – are structurally evaluated and described [*where (dbmH) = dibenzoylmethane and (tfbaH) = 4,4,4-trifluoro-1-phenyl-1,3-butanedione*]. Focus is placed on the influence of ligands when increasing the metallocycle from five (oxine-type ligands) to six (acac-type ligands) and using acac-type ligands containing different electron-donating properties. The effect of electron-withdrawing substituents on the ligand backbone with regards to coordination mode and coordination geometry. These examples show and conclude that hafnium-*β*-diketonato complexes also prefer a square-antiprismatic coordination geometry in the *D_2-corner* clipped isomer form. Moreover, all the hafnium(IV)- and zirconium(IV)-*β*-diketonato complexes are very similar with respect to their general geometry and corresponding bond lengths, angles and packing modes. Similar to the oxine-type complexes, this suggests that hafnium(IV) and zirconium(IV) has a certain preference for the chelation sites of the

coordinating atoms, regardless of the steric or electronic properties of the ligands as a whole.

Thirdly, a novel hafnium(IV) and zirconium(III) complex containing a *N,O,O,N*- and *N,N',N',N*-tetradentate ligand, respectively – **(9)** [Hf(salophen)$_2$·2(C_7H_8), **(10)** [Zr(pbp)(H_2O)$_2$]$_2$$NO_3$·(MeOH) – are structurally evaluated and compared with regard to the intimate geometric environment around the metal centres [*where (salophen) =N,N'-bis(salicylidene)-1,2-phenylene-diamine & (pbpH) = N,N'-(1,2-phenylene)bis-(pyridine-2-carboxamide)*]. It was found that the eight coordinated hafnium(IV) complex favours a square-antiprismatic coordination polyhedron. However, the six coordinated zirconium(III) complex formed a distorted octahedron as coordination polyhedron around the metal centre, as expected for many six coordinated metal complexes.

Finally, preliminary liquid-liquid extraction experiments are described herein, and it is concluded to in principle be considered a preliminary proof-of-concept for separation. The preliminary extraction investigation reported includes liquid-liquid extractions of zirconium- and hafnium-oxine complexes from methanol into dichloromethane and competition extractions, as qualitatively evaluated by **(I)** UV-Vis spectroscopy and **(II)** inductively coupled plasma optical emission spectroscopy.

Key words: *Hafnium; zirconium; nuclear industry; separation; N- and O- bi- and multidentate ligands; synthesis; solid-state crystallographic characterisation; liquid-liquid extraction.*

Chapter 1

Hafnium and the Nuclear Industry –

Introduction and Aim

Dirk Coster and George Charles, a Danish and Hungarian chemist, respectively, discovered hafnium in 1923 utilising X-ray spectroscopy.[1] However, the existence of the element was already predicted some 50 years earlier in 1869 by the Russian chemist, Dmitri Mendeleev, when he developed the Periodic Law of the Chemical Elements.[2] He hypothesised that the 72nd element (Hf) would be an element whose chemical properties would be very similar to zirconium and should have an atomic weight of approximately 180.

Pure hafnium was originally separated from zirconium through repeated recrystallisation with either potassium or ammonium fluorides and isolated by means of fractional crystallisation.[3] In 1925, van Arkel and de Boer first produced pure metallic hafnium and zirconium by vaporising the metal tetraiodides (HfI_4/ZrI_4) into a bulb containing a hot tungsten filament which caused the dissociation of the iodides, thus depositing the pure metals on the filament. This process became known as the "Crystal Bar Process" or "Iodide Process".[4] In 1938 these processes were further refined by William Kroll, where hafnium and zirconium metal was produced by

---

[1] D. Coster, *Phil. Mag.,* **46,** 856, 1923.
[2] M. Kaji, *Found. Chem.*, **5**, 189, 2003.
[3] G. von Hevesy, *Chem. Rev.*, **2**, 1, 1925.
[4] R. Nielsen & T.W. Chang; *"Zirconium and Zirconium Compounds"*, *Ullmann's Encyclopedia ofIndustrial Chemistry*, Wiley-VCH, Weinheim, 2005.

reducing the metal tetrachlorides ($HfCl_4/ZrCl_4$) with molten magnesium. This process later became known as the Kroll Process.[5]

It was later discovered that pure zirconium metal had very desirable applications in the nuclear industry as a *cladding material* for nuclear fuel rods due to its low thermal neutron absorption cross-section (NAC) and its outstanding anti-corrosion properties and thermal stability.[6] However, for zirconium to be used as a cladding material in nuclear reactors, it must be virtually hafnium free (< 100 ppm Hf)[7] due to the fact that hafnium has a thermal neutron absorption 600 times larger than that of zirconium, turning it into a “poison” in zirconium cladding materials. The high thermal neutron absorption cross-section of hafnium (capable of absorbing many neutrons without fissioning itself) makes it ideal to be used as *control rods* to control the rate of fission in nuclear reactors.[8]

Unfortunately, hafnium only occurs naturally in Zircon ($ZrSiO_4$) at an approximate ratio of 1:50 and has almost identical general chemical properties to that of zirconium. The chemical properties of these two elements are so similar that one could describe them as "chemical twins". In order for hafnium and zirconium to be utilised in the nuclear industry, it is apparent why the effective and economically viable separation of these metals to their pure chemical state is so vital. The chemical characteristics, applications, and separation of hafnium and zirconium will be discussed in detail in **Chapter 2**.

---

[5] W. J. Kroll, *J. Frankl. Inst*., **260**, 169, 1955.

[6] R. H. Nielsen, J .H. Schlewitz & H. Nielsen; *"Zirconium and Zirconium Compounds"*, *26*, Kirk-Othmer Encyclopaedia of Chemical Technology, John Wiley & Sons, Inc., 2000.

[7] M. Benedict, T. H. Pigford & H. W. Levi; *Nuclear Chemical Engineering*, McGraw-Hill, USA, 1981.

[8] D. R. Lide, ed.; *CRC Handbook of Chemistry and Physics* , *Section 4: Properties of the Elements and Inorganic Compounds*, Int.Vers. (http://www.hbcpnetbase.com), CRC Press, Boca Raton, FL, 2005.

1.1. Hafnium Production and Consumption

Hafnium production mainly relies on the production and refinement of zirconium, where nuclear-grade pure zirconium is required.[9] Hafnium would probably not be recovered if it is not used in the nuclear industry. To extract and separate only hafnium from zircon, which only contains between 1 and 5 % hafnium, would be too costly. However, hafnium also has a wide range of applications in various other industries. It is extensively used in the manufacturing process of superalloys to improve tensile strength due to its high melting point of 2233˚C and in the manufacturing of microprocessors. [10,11]

It is clear, as indicated above that the production and demand of hafnium are closely associated with the nuclear industry where essentially hafnium free nuclear-grade zirconium is required. Therefore, in order for these metals to be successfully used in the nuclear industry they have to be separated effectively.

In general, the manufacturing process of pure hafnium and zirconium from zircon ore is accomplished in 5 stages (*see* **Figure 1.1**):[12]

- Decomposition of the ore
- Separation of hafnium
- Calcination
- Chlorination
- Reduction by the Kroll proses

[9] H. Rosenberg & A. Sharif; *Encyclopedia of Materials: Science and Technology*, 3709, 2001.
[10] R. E. Smallman & R. J. Bishop; *"Modern Physical Metallurgy and Materials Engineering"*, 6th Ed., Elsevier Ltd., 1999.
[11] G. Gudivada & B. Kandasubramanian, *Ind. Eng. Chem. Res.*, **58**, 4711, 2019.
[12] L. Y. Wang & M. S. Lee, *J. Ind. Eng. Chem.*, **39**, 1, 2016.

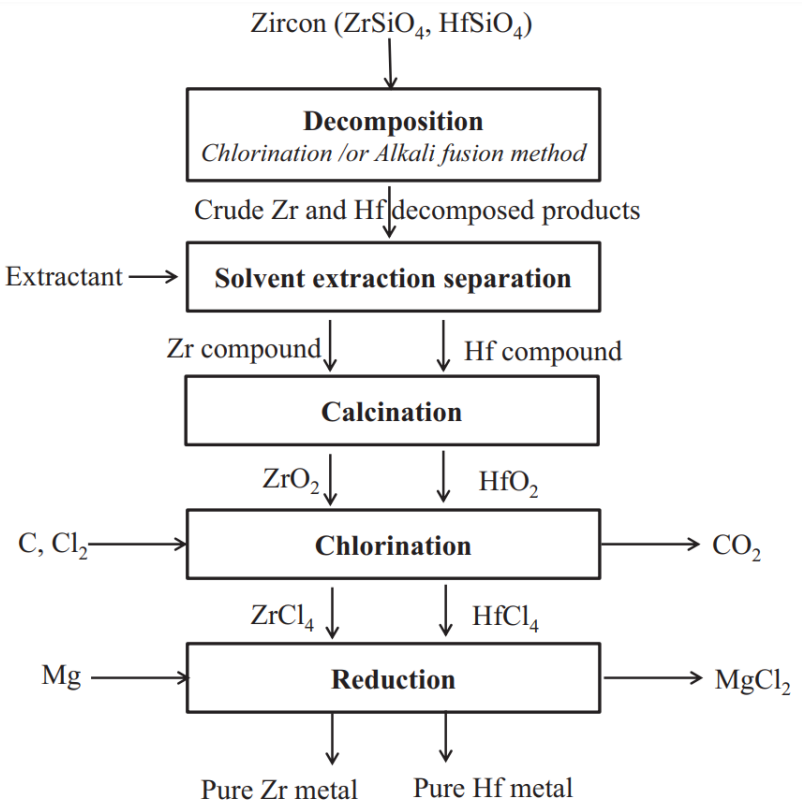

Figure 1.1: Flowsheet for the production of pure hafnium and zirconium from zircon ore.

At this stage, South Africa has approximately 30% of the global zircon reserves and currently supplies roughly 45% of the global demand. Despite all of these zircon (in sand deposits and established zircon-sand mines in South Africa), almost all beneficiation capacity for zircon sand is done in China.[13] This clearly creates significant beneficiation and separation opportunities for South Africa and the rest of the world.

[13] S. Lubbe, R. Munsami & D Fourie, *Journal of the Southern African Institute of Mining and Metallurgy*, **7A**, 584, 2012.

1.2. The aim of this study

The brief details indicated above makes it very reasonable to assume that there is room for improvement on the current processes. By investigating the nuances of the solid-state and solution behaviour of hafnium, with various *N*- and *O*-donating ligand systems may provide appropriate information that could be compared to available zirconium processes in literature to determine if metal separation is plausible in existing industrial methods. Following a literature search, it became clear that very little is known regarding the chelation behaviour of these metals with *N*- and *O*- donating multidentate ligands. The available pool of structural studies (X-ray crystallographic, NMR- and UV/Vis spectroscopy) is also very limited. This will thus be pursued by trying to identify the inherent preferences these metals have for coordination reactivity with specific and well understood ligands systems.

The three high-level overarching aims for this study, are thus summarised as:

(a) Synthesis of novel Hafnium(IV) coordination compounds with a range of *N*- and *O*-donating multidentate ligands followed by in-depth structural characterisation utilising analytical techniques, including IR-, UV/Vis- and NMR spectroscopies.

These *N*- and *O*-donating multidentate ligands are divided into three main groups:

i. 8-hydroxyquinolines / quinolinols / oxines (OxH)

During the precursor M.Sc. project,[14] the formation of *tetrakis*(*L,L'*-Bid)Hf(IV) complexes (*L,L'*-Bid=OxH) were confirmed, and a very preliminary formation kinetic evaluation of these *tetrakis*(8-hydroxyquinolinato)hafnium(IV)

[14] J. A. Viljoen; *Speciation And Interconversion Mechanism Of Mixed Halo and O,O- and N,O- Bidentate Ligand Complexes of Hafnium*, M.Sc. Dissertation (**2009**), University of the Free State,South Africa.

complexes was initiated. It is important to note that the oxine-type ligands coordinate via a five-membered metallocycle.

In this study, a step-wise mechanism for the coordination of the four oxine ligands to the Hf(IV) metal centre was postulated from experimental results (**Scheme 1.1 and 1.2**).

Fast reactions - Stopped-flow results:

$$Hf + (L,L') \underset{}{\overset{K_1}{\rightleftharpoons}} Hf(L,L')$$

$$Hf(L,L') + (L,L') \xrightarrow{k_2} Hf(L,L')_2$$

Scheme 1.1: The two fast proposed reactions for data obtained from stopped-flow spectroscopy (halide ligand omitted for simplicity). LL'H = bidentate ligand OxH.

Slower reactions - UV/Vis Results:

$$Hf(L,L')_2 + (L,L') \underset{k_{-3}}{\overset{k_3}{\rightleftharpoons}} (L,L')_2HfL{-\!\!-}L'$$

$$(L',L)_2Hf{-\!\!-}L,L' \overset{K_4}{\rightleftharpoons} (L',L)_2Hf\begin{array}{l}L\\|\\L'\end{array}$$

$$Hf(L,L')_3 + (L,L') \underset{k_{-5}}{\overset{k_5}{\rightleftharpoons}} Hf(L,L')_4$$

Scheme 1.2: The three slower proposed reactions for data obtained from UV/Vis spectroscopy. (halide ligand omitted for simplicity). LL'H = bidentate ligand OxH.

From this experience obtained and from the corresponding zirconium co-project by Dr. M Steyn[15] (UFS, 2009), wherein it was postulated that utilising various commercially available oxine-type ligands, in principle, could yield vital insights into the possible extraction of hafnium and zirconium complexes. Substituents in this ligand family range from halides, carboxylic acids and methyl groups.

ii. *β*-Diketones / acetylacetones / (acacH)

An integral part of this project is focused on also investigating aspects of the metallocycle formed by bidentate ligands, thus extending it to six-membered systems. To achieve this, different readily available acetylacetone (acacH) type ligands with various electron-withdrawing (CF_3-groups) and/or electron-donating (phenyl-groups) substituents on the 1 and 5 position of the ligand(acacH) back-bone, as illustrated below, were targeted.

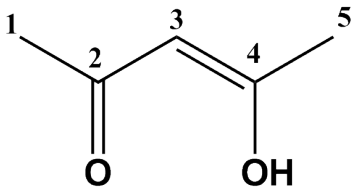

Figure 1.2: Schematic structure of acetylacetone (acacH).

The steric modification on the back-bone can potentially significantly influence the coordination modes around the hafnium metal centre to such an extent that the coordination of the 3rd and 4th acac-ligand complexes may be structurally isolated. This might allow selective interruption of *tetrakis*-coordination modes by selective intervention at appropriate time points, thus creating significant differences in carefully tuned hafnium and zirconium complexes, which may then be exploited for selective extraction. This

[15] M. Steyn; *Speciation And Interconversion Mechanism Of Mixed Halo And O,O- and O,N Bidentate Ligand Complexes of Zirconium*, M.Sc. Dissertation (**2009**), University of the Free State, South Africa.

approach, therefore, supports previous postulated mention of a ***step-wise reaction mechanism*** for the coordination around Hf/Zr metal centres.

iii. *N*- and *O*-donating Tetradentate Ligands

When planning a structural characterisation study, one needs to consider a number of other influencing factors that coordination ligands could potentially have on the final metal compounds. The steric and electronic influences of organic chelation substrates would give valuable insights to the aforementioned reactivity and final solid-state structures expected. A wide range of multidentate ligands can be commercially sourced for such a study, which would include all parameters to be considered. The added benefit of employing commercially available ligands, not only eliminates the trial-and-error of quality assurance during synthesis, but also economically favours the application of these chemical compounds if they were to be feasible chelators for industrial separation processes.

(b) Solid-state structural characterisation of crystalline products of the above, intended at elucidating the nuances of chelation that can be observed by means of single-crystal X-Ray Diffraction (XRD).

(c) Liquid-liquid extraction evaluation of synthesised and characterised hafnium(IV) and zirconium(IV) compounds in order to gain valuable data which can be used for separation between hafnium and zirconium.

In the following chapter, a literature overview of general chemistry of hafnium (and zirconium) relevant to this PhD investigation is presented and existing separation applications are discussed. Additionally, a technical description of selected organic coordination ligands as utilised in this project is presented as motivating rational for inclusion to the scope of the investigation to hafnium(IV) coordination trends.

Chapter 2

Theoretical Aspects:

Separation and Coordination

Studies of Hafnium(IV)

2.1. Introduction

In light of the discussion in the previous chapter, some theoretical aspects regarding the study will be discussed in this chapter to justify the need for the study and various techniques used.

This will include a brief overview of currently known methods of separation and purification of hafnium and zirconium in industry and the coordination chemistry of these metal centres with various organic chelators.

2.2. Hafnium and Zirconium

Hafnium and zirconium, which forms part of the titanium triad, are widely referred to in the literature as chemical twins due to lanthanide contraction.[1] The lanthanide elements collectively are theorised to fill the *4f*-electron subshell of the atomic electron model. The covalent radius (predicted bond length for an atom bound to another) decreases in a steady trend from cerium to lutetium, with a substantial total decrease over the lanthanide series. At the point where the *4f*-subshell is completely filled, the covalent radii of the transition elements from hafnium onwards are very similar to those elements of the preceding row in the periodic table. The covalent radius of hafnium (150 pm) is thus almost identical to that of zirconium (148 pm).[2] The only significant chemical difference between hafnium and zirconium is their density (**Table 2.1**). The density of zirconium is almost half that of hafnium, making their chemistries nearly identical and the separation of these two metals notoriously difficult.[3,4] The major sources of hafnium are found, as impurities, in zircon ($ZrSiO_4$) and baddeleyite, a natural form of zirconium oxide (ZrO_2).[5] Both hafnium and zirconium are considered as rare earth elements and is found widely distributed in the crust of the earth. Since zirconium comprises 0.013% of the earth's crusts, it is the ninth most abundant metal.[6] Hafnium, being an impurity in zirconium minerals, is less abundant but still more abundant than gold and silver and has an average concentration of 7 ng/L in sea water.[1]

---

[1] R. E. Krebs, *The History and Use of Our Earth's Chemical Elements: A Reference Guide*, Greenwood Press, Westport, CT, 1998.

[2] D. D. Ebbing & S. D. Gammon, *General Chemistry*, 7th Ed, Houghtoun Mifflin Company, Boston, New York, 2002.

[3] F. A. Cotton, G. Wilkinson, C. A. Murillo & M. Bochmann, *Advanced Inorganic Chemistry*, 6th Ed., Wiley-Interscience Publications, New York, 1999.

[4] N. N. Greenwood & A. Earnshaw; *"Chemistry of the Elements",* 2nd Ed., Reed Educational and Professional Publishing Ltd, Butterworth-Heinemann, Woburn, MA, 954-975, 1997.

[5] G. M. Bedinger, U.S. Geological Survey, Mineral Commodity Summaries, 2015 January.

[6] B. Mason, *Principles of Geochemistry*, 3rd ed., John Wiley & Sons, New York, 1966.

Table 2.1 *:* **Comparison between hafnium and zirconium chemical properties.**

Property	Hf	Zr
Group	4	4
Period	6	5
Block	d	d
Atomic number	72	40
Boiling point (°C, K)	2233, 2506.15	1854, 2127.15
Density ($kg.m^{-3}$)	13276	6507
Relative atomic mass	178.49	91.224
Common oxidation states	4	4
Atomic radius, non-bonded (Å)	2.23	2.23
Covalent radius (Å)	1.64	1.64
Electronegativity (Pauling scale)	1.3	1.33
Heat of fusion ($kJ.mol^{-1}$)	27.2	14
Heat of vaporization ($kJ.mol^{-1}$)	571	573
Molar heat capacity ($J.mol^{-1}.K^{-1}$)	25.73	25.36
Thermal conductivity ($W.m^{-1}.K^{-1}$)	23	22.6
Thermal expansion (@25 °C, $\mu m.m^{-1}.K^{-1}$)	5.9	5.7
Thermal Neutron Capture Cross Section (barns, 10^{-28} m^2)	0.184	104

The separation of hafnium from zirconium is paramount for both metals' relevant applications in the nuclear industry, since hafnium has an approximately 600 times larger affinity for thermal neutrons than zirconium, and therefore acts as a "poison" for zirconium in the nuclear industry (*Zircon, the primary ore for nuclear-grade zirconium contains about 65%ZrO_2, 33% SiO_2 and 1% HfO_2*). [7,8]

[7] R. C. Weast, *CRC Handbook of Chemistry and Physics*, 63rd Ed., The Chemical Rubber Publishing Company, USA, 1982.

[8] L. Poriel, A. Favre-Réguillon, S. Pellet-Rostaing & M. Lemaire*, Separation Science and Technology*, **41**, 1927, 2006.

The high neutron-absorbing properties and corrosion resistance of hafnium make it an ideal element for the use in control rods in nuclear reactors to control the rate of production of energy and also in case of emergency, to soak up the excess nuclear particles as illustrated in **Figure 2.1**.[9]

In turn, the unique low neutron-absorbing character feature of zirconium, together with high chemical stability at high temperatures, makes it an attractive element for cladding materials in nuclear reactors. The cladding material is the outer layer of the fuel rods in nuclear reactors, which separates the coolant from the nuclear fuel from one another. This prevents radioactive fission fragments from escaping from the fuel and thereby contaminating the coolant (**Figure 2.1**).[10]

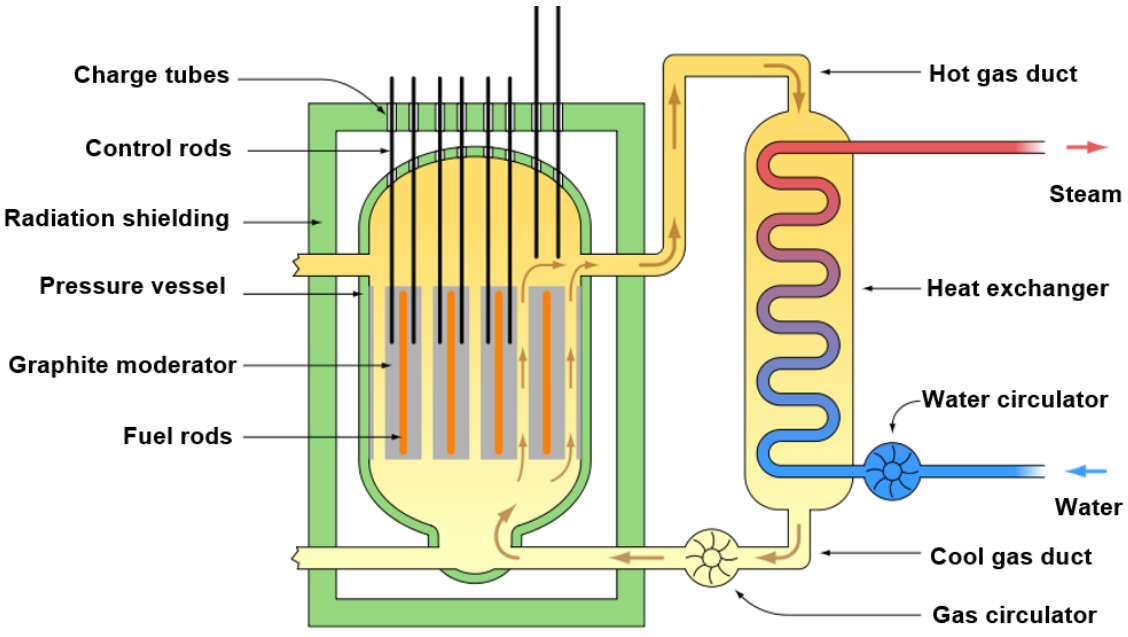

Figure 2.1: A diagrammatical representation of a water-cooled nuclear reactor.[11]

[9] D. R. Lide, *CRC Handbook of Chemistry and Physics*, *Section 4: Properties of the Elements and Inorganic Compounds*, Int. Vers. (http://www.hbcpnetbase.com), CRC Press, Boca Raton, FL, 4-14, 2005.

[10] H. W. Keller, J. M. Ballenberger, D.A. Hollein & C. Hott, *Nucl. Technol.*, **59**, 3, 476, 1982.

[11] Image of Nuclear Reactor adapted from : http://commons.wikimedia.org/wiki/Image: Magnox_ reactor_schematic.svg (Last accessed 21/02/2020).

2.2.1. Separation Methods

The separation of the chemical elements zirconium and hafnium was first carried out by de Hevesy and Coster in 1923,[12] but industrial applications for separating these two metals and the manufacturing of the pure metals started with the production of nuclear energy and the development of nuclear weapons in the 1950`s. The earliest known separation technique involved the fractional crystallisation of ammonium fluoride metal salts[13] and the fractional distillation of the metal chloride.[14] However, these methods are not suitable for industrial-scale production.

Unlike the many applications of zirconium for the production of glass, enamels, industrial catalysts, ceramics, etc. no expensive preliminary purification from hafnium is needed.[15,16,17,18] However, for the chain reactions of nuclear fission to be most effective, “reactor-grade” zirconium with as minimal as possible hafnium concentration, is required.[19,20]

It is obvious from the previous sections that it would be very beneficial to obtain hafnium and zirconium “isolates” as pure as possible for nuclear power applications.

A search of the available literature revealed that several separation techniques exist, and these are briefly summarised further in this chapter.[21,22,23,24 25]

---

[12] D. Coster, G. von Hevesy, *Nature,* **111**, 79, 1923.
[13] G. von Hevesy, *Chem. Rev*., **2**, 1, 1925.
[14] W. J. Kroll, *J. Frankl. Inst*., **260**, 169, 1955.
[15] J. Schwartz & J. A. Labinger, *Angew. Chem. Int. Ed,* **15**, 330, 2003.
[16] T. J. Pinnavaia & R. C. Fay, *Inorg. Chem.* **7**, 502-508, 1968.
[17] H. K. Chun, W. L. Steffen & R. C. Fay, *Inorg.Chem*. **18***,* 2458, 1979.
[18] A. Clearfield & D. S. Thakur; *Appl. Catal.,* **26**, 1, 1886.
[19] V. Shatalov, V. Nikonov & M.L. Kotsar, *At. Energy*, **4**, 242, 2008.
[20] L. Xu, Y. Xiao, A. V. Sandwijk, Q. Xu & Y. Yang*, J. Nucl. Mater.*, **466**, 21, 2015.
[21] L. Y. Wang, M. S. Lee, *Sep. Purif. Technol*., **142**, 83, 2015.
[22] K. A. Barawy, S. Z. Tawil, A. A. Francis, *Trans. Inst. Min. Metall. Sect. C,* **109**, 49, 2000.
[23] I. V. Vinarov, *Russ. Chem. Rev.*, **36**, 522, 1967.
[24] R. Mallikarjunan & J. C. Sehra, *Bulletin of Materials Science*, **12**, 407, 1989.
[25] B. R. Reddy, J. R. Kumar, A. V. Reddy*, Anal. Sci*., **20 (3)**, 501, 2004.

2.2.1.1. The Kroll Process

The Kroll process is a pyro-metallurgical industrial process initially used to produce metallic titanium[26] but was later refined in 1945 by W. J. Kroll for the purification of hafnium and zirconium. The first commercial production of zirconium metal was achieved in 1953.[27]

The Kroll process is a batch-technique and involves the following steps:

1. Sublimation of impure hafnium tetrachloride at 371 °C in an inert atmosphere to remove other non-volatile impurities and undesirable oxides.

2. Reduction of the $HfCl_4$ with magnesium by passing through molten magnesium heated in a furnace to produce a hafnium sponge.

$$HfCl_4 + 2Mg \rightarrow Hf + 2MgCl_4$$

3. Vacuum-distill treatment at 920 – 960 °C to remove the magnesium and magnesium chlorides. This part is carried out with the container inverted to allow partial drainage of the liquid Mg and MgCl from the solid hafnium sponge, which clings to the container wall.

After cooling and conditioning, the sponge is removed from the container wall and broken into smaller chunks using a hydraulic chisel. The chunks are graded and crushed to approximately 1cm diameter sizes before it is melted into ingots which will be used as cladding materials for the fissionable uranium in nuclear reactors.

[26] W. Kroll, *"Method for Manufacturing Titanium"* (**1940**), US Patent 2205854.
[27] G. Roza, *"Zirconium"*, Rosen Publishing Group, **2009**.

2.2.1.2. Fractional crystallisation

This method of separation makes use of comparatively small differences in the solubilities of individual compounds of zirconium and hafnium[28] containing oxide chlorides/bromides, citrates, acetylacetonates, sulphates or fluorides with ammonium and potassium. Flourozirconates and fluorihafnates systems which contain double fluorides of potassium or ammonium were the first to be utilised for the separation of hafnium and zirconium[29] and too some extents still retain their importance to this date.

In the fractional crystallisation of the flourozirconates and fluorihafnates (*double fluorides of potassium or ammonium*), the zirconium salt, which is less soluble than its hafnium counterpart, crystallises out more readily from the mother liquor, gradually purifying it from hafnium. Nevertheless, in order to obtain pure hafnium from the raw materials, hundreds of re-crystallisation steps are required. However, more modern technologies make it possible to produce "reactor-grade" zirconium containing not more than 0.05% hafnium impurity, in less than 20 re-crystallisation steps. While similar separation procedures were carried out followed by Kaweki[30] in the USA and Knaak *et al*.[31] in Germany, the original method is currently in use in the Prinieprovsky Chemical Plant in Dnieprod-zerzhinsk, Ukraine, to produce hafnium-free zirconium.[32]

2.2.1.3. Fractional Precipitation

Fractional precipitation exploits differences in solubility and/or stability of different zirconium and hafnium complexes. A variety of different versions of these methods utilises mostly organic compounds (benzoic, tartaric, salicylic, mandelic

---

[28] K. Reuter, G. N. Passing & S. Kirchmeyer, *"Process for Separating Zirconium and Hafnium"* U.S. Patent 7 635 396, May 2, 2007.
[29] G. von Hevesy, *Chem. Rev.* ***2,*** 1, 1925.
[30] H. C. Kawecki*, Nucleonics*, **14**, 47, 1956.
[31] H. Knaak & G. Knaak, *Chem. Abs*., **59**, 12438e, 1963.
[32] R. H. Nielsen & G. Wilfing, *Ullmann's Encyclopedia of Industrial Chemistry, John Wiley & Sons, Ltd., 2000.*

acids) and their derivatives. Separation has also been achieved using various inorganic compounds like phosphoric acid, sodium hexacyanoferrate(II), hydrogen peroxide and ammonia, among others. Knowledge gained from numerous separation studies undertaken pointed out that fractional precipitation is very time-consuming and tedious, considering the actual degree of separation achieved. The first systematic approach for the separation of zirconium and hafnium by fractional precipitation by means of phosphoric acid was developed by Larsen *et al*. [33] (*The Phosphate Method*). Subsequently, a more effective separation can be obtained using different varieties of phosphate (*Peter's method*)[34] and sodium hexacyanoferrate[35] (*Prandt's method*)[36] methods, but these methods were still not efficient enough for the production of pure zirconium and hafnium metal on an *industrial scale.*

In **Peter's method**, zirconium and hafnium is separated by dissolving the zirconium and hafnium hydroxides in diluted hydrochloric acid after which the solution is reacted with $NH_4H_2PO_4$ to produce insoluble zirconium and hafnium phosphates. The precipitates are washed in distilled water to remove the phosphate ions and then dissolved in 10% oxalic acid. An excess oxalic acid equal to that used for the dissolution is added to the reaction mixture and heated to *approximately* 50 °C, for a prolonged period, to form stable oxalate-complexes of zirconium and hafnium complexes which are fractionally decomposed with a hydrochloric acid and ammonium oxalate solution. The main disadvantage of this method is the time required for the stable oxalate-complexes to form.

In **Prandt's method**, the zirconium and hafnium hydroxides are dissolved in a dilute sulphuric acid solution which is then treated with ammonium sulphate and a solution of oxalic acid. To the resulting solution, adequate amounts of sodium hexacyanoferrate(II) is added to obtain partial precipitation of the zirconium and

[33] E. M. Larsen, W. C. Fernelius & L. L. Quill, *Ind. Eng. Chem. Anal*., **15**, 512, 1943.
[34] H. H. Willard & H. Freund, *Ind. Eng. Chem. Ana*l., **18**, 195, 1946.
[35] E. A. Ionova & I. V Tananaev, *Russ. J. Inorg. Chem*., 409, 1962.
[36] W. Prandtl, *Z. Anorg. Chem*., **206**, 420, 1932.

hafnium hexacyanoferrates(II). The hafnium rich hexacyanoferrate precipitation is left to stand for a period of time and then separated from the mother-liquor. The remaining solution is finally treated with NaOH to produce residual zirconium and hafnium hydroxides which are sent through the process again. It is claimed by Prandt's that only six precipitations are needed to yield 95% hafnium concentrates. Prandt's method was further refined by Schumb and Pittman[37] obtaining an 80% hafnium concentrate from a 12% concentrate just after four precipitation cycles.

2.2.1.4. Extractive Distillation

This type of separation is based on utilising difference in volatilities of various zirconium and hafnium compounds. Havesy and Dullenkopf[38] first began investigating the separation of zirconium and hafnium tetrachlorides ($ZrCl_4$ & $HfCl_4$) and tetrafluorides (ZrF_4 & HfF_4) by means of fractional distillation in the early 1930's. Although the efficiency of this method was found to be comparatively low in the beginning, a more effective separation was obtained when phosphorus(V)[39] -and phosphyrol(V)[40] chloride were reacted with $ZrCl_4$ and $HfCl_4$. This work led to extensive investigations into whether it could be possible to separate the metal tetrachlorides and tetrafluorides without the addition of phosphorus compounds (thereby making it possible to convert the separated zirconium and hafnium species directly to their corresponding metals). Three mainstream separation concepts based on the relative volatility of $ZrCl_4$ and $HfCl_4$ have been studied. The close similarity between zirconium and hafnium is reflected in the physical constants of their chlorides.[41]

---

[37] W. C. Schumb & F. K. Pittman, *Ind. Eng. Chem. Ana*l., **14**, 512, 1942.
[38] G. C. Havesy & W. Dullenkopf, *Z. Anorg. Chem*., **221**, 161, 1934.
[39] L. A. Nisel'son & L. E. Larionova, *Russ. J. Inorg. Chem*., 83, 1960.
[40] E. M. Larsen, J. Hovatson, A. M. Gammil & L. Wittenberg, *J. Am. Chem. Soc*., **74**, 3489, 1952.
[41] N. A. Lange, *Lange's Handbook of Chemistry*, 9th Ed., Handbook Publishers Inc., Sandusky, OH,1956.

Table 2.2: Physical constants of zirconium and hafnium tetrachlorides.

Properties	$ZrCl_4$	$HfCl_4$	Properties	$ZrCl_4$	$HfCl_4$
Sublimation temp. (°C)	331	317	Critical point:		
Triple point:			Temperature (°C)	505	449.2
Temperature (°C)	437	432	Pressure (kPa)	5766	5776
Pressure (kPa)	2236	4501	Volume (cm^3/mol)	319.3	303.6

Three mainstream separation concepts based on the relative volatility of $ZrCl_4$ and $HfCl_4$ have been studied;

- **Thin-film sublimation**[42,43]
  - $ZrCl_4$ and $HfCl_4$ have a relative volatility P_{HfCl4}/P_{ZrCl4} of 1.9 at 250 °C, enabling separation at 1atm.
- **Molten-salt distillation at 1 atm**[44,45]
  - The use of molten salts (K_2ZrCl_6/K_2HfCl_6 & Na_2ZrCl_6/Na_2HfCl_6) decreases the activity of the tetrachlorides and permits separation at atmospheric pressure and at temperatures below 400 °C.

- **High-pressure fractional distillation at 40 to 60 atm** [46,47]
  - At elevated pressures (*ca*. 5800 kPa), hafnium tetrachloride is more volatile than its zirconium counterpart enabling successful separation to occur.

[42] L. Jacque & P. Dumez, *Chim. Ind*., **97**, 1677, 1967.
[43] J. Gillot & W. M. Goldberger, *Chem. Eng. Prog. Symp*. Ser., **65,** 36, 1969.
[44] Anax Speciality Metal Corp., Greenwich C. T. *Separation of Zirconium and Hafnium*. U.S. Pat. 3 966 458, June 29, 1976.
[45] D. R. Spink & C. P. Vijayan, *J. Electrochem. Soc*., **121**, 879, 1974.
[46] N. D. Denisova, E. K Safronov, A. I Pustil'nik & O. N. Bystrova, *Russ. J. Phys. Chem.,* **41**, 30, 1967.
[47] R. H. Nielsen,*"Hafnium and Hafnium Compounds"*, Kirk-Othmer Encyclopedia of Chemical Technology, John Wiley & Sons, Inc., 2000.

2.2.1.5. Ion exchange separation

Ion Exchange separation is a type of extraction method which utilises chromatographic principles where ionic or polar analytes interact with an oppositely charged stationary phase (resin) to maintain the charge balance equilibrium in the system. This proses involves the release and retaining of differently charged ions in solution through the stationary phase, which usually consists of an appropriate substrate, the stationary phase, that is uniformly packed in a column for a desired experimental setup. The stationary phase is typically prepared from organic compounds with ionisable functional groups attached (fixed ions) which carry displaceable oppositely charged ions. The various analytes passed through the packed column at different rates depending on the type of stationary phase as well as the composition of the analytes to be separated[48] (**Figure 2.2**).

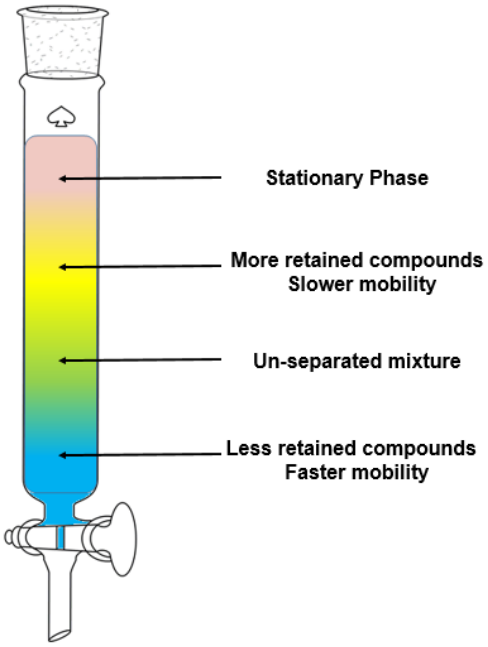

Figure 2.2: Schematic illustration of a basic Ion-exchange chromatography separation setup, indicating different separation of analytes over time.

[48] D. A. Skoog,. D. M. West, F. J. Holler, S. R. Crouch, *Fundamentals of Analytical Chemistry*, 8th ed., Thomson Brooks/Cole, 2004.

Hafnium has successfully been separated from zirconium on ion-exchange resins by exploiting the differences in their stabilities in different acids. Street and Seaborg published the first paper on the separation of hafnium and zirconium through ion-exchange chromatography, where the separation was achieved by dissolving a metal oxide mixture containing HfO_2 and ZrO_2 in sulfuric acid and passed along an ion-exchange separation column. [49]

The separation of zirconium and hafnium utilising cation-exchange resins together with sulphuric acid is primarily due to the noticeable differences in the stabilities of the sulphato-complexes of zirconium and hafnium in solution.

Ryabchikov *et al*.[50] determined that zirconium sulphato-complexes can be as much as three times more stable than its hafnium counterpart under certain conditions.

Studies performed by Benedict *et al*.[51] and Qureshi *et al*.[52] showed that a mixture of nitric acid and citric acid and formic acid could effectively be used, respectively, as acidifiers to achieved desirable separation. However, Machlan & Hague[53] showed by using a mixture of sulfuric and hydrofluoric acid; it is possible to separate hafnium and zirconium metal to reactor-grade specifications.

2.2.1.6. Liquid-liquid Extraction

Liquid-liquid extraction is a separation method which exploits relative solubilities of compounds in different immiscible liquids or solvents. This is mainly performed using water and various organic solvents, which is water-immiscible. Liquid-liquid extraction, or solvent extraction, processes exploit the differences in solubility of

[49] K. Street & G. T. Seaborg, *J. Amer. Chem. Soc*., 4268, 1948.
[50] D. I. Ryabchikov, A. N. Ermakov, V. N. Belaeva, I. N. Marov & Y. K'o-min, *Russ. J. Inorg. Chem*., **34**, 1962.
[51] J. T. Benedict, W.C. Schumb & C. D. Coryell, *J. Am. Chem. Soc.*, **76(8),** 2036, 1954.
[52] M. Qureshi & K. Husain, *Anal. Chem.* **43**, 447, 1971.
[53] L. A. Machlan & J.L. Hague, *J. Res. Nat. Bur. Stand.* **66A**, 517, 1962.

metal complexes, either hafnium of zirconium, to be extracted from the aqueous phase into the organic phase (**Figure 2.3**).

One of the modern versions of this process, zirconium and hafnium thiocyanate complexes are extracted from water using methyl isobutyl ketone (MIBK)[54] as extracting agent. The hafnium moiety has a slightly higher solubility in the organic phase, which allows for the extraction of the zirconium counterpart from the acidified (dilute sulphuric acid) aqueous phase. The hafnium and zirconium metals are then recovered by means of precipitation as zirconium sulphate ($Zr(SO_4)_{2)}$ and hafnium oxide (HfO_2). Vast quantities of purified HfO_2 can be obtained utilising this method. Hence it is widely used in the USA. [47]

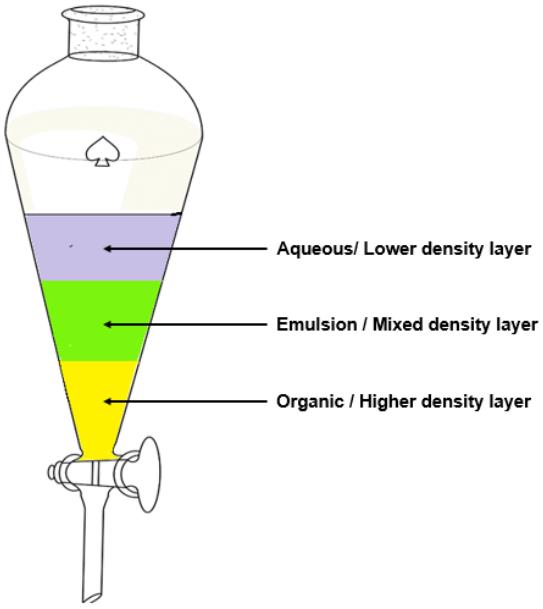

Figure 2.3: Schematic illustration of the basic laboratory setup of the liquid-liquid extraction technique. From initial agitation of the mixed solution, the emulsion or mixed density layer separates over time into a single density layer that can be run off individually.

[54] R. H. Nielsen, J. H. Schlewitz & H. Nielsen, *"Zirconium and Zirconium Compounds"*, Kirk-Othmer Encyclopedia of Chemical Technology, John Wiley & Sons, Inc., 2000.

Extractants utilised in solvent extraction for hafnium(IV) and zirconium(IV) are divided into three main groups;

1. **Acidic** extractants, where acidic organophosphorus extractants like **D2EHPA** ($CH_3(CH_2)_7O)_2POOH$) and **PC88A** ($CH_3(CH_2)_7O)(CH_3(CH_2)_7$) POOH) are used.[55]
2. **Solvating** extractants, when solvating extractants, such as **TBP**[56] ($CH_3(CH_2)_3O)_3PO$) or **TOPO**[57] ($CH_3(CH_2)_7)_3PO$) in hydrochloric acid solutions are used.
3. **Amine-based** extractants where Alamine 336 ($(C_8H_{17})_3N$) or Aliquat 336 ($(C_8H_{17})_3CH_3N^+Cl^-$ are utilised. [58,59]

2.3. Concluding Remarks – Separation Methods

It is evident from the overview, of known separation techniques used for the purification and separation of hafnium and zirconium, that each technique exploits, in one way or the other, small differences in the chemical behaviour of hafnium and zirconium in certain physical states.

- ***Fractional Crystallisation*** takes advantage of the ***difference in solubility*** of similar type hafnium and zirconium compounds in solution. By varying the temperature slowly, the least soluble compound will crystallise out first, leaving the other metal compound still in solution.

[55] B. R. Reddy, J. R. Kumar & A. V. Reddy, *Miner. Eng*., **17**, 553, 2004.

[56] Y. Kasamatsu, Y. Kikutani, A. Kino, Y. Komori, T. Yokokita, T. Yoshimura, N. Takahashi & A. Shinohara*, Radiochim. Acta*, **101**, 515, 2013.

[57] R. Banda, H. Y. Lee & M. S. Lee, *J. Radioanal. Nucl. Chem*., **298**, 259, 2013.

[58] L. Poriel, A. Favre-Reguillon, S. Pellet-Rostaing & M. Lemaire, *Sep. Sci. Technol*., **41**, 1927, 2006.

[59] R. Banda, H. W. Lee & M. S. Lee, *J. Radioanal. Nucl. Chem*., **295**, 537, 2013.

- ***Fractional Precipitation*** takes advantage of the ***difference in stability and solubility*** of hafnium and zirconium complexes, with very similar solubilities, by means of a series of analytical precipitations from a solution.

- ***Extractive Distillation*** takes advantage of the ***difference in volatility*** of hafnium and zirconium mixtures in a solvent which alters the boiling points of the metal compounds without directly reacting to the metal compounds.

- ***Ion Exchange Separation*** takes advantage of a ***difference in the rate of elution*** of different metal complex ions on a chromatographic separation setup. The hafnium and zirconium metal ions pass through the packed column at different rates depending on the type of stationary phase as well as the composition of the metal analytes.

- ***Liquid-Liquid Extraction*** takes advantage of relative solubility differences of chelated organometallic metal compounds in different immiscible liquids or solvents.

Taking these various separation techniques into consideration, it becomes quite apparent that with the proper understanding of how hafnium and zirconium react with different solvents, compounds, ligands or ions, it might be possible to develop cheaper and better purification techniques for hafnium and zirconium.

As a fundamental point, the proposal to study novel hafnium coordination compounds with various *N*- and *O*-donating ligand systems for the purification of this metal from its base ores, might therefore, provide valuable information that could be compared to zirconium equivalents to check if the metal separation is feasible for industrial applications. To do so, one would need to focus specifically on critical points like solubility, reactivity and volatility of the metal complexes, as highlighted previously.

Throughout this literature overview, it is apparent that a wide range of organic chelators are already intensively utilised in industrial-scale separation techniques.

This forms an ideal basis to investigate further, in-depth, the coordination chemistry of hafnium with different ligands systems and the effects thereof in terms of chemical behaviour. It is well known that the steric and electronic effects of organic ligands can have a significant impact on the chemical behaviour of metal complexes in solid state as well as in solution.

2.4. Hafnium and Organic Chelators

As stated earlier in **Chapter 1**, one of the main objectives of this study is to investigate possible means of separation by studying the coordination behaviour of different organic chelators with hafnium and to enable preparation of a range of novel complexes. Literature shows a few such complexes exist, and these are discussed in the following paragraphs.

2.4.1. 8-Hydroxyquinoline (N,O-Bidentate Ligand)

The *N,O*-bidentate ligand, 8-Hydroxyquinoline, **Figure 2.4(b)** is a heterocyclic organic compound with the formula C_9H_7NO and can be considered as a combination of catecholate and 2,2'-bipyridine.

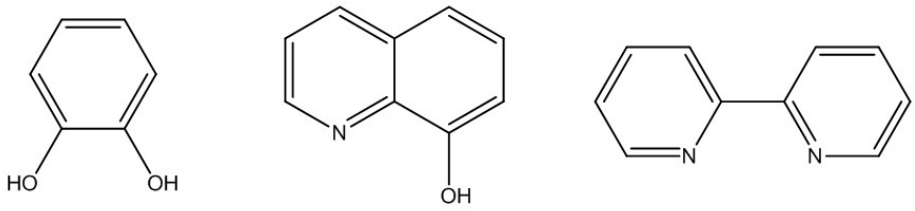

(a) **(b)** **(c)**

Figure 2.4: Comparison of the chelating elements of (a) catecholate, (b) 8-hydroxy-quinoline and (c) 2,2'-bipyridine.

Like other hydroxyquinolines, 8-hydroxyquinoline form an equilibrium mixture of the hydroxyl-form and the N-protonated zwitterionic form as shown in **Figure 2.5**).[60]

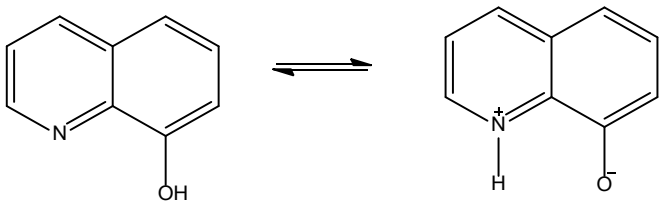

Figure 2.5: Zwitterionic form of 8-hydroxyquinoline.

8-Hydroxyquinoline and its derivatives are generally synthesised by the Friedländer[61] or the Skraup[62] synthesis methods (**Scheme 2.1**).

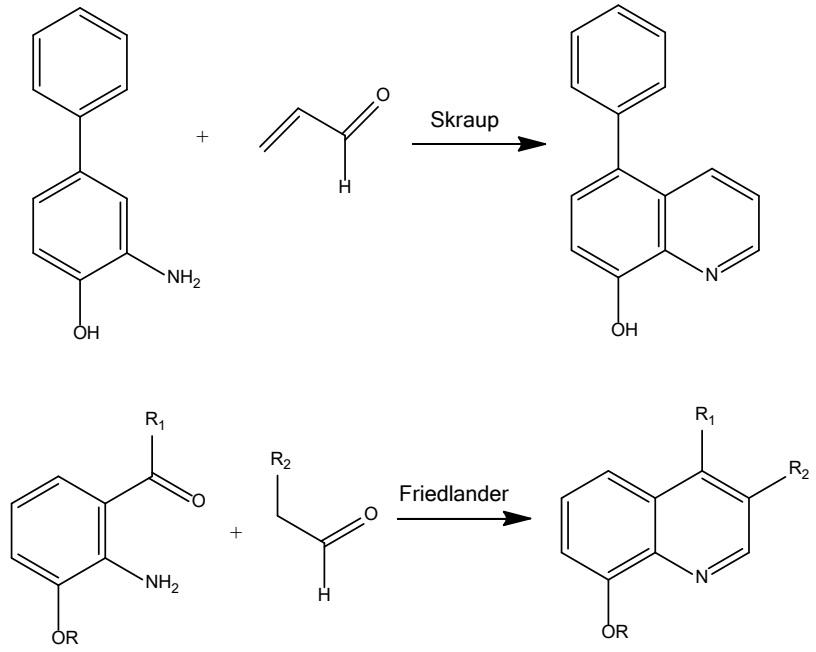

Scheme 2.1: General reaction scheme for the synthesis of 8-Hydroxyquinoline derivatives using Friedlander and Skraup methods.

[60] A. R. Katritzky & J. MLagowski, *Adv Heterocyclic Chem*., **2**, 27, 1963.

[61] C. C. Cheng & S. J Yan, *Org. React.,* **28**, 37, 1982.

[62] Z. H. Skraup, *Chem. Ber.,* **13**, 2086, 1880.

8-Hydroxyquinoline (OxH), in its deprotonated form, possesses one phenolate unit of catecholate and one pyridine donor of the bipyridine, thereby making it monoanionic and bridges the gap between the dianionic catecholate and the neutral bipyridine. Furthermore, 8-hydroxyquinoline can complex with metal ions as a neutral molecule[63] but complexes predominantly in its deprotonated anion form with the loss of the hydroxyl hydrogen.[64] As a result of the proximity of the hydroxyl group to the heterocyclic nitrogen, 8-hydroxyquinoline coordinate readily to the various metal ions to form different covalent metal complexes, e.g. [M(Ox)] (M = Mn, Cu, Ni),[65] [$M(Ox)_2$] (M = Cu, Ag),[66,67] [$M(Ox)_3$] (M = Al, Ga)[68] and [$M(Ox)_4$] (M = Zr Hf),[69,70] adducts as shown in **Figure 2.6**. A two-covalent metal complex requires 1 OxH molecule for each metal atom. Therefore, an eight-covalent metal complex requires four OxH molecules per metal centre.

The derivatives of 8-hydroxyquinoline have a wide range of applications as neurodegenerative, antimicrobial, antioxidant, anticancer and anti-inflammatory agents.[71,72,73] Furthermore, 8-hydroxyquinoline and some of its derivatives are well-proven precipitation agents and complexants in chemical analysis.[74] Vinogradov and Shpinel[75] are some of the first scientists to utilise 8-hydroxyquinoline for the separation of zirconium by means of precipitation.

---

[63] D. L. Huges & M. R. Truter, *Chem. Soc. Dalton Trans*., **520**, 1979.
[64] G. J. Palenik, *Acta Cryst*. **17**, 696, 1964.
[65] S. Prachayasittikul, A. Worachartcheewan & R. Pingaew*, Lett Drug Des Dis*. **9(3),** 282, 2012.
[66] H. Wu, X. Dong, H. Liu & J. Ma, *Acta Cryst.* E**62**, 281, 2006.
[67] S. Ammor, G. Coquerel, G. Perez. & F. Robert, *Eur. J. Solid State Inorg. Chem*., **29**, 445, 1992.
[68] F. Yue, A. Zhu, S. Zheng & X. Chen, *Eur. J. Inorg. Chem*., 32, 5076, 2008.
[69] M. Steyn, H. G. Visser & A. Roodt, *Acta Cryst.* E**68**, 1344, 2012.
[70] J. A. Viljoen, H. G. Visser & A. Roodt., *Acta Cryst*. E**66**, 603, 2010.
[71] V. Prachayasittikul, S. Prachayasittikul, S. Ruchirawat & V. Prachayasittikul, *Drug. Des. Dev. Ther*. **7**, 1157, 2013.
[72] J. Lazovic, L. Guo, J. Nakashima, L. Mirsadraei, W. Yong & H. J. Kim, *Neuro-Oncol***. 17 (1),** 53, 2015.
[73] K. G. Naber, H. Niggemann & G. Stein, *Infect. Dis*. **14**, 628, 2014.
[74] G. H Jeffery, J. Basset, J. Mendham & R. C. Denney, *Vogel's textbook of Quantitative Chemical Analysis*, 5th Ed., Longman Scientific and Technical, New York, 1989.
[75] A. V. Vinogradov & V. S. Shpinel, *Atom Energiya*, **3**, 130, 1957.

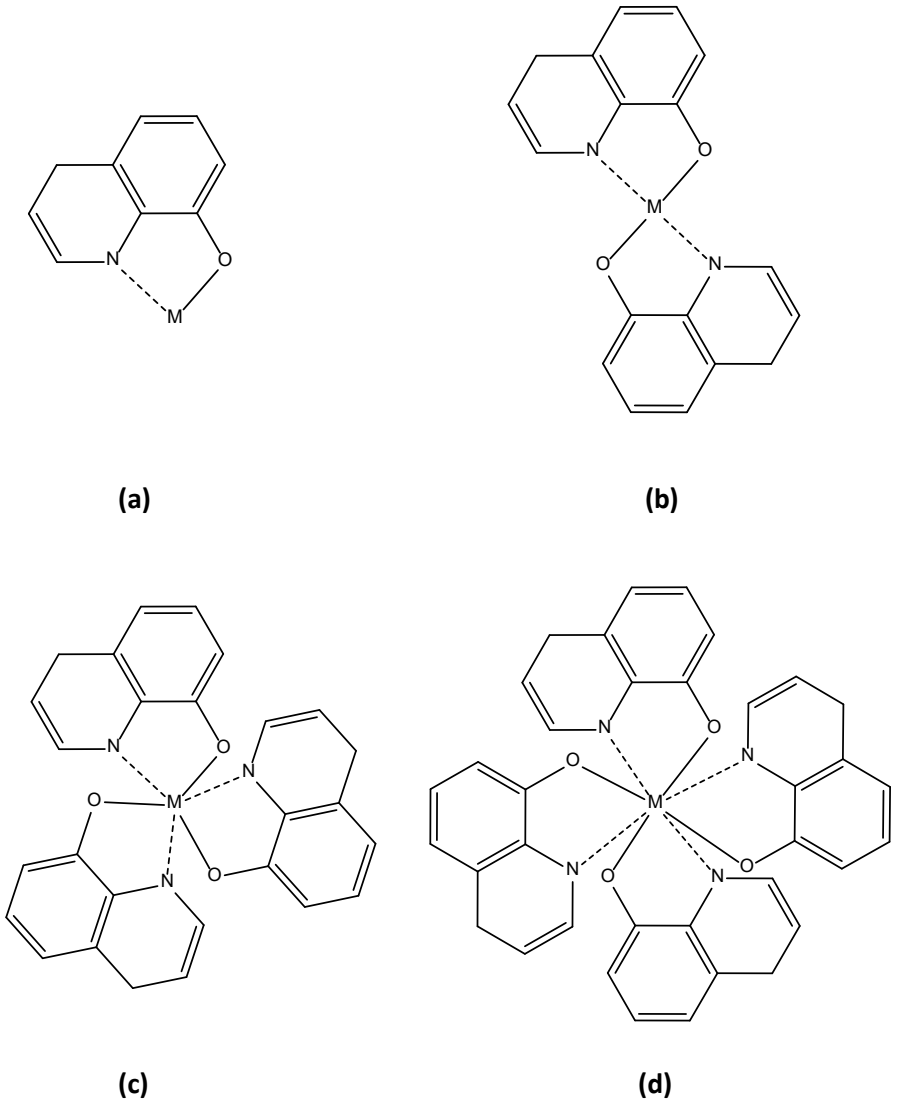

Figure 2.6: Graphical representation of **(a)** Two- **(b)** Four- **(c)** Six- **(d)** eight-covalent metal complexes of 8-hydroxyquinoline.

Recently, organic light-emitting diodes (OLEDs) have been under intensive investigation for applications in display technology due to their luminous efficiency and ability to emit full colours. Tang and Van Slyke were the first to exploit tris-(8-hydroxyquinolinolate) aluminium complexes ($[Al(Ox)_3]$) as an efficient green electroluminescent material. [76] Later it was discovered that different wavelength

[76] C. W. Tang & A. Van Slyke, *Appl. Phys. Lett*. **51**, 913, 1987.

light-emitters could be obtained by altering the chelated metal centre[77] and/or by modifying the quinoline's backbone.[78]

After studying various metal centres, it was discovered that zirconium *tetrakis*(8-hydroxyquinolinolate), $[Zr(Ox)_4]$, also acts as an excellent OLED with the added advantage of a better lifetime and greater efficiency compared to $[Al(Ox)_3]$ devices.[79] Conversely, in preliminary studies undertaken by Kathirgamanathan *et al.*,[80] it was determined that the hafnium *tetrakis*(8-hydroxy-quinolinolate) analogue ($[Hf(Ox)_4]$) on the other hand displays much poorer performance compared to $[Zr(Ox)_4]$. In summary, due to the unique chemical properties of 8-hydroxyquinoline and its derivatives, a large amount of these compounds have application in medical, OLEDs, agriculture, chemosensors, and metal extraction fields.

2.4.2. *β*-Diketones (*O,O'*-Bidentate Ligand)

β-Diketone ligands have now been widely used as classical metal coordination agents in coordination chemistry for more than a century.[81] Ligands of the type act as uni-negative *O*-*O'*-chelating donors enabling stabilisation of mono- or polynuclear complexes. Furthermore, these *β*-diketones can be readily deprotonated to produce either neutral or charged metal complexed when coordinated to metal ions.[82,83]

2,4-Pentanedione (acetylacetone, acacH) is the simplest *β*-diketone and is generally prepared by a base-catalysed condensation reaction. Claisen described

[77] T. A. Hopkins, K. Meerholz, S. Shaheen, M. L. Anderson, A. Schmidt, B. Kippelen, A. B. Padias, H. K. Hall, N. Peyghambarian & N. R. Armstrong, *Chem. Mater.*, **8**, 344, 1996.
[78] J. Xie, Z. Ning & H. Tian, *Tettrahedron Lett*., **46**, 8559, 2005.
[79] S. Kusano, M. Koike, A. Takesue & M. Anzai, *European Patent* 1698613A1, 06-09-2006.
[80] P. Kathirgamanathan, S. Surendrakumar, J. Antipan-Lara, S. Ravichandran, V. R. Reddy, S. Ganeshamurugan, M. Kumaraverl, V. Arkley, A. J. Blake & D. Bailey, *J. Mater. Chem*., **21**, 1762, 2011.
[81] A. J. Brock, J. K Clegg, F. Li & L. F Lindoy, *Coord. Chem. Rev*. **375**, 106, 2018.
[82] P. A. Vigato, V. Peruzzo & S. Tamburini, *Coord. Chem Rev*., **253**, 1099, 2009.
[83] D. J. Bray, J. K. Clegg, L. F Lindoy & D. Schilter, *Adv. Inorg. Chem*., **1**, 59, 2007.

this reaction in 1889,[84] whereby a desired ketone (*acetone)* is reacted with an appropriate acylation reagent (*ethyl acetate*) which is nowadays known as *Claisen condensation* (**Scheme 2.2**).

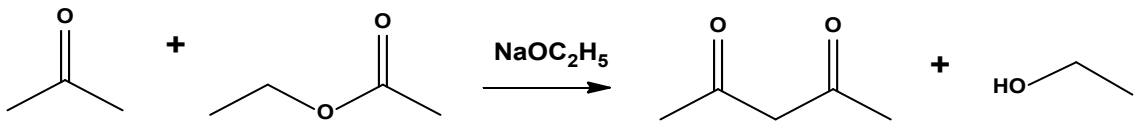

Scheme 2.2: Generalised synthetic scheme for acacH using the *Claisen condensation* route.

These type of *O,O'*-bidentate ligands can exist as both (**1**) enol and keto (**2**) tautomers, and due to the general ease in the preparation of these ligand systems, steric and electronic modification can easily be tuned by varying the R-substituents on the back-bone of the ligand system (**Scheme 2.3**)

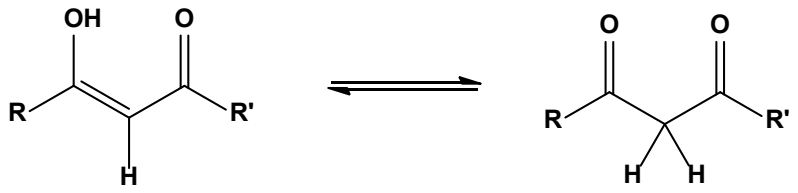

1, enol tautomer **2, keto tautomer**

Scheme 2.3: Keto-enol tautomerism in *β*-diketones.

The steric and electronic modification on the back-bone can drastically influence the coordination modes around the hafnium and zirconium metal centre so much that the coordination of the 3rd and 4th acac-ligand complexes can be observed[85,86] and structurally isolated. In vivo studies performed by Keppler et

[84] L. Claisen & E. F. Ehrhardt, *Chem. Ber*. **22**, 1009, 1889.
[85] R. M. Lord, J. J. Mannion, A. J. Hebden, A. Nako, B. D. Crossley, M. W McMullon, F. D. Janeway, R. M. Phillips & P. C. McGowan, *ChemMedChem.*, **9**, 1136, 2014.
[86] T. J. Pinnavaia & R. C. Fay, *Inorg. Chem.* **7**, 502, 1968.

al.,[87] on titanium *β*-diketonates, indicated that seven-coordinated complexes have lower cytotoxic activity when compared with the six-coordinate counterparts. However, in contrast, Lord et al. [88] showed that the tris diphenyl *β*-diketonate hafnium complex (seven-coordinated complex, **Figure 2.7(b)** exhibits superior cytotoxicity against human colon adenocarcinoma (HT-29) and human breast adenocarcinoma (MCF-7) when compared to cisplatin. Due to the antitumour activity and the easily '*tunable*' characteristics of acetylacetones, research with regards to functionalised acetylacetones coordinated to hafnium metal ions has found a fair amount of interest in literature.[89,90,91,92] Several more hafnium(IV) complexes were investigated and discussed in the previous M.Sc. dissertation parenting this project.[93] However, it was found that most of the hafnium and zirconium *β*-diketonate complexes in literature are predominantly *tetrakis*-chelated complexes with square-antiprismatic coordination geometries[94] around the metal centres and that only a handful of structural characterised examples of lesser coordinated complexes are available (**Figure 2.7**)

[87] B. K Keppler, C. Friesen, H. G. Moritz, H. Vongeriehten & E. Vogel, *Struct. Bond*., **78**, 97, 1991.
[88] G. Aromi, *Comments Inorg. Chem.* **32**, 163, 2011.
[89] S. V. Pasko, L. G. Hubert-Pfalzgraf, A. Abrutis, P. Richard, A. Bartasyte & V. Kaziauskiene, *J. Mater. Chem*., **14**, 1245, 2004.
[90] M. Steyn; *A Solid State and Mechanistic Study of Multidentate Ligand Zirconium(IV) Halido Complexes*, Ph.D Thesis, (**2014**), University of the Free State, South Africa.
[91] S. L. Benjamin, W. Levason, D. Pugh , G. Reid & W. Zhang, *Dalton Trans*., **41**, 12548, 2012.
[92] K. V. Zherikova, N. B Morozova, I. A. Baidina, E .V. Peresypkina & I. K. Igumenov, *J. Struct. Chem.*, **47**, 3, 570, 2006.
[93] J. A. Viljoen; *Speciation And Interconversion Mechanism Of Mixed Halo and O,O- and N,O-Bidentate Ligand Complexes of Hafnium*, M.Sc. Dissertation (**2009**), University of the Free State,South Africa.
[94] W. Clegg, *Acta Cryst., **C43***, 789, 1987.

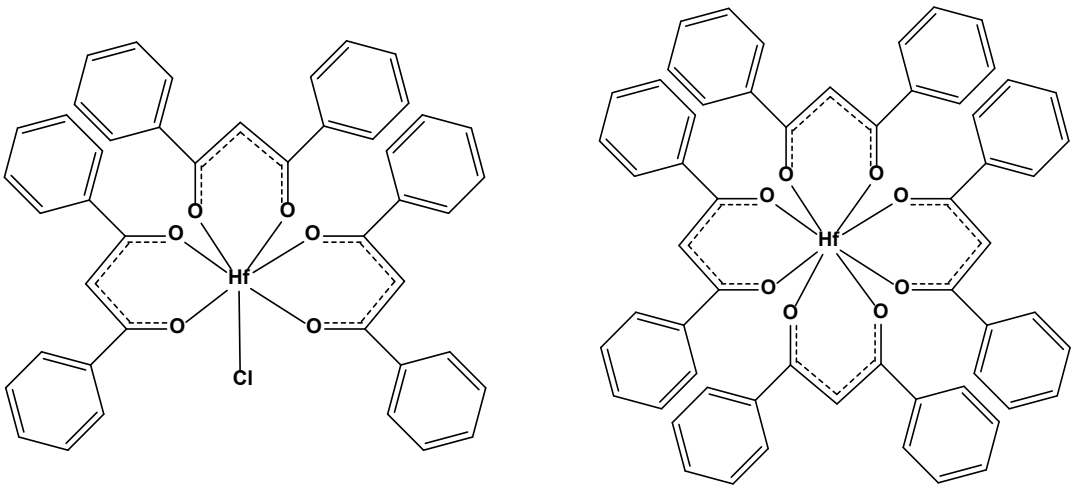

(a) **(b)**

Figure 2.7: Graphical representation of **(a)** *tris*-diphenyl β-diketonate hafnium complex, [Hf(dbm)$_3$Cl] and **(b)** *tetrakis*-diphenyl β-diketonate hafnium complex.

2.4.3. Tetradentate Ligands

In recent years, amine-based, tetradentate ligands have been used in a wide range of chemical applications as ion carries in liquid-liquid and solid-phase extractions[95,96,97,98] and in ion-selective PVC membrane electrodes.[99]

Schiff base ligands, *ligands that typically contain both oxygen and nitrogen and donors*, are able to coordinate metal ions through imine nitrogen and other groups usually linked to an aldehyde.

These Schiff base (Salen) ligands are many times referred to as “privileged ligands” in literature due to their high activity and ease of preparation through aldehyde-amine condensation reactions (**Scheme 2.4**).[100]

[95] S. Oshima, N. Hirayama, K. Kubono, H. Kokusen & T. Honjo, *Anal. Sci*., **18**, 1351, 2002.
[96] M. Mohammadhosseinia & M. S. Tehrani, *J. Chin. Chem. Soc*., **53**, 1119, 2006.
[97] M. R. Ganjali, M. R. Pourjavid, L. H. Babaei, *Quim. Nova*, **27**, 213, 2004.
[98] M. Shamsipur, A. R. Ghiasvand, H. Sharghi & H Naeimi, *Anal. Chim. Acta*, **408**, 271, 2000.
[99] M. R. Ganjali, T. Poursaberi, L. H. Babaei, S. Rouhani, M. Yousefi, M. Kargar-Razi, A. Moghimi, H. Aghabozorg & M. Shamsipur, *Anal. Chim. Acta*, **440,** 81, 2001.
[100] H. Schiff, *Ann Suppl*. **3**, 343, 1964.

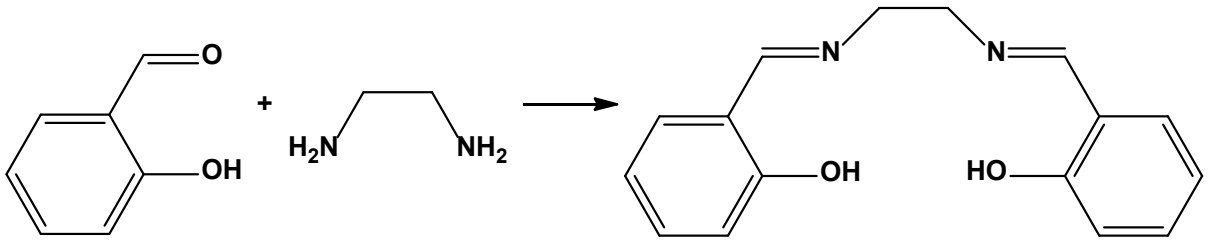

Scheme 2.4: Synthesis of Schiff base ligand, Salen - [N,N'-Ethylenebis-(salicylimine)].

Another advantage of these ligands is the fact that they are highly adjustable when modifying either the diamine or aldehyde portion of the ligand.[101,102] By varying these, both the steric and electronic properties of the ligand can be influenced dramatically as illustrated in **Scheme 2.5** below.

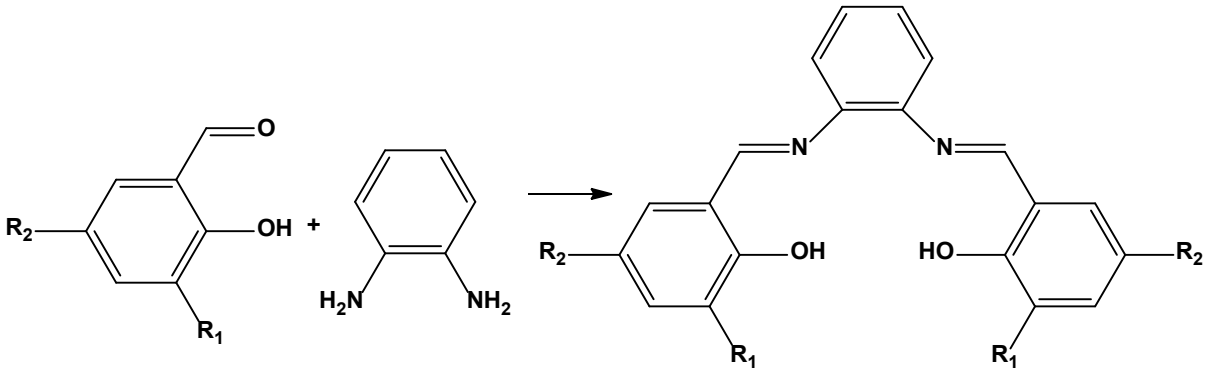

$R_1 = R_2 = H$

R_1 = Me (electron-donating group) ; R_2 = H

$R_1 = R_2$ = Cl (electron-withdrawing group)

$R_1 = R_2$ = *t*Bu (bulky electron-donating groups)

Scheme 2.5: Synthesis of Salophen ligands.

[101] E. J. Campbell & S. T. Nguyen, *Tetrahedron Lett., **42,*** 1221, 2001.
[102] H. Zhu, M. Wang, C. Ma, B. Li, C. Chen & L. Sun, *J. Organomet. Chem., **690,*** 3929, 2005.

In this regard, Salophen type ligands, which have an aromatic spacer between the two nitrogen donors, have been studied by several research groups, and its chelating behaviour with group IV metal ions are reported to be versatile. [103,104,105] Furthermore, titanium, zirconium and hafnium complexes containing salophen ligands have attracted a considerable amount of attention in recent years due to their excellent catalytic properties for olefin polymerisation.[106,107] However, in most of the studies performed, only the catalytic performances of the hafnium and zirconium compounds are compared and very rarely are they compared structurally. Keeping this and the aim of the study in mind, it is highly favourable to investigate some of these multidentate ligands as chelators when aiming to study and compare hafnium and zirconium complexes for separation endeavours.

2.5. A Brief Overview of the Coordination Polyhedrons of Eight Coordinated Hafnium(IV) and Zirconium(IV) Complexes

As mentioned earlier in this chapter (§ 2.4.2), most hafnium and zirconium complexes, containing bi- and tetradentate ligands) found in the literature are eight-coordinated (fully coordinated) complexes and adopt square-antiprismatic coordination geometries around the metal centres. It was previously postulated that these complexes have the lowest crystallisation state, therefore preferring maximum coordination.[93,108]

The two primary structural geometries of eight coordinated complexes are referred to as the α- and β forms, the dodecahedral and antiprismatic geometries,

[103] D. A. Atwood & D. Rutherford, *Organometallics*, **14**, 3988, 1995.
[104] S. Groysman, E. Sergeeva, I. Goldberg & M. Kol, *Eur. J. Inorg. Chem*, 2480, 2005.
[105] S. Gendler, A. L. Zelikoff, J. Kopilov, I. Goldberg & M. Kol*, J. Am. Chem. Soc*., **130**, 2144, 2008.
[106] X. Ji, X. Luo, W. Goa & Y. Mu, *Polyhedron*, **102,** 337, 2015.
[107] X. Ji, W. Yao, X. Luo, W. Goa & Y. Mu*, New J. Chem*., **40**, 2071, 2016.
[108] J. E Huheey, E. A Keiter & R. L Keiter; *Inorganic Chemistry - Principles of Structure and Reactivity,* 4th Ed. Harper Collins College Publishers, New York, 1993.

respectively,[109] The other geometry that these structures can adopt in the very rare cases, is the cubic geometry (**Figure 2.8**). A classic square antiprism is defined as an eight cornered structure, with sets of four corners on two parallel sides, where one set of corners is displaced away from the right-angled cube shape, so as to give triangle side planes connecting all corners.

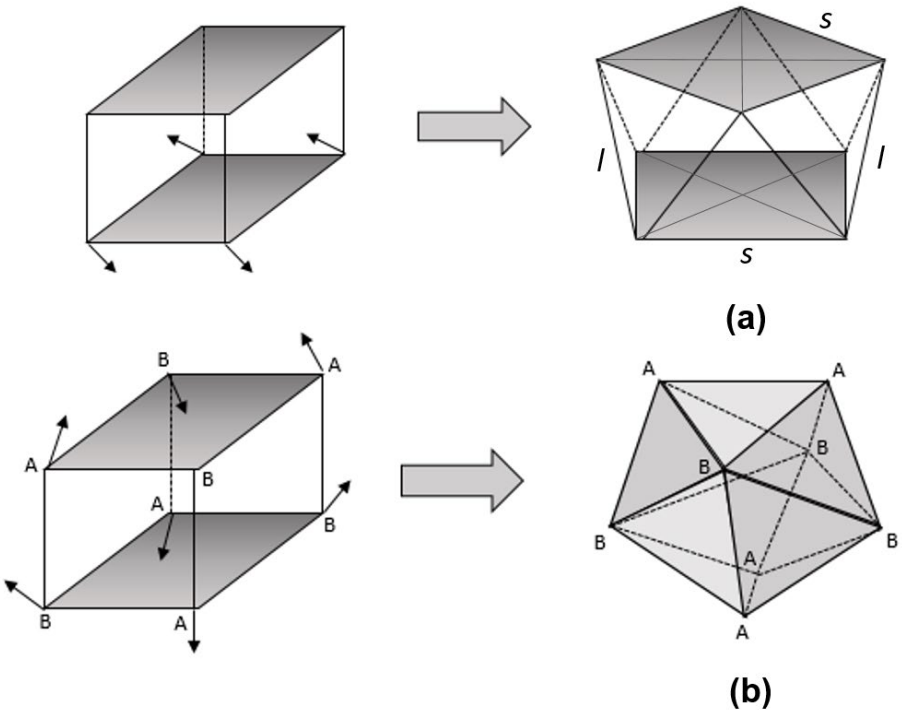

Figure 2.8: The three primary geometries for eight-coordinated complexes: The cube with its two principle distortions (**a**) Square antiprism (**b**) Dodecahedron.

From **Figure 2.8(a)** it is noticed that the 16 structural edges of the polyhedron is equally divided between two symmetry types (*s* and *l*), with the central metal atom being the intersection point of the 4 two-fold axes. Hoard and Silverton[110] reported that complexes with antiprismatic geometries can have three possible stereo-isomers, specifically for metal complexes containing symmetrical bidentate ligands like acetylacetone. The possible isomers and associated maximum point group symmetries are as follows;

[109] F. A Cotton, G Wilkinson & P. L Gauss P, *Basic Inorganic Chemistry,* 3rd Ed., John Wiley and Sons, New York, 1995.
[110] J. L. Hoard & J. V. Silverton, *Inorg.Chem.,* ***2***, 235, 1963.

The 1st possible isomer is defined as the **D_4-422 or D4-*llll*** isomer and for this to form all four symmetrical bidentate ligands has to coordinate vertically to the sides of the antiprism (*l*-edges, *side-bonded antiprism).*

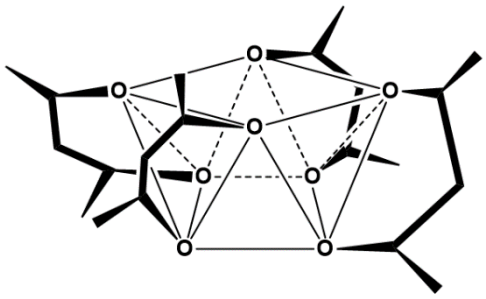

Figure 2.9: Illustration of the typical *D_4-side-bonded* square antiprismatic isomer.

Unfortunately, no *tetrakis*(acetylacetonato) complexes of hafnium and zirconium could be found in the literature which adopts this geometry. However, Pinnavaia et al.[111] reported a *tetrakis*(2,2,6,6-tetramethyl-3,5-heptanedionato)niobium(IV) adopting a D_4-422 square antiprismatic geometry.

The 2nd possible isomer, **C_2-2** or **C_2-*llss***, forms when two symmetrical bidentate ligands coordinate to the top and bottom corners (*s*-edges) and the two ligands coordinate vertically to the sides of the antiprism (*l*-edges, *mixed bonding antiprism)*.

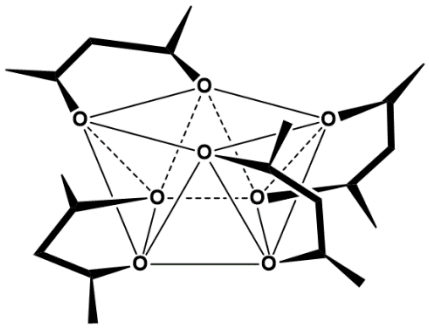

Figure 2.10: Illustration of the typical *C_2-mixed bonding* square antiprismatic isomer.

[111] T. J. Pinnavaia, B. Barnett, G. Podolsky & A. Tulinsky, *J. Am. Chem .Soc.* ***97***, 2712, 1975.

Published structures of this species include *tetrakis*(hexafluoroacetyl-acetonato)zirconium(IV)[112] and *tetrakis*(t-Butyl-3-oxobutanoato)zirconium(IV).[113] Unfortunately, no *tetrakis*(acetylacetonato) complexes of hafnium currently exist in literature.

The **3rd** and last possible isomer, **D_2-222 or D_2-*ssss***, forms when four symmetrical bidentate ligands coordinate on the top and bottom corners (*s*-edges) of the antiprism (*corner-bonded antiprism)*, as shown in **Figure 2.11**.

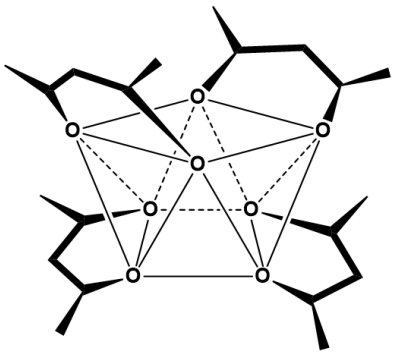

Figure 2.11: Illustration of the typical *D_2-corner-bonded* square antiprismatic isomer.

The D_2-222 isomer is the most preferred and commonly found. Published structures of this species include *tetrakis*(1,3-diphenyl-1,3-propanedionato) hafnium(IV),[114] *tetrakis*(trifluoroacetylacetonato)hafnium(IV),[115] Dihydrox-ido-bis-[trifluoro-phenylacetylacetonatohfnium(IV)],[116] *tetrakis*(acetyl-acetonato) zirconium(IV) ,[110] *tetrakis*(tri-fluoroacetylacetonato)zirconium(IV)[117] and *tetrakis*-(1,3-diphenyl-1,3-propanedionato)zirconium(IV).[118] Interestingly to note that of the very few hafnium and zirconium oxine complexes found, metal complexes coordinated to four 8-hydroxyquinoline ligands, all adopt the D_2-222 isomer

[112] M. Rahim, N. J. Taylor, S. Xin & S. Collins, *Organometallics, **17**,* 1315, 1998.

[113] U. K. Urs, M. S. Dharmaprakash, S. A. Shivashankar & T. N. G. Row, *Acta Cryst. **E59**,* m83, 2003.

[114] J. A. Viljoen, A. Roodt & H. G. Visser, *Acta Cryst. **E66**,* m1053, 2010.

[115] J. A. Viljoen, A. Muller & A. Roodt, *Acta Cryst.*, **E64**, m838, 2008.

[116] J. A. Viljoen, A. Muller & A. Roodt, *Acta Cryst.*, **E67**, m1822, 2011.

[117] M. Steyn, A. Roodt & G.Steyl, *Acta Cryst. **E64***, m827, 2008.

[118] H. K. Chun, W. L. Steffen & R. C. Fay, *Inorg. Chem., **18**,* 2458, 1979.

geometry.[119,120,121,122] However, since the available structural data pool of these *tetrakis*(oxine)-metal complexes are so small, speculating on trends is not yet possible.

2.6. Concluding Remarks

As has been noted throughout this section, fully coordinated (*tetrakis* or eight-coordinated) hafnium complexes adopt mainly three different geometry isomers. Therefore, it would be worth investigating, particular the crystallographic solid-state structure characterisation for various other symmetrical as well as unsymmetrical ligand systems to see if the same theory holds in this regards. The primary aim here is to identify ligands which can be modified sterically and electronically in order to manipulate the properties of these hafnium and zirconium complexes in such a way that subtle nuances in their chemical or physical behaviours can be induced and therefore be exploited for possible separation or extraction methods. However, it is of utmost importance for the development of such complexes, that sufficient data is collected to fully evaluate the root cause for the coordination behaviour observed.

To be able to successfully determine all specified aspects for this research project, the full characterisation of all novel hafnium compounds is required. When considering these inherent requirements, it becomes apparent that this project constitutes a significant challenge for the identification of the effects of ligand coordination on the solution- and solid-state behaviour of hafnium complexes.

[119] J. A. Viljoen, A Roodt & H. G. Visser, *Acta Cryst*., **E67,** m1428, 2011.
[120] M. Steyn, A. Roodt & & H. G. Visser, *Acta Cryst*., **E68**, m1344, 2012.
[121] J. A. Viljoen, A. Roodt & H. G. Visser, *Acta Cryst*., **E66**, m603, 2010.
[122] J. A. Viljoen, H. G. Visser, A Roodt & M. Steyn *Acta Cryst*., **E65**, m1514, 2009.

Chapter 3

Synthesis of Hafnium(IV) and Zirconium(IV) Complexes – Experimental Techniques & Preliminary Characterisation

---

3.1. Introduction

The synthesis of an extended range of new hafnium complexes is described in this chapter, which lays the foundation for the solid-state characterisation of these types of compounds. Complex characterisations were performed by using different techniques, including Infrared-, UV/Vis- and NMR spectroscopy.

As mentioned in **Chapter 2**, only a small number of hafnium complexes with *O,O'*- and *N,O*-multidentate ligands have been reported previously, and consequently, very little attention has been given to comparative identification of behavioural trends for this metal. If specific nuances in crystallisation between hafnium and zirconium complexes are found, it could be exploited in future extraction investigations. Thus, this part of the study aimed to explore the synthesis of hafnium and zirconium complexes with systematically selected nitrogen and oxygen donating ligands systems and to expand the knowledge base of their coordination behaviour in solution as well as in solid-state.[1,2,3]

[1] J. A. Viljoen, A. Muller and A. Roodt, *Acta Cryst*., **E64**, m838, 2008.
[2] J. A. Viljoen, H. G. Visser, A. Roodt & M. Steyn, *Acta Cryst.,* **E65**, m1367, 2009.
[3] J. A. Viljoen, H. G. Visser & A. Roodt, *Acta Cryst*., **E66**, m603, 2010.

3.2. Chemical and Equipment Details

3.2.1. Reagents and Solvents

All reagents used for the synthesis and characterisation were of analytical grade and were purchased from Sigma-Aldrich, South Africa. Reagents and solvents were used as received without further purification or drying, respectively.

3.2.2. Nuclear Magnetic Resonance (NMR) Spectroscopy

The ^{13}C- and ^{1}H- NMR solution-state spectra were recorded on a ***Bruker Advance II 600*** (^{1}H: 600.28 MHz; ^{13}C: 150.96 MHz, 5 mm DUAL ^{13}C-^{1}H/D probe with z-gradients) or ***Bruker Advance III*** 400 (^{1}H: 400.13 MHz; ^{13}C: 100.61 MHz, Solid-state probe = 4 mm VTN multinuclear double resonance magic angle spinning probe; Liquid-state probe = 5 mm BBI H-BB-D probe with z-gradients) or ***Bruker Fourier 300 MHz*** (^{1}H: 300.18 MHz; ^{13}C: 75.48 MHz, 5 mm ^{13}C/^{1}H high-resolution NMR probe equipped with Z-gradient coil) nuclear magnetic resonance spectrometer using the appropriate deuterated solvent at 25.0 °C. Chemical shifts, δ, are reported in ppm. ^{1}H NMR spectra were referenced internally using residual protons in the deuterated solvents, Benzene-d_6 [C_6D_6 = 7.16(1) ppm], Chloroform-d_1 [$CDCl_3$ = 7.26(5) ppm], Methanol-d_4 [MeOD = 4.78(1) ppm & 3.31(5) ppm] and Acetone-d_6 [C_3D_6O = 2.05(5) ppm]. ^{13}C NMR spectra were similarly referenced internally to the solvent resonance [C_6D_6 = 128(1)], [$CDCl_3$ = 77.26(4) ppm], [MeOD = 49.15(7) ppm] and [C_3D_6O = 29.92(7) ppm & 206.68(13) ppm] with values reported relative to tetramethylsilane (δ 0.0 ppm).

3.2.3. Infrared Spectroscopy

Solid-state FT-IR spectra were recorded as neat samples on a Digilab FTS 2000 Fourier transform spectrometer (ATR) utilising a He-Ne laser at 632.6 nm, in the range of 3000 to 600 cm^{-1}.

3.2.4. UV/Vis Spectroscopy

UV/Vis absorbance spectra were collected in a 1.000(1) cm tandem quartz cuvette on a Varian Cary 50 Conc. spectrophotometer, which was equipped with a Julabo F12-mV temperature cell regulator accurate within 0.1 °C. All λ_{max} values reported in this chapter were collected at 25.0 °C.

3.3. Syntheses of Hafnium(IV) Complexes

The general method for synthesising hafnium(IV) complexes was adopted from the previously determined procedure, as described in the related M.Sc. project concluded in 2009[4]. Metal complexation is achieved via a simple bench-top approach, under normal atmospheric conditions, by dissolving both the metal chloride ($HfCl_4$) and desired ligand in *N,N'*-dimethylformamide (DMF) or toluene, at slightly elevated temperatures (*ca. 60°C*). The reaction solutions are mixed and stirred for approximately 30 min and allowed to cool slowly to induce crystallisation. Specific amounts of reagents, other reaction conditions, and rate of crystallisation are described below.

[4] J. A. Viljoen; *Speciation And Interconversion Mechanism Of Mixed Halo and O,O- and N,O-Bidentate Ligand Complexes of Hafnium*, M.Sc. Dissertation (**2009**), University of the Free State,South Africa.

3.3.1. 8-Hydroxyquinolinato Complexes of Hafnium(IV)

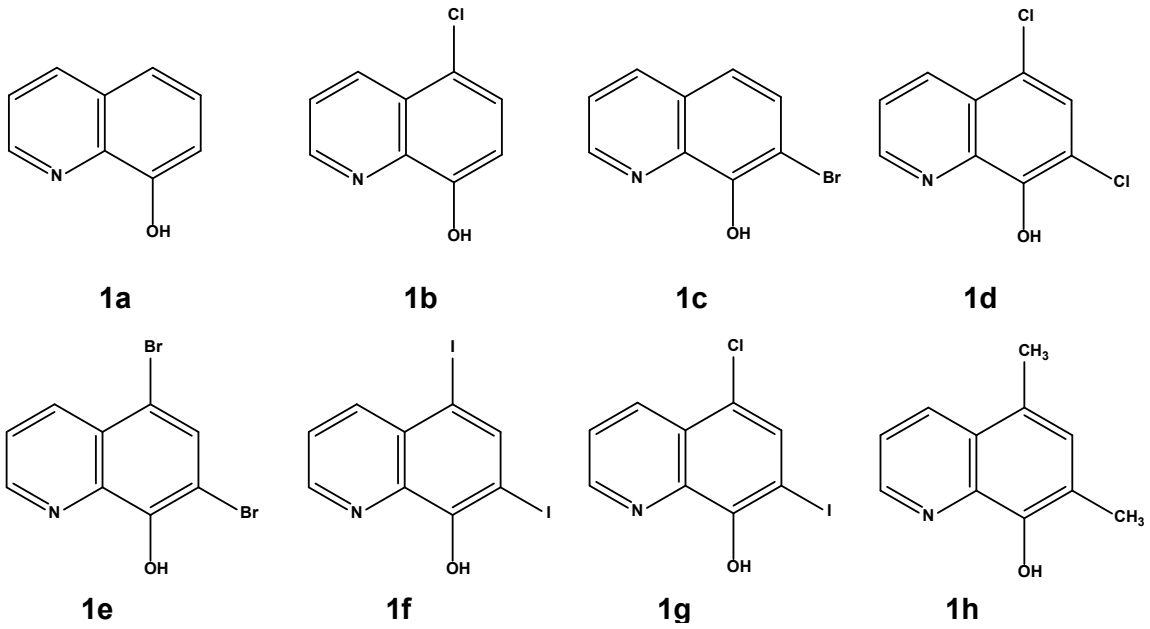

Figure 3.1. Graphical representation of the quinoline/oxine ligands utilised in the synthesis of hafnium(IV) complexes. (**1a**) 8-hydroxyquinoline (OxH), (**1b**) 5-chloro-8-hydroxyquinoline (5-ClOxH), (**1c**) 7-bromo-8-hydroxyquinoline (7-BrOxH), (**1d**) 5,7-dichloro-8-hydroxyquinoline (diClOxH), (**1e**) 5,7-dibromo-8-hydroxyquinoline (diBrOxH), (**1f**) 5,7-diiodo-8-hydroxyquinoline (diIOxH), (**1g**) 5-chloro-7-iodo-8-hydroxyquinoline (CliOxH), (**1h**) 5,7-dimethyl-8-hydroxy-quinoline (diMeOxH).

3.3.1.1. Tetrakis(quinolin-8-olato-κ²N,O)-hafnium(IV) – [Hf(Ox)₄] [5]

8-Hydroxyquinoline [OxH, **1a**] (191 mg, 1.311 mmol) was added to a suspension of hafnium tetrachloride [$HfCl_4$] (105 mg, 0.328 mmol) in toluene (20 ml). Upon dissolution, the solution turned slightly yellow after 10 min, and after stirring for 30 min at 60 °C, the crude product was filtered and left to crystallise at room temperature. After *ca.* ten days, yellow plate-like crystals (**Hf_1a,** § 4.4), suitable for single X-Ray diffraction, formed (***Yield*** 165 mg, 67%).

[5] J. A. Viljoen, H. G. Visser, A. Roodt & M. Steyn, *Acta Cryst.*, **E65**, m1514, 2009.

UV/Vis: λ^{MeOH}_{max} = 381 nm, ε = 430.4 $cm^{-1}.M^{-1}$; ***IR (ATR):*** $\nu_{C=O}$ = 1659 cm^{-1}; ***^{1}H NMR*** (300 MHz, C_6D_6) : δ = 8.13 (d, 1H), 7.36 (t, 2H), 7.29 (dd, 2H), 6.70 (d, 1H); ***^{13}C NMR*** (75 MHz, C_6D_6) : δ = 178.14(C), 166.98 (CH), 157.2 (C), 147.81 (CH), 131.23 (CH), 127.15 (C), 120.31 (CH), 117.05 (C), 110.76 (CH).

3.3.1.2. Tetrakis(5-chloroquinolin-8-olato-κ²N,O)hafnium(IV) – [Hf(5-ClOx)₄]

5-Chloro-8-hydroxyquinoline [5Cl-OxH, **1b**] (249 mg, 1.386 mmol) was added to a suspension of hafnium tetrachloride [$HfCl_4$] (111 mg, 0.347 mmol) in toluene (20 ml). The dissolution turned into a slightly yellow solution after 10 min, and after stirring for 30 min at 60 °C, the crude product was filtered and left to crystallise at room temperature. After *ca.* ten days, yellow needle-like crystals (**Hf_1b,** § 4.5), suitable for single X-Ray diffraction, formed (***Yield*** : 225 mg, 73%).

UV/Vis: λ^{MeOH}_{max} = 390 nm, ε = 496.8 $cm^{-1}.M^{-1}$; ***IR (ATR):*** $\nu_{C=O}$ = 1561 cm^{-1}; ***^{1}H NMR*** (400 MHz, $CDCl_3$) : δ = 8.94 (d, 1H), 8.29 (d, 1H), 7.39 (d, 1H), 7.29 (dd, 1H), 6.73 (d, 1H); ***^{13}C NMR*** (100 MHz, $CDCl_3$) : δ = 161.5 (C), 146.3 (CH), 142.2 (C), 134.8 (CH), 129.2 (CH), 127.1 (C), 122.1 (CH), 115.0 (C), 113.0 (CH).

3.3.1.3. Tetrakis(7-bromoquinolin-8-olato-κ²N,O)hafnium(IV) – [Hf(7-BrOx)₄]

Hafnium tetrachloride, [$HfCl_4$], (99 mg, 0.309 mmol) was dissolved in 10 ml DMF at room temperature. While stirring the $HfCl_4$ solution, 7-bromo-8-hydroxyquinoline ([7-BrOxH], **1c**) (277 mg, 1.236 mmol) dissolved in 10 ml DMF was slowly added. The transparent $HfCl_4$ solution turned yellow after the addition of the 7-BrOxH. The reaction mixture was stirred for 30 min at 60 °C

and left to crystallise at room temperature. However, no suitable crystals could be obtained for a crystallographic characterisation (***Yield*** : 201 mg, 61%).

UV/Vis: λ^{MeOH}_{max} = 386 nm, ε = 320.8 $cm^{-1}.M^{-1}$; ***IR (ATR):*** $\nu_{C=O}$ = 1571 cm^{-1}; ***^{1}H NMR*** (300 MHz, MeOD) : δ = 8.85 (dd, 1H), 8.28 (dd, 1H), 7.64 (d, 1H), 7.54 (dd, 1H), 7.33 (d, 1H); ***^{13}C NMR*** (75 MHz, MeOD) : δ = 151.4 (CH), 148.3 (C), 141.4 (C), 139.8 (CH), 132.4 (C), 129.9 (C), 126.1 (CH), 120.9 (C), 118.3 (CH).

3.3.1.4. Tetrakis(5,7-dichloroquinolin-8-olato-κ^{2}N,O)-hafnium(IV) – [Hf(diClOx)$_4$]

Hafnium tetrachloride, [$HfCl_4$], (101 mg, 0.315 mmol) was dissolved in 10 ml DMF at room temperature. While stirring the $HfCl_4$ solution, 5,7-dichloro-8-quinoline ([diClOxH], **1d**) (270 mg, 1.261 mmol) dissolved in 10 ml DMF was slowly added. The transparent $HfCl_4$ solution turned yellow instantly after the addition of the diClOxH. The reaction mixture was stirred for 30 min at 60°C and left to crystallise at room temperature. After *ca.* two weeks, yellow cubic-like crystals (**Hf_1d,** § 5.4), suitable for single X-Ray diffraction, formed (***Yield*** 238 mg, 73%).

UV/Vis: λ^{MeOH}_{max} = 406 nm, ε = 230.8 $cm^{-1}.M^{-1}$; ***IR (ATR):*** $\nu_{C=O}$ = 1593 cm^{-1}; ***^{1}H NMR*** (300 MHz, C_3D_6O) : δ = 8.99 (dd, 1H), 8.60 (dd, 1H), 7.78 (q, 1H), 7.74 (s, 1H); ***^{13}C NMR*** (75 MHz, C_3D_6O) : δ = 151.4 (CH), 148.3 (C), 141.4 (C), 139.8 (CH), 132.4 (C), 129.9 (C), 126.1 (CH), 120.9 (C), 118.3 (CH).

3.3.1.5. Tetrakis(5,7-dibromoquinolin-8-olato-κ²N,O)-hafnium(IV) – [Hf(diBrOx)₄] [6]

Hafnium tetrachloride, [$HfCl_4$], (108 mg, 0.337 mmol) was dissolved in 10 ml DMF at room temperature. While stirring the $HfCl_4$ solution, 5,7-dibromo-8-quinoline ([diBrOxH], **1e**) (409 mg, 1.354 mmol) dissolved in 10 ml DMF was slowly added. The transparent $HfCl_4$ solution turned yellowish after the addition of the diBrOxH. The reaction mixture was stirred for 30 min at 60°C and left to crystalise at room temperature. After *ca.* a week, yellow cubic-like crystals (**Hf_1e,** § 5.5), suitable for single X-Ray diffraction, formed (***Yield*** : 378 mg, 81%).

UV/Vis: λ^{MeOH}_{max} = 407 nm, ε = 281.9 $cm^{-1}.M^{-1}$; ***IR (ATR):*** $\nu_{C=O}$ = 1559 cm^{-1}; ***^{1}H NMR*** (600 MHz, C_3D_6O) : δ = 9.98 (d, 1H), 9.10 (d, 1H), 8.34 (s, 1H), 7.93 (m, 1H); ***^{13}C NMR*** (150 MHz, C_3D_6O) : δ = 179.50 (CH), 168.71 (CH), 142.74 (CH), 139.84 (C), 135.23 (C), 135.04 (CH), 128.26 (C), 122.68 (C) 118.89 (C).

3.3.1.6. Tetrakis(5,7-diiodoquinolin-8-olato-κ²N,O)hafnium(IV) – [Hf(diIOx)₄]

Hafnium tetrachloride, [$HfCl_4$], (101 mg, 0.315 mmol) was dissolved in 10 ml DMF at room temperature. While stirring the $HfCl_4$ solution, 5,7-diiodo-8-quinoline ([diIOxH], **1f**) (502 mg, 1.268 mmol) dissolved in 10 ml DMF was slowly added. The transparent $HfCl_4$ solution turned yellow after the addition of the diIOxH. The reaction mixture was stirred for 30 min at 60 °C and left to crystalise at room temperature. After *ca.* three weeks, yellow plate-like crystals (**Hf_1f,** § 5.6), suitable for single X-Ray diffraction, formed (***Yield*** : 388 mg, 72%).

[6] J. A. Viljoen, H. G. Visser, A. Roodt & I. Engelbrecht, *Z. Kristallog.*, NCS **228**, 485, 2013.

UV/Vis: λ^{MeOH}_{max} = 413 nm, ε = 402.8 $cm^{-1}.M^{-1}$; ***IR (ATR):*** $\nu_{C=O}$ = 1550 cm^{-1}; ***^{1}H NMR*** (600 MHz, C_3D_6O) : δ = 9.08 (d, 1H), 8.82 (d, 1H), 7.85 (t, 1H), 8.34 (s, 1H); ***^{13}C NMR*** (150 MHz, C_3D_6O) : δ = 151.32 (CH), 150.36 (CH), 136.26 (CH), 134.76 (C), 131.84 (C), 123.24 (CH), 121.28 (C), 120.89 (C) 119.89 (C).

3.3.1.7. Tetrakis(5-chloro-7-iodoquinolin-8-olato-κ²N,O)-hafnium(IV) –[Hf(5Cl-7I-Ox)$_4$]

Hafnium tetrachloride, [$HfCl_4$], (104 mg, 0.325 mmol) was dissolved in 10 ml DMF at room temperature. While stirring the $HfCl_4$ solution, 5-chloro-7-iodo-8-hydroxyquinoline ([5Cl-7I-OxH], **1g**) (397 mg, 1.301 mmol) dissolved in 10 ml DMF was slowly added. The transparent $HfCl_4$ solution turned yellowish after the addition of the 5Cl-7I-OxH. The reaction mixture was stirred for 30 min at 60°C and left to crystalise at room temperature. However, no suitable crystals could be obtained for a crystallographic description. (***Yield*** : 251 mg, 55%).

UV/Vis: λ^{MeOH}_{max} = 400 nm, ε = 998.6 $cm^{-1}.M^{-1}$; ***IR (ATR):*** $\nu_{C=O}$ = 1659 cm^{-1}; ***^{1}H NMR*** (600 MHz, MeOD) : δ = 8.91 (dd, 1H), 8.56 (dd, 1H), 7.93 (s, 1H), 7.45 (q, 1H). ***^{13}C NMR*** (75 MHz, MeOD) : δ = 156.41 (CH), 152.39 (C), 140.45 (C), 135.88 (CH), 134,43 (CH), 130.03 (C), 125.7 (C), 124.13 (CH), 96.56 (C).

3.3.1.8. Tetrakis(5,7-dimethylquinolin-8-olato-κ²N,O)-hafnium(IV) – [Hf(diMeOx)$_4$] [7]

Hafnium tetrachloride, [$HfCl_4$], (106 mg, 0.331 mmol) was dissolved in 10 ml DMF at room temperature. While stirring the $HfCl_4$ solution, 5,7-dimethyl-8-hydroxyquinoline ([diMeOxH], **1h**) (229 mg, 1.324 mmol) dissolved in 10 ml DMF was slowly added. The transparent $HfCl_4$ solution turned slightly orange after the addition of the diMeOxH. The reaction mixture was stirred for 30 min

[7] J. A. Viljoen, H. G. Visser & A. Roodt, *Acta Cryst.,* **E67**, m1428, 2011.

at 60°C and left to crystalise at room temperature. After *ca.* a week, reddish parallelepiped-like crystals (**Hf_1h,** § 4.5), suitable for single X-Ray diffraction, formed (***Yield*** : 265 mg, 91%).

UV/Vis: λ^{MeOH}_{max} = 403 nm, ε = 468.8 $cm^{-1}.M^{-1}$; ***IR (ATR):*** $\nu_{C=O}$ = 1550 cm^{-1}; ***^{1}H NMR*** (600 MHz, MeOD) : δ = 9.98 (d, 1H), 9.05 (d, 1H), 8.31 (t, 1H), 7.68 (s, 1H), 2.61 (s, 3H), 2.49(s, 3H); ***^{13}C NMR*** (150 MHz, MeOD) : δ = 145.8(CH), 143.2 (C), 140.6 (C), 136.8 (CH), 133.5 (CH), 130.5 (C), 128.7 (C), 123.2 (C), 121.2 (CH), 18.4 (CH3), 17.8 (CH3).

3.3.2. Acetylacetonato Complexes of Hafnium(IV)

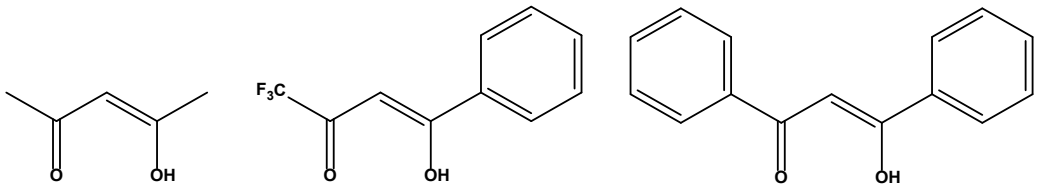

2a **2b** **2c**

Figure 3.2: Graphical representation of the *O,O'*-donating bidentate ligands employed in the synthesis of hafnium(IV) complexes. (**2a**) *Acetylacetone* (acacH), (**2b**), Trifluorophenyl-butanedione (tfbaH), (**2c**) *Dibenzoylmethane* (dbmH).

3.3.2.1. Tetrakis(acetylacetonato- κ^{2}O,O')hafnium(IV) – [Hf(acac)$_4$]

Hafnium tetrachloride, [$HfCl_4$], (207 mg, 0.646 mmol) was dissolved in 20 ml DMF at room temperature. While stirring the $HfCl_4$ solution, acetylacetone (acacH , **2a**) (261 mg, 2.61 mmol) dissolved in 20 ml DMF was slowly added. The reaction mixture was stirred for 30 min at 60°C and left to crystalise at room temperature. However, no suitable crystals could be obtained for a crystallographic description (***Yield*** : 59 mg, 11%).

UV/Vis: λ^{DMF}_{max} = 413 nm, ε = 2.134 x 10^3 $cm^{-1}.M^{-1}$; ***IR (ATR):*** $\nu_{C=O}$ = 1696 cm^{-1}

3.3.2.2. Di-μ-hydroxido-bis[tris(4,4,4-trifluoro-1-phenyl-acetylacetonato-κ²O,O')-hafnium(IV)] dimethylformamide disolvate – [Hf(OH)(tfba)₃]₂ [8]

Hafnium tetrachloride, [$HfCl_4$], (201 mg, 0.626 mmol) was dissolved in 25 ml DMF at room temperature. While stirring the $HfCl_4$ solution, 4,4,4-trifluoro-1-phenyl-1,3-butanedione ([tfbaH], **2b**) (540 mg, 2.532 mmol) dissolved in 25 ml DMF was slowly added. The reaction mixture was refluxed for 12 hours and left to crystalise at room temperature. After *ca.* two weeks, colourless crystals (**Hf_2c,** § 6.5), suitable for single X-Ray diffraction, formed (***Yield*** : 398 mg, 76%).

UV/Vis: λ^{DMF}_{max} = 382 nm, ε = 2.564 x 10^3 $cm^{-1}.M^{-1}$; ***IR (ATR):*** $\nu_{C=O}$ = 1664 & 1596cm^{-1}; ***^{1}H NMR*** (300 MHz, MeOD) : δ = 8.05 (s, 1H), 7.68 (t, 2H), 7.55 (d, 2H), 7.29 6.99 (m, 1H) 5.16 (s, 1H); ***^{13}C NMR*** (75 MHz, MeOD) : δ = 206.67 (1C), 203.40 (1C), 133.15 (1C), 128.92 (2C), 128.69 (2C), 117.05 (1C), 75.25 (1C).

[8] J. A. Viljoen, H. G. Visser & A. Roodt, *Acta Cryst.*, **E67**, m1822, 2011.

3.3.2.3. Tetrakis(1,3-diphenylpropane-1,3-dionato- κ^2O,O')-hafnium(IV) – [Hf(dbm)$_4$] [9]

Hafnium tetrachloride, [$HfCl_4$], (203 mg, 0.634 mmol) was dissolved in 10 ml DMF at room temperature. While stirring the $HfCl_4$ solution, dibenzoylmethane ([dbmH], **2c**) (568 mg, 2.535 mmol) dissolved in 10 ml DMF was slowly added. The reaction mixture was stirred for 30 min at 60°C and left to crystalise at room temperature. After *ca.* two weeks, colourless cubic-like crystals (**Hf_2c,** § 6.4), suitable for single X-Ray diffraction, formed (***Yield*** : 654 mg, 83%).

UV/Vis: λ^{DMF}_{max} = 349 nm, ε = 2.954 x 10^3 $cm^{-1}.M^{-1}$; ***IR (ATR):*** $\nu_{C=O}$ = 1595 & 1529 cm^{-1}; ***^{1}H NMR*** (600 MHz, C_3D_6O) : δ = 8.35 (d, 4H), 7.63 (t, 2H), 7.51 (t, 4H) 7.29 (s, 1H); ***^{13}C NMR*** (600 MHz, C_3D_6O) : δ = 182.67 (2C), 138.39 (2C), 131.58 (2C), 128.20 (2C), 127.98 (2C), 95.08 (1C).

3.3.3. Tetradentate Complexes of Hafnium(IV)

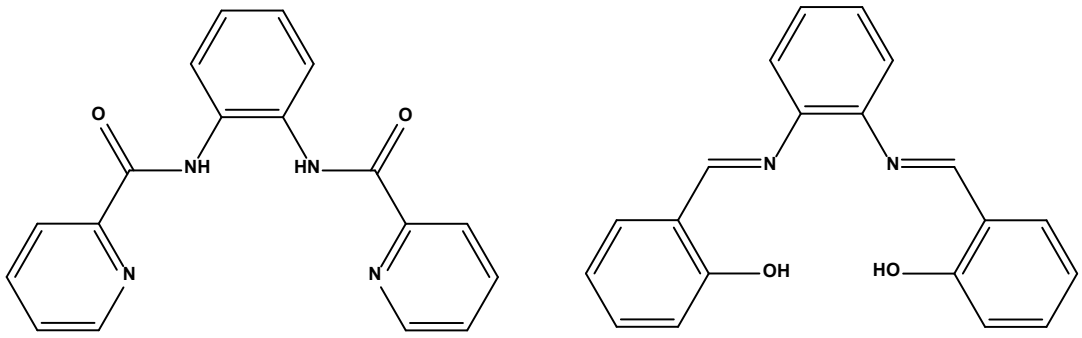

3a **3b**

Figure 3.3: Graphical representation of the *N*- & *O*-donating tetradentate ligands employed in the synthesis of hafnium(IV) complexes. (**3a**) *N,N'*-(1,2-phenylene)bis(pyridine-2-carboxamide), (bpbH), (**3b**) *N,N'*-Bis(salicylidene)-1,2-phenylenediamine (SalophenH).

[9] J. A. Viljoen, H. G. Visser & A. Roodt, *Acta Cryst.*, **E66**, m1053, 2010.

3.3.3.2. Diaqua-(N,N'-(o-phenylene)bis(pyridine-2-carbox-amidato)- κ^4N,N',N'',N''')zirconium(IV) nitrate - (Zr(bpb)(H_2O)$_2$]NO_3

Zirconium tetrachloride ([$ZrCl_4$] 203 mg, 0.897 mmol) was dissolved in 20 ml methanol at room temperature. While stirring the $ZrCl_4$ solution, 1,2-phenylene-bis(pyridine-2-carboxamide) (bpbH, **3a**) (286 mg, 0.899 mmol) dissolved 20 ml methanol was slowly added and refluxed overnight. After cooling, the yellow precipitate was filtered off and washed with chloroform. The filtrate was slowly recrystallised in methanol at room temperature (**Yield** : 34 mg, 9%). Crystallographic structural characterisation of **Zr_3a** is discussed in §7. 5.

UV/Vis: λ^{DMF}_{max} = 367 nm, ε = 6.532 x 10^3 $cm^{-1}.M^{-1}$; ***IR (ATR):*** $\nu_{C=O}$ = 1625 cm^{-1}; ***^{1}H NMR*** (600 MHz, C_2D_6OS) : δ = 9.23 (d, 2H), 8.77 (dt, 2H), 8.54 (d, 4H), 8.10 (m, 2H), 7.09 (m, 2H); ***^{13}C NMR*** (150 MHz, C_2D_6OS) : δ = 158.45 (2C), 149.55 (2C), 145.58 (2C), 143.70 (2CH), 134.70 (2CH), 128.65 (2CH), 124.17 (2CH), 123.41 (2CH), 119.25 (2CH).

3.3.3.1. Bis(N,N'-disalicylidene-1,2-phenylenediamino-κ^4N,N',O,O')hafnium(IV) – [Hf(Salophen)$_2$]·2(C_7H_8)

N,N'-bis(salicylidene)-1,2-phenylene-diamine, [salophenH_2, **3b**] (395 mg, 1.253 mmol) was added to a suspension of hafnium tetrachloride, [$HfCl_4$], (202 mg, 0.631 mmol) in toluene (20 ml). The reaction mixture was refluxed for 12 hours and left to crystallise at room temperature. After several days yellow cubic-like crystals (**Hf_3a,** § 7.4), suitable for single X-Ray diffraction, formed (***Yield*** : 283 mg, 56%)

UV/Vis: λ^{DMF}_{max} = 375 nm, ε = 7.86 x 10^3 $cm^{-1}.M^{-1}$; ***IR (ATR):*** $\nu_{C=O}$ = 1678 cm^{-1}; ***^{1}H NMR*** (300 MHz, $CDCl_3$) : δppm = 8.54 (s, 2H), 7.46 (m, 2H), 7.41 (m, 2H), 7.21 (dd, 2H,), 7.01 (m, 2H), 6.45 (td, 2H), 5.98 (d, 2H); ***^{13}C NMR*** (75 MH. $CDCl_3$) : δ = 163.13 (2CH), 147.34 (2C), 138.23 (CH), 135.53 (CH), 134.81 (CH), 132.45 (CH), 131.87 (CH), 130.11 (CH), 129.88 (2CH), 123.71 (2C), 121.45 (CH), 121.05 (CH), 119.93 (C), 119.15 (C), 117.23 (CH), 116.80 (CH).

3.4. Conclusion

The synthesis of a series of novel hafnium(IV) and zirconium(IV) coordination compounds, obtained from a systematic range of *N*- and *O*- bi- and multidentate ligands, have been successfully carried out. However, the more significant focus area revolved around the synthesis and crystallisation of [Hf(*N,O*-bid)$_4$] (*N,O*-bid = oxinate) complexes, of which no single-crystal X-Ray data were available in literature prior to this PhD study. It was clearly illustrated in this study that it is possible to synthesise hafnium(IV) and zirconium(IV) complexes containing various *N,O*- and *O,O'*-bidentate ligand systems as well as *N,O,O,N*- and *N,N',N',N*-tetradentate ligand systems under simple aerobic conditions, contradicting the available literature where it is reported that hafnium(IV) and zirconium(IV) complexes could only be synthesised under anhydrous and inert oxygen-free (Schlenk) conditions to avoid hydrolysis of the tetrachloridohafnium(IV) starting reagent ($HfCl_4$).[10] Although excessive water should still be avoided, the presence of oxygen in the system is not relevant since both the metals are already in the highest oxidation state.

In the following **Chapters (4-9)**, the crystallographic characterisation of the systematic range of these compounds is described in detail and structurally evaluated and correlated. Furthermore, a preliminary solution extraction study of some of these oxinato-metal complexes are also evaluated in **Chapter 11**.

[10] Z. Fang & D. A. Dixon*, J. Phys. Chem*., 117, **15**, 7459, 2013.

Chapter 4

X-Ray Diffraction Studies of Hafnium(IV) Complexes Containing Non- and Substituted 8-Hydroxyquinoline Ligands

---

4.1. Introduction

An extensive literature study revealed that only two hafnium(IV)-oxinato complexes had been structurally characterised before this overarching crystallographic study.[1,2] However, none of these studies revealed any specific details regarding solid-state comparisons between Hf(IV) -and Zr(IV)-oxinato complexes.

The 8-hydroxyquinoline (oxine) ligand and its derivates have a wide range of applications such as in neurodegenerative, antimicrobial, antioxidant, anticancer and anti-inflammatory agents.[3,4,5]

---

[1] I. Demakopoulos, N. Klouras, C. P. Raptopoulou & A. Terzis, *Z. Anorg. Allg .Chem*., **621**, 1761, 1995.

[2] M. Mirzaee, M. Armaghan, M. Norouzi, M. M.Amini & H. R. Khavasi, *Aust. J. Chem.*, **66,** 1587, 2013.

[3] V. Prachayasittikul, S. Prachayasittikul, S. Ruchirawat & V. Prachayasittikul, *Drug. Des. Dev. Ther*., **7**, 1157, 2013.

[4] J. Lazovic, L. Guo, J. Nakashima, L. Mirsadraei, W. Yong & H. J. Kim, *Neuro-Oncol*., **17 (1),** 53, 2015.

[5] K. G. Naber, H. Niggemann & G. Stein, BMC *Infect. Dis*., **14**, 628, 2014.

Moreover, oxine ligands and some of its derivatives are well-proven complexants and precipitation agents in chemical analysis.[6,7] For example, Vinogradov and Shpinel[8] showed that 8-hydroxyquinoline could be used to separate zirconium from hafnium through precipitation.

This crystallographic study focuses on the modification of the electronic and steric properties of 8-hydroxyquinoline as ligand for potential further application in separation studies, or, more specifically, the manipulation of the electronic influence of electron-withdrawing substitutes (chloro moieties,) *vs.* electron-donating substituents (methyl moieties) on the 5 and/or 7 position of the quinoline back-bone when coordinated to hafnium(IV) metal centres, see below.

As a result, this chapter contains a detailed discussion of the single-crystal structures of three hafnium(IV) complexes containing non- and substituted 8-hydroxyquinoline ligands as well as the preliminary intercorrelation of each structure. (**Figure 4.1**).

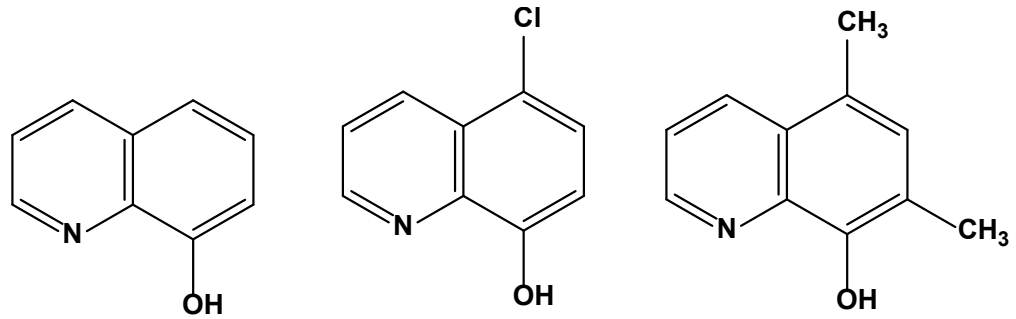

Figure 4.1: 8-Hydroxyquinoline type ligands chelated to hafnium(IV) and discussed in this chapter. (**a**) 8-hydroxyquinoline (OxH); (**b**) 5-Chloro-8-hydroxyquinoline (5-ClOxH); (**c**) 5,7-Dimethyl-8-hydroxyquinoline (diMeOxH).

The importance of the structural characterisation of these hafnium type complexes lies in the possibility of observing small differences in the chemical behaviours

[6] G. H. Jeffery, J. Basset, J. Mendham & R. C. Denney, *Vogel's textbook of Quantitative Chemical Analysis*, 5th Ed., New York, Longman Scientific and Technical, 1989.
[7] D. L. Huges & M. R. Truter, *J. Chem. Soc. Dalton Trans.*, **3**, 520, 1979.
[8] A. V. Vinogradov & V. S. Shpinel, *Atom Energiya*, **3**, 130, 1957.

between hafnium and zirconium, which could, in principle, be exploited for designing novel separation techniques.

4.2. Experimental

The X-ray intensity data was collected on a Bruker X8 ApexII 4K Kappa CCD area detector diffractometer, equipped with a graphite monochromator and Mo$K\alpha$ fine-focus sealed tube (λ = 0.71069 Å, T = 100(2) K) operated at 2.0 kW (50 kV, 40 mA). The initial unit cell determinations and data collections were done by the SMART[9] software package. The collected frames were integrated using a narrow-frame integration algorithm and reduced with the Bruker SAINT-Plus and XPREP software packages[10] respectively. Analysis of the data showed no significant decay during the data collection. Data was corrected for absorption effects using the multi-scan technique SADABS[11], and the structure was solved by the direct methods package SIR97[12] and refined using the WinGX[13] software incorporating SHELXL[14]. The final anisotropic full-matrix least-squares refinement was done on F^2. The methyl and aromatic protons were placed in geometrically idealised positions (C–H = 0.93 – 0.98 Å) and constrained to ride on their parent atoms with $U_{iso}(H) = 1.2U_{eq}(C)$. All non-hydrogen atoms were refined with anisotropic displacement parameters. The graphics were obtained with the DIAMOND[15] program with 50% probability ellipsoids for all non-hydrogen atoms.

---

[9] Bruker SMART-NT Version 5.050, *Bruker AXS Inc. Area-Detector Software Package*; Madison, Winconsin, United States of America, 1998.

[10] Bruker SAINT-Plus Version 6.02 (including XPREP), *Bruker AXS Inc. Area-Detector Integration Software*, Madison, Winconson, United States of America, 1999.

[11] Bruker SADABS Version 2004/1, *Bruker AXS Inc. Area Detector Absorption Correction Software*, Madison, Wisconsin, United States of America, 1998.

[12] A. Altomare, M. C. Burla, M. Camalli, G. L. Cascarano, C. Giacovazzo, A. Guagliardi, A. G. G. Moliterni, G. Polidori & R. Spagna, *J. Appl. Cryst.,* **32**, 115, 1999.

[13] L. J. Farrugia, *J. Appl. Cryst., **32***, 837, 1999.

[14] G. M. Sheldrick; SHELXL97, (1997). *Program for Crystal Structure Refinement*, University of Göttingen, Germany.

[15] K. Brandenburg & H. Putz; DIAMOND, *Release 3.0e, Crystal Impact GbR*, Bonn, Germany, 2006.

Table 4.1. Crystallographic and refinement details for structures discussed in this chapter.

Crystal Formula	$[Hf(Ox)_4]\cdot 2(C_7H_8)$ (Hf_1a)[16]	$[Hf(5\text{-}ClOx)_4]\cdot 2(C_7H_8)$ (Hf_1b)	$[Hf(diMeOx)_4]\cdot 2(DMF)$ (Hf_1h) [17]
Formula weight	939.35	1031.05	1013.48
Crystal system	Triclinic	Monoclinic	Monoclinic
Space group	$P\bar{1}$	*C*2/*c*	*P*2/*c*
Unit cell dimensions: ***a,*** ***b,*** ***c* (Å)**	11.3323(5), 12.5539(5), 15.7126(7)	26.967(7), 21.304(5), 18.665(5)	9.978(2), 16.059(3), 28.509(5)
α, ***β,*** ***γ* (°)**	69.746(2), 69.700(2), 75.787(2)	90, 130.746(5), 90	90, 101.582(1), 90
Volume (Å^3) / *Z*	1946.79(14) / 2	8214(3) / 4	4475.2(15) / 4
Density (calculated) (mg/cm^3)	1.602	1.686	1.504
Absorption coefficient (mm^{-1})	2.734	2.883	2.388
F(000)	944	4088	2064
Crystal size (mm)	0.22 x 0.10 x 0.04	0.23 x 0.06 x 0.04	0.26x 0.22 x 0.18
Theta range for data collection (°)	1.44 to 27.00	1.91 to 28.00	1.87 to 27.00
Index ranges	-14<=h<=14, -16<=k<=16, -20<=l<=20	-35 <= h <= 35, -27 <=k<= 28, -22 <= l <= 24	-13<=h<=13, -21<=k<=21, -38<=l<=38
Reflections collected	22928	80849	76225
Independent reflections/R_{int}	8458 [R_{int} = 0.0442]	9813 [R_{int} = 0.0473]	11107 [R_{int} = 0.0581]
Completeness (θ = 28.35°) (%)	99.60	99.90	99.7
Refinement method	Full-matrix least-squares on F^2	Full-matrix least-squares on F^2	Full-matrix least-squares on F^2
Data / restraints / parameters	8458 / 0 / 534	8215 / 48 / 599	11107 / 0 / 581
The goodness of fit on F^2	1.037	1.062	1.040
Final R indices [I>2sigma(I)]	R_1 = 0.0328, wR_2 = 0.0933	R_1 = 0.0216, wR_2 = 0.0490	R_1 = 0.0288, wR_2 = 0.0608
R indices (all data)	R_1 = 0.0383, wR_2 = 1003	R_1 = 0.0323, wR_2 = 0.0542	R_1 = 0.0418, wR_2 = 0.0657
Largest diff. peak and hole (e.Å^{-3})	1.161 / -0.809	0.901 / -0.563	1.440 / -0.671

[16] J .A. Viljoen, H. G. Visser, A. Roodt & M. Steyn, *Acta Cryst.,* **E65,** m1514, 2009.

[17] J. A. Viljoen, H. G. Visser & A. Roodt, *Acta Cryst.,* **E67,** m1428, 2011.

4.3. General Considerations for Chapter 4

Note: The following general considerations which enables a systematic comparison and standardised geometry for the complexes as discussed, are used throughout the text below. It is further important to take into account that although the symmetry elements are formally defined as “inversion centres”, “rotation axes”, “mirror planes”, etc., these are all to be considered “*pseudo*” elements, since they all describe solid-state observations.

- Coordinated oxine ligands are numbered starting from the N-atom. In structures containing multiple complexes / dinuclear compounds, the first digit of carbon/oxygen/nitrogen atoms indicates the oxine ligand associated with the N-atom and the second digit indicates the position of the atom in the ring (**Figure 4.2(a)**).

- Each independent oxine ligand *(identified by the numbering of the oxygen and nitrogen atoms, where appropriate*) coordinated to the metal centre is numbered consecutively and abbreviated to "***Lig#***" with # = 1-4 (**Figure 4.2(b)**).

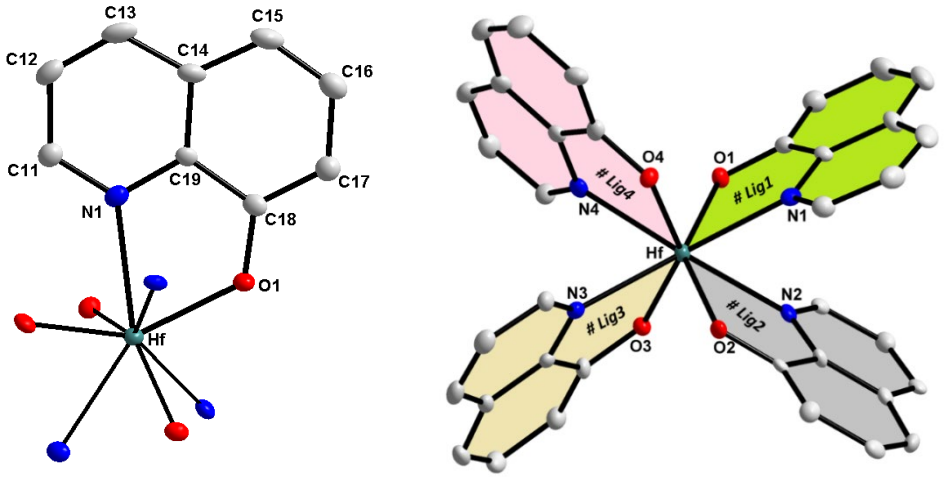

(a) **(b)**

Figure 4.2: **(a)** General numbering scheme for oxine ligands coordinated to hafnium(IV), illustrated within **(b)** a pseudo ***centrosymmetrically inverted isomer***

- Eight coordinated hafnium(IV) structures (*tetrakis*-coordinated, **Figure 4.2(b)** and **Figure 4.3** are described as two types of isomeric forms.

  The spatial arrangement of the oxine ligands allows the formation of two geometrical isomers. The placement of the nitrogen and oxygen coordination atoms are observed as either a:

  - **(a) *centrosymmetrically inverted*** isomer (**Figure 4.2 (b);** or
  - **(b) *(multiple) two-fold rotated*** isomer (**Figure 4.3**)

    The latter may be via multiple two-fold rotation axes through the metal centre as shown in **Figure 4.3** (illustrating three ***pseudo two-fold*** rotation axes, defined along the classic x, y, and z-axes as reference).

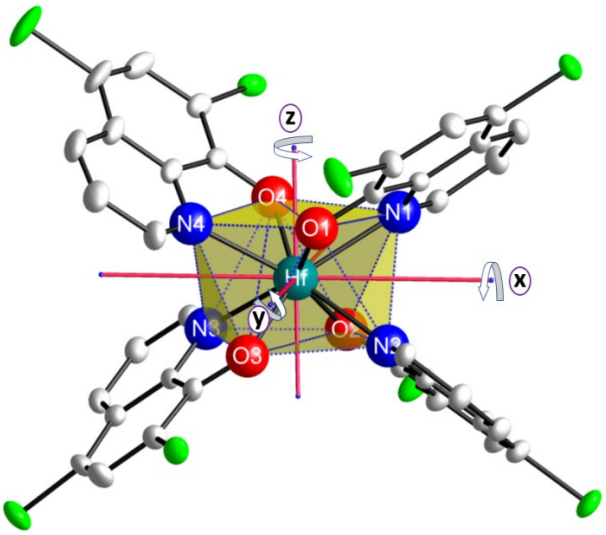

Figure 4.3: Coordinate functionalised ox-ligand arrangement around the metal centre when considering the *N*- and *O*- coordination sites via three ***pseudo two-fold*** rotation axes, i.e. a *two-fold rotated-isomer*. It is illustrated for the unsymmetrical oxine ligand, even functionalised by two chloro substituents

As discussed earlier in **Chapter 2** (§ 2.5), most hafnium and zirconium complexes, containing bidentate ligands adopt **square-antiprismatic** coordination geometries around the metal centres. However, in addition, it was also noted that this geometry exhibits three possible stereo-isomers, often for metal complexes containing symmetrical bidentate ligands like acetylacetonate.

The three possible isomers, containing simplified ligand entities, are illustrated in **Figure 4.4** and may exhibit a:

(a) ***D_2-corner-clipped*** ligand placement;

(b) ***D_4-side-clipped*** coordination;

(c) ***C_2-isomer*** (combination of D_2 -and D_4 isomers).

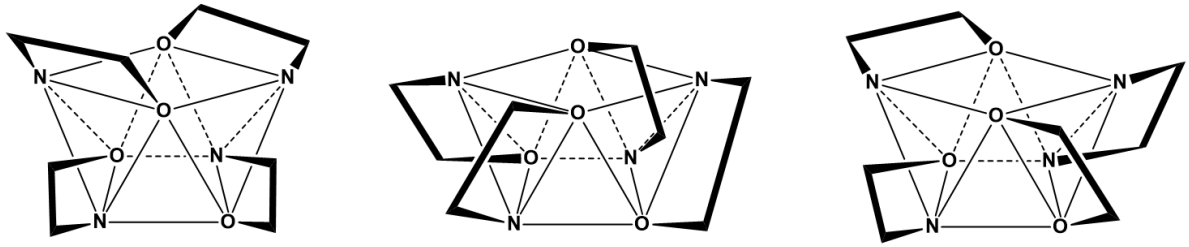

(a) **(b)** **(c)**

Figure 4.4: Coordination isomers as defined for tetrakis(oxinato)metal complexes exhibiting a square antiprismatic coordination polyhedron. **(a)** ***D_2***-corner-clipped ligands; **(b)** ***D_4***-side-clipped ligands; **(c)** ***C_2***-combination of corner- and side-clipped ligands.

4.4. Crystal Structure of Tetrakis(quinolin-8-olato-κ^2N,O)-hafnium(IV) toluene disolvate – $[Hf(Ox)_4]\cdot 2C_7H_8$

The structure of this *tetrakis*-oxinato coordinated hafnium complex (**Hf_1a**)[16] was the first structural study of such a compound published and is currently one of only four structures available in the Cambridge Structural Data Base.[18] The title compound, $[Hf(C_9H_6NO)]_4 \bullet 2(C_7H_8)$, where (C_9H_6NO) = 8-hydroxy-quinolate, Ox^-, crystallises in the triclinic space group $P\bar{1}$ with two formula units per unit cell (Z=2). Synthesis of **Hf_1a** and the resulting yellow crystals obtained were discussed in § 3.3.1.1.

[18] Cambridge Structural Database (CSD) Version 5.42, November 2020 update. C. R. Groom, I. J. Bruno, M. P. Lightfoot & S. C. Ward, *Acta Cryst.*, **B72**, 171, 2016.

The asymmetric unit contains one independent complex molecule together with two toluene solvate molecules and is represented in **Figure 4.5** with the atom numbering scheme.

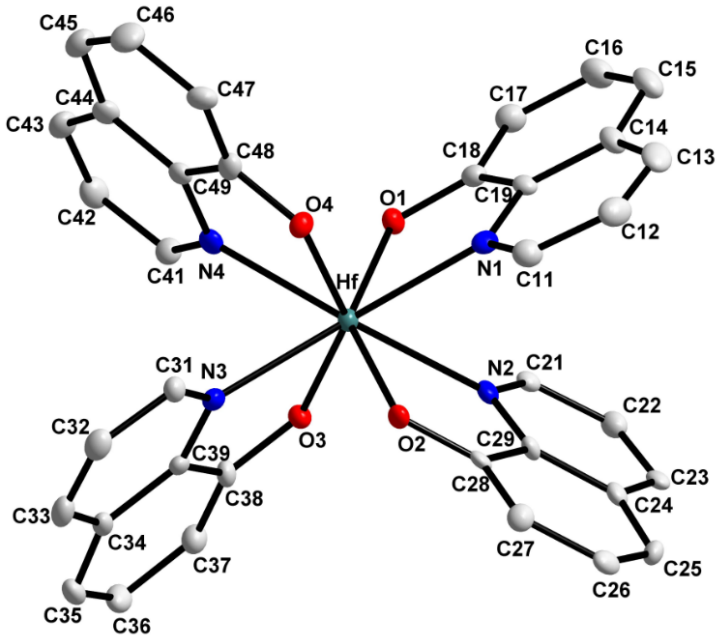

Figure 4.5. Representation of the title compound (**Hf_1a**), showing the numbering scheme and displacement ellipsoids *(50 % probability, solvent molecules and hydrogen atoms omitted for clarity*).

A summary of the general crystal data is given in **Table 4.1**, while **Table 4.2** presents selected bond lengths and angles of the title compound. Atomic coordinates, anisotropic displacement parameters, bond distances and angles and hydrogen coordinates are given in the supplementary data (**Appendix A.1**).

Table 4.2: Selected geometry parameters of $[Hf(Ox)_4]\cdot 2C_7H_8$ (Hf_1a).

Selected Bond Lengths (Å)			
Hf—O1	2.0978(2)	Hf—N1	2.3951(2)
Hf—O2	2.0951(1)	Hf—N2	2.4044(1)
Hf—O3	2.1027(2)	Hf—N3	2.3906(2)
Hf—O4	2.0848(1)	Hf—N4	2.4001(1)
Selected Bite Angles (°)			
O1—Hf—N1	70.734(2)	N1—Hf—N3	138.187(3)
O2—Hf—N2	70.843(2)	N2—Hf—N4	138.569(2)
O3—Hf—N3	71.160(2)	O1—Hf—O3	94.853(2)
O4—Hf—N4	71.045(2)	O2—Hf—O4	94.4497(2)
Selected Torsion Angles (°)			
O1—C18—C19—N1	1.445(6)	O3—C38—C39—N3	10.920(6)
O2—C28—C29—N2	0.155(6)	O4—C48—C49—N4	1.260(6)

Selected Dihedral Angles within the Anti-prism (°)

Bending		Rotation	
[N1—O1—O4] — [N4—O1—O4]	14.49(6)	[O1—Hf—O4] — [O2—Hf—O3]	51.23(7)
[N2—O2—O3] — [N3—O2—O3]	15.85(5)	[N1—Hf—N4] — [N2—Hf—N3]	47.06(8)

Figure 4.6 visually shows the duplicated placement of opposing coordinated ligands, illustrating the cross-facing orientation across the hafnium metal center by a *ca.* 180° rotation. Considering the fact that these ligands are not found to be placed in a planar arrangement relative to any other, we can see that they are bound to the metal center with a (multiple) ***pseudo two-fold rotated isomer*** placement of the *N*- and *O*- coordinating site [Option (b); **Figure 4.3**]. It therefore yields average O—Hf—O and N—Hf—N bond angles of 94.652(3)° and 138.378(5)°, respectively (individual O—Hf—O and N—Hf—N bond angles are given in **Table 4.2**)

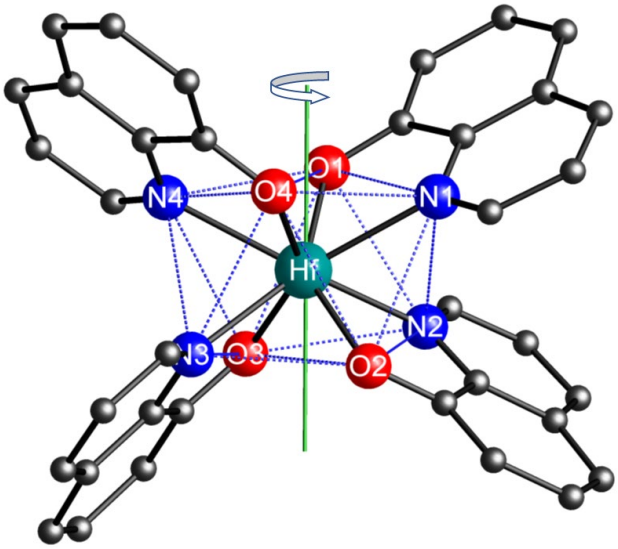

Figure 4.6: Graphical illustration of the ***pseudo two-fold rotated*** isomer of the oxine ligands across the metal centre in the **Hf_1a** title molecule (*Hydrogen atoms and solvent molecules omitted for clarity*). When compared to **Figure 4.3**, the principal rotation axis is considered to be approximately perpendicular to the top/bottom planes of the anti-prism, i.e. along the z-axis.

The Hf—O and Hf—N bond lengths vary from 2.0848(1) Å to 2.1027(2) Å and 2.3906(2) Å to 2.4044(1) Å, respectively, and the O—Hf—N bite angles vary from 70.73(11)° to 71.16(11)° (*see* **Table 4.2**). The dihedral angles between the two phenyl rings of the coordinated quinolinato ligands are all less than 1°, indicating little or negligible distortion due to coordination or packing. The solvate molecule seems to have no effects on the different Hf—O and H—N bond distances as they are all in the same magnitude as listed in **Table 4.2.**

The hafnium metal centre in **Hf_1a**, in which the four *N,O*-donating bidentate oxine-ligands are arranged in a fan-like manner around the metal centre produces a square antiprismatic coordination polyhedron, with a small bending distortion towards dodecahedral geometry. With regard to the overall coordination description of the ligands as viewed in the square anti-prism (**Figure 4.7(a)**), the title compound therefore clearly crystallises as a ***D_2-corner-bonded isomer*** (**Figure 4.4(a)** and **Figure 4.7(b)**).

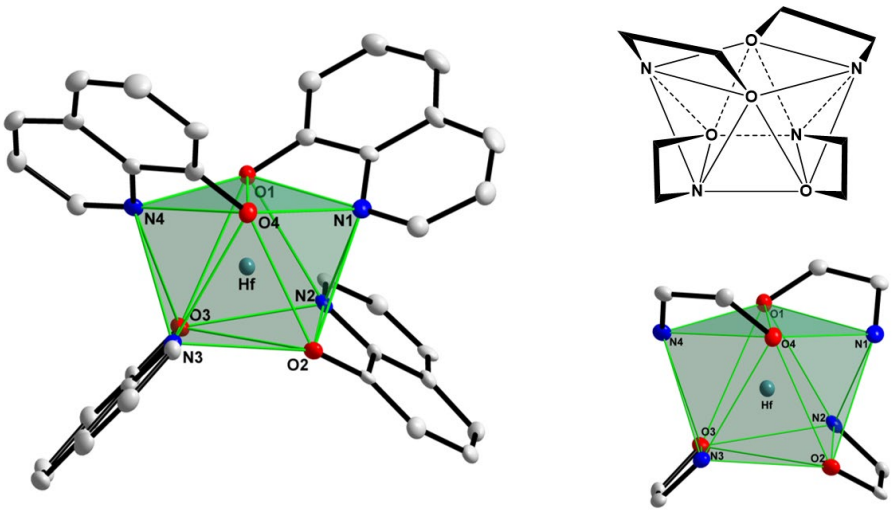

(a) **(b)**

Figure 4.7: **(a)** Graphic illustration of the square-antiprismatic coordination polyhedron of $[Hf(Ox)_4]$ (**Hf_1a**, hydrogen atoms omitted for clarity, 50% probability displacement ellipsoids). **(b)** Illustration of the typical D_2-corner-bonded square antiprismatic isomer.

In order to define the total distortion at the metal centre, two orientations for the metal complex are considered, as shown in **Figure 4.8** to allow the evaluation of the geometric parameters from the different planes; see **Figure 4.8 (a)** and **(b).** The orientations allow for the consideration of the relative distortions on the identified sets of two planes describing the "top" and the "base" of the complex.

Therefore, the dihedral angles between the yellow (N1—O1—O4 and N2—O2—O3), and green planes (N4—O1—O2 and N3—O2—O3), are illustrated in **Figure 4.8**, indicative of a bending distortion, measured as 14.49(6)° and 15.85(5)°, respectively for the top and bottom two sets of *N,O* donor atoms describing the coordination polyhedron.

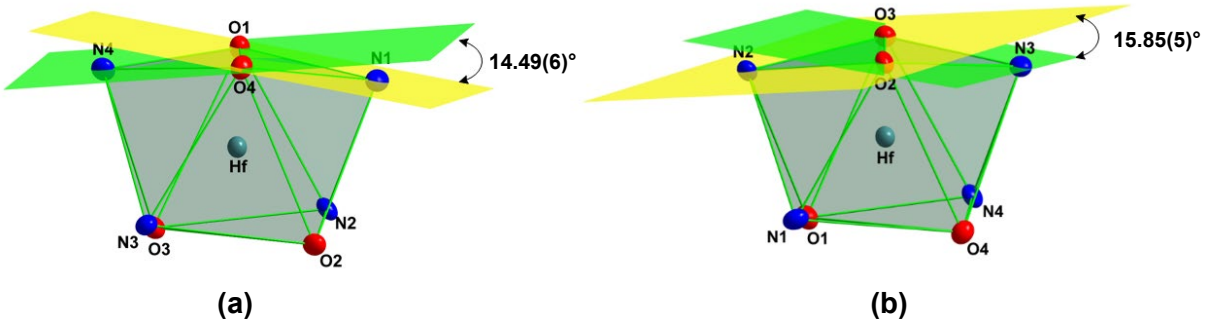

Figure 4.8*:* A graphical representation of the bending distortion (observed from the dihedral panes) in the antiprismatic coordination polyhedron surrounding the hafnium metal atom (*C and H atoms are omitted for clarity*).

A further indication of the distortion within the **Hf_1a** complex is observed from the amount of rotation observed between the two sets of *N,O* donor atoms describing the antiprismatic coordination polyhedron. Therefore, when viewing the coordination polyhedron from above, the dihedral angles between planes ([O1—Hf—O4] and [O2—Hf—O3]) and ([N1—Hf—N4] and [N2—Hf—N3]) were measured as 51.23(7)° and 47.06(8)°, respectively, signifying the rotation distortion observed (**Figure 4.9**). Ideally, these angles should be 45°.

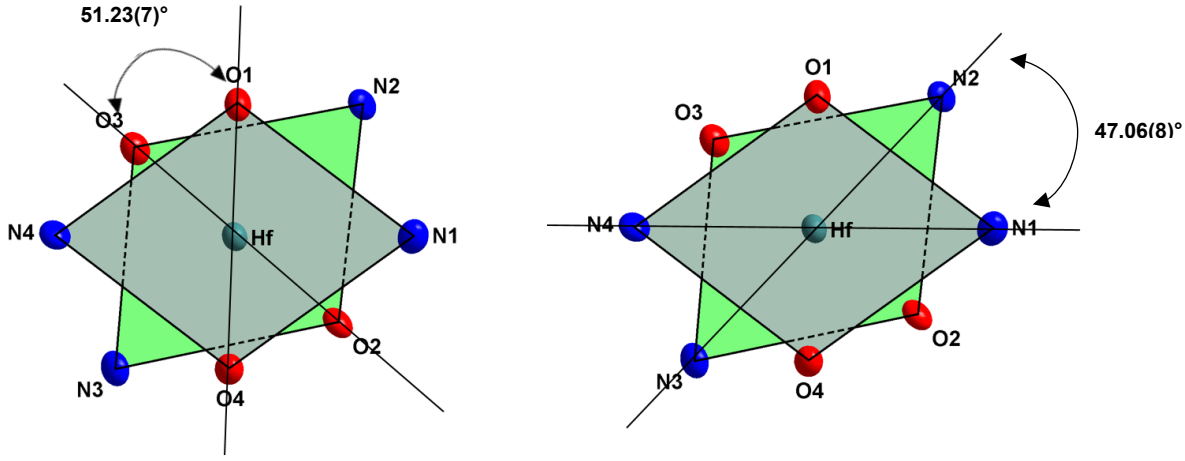

Figure 4.9: A graphical representation of the top view of the antiprismatic coordination polyhedron indicting the rotation distortion observed. (*C and H atoms are omitted for clarity*).

In **Hf_1a** the dihedral angle between the metal coordination plane (Hf, N3 and O3) and the plane formed by the quinolinato ligand is only 2.72 (1)° for ***Lig3***. However, the dihedral angles between the metal coordination plane and the plane formed by the other three oxinato ligands are 8.51(1), 6.22(2) and 5.15(1)°, respectively for ***Lig1***, ***Lig2*** and ***Lig4*** as shown in **Figure 4.10.**

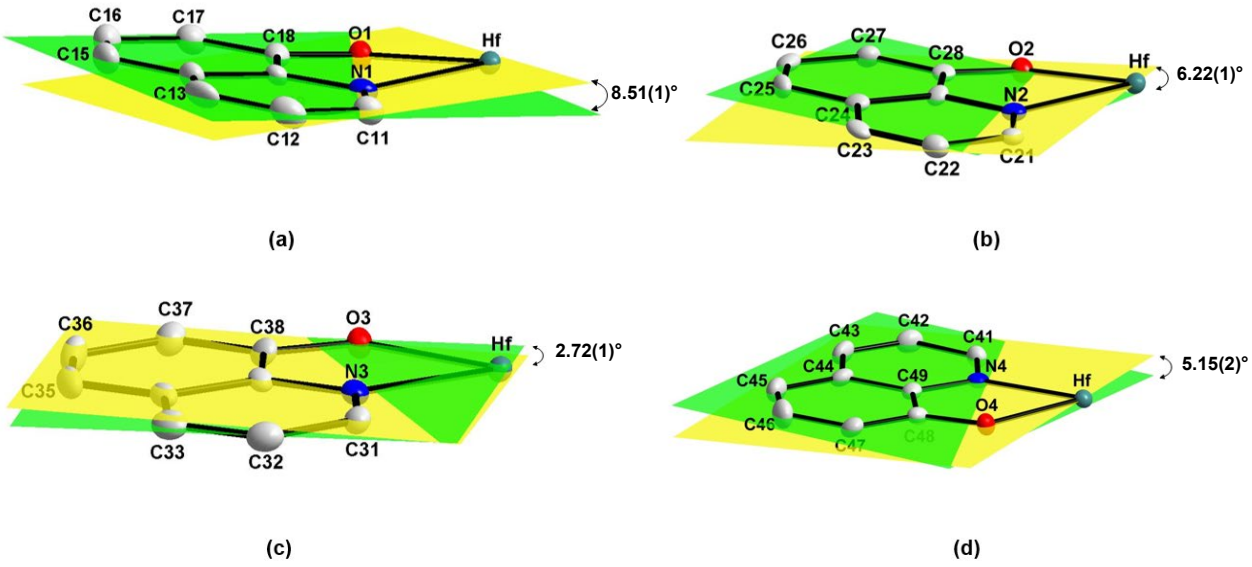

Figure 4.10: Partial structures of $[Hf(Ox)_4]$ (**Hf_1a)** graphically illustrating the dihedral angle between the metal coordination plane and the plane formed by the four quinolinato ligands. **(a)** ***Lig1*** – 8.51(1)°; **(b)** ***Lig2*** – 6.22(1)°; **(c)** ***Lig3*** – 2.72(1)° and **(d)** ***Lig4*** – 5.15(2)° *(Hydrogen atoms omitted for clarity, 50% probability displacement ellipsoids*).

In **Hf_1a** these slight distortions, although packing effects cannot be excluded, are possibly due to hydrogen- and π-π-interaction observed in the unit cell. The molecular units are connected by π-π interactions between different oxinato ligands of neighbouring molecules to produce a three-dimensional network, with interplanar distances varying between 3.1433(3) Å and 3.2103(3) Å and centroid-to-centroid distances from 3.5761(13) Å and 4.0373(1) Å. The various π-π-stacking interactions observed in the unit cell, are shown and reported in **Figure 4.11** and **Table 4.3**.

A strong C—H···O hydrogen bonding interaction is observed between one toluene solvent molecule and one of the oxygen donor atoms atoms from a neighbouring metal complex. Theoretically, this occurrence might be the cause for the larger dihedral angle observed for ***Lig1*** as described earlier. The bond distances and angles for the hydrogen bonding are given in **Table 4.4** and illustrated in **Figure 4.12**. The molecules pack in a "head-to-tail" fashion along the *b*-axis (**Figure 4.13**).

Table 4.3: π-π-Stacking properties of [Hf(Ox)$_4$] (Hf_1a).

Ligand no.	Interplanar distance (Å)	Centroid to centroid distance (Å)
2	3.1433(3)	3.5761(13)
3	3.2103(3)	4.0373(11)

Symmetry code: *(') 1-x,1- y, 1- z; (") 1-x, -y, 1-z*

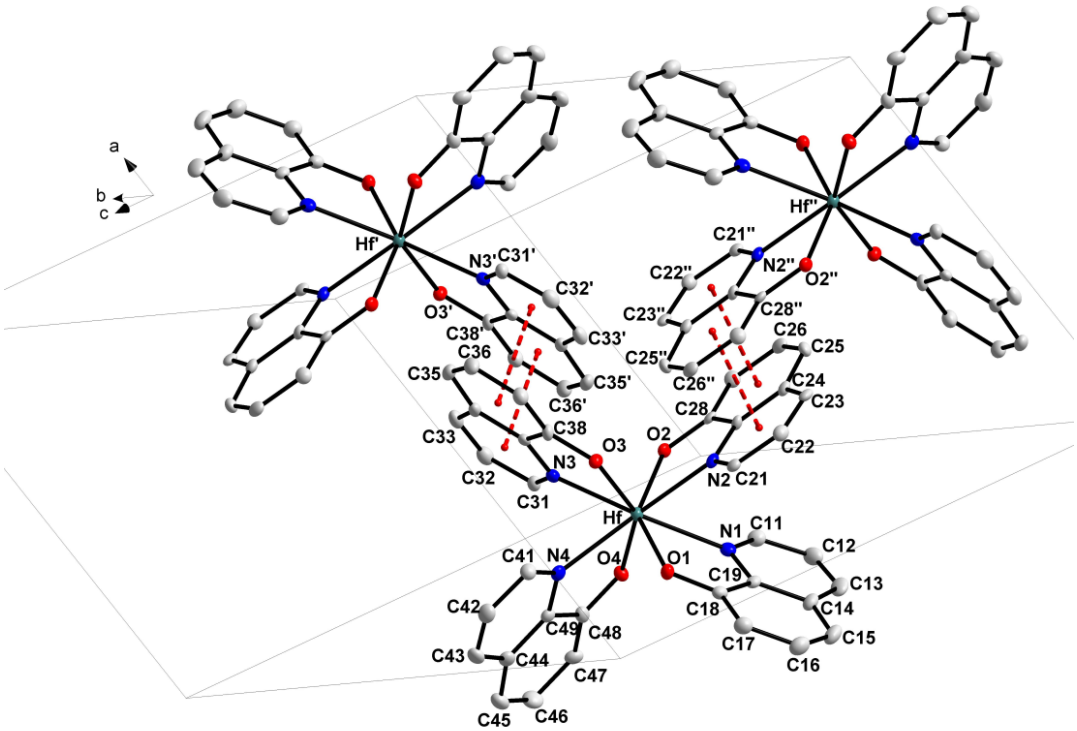

Figure 4.11: Partial structures [Hf(Ox)$_4$] (**Hf_1a)** showing π-π-stacking between the oxine ligands coordinated to the hafnium metal centre (S*olvent molecules and hydrogen atoms omitted for clarity*, *50% probability displacement ellipsoids*).

Table 4.4: Hydrogen-bond geometries (Å, ˚) of [Hf(Ox)$_4$] (Hf_1a).

D-H...A	d (D-H)	d (H...A)	d (D...A)	D-H…A angle
C105—H105···O1'	1.00(4)	1.89(4)	2.865(3)	165(3)

Symmetry code: *(') x, y+1, z*

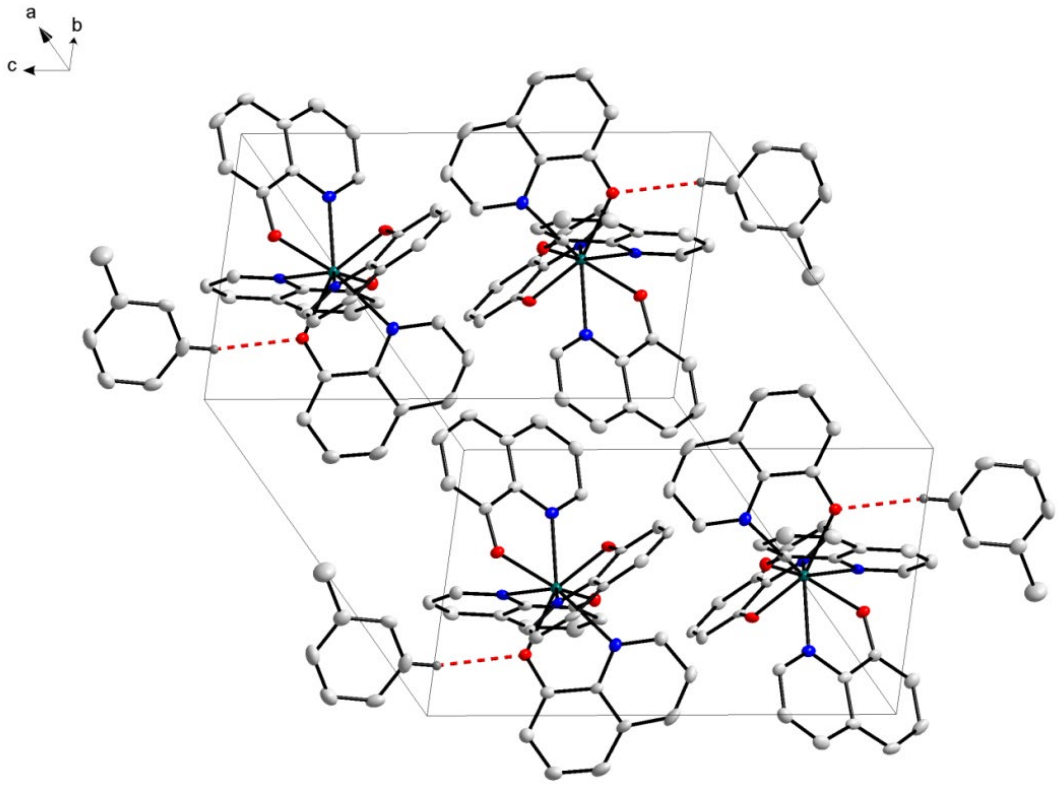

Figure 4.12: Partial structures [Hf(Ox)$_4$] (**Hf_1a)** indicating the C—H···O hydrogen bonding interaction observed in the unit cell (Hydrogen atoms omitted for clarity, 50% probability displacement ellipsoids).

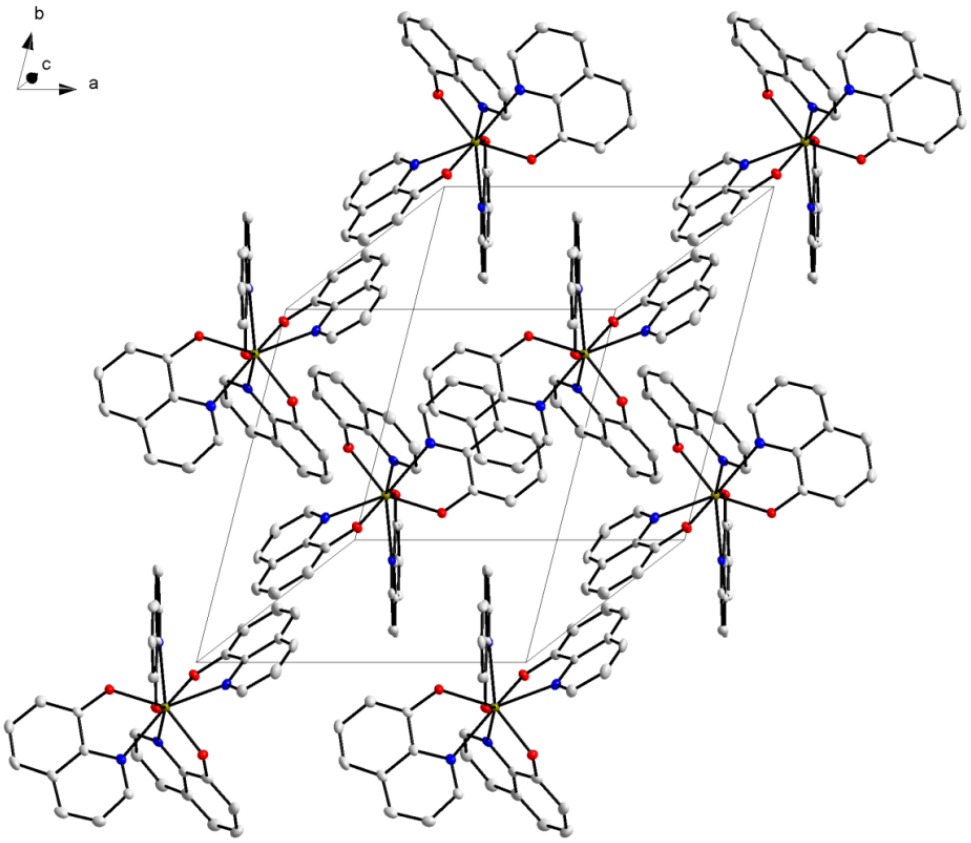

Figure 4.13: Packing of molecules (**Hf_1a**) in the crystal structure, illustrating the head-to-head packing of the individual molecules along the *c*-axis in the unit cell.

4.5. Crystal Structure of Tetrakis(5-chloroquinolin-8-olato-κ^2N,O)hafnium(IV) toluene disolvate – [Hf(5-ClOx)$_4$]·2C$_7$H$_8$

The title compound (**Hf_1b, Figure 4.14**), *tetrakis*(5-chloroquinolin-8-olato-κ^2*N,O*)hafnium(IV) toluene disolvate, crystallises in the monoclinic space group, *C*2/*c* with four formula units per unit cell (*Z*=4). The asymmetric unit consists of a Hf(IV) metal centre coordinated to four 5-chloroquinolin-8-olate bidentate ligands (5-ClOx$^-$). Two crystallographically independent toluene solvent molecules fill the rest of the asymmetric unit, where one of the toluene solvent molecules is disordered over two positions in a 55% : 45 % ratio as depicted in **Figure 4.15**. The synthesis of **Hf_1b** and the resulting yellow needle crystals obtained for this was discussed in § 3.3.1.2.

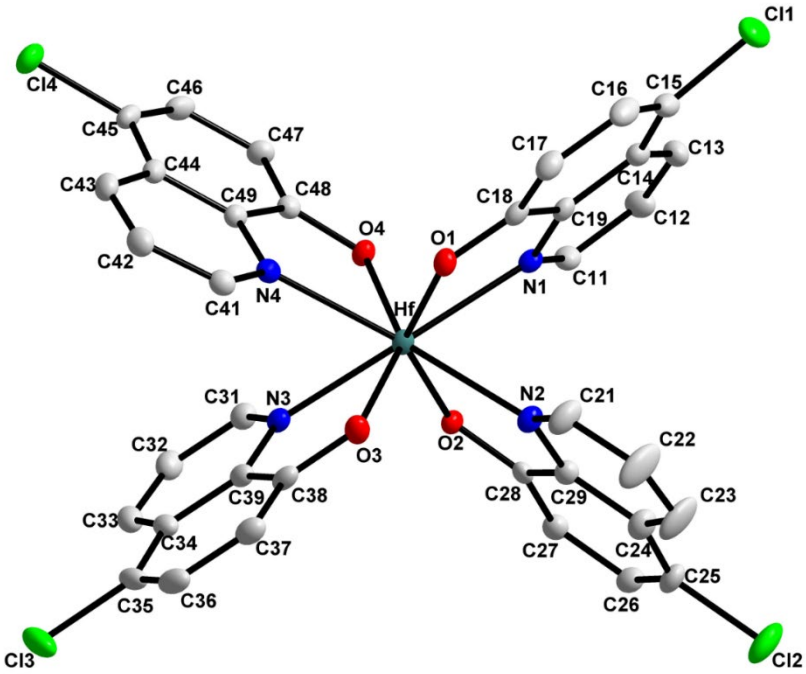

Figure 4.14: Representation of the title compound (**Hf_1b**), showing the numbering scheme and displacement ellipsoids (*50 % probability, solvent and hydrogen atoms omitted for clarity*).

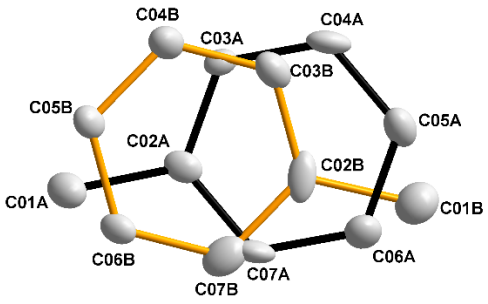

Figure 4.15: Representation of the disorder found in of one of the toluene solvent molecules is over two positions (*Ratio : black 55% : brown 45%*, *hydrogen atoms omitted for clarity*).

A summary of the general crystal data is given in **Table 4.1**, while the numbering scheme of the solvated complex is shown in **Figure 4.14**. **Table 4.5** presents selected bond lengths and angles of the title compound (**Hf_1b**). Atomic coordinates, anisotropic displacement parameters, bond distances and angles and hydrogen coordinates, are given in the supplementary data (**Appendix A.2**). Hydrogen atoms and/or solvent molecules are omitted in some molecular presentations for clarity.

Figure 4.16 visually shows the duplicated placement of opposing coordinated ligands, illustrating the cross-facing orientation across the hafnium metal center by a *ca.* 180° rotation. Considering the fact that these ligands are not found to be placed in a planar arrangement relative to any other, we can see that they are bound to the metal center with a (multiple) ***pseudo two-fold rotated isomer*** placement of the *N*- and *O*- coordinating sites, similar to **Hf_1a**, see **Figure 4.6**. It therefore yields average O—Hf—O and N—Hf—N bond angles of 87.54(10)° and 143.16(11)°, respectively (individual O—Hf—O and N—Hf—N bond angle are given in **Table 4.5**)

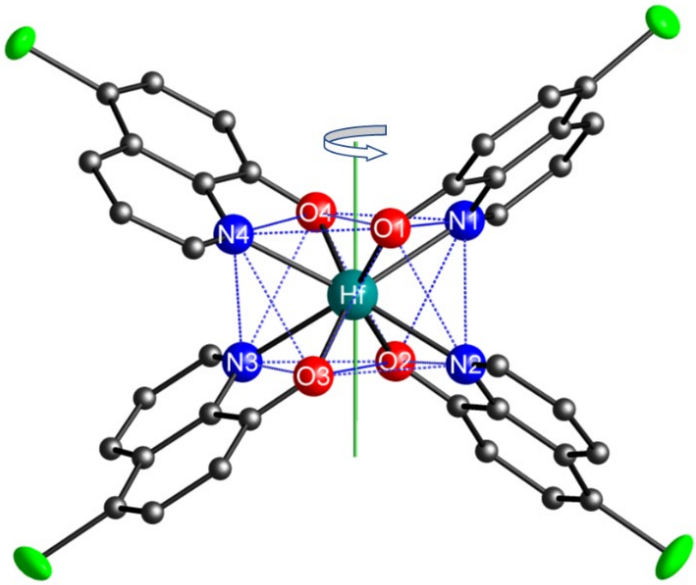

Figure 4.16: Graphical illustration of the ***pseudo two-fold rotated*** isomer of the oxine ligands across the metal centre in the **Hf_1b** title molecule (*Hydrogen atoms and solvent molecules omitted for clarity*). When compared to **Figure 4.3**, the principal rotation axis is considered to be approximately perpendicular to the top/bottom planes of the anti-prism, i.e., along the z-axis.

The Hf—O and Hf—N bond lengths vary from 2.080(2) Å to 2.109(2) Å and 2.396(2) Å to 2.420(2) Å, respectively, whereas the O—Hf—N bite angles vary from 70.30(8)° to 70.859)° (*presented in* **Table 4.5**). The measured N—C—C—O torsion angles of the ligand frame facing the N—Hf—O bite angles are found to range from 0.091(81)° to 3.0(3)°, showing minimal deviation from the planarity of the ligands themselves.

Table 4.5. Selected Geometric Parameters for $[Hf(5\text{-}ClOx)_4]\cdot 2C_7H_8$ (Hf_1b).

Selected Bond Lengths (Å)			
Hf—O1	2.098(2)	Hf—N1	2.402(2)
Hf—O2	2.102(2)	Hf—N2	2.396(2)
Hf—O3	2.109(2)	Hf—N3	2.396(2)
Hf—O4	2.080(2)	Hf—N4	2.420(2)
Cl1—C15	1.746(3)	Cl3—C35	1.742(3)
Cl2—C25	1.746(3)	Cl4—C45	1.775(2)
Selected Bite Angles (°)			
O1—Hf—N1	70.78(9)	N1—Hf—N3	142.35(10)
O2—Hf—N2	70.66(9)	N2—Hf—N4	143.97(10)
O3—Hf—N3	70.85(9)	O1—Hf—O3	86.78(8)
O4—Hf—N4	70.30(8)	O2—Hf—O4	88.29(8)
Selected Torsion Angles (°)			
O1—C18—C19—N1	3.0(3)	O3—C38—C39—N3	2.0(3)
O2—C28—C29—N2	0.1(3)	O4—C48—C49—N4	0.4(3)

Selected Dihedral Angles of Anti-prism (°)			
Bending		**Twisting**	
[N1—O1—O4] — [N4—O1—O4]	7.01(7)	[O1—Hf—O4] — [O2—Hf—O3]	47.96(7)
[N2—O2—O3] — [N3—O2—O3]	5.21(6)	[N1—Hf—N4] — [N2—Hf—N3]	42.43(11)

The hafnium metal centre, in which the four 5-chloroquinolin-8-olate ligands are fan-like arranged around the metal centre produces a square antiprismatic coordination polyhedron, with a small distortion towards dodecahedral geometry.

With regard to the overall coordination description of the ligands as viewed in the square anti-prism (**Figure 4.17 (a)**), the title compound ([Hf(5-ClOx)$_4$], **Hf_1b**) crystallises as a ***D_2-corner-bonded isomer*** (**Figure 4.17 (b)**).

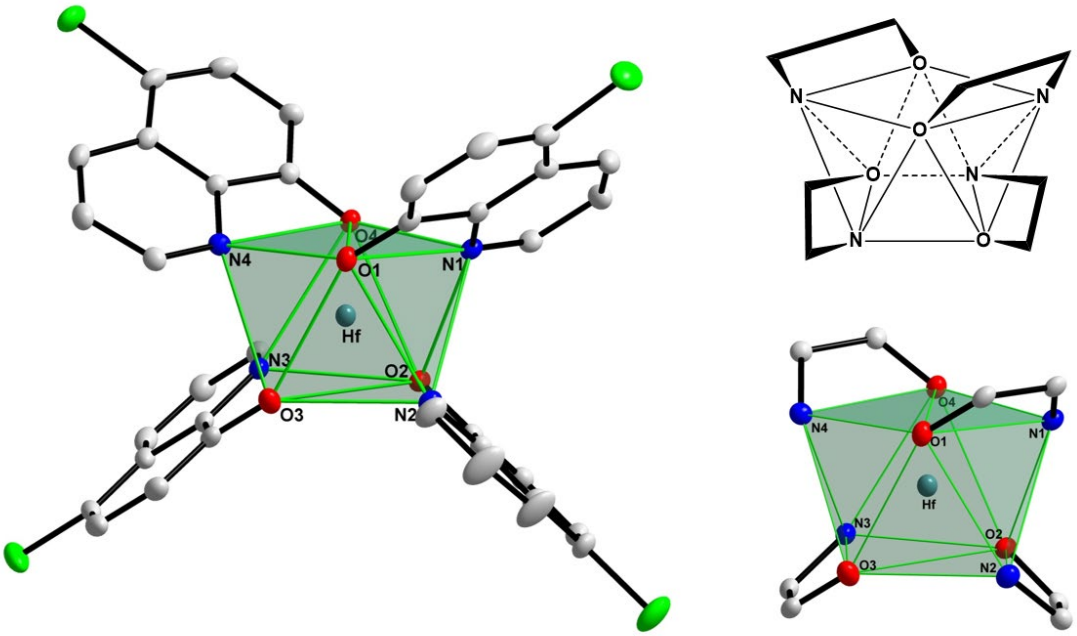

(a) **(b)**

Figure 4.17. **(a)** Graphic illustration of the square-antiprismatic coordination polyhedron of [Hf(5-ClOx)$_4$] (**Hf_1b**, Hydrogen atoms omitted for clarity, 50% probability displacement ellipsoids). **(b)** Illustration of the typical D_2-corner-bonded square antiprismatic isomer.

Again, in order to define the total distortion at the metal centre, two orientations for the metal complex are considered, as shown in **Figure 4.18** to allow the evaluation of the geometric parameters from the different planes; see **(a)** and **(b)**. The orientations allow for the consideration of the relative distortions on the identified sets of two planes describing the "top" and the "base" of the complex.

The dihedral angle between the yellow (N1—O1—O4 and N2—O2—N3), and green planes (N4—O1—N4 and N3—O2—O3), indicative of distortion, was measured as 7.01(7)° and 5.21(6)°, respectively for the top and bottom two sets of *N,O* donor atoms describing the polyhedron as illustrated in **Figure 4.18**.

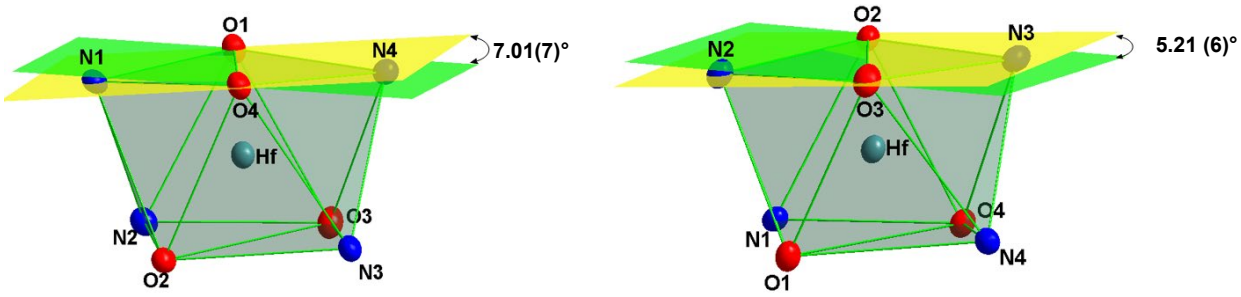

Figure 4.18. A graphical representation of the slightly distorted antiprismatic coordination polyhedron surrounding the hafnium metal atom (*C, H and Cl atoms are omitted for clarity*).

Furthermore, when viewing the coordination polyhedron from above, the dihedral angles between planes [O1—Hf—O4] and [O2—Hf—O3] and [N1—Hf—N4] and [N2—Hf—N3] was measured as 47.96(7)° and 42.43(11)°, respectively, signifying the rotation distortion away from the ideal 45° found in square antiprismatic polyhedrons as shown in **Figure 4.19**.

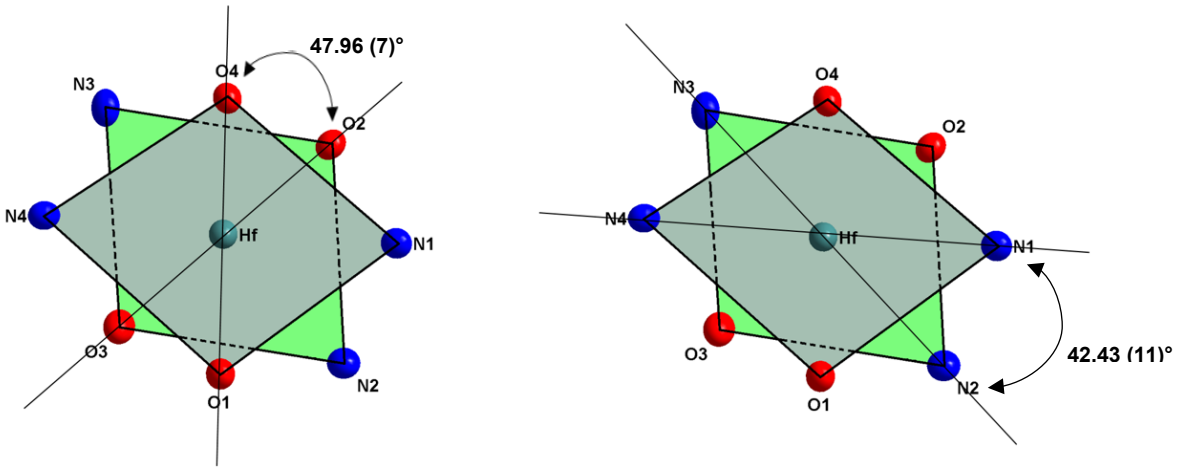

Figure 4.19: A graphical representation of the top view of the antiprismatic coordination polyhedron indicting the rotation distortion.(*C and H atoms are omitted for clarity*).

In **Hf_1b** the dihedral angle between the metal coordination plane (Hf, N2 and O2) and the plane formed by the quinolinato ligand are negligible for ***Lig2.*** However, the dihedral angles between the metal coordination plane and the plane formed by the other three oxinato ligands are 3.32(6), 4.20(6) and 4.78(5)°, respectively for ***Lig1***, ***Lig3*** and ***Lig4*** as shown **Figure 4.20**.

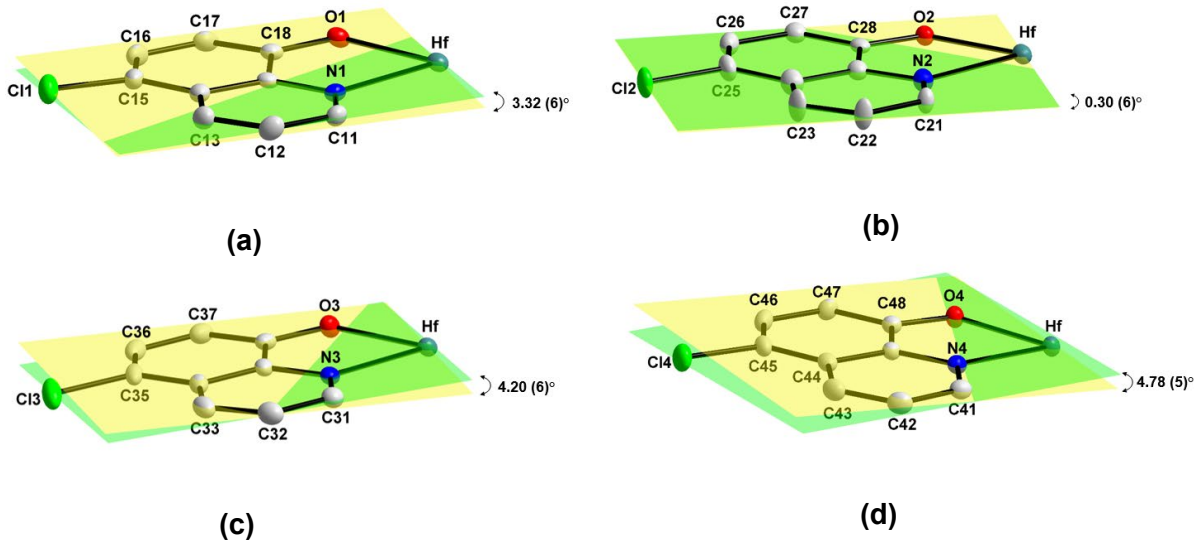

Figure 4.20: Partial structures of [Hf(5-ClOx)$_4$] (**Hf_1b)** graphically illustrating the dihedral angle between the metal coordination plane and the plane formed by the four quinolinato ligands **(a)** ***Lig1*** – 3.32(6)°; **(b)** ***Lig2*** – 0.30(6)°; **(c)** ***Lig3*** – 4.20(6)° and **(d)** ***Lig4*** – 4.78(5)° (*Hydrogen atoms omitted for clarity, 50% probability displacement ellipsoids).*

Inter- and intramolecular C—H···O (**Table 4.6**) hydrogen bonding interactions are observed in this structure. As illustrated in **Figure 4.21**, the intramolecular hydrogen bonding interaction are linked to a neighbouring 5-ClOx-ligand (***Lig4***), with C47'—H47'···O4 (' = 1-x, y, 0.5-z) from symmetry generated molecule.

Table 4.6: Hydrogen-bond geometries in [Hf(5-ClOx)$_4$], (Hf_1b, (Å, ˚))

D-H...A	d (D-H)	d (H...A)	d (D...A)	D-H…A angle
C21—H21···O1	0.930	2.555(1)	3.014(3)	110.75(17)
C47'—H47'···O4	0.930	2.506(3)	3.309(5)	144.73(22)
C15—Cl1··· π''	1.745(2)	2.506(3)	3.692(1)	144.73(22)
C45'—C4··· π'	1.745(2)	2.506(3)	3.692(1)	144.73(22)

Symmetry code: *(') 1-x, y, 0.5-z; (") 0.5-x,1.5-y,-z*

The crystal lattice is further stabilised by C-Cl–π interactions between some of the benzene rings of the 5-ClOx-ligands (***Lig1*** & ***Lig2***) and symmetry generated counterparts (' = 1-x,2-y,1-z; " = 0.5-x,1.5-y,-z) of neighbouring molecules, with chlorine-to-centroid distances of 3.6922(9) Å and 3.4202(10) Å, respectively, (**Figure 4.22**) linking the crystal lattice as a whole.

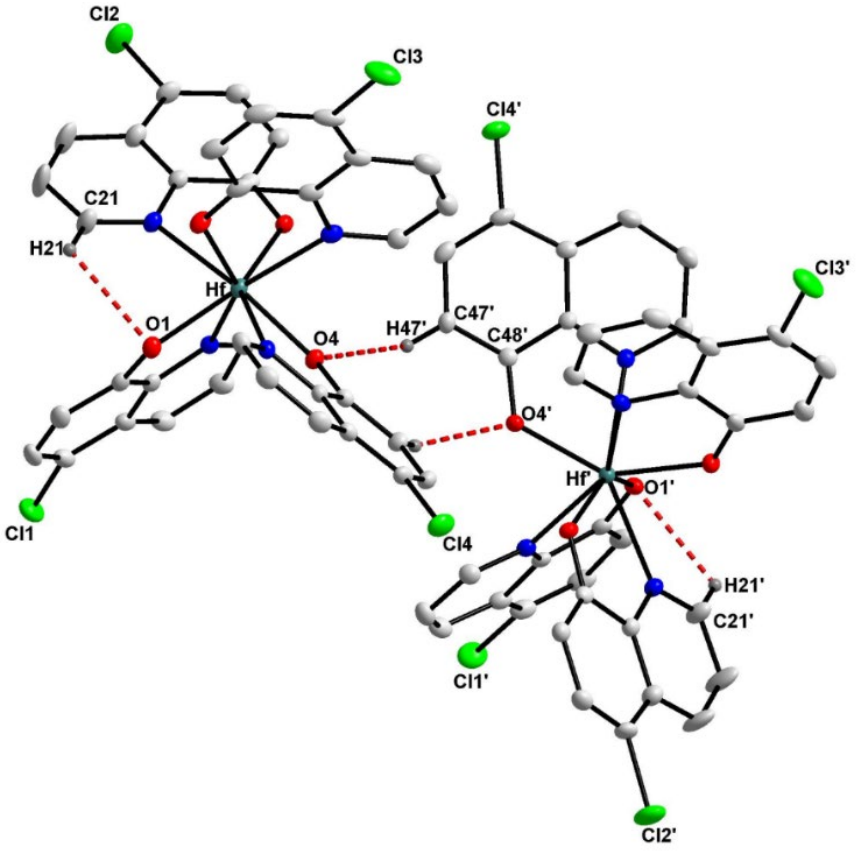

Figure 4.21: Illustration of the *inter*- and *intra*-molecular hydrogen bonding interaction found in the title molecule (**Hf_1b,** *Some hydrogen atoms and solvent molecules omitted for clarity, 50% probability displacement ellipsoids).*

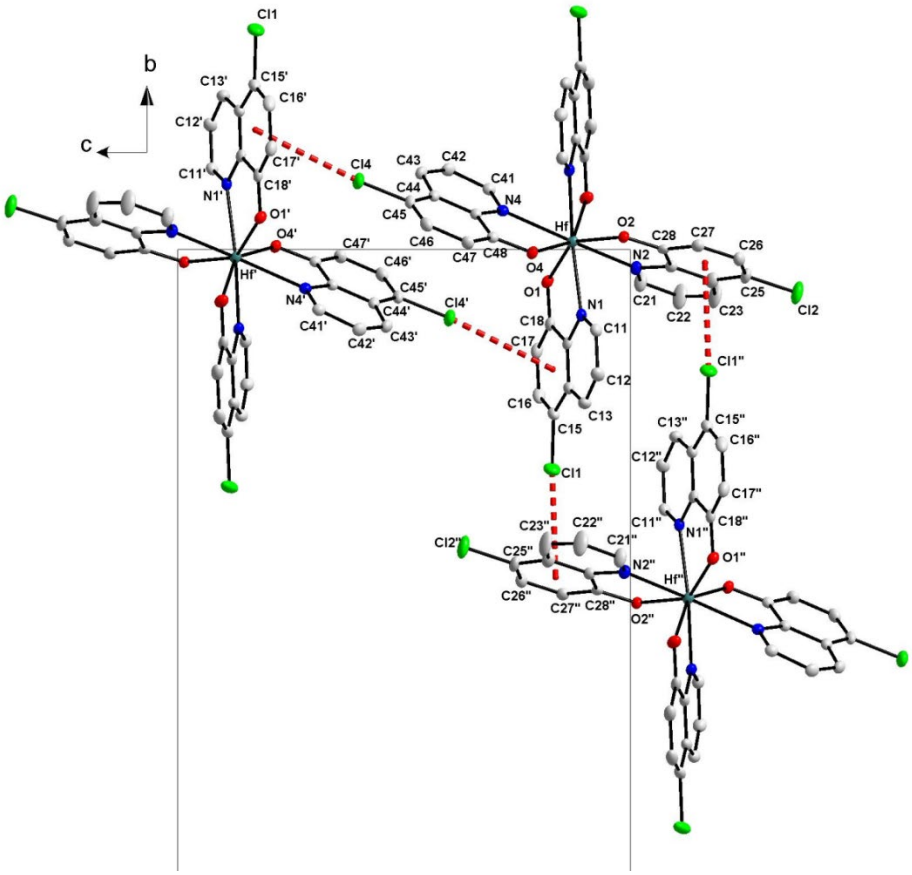

Figure 4.22: Illustration of the i*ntermolecular* hydrogen bonding interaction found in the title molecule (**Hf_1b,** *Some hydrogen atoms and solvent molecules omitted for clarity, 50% probability displacement ellipsoids).*

4.6. Crystal Structure of Tetrakis(5,7-dimethylquinolin-8-olato-κ²N,O)hafnium(IV) dimethylformamide disolvate – [Hf(diMeOx)₄]·2DMF

The published structure of this *tetrakis*(5,7-dimethylquinolin-8-olato-κ^2N,O)hafnium(IV) dimethylformamide disolvate[17] (**[Hf(diMeOx)$_4$]·2DMF**) is one of four *tetrakis* examples of hafnium-oxine structures available in the literature to date.[18] The synthesis of Hf(diMeOx)$_4$ (**Hf_1h**) was discussed in § 3.3.1.8. Red parallelepiped-like crystals of the title compound crystallises in the monoclinic crystal system $P2_1/c$ with four formula units per unit cell (Z=4). The asymmetric unit contains one independent molecule together with two dimethylformamide (DMF) solvate molecules and is represented in **Figure 4.23**.

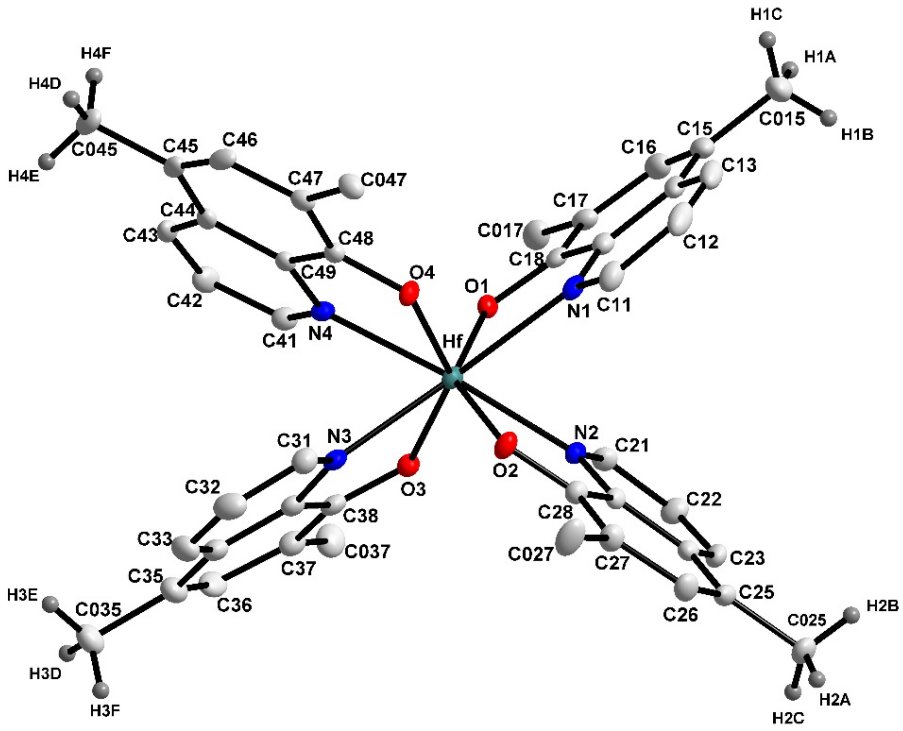

Figure 4.23: Representation of the title compound (**Hf_1h**), showing the numbering scheme and displacement ellipsoids (*50% probability, solvent molecules and some hydrogen atoms omitted for clarity).*

A summary of the general crystal data is given in **Table 4.1**, while **Table 4.7** presents selected bond lengths and angles of the title compound. Atomic coordinates, anisotropic displacement parameters, bond distances and angles and hydrogen coordinates, are given in the supplementary data (**Appendix A.3**).

Table 4.7: Selected geometry parameters of [Hf(diMeOx)$_4$] (Hf_1h).

Selected Bond Lengths (Å)			
Hf—O1	2.094(2)	Hf—N1	2.413(2)
Hf—O2	2.098(2)	Hf—N2	2.377(2)
Hf—O3	2.104(2)	Hf—N3	2.409(2)
Hf—O4	2.096(2)	Hf—N4	2.393(2)
C015—C15	1.518(4)	C025—C25	1.515(4)
C017—C17	1.504(4)	C027—C27	1.504(4)
C035—C35	1.530(4)	C045—C45	1.519(4)
C037—C37	1.504(4)	C047—C47	1.507(4)
Selected Bite Angles (°)			
O1—Hf—N1	69.92(8)	N1—Hf—N3	146.09(8)
O2—Hf—N2	70.87(8)	N2—Hf—N4	143.72(8)
O3—Hf—N3	69.58(8)	O1—Hf—O3	83.35(8)
O4—Hf—N4	70.39(7)	O2—Hf—O4	84.51(8)
Selected Torsion Angles (°)			
O1—C18—C19—N1	4.2(4)	O3—C38—C39—N3	3.8(4)
O2—C28—C29—N2	1.0(4)	O4—C48—C49—N4	0.08(4)

Selected Dihedral Angles of Anti-prism (°)			
Bending		**Twisting**	
[O1—N1—O4] — [O1—N4—O4]	0.44(10)	[O1—Hf—O4] — [O2—Hf—O3]	47.63(6)
[O2—N2—O3] — [O2—N3—O3]	0.44(10)	[N1—Hf—N4] — [N2—Hf—N3]	41.21(6)

The Hf—O and Hf—N bond lengths vary from 2.094(2) Å to 2.104(2) Å and 2.377(2) Å to 2.413(2) Å, respectively, and the O—Hf—N bite angles vary from 69.58(8)° to 70.87(1)° (*presented in* **Table 4.7**).

It is clear from **Figure 4.24** that each independently coordinated oxine-ligand is duplicated by an opposite facing one, *via ca.* 180**°** rotation through the metal centre. Although these ligands do not lie in a flat plane opposite each other, it is evident that the ligands are chelated to the metal centre with a (multiple) ***pseudo two-fold rotated*** isomer placement of the *N*- and *O*- coordinating sites [Option **(b)**; **Figure 4.3**]. Thus, giving average O—Hf—O and N—Hf—N bond angles of 83.93(10)° and 144.91(11)°, respectively (individual O—Hf—O and N—Hf—N bond angles are given in **Table 4.7**.

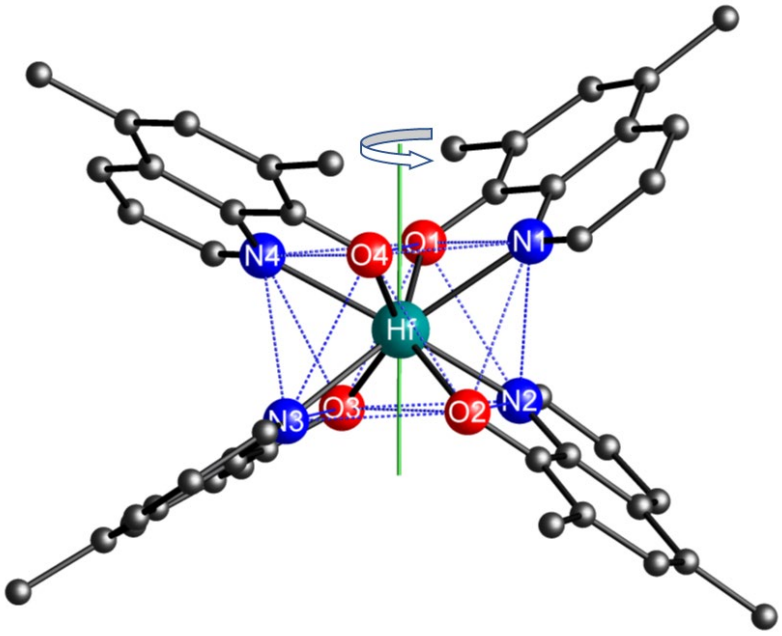

Figure 4.24: Graphical illustration of the ***pseudo two-fold rotated*** *isomer defined by* the oxine ligands across the metal centre in [Hf(diMeOx)$_4$] molecule (**Hf_1h**, *Hydrogens and solvent molecules omitted for clarity*). When compared to Figure 4.3, the principal rotation axis is considered to be approximately perpendicular to the top/bottom planes of the anti-prism, i.e., along the z-axis.

The hafnium metal centre, in which the four *N,O*-donating bidentate oxine ligands are fan-like arranged around the metal centre produces a square antiprismatic coordination polyhedron. With regard to the overall coordination description of the ligands as viewed in the square anti-prism (**Figure 4.25 (a)**), the title compound ([Hf(diMeOx)$_4$], **Hf_1h**) crystallises as a ***D$_2$-corner-bonded isomer*** (**Figure 4.25 (b)**).

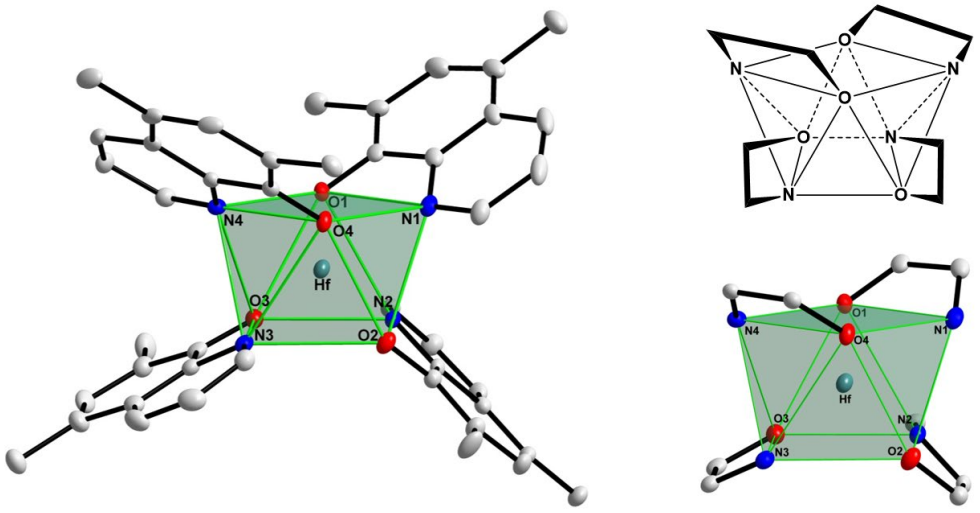

(a) **(b)**

Figure 4.25: (a) Graphic illustration of the square-antiprismatic coordination polyhedron of [Hf(diMeOx)$_4$] (**Hf_1h**, hydrogen atoms omitted for clarity, 50% probability displacement ellipsoids). **(b)** Illustration of the typical *D$_2$-corner-bonded* square antiprismatic isomer.

Contrary to the above described [Hf(Ox)$_4$] and the [Hf(Cl-Ox)$_4$] complexes, the resulting square anti-prism in the case of the [Hf(diMeOx)$_4$] (**Hf_1h**), has an almost negligible bending distortion towards the dodecahedral geometry. The top and bottom two sets of *N,O* donor atoms describing top and bottom bases (planes) are planar and nearly parallel to each other with only a dihedral angle of only 0.44(10)° between the two planes. However, some rotation distortion is observed between the top and bottom two sets of *N,O* donor atoms describing the N_2O_2 coordination sites as indicated in **Figure 4.26**.

Furthermore, the dihedral angles between the metal coordination plane and the plane formed by the coordinated oxine ligands are 5.52(1), 0.98(8), 13.33(7) and 5.96(9)° for coordinating ligand 1, 2, 3 and 4, respectively (dihedral angles are graphically illustrated **Figure 4.27**.

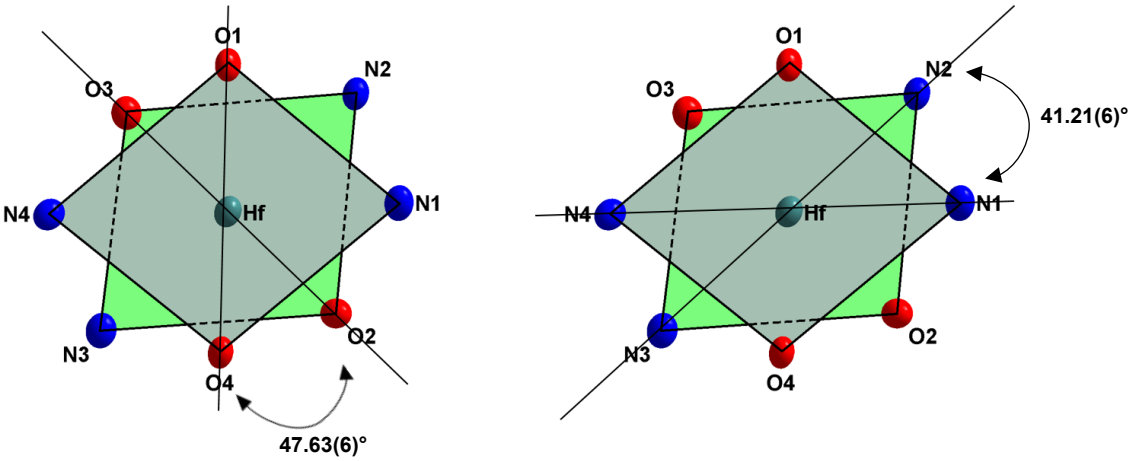

Figure 4.26: A graphical representation of the top view of the antiprismatic coordination polyhedron showing the rotation distortion.(*C and H atoms are omitted for clarity*).

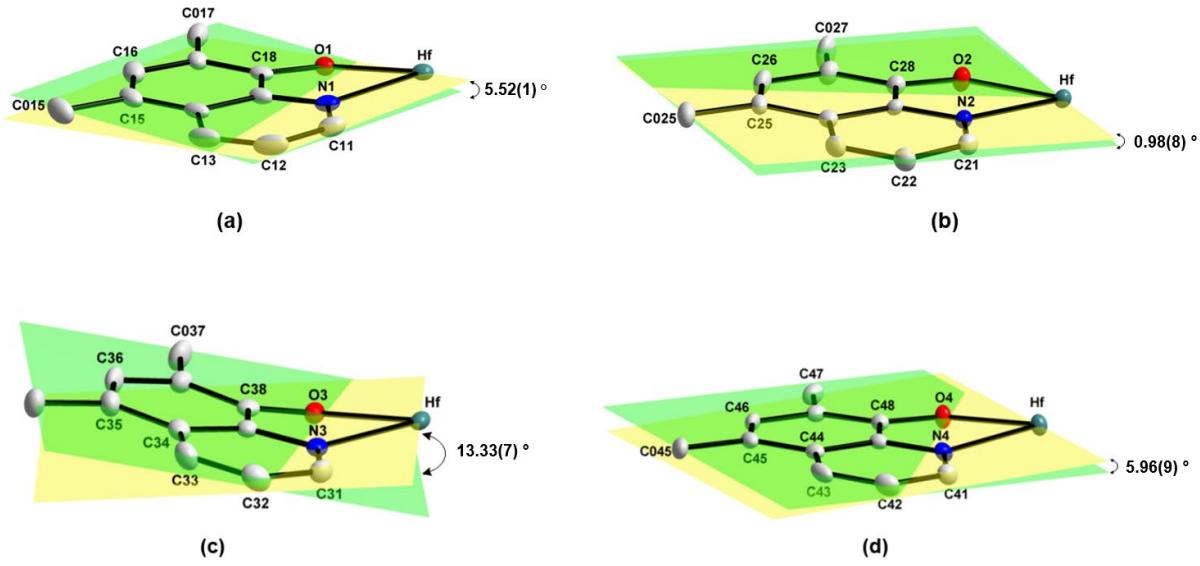

Figure 4.27. Partial structures of [Hf(diMeOx)$_4$] (**Hf_1h**), showing graphical illustration of the dihedral angles between the metal coordination plane and the plane formed by the oxine ligands **(a)** ***Lig1*** - 5.52(1)°; **(b)** ***Lig2*** – 0.95(8)°; **(c)** ***Lig3*** – 13.33(7)° and **(d)** ***Lig4*** - 5.96(9)° (*Hydrogen atoms omitted for clarity, 50% probability displacement ellipsoids).*

These slight distortions are possibly due to hydrogen- and π-π interactions observed in the unit cell. The molecular units are connected by π-π-interactions between the pyridine and phenyl rings of the different quinoline ligands of neighbouring molecules to produce a three-dimensional network. The interplaner- and centroid-to-centroid distances vary between 3.668(1) Å and 3.759(1) Å and 3.668(1) Å and 3.759(1) Å, respectively (**Table 4.8**). The various π-π-stacking, which is observed in the unit cell, are shown in **Figure 4.28** and reported in **Table 4.8**.

Table 4.8: π-π-Stacking properties of [Hf(diMeOx)$_4$] (Hf_1h).

π-π- Interaction	Interplanar distance (Å)	Centroid to centroid distance (Å)
Pyridine – pyridine'	3.492(1)	3.668(1)
Phenyl – phenyl'	3.507(2)	3.759(1)

Symmetry code: *(') 1-x, 0.5+y, 1.5-z; (") 1-x, 1-y, 1-z; ("') x, 0.5-y, -0.5+z*

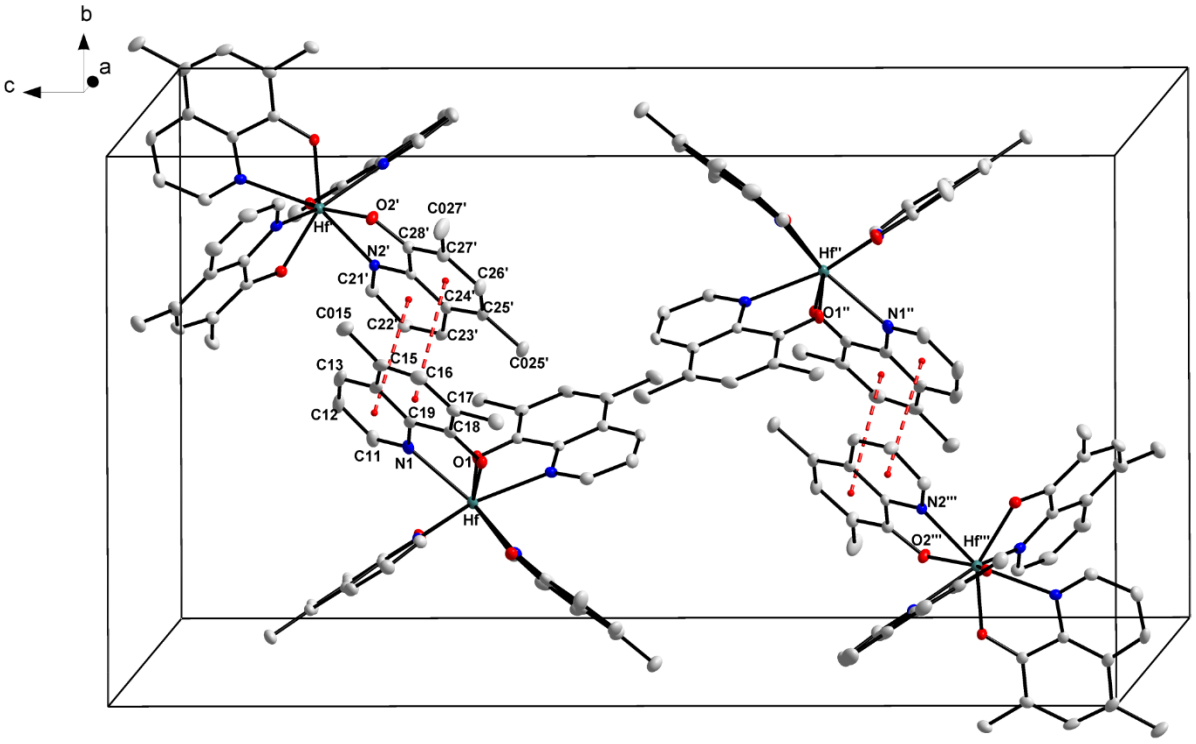

Figure 4.28: Graphic illustration of π-π-stacking inside the unit cell showing π-π-stacking between the oxine ligands (***Lig1*** and ***Lig2***) coordinated to the hafnium metal centre (**Hf_1h**, hydrogen atoms omitted for clarity, 50% probability displacement ellipsoids).

A non-classical C—H···O hydrogen bonding interaction is observed between the complex and one of the solvent molecules (**Figure 4.29**). Theoretically, this occurrence might be the cause for the higher dihedral angles seen and described earlier. Furthermore, the molecules pack in a "head-to-head" fashion when viewed along the diagonal axis of the *bc*-plane (**Figure 4.30**).

Table 4.9: Hydrogen-bond geometries of [Hf(diMeOx)$_4$] (Hf_1h, (Å, ˚)).

D-H...A	d (D-H)	d (H...A)	d (D...A)	D-H…A angle
C42—H42···O5	0.93(4)	2.55(4)	3.348(4)	144(2)

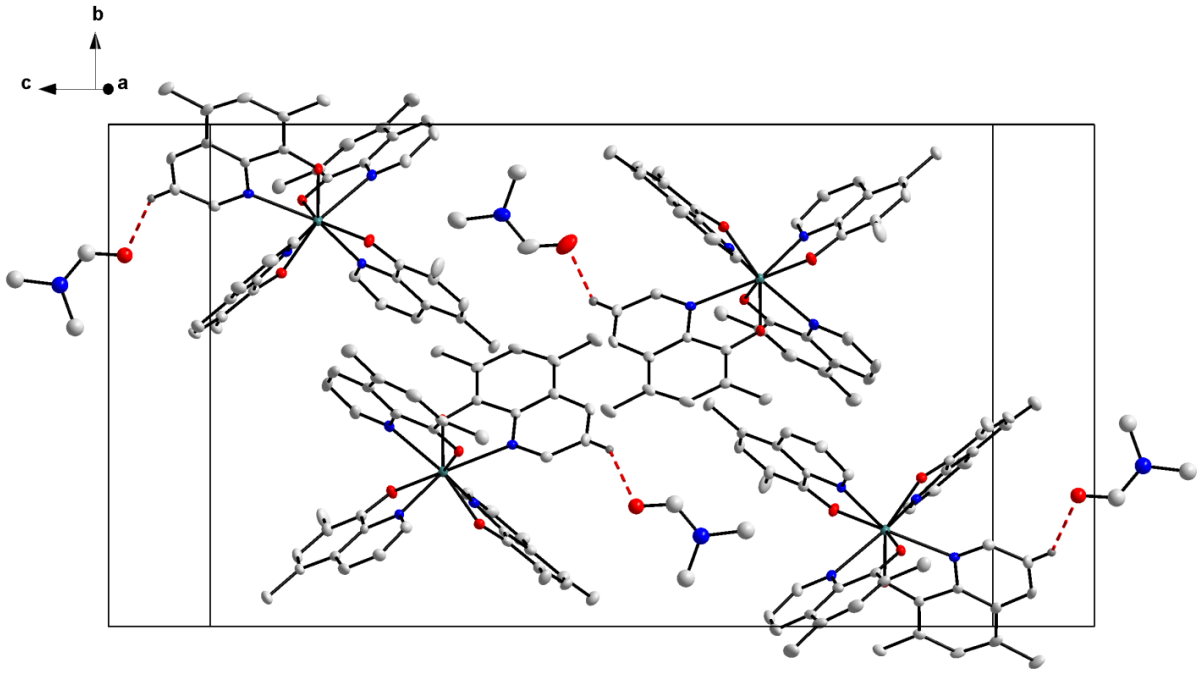

Figure 4.29: Partial structures [Hf(diMeOx)$_4$].2DMF (**Hf_1h**), indicating the C—H···O hydrogen bonding interaction observed in the unit cell (*Hydrogen atoms omitted for clarity, 50% probability displacement ellipsoids*).

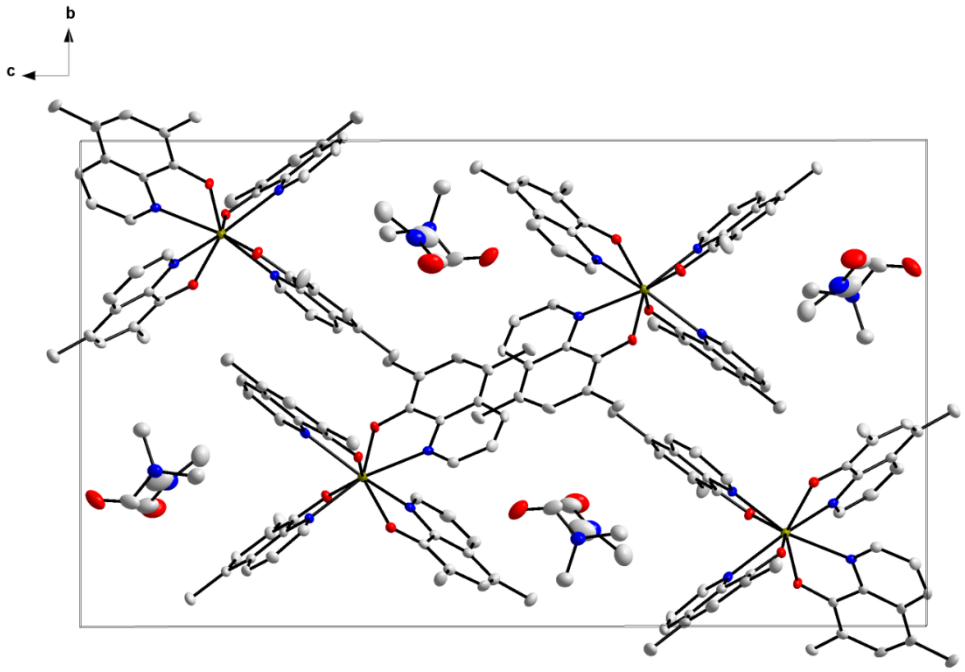

Figure 4.30: Packing of molecules in the [Hf(diMeOx)4].2DMF (**Hf_1h**), crystal structure, illustrating the head-to-head packing of the individual molecules along the a-axis in the unit cell (Hydrogen atoms omitted for clarity, 50% probability displacement ellipsoids).

4.7. Correlation of Structural Parameters for Compounds Hf_1a, Hf_1b and Hf_1h

Three additional Hf(IV)-oxinato complexes have been evaluated and described thus far in the preceding sections (**Figure 4.31**). The general structural parameters, bond distances and angles from the various complexes are given in **Table 4.10**.

As described in **Chapter 3**, these complexes' synthesis seems to afford these types of compounds with relative ease, reproducibly and with very high yields. An added advantage is that these complexes form rapidly, without any special manipulations needed, as described in previously published literature.[19] Therefore, this approach is much more cost-effective, environmentally friendly, and ideal to further a separation study.

[19] P. Kathirgamanathan, S. Surendrakumar, J. Antipan-Lara, S. Ravichandran, V .R. Reddy, S. Ganeshamurugan, M.Kumaraverl, V. Arkley, A. J. Blake & D. Bailey, *J. Mater. Chem. ,* **21,** 1762, 2011.

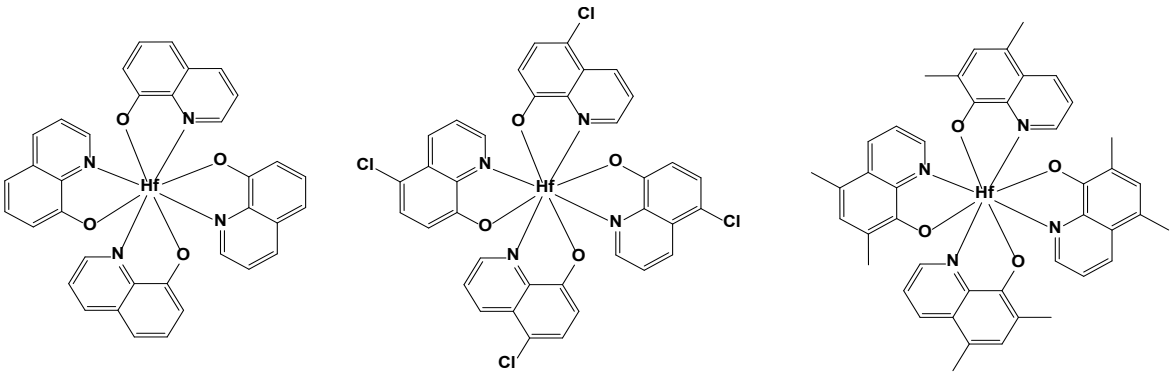

(a) **(b)** **(c)**

Figure 4.31: The three hafnium complexes discussed in this single crystal X-ray diffraction chapter. **(a)** [Hf(Ox)$_4$] (**Hf_1a**), **(b)** [Hf(5-ClOx)$_4$] (**Hf_1h**) and **(c)** [Hf(diMeOx)$_4$] (**Hf_1b**).

In this chapter, three novel hafnium(IV) complex structures with different coordinated oxine ligands were presented. All three structures are very similar in relation to bond lengths and angles to the only other hafnium(IV)-oxine structure found in literature.[19] In general, it is observed that *tetrakis*(oxinato)metal complexes do not show any particular preference towards a specific space group. However, with regards to the coordination environment around the metal centre, all the oxine complexes favour a square-antiprismatic geometry (***D$_2$-corner-clipped isomer***) with a minimal distortion towards dodecahedral geometry. Furthermore, the comparison of the data currently available, the average Hf—O and Hf—N bond lengths are 2.097(3) Å and 2.400(2) Å, respectively, with an average N—Hf—O bite angle of 70.60(8) °.

In this regard, a more detailed comparative relation study of these Hf(IV)-oxinato complexes and additional structures will be undertaken in **Chapter 8** and **Chapter 9**. Properties such as steric bulk and electronic properties of the Hf(IV)-oxinato complexes will be correlated to various aspects such as complex stability and structural effects.

Table 4.10: Unit cell and structure overview of presented Hf(IV)-oxinato complexes.

	[Hf(Ox)]$_4$ •2(C_7H_8) Hf_1a	[Hf(5-ClOx)]$_4$ •2(C_7H_8) Hf_1b	[Hf(diMeOx)$_4$] •2DMF Hf_1h
Crystal system	Triclinic	Monoclinic	Monoclinic
Space group	$P\bar{1}$	$C2/c$	$P2_1/c$
	Square-antiprismatic Polyhedron		
Isomer	*D_2-corner clip*	*D_2-corner clip*	*D_2-corner clip*
Geometrical Isomer	*pseudo two-fold rotated*	*pseudo two-fold rotated*	*pseudo two-fold rotated*
Avg. bending distortion (°)	15.17(6)	6.11(7)	0.44(10)
Avg. rotation distortion (°)	49.12(8)	45.20(11)	44.42(9)
	Selected Bond Lengths (Å)		
Hf—O1	2.0978(2)	2.098(2)	2.094(2)
Hf—O2	2.0951(1)	2.102(2)	2.098(2)
Hf—O3	2.1027(2)	2.1097(2)	2.104(2)
Hf—O4	2.0848(1)	2.080(2)	2.096(2)
Hf—N1	2.3951(2)	2.402(2)	2.413(2)
Hf—N2	2.4044(1)	2.396(2)	2.377(2)
Hf—N3	2.3906(2)	2.396(2)	2.409(2)
Hf—N4	2.4001(1)	2.420(2)	2.393(2)
	Bond Angles (°)		
O1—Hf—N1	70.734(2)	70.78(9)	69.92(8)
O2—Hf—N2	70.843(2)	70.66(9)	70.87(8)
O3—Hf—N3	71.160(2)	70.85(9)	69.58(8)
O4—Hf—N4	71.045(2)	70.30(8)	70.39(7)

4.8. Conclusion

In this chapter, three new hafnium(IV) structures with different coordinated 8-hydroxyquinoline ligands were presented, increasing the available pool of hafnium-oxinato single-crystal data fourfold. After consideration of the information presented, a number of conclusions can be surmised regarding the solid-state characteristics of hafnium(IV) complexes with chelated oxine ligands.

Firstly, as discussed in **Chapter 2**, section 5, it is a well-known fact that eight coordinated hafnium complexes, particularly the *tetrakis*(*β*-diketone)hafnium(IV) complexes, prefer the square-antiprismatic coordination geometry. From the details described in this chapter, we can extent this observation to also be the case for *tetrakis*(oxinato)hafnium(IV) complexes so far.

Additionally, the structures described in this chapter compare well in regards to physical properties such as bond lengths and angles as well as packing modes. All of the complexes display intermolecular interactions to some extent, with π-π- and Cl-π staking being most recurrent within the crystal lattices.

This chapter is the first in a series of crystallographic investigations on various *N*- and *O*-donating multidentate ligands coordination to Hf(V) metal centres. A comprehensive comparison of all available data from this crystallographic structural evaluation will be discussed at the end of **Chapter 8**.

In the following chapter, the structural evaluation and description of three additional hafnium(IV) complexes containing different halogenated substituted 8-hydroxyquinoline ligands, is presented. The focus shift in the next chapter is on the effect of similar dihalogen substituents on the outer periphery of the ligand back-bone on the coordination mode and coordination geometry (ligand plane angles, square anti-prism deviations, etc.) of the obtained solid-state structures.

Chapter 5

X-Ray Diffraction Studies of Hafnium(IV) Complexes Containing Di-halogen Substituted 8-Hydroxyquinoline Ligands

---

5.1. Introduction

This chapter contains a detailed discussion of hafnium(IV) complexes with other, dihalogen substituted, variations of 8-hydroxyquinoline (oxine; ox) ligands. As mentioned previously in **Chapter 2** and **Chapter 4**, 8-hydroxyquinoline and some of its derivatives are well-proven precipitation agents and could be used to extract zirconium from hafnium.[1]

This crystallographic section's primary focus will be placed on the potential influence that the substituents on the periphery of the oxine ligand backbone may have on the coordination mode and coordination geometry of hafnium(IV) complexes after coordination.

The importance of the structural characterisation of these hafnium type complexes lies, again, in the possibility of finding or observing small anomalies in the solid-state behaviours between hafnium and zirconium, with an overarching aim of exploiting these differences for separation purposes.

[1] A. V. Vinogradov & V.S Shpinel, *Atom Energiya*, **3**, 130, 1957.

In the following paragraphs, a detailed discussion of the single-crystal structures of three novel hafnium(IV) complexes containing dihalogen substituted 8-hydroxyquinoline ligands as well as the preliminary intercorrelation of each structure. (**Figure 5.1**).

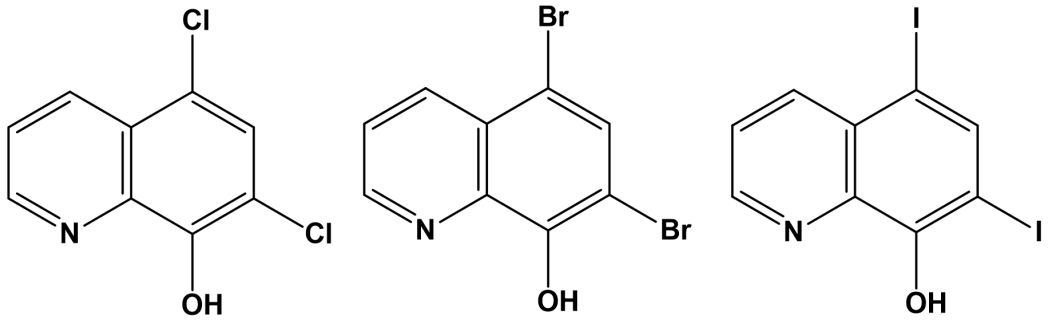

(a) **(b)** **(c)**

Figure 5.1: Functionalized oxine ligands chelated to hafnium(IV) and discussed in this chapter. (**a**) 5,7-dichloro-8-hydroxyquinoline (diClOxH); (**b**) 5,7-dibromo-8-hydroxyquinoline (diBrOxH); (**c**) 5,7-diiodo-8-hydroxyquinoline (diIOxH).

5.2. Experimental

The X-ray intensity data was collected on a Bruker X8 ApexII 4K Kappa CCD area detector diffractometer, equipped with a graphite monochromator and Mo$K\alpha$ fine-focus sealed tube (λ = 0.71069 Å, T = 100(2) K) operated at 2.0 kW (50 kV, 40 mA). The initial unit cell determinations and data collections were done by the SMART[2] software package. The collected frames were integrated using a narrow-frame integration algorithm and reduced with the Bruker SAINT-Plus and XPREP software packages[3] respectively. Analysis of the data showed no significant decay during the data collection. Data was corrected for absorption effects using the multi-scan technique SADABS[4], and the structure was solved by the direct methods package SIR97[5] and refined using the WinGX[6] software incorporating SHELXL[7]. The final anisotropic full-matrix least-squares refinement was done on F^2. The methyl and aromatic protons were placed in geometrically idealised positions (C–H = 0.93 – 0.98 Å) and constrained to ride on their parent atoms with $U_{iso}(H) = 1.2U_{eq}(C)$. Non-hydrogen atoms were refined with anisotropic displacement parameters. The graphics were obtained with the DIAMOND[8] program with 50% probability ellipsoids for all non- hydrogen atoms.

---

[2] Bruker SMART-NT Version 5.050.Bruker AXS Inc. Area-Detector Software Package; Madison, WI, USA, 1998.

[3] Bruker SAINT-Plus Version 6.02 (including XPREP), Bruker AXS Inc. Area-Detector Integration
Software, Madison, WI, USA, 1999.

[4] Bruker SADABS Version 2004/1.Bruker AXS Inc. Area Detector Absorption Correction Software, Madison, WI, USA, 1998.

[5] A. Altomare, M.C. Burla, M. Camalli, G.L. Cascarano, C. Giacovazzo, A. Guagliardi, A.G.G. Moliterni, G. Polidori & R. Spagna; *J. Appl. Cryst.* ***32***, 115, 1999.

[6] L.J. Farrugia; *J. Appl. Cryst.* ***32***, 837, 1999.

[7] G.M. Sheldrick; SHELXL97. *Program for crystal structure refinement*, University of Göttingen, Germany, 1997.

[8] K. Brandenburg & H. Putz; DIAMOND, *Release 3.0e, Crystal Impact GbR*, Bonn, Germany, 2006.

Table 5.1. Crystallographic and refinement details for structures discussed in this chapter.

Compound	[Hf(diClOx)$_4$]·3DMF	[Hf(diBrOx)$_4$]·3DMF	[Hf(diIOx)$_4$]·DMF
Formula weight	2426.72	1605.51	3670.63
Crystal system	Monoclinic	Monoclinic	Triclinic
Space group	$P2_1/c$	$P2_1/c$	$P\bar{1}$
Unit cell dimensions: ***a,*** ***b,*** ***c* (Å)**	22.428(2), 15.790(1), 28.618(1)	9.600(1), 38.598(2), 13.621(1)	15.208(2), 17.490(5), 20.262(1)
α, ***β,*** ***γ* (°)**	90, 113.853(2), 90	90, 98.672(2), 90	71.119(2), 89.842(3), 89.764(2)
Volume (Å^3) / Z	9269.1(11) / 4	4989.6(4) / 4	5099.4(12) / 2
Density (calculated) (mg/m^3)	1.739	2.137	2.391
Absorption coefficient (mm^{-1})	2.769	8.554	6.931
F(000)	4800	3056	3312
Crystal size (mm)	0.19 x 0.15 x 0.05	0.33 x 0.16 x 0.14	0. 2 x 0.084 x 0.284
Theta range for data collection (°)	0.99 to 28.00	3.20 to 28.40	1.10 to 28.00
Index ranges	-30<=h<=29, -12<=k<=21, -37<=l<=38	-12 <= h <= 8, -48<=k<= 51, -18 <= l <= 17	-20<=h<=20, -23<=k<=23, -25<=l<=26
Reflections collected	187649	65172	89282
Independent reflections/R_{int}	22345 [R_{int} = 0.0703]	12395[R_{int} = 0.0617]	24273 [R_{int} = 0.0616]
Completeness (θ = 28.35°) (%)	99.90	99.50	99.60
Refinement method	Full-matrix least-squares on F^2	Full-matrix least-squares on F^2	Full-matrix least-squares on F^2
Data / restraints / parameters	22345 / 0 / 1181	12395 / 0 / 619	24273 / 39 / 655
The goodness of fit on F^2	1.079	1.036	1.092
Final R indices [I>2sigma(I)]	R_1 = 0.498, wR_2 = 0.1169	R_1 = 0.033, wR_2 = 0.067	R_1 = 0.0815, wR_2 = 0.1910
R indices (all data)	R_1 = 0.0836, wR_2 = 0.1402	R_1 = 0.045, wR_2 = 0.070	R_1 = 0.1178, wR_2 = 0.2105
Largest diff. peak and hole (e.Å^{-3})	2.385 and -1.578	1.340 and -1.690	3.810 and -3.860

5.3. General Considerations for Chapter 5

Note: As indicated in **Chapter 4**, the following general considerations which enables a systematic comparison and standardised geometry for the complexes as discussed, are used throughout the text below. It is further important to take into account that although the symmetry elements are formally defined as “inversion centres”, “rotation axes”, “mirror planes”, etc., these are all to be considered “***pseudo***” elements, since they all describe **solid-state** observations.

- Coordinated oxine ligands are numbered starting from the N-atom. In structures containing multiple complexes/ dinuclear compounds, the first digit of carbon/oxygen/nitrogen atoms indicates the oxine ligand associated with the N-atom and the second digit indicates the position of the atom in the ring (**Figure 5.2(a)**).

- Each independent oxine ligand *(identified by the numbering of the nitrogen and oxygen atoms, where appropriate*) coordinated to the metal centre is numbered consecutively and abbreviated to "***Lig#***" with # = 1-4 (**Figure 5.2(b)**).

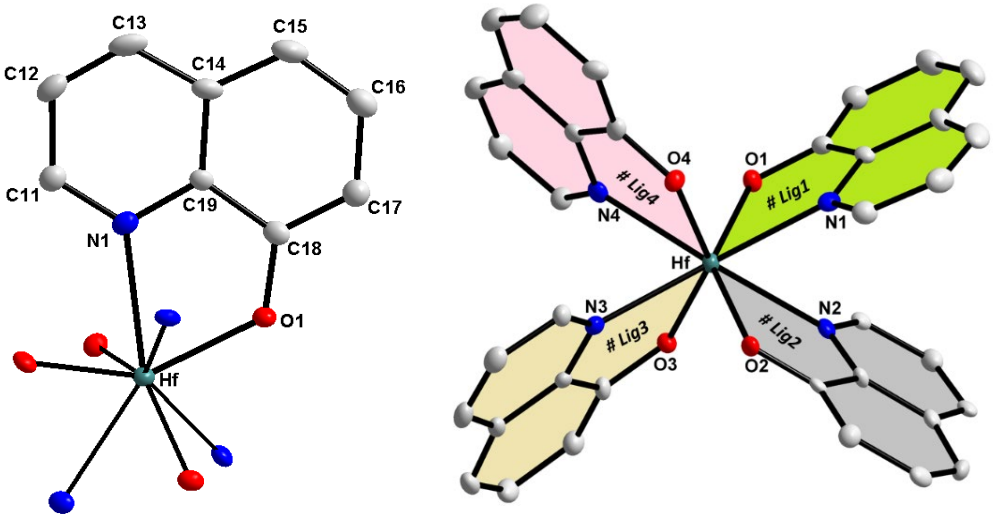

(a) **(b)**

Figure 5.2: (a) General numbering scheme for oxine ligands coordinated to hafnium(IV), illustrated within **(b)** a pseudo ***centrosymmetrically inverted isomer***

- Eight coordinated hafnium(IV) structures (*tetrakis*-coordinated, **Figure 5.2(b)** and **Figure 5.3** are described as two types of isomeric forms.

  The spatial arrangement of the oxine ligands allows the formation of two geometrical isomers. The placement of the nitrogen and oxygen coordination atoms are observed as either a:

  - **(a) *centrosymmetrically inverted*** isomer (**Figure 5.2 (b)**; or
  - **(b) *(multiple) two-fold rotated*** isomer (**Figure 5.3**)

    The latter may be via multiple two-fold rotation axes through the metal centre as shown in **Figure 5.3** (illustrating three ***pseudo two-fold*** rotation axes, defined along the classic x, y, and z-axes as reference).

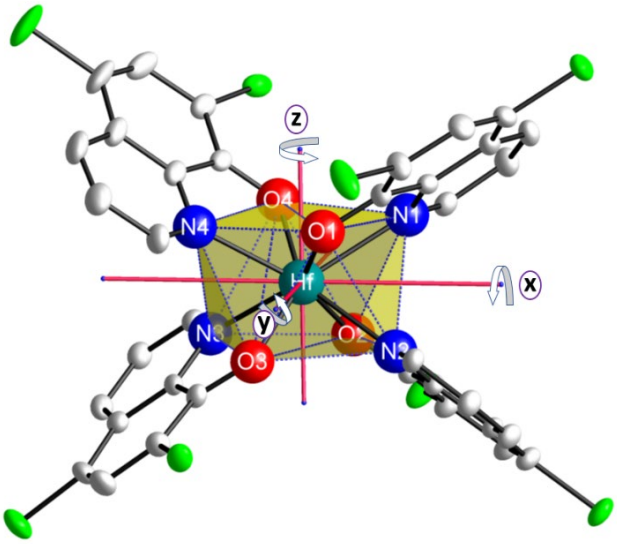

Figure 5.3: Coordinate functionalised ox-ligand arrangement around the metal centre when considering the *N*- and *O*- coordination sites via three ***pseudo two-fold*** rotation axes, i.e. a *two-fold rotated-isomer*. It is illustrated for the unsymmetrical oxine ligand, even functionalised by two chloro substituents.

As discussed earlier in **Chapter 2** (§ 2.5), most hafnium and zirconium complexes, containing bidentate ligands adopt **square-antiprismatic** coordination geometries around the metal centres. However, in addition, it was also noted that this geometry exhibits three possible stereo-isomers, often for metal complexes containing symmetrical bidentate ligands like acetylacetonate.

The three possible isomers, containing simplified ligand entities, are illustrated in **Figure 5.4** and may exhibit a:

(a) ***D_2-corner-clipped*** ligand placement;

(b) ***D_4-side-clipped*** coordination;

(c) ***C_2-isomer*** (combination of D_2 -and D_4 isomers).

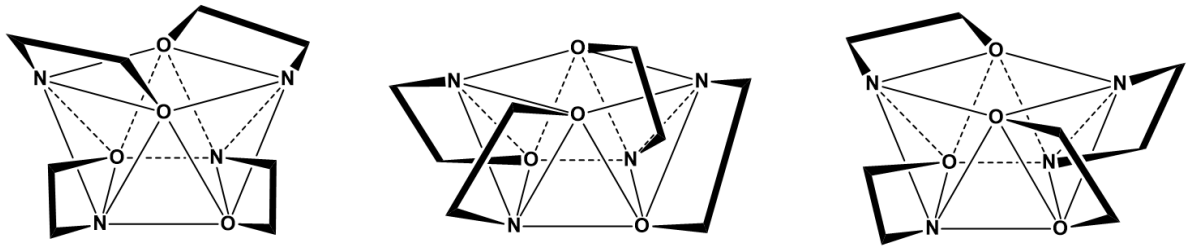

(a) **(b)** **(c)**

Figure 5.4: Coordination isomers as defined for *tetrakis*(oxinato)metal complexes exhibiting a square antiprismatic coordination polyhedron. **(a)** ***D_2***-corner-clipped ligands; **(b)** ***D_4***-side-clipped ligands; **(c)** ***C_2***-combination of corner- and side-clipped ligands.

5.4. Crystal Structure of Tetrakis(5,7-dichloro-quinolin-8-olato-κ^2N,O)-hafnium(IV) dimethylformamide trisolvate – $[Hf(diClOx)_4]\cdot 3C_3H_7NO$

The structure of this *tetrakis*-coordinated hafnium – 5,7-dichloro-8-hydroxyquinoline complex (**Hf_1d**) is one of few examples of hafnium-oxinato structures exhibiting two unique molecules in the asymmetric unit. Synthesis of **Hf_1d** and the resulting yellow cubic-like crystals obtained for this was discussed in § 3.3.1.4.

The title compound, $[Hf(C_9H_4Cl_2NO)_4]\bullet 3(C_3H_7NO)$, where $C_9H_4Cl_2NO$ = 5,7-dichloro-8-hydroxyquinoline = diClOx$^-$ and C_3H_7NO = dimethylformamide = DMF), crystallises in the monoclinic crystal system $P2_1/c$ with four formula units per unit cell (Z=4). The asymmetric unit consists of two hafnium(IV) metal centres, each coordinated to four bidentate ligands (diClOx$^-$). Six crystallographically independent DMF solvent molecules fill the rest of the asymmetric unit. A summary of the general crystal data is given in **Table 5.1**, while the numbering scheme of the solvated complexes is represented **Figure 5.5**.

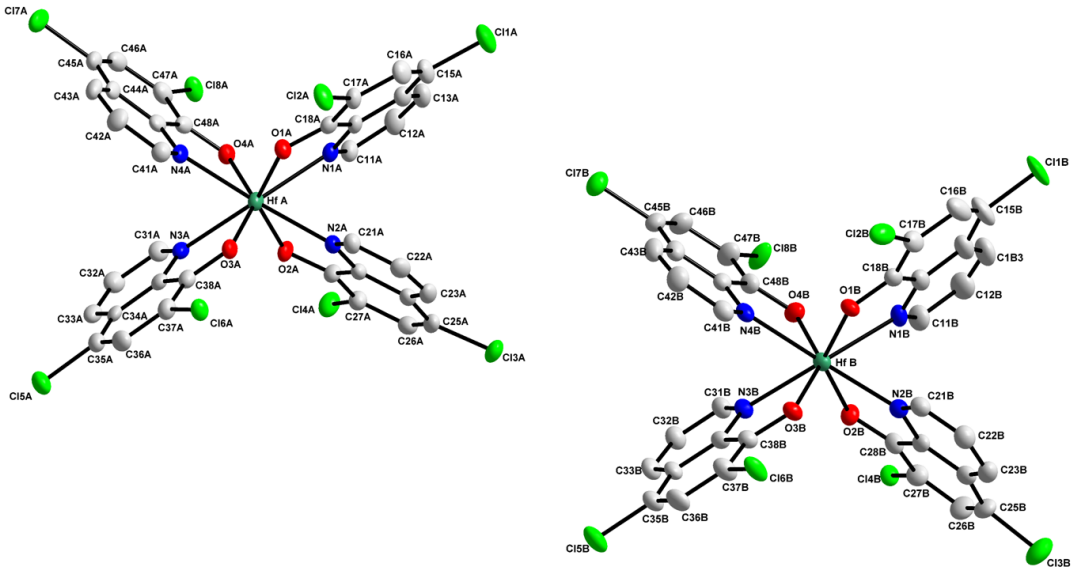

Figure 5.5: Representation of the title compound (**Hf_1d**), showing the two independent molecules in the asymmetric unit and the numbering scheme and displacement ellipsoids *(50 % probability, solvent molecules and hydrogen atoms omitted for clarity*)

Table 5.2 presents selected bond lengths and angles of the title compound. Atomic coordinates, anisotropic displacement parameters, bond distances and angles and hydrogen coordinates, are given in the supplementary data (**Appendix A.4**).

Table 5.2: Selected geometry parameters of $Hf(diClOx)_4]\cdot 3C_3H_7NO$ (Hf_1d).

Selected Bond Lengths (Å)					
Molecule	**A**	**B**	**Molecule**	**A**	**B**
Hf—O1	2.1025(1)	2.0989(1)	Hf—N1	2.4048(2)	2.3846(1)
Hf—O2	2.1029(1)	2.1058(1)	Hf—N2	2.3695(1)	2.3835(1)
Hf—O3	2.1023(2)	2.1013(1)	Hf—N3	2.3751(1)	2.3888(1)
Hf—O4	2.0880(1)	2.0861(2)	Hf—N4	2.3911(1)	2.3877(1)
C15—Cl1	1.755(1)	1.7357(1)	C35— Cl5	1.7476(1)	1.7383(1)
C17— Cl2	1.7422(1)	1.7297(1)	C37— Cl6	1.7351(1)	1.7301(1)
C25— Cl3	1.7422(1)	1.7472(1)	C45— Cl7	1.7508(1)	1.7427(1)
C27— Cl4	1.7334(1)	1.7224(1)	C47— Cl8	1.7092(1)	1.7285(1)
Selected Bite Angles (°)					
O1—Hf—N1	70.48(1)	70.94(1)	N1—Hf—N3	142.56(1)	140.30(2)
O2—Hf—N2	70.99(1)	70.99(1)	N2—Hf—N4	140.99(1)	141.15(1)
O3—Hf—N3	70.82(1)	70.78(2)	O1—Hf—O3	85.90(1)	88.85(2)
O4—Hf—N4	70.82(1)	70.96(2)	O2—Hf—O4	86.57(1)	87.38(2)
Selected Torsion Angles (°)					
O1—C18—C19—N1	3.63(2)	1.85(1)	O3—C38—C39—N3	1.83(1)	1.87(1)
O2—C28—C29—N2	3.24(2)	5.31(2)	O4—C48—C49—N4	0.47(2)	2.38(2)
Selected Dihedral Angles of Anti-prism (°)					
Bending			**Twisting**		
[O1—N1—O4]—[O1—N4—O4]	1.97(3)	5.57(4)	[O1—Hf—O4]—[O2—Hf—O3]	49.63 (1)	49.83(1)
[O2—N2—O3]—[O2—N3—O3]	3.96(4)	6.00(5)	[N1—Hf—N4]—[N2—Hf—N3]	44.45(1)	45.43(1)

For both molecules in the asymmetric unit, the central hafnium metal coordinates with the nitrogen and oxygen atoms of oxine (diClOx$^-$) ligands to form eight different six-membered metallacycle rings. Moreover, it is clear from **Figure 5.5,** that each coordinated ligand, for both independent molecules, is duplicated by an opposite facing ligand by *ca*. 180° rotation, through the hafnium metal centre. Although these ligands do not lie in a flat plane opposite each other, it is evident that these ligands are chelated to the metal centre in a (multiple) ***pseudo two-fold rotated-isomer*** geometry by the N- and O-coordinating sites (**Figure 5.3**). This yields average O—Hf—O and N—Hf—N bond angles of 87.12(3)° and 141.25(2)°, respectively (individual O—Hf—O and N—Hf—N bond angle are given in **Table 5.2**.

The diClOx-ligands lie around the metal centre in a space filling, fan-like arrangement to give an approximate square-antiprismatic coordination polyhedron (**Figure 5.6**), with an almost negligible outward distortion towards dodecahedral geometry. Concerning the overall coordination description of the ligands as viewed in the square antiprism (**Figure 5.6 (a)**), the title compound (**Hf_1d**) crystallises as a ***D_2-corner-bonded isomer*** ((**Figure 5.6 (b)**)***.***

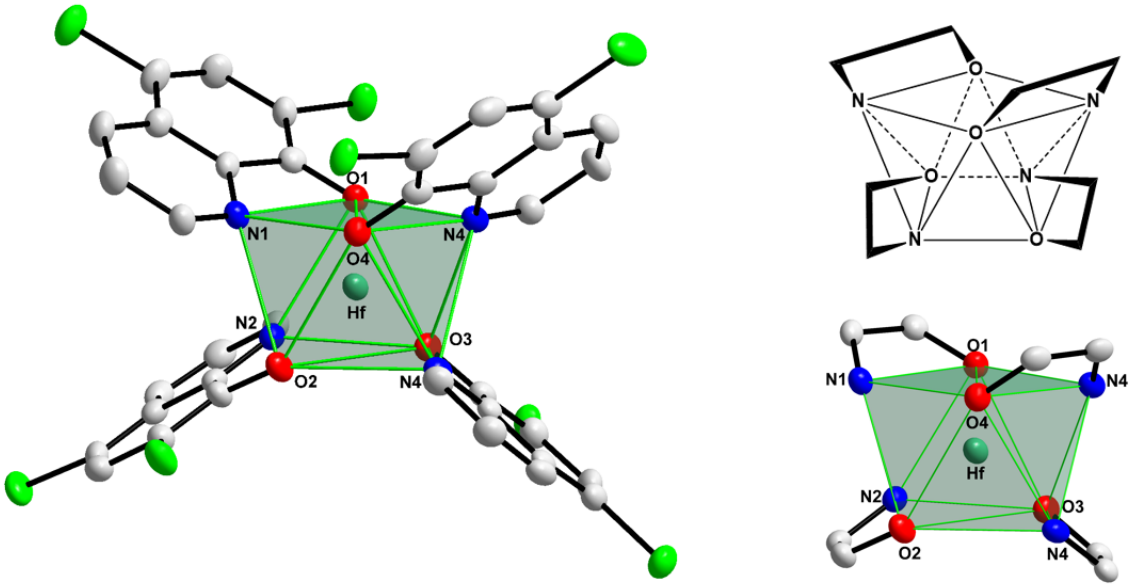

(a) **(b)**

Figure 5.6: **(a)** Graphic illustration of the square-antiprismatic coordination polyhedron of [Hf(diClOx)$_4$ (**Hf_1d**, hydrogen atoms omitted for clarity, 50% probability displacement ellipsoids). **(b)** Illustration of the typical D_2-corner-bonded square antiprismatic isomer.

This distortion from the ideal square antiprism is associated with an outward bend of the N_2O_2 bases, as illustrated in **Figure 5.7**. The dihedral angles between the yellow (N1—O1—O4 & N3—O2—O3) and green planes **(**N4—O1—O2 & 4: N2—O2—O3), indicative of a bending distortion, was measured as 1.97(3)° and 3.96(4)° for molecule A and 5.57(4)° and 6.00(5)° for molecule B, respectively for the top and bottom N_2O_2 bases of the coordination polyhedron.

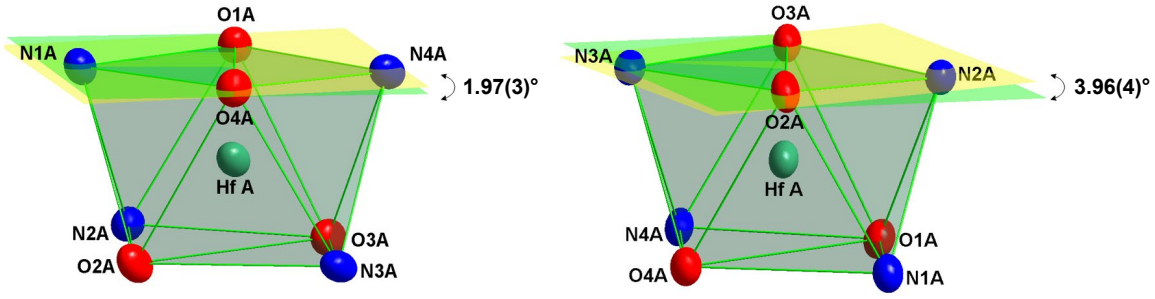

(a)

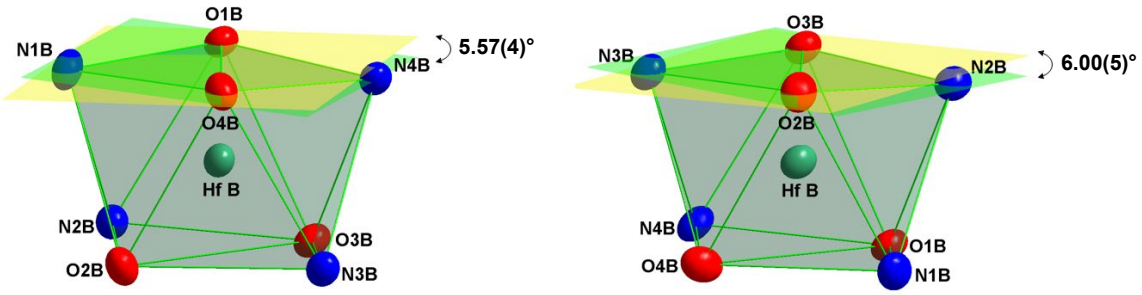

(b)

Figure 5.7: A graphical representation of the outward bending observed in the antiprismatic coordination polyhedron surrounding the hafnium metal **(a) -** Hf A & **(b) -** Hf B (*C, H and Cl atoms and solvent molecules are omitted for clarity*).

A further indication of distortion is the amount of rotation observed between the top and bottom N_2O_2 bases of the antiprismatic coordination polyhedron. Ideally, these angles should be 45°. Therefore, when viewing the coordination polyhedron from above, the dihedral angles between planes [O1—Hf—O4] & [O2—Hf—O3] and [N1—Hf—N4] & [N2—Hf—N3] was measured as 49.63(1)° and 44.45(1)° for molecule A and 49.83(1)° and 45.43(1)° for molecule B, respectively, indicating the rotation distortion observed within the coordination polyhedron (**Figure 5.8**).

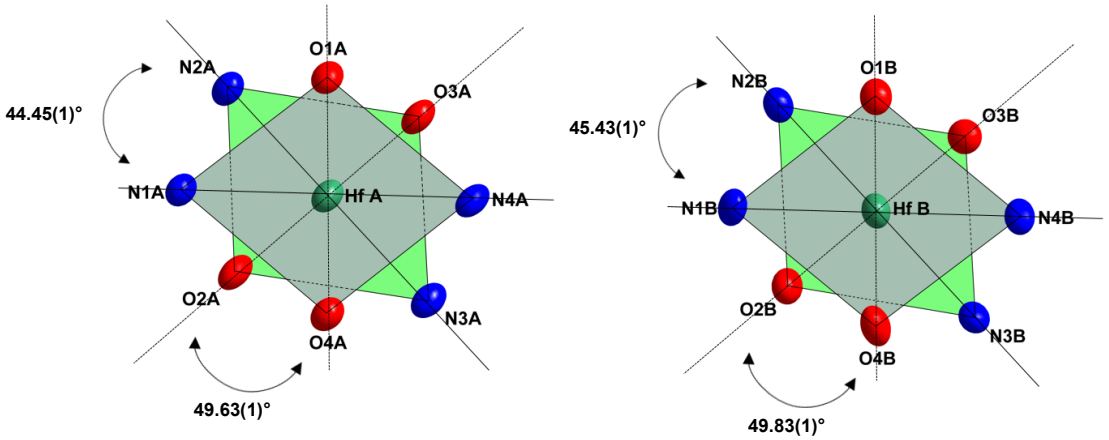

(a) **(b)**

Figure 5.8: A graphical representation of the top view of the antiprismatic coordination polyhedron indicting the rotation distortion observed in molecule A and B. (*C, H and Cl atoms and solvent molecules are omitted for clarity*).

In these structures, the average Hf—N and Hf—O bond distances are 2.3856(1) Å and 2.0985(3) Å, respectively, and the average N—Hf—O bite angle is found to be 70.85(3)° (**Table 5.2**). The measured N—C—C—O torsion angles of the ligand frame facing the N—Hf—O bite angles are found to range from 1.87(1)° to 5.31(2)°, indicating very little deviation from the planarity of the ligands themselves. However, the dihedral angle between the metal coordination plane and the plane formed by the oxine ligands range from 2.46(1)° to 11.56(1)° as shown in **Figure 5.9**.

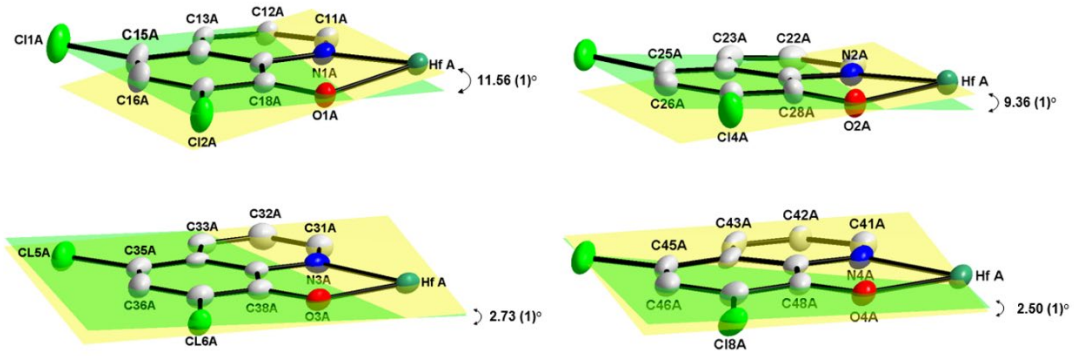

(a)

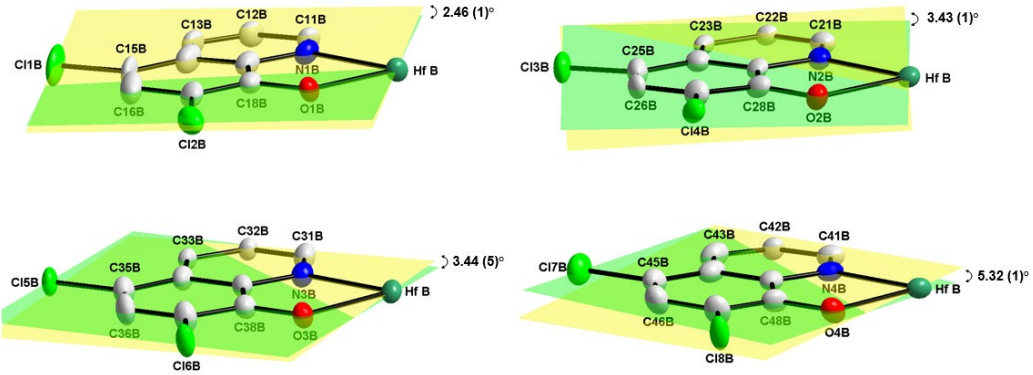

(b)

Figure 5.9: Graphical illustration of the dihedral angles between the hafnium metal coordination planes and the planes formed by the coordinating backbone of the oxine (diClOx) ligands. **(a)** – Molecule A; ***Lig1- Lig4*. (b)** – Molecule B; ***Lig1- Lig4*** (*C, H and Cl atoms and solvent molecules are omitted for clarity*).

Crystal lattice packing is stabilised by π–π interactions between the benzene and pyridene rings of the diClOx ligand groups 3 and 4 (***Lig3 & Lig4)*** with symmetry generated of neighbouring molecules, with interplanar and averaged centroid-to-centroid distances of 3.345(9) Å and 3.606(3) Å for molecule A and 3.355(7) Å and 3.687(4) Å for molecule B, respectively (Red dotted line, **Figure 5.10(a) & (b)**).

Crystal lattice packing is further stabilised by Cl···π interactions between Cl_{7A} (***Lig4***) to the pyridne ring of ***Lig2*** (Cl_{7A}···Py2 = 3.723(1) Å, 165.97(3)° (Green dotted line, **Figure 5.10(a)**. This tightly knit two-dimensional interaction network rigidly ties the crystal lattice together, influencing the overall packing in pairs of these two hafnium molecules dispersed in a head-to-head manner when viewed along the diagonal axis of the *bc*-plane (**Figure 5.11**). No classical hydrogen bonding is found within the molecules (*intramolecular interactions*) or between neighbouring molecules (*intermolecular interactions*) in the unit cell.

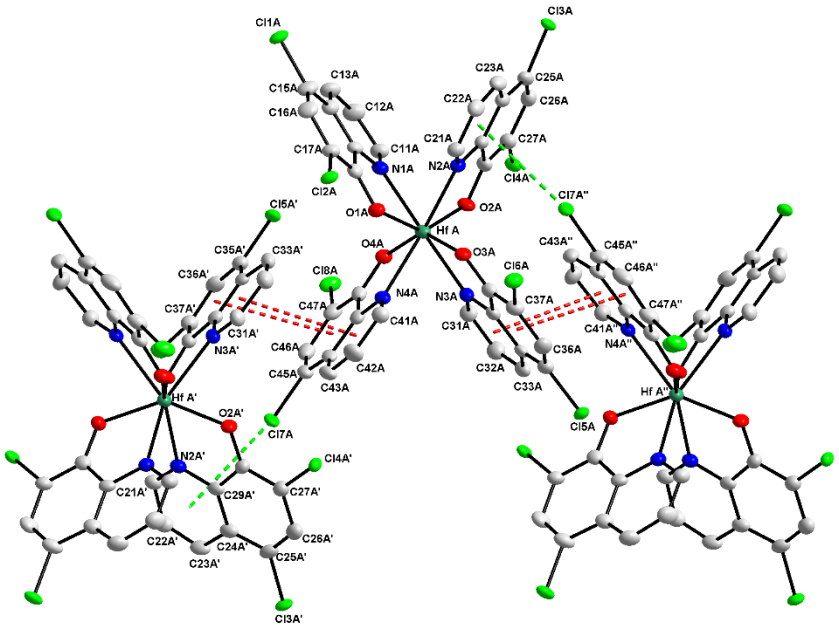

Symmetry code *:(') = 1-x, -1/2+y, 1/2-z*
(") =1-x, 1/2+y, 1/2-z

(a)

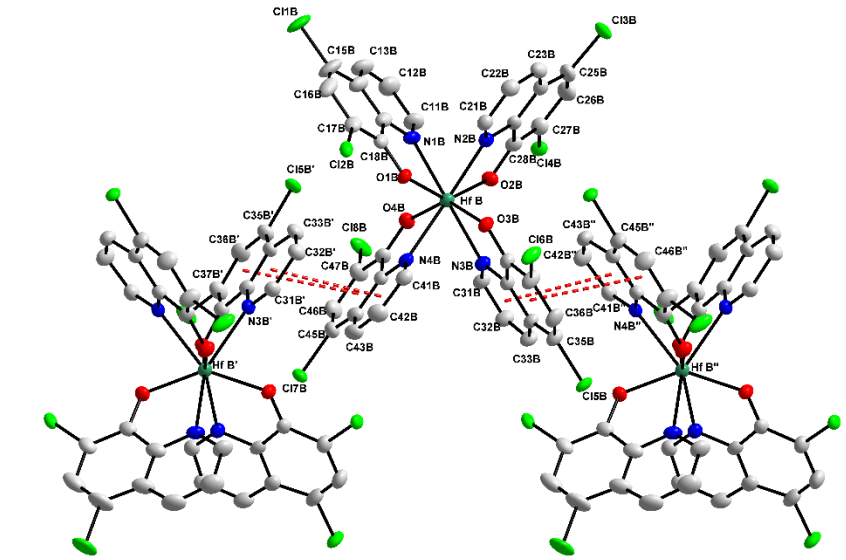

Symmetry code *: (') = -x, -1/2+y, 1/2-z*
(") =-x, 1/2+y, 1/2-z

(b)

Figure 5.10: Graphical illustration depicting the paired π–π interactions between the benzene and pyridine rings of the diClOx ligands **(a)** – Molecule A; **(b)** – Molecule B (*C and H atoms and solvent molecules are omitted for clarity*).

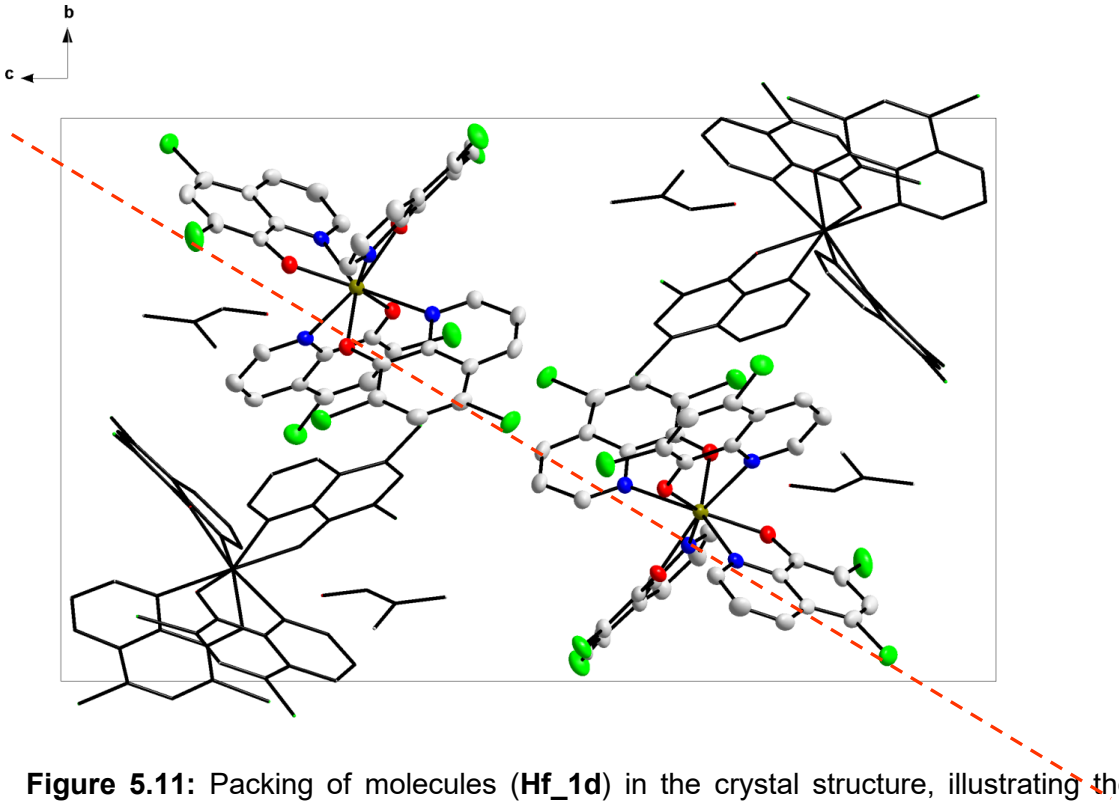

Figure 5.11: Packing of molecules (**Hf_1d**) in the crystal structure, illustrating the head-to-head packing of the individual molecules when viewed along the diagonal axis of the *bc*-plane.

5.5. Crystal Structure of Tetrakis(5,7-dibromo-quinolin-8-olato-κ²N,O)-hafnium(IV) dimethylformamide trisolvate – [Hf(diBrOx)$_4$]·3C$_3$H$_7$NO

The structure of this *tetrakis*-coordinated hafnium complex (**Hf_1e**)[9] was the last *tetrakis* hafnium-oxine crystal structure to be published and is now one of four structures available in the Cambridge Structural Data Base.[10] The title compound, [Hf(diBrOx)$_4$]·3C$_3$H$_7$NO where (diBrOx) = 5,7 dibromeo-8-hydroxy-quinoline, Ox^-, crystallises in the monoclinic space group $P2_1/c$ with four formula units per unit cell (Z=4). Synthesis of **Hf_1e** and the resulting yellow needle crystals obtained for this was discussed in § 3.3.1.5.

[9] J. A. Viljoen, H. G Visser, A Roodt & I Engelbrecht, *Z. Kristallogr. NCS*., **228**, 485, 2013.

[10] Cambridge Structural Database (CSD) Version 5.42, November 2020 update. C. R. Groom, I. J. Bruno, M. P. Lightfoot & S. C. Ward, *Acta Cryst*., **B72**, 171, 2016.

The asymmetric unit contains one independent molecule together with three dimethylformamide (DMF) solvate molecules and is represented in **Figure 5.12** with the atom numbering scheme.

A summary of the general crystal data is given in **Table 5.1**, while **Table 5.3** presents selected bond lengths and angles of the title compound. Atomic coordinates, anisotropic displacement parameters, bond distances and angles and hydrogen coordinates, are given in the supplementary data (**Appendix A.5**).

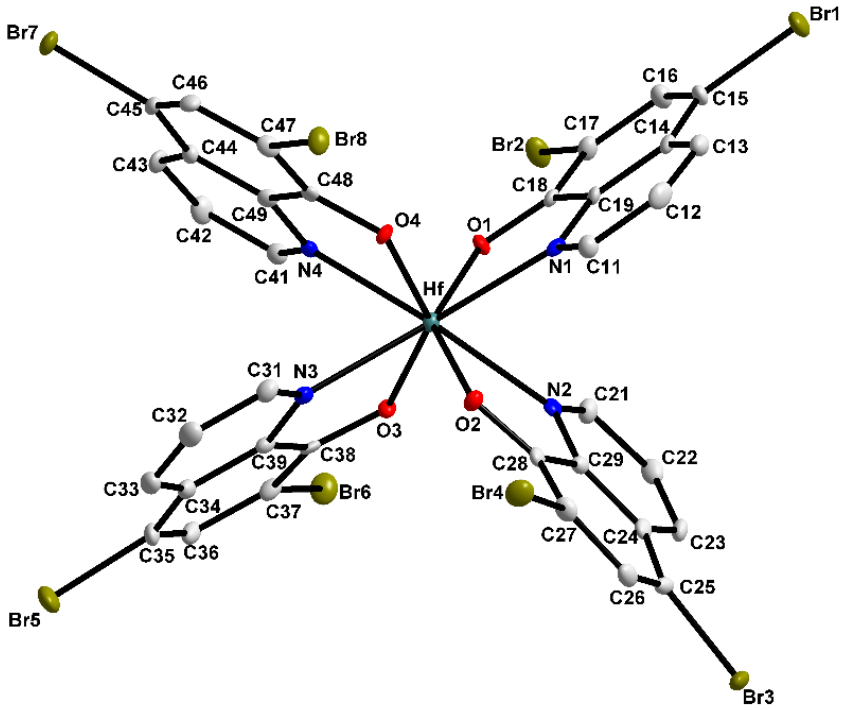

Figure 5.12: Representation of the title compound (**Hf_1e**), showing the numbering scheme and displacement ellipsoids *(50 % probability, solvent molecules and hydrogen atoms omitted for clarity*).

Table 5.3: Selected geometry parameters of $[Hf(diBrOx)_4]\cdot 3C_3H_7NO$ (Hf_1e).

Selected Bond Lengths (Å)			
Hf—O1	2.095(2)	Hf—N1	2.389(3)
Hf—O2	2.095(3)	Hf—N2	2.410(3)
Hf—O3	2.083(2)	Hf—N3	2.413(3)
Hf—O4	2.080(3)	Hf—N4	2.383(3)
C15—Br1	1.901(4)	C35—Br5	1.895(4)
C17—Br2	1.888(4)	C37—Br6	1.885(4)
C25—Br3	1.891(4)	C45—Br7	1.899(4)
C27—Br4	1.890(4)	C47—Br8	1.890(4)
Selected Bite Angles (°)			
O1—Hf—N1	70.69(10)	N1—Hf—N3	140.57(11)
O2—Hf—N2	70.65(10)	N2—Hf—N4	139.41(10)
O3—Hf—N3	70.48(10)	O1—Hf—O3	88.95(10)
O4—Hf—N4	70.97(10)	O2—Hf—O4	88.89(10)
Selected Torsion Angles (°)			
O1—C18—C19—N1	1.99(5)	O3—C38—C39—N3	5.38(5)
O2—C28—C29—N2	4.22(5)	O4—C48—C49—N4	2.72(5)

Selected Dihedral Angles of Anti-prism (°)			
Bending		**Twisting**	
[O1—N1—O4] — [O1—N4—O4]	7.37(11)	[O1—Hf—O4] — [O2—Hf—O3]	50.97(8)
[O2—N2—O3] — [O2—N3—O3]	2.83(12)	[N1—Hf—N4] — [N2—Hf—N3]	46.29(7)

It is evident from **Figure 5.13** and **Figure 5.14** that each coordinated oxinato ligand is duplicated by an opposite facing ligand by *ca*. 180° rotation, through the hafnium metal centre. Although these ligands do not lie in a flat plane opposite each other, it is clear that the ligands are chelated to the metal centre with a ***two-fold rotated-isomer*** placement of the N- and O-coordinating sited similar to **Hf_1e**, *see* **Figure 5.13**. Thus, it yields average O—Hf—O and N—Hf—N bond angles of 88.92(10)° and 139.99(11)°, respectively (individual O—Hf—O and N—Hf—N bond angle are given in **Table 5.3**.

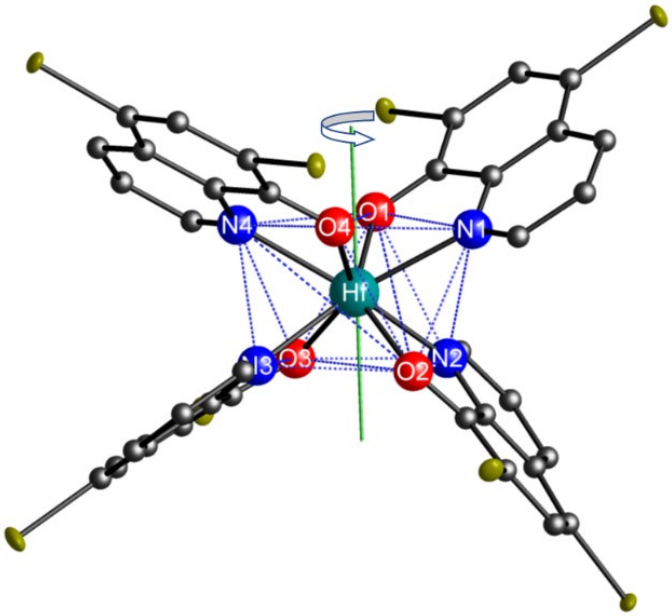

Figure 5.13: Graphical illustration of the **multiple *two-fold rotated*-isomer** of the dibromo oxine ligands across the metal centre in the title molecule (**Hf_1e**), (*Hydrogen atoms and solvent molecules omitted for clarity*). Only shown here is the two-fold rotation around the z-axis.

The hafnium metal centre, in which the four *N,O*-donating bidentate ox-ligands are fan-like arranged around the metal centre produces a square antiprismatic coordination polyhedron, with a small bending distortion towards dodecahedral geometry. With regard to the overall coordination description of the ligands as viewed in the square antiprism (**Figure 5.14 (a)**), the title compound crystallises as a ***D_2-corner-bonded isomer*** ((**Figure 5.14 (b)**)*.*

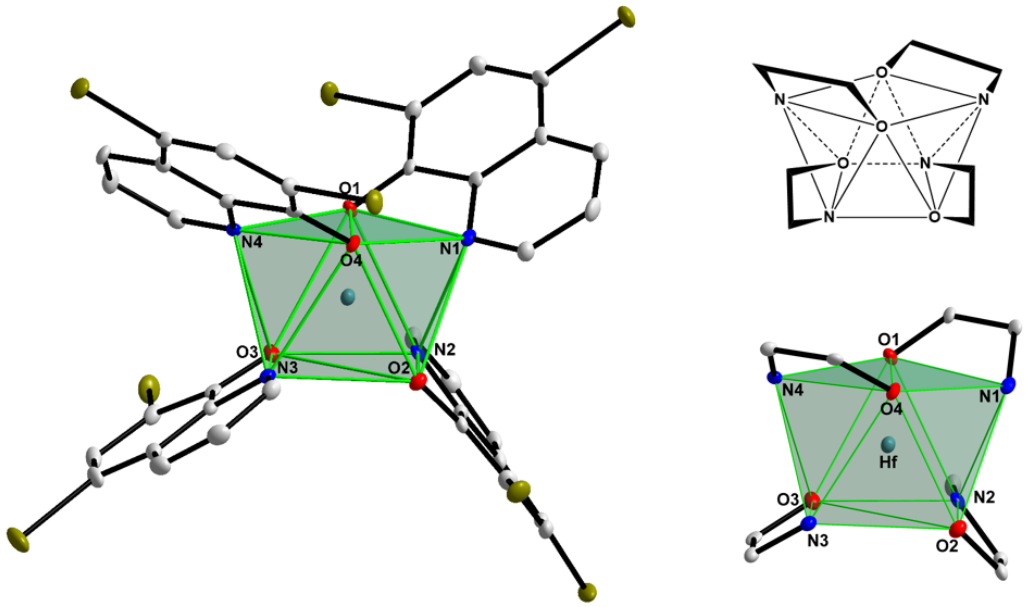

Figure 5.14: **(a)** Graphic illustration of the square-antiprismatic coordination polyhedron of [Hf(diBrOx)$_4$] (**Hf_1e**, Hydrogen atoms omitted for clarity, 50% probability displacement ellipsoids). **(b)** Illustration of the typical ***D$_2$-corner-bonded*** square antiprismatic isomer.

The dihedral angles between the green (N1—O1—O4 & N3—O2—O3) and yellow planes **(**N4—O1—O2 & 4: N2—O2—O3) in illustrated **Figure 5.15**, indicative of a bending distortion, was measured as 7.37(11)° and 2.83(11)°, respectively for the top and bottom N_2O_2 bases of the coordination polyhedron.

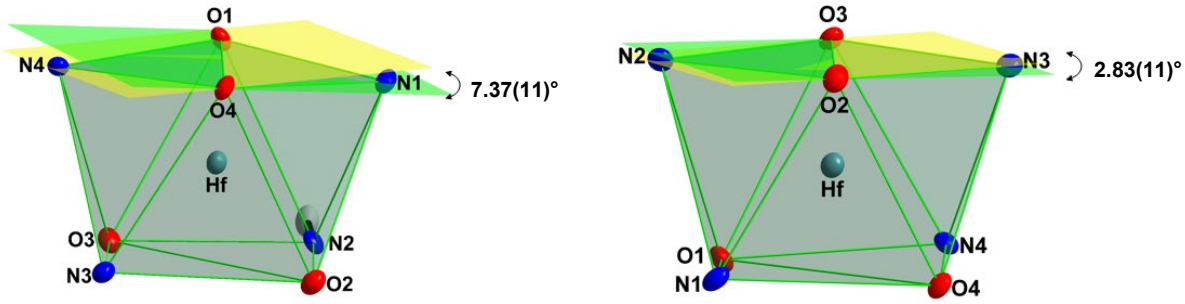

Figure 5.15*:* A graphical representation of the bending distortion observed in the antiprismatic coordination polyhedron surrounding the hafnium metal atom (*C and H atoms and solvent molecules are omitted for clarity*).

A further indication of distortion is the amount of rotation observed between the top and bottom N_2O_2 bases of the antiprismatic coordination polyhedron. Ideally, these angles should be 45°. Therefore, when viewing the coordination polyhedron from above, the dihedral angles between planes [O1—Hf—O4] & [O2—Hf—O3] and [N1—Hf—N4] & [N2—Hf—N3] was measured as 50.97(8)° and 46.29(7)°, respectively, signifying the rotation distortion observed (**Figure 5.16**).

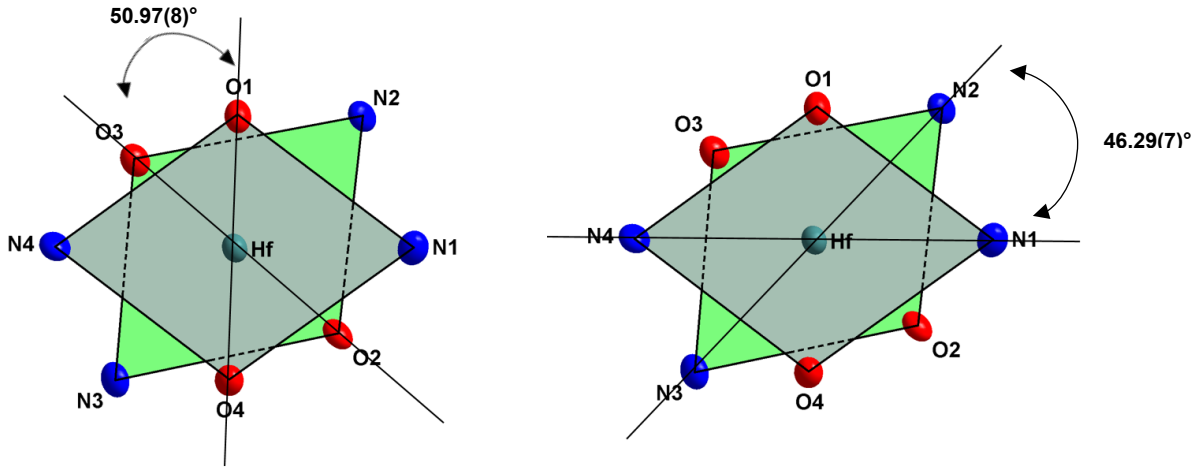

Figure 5.16: A graphical representation of the top view of the antiprismatic coordination polyhedron indicting the rotation distortion observed. (*C and H atoms are omitted for clarity*).

The Hf—O and Hf—N bond lengths vary from 2.080(3) Å to 2.095(2) Å and 2.383(3) Å to 2.413(3) Å, respectively, and the O—Hf—N bite angles vary from 70.48(10)° to 70.97(10)°. The dihedral angles between the two phenyl rings of the quinoline ligands coordinated are all less than 1°, indicating little or negligible distortion due to coordination or packing. The solvate molecule seems to have no effects on the different Hf—O and H—N bond distances as they are all in the same magnitude as listed in **Table 5.3**. The dihedral angle between the metal coordination plane and the plane formed by the quinoline ligands are considered negligible for ***Lig1*** at 2.10(1)° (see **Figure 5.17**). However, the dihedral angles formed between the metal coordination plane and the plane formed by the other oxine ligands are measured at 5.43(6), 9.73(8) and 9.42(8)°, respectively for ***Lig2***, ***Lig3*** and ***Lig4*** as shown in **Figure 5.17**.

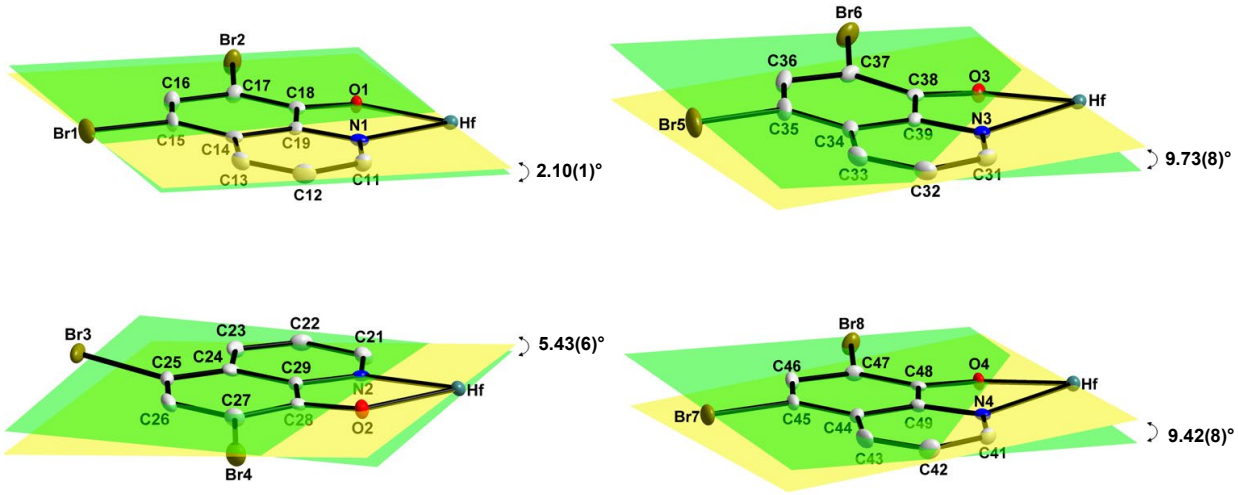

Figure 5.17: Partial structures of [Hf(diBrOx)$_4$] (**Hf_1e**) graphical illustration the dihedral angle between the metal coordination plane and the plane formed by the quinoline ligands (Hydrogen atoms omitted for clarity, 50% probability displacement ellipsoids).

No π-π-stacking is observed between neighbouring molecules. However, strong C—H···O hydrogen bonding interaction is observed between the solvent molecules and the oxygen atoms from the neighbouring metallic molecular group to produce a three-dimensional network. Theoretically, this occurrence might be the cause for the higher dihedral angle observed for ***Lig3 and Lig4*** as described earlier (**Figure 5.17**). The bond distances and angles for the hydrogen bonding are given in **Table 5.4** and illustrated in **Figure 5.18**.

Table 5.4: Hydrogen-bond geometries of [Hf(diBrOx)$_4$]·3DMF (Hf_1e, (Å, ˚))

D-H...A	d (D-H)	d (H...A)	d (D...A)	D-H…A angle
C62—H62B···O5	0.96	2.577(2)	3.334(1)	136
C70—H70···O5	0.93	2.533(2)	3.406(1)	156
C72—H72A···O5	0.96	2.482(1)	3.411(1)	136
C42—H42···O6	0.96	2.448(2)	3.412(1)	163
C36—H36···O7	0.93	2.424(1)	3.185(1)	139
C60—H60···O7	0.93	2.497(1)	3.351(2)	152

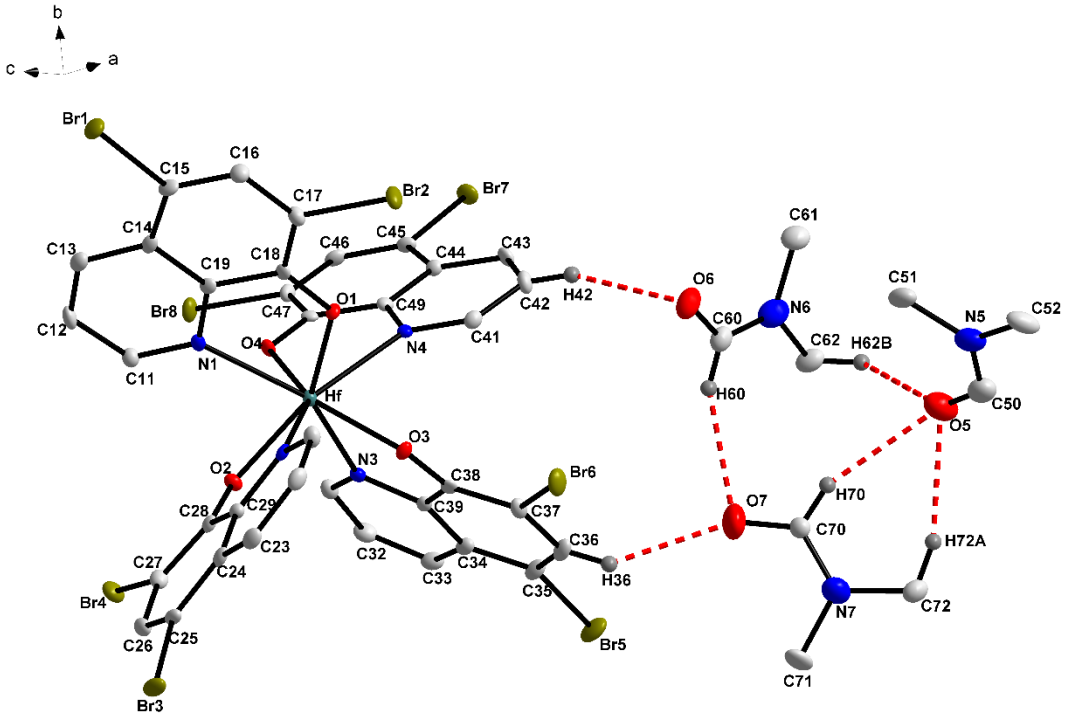

Figure 5.18: Partial structures [Hf(Ox)$_4$] (**Hf_1e**) indicating the C—H···O hydrogen bonding interaction observed in the unit cell (Hydrogen atoms omitted for clarity, 50% probability displacement ellipsoids).

5.6. Crystal Structure of Tetrakis(5,7-dilodoquinolin-8-olato-κ²N,O)-hafnium(IV) dimethylformamide solvate – [Hf(dilOx)₄]·C₃H₇NO

The structure of this *tetrakis*-coordinated hafnium – 5,7-dilodo-8-hydroxyquinoline complex (**Hf_1f**) is one of few examples of hafnium-oxine structures exhibiting two unique molecules in the asymmetric unit. Synthesis of **Hf_1f** and the resulting yellow plate-like crystals obtained for this was discussed in § 3.3.1.6.

The title compound, $[Hf(C_9H_4I_2NO)_4]\bullet 2(C_3H_7NO)$, where $C_9H_4I_2NO$ = 5,7-dilodo-8-hydroxyquinoline = $dilOx^-$ and C_3H_7NO = dimethylformamide = DMF), crystallises in the triclinic crystal system $P\bar{1}$ with two formula units per unit cell (Z=2). The asymmetric unit consists of two hafnium(IV) metal centres, each coordinated to four bidentate oxine ligands ($dilOx^-$). Two crystallographically independent DMF solvent molecules fill the rest of the asymmetric unit. A summary of the general crystal data is given in **Table 5.1**, while the numbering scheme of the complex is shown in the perspective drawing in **Figure 5.19**.

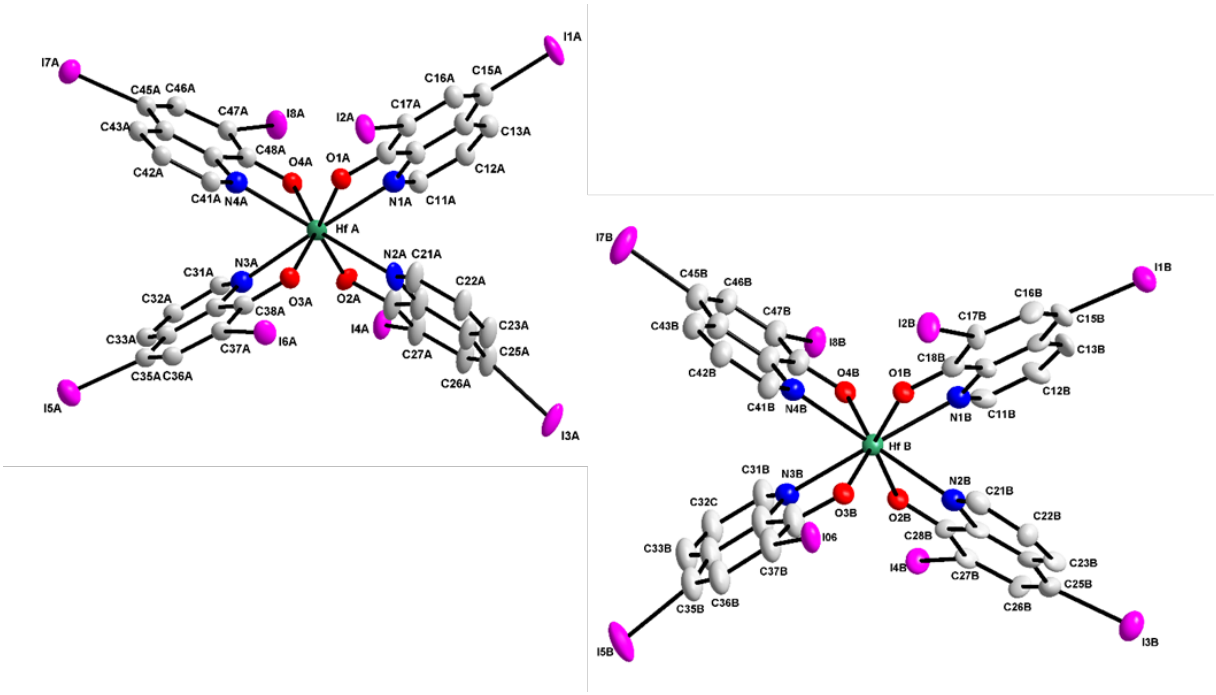

Figure 5.19: Representation of the title compound (**Hf_1f**), showing the numbering scheme and displacement ellipsoids. (*50% probability, solvent molecules and some hydrogen atoms omitted for clarity).*

Table 5.5 presents selected bond lengths and angles of the title compound. Atomic coordinates, anisotropic displacement parameters, bond distances and angles and hydrogen coordinates are given in the supplementary data (**Appendix A.6**).

Table 5.5: Selected geometry parameters of Hf(dilOx)$_4$] (Hf_1f).

Selected Bond Lengths (Å)					
Molecule	**A**	**B**	**Molecule**	**A**	**B**
Hf—O1	2.112(13)	2.099(9)	Hf—N1	2.370(14)	2.403(14)
Hf—O2	2.088(11)	2.110(10)	Hf—N2	2.407(13)	2.389(14)
Hf—O3	2.089(13)	2.084(11)	Hf—N3	2.401(14)	2.412(14)
Hf—O4	2.103(12)	2.109(10)	Hf—N4	2.408(14)	2.382(14)
C15—I1	2.09(2)	2.110(15)	C35— I5	2.111(15)	2.135(19)
C17— I2	2.09(2)	2.073(13)	C37— I6	2.111(14)	2.083(18)
C25— I3	2.194(19)	2.119(16)	C45— I7	2.106(15)	2.109(16)
C27— I4	2.076(18)	2.101(13)	C47— I8	2.098(15)	2.093(16)
Selected Bite Angles (°)					
O1—Hf—N1	69.7(5)	70.2(4)	N1—Hf—N3	146.0(5)	147.0(4)
O2—Hf—N2	70.4(4)	70.4(4)	N2—Hf—N4	147.3(5)	146.3(5)
O3—Hf—N3	70.9(5)	70.7(4)	O1—Hf—O3	83.4(5)	82.4(4)
O4—Hf—N4	70.0(5)	70.3(4)	O2—Hf—O4	82.7(5)	82.9(4)
Selected Torsion Angles (°)					
O1—C18—C19—N1	2.33 (28)	0.19 (20)	O3—C38—C39—N3	0.98 (20)	2.77 (26)
O2—C28—C29—N2	1.65 (27)	1.58 (20)	O4—C48—C49—N4	1.97 (20)	1.76 (23)
Selected Dihedral Angles of Anti-prism (°)					
Bending			**Twisting**		
[O1—N1—O4]—[O1—N4—O4]	1.63 (1)	1.62 (1)	[O1—Hf—O4]—[O2—Hf—O3]	45.02 (40)	45.50 (34)
[O2—N2—O3]—[O2—N3—O3]	0	0	[N1—Hf—N4]—[N2—Hf—N3]	38.92 (35)	38.88 (34)

For both molecules in the asymmetric unit, the central hafnium metal coordinates with the nitrogen and oxygen atoms of oxine ($dilOx^-$) ligands to form eight different six-membered metallacycle rings. Moreover, it is clear from **Figures 5.19** and **Figure 5.20** that each coordinated ligand, for the molecules, is duplicated by an opposite facing ligand by *ca*. 180° *rotation*, through the hafnium metal centre. Although these ligands do not lie in a flat plane opposite to one another, it is evident that these ligands are chelated to the metal centre with a ***two-fold rotated-isomer*** placement of the *N*- and *O*-coordinating sites. Thus, it yields average O—Hf—O and N—Hf—N bond angles of 82.85(6)° and 146.65(5)°, respectively (individual O—Hf—O and N—Hf—N bond angles are given in **Table 5.5**).

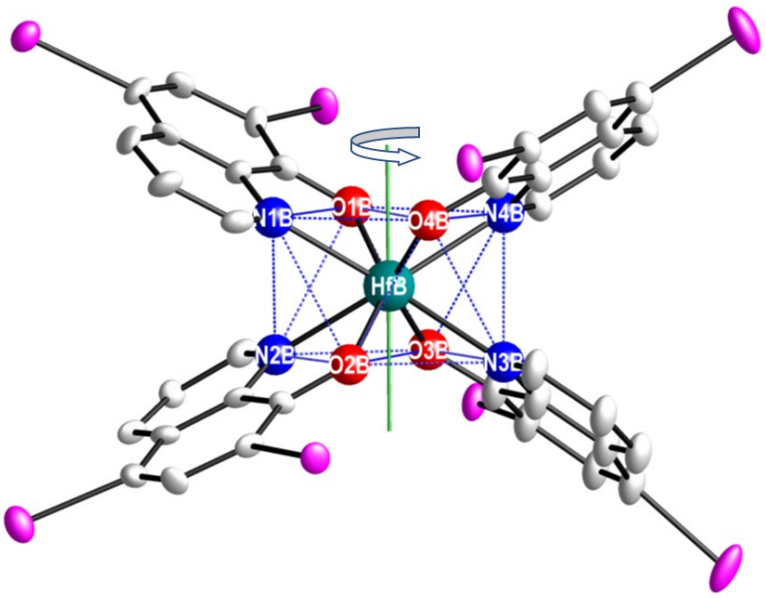

Figure 5.19: Graphical illustration of the ***two-fold rotated***-isomer of the oxine ligands across the metal centre in the title molecule (**A**) and (**B**) (**Hf_1f**, *hydrogens and solvent molecules omitted for clarity*). Only shown here is the two-fold rotation around the z-axis.

The dilOx-ligands lie around both metal centres in a space-filling, fan-like arrangement to give an approximate square-antiprismatic coordination polyhedron (**Figure 5.20**), with an almost negligible outward distortion towards dodecahedral geometry. Concerning the overall coordination description of the ligands as viewed in the square antiprism (**Figure 5.20 (a)**), the title compound crystallises as a ***D_2-corner-bonded*** isomer ((**Figure 5.20 (b)**)*.*

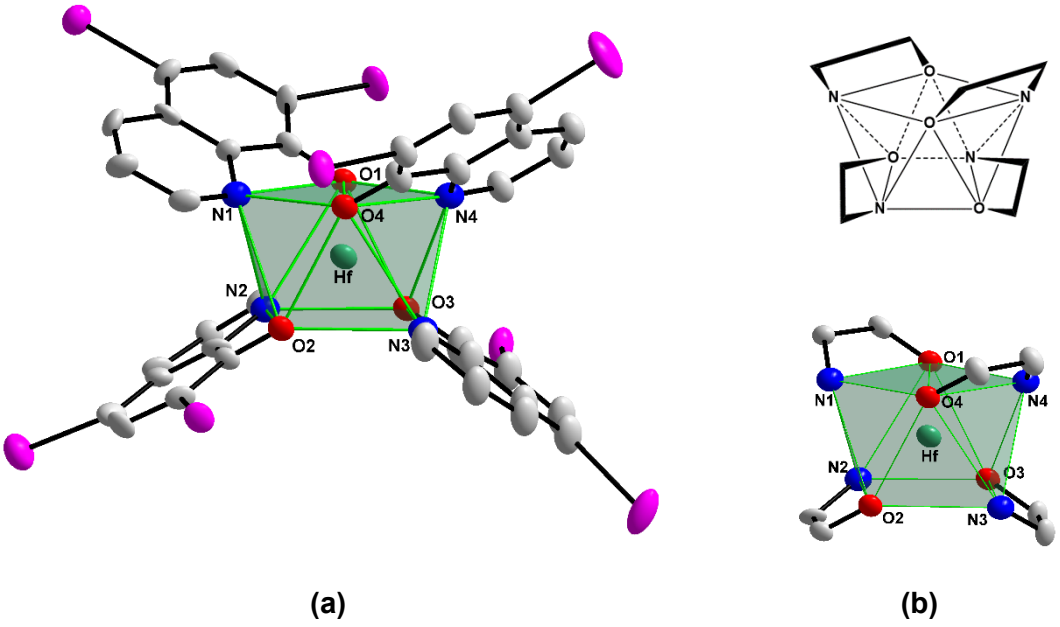

(a) **(b)**

Figure 5.20: **(a)** Graphic illustration of the square-antiprismatic coordination polyhedron of [Hf(dilOx)$_4$] (**Hf_1f**) (Solvent molecules and some carbon and hydrogen atoms omitted for clarity, 50% probability displacement ellipsoids). **(b)** Illustration of the typical ***D_2-corner-bonded*** square antiprismatic isomer.

This distortion from the ideal square antiprism is associated with an outward bend of the N_2O_2 bases, as illustrated in **Figure 5.21**. The dihedral angles between the yellow plane (N1—O1—O4) and the green plane **(**N4—O1—O4), indicative of a bending distortion, was measured as 1.625(3)° and 1.621(3)° for molecule A and and molecule B, respectively.

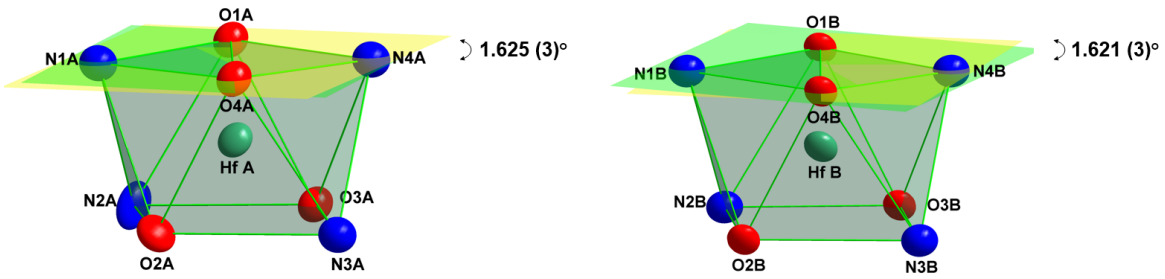

(a) **(b)**

Figure 5.21: A graphical representation of the outward bending observed in the antiprismatic coordination polyhedron surrounding the hafnium metal atoms (**(a) -** Hf A *&* **(b) -** Hf B) (*Solvent, C, H and I atoms are omitted for clarity*).

A further indication of distortion is the amount of rotation observed between the top and bottom N_2O_2 bases of the antiprismatic coordination polyhedron. Ideally, these angles should be 45°. Therefore, when viewing the coordination polyhedron from above, the dihedral angles between planes [O1—Hf—O4] & [O2—Hf—O3] and [N1—Hf—N4] & [N2—Hf—N3] was measured as 45.02(40)° and 38.92(35)° for molecule A and 45.50(34)° and 38.88(34)° for molecule B, respectively, indicating the rotation distortion observed within the coordination polyhedron (**Figure 5.22**).

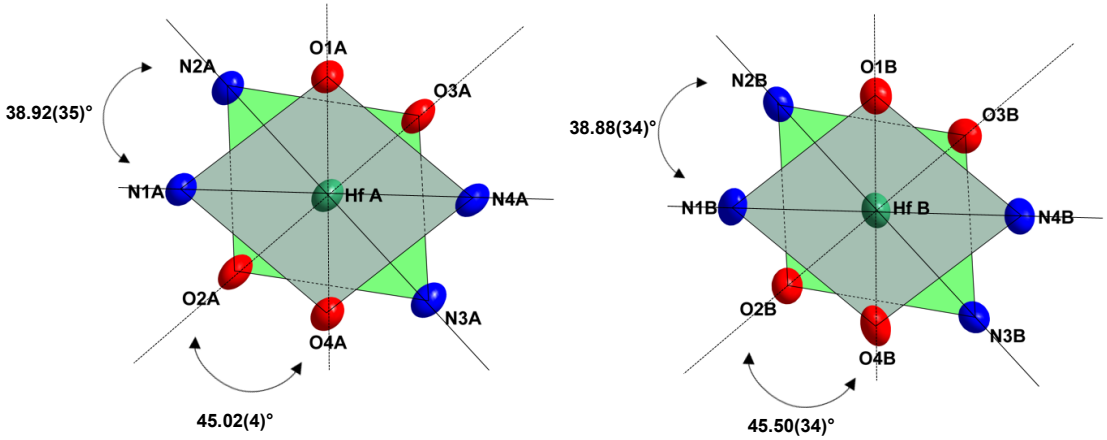

(a) **(b)**

Figure 5.22: A graphical representation of the top view of the antiprismatic coordination polyhedron indicting the rotation distortion observed in molecule A and B. (*Solvent, C, H and I atoms are omitted for clarity*).

The Hf—O and Hf—N bond lengths vary from 2.088(11) Å to 2.112(13) Å and 2.370(14) Å to 2.408(14) Å, respectively, and the O—Hf—N bite angles vary from 69.7(5)° to 70.9(5)°. The dihedral angles between the two phenyl rings of the quinoline ligands coordinated are all less than 1°, indicating little or negligible distortion due to coordination or packing. The solvate molecule seems to have no effects on the different Hf—O and H—N bond distances as they are all in the same magnitude as listed in **Table 5.3**. However, the dihedral angles formed between the metal coordination plane and the plane formed by the coordinated oxine ligands are measured at 8.08(3), 7.47(3), 10.71(3) and 8.53(3)° for structure A (**Figure 5.23(a)**), and 8.84(3), 10.33(3), 6.30(3) and 7.62(3)° for structure B (**Figure 5.23(b)**), respectively for ***Lig1***, ***Lig2***, ***Lig3*** and ***Lig4*** as shown below

.

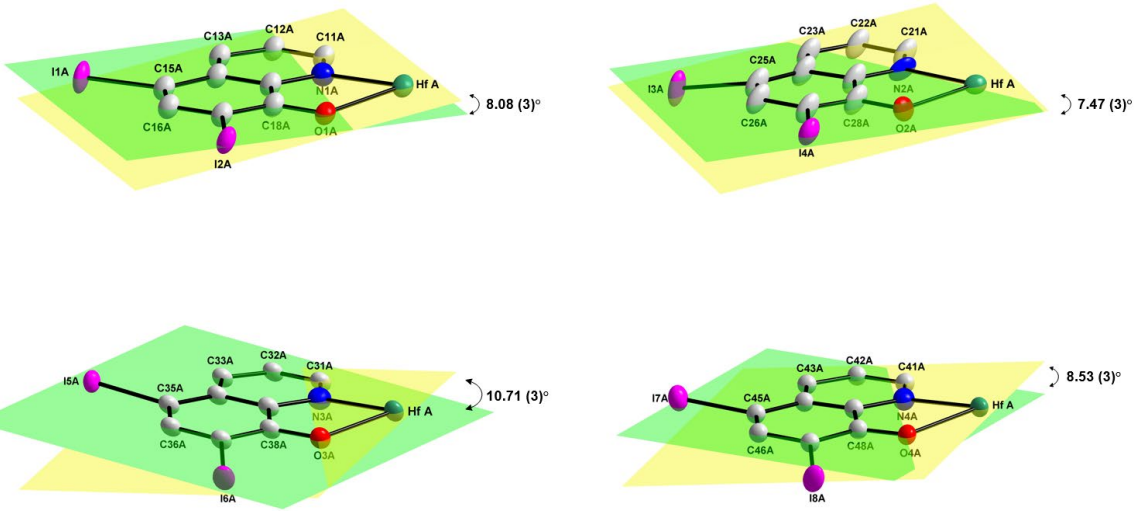

(a)

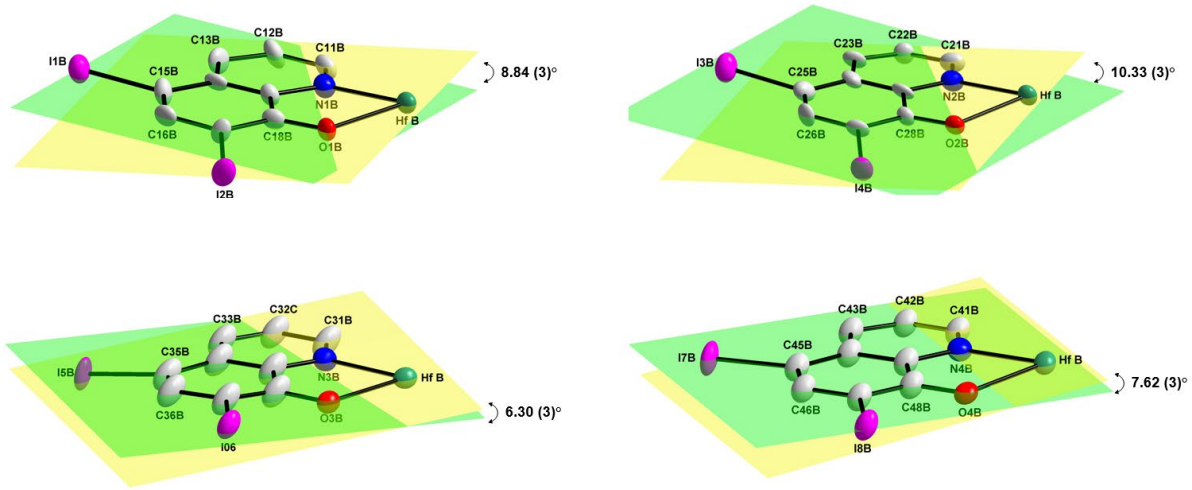

(b)

Figure 5.23: Partial structures of [Hf(diIOx)$_4$] showing graphical illustration of the dihedral angle between the metal coordination plane and the plane formed by the quinoline ligands (*Solvent and some carbon and hydrogen atoms omitted for clarity, 50% probability displacement ellipsoids*): **(a)** Molecule 1; **(b)** Molecule 2.

The solid-state crystal lattice packing is further stabilised by I···π interactions between iodine atoms ($I_{A/B}$) and pyridine rings of neighbouring molecules (**Table 5.6** and **Figure 5.24**). This tightly knit two-dimensional interaction network rigidly ties the crystal lattice together, influencing the overall packing in pairs of these two independent hafnium molecules dispersed in a head-to-tail packing fashion throughout the system when viewed along the *a*-axis (**Figure 5.25**). In other words, each of the crystallographically independent Hf-molecules interacts with one another in such a way as to form tandem pairs of metallic molecule units. No classical hydrogen bonding is found within the molecules (intramolecular interactions) or between neighbouring molecules (intermolecular interactions) in the unit cell.

Table 5.6: I•••π interactions bond geometry in the title compound (Hf_1f (Å, °)).

D-H...A	d (D-H)	d (H...A)	d (D...A)	D-H…A angle
C35A—I5A···*Py_{4B}	2.111(15)	3.567(1)	5.432(14)	145
C45A—I7A·· Py_{3B}	2.110(15)	3.581(1)	5.452(17)	145
C15B—I1B··· Py_{2A}	2.119(16)	3.586(1)	5.443(16)	143
C25—I3B··· Py_{1A}	2.106(15)	3.556(1)	5.407(16)	144

* *Py_{NX}: Py = pyridine ring*
N = Lig # (1-4)
X = Molecule A or B

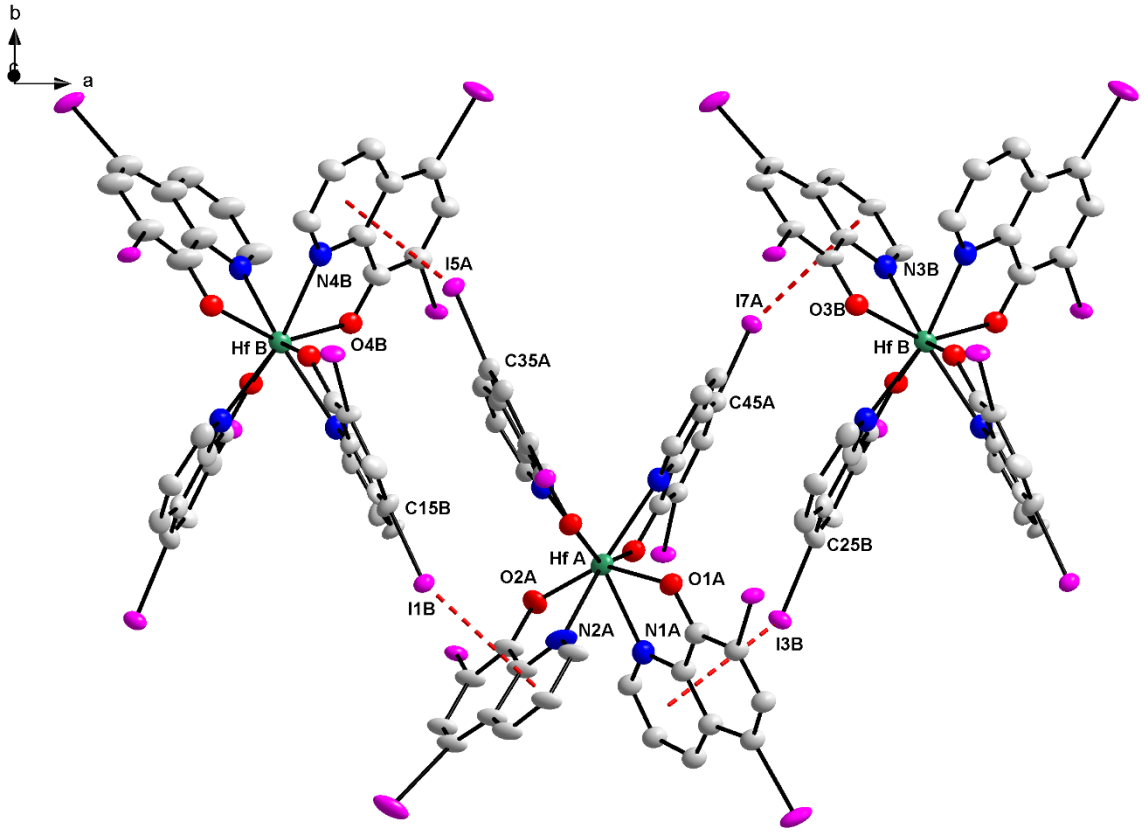

Figure 5.24: Graphical illustration depicting the paired I–π interactions between the pyridine rings of the dilOx Ligands (red dotted line) linking the entire crystal lattice into a tightly packed network. (Only necessary atoms are illustrated for the sake of clarity).

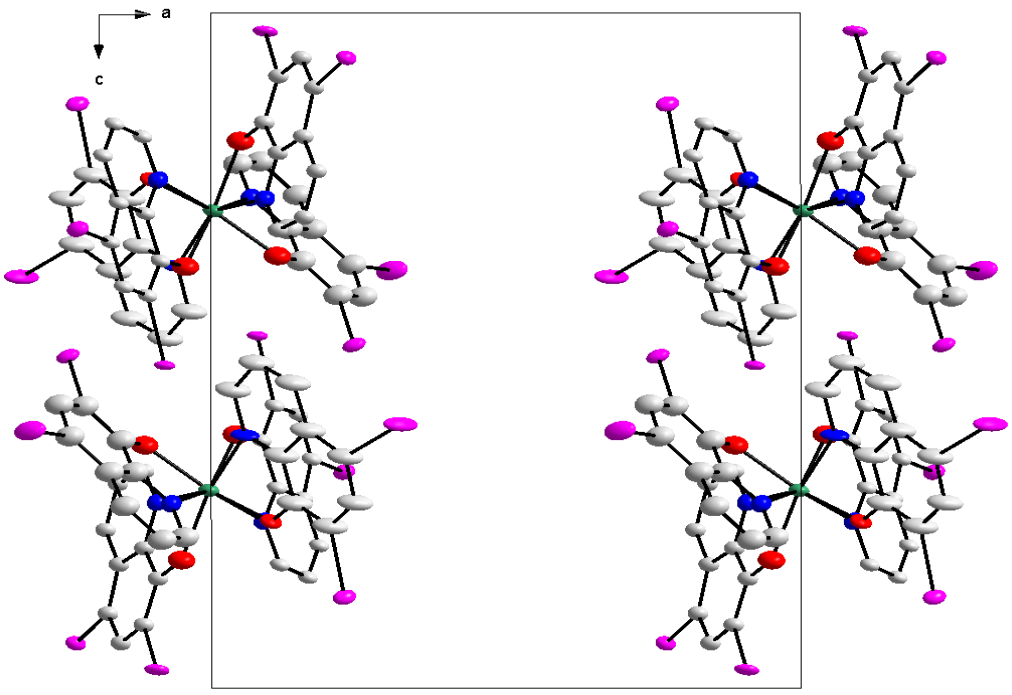

Figure 5.25: Graphical illustration of the head-to-tail packing found in the title compound (**Hf_1f**) along the *a*-axis.

5.7. Correlation of Structural Parameters for Compounds Hf_1d, Hf_1e and Hf_1f

Three additional Hf(IV)-*oxinato* complexes have been investigated and described thus far in the preceding sections (**Figure 5.26**). The general structural parameters, bond distances and angles from the various complexes are given in **Table 5.7**. As described in **Chapter 3**, these complexes' synthesis seems to afford these types of compounds with relative ease, reproducibly and with very high yields. An added advantage is that these complexes form rapidly, without any special manipulations needed, as described in previously published literature.[11] Therefore, this approach is much more cost-effective, environmentally friendly, and ideal to further a separation study.

[11] P. Kathirgamanathan, S. Surendrakumar, J. Antipan-Lara, S. Ravichandran, V .R. Reddy, S. Ganeshamurugan, M.Kumaraverl, V. Arkley, A. J. Blake & D. Bailey, *J. Mater. Chem. ,* **21,** 1762, 2011.

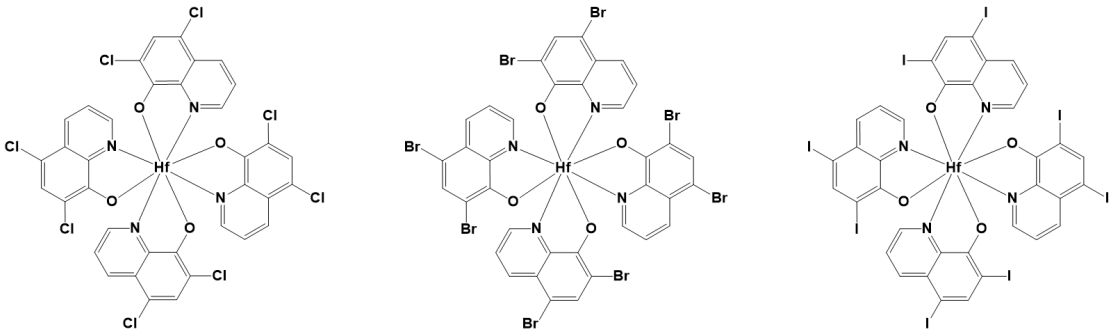

(a) **(b)** **(c)**

Figure 5.26: The three hafnium complexes discussed in this single crystal X-ray diffraction chapter. **(a)** [Hf(diClOx)$_4$] (**Hf_1d**), **(b)** [Hf(diBrOx)$_4$] (**Hf_1e**) and **(c)** [Hf(diIOx)$_4$] (**Hf_1f**).

In this chapter, three novel hafnium(IV) complex structures with different coordinated **oxine** ligands were presented. All three structures are very similar in relation to bond lengths and angles to other hafnium(IV)-oxine structure presented in Chapter 4 and found in literature.[11] In general, it is observed that *tetrakis*(oxinato)metal complexes do not show any particular preference towards a specific space group. However, with regards to the coordination environment around the metal centre, all the oxine complexes favour a square-antiprismatic geometry (***D$_2$-corner-clipped isomer***) with a minimal distortion towards dodecahedral geometry. Furthermore, the comparison of the data currently available, the average Hf—O and Hf—N bond lengths are 2.095(3) Å and 2.394(2) Å, respectively, with an average N—Hf—O bite angle of 70.61(8) °.

In this regard, a more detailed comparative relation study of these Hf(IV)-oxinato complexes and additional structures will be undertaken in **Chapter 8** and **Chapter 9**. Properties such as steric bulk and electronic properties of the Hf(IV)-oxinato complexes will be correlated to various aspects such as complex stability and structural effects.

Table 5.7: Unit cell and structure overview of presented Hf(IV)-oxinato complexes.

	[Hf(diClOx)]$_4$ •3DMF Hf_1d	[Hf(diBrOx)]$_4$ •3DMF Hf_1e	[Hf(diIOx)$_4$] •1DMF Hf_1f
Crystal Formula			
Crystal system	Monoclinic	Monoclinic	Triclinic
Space group	$P2_1/c$	$P2_1/c$	$P\bar{1}$
Square-antiprismatic Polyhedron			
Isomer	*D_2-corner clip*	*D_2-corner clip*	*D_2-corner clip*
Geometrical Isomer	*pseudo two-fold rotated*	*pseudo two-fold rotated*	*pseudo two-fold rotated*
Avg. bending distortion (°)	4.38(6)	5.10(5)	1.62(3)
Avg. rotation distortion (°)	47.34(9)	48.15(8)	41.97(9)
Selected Bond Lengths (Å)			
Hf—O1	2.101(1)	2.095(2)	2.106(12)
Hf—O2	2.104(1)	2.095(3)	2.099(13)
Hf—O3	2.102(1)	2.083(2)	2.087(13)
Hf—O4	2.087(1)	2.080(3)	2.106(12)
Hf—N1	2.395(2)	2.389(3)	2.387(15)
Hf—N2	2.377(2)	2.410(3)	2.398(15)
Hf—N3	2.382(3)	2.413(3)	2.407(14)
Hf—N4	2.389(2)	2.383(3)	2.395(15)
Bond Angles (°)			
O1—Hf—N1	70.71(2)	70.78(9)	69.95(5)
O2—Hf—N2	70.99(2)	70.66(9)	70.40(5)
O3—Hf—N3	70.80(2)	70.85(9)	70.80(5)
O4—Hf—N4	70.89(2)	70.30(8)	70.15(5)

5.8. Conclusion

In this chapter, three new hafnium(IV) structures with different halogenated coordinated 8-hydroxyquinoline ligands were presented, almost doubling the available pool of hafnium-oxinato single-crystal data. By considering all of the structural detail discussed, some conclusions are possible with regard to all these endeavours of identifying the solid-state properties of hafnium complexes containing oxine-ligands.

Firstly, as already discussed in **Chapter 4**, it is evident also from **Chapter 5**, thus from a total of six complexes studied, that *tetrakis*(oxinato)hafnium(IV) complexes prefer the square-antiprismatic coordination geometry in the ***D_2-corner*** clipped isomer form, or at least for all the complexes structurally characterised thus far.

Furthermore, all three structures are very similar with relation to bond lengths, angles and packing modes. All of the complexes display intermolecular interactions to some extent, with π-π- and halogen-π staking being most recurrent within the crystal lattices.

This chapter forms part of an overarching crystallographic investigation on various *N*- and *O*-donating multidentate ligands coordination to Hf(V) metal centres. A comprehensive discussion of all the complexes evaluated during this crystallographic study will be presented in **Chapter 8**, including the three structures presented in this chapter. In the following chapter, two hafnium-*β*-diketonato complexes are reported, structurally evaluated and described. A next focus will be placed on the influence of these types of ligands when increasing the metallocycle from five (oxines, **Chapters 4** and **5**) to six (**Chapter 6**), and using ligands containing different electron-donating *and* electron-withdrawing substituents on the ligand backbone with regards to coordination mode and coordination geometry of the obtained solid-state structures.

Chapter 6

X-Ray Diffraction Studies of Hafnium(IV) Complexes Containing Substituted Acetylacetone Ligands

---

6.1. Introduction

One of the main aims of this research project was to synthesise and characterise novel hafnium(IV) complexes (see Chapter 1) containing different L,L'-Bid ligands (L,L'-Bid = bidentate ligands with L, L' donor atoms). Various *O*,*O'* and *N*,*O* ligands were utilised to achieve the aim as was discussed previously in Chapter 3. An integral part of this project has been focused on utilising different commercially available acetylacetone (acacH) type ligands with various electron-withdrawing (CF_3-groups) and/or electron-donating (*phenyl*-groups) substituents on the 1 and 5 position of the ligand's backbone, as illustrated in **Figure 6.1**.

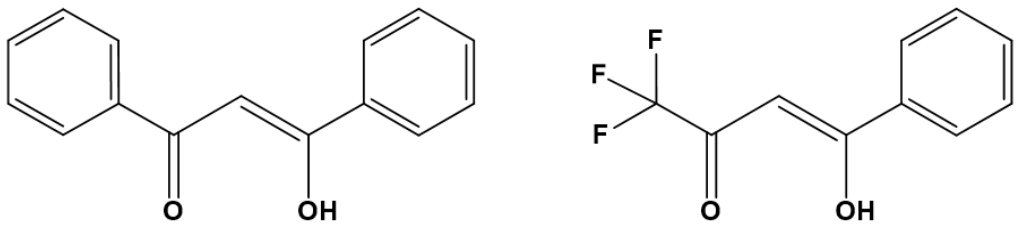

(a) **(b)**

Figure 6.1: *O,O'*-bidentate ligands chelated to hafnium(IV) and discussed in this chapter. **(a)** 1,3-diphenyl-1,3-propandione (dbmH / dibenzoylmethane, electron donating); **(b)** 4,4,4-trifluoro-1-phenyl-1,3-butanedione (tfbaH / benzoyltrifluoro-acetone, electron withdrawing)

These modifications on the ligand's backbone may possibly influence the electronic and steric properties of the final metal complexes, hafnium compared to zirconium, in such a way that it might be exploited as a novel extractive compound for the separation of hafnium and zirconium from solution.

This chapter contains a detailed discussion of the single-crystal structures of two hafnium(IV) complexes containing substituted acetylacetone (acacH) ligands as well as the correlation between these two structures (**Figure 6.2**). More in-depth correlations of each structure with similar hafnium structures from the literature will be discussed in **Chapter 8**.

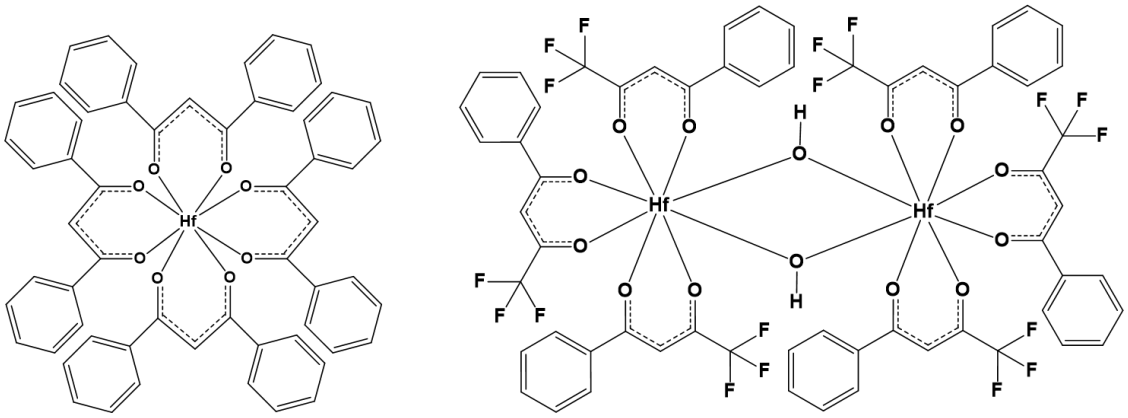

(a) **(b)**

Figure 6.2: The chelated hafnium complexes discussed in this single crystal X-ray diffraction chapter. (a) $[Hf(dbm)_4]$, (b) $[Hf(OH)(tfba)_3]_2$.

6.2. Experimental

The X-ray intensity data was collected on a Bruker X8 ApexII 4K Kappa CCD area detector diffractometer, equipped with a graphite monochromator and Mo$K\alpha$ fine-focus sealed tube (λ = 0.71069 Å, T = 100(2) K) operated at 2.0 kW (50 kV, 40 mA). The initial unit cell determinations and data collections were done by the SMART[1] software package. The collected frames were integrated using a narrow-frame integration algorithm and reduced with the Bruker SAINT-Plus and XPREP software packages[2] respectively. Analysis of the data showed no significant decay during the data collection. Data was corrected for absorption effects using the multi-scan technique SADABS,[3] and the structure was solved by the direct methods package SIR97[4] and refined using the WinGX[5] software incorporating SHELXL.[6] The final anisotropic full-matrix least-squares refinement was done on F^2. The methyl and aromatic protons were placed in geometrically idealised positions (C–H = 0.93 – 0.98 Å) and constrained to ride on their parent atoms with $U_{iso}(H) = 1.2U_{eq}(C)$. Non-hydrogen atoms were refined with anisotropic displacement parameters. The graphics were obtained with the DIAMOND[7] program with 50% probability ellipsoids for all non-hydrogen atoms.

A summary of the general crystal data and refinement parameters are given in **Table 6.1** for both structures. Supplementary data for the atomic coordinates, anisotropic displacement parameters, all bond distances and angles and hydrogen coordinates are given in the **Appendix B** for each individual dataset.

---

[1]Bruker SMART-NT Version 5.050.Bruker AXS Inc. Area-Detector Software Package; Madison, WI, USA, 1998.

[2]Bruker SAINT-Plus Version 6.02 (including XPREP), Bruker AXS Inc. Area-Detector Integration Software, Madison, WI, USA, 1999.

[3]Bruker SADABS Version 2004/1.Bruker AXS Inc. Area Detector Absorption Correction Software, Madison, WI, USA, 1998.

[4] A. Altomare, M. C. Burla, M. Camalli, G. L. Cascarano, C. Giacovazzo, A. Guagliardi, A .G. G. Moliterni, G. Polidori & R. Spagna, *J. Appl. Cryst.,* **32**, 115, 1999.

[5] L. J. Farrugia, *J. Appl. Cryst.,* **32,** 837, 1999.

[6]G. M. Sheldrick; SHELXL97. Program for crystal structure refinement, University of Göttingen, Germany, 1997.

[7] K. Brandenburg & H. Putz; DIAMOND, Release 3.0e, Crystal Impact GbR, Bonn, Germany, 2006.

Table 6.1: Crystallographic and refinement details for structures discussed in this chapter.

Compound	$[Hf(dbm)_4]$	$[Hf(OH)(tfba)_3]_2 \cdot 2DMF$
Formula weight	1071.44	1828.08
Crystal system	Monoclinic	Monoclinic
Space group	$P2_1/c$	$P2_1/c$
Unit cell dimensions: ***a,*** ***b,*** ***c* (Å)**	 24.846(2), 10.224(1), 19.316(1)	 12.414(1), 19.244(5), 17.503(5)
α, ***β,*** ***γ* (°)**	90, 101.62(1), 90	90, 122.94(1), 90
Volume (Å^3) / *Z*	4805.8(5) / 4	3509(2) / 2
Density (calculated) (mg/m^3)	1.481	1.730
Absorption coefficient (mm^{-1})	2.229	3.071
F(000)	2160	1792
Crystal size (mm)	0.20 x 0.19 x 0.11	0.28 x 0.23 x 0.21
Theta range for data collection (°)	0.84 to 28.00	2.97 to 28.33
Index ranges	-23<=h<=32, -11<=k<=13, -25<=l<=24	-16 <= h <= 16, -25 <=k<= 25, -23 <= l <= 22
Reflections collected	11555	41903
Independent reflections/R_{int}	11555 [R_{int} = 0.0360]	8726 [R_{int} = 0.0496]
Completeness (θ = 28.35°) (%)	99.50	99.60
Refinement method	Full-matrix least-squares on F^2	Full-matrix least-squares on F^2
Data / restraints / parameters	11555 / 0 / 623	8726 / 1* / 475
Goodness of fit on F^2	1.158	1.030
Final R indices [I>2sigma(I)]	R_1 = 0.0374, wR_2 = 0.0950	R_1 = 0.0303, wR_2 = 0.0653
R indices (all data)	R_1 = 0.0531 wR_2 = 0.1218	R_1 = 0.0467 wR_2 = 0.0716
Largest diff. peak and hole (e.Å^{-3})	1.17 and -1.29	1.32 and -0.97

* H atoms treated by a mixture of independent and constrained refinement.

6.3. General Considerations for Chapter 6

Note: The following general considerations are used throughout the text below, which enables a systematic comparison and standardised geometry for the complexes as discussed. It is further important to take into account that although the symmetry elements are formally defined as “inversion centres”, “rotation axes”, “mirror planes”, etc., these are all to be considered “pseudo” elements, since they all describe solid-state observations.

- Each independent acac ligand coordinated to the metal centre is numbered consecutively and abbreviated to "Lig #" with # = 1 - 4 (**Figure 6.3)**).

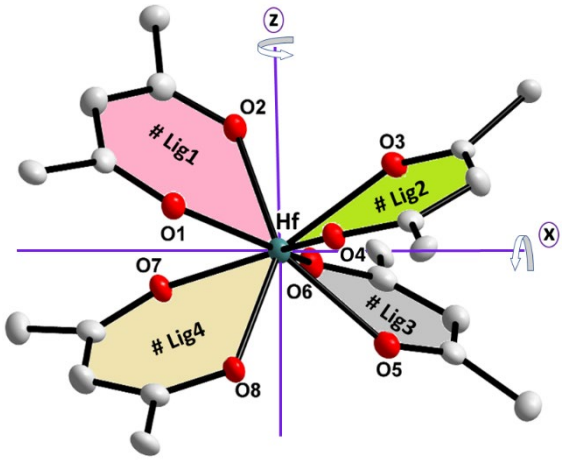

Figure 6.3: (a) General acac ligand abbreviation of mononuclear *tetrakis* acac-coordinated hafnium(IV) complex, also showing potential two-fold rotation axes.

As discussed earlier in Chapter 2 (§ 2.5), most hafnium and zirconium complexes, containing bidentate ligands adopt square-antiprismatic coordination geometries around the metal centres. It was also noted that this geometry exhibits three possible stereo-isomers, specifically for metal complexes containing symmetrical bidentate ligands like acetylacetone. The possible isomers, **(a)** ***D_2-corner-clipped*** ligand placement; **(b)** ***D_4-side-clipped*** coordination and **(c)** ***C_2-isomer*** which is a combination of ***D_2*** -and ***D_4*** isomers, is illustrated in **Figure 6.4.**

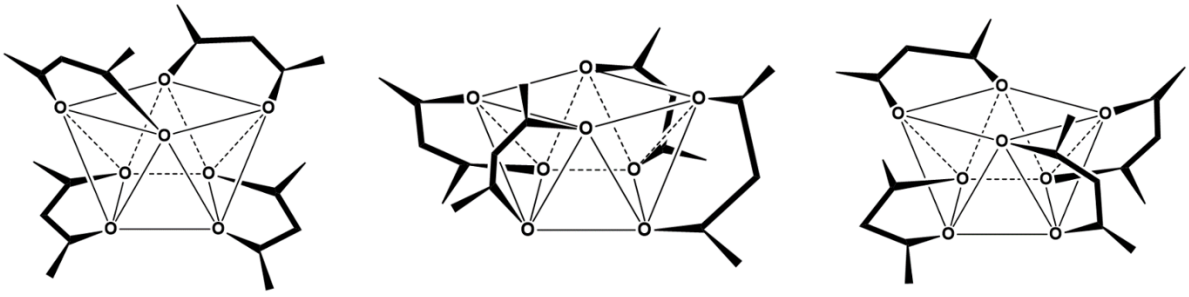

(a) **(b)** **(c)**

Figure 6.4: Coordination isomers as defined for *tetrakis*(*β*-diketone)metal complexes exhibiting a square antiprismatic coordination polyhedron. **(a)** D_2-corner-clipped ligands; **(b)** D_4-side-clipped ligands; **(c)** C_2-combination of corner- and side-clipped ligands.

6.4. Crystal Structure of Tetrakis(1,3-diphenyl-1,3-propane dionato)hafnium(IV) – [Hf(dbm)$_4$] [8]

The title compound (**Hf_2c**) *tetrakis(1,3-diphenyl-1,3-propanedionato)*, crystallises in the monoclinic space group, $P2_1/c$ with four formula units per unit cell (Z=4). The asymmetric unit consists of a Hf(IV) metal centre coordinated to four unique bidentate, oxygen donating ligands, dibenzoylmethane (dbmH) ligands. No solvent molecule is present in the crystal lattice, even though the compound was synthesised and crystallised in toluene. Synthesis of **Hf_2c** and the resulting colourless cubic-like crystals obtained for this was discussed in § 3.3.2.3. A summary of the general crystal data is given in **Table 6.1**, while the numbering scheme of the complex is shown in the perspective drawing in **Figure 6.5**. **Table 6.2** presents selected bond lengths and angles of the title compound. Atomic coordinates, anisotropic displacement parameters, all bond distances and angles and hydrogen coordinates, are given in the supplementary data (**Appendix B.1**). Hydrogen atoms and/or solvent molecules are omitted in some molecular presentations for clarity.

[8] J. A. Viljoen, H. G. Visser & A. Roodt, *Acta Cryst*., **E66**, m1053, 2010.

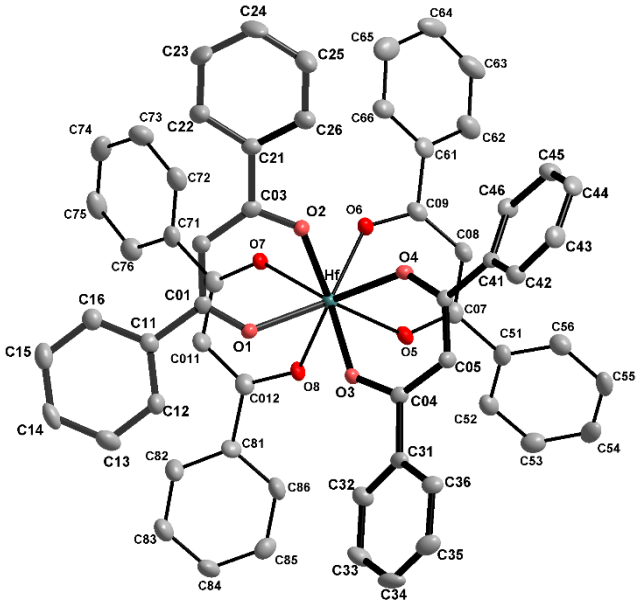

Figure 6.5: Representation of the title compound (**Hf_2c**), showing the numbering scheme and displacement ellipsoids *(50 % probability, hydrogen atoms omitted for clarity*).

The hafnium metal centre, in which the four 1,3-diphenyl-1,3-propanedionato ligands are fan-like arranged around the metal centre produces a square antiprismatic coordination polyhedron, with a small distortion towards dodecahedral geometry.

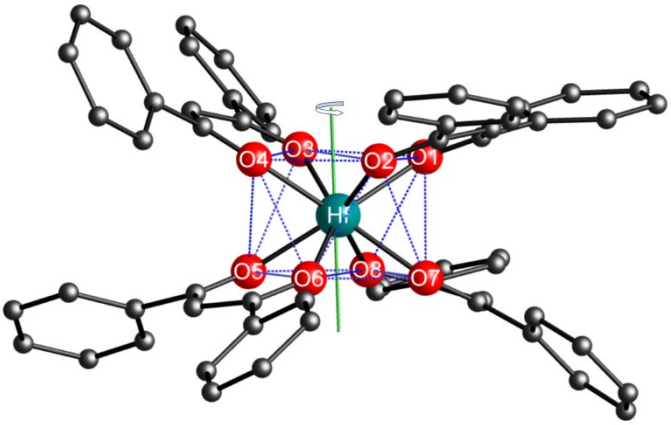

Figure 6.6: Graphical illustration of the ***pseudo two-fold rotated*** isomer of the dbm ligands across the metal centre in the **Hf_2c** title molecule (*Hydrogen atoms and solvent molecules omitted for clarity*). When compared to **Figure 6.3**, the principal rotation axis is considered to be approximately perpendicular to the top/bottom planes of the square antiprism, i.e., along the *z*-axis.

Table 6.2: Selected bond distances, angles and torsion angles of Hf(dbm)$_4$] (Hf_2c).

Selected Bond Lengths (Å)			
Hf—O1	2.197(3)	C01—C11	1.503(5)
Hf—O2	2.142(3)	C03—C21	1.482(6)
Hf—O3	2.133(2)	C04—C31	1.501(5)
Hf—O4	2.200(2)	C06—C41	1.495(5)
Hf—O5	2.180(3)	C07—C51	1.496(5)
Hf—O6	2.154(2)	C09—C61	1.503(5)
Hf—O7	2.189(2)	C010—C71	1.500(6)
Hf—O8	2.154(2)	C012—C81	1.496(5)
Selected Bite Angles (°)			
O1—Hf—O2	74.45(10)	O1—Hf—O5	140.72(10)
O3—Hf—O4	75.02(9)	O2—Hf—O6	77.42(10)
O5—Hf—O6	74.71(10)	O3—Hf—O8	79.05(10)
O7—Hf—O8	74.79(9)	O4—Hf—O7	138.39(9)
Selected Torsion Angles (°)			
O1—C01—C03—O2	1.12(3)	O5—C07—C09—O6	1.32(3)
O3—C04—C06—O4	-4.86(3)	O7—C010—C012—O8	-10.46(3)
Selected Dihedral Angles within the Anti-prism (°)			
Bending distortion			
[O1—O2—O3] — [O4—O2—O3]	3.65(1)	[O8—O5—O7] — [O6—O5—O7]	0.74(1)
Rotation distortion			
[O1—Hf—O4] [O6—Hf—O8]	44.19(9)	[O5—Hf—O7] — [O2—Hf—O3]	43.97(8)

With regard to the overall coordination description of the ligands as viewed in the square antiprism (**Figure 6.6**. and **Figure 6.7(a)**), the title compound ([Hf(dbm)$_4$], **Hf_2c**) crystallises as a ***D_2-corner-bonded isomer*** (**Figure 6.7(b)**)***.***

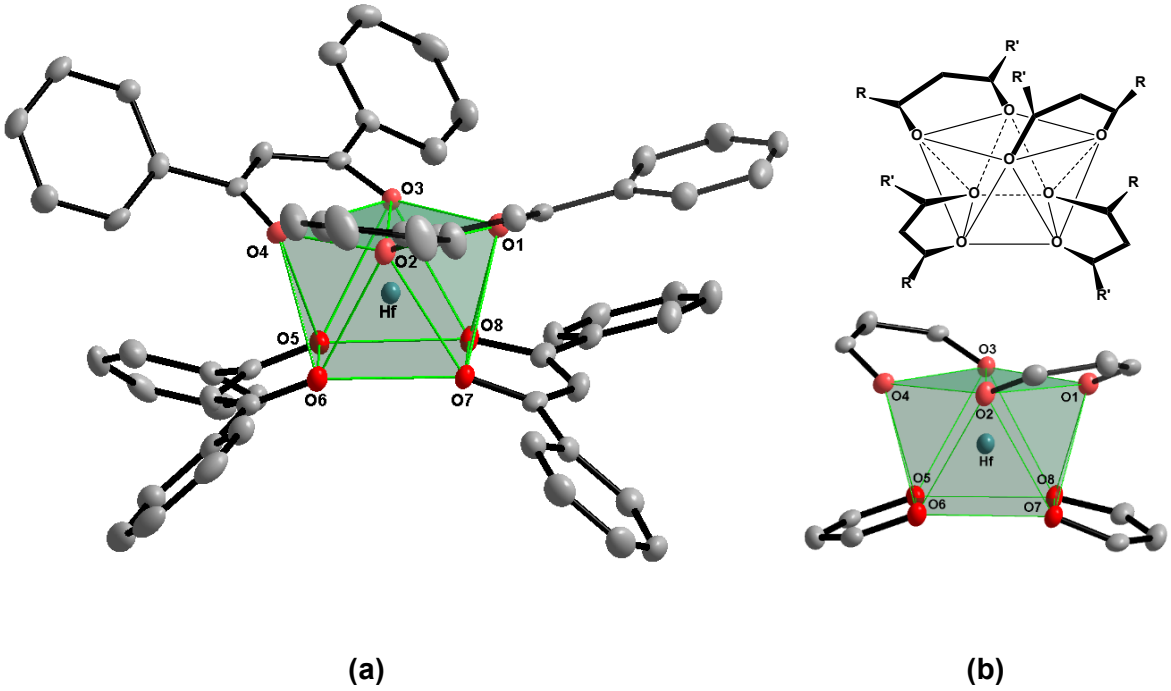

(a) **(b)**

Figure 6.7: (a) Graphic illustration of the square-antiprismatic coordination polyhedron of [Hf(dbm)$_4$] (**Hf_2c**) (Hydrogen atoms omitted for clarity, 50% probability displacement ellipsoids). **(b)** Illustration of the typical D_2-corner-bonded square antiprismatic isomer.

In order to define the total distortion at the metal centre, two orientations for the metal complex are considered, as shown in **Figure 6.8** to allow the evaluation of the geometric parameters from the different planes; see **(a)** and **(b).** The orientations allow the consideration of the relative distortions on the identified sets of two planes describing the "top" and the "base" of the complex.

Therefore, the dihedral angles between the green (O1—O2—O3 and O8—O5—O7), and yellow planes **(**O4—O2—O3 and O6—O5—O7), are illustrated in **Figure 6.8**, indicative of a ***bending distortion***, measured as 3.65(9)° and 0.74(1)°, respectively for the top and bottom two sets of *O,O* donor atoms describing the coordination polyhedron.

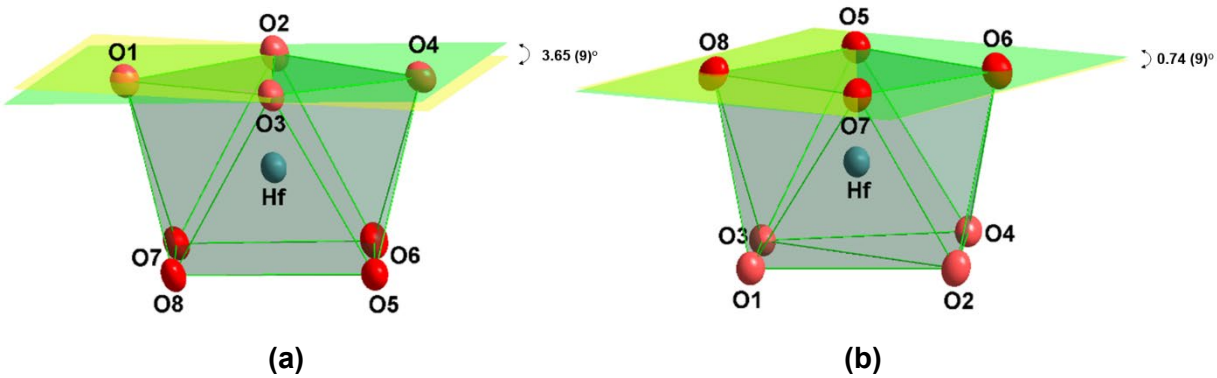

Figure 6.8: A graphical representation of the bending distortion (observed from the dihedral panes) in the antiprismatic coordination polyhedron surrounding the hafnium metal atom (*C and H atoms are omitted for clarity*).

A further indication of the distortion within the **Hf_2c** complex is observed from the amount of rotation observed between the two sets of *O,O* donor atoms describing the antiprismatic coordination polyhedron. Therefore, when viewing the coordination polyhedron from above, the dihedral angles between planes ([O1—Hf—O4] and [O8—Hf—O6]) and ([O5—Hf—O7] and [O2—Hf—O3]) were measured as 44.19(9)° and 43.97(8)°, respectively, signifying the rotation distortion observed (**Figure 6.9**). Ideally, these angles should be 45°.

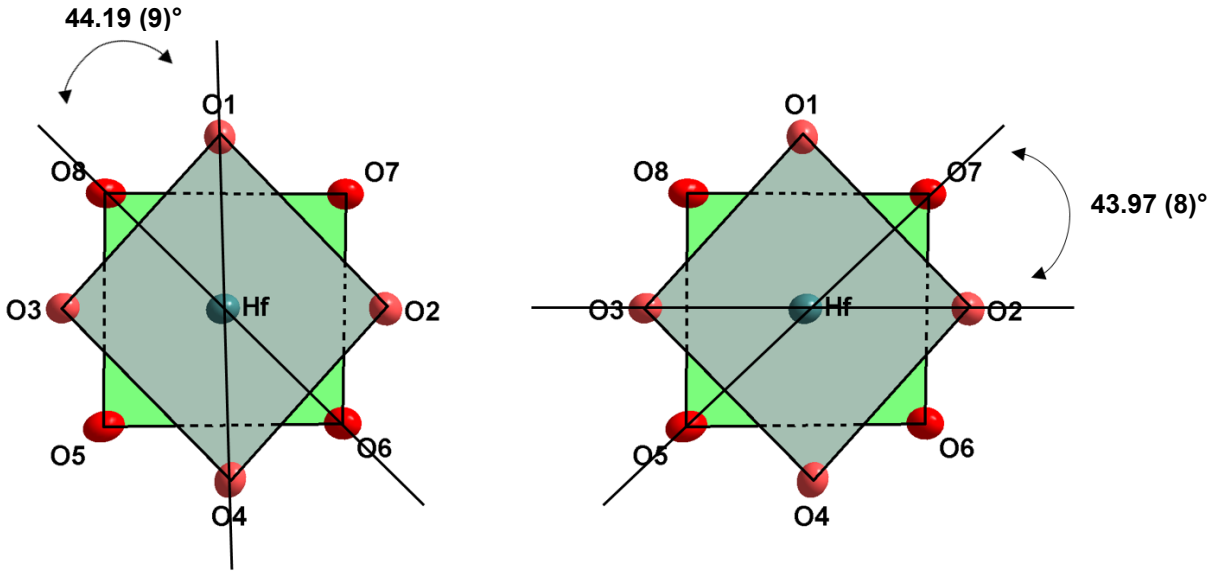

Figure 6.9: A graphical representation of the top view of the antiprismatic coordination polyhedron indicting the rotation distortion observed in **Hf_2C**. (C and H atoms are omitted for clarity).

The Hf—O bond lengths vary from 2.133(2) Å to 2.200(2) Å, with the average Hf—O distance being 2.169(3) Å. This average Hf—O bond distance is somewhat larger than the average of 2.159(5) Å obtained from the Cambridge Structural Database[9] (Groom *et al.*, (2016), data extracted from 22 hits, yielding 60 observations ranging from 2.079 to 2.262 Å). The O—Hf—O bite angles vary between 74.45(10) and 75.02(9)° (**Table 6.2**).

A noteworthy characteristic of the hafnium metal centre is observed in this structure, in that it distorts the backbone of the bidentate (acac-type) ligands from its preferred coordination geometry of ca. 180° towards a highly distorted bent-like geometry to accommodate the overall polyhedron geometry around the metal centre. (**Figure 6.10**). In **Hf_2c** the dihedral angles between the metal coordination plane (O—Hf—O) and the plane formed by the ligands backbone (O—C—C—C—O) ranges from 16.2(1) to 24.6(1)° (**Table 6.3**)

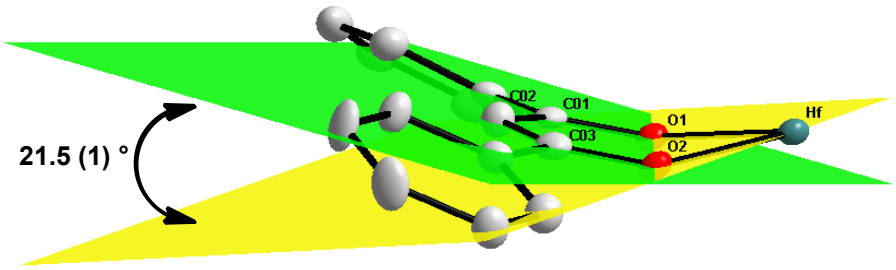

Figure 6.10: Partial structures of [Hf(dbm)4] (**Hf_2c**) graphically illustrating the dihedral angle between the metal coordination plane and the plane formed by ***Lig1*** (Hydrogen atoms omitted for clarity, 50% probability displacement ellipsoids).

[9] Cambridge Structural Database (CSD) Version 5.42, November 2020 update. C. R. Groom, I. J. Bruno, M. P. Lightfoot & S. C. Ward, *Acta Cryst.*, **B72**, 171, 2016.

These *dbm*-ligands are not only bent but also slightly twisted due to the extreme constraints exerted on them. All relevant torsion angles concerning these disorders are listed in **Table 6.2.**

Furthermore, the angle at which each phenyl pair are swivelled away from each other over the *β*-diketone backbone plane ranges from 120.25(2) to 158.77(1)° (**Table 6.3**). This planar swivelling found for each individual phenyl ring is directly related to the way the crystal lattice packing is arranged, as described below.

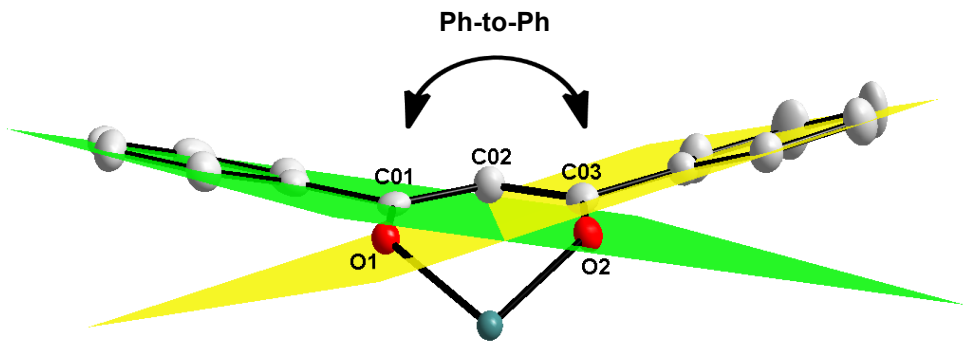

Figure 6.11: Partial structure of $[Hf(dbm)_4]$ (**Hf_2c**) illustrating phenyl-to-phenyl plane swivel observed in the dbm ligand structure.

There are no classical hydrogen bonds observed in this structure, however the molecules pack in horizontal layers along the *bc*-plane and are stabilised by weak C—H···O interactions. The bond distances and angles for all the hydrogen bonds are given in **Table 6.4** and illustrated in **Figure 6.12**. Molecules in the unit cell pack in a "head-to-tail" fashion when viewed along the *b*-axis (**Figure 6.13**)

Table 6.3: Selected dihedral angles for phenyl swivelling on individual dbm ligands as observed in the title compound (Hf_2c).

Atoms in plane	Atoms in plane	Dihedral Angles (°)
O1—Hf—O2	O1—C01—C02—C03—O2	21.5(1)
O3— Hf —O4	O3—C04—C05—C06—O4	16.2(1)
O5— Hf —O6	O5—C07—C08—C09—O6	22.7(2)
O7— Hf —O8	O7—C10—C11—C12—O8	24.6(1)
Atoms in ring	**Atoms in ring**	**Dihedral Angles (°)**
C11 — — C16	C21 — — C26	154.10(1)
C31 — — C36	C41 — — C46	158.77(1)
C51 — — C56	C61 — — C66	120.25(2)
C71 — — C76	C81 — — C86	123.48(1)

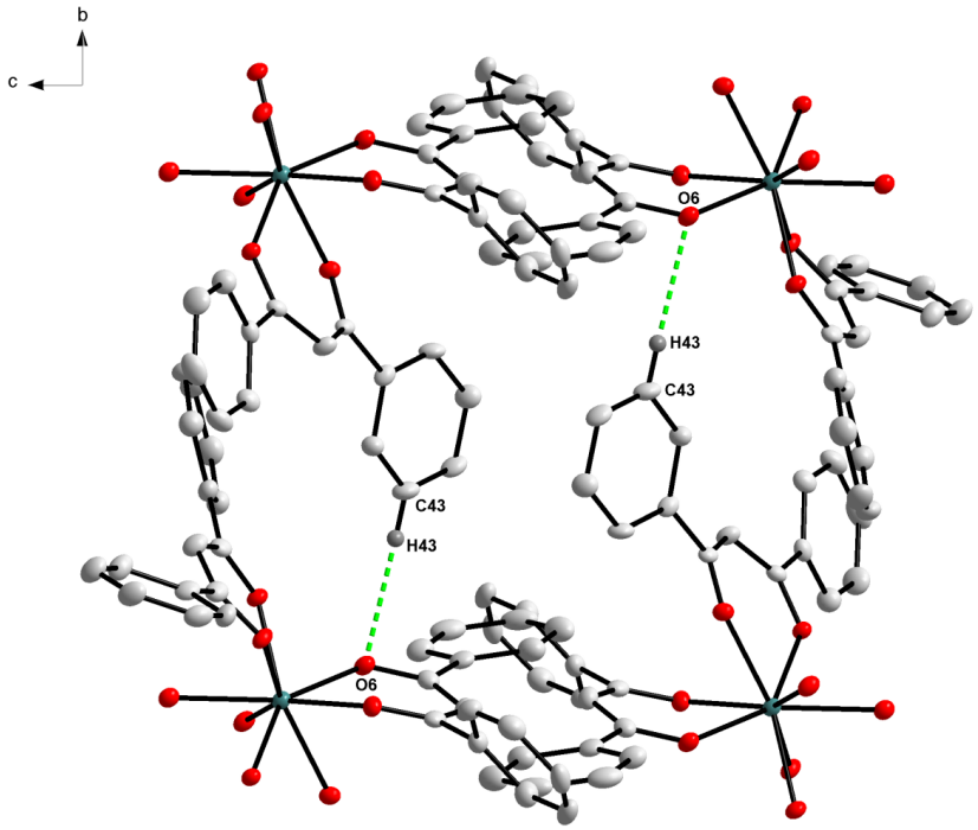

Figure 6.12: Partial structures [Hf(dbm)$_4$] (**Hf_2c**) indicating the C—H···O hydrogen bonding interaction observed in the unit cell (Non-interacting molecule portions and hydrogens omitted for clarity, 50% probability displacement ellipsoids).

Table 6.4: Hydrogen-bond geometry for [Hf(dbm)$_4$] (Hf_2c) (Å, ˚)

D—H···A	d(D—H)	d(H···A)	d(D···A)	D—H···A
C43—H43···O6^{i}	0.95	2.6	3.538(5)	169.5

***Symmetry code**: (i) x, y+1, z.*

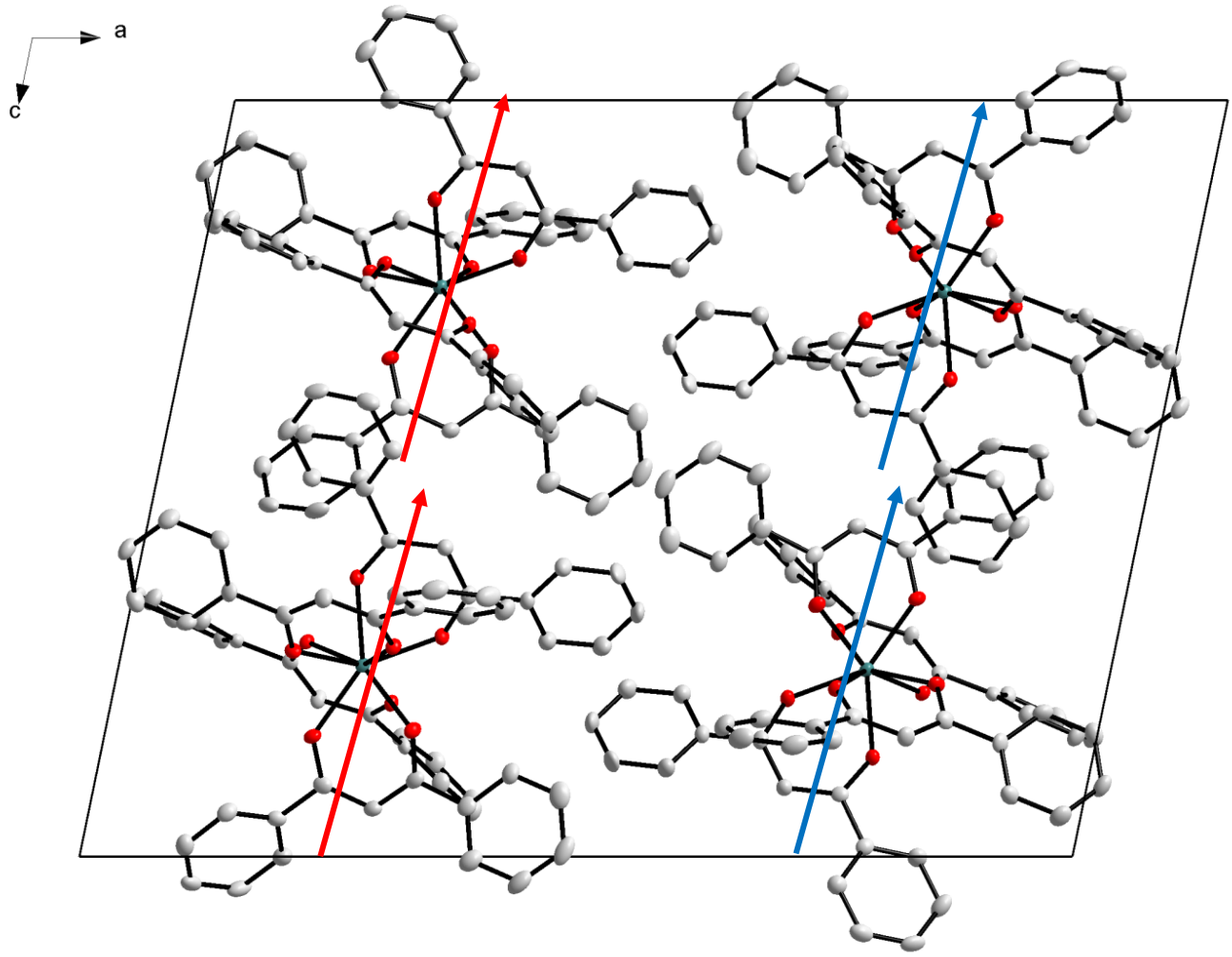

Figure 6.13: Graphical representation of molecular packing within the unit cell for the title compound (**Hf_2c**) viewed along the *b*-axis, showing "*head-to-tail*" packing along the *c-axis* (arrow direction). Hydrogen atoms omitted for clarity, 50% probability displacement ellipsoids.

6.5. Crystal Structure of Di-μ-hydroxido-bis[tris(4,4,4-trifluoro-1-phenyl-acetylacetonato-κ²-O,O')-hafnium(IV) dimethylformamide disolvate - [Hf(OH)(tfba)₃]₂·2(DMF) [10]

The title compound (**Hf_2b**) Di-*μ*-hydroxido-bis[tris(4,4,4-trifluoro-1-phenyl-acetylacetonato-κ^2-O,O')-hafnium(IV) dimethylformamide disolvate, crystallises in the monoclinic space group, $P2_1/c$ with two formula units per unit cell ($Z = 2$). The binuclear title compound, $[Hf(OH)(tfba)_3]_2 \cdot 2(C_3H_7NO)$, where $tfba^-$ = $CF_3C(O)CHC(O)C_6H_6$ and DMF = (C_3H_7NO)), lies across an inversion centre and contains a Hf(IV) atom which is eight coordinated and surrounded by three chelating *β*-diketonato $tfba^-$ ligands and two bridging OH-groups, thereby adopting a slightly distorted anti-prismatic coordination geometry.

Synthesis of **Hf_2b** and the resulting colourless crystals obtained for this was discussed in § 3.3.2.2. A summary of the general crystal data is given in **Table 6.1**, while the numbering scheme of the complex is shown in the perspective drawing in **Figure 6.14**. **Table 6.5** presents selected bond lengths and angles of the title compound. Atomic coordinates, anisotropic displacement parameters, all bond distances and angles and hydrogen coordinates, are given in the supplementary data (**Appendix B.2**). Hydrogen atoms and/or solvent molecules are omitted in some molecular presentations for clarity.

[10] J. A. Viljoen, H. G. Visser & A. Roodt. *Acta Cryst*., **E67**, m1822, 2011.

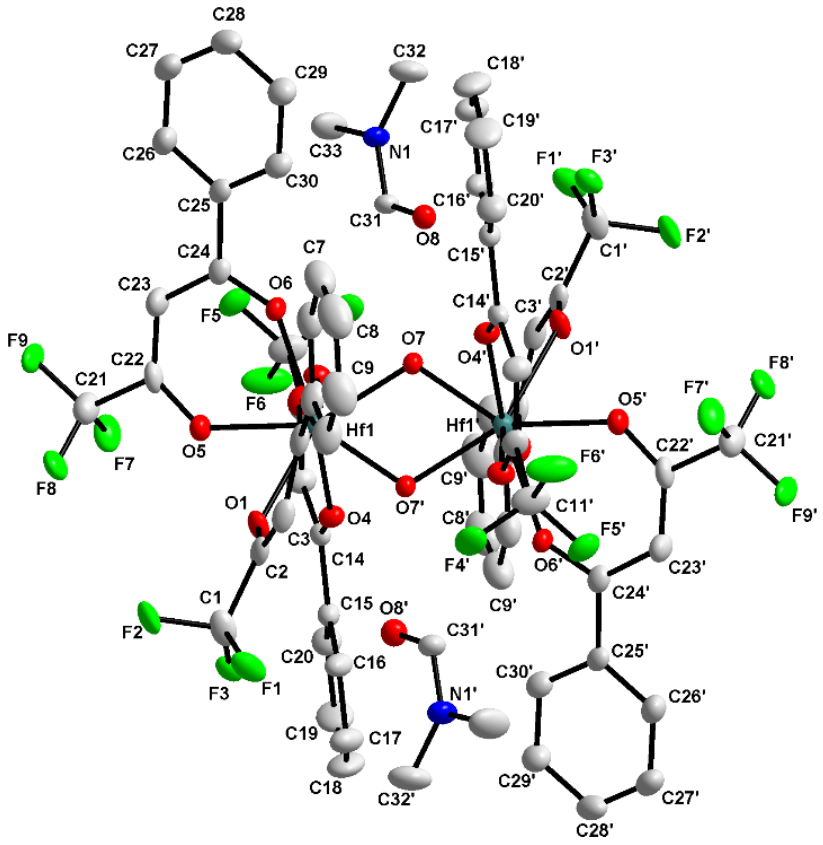

Figure 6.14: Representation of the title compound $[Hf(OH)(tfba)_3]_2 \cdot 2(C_3H_7NO)$, (**Hf_2b**), showing the numbering scheme and displacement ellipsoids (50 % probability, hydrogen atoms omitted for clarity).

Table 6.5: Selected bond distances, angles and torsion angles of $[Hf(OH)(tfba)_3]_2$ (Hf_2b) [Å and °].

Selected Bond Lengths (Å)			
Hf—O1	2.232(2)	Hf—Hf’	3.495(8)
Hf—O2	2.167(2)	C1—C2	1.529(5)
Hf—O3	2.244(2)	C4—C5	1.493(5)
Hf—O4	2.146(2)	C11—C12	1.535(5)
Hf—O5	2.170(2)	C14—C15	1.484(5)
Hf—O6	2.207(2)	C21—C22	1.592(5)
Hf—O7	2.073(2)	C24—C25	1.492(5)
Hf—O7'	2.135(2)		
Selected Bite Angles (°)			
O1—Hf—O2	74.69(9)	O7—Hf—O7’	67.11(11)
O3—Hf—O4	73.49(9)	Hf—O7—Hf'	112.34(11)
O5—Hf—O6	75.60(9)		
Selected Torsion Angles (°)			
O1—C2—C4—O2	2.46(32)	O5—C22—C24—O6	5.52(32)
O3—C12—C14—O4	3.87(31)	Hf—O7—Hf’—O7'	0
Selected Dihedral Angles within the Anti-prism (°)			
Bending distortion			
[O1—O2—O5] — [O2—O5—O6]	20.70(10)	[O3—O4—O7] — [O4—O7—O7']	12.06(10)
Rotation distortion			
[O1—Hf—O6] [O3—Hf—O7’]	54.06(9)	[O4—Hf—O7] — [O2—Hf—O5]	46.61(9)

With regard to the overall coordination description of the ligands and bridging OH-groups as viewed in the square antiprism (**Figure 6.15** and **Figure 16(a)**), the title compound $[Hf(OH)(tfba)_3]_2 \cdot 2(C_3H_7NO)$, (**Hf_2b**) crystallises as a ***D₂-corner-bonded*** isomer (**Figure 6.15(b)**).

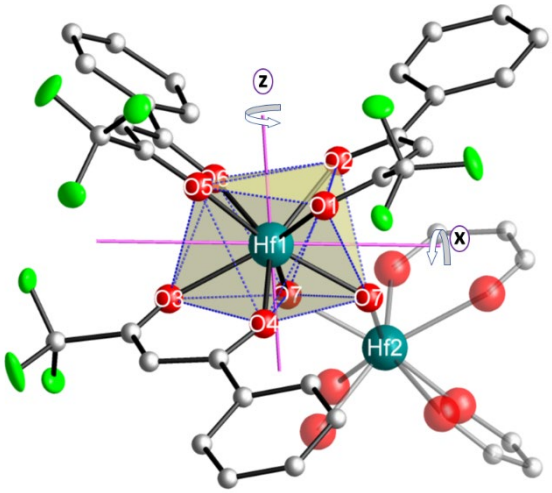

Figure 6.15: Half a fragment of the dinuclear complex bridged by two hydroxido ligands (O7 and O7' respectively), with a tris coordination at each hafnium(IV) centre, illustrating potential ***pseudo two-fold*** axes (x- and z-direction), depending on relative coordination of the acac-type ligand [note: the Hf(2) centre 'imitate' a 4th acac-type ligand, indicated in semi-transparent mode].

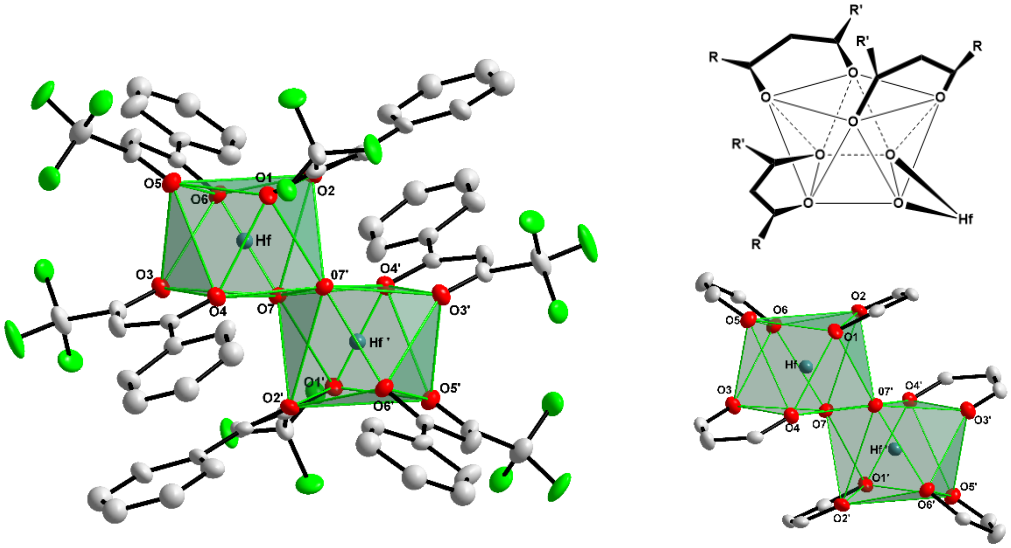

(a) **(b)**

Figure 6.16: (a) Graphic illustration of the square-antiprismatic coordination polyhedron of $[Hf(OH)(tfba)_3]_2$ (**Hf_2b**) **(b)** Illustration of the typical ***D₂-corner-bonded*** square antiprismatic isomer. (Hydrogen atoms omitted for clarity, 50% probability displacement ellipsoids).

In order to define the total distortion at the metal centre, two orientations for the metal complex are considered, as shown in **Figure 6.17** to allow the evaluation of the geometric parameters from the different planes; see **(a)** and **(b).** The orientations allow to consider the relative distortions on the identified sets of two planes describing the "top" and the "base" of the complex.

Therefore, the dihedral angles between the green (O1—O2—O5 and O3—O4—O7), and yellow planes **(**O6—O2—O5 and O7'—O4—O7), are illustrated in **Figure 6.17**, indicative of a ***bending distortion***, measured as 20.70(10)° and 12.06(10)°, respectively for the top and bottom two sets of O,O donor atoms describing the coordination polyhedron.

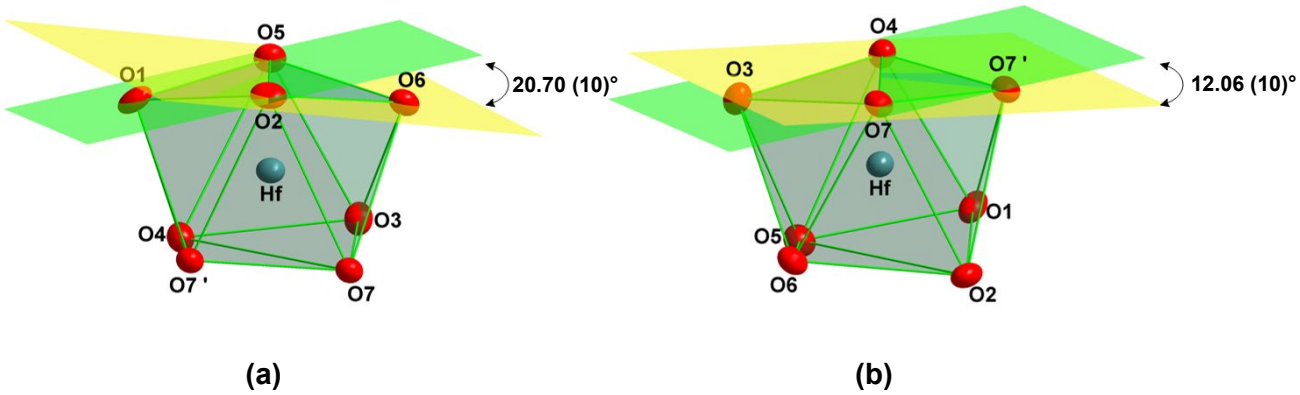

Figure 6.17: A graphical representation of the bending distortion (observed from the dihedral panes) in the antiprismatic coordination polyhedron surrounding the hafnium metal atom (C and H atoms are omitted for clarity).

A further indication of the distortion within the **Hf_2b** complex is observed from the amount of rotation observed between the two sets of O,O donor atoms describing the antiprismatic coordination polyhedron. Therefore, when viewing the coordination polyhedron from above, the dihedral angles between planes ([O1—Hf—O6] and [O7'—Hf—O3]) and ([O4—Hf—O7] and [O2—Hf—O5]) were measured as 54.06(9)° and 46.61(9)°, respectively, signifying the rotation distortion observed (**Figure 6.18**).

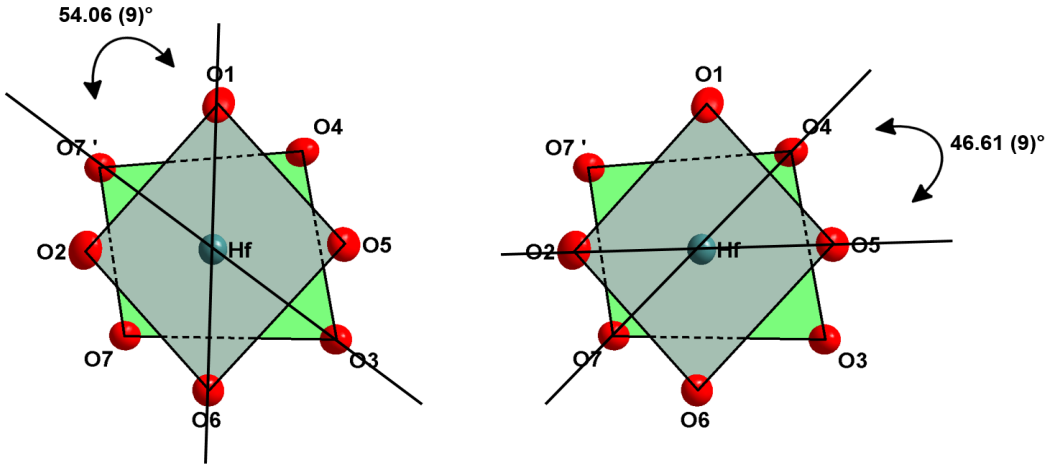

Figure 6.18: A graphical representation of the top view of the antiprismatic coordination polyhedron indicting the rotation distortion observed **Hf_2b**. (C and H atoms are omitted for clarity).

The dinuclear skeleton in **Hf_2b** presents a flat diamond-like structure with Hf—O7, Hf—O7' and Hf—Hf' distances of 2.073(2), 2.135(2) and 3.495(8) Å respectively, and a bite angle of 67.11(11) ° (**Figure 6.19**).

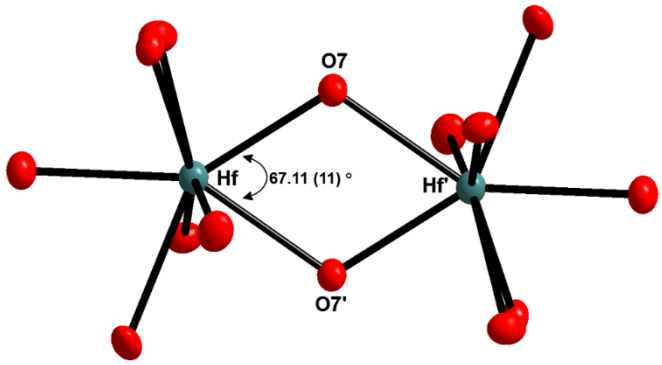

Figure 6.19: Partial structure of $[Hf(OH)(tfba)_3]_2 \cdot 2(C_3H_7NO)$, (**Hf_2b**) indicating the flat diamond-like dinuclear skeleton(Carbons, hydrogens and fluorine atoms are omitted for clarity, 50% probability displacement ellipsoids).

Furthermore, the dihedral angles between the metal coordination plane (*yellow planes*) and the plane formed by the three acetylacetonato ligands (*green planes*) are 23.67(13), 17.57(12) and 8.11(12)°, respectively for ***Lig1***, ***Lig2*** and ***Lig3*** as shown **Figure 6.20**. Again, illustrating the hafnium metal centre's ability to distort the backbone of the bidentate (acac-type) ligands from its preferred coordination

geometry of ca. 180° towards a highly distorted bent-like geometry to accommodate the overall polyhedron geometry around the metal centre.

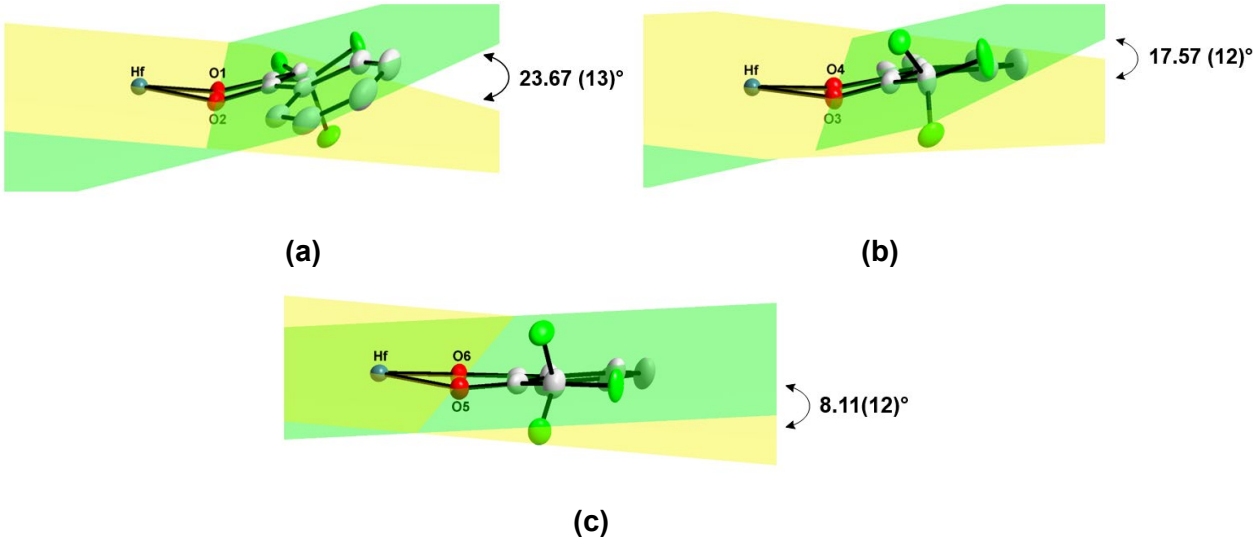

Figure 6.20: Partial structures of $[Hf(OH)(tfba)_3]_2$ (**Hf_2b**) graphically illustrating the dihedral angle between the metal coordination plane and the plane formed by the three acetylacetonato ligands. **(a)** ***Lig1*** – 23.67(13)°; **(b)** ***Lig2*** – 17.57(12)° and **(c)** ***Lig3*** – 8.11(12)°. (Hydrogen atoms omitted for clarity, 50% probability displacement ellipsoids).

Intermolecular O—H···O, as well as intramolecular C—H···O, hydrogen bonding interactions, are observed and may add some of the geometrical strain of the $[Hf(OH)(tfba)_3]_2{\cdot}2(C_3H_7NO)$ complex. The O—H···O intermolecular interaction are found between O7—H1A and the DMF solvent molecule, whereas the C—H···O interaction is found within the DMF solvent molecules (**Table 6.6**) as illustrated in **Figure 6.21**. Lastly, the molecules pack in a "head-to-tail" fashion when viewed along the *c*-axis (**Figure 6.22).**

Table 6.6: Hydrogen-bond geometry for $[Hf(OH)(tfba)_3]_2.2.(C_3H_7NO)$ (Hf_2b) (Å, ˚).

D—H···A	d(D—H)	d(H···A)	d(D···A)	D—H···A
O7—H1A···O8	0.78(2)	1.94(2)	2.712(3)	171(1)
$O7^i$—$H1A^i$···$O8^i$	0.78(2)	1.94(2)	2.712(3)	171(1)
C32—H32A···O8	0.98	2.365(3)	2.785(6)	105(1)
$C32^i$—$H32A^i$···$O8^i$	0.98	2.365(3)	2.785(6)	105(1)

***Symmetry code**: (i) 1-x,1-y,1-z.*

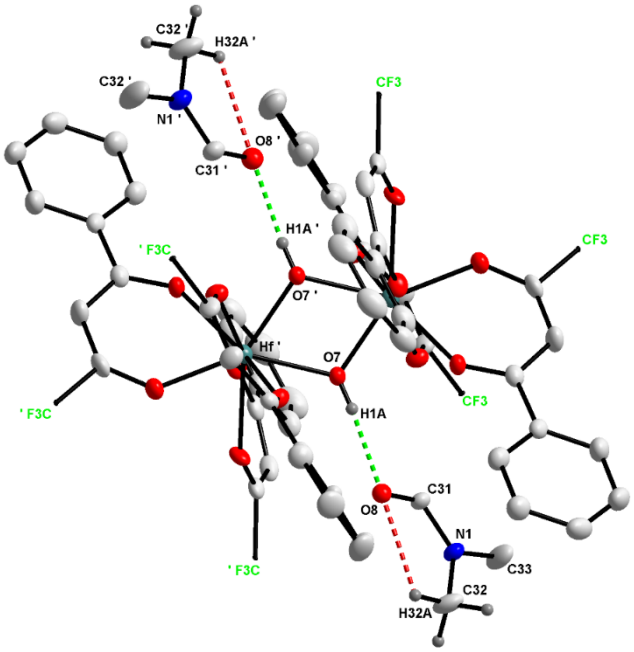

Figure 6.21: Partial structures $[Hf(OH)(tfba)_3]_2 \cdot 2(C_3H_7NO)$, (**Hf_2b**) indicating the O—H···O and C—H···O hydrogen bonding interaction observed in the unit cell (Hydrogens and fluorine atoms are omitted for clarity, 50% probability displacement ellipsoids).

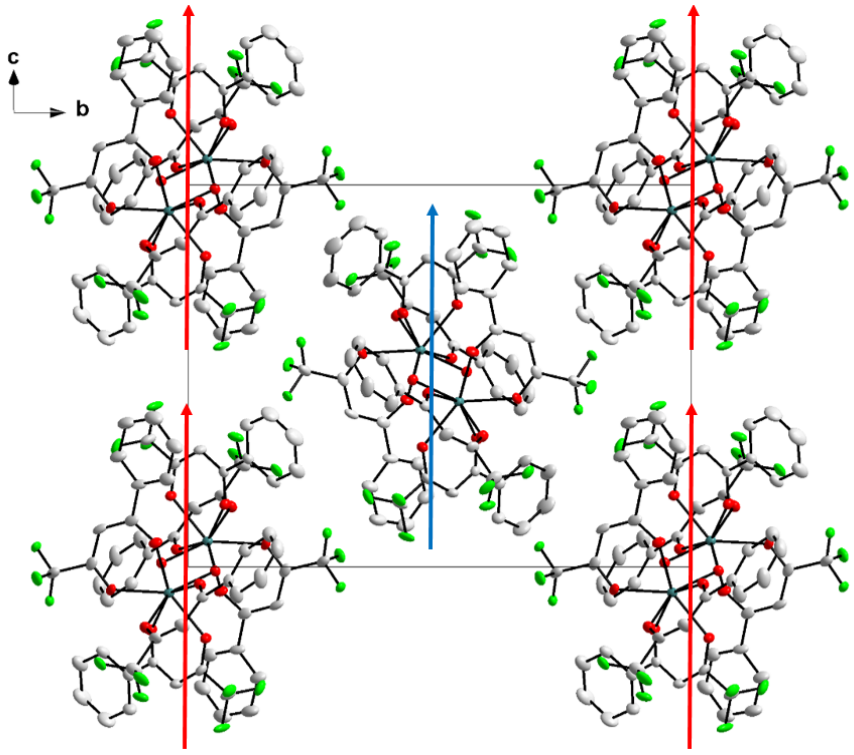

Figure 6.22: Graphical representation of molecular packing viewed along the a-axis within the unit cell for the title compound (**Hf_2b**), showing head-to-tail packing along the *c-axis* (arrow direction). Hydrogen atoms omitted for clarity, 50% probability displacement ellipsoids.

6.6. Discussion

Two additional Hf(IV)-*β*-diketonate complexes have been investigated and described thus far in the preceding sections (**Figure 6.21**). The general structural parameters, bond distances and angles from the various complexes are given in **Table 6.7**. As described in Chapter 3, these complexes' synthesis seems to afford these types of compounds with relative ease, reproducibly and with very high yields. An added advantage is that these complexes form rapidly, without any special manipulations needed, as described in previously published literature.[11,12,13,14] Therefore, this approach is much more cost-effective, environmentally friendly, and ideal to further a separation study.

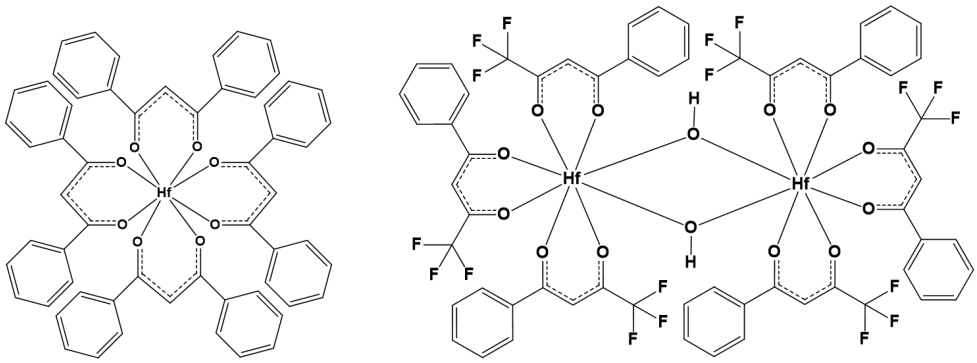

(a) **(b)**

Figure 6.23: The two hafnium complexes discussed in this single crystal X-ray diffraction chapter. **(a)** $[Hf(dbm)_4]$ (**Hf_2c**), **(b**) $[Hf(OH)(tfba)_3]_2$ (**Hf_2b**).

In this chapter, two additional hafnium(IV) complex structures with different coordinated *β*-diketonate ligands were presented. Both these structures are very similar in relation to bond lengths and angles to the structures found in literature.[15,16]

[11] T. J. Pinnavaia & C. Fray, *Inorg. Chem.*, **5**, 233, 1968.
[12] K. V. Zherikova, N. B. Morozova, N. V. Kurat'eva, I. A. Baidina, P. A. Stabnikov & I. K. Igumenov, *J. Struct. Chem.*, **46**, 6, 1039, 2005.
[13] K. V. Zherikova, N. B. Morozova I. A. Baidina, E.V. Peresypkina & I. K. Igumenov, *J. Struct. Chem.*, **47**, 3, 570, 2006.
[14] K. V. Zherikova, N. B. Morozova, I. A. Baidina, V. I. Alekseev & I. K. Igumenov, *J. Struct. Chem.*, **47**, 1, 82, 2006.
[15] J. A. Viljoen, A. Muller & A. Roodt., *Acta Cryst.* **E64**, m838, 2008.
[16] J. A. Viljoen, H. G. Visser, A. Roodt & M. Steyn., *Acta Cryst*., **E65**, m1367, 2009.

Table 6.7: Cell and structure overview of presented Hf(IV)-*β*-diketonate complexes.

Crystal Formula	**$[Hf(dbm)_4$**	**$[Hf(OH)(tfba)_3]_2$**
Crystal system	Monoclinic	Monoclinic
Space group	$P2_1/c$	$P2_1/c$
Square-antiprismatic Polyderon		
Isomer	*D_2-corner clip*	*D_2-corner clip*
Geometrical Isomer	*pseudo* t*wo-fold rotated*	*pseudo* t*wo-fold rotated*
Avg. bending distortion (°)	2.2(1)	16.38(10)
Avg. rotation distortion (°)	44.07(9)	50.34(10)
Selected Bond Lengths (Å)		
Hf—O1	2.197(3)	2.232(2)
Hf—O2	2.142(3)	2.167(2)
Hf—O3	2.133(2)	2.244(2)
Hf—O4	2.200(2)	2.146(2)
Hf—O5	2.180(3)	2.170(2)
Hf—O6	2.154(2)	2.207(2)
Hf—O7	2.189(2)	2.073(2)
Hf—O7'	---	2.135(2)
Hf—O8	2.154(2)	---
Bond Angles (°)		
O1—Hf—O2	74.45(10)	74.69(9)
O3—Hf—O4	75.02(9)	73.49(9)
O5—Hf—O6	74.71(10)	75.60(9)
O7—Hf—O8	74.79(9)	---
O7—Hf—O7’	---	67.11 (11)

In this regard, a more detailed comparative relation study of these Hf(IV)-*β*-diketonate complexes and additional structures will be undertaken in Chapter 8. Properties such as steric bulk and electronic properties of the Hf(IV)-*β*-diketonate complexes will be correlated to various aspects such as complex stability and structural effects.

6.7. Conclusion

By considering all of the structural detail discussed in this and previous chapters, some conclusions are attempted with regard to all these endeavours of identifying the solid-state tendencies of hafnium(IV) complexes containing *O,O'*-bidentate-ligands. Firstly, it is a well-known fact that hafnium-*β*-diketone complexes in general always show a square-antiprismatic coordination polyhedron.

As was found for the complexes in **Chapter 4** and **Chapter 5,** the coordination environment around the Hf(IV) metal centre for both complexes, discussed in this chapter, favours the ***D_2-clipped isomer***, with noticeable distortions. This suggests that hafnium(IV) has a certain preference for the chelation sites of the coordinating atoms, regardless of the steric properties of the ligands as a whole.[17] In theory, this could be mainly due to the fact that hafnium(IV) tends towards a maximum state of coordination, as a preference, or as lowest crystallisation state, which is in accordance with what is expected in these symbiotic systems.[18]

This chapter forms part of an overarching crystallographic investigation on different *N*- and *O*-donating multidentate ligands coordination to Hf(V) metal centres. A comprehensive discussion of all the complexes evaluated during this crystallographic study will be presented in **Chapter 8**, including the two structures

---

[17] J. A. Viljoen. (2009). *Speciation And Interconversion Mechanism Of Mixed Halo And O,O- And N,O- Bidentate Ligand Complexes Of Hafnium*, M.Sc. Dissertation, University of the Free State, South Africa.

[18] J. E. Huheey, E. A. Keiter & R. L. Keiter. (1993). *Inorganic Chemistry : Principles of Structure and Reactivity,* 4th Ed. New York: HarperCollins College Publishers.

presented in this chapter. The comparative nature of this subdivision will allow for a better evaluation of the effect that subtle changes on the coordinating *β*-diketonato ligands may have on the solid and solution state properties of the compounds.

In the following chapter, various Hf(IV) complexes coordinated to tetradenate ligands systems are structurally evaluated and described. The main focus will be placed on the influence of ligands on the coordination modes and coordination geometry of the obtained solid-state structures.

Chapter 7

X-Ray Diffraction Studies of Hafnium and Zirconium Complexes Containing Tetradentate *N,O*- and *N,N'*-donor ligands.

7.1. Introduction

The chemical behaviour of a metal site or any functionality attached to it as a function of the coordination environment for group 4 metals have received moderate amounts of interest from research groups worldwide due to their impact in organometallic chemistry and catalysis.[1,2,3] However, very few hafnium(IV)- and zirconium(IV) complexes containing tetradentate Schiff-base type ligands exist in literature.[4,5,6] Furthermore, after a comprehensive literature study, no structural data could be obtained of hafnium or zirconium complexes containing carboxamide type ligands.

---

[1] A. K. Singh & S. Mehtab, *Talanta*, **74**, 806, 2008.
[2] L. Gorski, A. Saniewska, P. Parzuchowski, M.E. Meyerhoff & E. Malinowska, *Anal. Chim. Acta*, **551**, 37, 2005.
[3] B. M. Trost & Hachiya, *J. Am. Chem. Soc.*, **120**, 1104, 1998.
[4] S. Gendler, A. L. Zelikoff, J. Kopilov & I. M. Goldberg*, J. Am. Chem. Soc.*, **130**, 2144, 2008.
[5] B. E. Klamm, C. J. Windorff, C. Celis-Barros, M. L. Marsh, D.S. Meeker & T. E. Albrecht-Schmitt, *Inorg.Chem*. ,**57**,15389, 2018.
[6] M. D. Jones, M. G. Davidson & G. Kociok-Kohn, *Polyhedron,* **29,** 697, 2010.

As mentioned in **Chapter 1**, one of the main aims of this research project was to synthesise and characterise novel hafnium(IV) complexes containing different tetradentate *N,O′*- and *N,N′*- donor ligands. Moreover, an integral part of this research has been focused on utilising commercially available ligands with various electronic and steric properties.

If one were to design novel tetradentate ligands for a comparative study, one would have to consider a range of ligands with different electronic properties and a wide range of steric characteristics. Two groups of tetradentate ligands that fall directly within these categories are the salophen and carboxamide family of chelators (**Figure 7.1**).

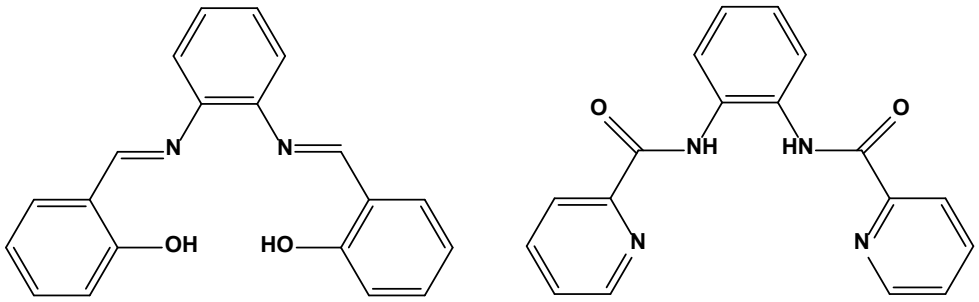

(a) **(b)**

Figure 7.1: Graphical representation of **(a)** - N,N′-bis(salicylidene)-1,2-phenylene-diamine (**SalophenH$_2$**) and **(b)** - N,N'-(1,2-phenylene)bis(pyridine-2-carboxamide) (**pbpH$_2$**) ligands.

These ligands are highly adjustable when modifying the diamine (o-phenylenediamine) fragment at the centre of the tetradentate chelator,[7,8,9] and can be prepared by simply altering the initial diamine **(a)** that is condensed either with salicylaldehyde **(b)** or picolinic acid **(c)** (**Figure 7.2**).

[7] E. J. Campbell & S. T. Nguyen, *Tetrahedron Lett.,* **42***,* 1221, 2001.

[8] H. Zhu, M. Wang, C. Ma, B. Li, C. Chen & L. Sun, *J. Organomet. Chem.,* **690** , 3929, 2005.

[9] P. C. W. Van der Berg, H. G. Visser, A. Roodt & T.J. Muller, *Acta Cryst.*, **E68**, o2739, 2012.

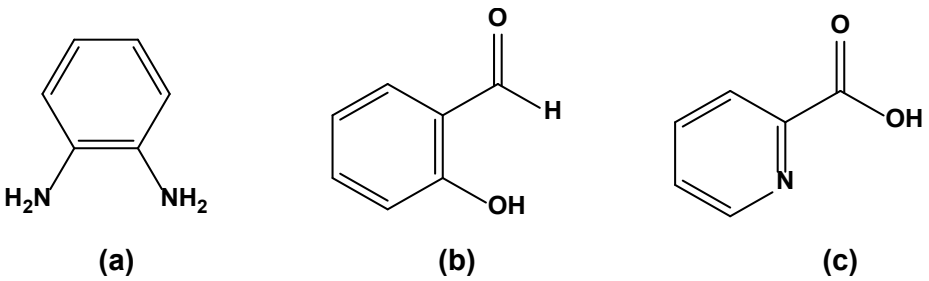

(a) (b) (c)

Figure 7.2: Graphical representation of common **(a)** - diamine (o-phenylenediamine; **(b)** - salicylaldehyde (2-hydroxybenzaldehyde); **(c)** - picolinic acid (pyridine-2-carboxylic acid)

These unique characteristics allow for even broader electronic and steric contributors to organometallic complexes of hafnium and zirconium, yielding valuable information on these metals' chelation preferences. Furthermore, when considering the limited database entries for these types of hafnium and zirconium complexes that have been structurally characterised,[10] it becomes apparent that a crystallographic study of metal complexes containing theses ligand families could shed (i) considerable light on characteristics of complexes and (ii) thus on experimental design regarding possible separation studies utilising such ligands.

This chapter contains a detailed discussion of the single-crystal structure of a hafnium and zirconium complex containing *N,O'*- and *N,N'*- tetradentate ligand, respectively, as well as the correlation between these two structures (**Figure 7.3**). More in-depth correlations of each structure with similar structures from the literature will be discussed in **Chapter 8** and **Chapter 9**.

[10] Cambridge Structural Database (CSD) Version 5.42, November 2020 update. C. R. Groom, I. J. Bruno, M. P. Lightfoot & S. C. Ward, *Acta Cryst.*, **B72**, 171, 2016.

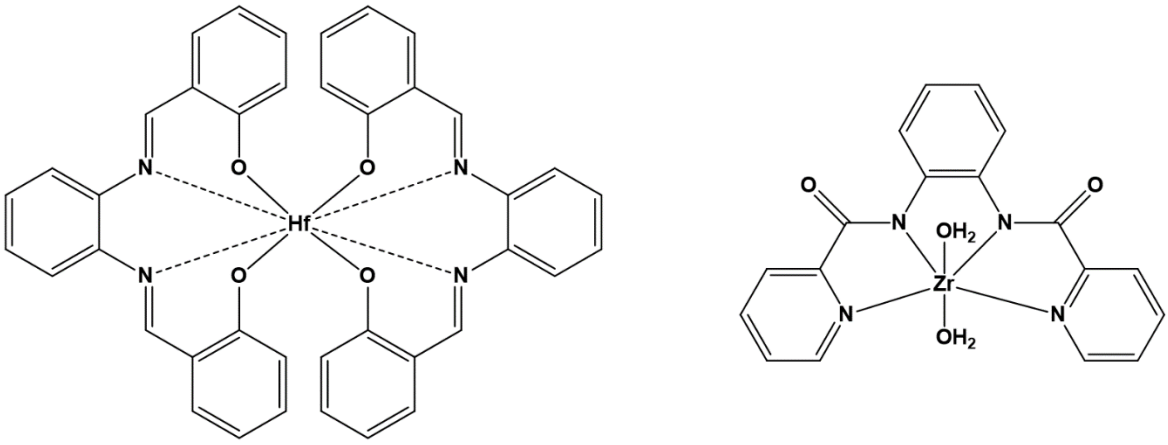

(a) **(b)**

Figure 7.3: The chelated hafnium complexes discussed in this single crystal X-ray diffraction chapter **(a) -** [Hf(salophen)$_2$], **(b)** - [Zr(pbp)(H_2O)$_2$].

7.2. General Considerations for Chapter 7

Note: The following general considerations are used throughout the text below, which enables a systematic comparison and standardised geometry for the complexes as discussed. It is further important to take into account that although symmetry elements are formally defined as “inversion centres”, “rotation axes”, “mirror planes”, etc., these are all to be considered “*pseudo*” elements, since it all describe solid-state observations.

The spatial arrangement of the tertradentate ligands allows the formation of various geometrical isomers. The placement of the nitrogen and oxygen coordination atoms are observed as potentially a ***two-fold rotated*** isomer (**Figure 7.4**). The latter may be via two-fold rotation axes through the metal centre as depicted below, defined along the classic *z*-axis as reference.

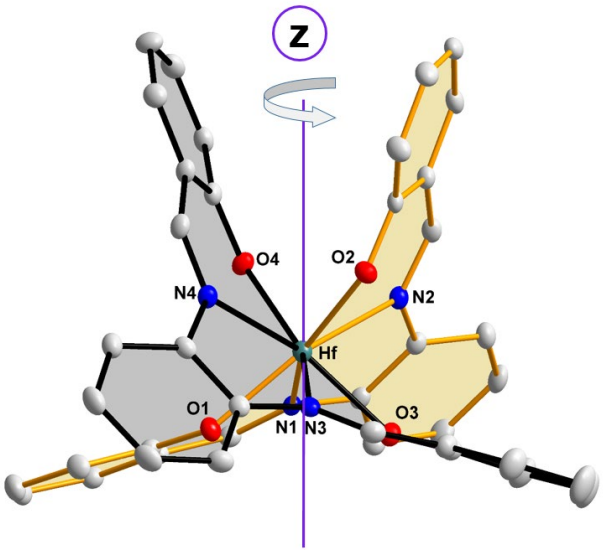

Figure 7.4: Coordinated salophen-ligand arrangement around the metal centre when considering the N- and O- coordination sites via a *pseudo two-fold* rotation axes, i.e. a *two-fold rotated-isomer*.

7.3. Experimental

The X-ray intensity data was collected on a Bruker X8 ApexII 4K Kappa CCD area detector diffractometer, equipped with a graphite monochromator and Mo*Kα* fine-focus sealed tube (*λ* = 0.71069 Å, T = 100(2) K) operated at 2.0 kW (50 kV, 40 mA). The initial unit cell determinations and data collections were done by the SMART[11] software package. The collected frames were integrated using a narrow-frame integration algorithm and reduced with the Bruker SAINT-Plus and XPREP software packages[12] respectively. Analysis of the data showed no significant decay during the data collection. Data was corrected for absorption effects using the multi-scan technique SADABS,[13] and the structure was solved by the direct

[11] Bruker SMART-NT Version 5.050.Bruker AXS Inc. Area-Detector Software Package; Madison, WI, USA, **1998.**

[12] Bruker SAINT-Plus Version 6.02 (including XPREP), Bruker AXS Inc. Area-Detector Integration Software, Madison, WI, USA, **1999.**

[13] Bruker SADABS Version 2004/1.Bruker AXS Inc. Area Detector Absorption Correction Software, Madison, WI, USA, **1998.**

methods package SIR97[14] and refined using the WinGX[15] software incorporating SHELXL.[16] The final anisotropic full-matrix least-squares refinement was done on F^2. The methyl and aromatic protons were placed in geometrically idealised positions (C–H = 0.93 – 0.98 Å) and constrained to ride on their parent atoms with $U_{iso}(H) = 1.2U_{eq}(C)$. Non-hydrogen atoms were refined with anisotropic displacement parameters. The graphics were obtained with the DIAMOND[17] program with 50% probability ellipsoids for all non-hydrogen atoms.

A summary of the general crystal data and refinement parameter is given in **Table 7.1** for both structures. Supplementary data for the atomic coordinates, anisotropic displacement parameters, all bond distances and angles and hydrogen coordinates are given in the **Appendix C** for each individual dataset.

[14] A. Altomare, M. C. Burla, M. Camalli, G. L. Cascarano, C. Giacovazzo, A. Guagliardi, A.G.G. Moliterni, G. Polidori & R. Spagna, *J. Appl. Cryst.,* **32**, 115, 1999.
[15] L. J. Farrugia, *J. Appl. Cryst.,* **32***,* 837, 1999.
[16] G. M. Sheldrick; SHELXL97. Program for crystal structure refinement, University of Göttingen, Germany, 1997**.**
[17] K. Brandenburg & H. Putz; DIAMOND, Release 3.0e, Crystal Impact GbR, Bonn, Germany, 2006.

Table 7.1: Crystallographic and refinement details for structures discussed in this chapter

Compound	[Hf(salophen)$_2$] •2C$_7$H$_8$	[Zr(pbp)(H$_2$O)$_2$] NO$_3$•MeOH
Formula weight	945.35	1039.16
Crystal system	Triclinic	Orthorhombic
Space group	$P\bar{1}$	*Pbca*
Unit cell dimensions:		
a,	10.785(5),	15.479(2),
b,	13.969(5),	13.386(2),
***c* (Å)**	14.082(5)	19.872(3)
α,	84.248(3),	90,
β,	76.052(2),	90,
γ (°)	80.719(5)	90
Volume (Å^3) / *Z*	2027.9(14) / 2	4117.3(11) / 4
Density (calculated) (mg/m^3)	1.548	1.676
Absorption coefficient (mm^{-1})	2.625	2.229
F(000)	950	2100
Crystal size (mm)	0.189 x 0.204 x 0.309	0.300 x 0.150 x 0.100
Theta range for data collection (°)	1.97 to 28.00	3.040 to 28.00
Index ranges	-14 <= h <= 14, -18 <=k<= 18, -18 <= l <= 18	-20<=h<=20, -17<=k<=17, -26<=l<=26
Reflections collected	31646	211393
Independent reflections/R(int)	9729 [R(int) = 0.0351]	4970 [R(int) = 0.0792]
Completeness (θ = 28.35°) (%)	99.10	99.80
Refinement method	Full-matrix least-squares on F^2	Full-matrix least-squares on F^2
Data / restraints / parameters	9729 / 15* / 559	4970 / 0 / 304
Goodness of fit on F^2	1.063	1.076
Final R indices [I>2sigma(I)]	R_1 = 0.0255, wR_2 = 0.0597	R_1 = 0.0292 wR_2 = 0.0696
R indices (all data)	R_1 = 0.0298 wR_2 = 0.0614	R_1 = 0.0349 wR_2 = 0.0734
Largest diff. peak and hole (e.Å^{-3})	1.002; -0.983	0.32; -0.530

*Unusual anisotropic displacement values are found for the solvent molecule toluene (atoms C41-- C47) due to a disorder and due to its location on a special position.

7.4. Crystal Structure of Bis(N,N'-disalicylidene-1,2-phenylene-diamino)hafnium(IV) Toluene Disolvate – [Hf(salophen)$_2$]•2C$_7$H$_8$

Most literature reports on the synthesis of hafnium(IV) compounds emphasise the importance of working under anaerobic conditions employing Schlenk-type apparatus.[18,19,20] This is not viable in industrial applications and forced us to look for synthetic procedures under normal aerobic conditions. Moreover, since the Hf(IV) starting material is already in the highest oxidation state, preventing oxygen to enter the synthesis setup is irrelevant. The synthesis, as described in § 3.3.2.1, of the title compound (**Hf_3a**) in toluene under aerobic conditions opens up new possibilities in the rich coordination chemistry of hafnium complexes.

The **Hf_3a** compound crystallises in the triclinic space group $P\bar{1}$, with two [Hf(salophen)$_2$] entities in the unit cell (Z = 2). The asymmetric unit consists of a Hf(IV) metal ion coordinated to two *N*,*N*',*O*,*O*'-tetradentate (Salophen^{2-}) ligands in a meridional fashion, one complete toluene and one half toluene solvate molecule. The rest of the mentioned half toluene molecule is generated by an inversion centre coupled with 50% positional disorder.

The crystal structure as well as the numbering scheme of the complex is represented in **Figure 7.5**. General crystallographic information pertaining to the crystal structure is referred to in **Table 7.1** and selected bond lengths and angles are given in **Table 7.2.** For comprehensive information regarding bond distances, angles, atomic coordinates and anisotropic displacement parameters related to the structure, refer to **Appendix C1**.

---

[18] J. V. Silverton & J. L. Hoard., *Inorg. Chem.,* **2**, 243, 1963.
[19] F. Corazza, E. Solari, C. Floriani, A. Chiesi-Villa & C Guastini., *J. Chem. Soc., Dalton Trans.*, 1335, 1990.
[20] B. E. Klamm, C. J. Windorff, C. Celis-Barros, M. L. Marsh, D. S. Meeker & T. E. Albrecht-Schmitt, *Inorg. Chem*., 57, **24**, 15389, 2018.

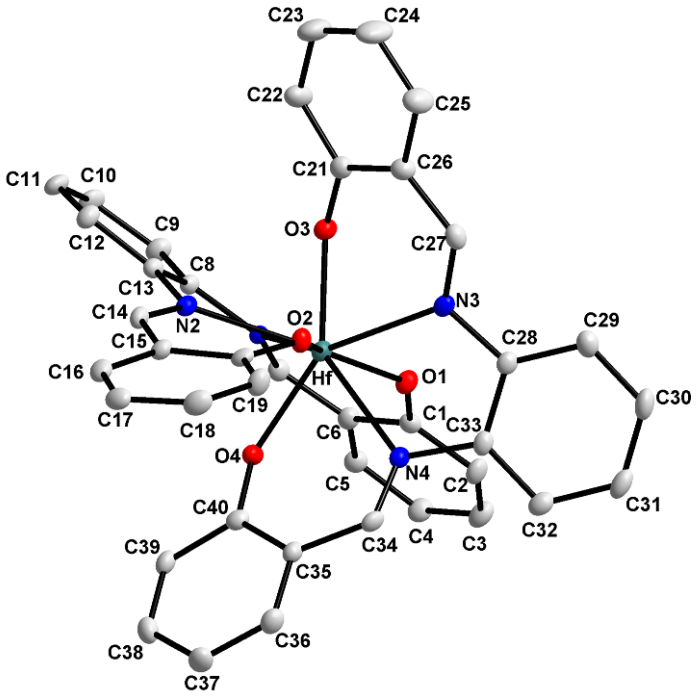

Figure 7.5: Representation of the title compound (**Hf_3a**), showing the numbering scheme and displacement ellipsoids *(50 % probability, solvent molecules and hydrogen atoms omitted for clarity)*

The hafnium metal centre, in which the two *mer* coordinated salophen ligands are fan-like arranged around the metal centre (**Figure 7.5)**, intersecting nearly perpendicular to one another (89.98(5)°, **Figure 7.6),** produces a distorted square antiprismatic coordination polyhedron, with a slight distortion towards dodecahedral geometry as shown in **Figure 7.7** and **Figure 7.8 (a).**

In the title compound (**Hf_3a**), the Hf—O and Hf—N bond lengths vary from 2.055(2) Å to 2.095(2) Å and 2.379(2) Å to 2.42(2) Å, respectively, with average O—Hf—N and N—Hf—N bite angles of 74.22(2)° and 67.53(2)°, respectively (**Table 7.2**).

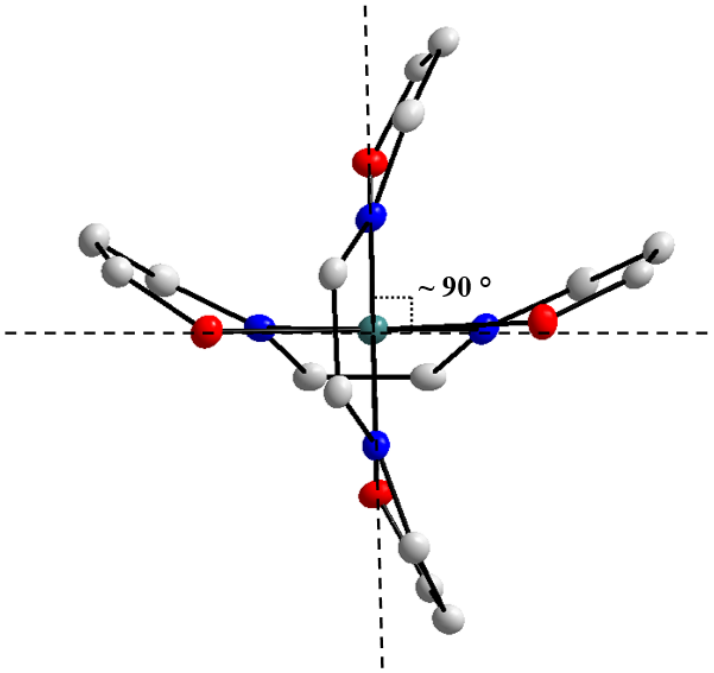

Figure 7.6: Graphical illustration of the tetradentate ligands in [Hf(salophen)$_2$] (**Hf_3a**), intersecting practically perpendicular to each other. (Hydrogen atoms and solvent molecules are omitted for clarity, 50% probability displacement ellipsoids)

Figure 7.7 illustrates that each coordinated ligand is duplicated by an opposite facing ligand by *ca*. 180° rotation through the hafnium metal centre. Although these ligands do not lie in a flat plane relative to one another, it is clear that the two salophen ligands are chelated to the metal centre with a ***pseudo two-fold rotated isomer*** placement of the *N*- and *O*-coordinating site.

The overall coordination description of the salophen ligands as viewed in the distorted square antiprism (**Figure 7.8(a)**), the title compound [Hf(salophen)$_2$] (**Hf_3a**) crystallises as a ***C$_2$-corner -and side clipped*** bonded isomer (**Figure 7.8(b)**).

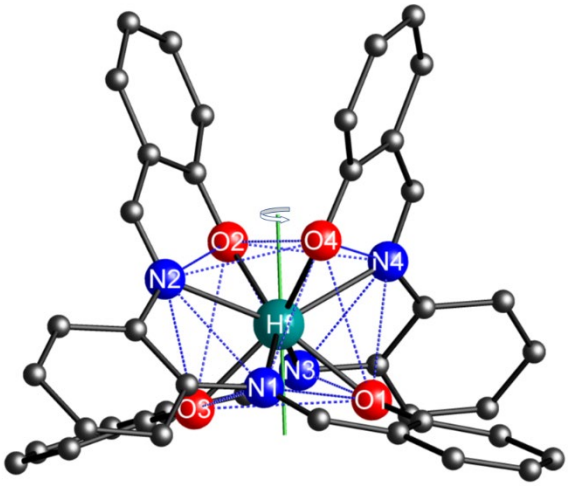

Figure 7.7: Graphical illustration of the *pseudo two-fold rotated* isomer of the salophen ligands across the metal centre in the **Hf_3a** title molecule (*Hydrogen atoms and solvent molecules omitted for clarity*). When compared to **Figure 7.4**, the principal rotation axis is considered to be approximately perpendicular to the top/bottom planes of the antiprism, i.e., along the z-axis.

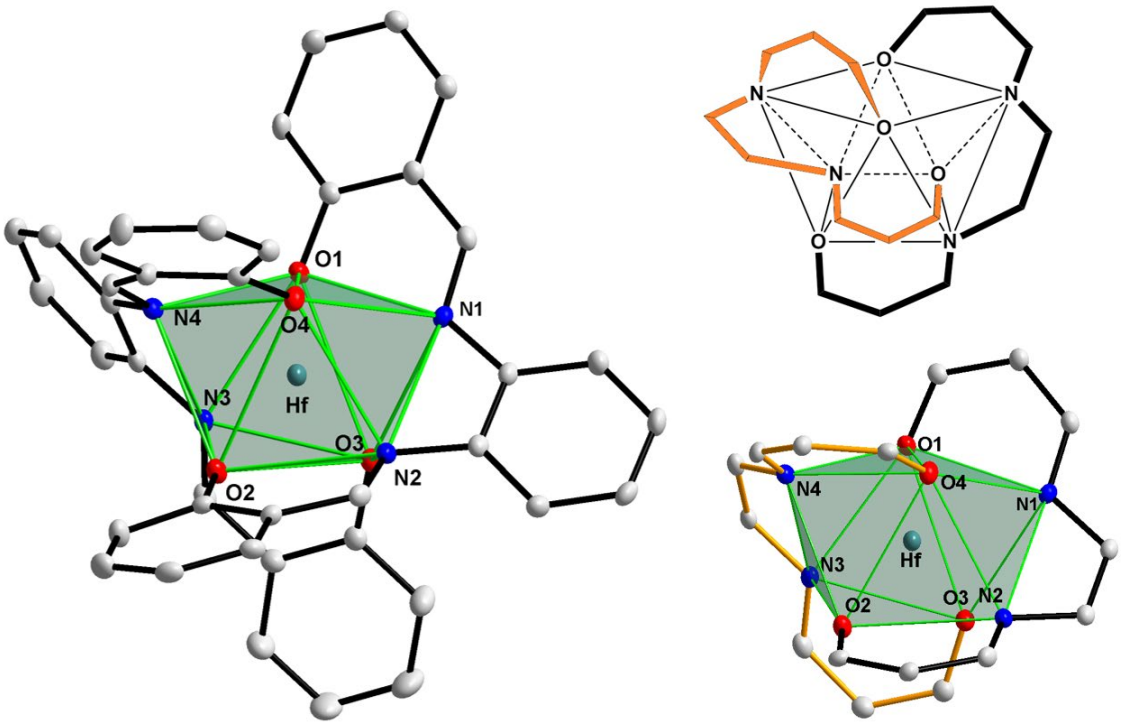

Figure 7.8 (a) Graphic illustration of the square-antiprismatic coordination polyhedron of [Hf(salophen)$_2$] (**Hf_3a**); **(b)** Illustration of the typical ***C$_2$-corner and side-clipped*** bonded square antiprismatic isomer. (Hydrogen atoms and solvent molecules are omitted for clarity, 50% probability displacement ellipsoids).

Table 7.2: Selected bond distances, angles and torsion angles of [Hf(salophen)$_2$] (Hf_3a).

Selected Bond Lengths (Å)			
Hf—O1	2.055(2)	C01—C11	1.503(5)
Hf—O2	2.077(2)	C03—C21	1.482(6)
Hf—O3	2.070(2)	C04—C31	1.501(5)
Hf—O4	2.095(2)	C06—C41	1.495(5)
Hf—N1	2.410(2)	C07—C51	1.496(5)
Hf—N2	2.398(2)	C09—C61	1.503(5)
Hf—N3	2.379(2)	C010—C71	1.500(6)
Hf—N4	2.423(2)	C012—C81	1.496(5)
Selected Bite Angles (°)			
O1—Hf—N1	74.28(7)	O3—Hf—N3	74.38(8)
O2—Hf—N2	74.43(8)	O4—Hf—N4	73.78(7)
N1—Hf—N2	68.14(8)	N3—Hf—N4	66.91(8)
O1—Hf—O2	143.15(7)	O3—Hf—O4	144.9(7)
Selected Torsion Angles (°)			
O1—N2—N3—O3	-0.13(11)	O3—N3—N4—O4	-2.87(12)
Selected Dihedral Angles regarding the Anti-prism (°)			
Bending distortion (°)			
[N1—O1—O4] — [N4—O1—O4]	22.63(10)	[N2—O2—O3] — [N3—O2—O3]	22.80(7)
Rotation distortion (°)			
[N1—Hf—O4] [O3—Hf—O2]	49.10(7)	[N1—Hf—N4] — [N2—Hf—N3]	50.02(7)

In order to define the total distortion at the metal centre, two orientations for the metal complex are considered, as shown in **Figure 7.9,** to allow the evaluation of the geometric parameters from the different planes; see **Figure 7.9 (a)** and **(b).** The orientations allow to consider the relative distortions on the identified sets of two planes describing the "top" and the "base" of the complex.

Hence, the dihedral angles between the green planes (N1—O1—O4 and N2—O2—O3) and yellow planes **(**N4—O1—O4 and N3—O2—O3), as illustrated in **Figure 7.9**, indicative of a bending distortion, measured as 21.63(10)° and 22.80(10)°, respectively for the top and bottom two sets of N,O donor atoms describing the coordination polyhedron.

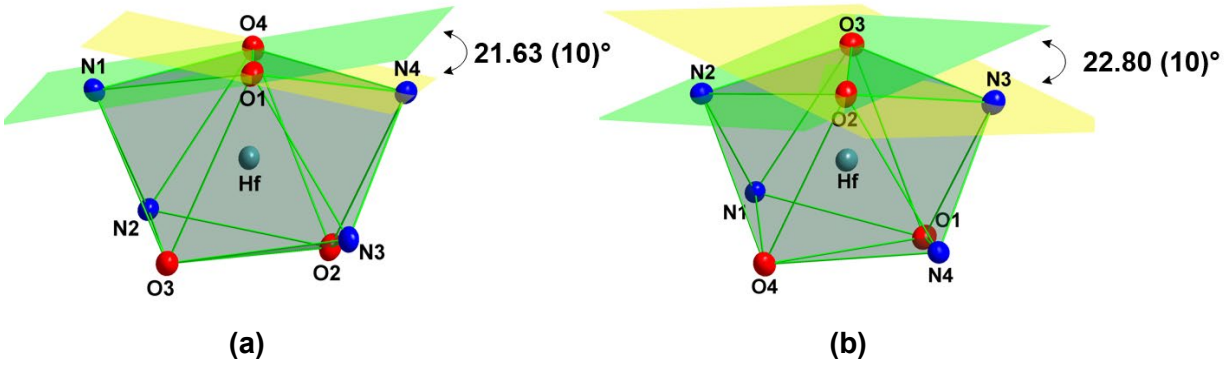

Figure 7.9: A graphical representation of the bending distortion (observed from the dihedral panes) in the antiprismatic coordination polyhedron surrounding the hafnium metal atom (C and H atoms are omitted for clarity).

A further indication of the distortion within the **Hf_3a** complex is observed from the amount of rotation observed between the two sets of N,O donor atoms describing the antiprismatic coordination polyhedron. Therefore, when viewing the coordination polyhedron from above, the dihedral angles between planes ([O1—Hf—O4] and [O2—Hf—O3]) and planes ([N1—Hf—N4] and [N2—Hf—N3]) were determined as 49.10(7)° and 50.02(7)°, respectively, signifying the rotation distortion observed (**Figure 7.10, Table 7. 2**). Ideally, these angles should be 45°.

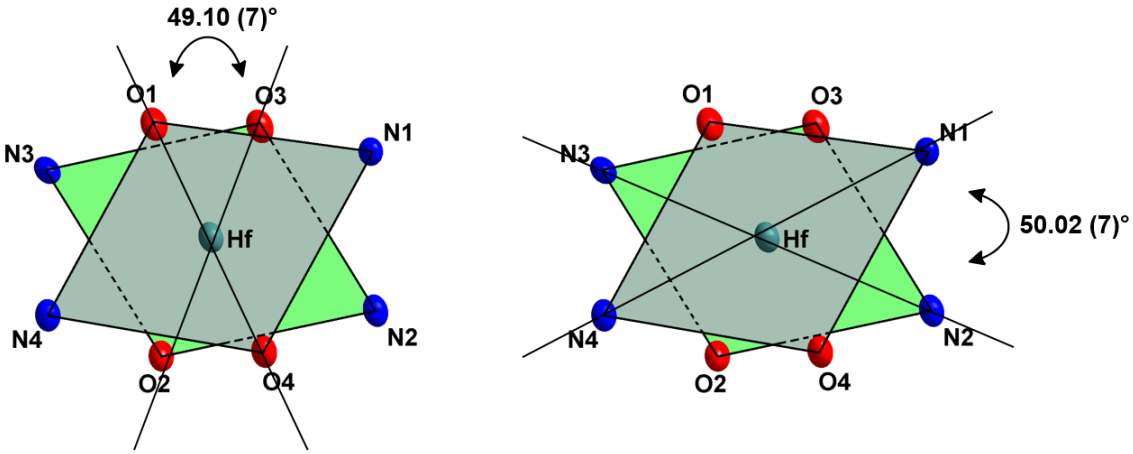

Figure 7.10: A graphical representation of the top view of the antiprismatic coordination polyhedron indicting the rotation distortion observed. (*Carbon and hydrogen atoms are omitted for clarity*).

When constructing an equatorial plane through the Hf(IV) metal centre and the coordinated *N* -and *O* atoms of each individual salophen ligand, it is observed that all the atoms lie either in or just slightly off this plane, **Figure 7.11**. yielding small torsion angles of -0.13(11) and -2.87(12)° for atoms O1—N1—N2—O2 and O3—N3—N4—O4, respectively, (**Table 7.2**) even though the ligands as a whole is quite distorted from planarity.

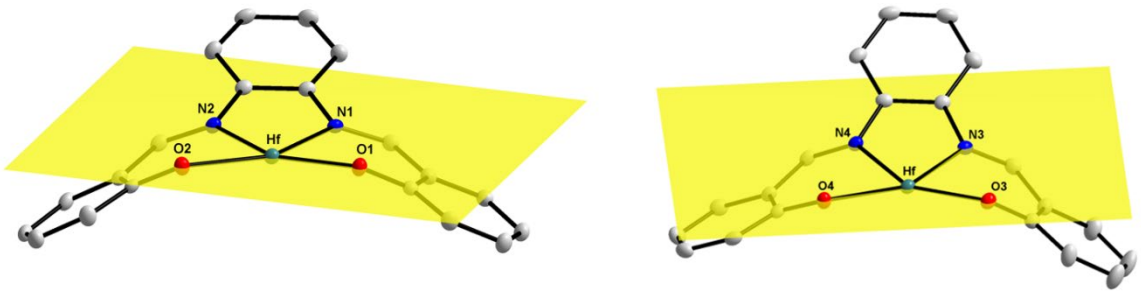

Figure 7.11: A graphical representation of the two coordinated salophen ligands coordinated to Hf(IV), showing the planarity of the O-N-N-O donor atom set and the puckering of the ligand backbone (*Carbon and hydrogen atoms are omitted for clarity*).

As mentioned, a noteworthy characteristic of the hafnium metal centre is observed in this structure, in that it distorts the backbone of the salophen ligand from its preferred coordination geometry of *ca*. 180° towards a highly distorted bent-like geometry to accommodate the overall polyhedron geometry around the metal centre. In **Hf_3a** the dihedral angles between the metal coordination plane (O—N—Hf—N—O) and the planes formed by the phenylenediamine and salicylaldehyde parts of the ligands' backbone are illustrated in **Figure 7.12** and reported in **Table 7.3**.

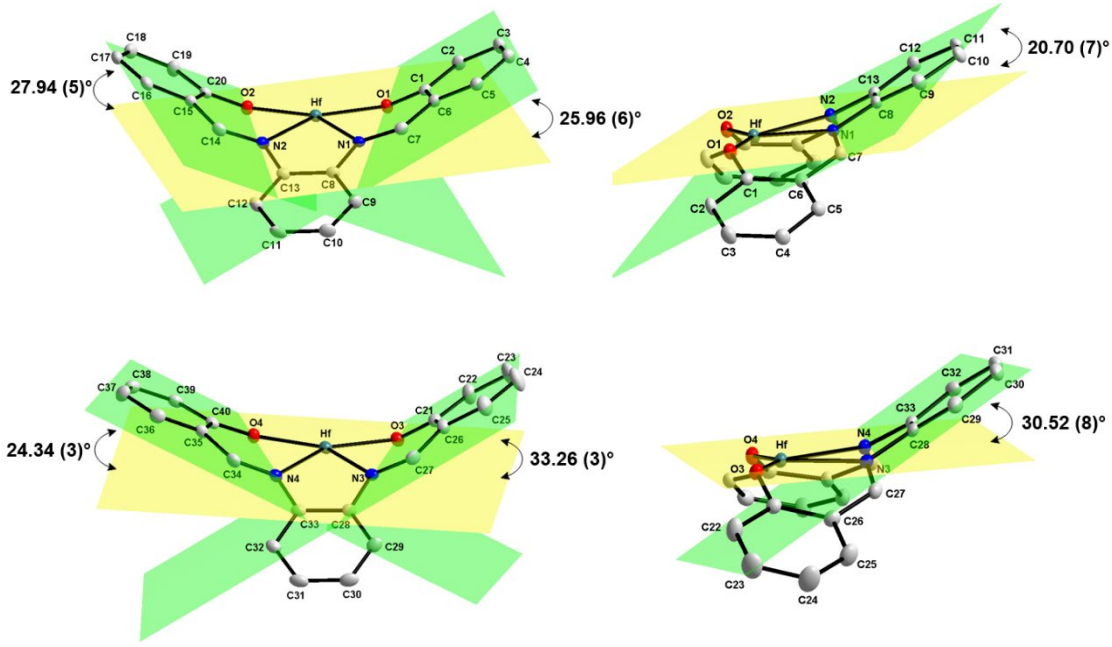

Figure 7.12: A graphical representation of the two coordinated salophen ligands coordinated to Hf(IV), showing dihedral angles between the metal coordination plane (O—N—Hf—N—O) and the planes formed by **(a)** salicylaldehyde and **(b)** phenylenediamine parts of the ligands' backbone (*Hydrogen atoms are omitted for clarity).*

The **Hf_3a** molecules in the unit cell pack in a "head-to-tail" fashion in vertical layers when viewed along the *b*-axis. No classical intermolecular hydrogen bonding nor π-π interactions occurs within the unit cell, with only van der Waals forces stabilising the crystal structure.

Table 7.3: Selected dihedral angles between the metal coordination plane (O—N—Hf—N—O) and the planes formed by phenylenediamine and salicylaldehyde parts of the salophen ligands as observed in the title compound (Hf_3a).

Atoms in plane (Yellow plane)	Atoms in plane (Green Plane)	Dihedral Angles (°)
O1—N1—Hf—N2—O2	O1—C1—C2 - - - C6—C7—N1	25.96(6)
O1—N1—Hf—N2—O2	N2—C14—C15 - - - C19—C20—O2	27.94(5)
O1—N1—Hf—N2—O2	N1—C8—C9 - - - C12—C13—N2	20.70(7)
O3—N3—Hf—N4—O4	O3—C21—C22 - - - C26—C27—N4	33.26(3)
O3—N3—Hf—N4—O4	N4—C34—C35 - - - C39—C40—O4	24.34(3)
O3—N3—Hf—N4—O4	N1—C28—2C9 - - - C32—C33—N4	30.52(8)

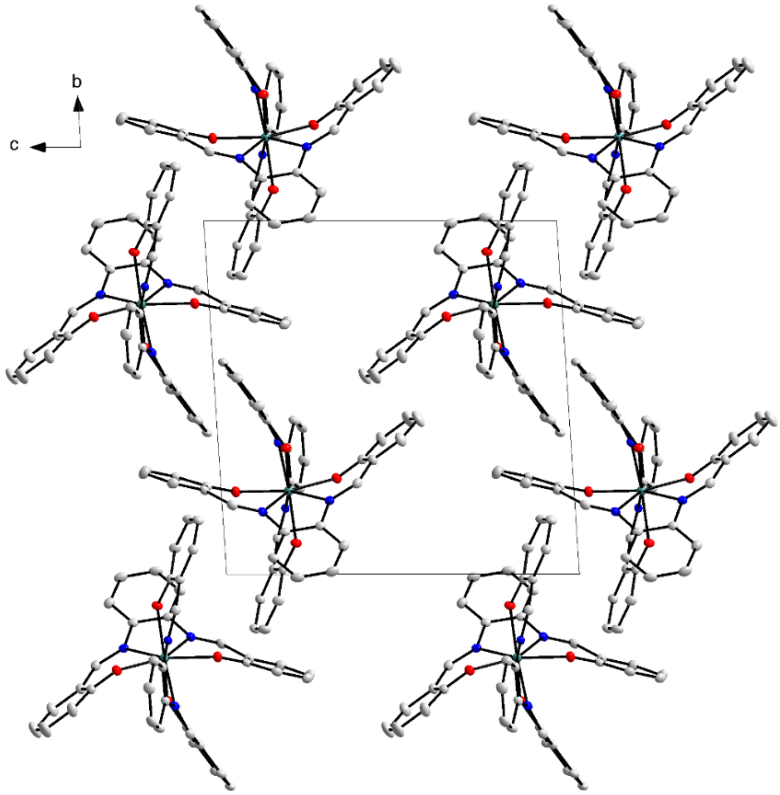

Figure 7.13: Graphical representation of molecular packing within the unit cell for the title compound (**Hf_3a**), showing "*head-to-tail*" packing fashion in vertical layers along the *b*-axis. Solvent and hydrogen atoms omitted for clarity, 50% probability displacement ellipsoids.

7.5. Crystal Structure of Diaqua-(N,N'-(o-phenylene)-bis(pyridine-2-carbox-amidato)-κ⁴N,N',N'',N''')-zirconium(III) nitrate - (Zr(pbp)(H₂O)₂]NO₃

The structure of this six coordinated zirconium – (1,2-phenylene)bis-(pyridine-2-carboxamide) (*pbp*$^{2-}$) complex **Zr_1a** was produced in an attempt at the re-synthesis of a published isomorphic structure reported with a methanol solvent and nitrate anion in the asymmetric unit.[21] Due to the recent successes with the synthetic methodology employing methanol (CH_3OH) as solvent under aerobic conditions, the synthesis of new hafnium and zirconium - pbp structures were deemed a potential important addition to hafnium(IV) coordination chemistry. The broader interest in a new structure with a different solvate and different distortion characteristics in the backbone (than the salophen system described in Par. 7.2) in the crystal lattice could give additional insight into the ligand coordination and solvent effects on these metal complexes' solid-state characteristics as a whole.

The synthesis of **Zr_1a** and the resulting yellow needle-like crystals obtained for this was discussed in § 3.2.2.1.

It is important to note that although Zr(III) mononuclear coordination compounds are not that frequently encountered,[22] **Zr_1a** is presented here as the Zr(III) to ensure charge in the compound is counterbalanced by the nitrate ion and the deprotonated pbp. Based on the synthesis, the fact that the starting pbp reactant contained a Ga(III) from a previous study, the possibility of the compound being the corresponding Ga(III) complex, cannot be ruled out. Nevertheless, it is presented herein as the Zr(III) and refined as such, and in following paragraphs

[21] P. W. C. van der Berg. (2013). *Development and Assessment of Metal Containing Drugs as Model Radiopharmaceuticals for Cancer Treatment*, M.Sc Dissertation, University of the Free State, South Africa.
[22] L. Pan, R. Heddy, J. Li, C. Zheng, X. Huang, X. Tang & L..Kilpatrick, *Inorg.Chem*., **47**, 5537, 2008.

some speculation as to whether in might be a Ga(III) compound instead of a Zr(III) entity is presented.

A summary of the general crystal data is given in **Table 7.1**, while the numbering scheme of the solvated complex is shown in the perspective drawing in **Figure 7.14**. **Table 7.4** presents selected bond lengths and angles of the title compound. Atomic coordinates, anisotropic displacement parameters, all bond distances and angles and hydrogen coordinates, are given in the supplementary data (**Appendix C.2**). Hydrogen atoms and/or solvent molecules are omitted in some molecular presentations for clarity.

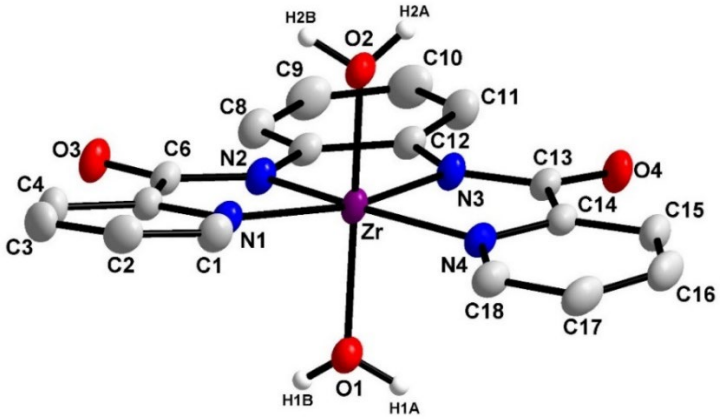

Figure 7.14: Representation of the title compound (**Zr_1a**), showing the numbering scheme and displacement ellipsoids *(50 % probability, some hydrogen atoms omitted for clarity*).

The title compound **Zr_1a** compound crystallises in a centrosymmetric, orthorhombic *Pbca* space group, with four [(Zr(pbp)(H_2O)$_2$] entities in the unit cell (Z = 4). The asymmetric unit consists of a Zr(III) metal centre coordinated to the four nitrogen atoms of the *pbp*-tetradentate ligand and two water molecules *trans* to each other, producing a distorted octahedron as shown in **Figure 7.15.** This distortion is illustrated in **Figure 7.15** by means of evaluating the base angles of the octahedron (N4—N1—N2 = 80.47(1)°; N1—N2—N3 = 99.19(1)°; N2—N3—N4 = 99.38(1)° and N3—N4—N1 = 80.07(1)°) and the angle between the trans water molecules and the metal centre (O1—Zr—O2 = 161.68(1)°, **Table 7.4**)

Table 7.4: Selected bond distances, angles and torsion angles of [(Zr(pbp)(H_2O)$_2$]NO_3.MeOH (Zr_1a) [Å and °].

Selected Bond Lengths (Å)			
Zr—O1	2.0418(3)	N1—C1	1.3423(2)
Zr—O2	2.0474(3)	N1—C5	1.3466(1)
Zr—N1	2.0420(2)	N2—C6	1.3238(1)
Zr—N2	1.9620(2)	N2—C7	1.4104(2)
Zr—N3	1.9631(2)	N3—C12	1.4067(2)
Zr—N4	2.0538(2)	N3—C13	1.3230(1)
O3—C6	1.2445(1)	N4—C14	1.3534(1)
O4—C13	1.2430(1)	N4—C18	1.3404(2)
Selected Bite Angles (°)			
N1—Zr—N2	81.48(1)	N2—Zr—N3	82.46(1)
N3—Zr—N4	81.45(1)	O1—Zr—O2	161.68(1)
N4—N1—N2	80.47(1)	N2—N3—N4	99.38(1)
N1—N2—N3	99.19(1)	N3—N4—N1	80.07(1)
Selected Torsion Angles (°)			
N1—N2—N3—N4	8.80(1)	N2—C7—C12—N3	4.84(1)
N1—C5—C6—N2	1.20(1)	N3—C13—C14—N4	4.98(1)

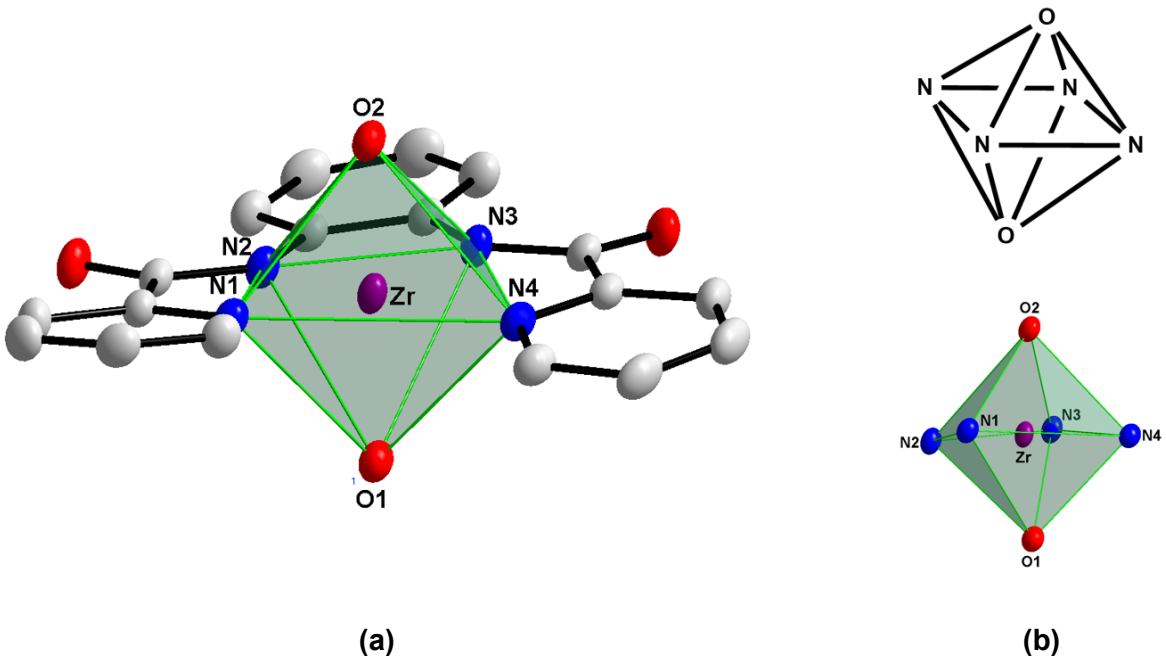

Figure 7.15: (a) Graphic illustration of the octahedron coordination polyhedron of **[(Zr(pbp)(H$_2$O)$_2$]** (**Zr_1a**) **(b) Top**: Illustration of the typical octahedron coordination polyhedron; **Bottom**: Octahedron polyhedron formed by the nitrogen atoms of the *pbp*-tetradentate ligand and the two water molecules (Hydrogen atoms and solvent molecules are omitted for clarity, 50% probability displacement ellipsoids).

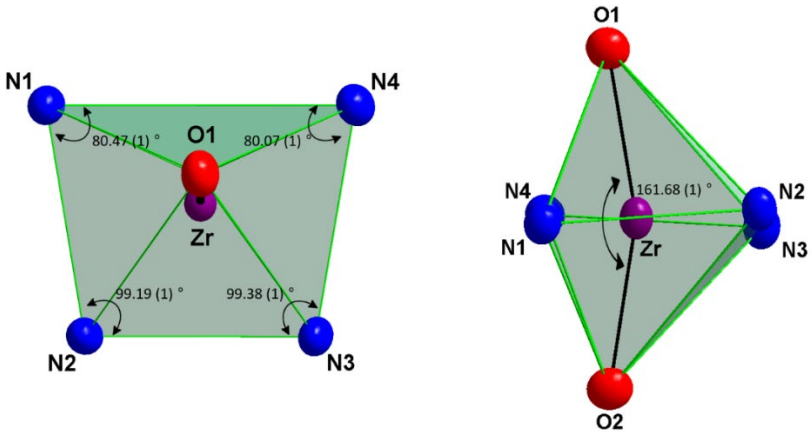

Figure 7.16: A graphical representation of the distortion observed in the octahedron coordination polyhedron. (Carbon and hydrogen atoms are omitted for clarity).

In this structure (**Zr_1a**), the Zr—N bond distances range from 1.9620(2) to 2.0538 Å, with an overall average of 2.00(2) Å (**Table 7.4**). The average N—Zr—N bite angle is found to be 80.80(1)°.

When constructing an equatorial plane through the Zr(III) metal centre and the coordinated *N* atoms of the *pbp* ligand, it is observed that all the atoms lie either in or just slightly off this plane, **Figure 7.17**. The measured N—C—C—N torsion angles of the ligand frame facing the N—Zr—N bite angles are found to range from 1.20(1)° to 4.98(1)° (**Table 7.4**), indicating very little deviation from the planarity of the ligands themselves.

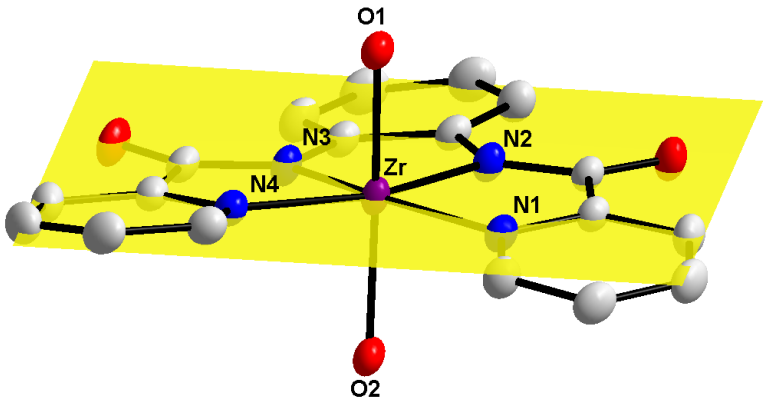

Figure 7.17: A graphical representation of the coordinated *pbp* ligands coordinated to Zr(III), showing the planarity of the N—N'—N'—N donor atom set and the puckering of the ligand backbone (Carbon and hydrogen atoms are omitted for clarity).

The dihedral angle between the central phenyl ring and the two picoline rings are calculated as 12.00(2)° and 7.15(1)° (**Figure 7.18**), while the dihedral angle between the two picoline rings is calculated as 14.04(2)° (**Figure 7.19**).

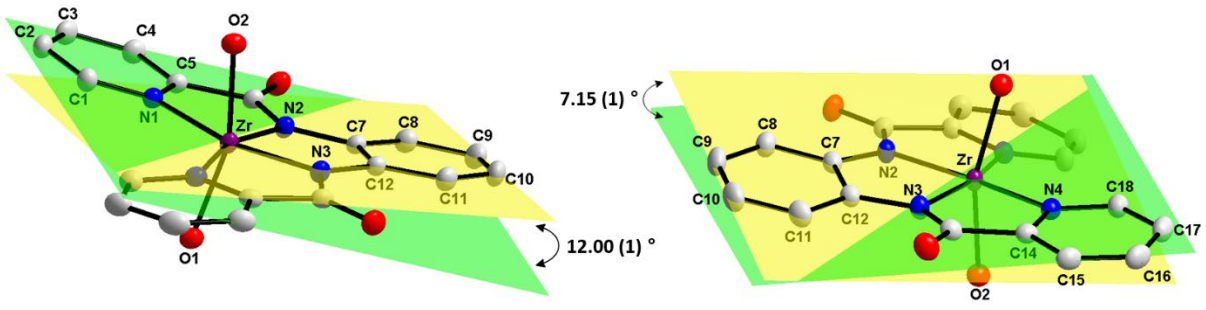

(a) **(b)**

Figure 7.18: A graphical representation that displays the planarity and the dihedral angle between the central phenyl plane (C7-C8-C9-C10-C11-C12) and **(a)** *picoline ring1* (N1-C1-C2-C3-C4-C5) and **(b)** *picoline ring 2* (N4-C14-C15-C16-C17-C18-C19) at 50 % probability level (*Hydrogen atoms are omitted for clarity*)

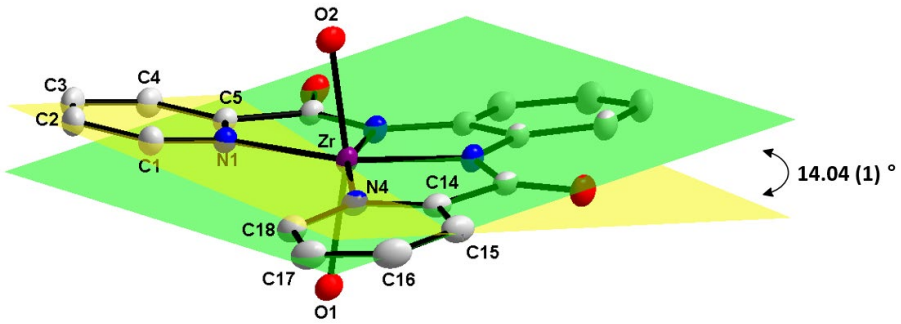

Figure 7.19: A graphical representation that displays the the dihedral angle between *picoline ring1* (N1-C1-C2-C3-C4-C5) and *picoline ring 2* (N4-C14-C15-C16-C17-C18-C19) at 50 % probability level (*Hydrogen atoms are omitted for clarity*)

Weak O-H···O and C-H···O hydrogen bonding interactions are observed and contribute to the stability of the crystal structure. All the bond distances and angles of these interactions are listed in **Table 7.5** and **Figure 7.20** illustrates these interactions. The packing diagram of the crystal structure displays a "head-to-tail" packing fashion in vertical layers along the *b*-axis as shown in **Figure 7.21**.

Table 7.5: Hydrogen-bond geometry for $[Zr(pbp)(H_2O)_2]NO_3 \cdot CH_3OH$ (Zr_1a) (Å, °)

D—H···A	d(D—H)	d(H···A)	d(D···A)	D—H···A
O1—H1A···O3'	0.85	1.84	2.681(2)	173
O1—H1B···O7	0.85	1.89	2.713(2)	163
O2—H2A···O5	0.85	1.80	2.644(2)	169
O2—H2B···O4"	0.85	1.81	2.654(2)	174
O5—H5···O8""	0.8(4)	2.11(4)	2.850(2)	152
O5—H5···O7""	0.81 (4)	2.40(4)	3.093(2)	145
C15—H15···O8"'	0.95	2.52	3.145(2)	124
C17—H17···O5"""	0.95	2.41	3.349(3)	169

Symmetry code: (i) 3/2-x, 1/2+y, z; (ii) 3/2-x, -1/2+y, z; (iii) 3/2-x, 1-y, 1/2+z; (iiii) x, 1/2-y, 1/2+z; (iiiii) 2-x, 1-y, 1-z.

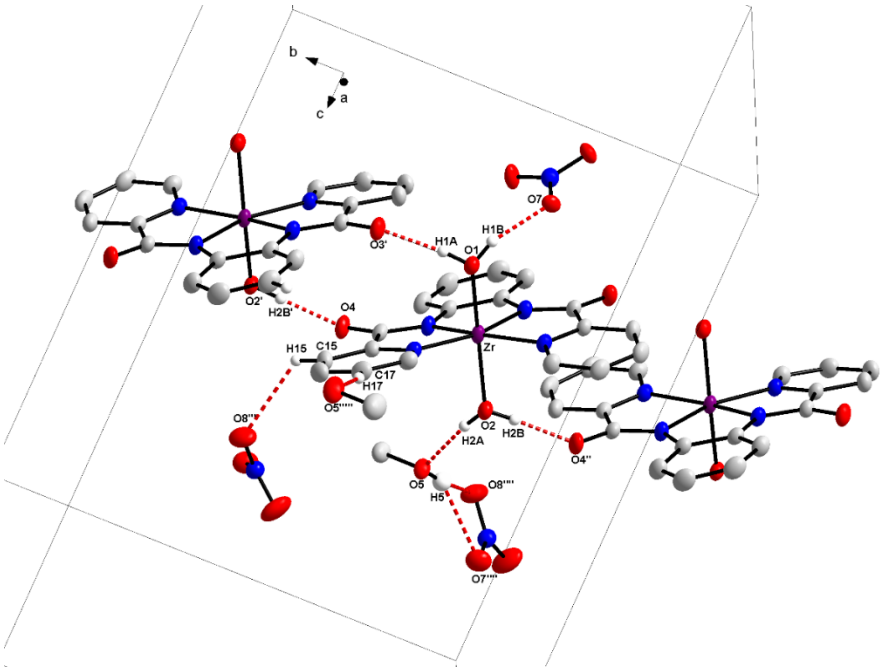

Figure 7.20: Molecular structure of $[Zr(pbp)(H_2O)_2]NO_3 \cdot CH_3OH$, displaying O-H···O and C-H···O hydrogen bonding interactions at 50 % probability level). Hydrogen atoms that are not part of the interactions are omitted for clarity.

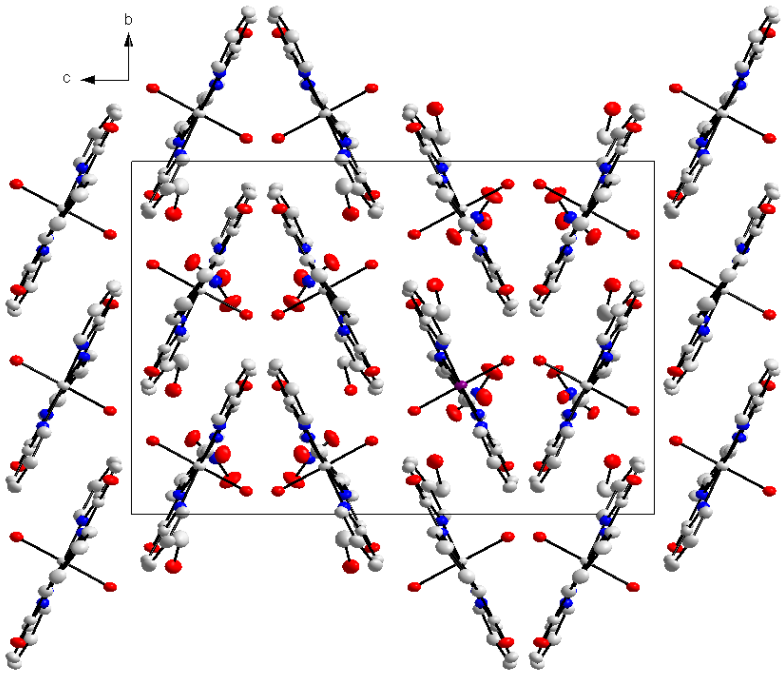

Figure 7.21: Graphical representation of molecular packing within the unit cell for the title compound (**Zr_1a**), showing "*head-to-tail*" packing fashion in vertical layers along the *b*-axis. Solvent and hydrogen atoms omitted for clarity, 50% probability displacement ellipsoids.

7.6. Discussion

Two novel complexes have been investigated and described thus far in the preceding sections (**Figure 7.22**). The general structural parameters, bond distances and angles from the various complexes are given **Table 7.6.** As described in **Chapter 3**, these complexes' synthesis seems to afford these types of compounds with relative ease and with the added advantage is that no special manipulations during synthesis are needed, as described in literature.[23,24,25,26] Therefore, this approach is much more cost-effective, environmentally friendly, and ideal to further a separation study.

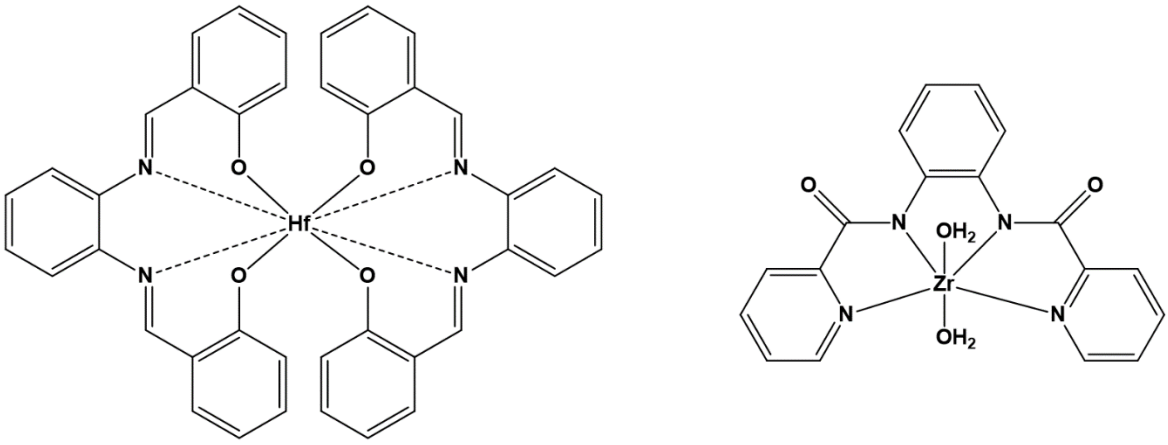

(a) **(b)**

Figure 7.22: The chelated hafnium complexes discussed in this single crystal X-ray diffraction chapter **(a)** [Hf(salophen)$_2$], **(b)** - [Zr(pbp)(H_2O)$_2$].

[23] M. L. Illingsworth, B. P. Cleary, A. J. Jensen, L. J. Schwartz & A. L. Rheingold, *Inorg. Chim. Acta,* **207**, 147, 1993.
[24] H. Zhu, M. Wang, K. Jin, D. Dai, L.Sun & C. Chen, *Transition Met. Chem*., **30**, 517 ,2005.
[25]L. He, S.R. Wagner, M. L. Illingsworth, A. J. Jensen, G. P. Yap & A. L. Rheingold, *Chem. Mater.,* **9**, 3005, 1997.
[26] B. E. Klamm, C. J. Windorff, C. Celis-Barros, M. L.Marsh, D. S. Meeker & T. E. Albrecht-Schmitt, *Inorg.Chem*., **57**, 15389, 2018.

Table 7.6: Cell and structure overview of the hafnium and zirconium complexes presented herein.

Crystal Complex	**[Hf(salophen)$_2$],**	**[Zr(pbp)(H$_2$O)$_2$].**
Crystal system	Triclinic	Orthorhombic
Space group	$P\bar{1}$	*Pbca*
Coordination Polyderon		
Type	Square-antiprismatic	Octahedron
Isomer	C_2-corner side clipped	trans
Avg. bending distortion (°)	22.72(10)	161.68(1)
Avg. rotation distortion (°)	49.56(7)	—
Selected Bond Lengths (Å)		
M—O1	2.055(2)	2.0418(3)
M—O2	2.077(2)	2.0474(3)
M—O3	2.070(2)	—
M—O4	2.095(2)	—
M—N1	2.410(2)	2.0420(2)
M—N1	2.398(2)	1.9620(2)
M—N3	2.379(2)	1.9631(2)
M—N4	2.423(2)	2.0538(2)
Bond Angles (°)		
N1—M—N2	68.14(8)	81.48(1)
N2—M—N3	—	82.46(1)
N3—M—N4	66.91(8)	81.45(1)
N1—M—O1	74.28(7)	—
N2—M—O2	74.43(8)	—
N3—M—O3	74.38(8)	—
N4—M—O4	73.78(7)	—
O1—M—O2	143.15(7)	161.68(1)

The first complex presented, in this chapter **(Hf_3a), (Figure 7.22(a))**, involves an eight-coordinated hafnium(IV) metal centre, where two salophen tetradentate ligands are coordinated to the metal centre. The second complex described **(Zr_1a), (Figure 7.22(b))**, is a six-coordinated zirconium complex, where the asymmetric unit consists of a zirconium(III) metal centre coordinated to the four nitrogen atoms of the *pbp*-tetradentate ligand and two water molecules *trans* to each other. Both these structures are very similar in relation to bond lengths and angles to polymorphic -and isomorphic structures found in literature.[27]

In this regard, a more detailed comparative relation study of these hafnium and zirconium complexes, and additional structures will be presented in **Chapter 8**. Properties such as steric bulk and electronic properties of the Hf(IV)-*β*-diketonate complexes will be correlated to various aspects such as complex stability and structural effects.

7.7. Conclusion

By considering all of the structural detail discussed in this and previous chapters, some conclusions are attempted with regard to all these endeavours of identifying the solid-state tendencies of zirconium and hafnium complexes containing multidentate-ligands.

Firstly, it is a well-known fact that eight coordinated zirconium and hafnium complexes, in general, always show a square-antiprismatic coordination polyhedron. Thus, as was found for the complexes in **Chapter 4**, **5** and **6,** the eight coordinated hafnium complex, discussed in this chapter, also favours a square-antiprismatic coordination polyhedron. However, the six coordinated (assumed) zirconium(III) complex, discussed above, formed an octahedron as coordination polyhedron around the metal centre, as would be expected for any normal six coordinated metal complex.

[27] M. Mandal, V. Ramkumar & D. Chakraborty, *Polym. Chem.*, **10**, 3444, 2019.

This suggests that zirconium and hafnium have a certain preference for the chelation sites of the coordinating atoms, regardless of the steric properties of the ligands as a whole.[28]

To conclude, this chapter forms part of an overarching crystallographic investigation on different *N*- and *O*-donating multidentate ligands coordination to zirconium and hafnium metal centres. A comprehensive discussion of all the complexes evaluated during this crystallographic study, will be presented in the following chapter, **Chapter 8**, including the two structures presented here. The comparative nature of this subdivision will allow for a better evaluation of the effect that subtle changes on the coordinating ligands may have on the solid-state properties of the compounds.

[28] J. A. Viljoen. (2009). *Speciation And Interconversion Mechanism Of Mixed Halo And O,O- And N,O- Bidentate Ligand Complexes Of Hafnium*, M.Sc. Dissertation, University of the Free State, South Africa.

Chapter 8

Evaluation and Structural Correlation of Hafnium(IV) Bi- and Multidentate Ligand Complexes

---

8.1. Introduction

In the four preceding chapters, important emphasis has been placed on elaborate but concise structural identification of various hafnium complexes containing *O,O'* – and *N,O*-bidentate, and *O,N,N,O*-tetradentate ligand systems. As was discussed in **Chapter 2**, a complete understanding of these compounds' solid-state behaviour was deemed necessary for proper correlation studies, with the intent of identifying subtle nuances within the structural features that might be exploited in future separation studies.

However, to effectively assess all the structural data presented in this PhD study, a comparison of relevant structural aspects of these metal complexes needs to be taken into consideration. Therefore, the general sub-foci when discussing hafnium complexes are the following:

1. **Ligand systems considered:**
    a. *N,O*-bidentate ligands (Oxine type ligands) [**Chapter 4** and **5**];
    b. *O,O'-β*-diketone ligands (Acac type ligands) [**Chapter 6**];
    c. *N,N',O,O'* –and *N,N',N',N*-tetradentate ligands [**Chapter 7**].
        i. *Since no polymorphic, isostructural nor similar hafnium type complexes, containing N,N',N',N*-tetradentate ligand (bpbH_2), *are*

found in literature[1], this ligand system will not be discussed and correlated in this chapter

2. **Metal coordination number** – The number of coordinated atoms to the metal centre (*number of ligands (L) surrounding the metal (M)*).

3. **Coordination geometry** (*coordination polyhedra*) – Defining the arrangement of the ligands around the metal centre.

4. **Nature of specific bond lengths and bond angles** - Characteristics observed in bond length and bond angle comparisons.

5. **Packing/stabilisation** – Describing specific influencers of hydrogen bonding interaction, π-π-interactions and solvent molecules.

6. **Distortions observed** – As defined by general ideal geometries for six-and eight coordination.

With these factors in mind, a comparative evaluation of the presented hafnium solid-state structures will be discussed and summarised.

[1] Cambridge Structural Database (CSD) Version 5.42, November 2020 update. C. R. Groom, I. J. Bruno, M. P. Lightfoot & S. C. Ward, *Acta Cryst.*, **B72**, 171, 2016.

8.2. Inter-Structural Evaluation of Hafnium(IV) N,O-Bidentate (Oxine) Ligand Complexes

The crystallographic studies in the previous chapters focused on the modification of the electronic and steric properties of 8-hydroxyquinoline as ligand for further potential application in separation studies, or, more specifically:

(i) electronic influences of electron-withdrawing substituents (halo moieties,) *vs.* electron-donating substituents (methyl moieties) on the 5th and/or 7th position of the quinoline back-bone when coordinated to hafnium(IV) metal centers (**Figure 8.1**);

(ii) Spacial effects induced exhibited by the substituents on the outer periphery of the metal complexes.

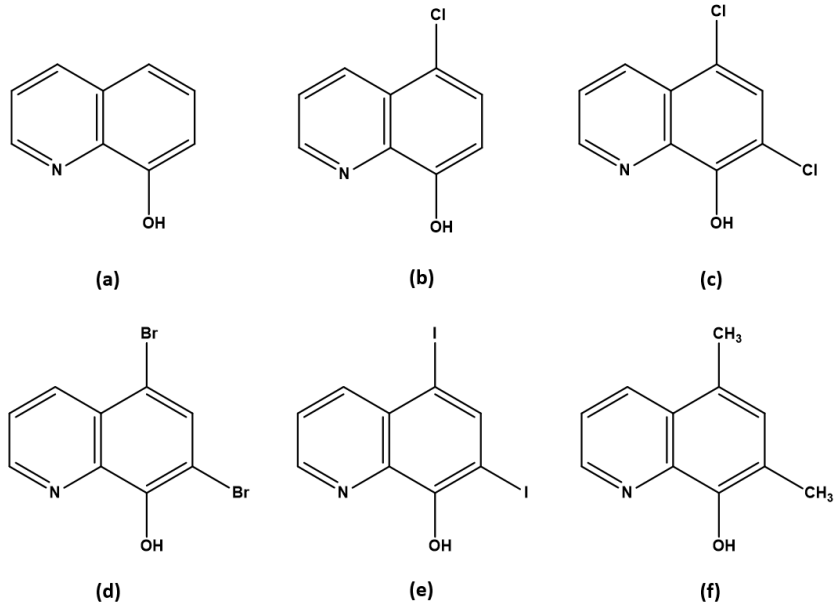

Figure 8.1. Graphical representation of the quinoline/oxine ligands employed in synthesis of hafnium(IV) complexes. **(a)** 8-hydroxyquinoline (OxH), **(b)** 5-Chloro-8-hydroxyquinoline (5-ClOxH), **(c)** 5,7-Dichloro-8-hydroxyquinoline (diClOxH), **(d)** 5,7-Dibromo-8-hydroxyquinoline (diBrOxH), **(e)** 5,7-Diiodo-8-hydroxyquinoline (diIOxH), **(h)** 5,7-Dimethyl-8-hydroxyquinoline (diMeOxH).

Therefore, this section contains a detailed evaluation of presented hafnium(IV) complexes containing non- and substituted 8-hydroxyquinoline ligands, as well as the correlation of each structure with similar hafnium structures from literature. A detailed evaluation and correlation study with similar *zirconium* complexes will be discussed in **Chapter 9**.

A search conducted on the Cambridge crystallographic database[1] (CSD) revealed that there are only six crystal structures in literature where 8-hydroxyquinoline (OxH) is coordinated to a hafnium metal centre. However, after refining the CSD search to search for eight-coordinated hafnium complexes containing 8-hydroxyquinoline, only four structures are available in the literature. Interestingly, these four structures have already been presented in **Chapter 4** and **Chapter 5** and were thus reported *at the UFS research facility and by the author of this PhD study*, demonstrating how little is known about these complexes' solid-state behaviour, and highlighting the relevance of this crystallographic study.

With these factors in mind, a comparative evaluation of the presented hafnium solid-state characteristics, typical of the coordination mode(s) and carefully selected distortion descriptors are summarised in **Table 8.1**. In general, with the larger group of structurally characterised complexes available from this study in particular, a more expanded set of descriptors can now be formulated, relevant to this extended series of hafnium(IV) complexes containing oxine-type ligands.

Table 8.1: Selected crystallographic characteristics, bond lengths and angles of hafnium(IV) - oxine complexes.

Compound	$[Hf(Ox)]_4 \cdot 2(C_7H_8)$ Hf_1a	$[Hf(diBrOx)_4] \cdot 3DMF$ Hf_1e	$[Hf(diClOx)_4] \cdot 3DMF$ Hf_1d	$[Hf(5\text{-}ClOx)]_4 \cdot 2(C_7H_8)$ Hf_1b	$[Hf(diMeOx)_4] \cdot 2DMF$ Hf_1h	$[Hf(diIOx)_4] \cdot DMF$ Hf_1f
Reference	§4.4	§5.5	§5.4	§4.5	§4.6	§5.6
Crystal system	Triclinic	Monoclinic	Monoclinic	Monoclinic	Monoclinic	Triclinic
Space group	$P\bar{1}$	$P2_1/c$	$P2_1/c$	$C2/c$	$P2_1/c$	$P\bar{1}$
Unit cell dimensions: *a, b, c* (Å)	11.3323(5), 12.5539(5), 15.7126(7)	9.600(1), 38.598(2), 13.622(1)	22.429(2) 15.789(1), 28.335(2)	26.967(7), 21.304(5), 18.665(5)	9.978(2), 16.059(3), 28.509(5)	15.208(4), 17.490(5), 20.262(4)
***α, β, γ* (°)**	69.746(2), 69.700(2), 75.787(2)	90, 98.672(2), 90	90, 113.853(2), 90	90, 130.746(5), 90	90, 101.582(1), 90	71012(4), 89.84(5), 89.76(3)
Volume (Å^3)	1946.79(14)	4989.6 (4)	9269.1(11)	8214(4)	4475.2(15)	5099.4(12)
Z	2	4	8	4	4	2
Geometrical Isomer	*twofold rotated*	*twofold rotated*	*twofold rotated*	*twofold rotated*	*twofold rotated*	*twofold rotated*
Coordination Polyhedra	Sq-Anti prismatic	Sq-Anti prismatic	Sq-Anti prismatic	Sq-Anti prismatic	Sq-Anti prismatic	Sq-Anti prismatic
& Isomer	D_2-corner	D_2-corner	D_2-corner	D_2-corner	D_2-corner	D_2-corner
Avg. Bending (°) [a]	15.17(6)	5.10(9)	4.38(8)	6.11(7)	0	1.62(4)
Avg. Rotation (°) [b]	49.15(8)	48.15(7)	47.34(9)	45.20(11)	44.42(9)	41.97(10)
Avg. Hf–N (Å)	2.3976(2)	2.399(3)	2.3856(2)	2.4035(3)	2.398(2)	2.397(15)
Avg. Hf–O (Å)	2.0951(2)	2.088(3)	2.0985(2)	2.0974(2)	2.098(2)	2.099(14)
Avg. N–Hf–O (°)	70.95(9)	70.70(10)	70.85(8)	70.65(9)	70.19(9)	70.33(4)

(a) Defined as (x˚+ y˚)/2, see ***Figure 8.2(c)***; **(b)** defined as (x˚+ y˚)/2, see ***Figure 8.2(d)***.

A number of general observations come to the fore from **Table 8.1** and are illustrated in **Figure 8.2**.

(i) *Tetrakis*(oxinato)metal complexes do not show any particular preference towards a specific space group, although the lower symmetry crystal systems (monoclinic and triclinic) were the only ones observed.

(ii) However, with regards to the coordination environment around the metal centre, all the oxine complexes favour a distorted square-antiprismatic geometry (***D_2-corner-clipped isomer,*** **Figure 8.2 (a)**) with a minimal distortion towards dodecahedral geometry.

(iii) Furthermore, it is observed that each coordinated ligand is duplicated by an opposite facing ligand by *ca*. 180° rotation through the hafnium metal centre. Although these ligands do not lie in a flat plane opposite one another, it is clear that all the ligands are chelated to the metal centres with a ***twofold rotated isomer*** as illustrated in **Figure 8.2 (b).**

(iv) In addition, although not completely consistent, there are seemingly two rough tendencies emerging when considering the ***average bending*** and ***average rotation*** as presented in **Table 8.1**:

(a) The average ***bending*** varies from ca. 15° for the unmodified Ox ligand, to around ca. 4-6° for the 'smaller halido' (Cl, Br) substituents, to only ca. 0-1° for the larger substituents (I, Me);

(b) Similarly, although less prominent, the average ***rotation*** decreases from ca. 49° for the unmodified Ox ligand, to around ca. 45-48° for the 'smaller halido' (Cl, Br) substituents, to only ca. 42-44° for the larger substituents (I, Me).

This suggests a relationship between substituents on the outer periphery and the relative distortion of the polyhedron.

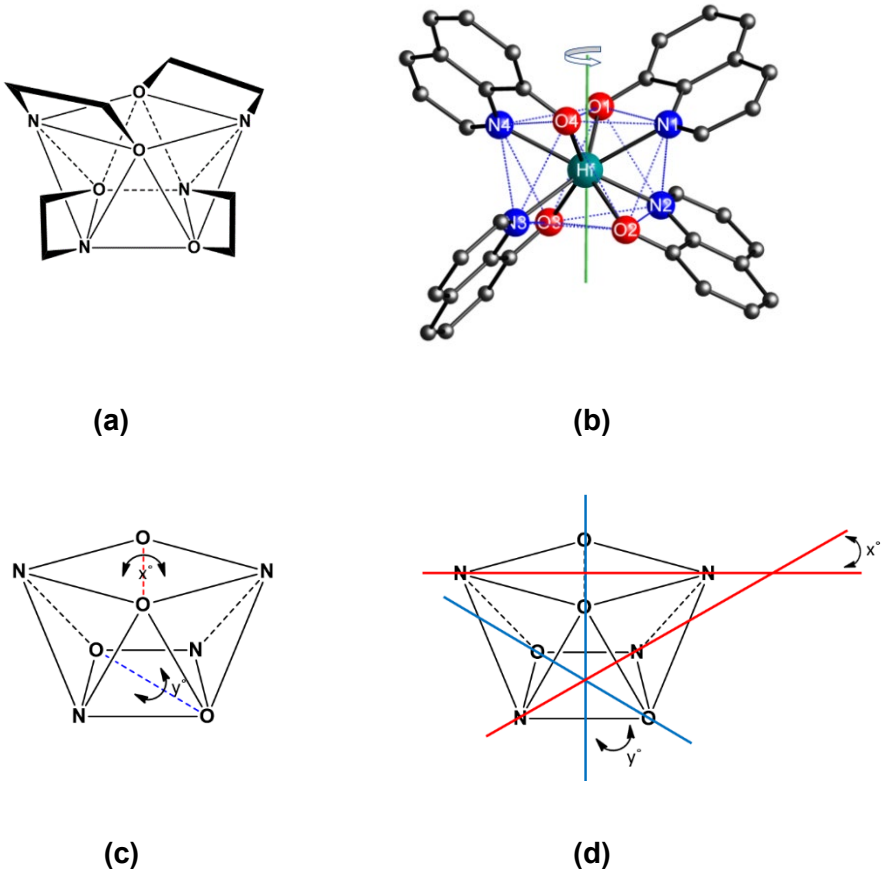

Figure 8.2. Graphical illustration of **(a)** Coordination ***D*$_2$-isomer** as defined for *tetrakis*(oxinato)metal complexes exhibiting a square antiprismatic coordination polyhedron and **(b)** Coordinate ox-ligand arrangement around the metal centre when considering the *N*- and *O*- coordination sites; ***pseudo two-fold rotated isomer***; **(c)** average bending distortion defined as (x˚+ y˚)/2; and **(d)** averaged rotation distortion defined as (x˚+ y˚)/2 for *tetrakis*-(oxinato)metal complexes exhibiting a small distortion towards dodecahedral geometry.

The behaviour observed above (although limited to only six similar *N,O*-bidentate ligands) allows for some *speculation/prediction* regarding general solid-state behaviour of hafnium(IV) *N,O*-bidentate ligand complexes. Hoard and Silverton[2] have reported some six decades ago that metal(IV) *O,O'*-bidentate ligand complexes, in particular the *tetrakis*(*β*-diketone)hafnium(IV) complexes, prefer the square-antiprismatic coordination mode. Now the same conclusion can be made

[2] J. L. Hoard & J. V. Silverton; *Inorg.Chem.,* ***2***, 235, 1963.

for *N,O*-bidentate ligand complexes, or at the very least for oxine-complexes in general, with small variations in the geometric descriptors, see **Table 8.1.**

When comparing the various bond lengths and bite angles of the data currently available, the average Hf—N and Hf—O bond lengths are 2.397(5) Å and 2.096(5) Å, respectively, with an average N—Hf—O bite angle of 70.61(8) °. With respect to other structural properties, all the hafnium oxine complexes are, in general, very similar, although the seemingly systematic tendencies in the ***rotation*** and ***bending*** were pointed out above. The only noticeable difference between the oxine complexes are the large antiprismatic geometry distortion found in $[Hf(Ox)_4]•2(C_7H_8)$, with a bending -and rotation distortion of 5.17(6) and 49.15(8)°, respectively, even though 8-hydroxyquinoline is the least steric ligand in this study. However, the large distortion is assumed to be due to packing effects but more importantly, to the π-π stacking between coordinated ligands and the C—H···O hydrogen bonding interaction observed between the complex and one of the toluene solvate molecules (**Figure 8.3**; see also **Par. 4.2**).

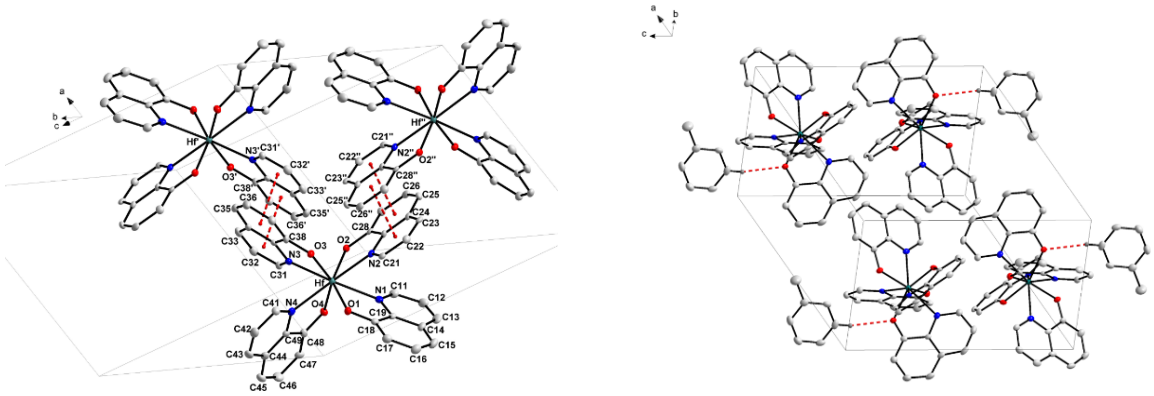

(a) **(b)**

Figure 8.3. Partial structures $[Hf(Ox)_4]$ (**Hf_1a) (a)** showing π-π-stacking between the quinoline ligands coordinated to the hafnium metal centre; **(b)** indicating the C—H···O hydrogen bonding interaction observed in the unit cell (Hydrogen atoms omitted for clarity, 50% probability displacement ellipsoids).

Finally, the influence of solvate molecules in the effective packing of these organometallic molecules shows that hydrogen bonding between these entities and the coordinated oxine-ligands influences the lattice's stability as a whole. However, the most significant packing stabiliser seems to the π-stacking interactions observed in all structures characterised. In some cases, direct π-π stacking between coordinated ligands are clear ([Hf(ox)$_4$], [Hf(diMeOx) and [Hf(diClOx)$_4$]), while in others halogen-π stacking ([Hf(5-ClOx)$_4$], [Hf(diClOx)$_4$] and [Hf(dilOx)$_4$]) are observed. This stacking dictates the overall stability and arrangement in the crystal lattice as a whole, as is evident from the structural descriptions emphasised above.

8.3. Inter-Structural Evaluation of Hafnium(IV) O,O'–Bidentate (acac type) Ligand Complexes

β-Diketone ligands have now been widely used as classical metal coordination agents in coordination chemistry for more than a century.[3] Ligands of this type act as uni-negative *O,O'*-chelating donors enabling stabilisation of mono- or polynuclear complexes. Furthermore, these *β*-diketones can be readily deprotonated to produce either neutral or charged metal complexed when coordinated to metal ions.[4,5]

2,4-Pentanedione (acetylacetone, acacH) is the simplest *β*-diketone and is generally prepared by a base-catalysed condensation reaction. Claisen described this reaction in 1889, whereby a desired ketone (*acetone)* is reacted with an appropriate acylation reagent (*ethyl acetate*) which is nowadays known as *Claisen condensation.*[6]

[3] A. J. Brock , J. K. Clegg, F. Li & L. F. Lindoy, *Coord. Chem. Rev*. **375**, 106, 2018.
[4] P. A. Vigato, V. Peruzzo & S. Tamburini, Coord. Chem Rev., **253**, 1099, 2009.
[5] D. J. Bray, J. K. Clegg, L. F. Lindoy & D. Schilter, *Adv. Inorg. Chem*., **1**, 59, 2007.
[6] L. Claisen & E. F. Ehrhardt, *Chem. Ber*., **22**, 1009, 1889.

As discussed in **Chapter 1**, an integral part of this project is focused on utilising different readily available acetylacetone (acacH) type ligands with various electron-withdrawing (CF_3-groups) and/or electron-donating (phenyl-groups) substituents on the 1 and 5 position of the ligand's (acacH) back-bone, as illustrated below.

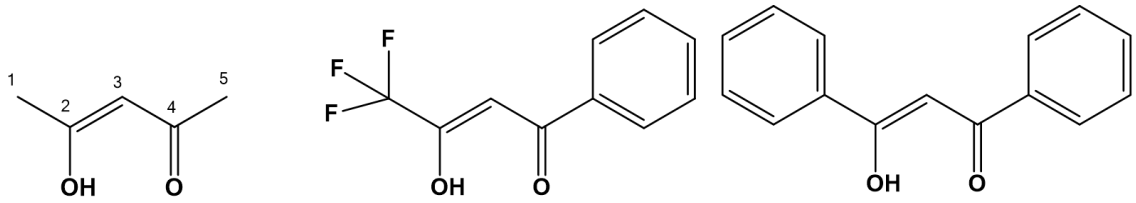

(a) **(b)** **(c)**

Figure 8.4. Graphical representation of **(a)** acetylacetone (acacH); **(b)** 4,4,4-trifluoro-1-phenyl-1,3-butanedione (tfbaH / benzoyltrifluoroacetone, *electron withdrawing*); **(c)** 1,3-diphenyl-1,3-propandione (dbmH / dibenzoylmethane, *electron donating*)

The steric and electronic modification on the back-bone can significantly influence the coordination modes around the hafnium and zirconium metal centre so much that the coordination of the 3rd and 4th acac-ligand complexes can be observed and structurally isolated.[7]

Therefore, this section contains an evaluation of presented hafnium(IV) complexes containing non- and substituted acetylacetone (acac) ligands, as well as the correlation of each structure with similar hafnium structures from literature, see **Table 8.2.** A detailed evaluation and correlation study with similar zirconium complexes will be discussed in **Chapter 9**.

[7] R. M. Lord, J. J. Mannion, A. J. Hebden, A Nako, B. D. Crossley, M. W. McMullon, F. D. Janeway, R. M. Phillips & P. C. McGowan, *ChemMedChem*, **9**, 1136, 2014.

Table 8.2: Selected crystallographic characteristics, bond lengths and angles of hafnium(IV) - acetylacetonate complexes

Compound	$[Hf(OH)(tfba)_3]_2$ •2(DMF) Hf_2b	$[Hf(tfaa)]_4$ •2(C_7H_8)	$[Hf(hfaa)_4]$	$[Hf(acac)]_4$	$[Hf(dbm)_4]$ Hf_2c	$[Hf(OH)(hfaa)_3]_2$ •$(CH_3)CO$
Reference	§6.5	8	9	10	§6.4	11
Crystal system	Monoclinic	Monoclinic	Monoclinic	Monoclinic	Monoclinic	Monoclinic
Space group	$P2_1/c$	$C2/c$	$C2/c$	$C2/c$	$P2_1/c$	$C2/c$
Unit cell dimensions: *a, b, c* (Å)	12.414(1), 19.244(5), 17.503(5)	22.492(15), 8.0642(5), 22.712(2)	15.304(2), 20.072(3), 19.494(5)	21.610(4), 8.354(1), 14.091(2)	24.846(2), 10.224(1), 19.316(1)	22.129(2) 12.410(1), 19.501(2)
***α, β, γ* (°)**	90, 122.94(1), 90	90, 118.211(5), 90	90, 96.16(1), 90	90, 116.321(5), 90	0, 101.62(1), 0	90, 105.197(5), 90
Volume (Å^3)	4805.8(5)	3631(4)	5953(15)	2269(1)	3509(2)	5168(12)
Z	2	4	8	4	4	4
Geometrical Isomer	*twofold rotated*	*twofold rotated*	*twofold rotated*	*twofold rotated*	*twofold rotated*	*twofold rotated*
Coordination Polyhedra	Sq-Anti prismatic	Sq-Anti prismatic	Sq-Anti prismatic	Sq-Anti prismatic	Sq-Anti prismatic	Sq-Anti prismatic
& Isomer	D_2-corner	D_2-corner	C_2-comb.	D_2-corner	D_2-corner	D_2-corner
Avg. Bending (°) [a]	16.38(8)	7.94(8)	4.15(9)	3.67(8)	2.20(1)	18.73(9)
Avg. Rotation (°) [b]	50.34(7)	46.51(5)	45.81(8)	46.21(8)	44.07(9)	47.28(8)
Avg. Hf–O (Å)	2.1943(3)	2.172(15)	2.1645(26)	2.1730(18)	2.1686(4)	2.190(21)
Shortest Hf–O (Å)	2.146(2)	2.1571(13)	2.1396(26)	2.1619(13)	2.1330(3)	2.136(9)
Longest Hf–O (Å)	2.244(2)	2.1933(13)	2.2022(26)	2.1865(16)	2.2000(3)	2.258(9)
Avg. O–Hf–O (°)	74.59(9)	75.61(5)	76.75(10)	75.10(9)	74.74(9)	75.3(5)

(a) Defined as (x˚+ y˚)/2, see **Figure 8.5(c); (b)** defined as (x˚+ y˚)/2, see **Figure 8.5(d).**

[8] J. A. Viljoen, A. Muller & A. Roodt, *Acta Crystallogr.,* **E64,** m838, 2008.
[9] W. F. Schwandt, T. J. Woods & G .S. Girolami, *Acta Crystallogr.*, **E74**, 1182, 2018.
[10] F. Hentschel, V. V. Vinogradov, A. V. Vinogradov, A. V. Agafonov, V. V. Guliants, I. Persson, G. A. Seisenbaeva & V. G. Kessler, *Polyhedron,* **89,** 297, 2015.
[11] J. A .Viljoen, H. G. Visser, A. Roodt & M. Steyn, *Acta Crystallogr.,* **E65,** m1367, 2009.

A number of general observations are again possible when considering the summarised data in **Table 8.2**, and illustrated in **Figure 8.5**:

(i) All hafnium(IV) *β*-diketonato complexes seemingly prefer lower symmetry monoclinic crystal systems with relative low symmetry in the solid-state.

(ii) The coordination environment around the metal centre in all the hafnium *β*-diketonato complexes favour a square-antiprismatic geometry (***D_2-corner-clipped isomer,*** **Figure 8.5**) with a small distortion towards dodecahedral geometry. As mentioned previously, it has been established in literature that hafnium *β*-diketonate complexes, particularly the *tetrakis*(*β*-diketonate)hafnium(IV) complexes, prefer the square-antiprismatic coordination mode.[2]

(iii) Furthermore, it is observed that each coordinated acac-type ligand is duplicated by an opposite facing ligand by *ca*. 180° rotation through the hafnium metal centre. Although these ligands do not lie in a flat plane opposite one another, it is clear that all the ligands are chelated to the metal centres with a ***twofold rotated-isomer*** as illustrated in **Figure 8.5 (b).** The exception is the dinuclear $[Hf(OH)(hfaa)_3]_2.(CH_3)_2CO$, which does not contain four hfaa ligands.

(iv) In addition, similar to the oxine-type complexes described above, although not completely consistent, there are seemingly two rough tendencies emerging when considering the ***average bending*** and ***average rotation*** for the acac-type ligand containing complexes listed in **Table 8.2**:

(a) The average ***bending*** varies from ca. 16° for the *unsymmetric* tbfa ligand, to around ca. 8° for the *symmetric* bis-CF_3 ligand (hfaa), to only ca. 2-4° for the acac and dbm ligands.

(b) Similarly, although less prominent, the average ***rotation*** decreases from ca. 50° for the *unsymmetric* tbfa ligand, to around ca. 46-47° for the hfaa and acac ligands, to only ca. 44° for the larger dbm ligand.

(c) The dinuclear $[Hf(OH)(hfaa)_3]_2.(CH_3)_2CO$ complex is inconsistent with (a) and (b), displaying an average bending of ca. 19°, shows the smallest average rotation of only ca. 43°.

It is clear that similar to the oxine-type ligand complexes, the substituents on the outer periphery of the ligands in the acac-type complexes clearly show an influence on the distortions in the complexes, although different in the sense that there is some indication that the substituents, when equivalent, effects the symmetry potentially different.

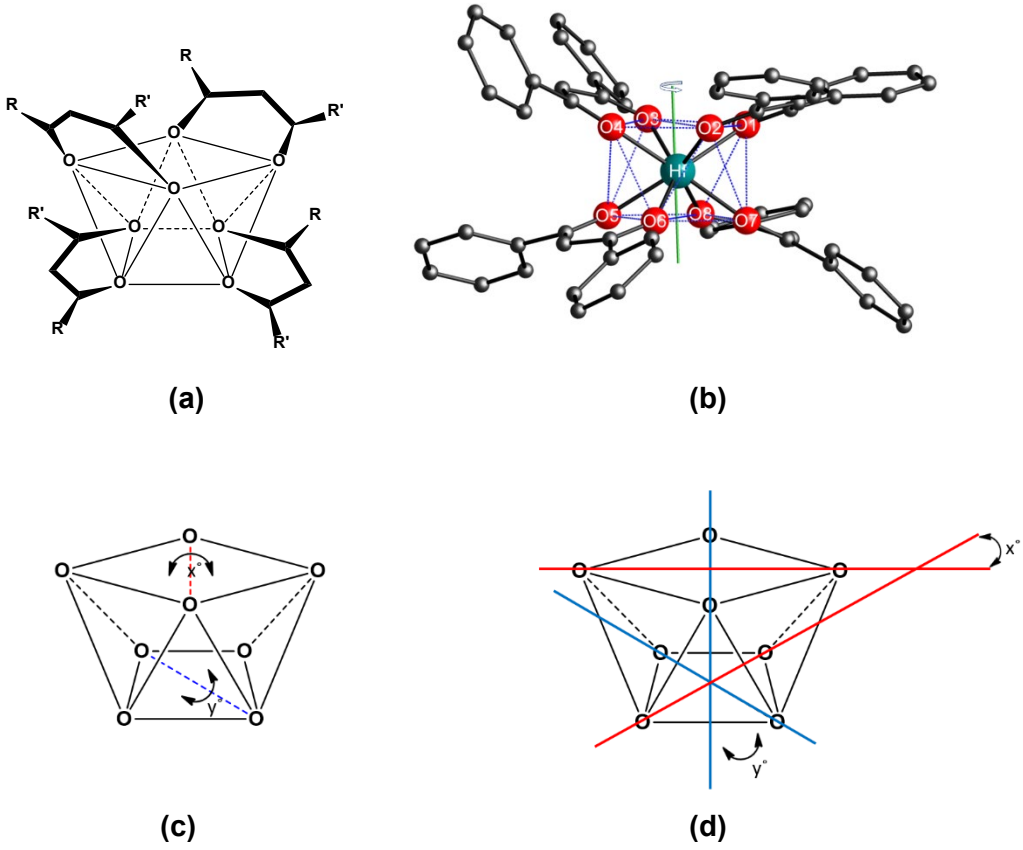

Figure 8.5. Graphical illustration of **(a)** a coordinated D_2-isomer as defined for *tetrakis*-(*β*-diketonate)metal complexes exhibiting a square antiprismatic coordination polyhedron; **(b)** Coordinate acac-ligand arrangement around the metal centre when considering the O,O'-coordination sites; *pseudo two-fold rotated isomer*; **(c)** the average bending distortion defined as (x˚+ y˚)/2; and **(d)** averaged rotation distortion defined as (x˚+ y˚)/2 for *tetrakis*(*β*-diketonato)metal complexes exhibiting a small distortion towards dodecahedral geometry.

When comparing the various bond lengths and bite angles of the data currently available, an average Hf—O bond length of 2.1771 Å and an average O—Hf—O bite angle of 75.35° are obtained. With respect to other structural properties, it is noted that both the binuclear hafnium *β*-diketonato complexes $[Hf(OH)(hfaa)_3]_2$ &

[Hf(OH)(tfba)$_3$]$_2$) display large bending deviations away from the ideal square antiprismatic geometry ([Hf(OH)(hfaa)$_3$]$_2$ = 18.73(9)° & [Hf(OH)(tfba)$_3$]$_2$ = 16.38(8)°). The dimer formation, where hafnium(IV) atoms are bridged by two hydroxo groups, cannot be clearly explained at this stage. It is worth noting that the monomer, [Hf(hfaa)$_4$], and the dimer [Hf(OH)(hfaa)$_3$]$_2$ complexes were both obtained under similar aerobic conditions by mixing $HfCl_4$ and hfaaH in diether ether and toluene, respectively. The solutions were filtered, and the filtrate was taken to dryness under vacuum. However, monomer crystals were obtained *via* sublimation (15 mTorr and 303 K) of the dry product, whereas the dimeric structure was obtained via recrystallisation in acetone at room temperature. Therefore, at this stage, it can only be speculated that the properties of the solvent used (polarity, Bronsted *pKa* value, etc.), or the lack thereof during synthesis and recrystallisation, are contributing factors for the dimer formations observed. With respect to other physical structural characteristics of the *tetrakis*(*β*-diketone)hafnium(IV) complexes are concerned, all aspects are in good comparison to other published structures containing such ligands (**Table 8.2**). All coordination bond lengths are in the average range of 2.1-2.2 Å and bite angles average the standard angle of 74-76 °.

Finally, the influence of solvent molecules in the effective packing of these organometallic molecules shows that hydrogen bonding between these solvent molecules, coordinated acac-ligands and bridging hydroxo-groups influences the lattice stability as a whole. Therefore, the extent of coordination and even the intimate geometry around the metal centre is governed directly by solvent interactions and the hafnium(IV) tending towards a maximum state of coordination, as a preference, or as lowest energy crystallisation state.

8.4. Inter-Structural Evaluation of Hafnium(IV) O,N,N,O-tetradentate Ligand Complexes

Schiff bases are one of the most established ligands in coordination chemistry. Their metal complexes have a variety of biological, medicinal and analytical applications, in addition to their important roles in organic syntheses.[12] Nitrogen and oxygen donor Schiff bases are excellent chelating agents for both transition and non-transition metals and have been heavily utilised for their ability to stabilise metals in various oxidation states and control the behavior of metals during catalysis.[13] Furthermore, the steric and electronic properties of these tetradentate N_2O_2 donor Schiff base ligands are highly modular.

These unique characteristics allow for much broader electronic and steric contributors to organometallic complexes of hafnium and zirconium, yielding valuable information on these metals' chelation preferences. Furthermore, when considering the limited database entries for these types of hafnium and zirconium complexes that have been structurally characterised,[14] it becomes apparent that a crystallographic study of metal complexes containing theses ligand families could shed considerable light on characteristics of complexes and thus on experimental design regarding possible separation studies utilising such ligands.

Therefore, this section contains a detailed evaluation of the presented hafnium(IV) complexes containing two *N,N'*-bis(salicylidene)-1,2-phenylene-diamine (SalophenH_2, **Figure 8.6**) ligands, as well as the correlation of this structure with the only other similar hafnium structure from literature. A detailed evaluation and correlation study with similar zirconium complexes will be discussed in **Chapter 9**.

[12] M. Mandal, V. Ramkumar & D. Chakraborty, *Polym.Chem*., **10**, 3444, 2019.
[13] A. Sahraei, H. Kargar, M. Hakimi, & M. N. Tahir, *Transit. Met. Chem*., **42**, 483, 2017.
[14] B. E. Klamm, C. J. Windorff, C. Celis-Barros, M. L. Marsh, D. S. Meeker & T. E. Albrecht-Schmitt, *Inorg.Chem*., **57**, 15389, 2018.

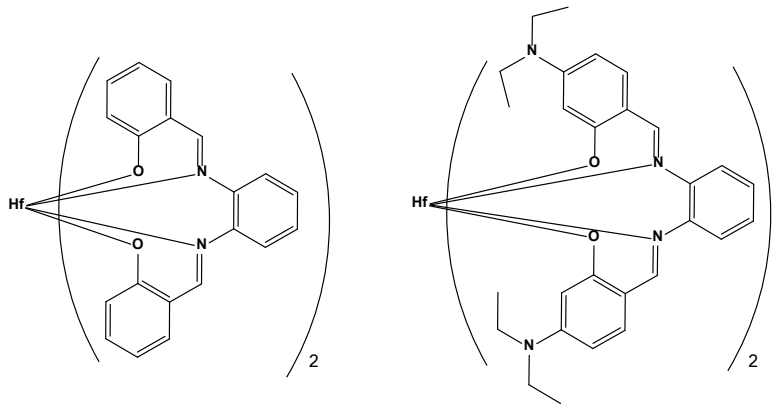

(a) **(b)**

Figure 8.6. Graphical representation of **(a)** bis(N,N'-disalicylidene-1,2-phenylene-diamino) hafnium(IV) **[Hf(salophen)$_2$]** and **(b)** bis[2,2'-(1,2-phenylenebis[(azanylylidene)methylylidene]) bis[5-(diethylamino)phenolato]]-hafnium(IV) **[Hf(eda-salophen)$_2$]**

Table 8.3: Selected crystallographic characteristics, bond lengths and angles of hafnium(IV) - salophen complexes.

Compound	[Hf(salophen)]$_2$•2C$_7$H$_8$ Hf_3a	[Hf(eda-salophen)]$_2$ •THF
Reference	§7.4	14
Crystal system	Triclinic	Monoclinic
Space group	$P\bar{1}$	$P2_1/c$
Unit cell dimensions: *a, b, c* (Å)	10.785(5), 13.969(5), 14.082(5)	14.853(1), 19.6863), 35.692(5)
***α, β, γ* (°)**	84.248(3), 76.052(2), 80.719(5)	90, 91.4(5), 90
Volume (Å^3)	2027.914)	10434.47(15)
Z	1	8
Coordination Polyhedra	Sq-Antiprismatic	Sq-Antiprismatic
& Isomer	C_2-corner & side	D_2-corner
Avg. Bending [a]	22.72(8)	6.61(9)
Avg. Rotation [b]	49.56(8)	47.31(9)
Avg. Hf–O (Å)	2.074(2)	2.110(3)
Avg. Hf–N (Å)	2.403(2)	2.353(3)
Avg. N–Hf–O (°)	74.22(2)	74.968(2)
Avg. N–Hf–N (°)	67.53(2)	66.67(5)

(a) Defined as (x˚+ y˚)/2, see ***Figure 8.2(c)***; **(b)** defined as (x˚+ y˚)/2, see ***Figure 8.2(d)***.

When considering the summarised data in **Table 8.3**, it is evident that hafnium(IV) complexes containing salophen type ligand systems prefer crystal systems with relative low symmetry in solid-state. Furthermore, as was the case for oxine and acac ligand systems, these complexes favour a square-antiprismatic coordination polyhedron with a slight distortion towards dodecahedron geometry. This again suggests that hafnium has a particular preference to form maximum coordinated (eight-coordinated) metal complexes, regardless of the steric properties of the ligands as a whole. However, even though both complexes prefer an antiprismatic polyhedron geometry, **[Hf(salophen)$_2$]** crystalised as a *C_2-corner & side capped* polyhedron isomer, whereas **[Hf(eda-salophen)$_2$]** crystalised in the more predominantly occurring *D_2-corner capped* isomer.

Again, similar to the oxine- and acac-type complexes described above, although not completely consistent, the two rough tendencies when considering the ***average bending*** and ***average rotation*** for the two tetradentate ligands described here, contained in the complexes listed in **Table 8.2**, emerge:

(a) The average ***bending*** decreases from ca. 23° for the *salophen* ligand, to only ca. 7° for the *eda-salophen* ligand.

(b) Similarly, although less prominent, the average ***rotation*** decreases from ca. 50° for the *salophen* ligand, to only ca. 47° for the *eda-salophen* ligand.

This observation again highlights the fact that when larger substituents are seemingly present on the outer periphery of the ligands, a systematic change in distortion at the coordination polyhedron is potentially present.

When comparing the various bond lengths, bite distances and bond angles listed in **Table 8.3** some trends are noticed. As expected, the average Hf—O (2.074(2) Å *vs* 2.110(3) Å) and Hf—N (2.403(2) Å *vs* 2.353(3) Å) bond distances correlate very well with each other. Similar average Hf—O and Hf—N bond lengths have been noted for the hafnium-oxine complexes (Hf—O = 2.096(5) Å and Hf—N = 2.397(5) Å). The average N—Hf—O and N—Hf—N angels for **[Hf(salophen)$_2$]** are 74.22(2) and

67.53(2)°, respectively and compare well with **[Hf(eda-salophen)$_2$]** corresponding angles of 74.968(2) and 66.67(5)°, respectively.

Lastly, the influence of solvate molecules in the effective packing of these organometallic molecules shows that hydrogen bonding between these solvent molecules and coordinated salophen-ligands influences the lattice stability as a whole.

8.5. Conclusion

The essential parameters of the Hf(IV) complexes as described in **Par. 8.2-8.4** are all compared in **Table 8.4**.

Table 8.4: Selected crystallographic characteristics, bond lengths and angles of hafnium(IV) complexes containing *N,O*- and *O,O'*-bidentate, and *O,N,N,O*-tetradentate ligands.

Compound	$[Hf(Ox)]_4$	$[Hf(5\text{-}ClOx)]_4$	$[Hf(diMeOx)_4]$	$[Hf(diClOx)_4]$	$[Hf(diBrOx)_4]$	$[Hf(dilOx)_4]$	$[Hf(acac)]_4$	$[Hf(tfaa)]_4$	$[Hf(hfaa)_4]$	$[Hf(OH)(hfaa)_3]_2$	$[Hf(OH)(tfba)_3]_2$	$[Hf(dbm)_4]$	[Hf(salo-phen)$_2$]
Par	§4.4	§4.5	§4.6	§5.4	§5.5	§5.6	§8.3	§8.3	§8.3	§8.3	§6.5	§6.4	§7.4
Crystal system	Triclinic	Monoclinic	Monoclinic	Monoclinic	Monoclinic	Triclinic	Monoclinic	Monoclinic	Monoclinic	Monoclinic	Monoclinic	Monoclinic	Triclinic
Space group	$P\bar{1}$	*C*2/*c*	*P*2$_1$/*c*	*P*2$_1$/*c*	*P*2$_1$/*c*	$P\bar{1}$	*C*2/*c*	*C*2/*c*	*C*2/*c*	*C*2/*c*	*P*2$_1$/*c*	*P*2$_1$/*c*	$P\bar{1}$
Unit cell Dimensions: a, b, c (Å)	11.332(1), 12.554(1), 15.713(1)	26.967(7), 21.304(5), 18.665(5)	9.978(2), 16.059(3), 28.509(5)	22.429(2) 15.789(1), 28.335 2)	9.600(1), 38.598(2), 13.622(1)	15.208(4), 17.490(5), 20.262(4)	21.610(4), 8.354(1), 14.091(2)	22.492(15), 8.0642(5), 22.712(2)	15.304(2), 20.072(3), 19.494(5)	22.129(2) 12.410(1), 19.501(2)	12.414(1), 19.244(5), 17.503(5)	24.846(2), 10.224(1), 19.316(1)	10.785(5) 13.969(5), 14.082(5)
Z	2	4	4	8	4	2	4	4	8	4	2	4	1
Coordination Polyhedra	Sq-Anti prismatic	Sq-Anti prismatic	Sq-Anti prismatic	Sq-Anti prismatic	Sq-Anti prismatic	Sq-Anti prismatic	Sq-Anti prismatic	Sq-Anti prismatic	Sq-Anti prismatic	Sq-Anti prismatic	Sq-Anti prismatic	Sq-Anti prismatic	Sq-Anti prismatic
& Isomer	D_2-corner	D_2-corner	D_2-corner	D_2-corner	D_2-corner	D_2-corner	D_2-corner	D_2-corner	C_2-comb.	D_2-corner	D_2-corner	D_2-corner	C_2-comb
Avg. Bending (°)	15.17(6)	6.11(7)	0	4.38(7)	5.1(8)	1.62(9)	3.67(8)	7.94(8)	4.15(9)	18.73(9)	16.38(8)	2.20(1)	22.72(8)
Avg. Rotation (°)	49.15(8)	45.20(11)	44.42(9)	47.34(9)	48.15(7)	41.97(10)	46.21(8)	46.51(5)	45.81(8)	47.28(8)	50.34(7)	44.07(9)	49.56(7)
Hf–O (Å)	2.0951(2)	2.0974(2)	2.098(2)	2.0985(2)	2.088(3)	2.099(14)	2.1730(18)	2.172(15)	2.1645(26)	2.190(21)	2.1943(3)	2.1686(4)	2.074(2)
Hf–N (Å)	2.3976(2)	2.4035(3)	2.398(2)	2.3856(2)	2.399(3)	2.397(15)	-	-	-	-	-	-	2.403(2)
Hf bite angle (°)	70.95 (9)	70.65(9)	70.19(9)	70.85(8)	70.70(10)	70.33(12)	75.10(9)	75.61(5)	76.75(10)	75.30(5)	74.59(9)	74.74(9)	74.22(2)

By considering all of the single x-ray structural data discussed in this chapter, some conclusions are possible with regard to all these endeavours of identifying the solid-state properties of hafnium(IV) complexes containing various *N,O*- and *O,O'*-multidentate ligands.

Some general trends, or tendencies of trends, are discussed below.

However, it is worth noting that there is a clear general trend between the ***average* rotation** and the ***average bending*** within the coordination polyhedron. This is highlighted in **Figure 8.7.** below. The exception comes from the dinuclear species, $[Hf(OH)(hfaa)_3]_2$, illustrated to the far right in **Figure 8.7** below.

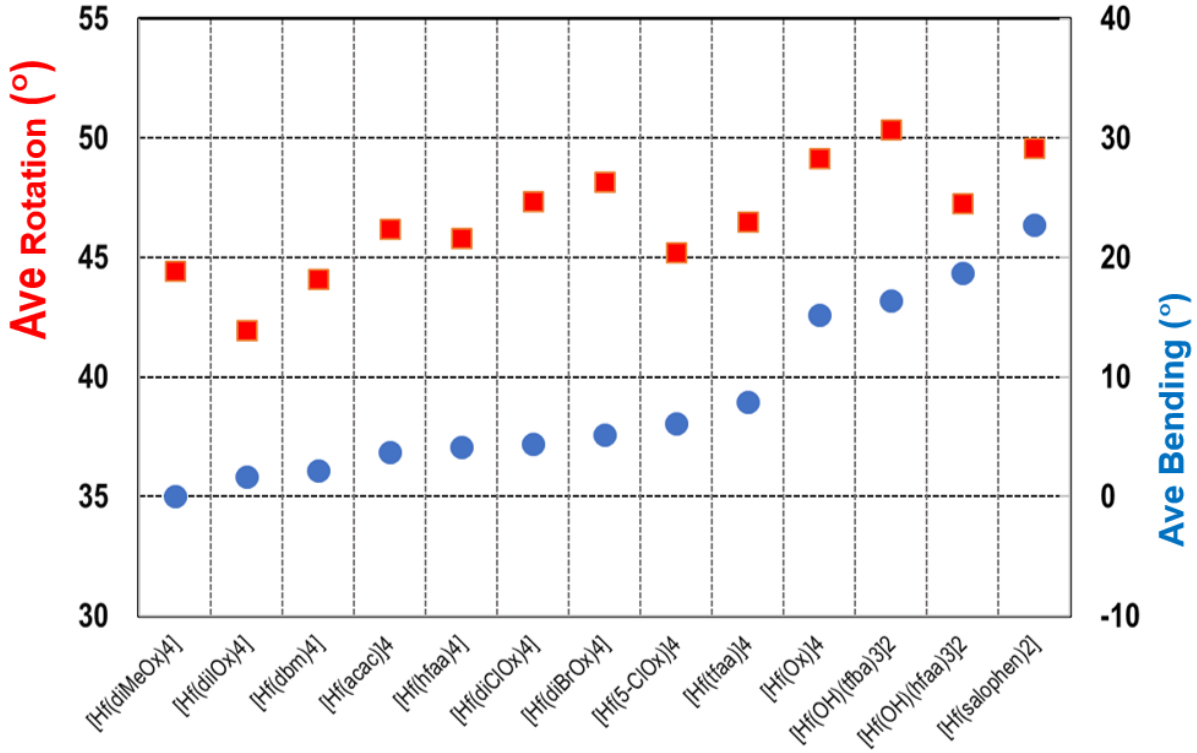

Figure 8.7. Correlation between the *average rotation* (red) and *average bending* (blue) within the coordination polyhedral within the compounds listed in **Table 8.4**.

Additional trends are also observable as far as general structural aspects (crystal systems, bond lengths and bite angles) and crystal lattice packing stabilisation (π-stacking, hydrogen and halogen bonding) are considered.

Firstly, the comparison of the data available, the average Hf—O and Hf—N bond lengths are 2.128(26) Å and 2.398(5) Å, respectively, yielding average N—Hf—O and O—Hf—O bite angles of 70.61(14)° and 75.19(12)°, respectively.

Furthermore, it is observed that eight coordinated hafnium metal complexes show a particular preference towards low symmetry crystal systems, e.g. triclinic and monoclinic systems. With regard to the expected lattice/crystalline network stabilisation, it has become apparent in these systems to expect a certain degree of π-π- and/or halogen-π staking to be present.

Moreover, it has been shown, elaborately in **Chapters 4-7,** that *N,O-, O,O'-* and O,*N,N,O*-donating ligands (oxine, acac and salophen type ligands) chelate around hafnium metal centres in a square antiprismatic polyhedral fashion, with slight distortions towards dodecahedral geometries in all cases studied. This suggests that chelation geometry is mainly governed by intermolecular forces rather than that of the ligands internal geometries and properties.

Even though square antiprismatic coordination geometries are always observed, with very comparable physical properties (bond lengths and bite angles), there are some aspects of these structures' geometries that display different tendencies. Firstly, the range of coordination isomers (***D_2, C_2 & D_4, see*** **Par. 2.5**) defined for each structure indicates that there are aspects of hafnium(IV) ligand chelation that allows for manipulation to obtain chemically different metal complexes. It was noted that by modifying recrystallisation techniques, especially for the hafnium *β*-diketonato complexes, it is possible to produce either monomeric or dinuclear complexes. However, with regard to the explicit affinity of a ligand to finally coordinate in any specific isomer, no broad generalisation or argument can be made with the data available at this stage, and lastly, it seems, ***steric bulk*** does not influence this trend either, when considering the data presented in **Table 8.4**. Although not definitively proven, the significance here is that these observations can assist a great deal when designing/choosing ligands for future separation studies.

In **Chapter 9**, a detailed evaluation and correlation study with similar zirconium complexes will be discussed with regard to the nature of these hafnium complexes. With comparable structures between hafnium and zirconium, a broader understanding of the solid-state behaviours of these organometallic complexes can be drawn.

Chapter 9

Evaluation and Structural Correlation of Hafnium(IV)- and Zirconium(IV) Bi- and Multidentate Ligand Complexes

---

9.1. Introduction

In the previous **Chapter 8**, significant emphasis has been placed on concise structural identification and correlation of **hafnium** complexes containing *O,O'*- and *N,O*-bidentate, and *O,N,N,O*-tetradentate ligand systems. As discussed therein, a broad understanding of these compounds' solid-state behaviour is necessary for correlation studies, with the intent of discovering subtle nuances within these crystal structures that might be exploited in future separation and/or extraction studies. With this in mind, the main aim here is to identify specific ligands that can manipulate solid-state structural properties to induce different physical or chemical behaviours for both **zirconium** and **hafnium**.

However, to effectively assess all the structural data presented in this PhD study and corresponding zirconium co-project,[1] a comparison of certain structural aspects of these metal complexes needs to be taken into consideration. Therefore, the general sub-foci when discussing hafnium and zirconium complexes are the following:

[1] M. Steyn; *A Solid State and Mechanistic Study of Multidentate Ligand Zirconium(IV) Halido Complexes*, Ph.D. Dissertation (**2014**), University of the Free State, South Africa.

1. **Ligand systems considered:**
    a. *N,O*-bidentate ligands (Oxine type ligands) [**Chapter 4** and **5**];
    b. *O,O'-β*-diketone ligands (Acac type ligands) [**Chapter 6**];
    c. *N,N',O,O'* –and *N,N',N',N*-tetradentate ligands [**Chapter 7**].
        i. *Since no similar hafnium type complex of the form of* [(Zr(bpb)(H_2O)$_2$] *are found in literature*[2]*, this ligand system complex will not be discussed and correlated in this chapter.*

2. **Metal coordination number** – The number of coordinated atoms to the metal centre (*number of ligands (L) surrounding the metal (M); i.e. monodentate, bidentate, or tetradentate*).

3. **Coordination geometry** (*coordination polyhedra*) – Defining the arrangement of the ligands around the metal centre.

4. **Nature of specific bond lengths and bond angles** - Characteristics observed in bond length and bond angle comparisons.

5. **Packing/stabilization** – Describing specific influencers of hydrogen bonding interaction, π-π-interactions and solvent molecules.

6. **Distortions observed** – As defined by general ideal geometries for eight coordination.

With these factors in mind, a comparative evaluation of the presented hafnium, and related zirconium, solid-state structures will be discussed and summarised.

[2] Cambridge Structural Database (CSD) Version 5.42, November 2020 update. C. R. Groom, I. J. Bruno, M. P. Lightfoot & S. C. Ward, *Acta Cryst.*, **B72**, 171, 2016.

9.2. Inter-Structural Evaluation of Hafnium(IV)- and Zirconium(IV) N,O-Bidentate (Oxine) Ligand Complexes

The crystallographic studies in the previous chapters focused on the modification of the electronic and steric properties of 8-hydroxyquinoline as ligand (forming five-membered metallacycles) for further potential application in separation and/or extraction studies, but more specifically:

(i) electronic influences of electron-withdrawing substituents (halo moieties,) *vs.* electron-donating substituents (methyl moieties) on the 5th and/or 7th position of the quinoline back-bone when coordinated to hafnium(IV) metal centers (**Figure 9.1**);

(ii) Spacial effects induced by the substituents on the outer periphery of the metal complexes.

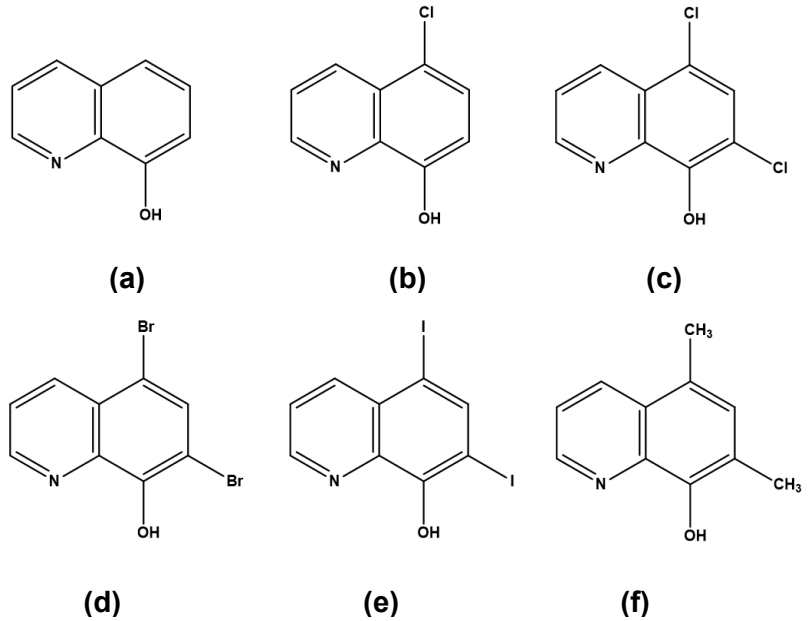

Figure 9.1: Graphical representation of the quinoline/oxine ligands employed in synthesis of hafnium(IV)– and zirconium(IV) complexes. **(a)** 8-hydroxyquinoline (OxH), **(b)** 5-Chloro-8-hydroxyquinoline (5-ClOxH), **(c)** 5,7-Dichloro-8-hydroxyquinoline (diClOxH), **(d)** 5,7-Dibromo-8-hydroxyquinoline (diBrOxH), **(e)** 5,7-Diiodo-8-hydroxyquinoline (diClOxH), **(f)** 5,7-Dimethyl-8-hydroxy-quinoline (diMeOxH).

Therefore, this section contains a detailed evaluation of presented hafnium(IV) complexes containing non- and substituted 8-hydroxyquinoline ligands (**Figure 9.1**) and the correlation with similar zirconium(IV) structures from the corresponding zirconium co-project[1] and structures from literature.

As mentioned in **Chapter 8**, a search conducted on the Cambridge crystallographic database[2] (CSD) revealed that this PhD and the preceding study[3] had contributed all known eight-coordinated hafnium complexes containing 8-hydroxyquinoline single-crystal structures in literature. Furthermore, after refining the CSD search to search for eight-coordinated zirconium complexes containing 8-hydroxyquinoline, only three available structures could be found in the literature. Interestingly, two of these structures have already been reported in the corresponding zirconium co-project,[1] yet again, demonstrating how little is known about these complexes' solid-state behaviour, and highlighting the relevance of this crystallographic study.

Thus, here a comparative evaluation of the available zirconium(IV) and hafnium(IV) solid-state characteristics, typical of the coordination mode(s) and carefully selected distortion descriptors, as summarised in **Table 9.1**, is done. In general, with the more significant group of structurally characterized complexes available at this stage, an expanded set of descriptors can now be formulated, relevant to the extended series of zirconium(IV) and hafnium(IV) complexes containing oxine-type ligands.

[3] J. A. Viljoen; *Speciation And Interconversion Mechanism Of Mixed Halo And O,O- And N,O-Bidentate Ligand Complexes Of Hafnium*, M.Sc. Dissertation (**2009**), University of the Free State, South Africa.

Table 9.1: Selected crystallographic characteristics, bond lengths and angles of hafnium(IV) and zirconium(IV) - oxine complexes.

Compound	$[Hf(diMeOx)_4]$	$[Hf(dilOx)_4]$	$[Zr(5ClOx)]_4$	$[Hf(diClOx)_4]$	$[Zr(diMeOx)_4]$	$[Hf(diBrOx)_4]$	$[Hf(5ClOx)]_4$	$[Zr(diClOx)_4]$	$[Zr(Ox)]_4$	$[Hf(Ox)]_4$
Reference	§4.6	§5.6	1	§5.4	4	§5.5	§4.5	5	6	§4.4
Crystal system	Monoclinic	Triclinic	Monoclinic	Monoclinic	Orthorhombic	Monoclinic	Monoclinic	Monoclinic	Triclinic	Triclinic
Space group	$P2_1/c$	$P\bar{1}$	$P2_1/c$	$P2_1/c$	$Pca2_1$	$P2_1/c$	$C2/c$	$C2/c$	$P\bar{1}$	$P\bar{1}$
Geometrical Isomer	*twofold rotated*	*twofold rotated*	*twofold rotated*	*twofold rotated*	*twofold rotated*	*twofold rotated*	*twofold rotated*	*twofold rotated*	*twofold rotated*	*twofold rotated*
Coordination Polyhedra	Sq-Anti prismatic	Sq-Anti prismatic	Sq-Anti prismatic	Sq-Anti prismatic	Sq-Anti prismatic	Sq-Anti prismatic	Sq-Anti prismatic	Sq-Anti prismatic	Sq-Anti prismatic	Sq-Anti prismatic
Polyhedra Isomer	D_2-corner	D_2-corner	D_2-corner	D_2-corner	D_2-corner	D_2-corner	D_2-corner	D_2-corner	D_2-corner	D_2-corner
Avg. Bending (°) [a]	0	1.62(4)	3.54(10)	4.38(8)	4.66(9)	5.10(9)	6.11(7)	11.90(8)	12.83 (1)	15.17(6)
Avg. Rotation (°) [b]	44.42(9)	41.97(10)	45.27(13)	47.34(9)	43.39(6)	48.15(7)	45.20(11)	47.44(7)	48.15(8)	49.15(8)
Avg. Hf–N (Å)	2.398(2)	2.397(15)	2.427(4)	2.3856(2)	2.418(3)	2.399(3)	2.4035(3)	2.452(2)	2.420(2)	2.3976(2)
Avg. Hf–O (Å)	2.098(2)	2.099(14)	2.100(3)	2.0985(2)	2.104(2)	2.088(3)	2.0974(2)	2.095(2)	2.106(2)	2.0951(2)
Avg. N–Hf–O (°)	70.19(9)	70.33(4)	70.65(9)	69.77(7)	70.16(8)	70.85(8)	69.97(14)	70.95(9)	70.70(10)	70.43(7)

(a) Defined as (x˚+ y˚)/2, see ***Figure 9.4(a)***; **(b)** defined as (x˚+ y˚)/2, see ***Figure 9.4(b).***

[4] M. Steyn, H. G. Visser & A. Roodt, *Acta Cryst.,* **E68,** m1344, 2012.
[5] M. Steyn, H. G. Visser & A. Roodt, *Z.Kristallogr. New Cryst.Struct.,* **228,** 413, 2013.
[6] M. Steyn, H. G. Visser & A. Roodt; *J. S. Afr. Inst. Min. Metall.* ***113*** , 105, 2013.

A number of general observations come to the fore from **Table 9.1**, as further illustrated in **Figure 9.2** to **Figure 9.4**:

(i) *Tetrakis*(oxinato)metal complexes do not show any particular preference for a specific space group. Furthermore, no specific crystal systems are preferred either when considering the wide range of monoclinic, triclinic and orthorhombic examples presented.

(ii) However, with regards to the coordination environment around the metal centre, all the oxine complexes favour a distorted square-antiprismatic geometry (***D_2-corner-clipped isomer,*** **Figure 9.2**) with a fairly small distortion towards dodecahedral geometry. Therefore it can be theorized that hafnium(IV) and zirconium(IV) complexes containing oxine-type ligands should yield a square-antiprismatic geometry around the metal centre.

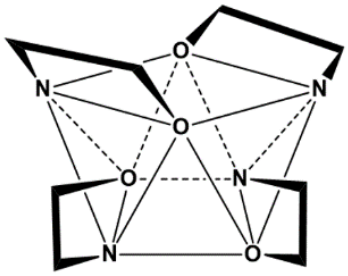

Figure 9.2: Graphical illustration of coordination ***D_2*-isomer** as defined for *tetrakis*(oxinato)-metal complexes exhibiting a square antiprismatic coordination polyhedron.

(iii) Furthermore, it is observed that each coordinated ligand is duplicated by an opposite facing ligand by *ca*. 180° rotation through the metal centre. Although these ligands do not lie in a flat plane opposite one another, it is clear that all the ligands are chelated to the metal centres with a geometry defined as a ***twofold rotated-isomer*** as illustrated **Figure 9.3.**

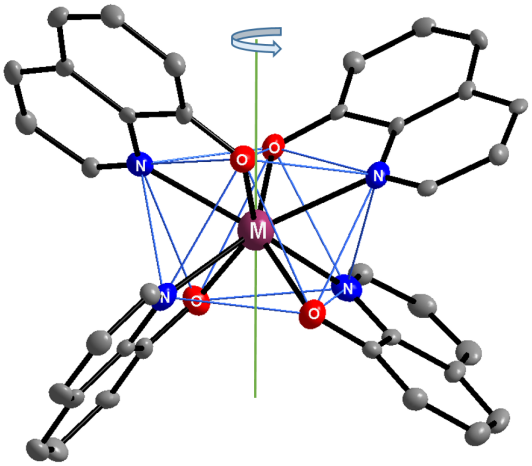

Figure 9.3: Graphical illustration of the coordinate oxine-ligand arrangement around the metal centre when considering the *N*- and *O*- coordination sites; *pseudo two-fold rotated isomer*.

(iv) In addition, although not completely consistent, there are seemingly two approximate tendencies emerging when considering the ***average bending*** and ***average rotation distortions*** as presented in **Table 9.1** (*as defined by* **Figure 9.4**).

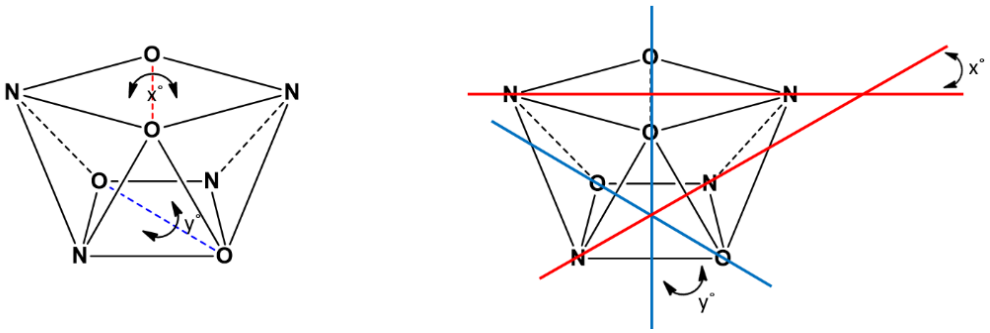

Figure 9.4: Graphical illustration of **(a)** average bending distortion defined as (x˚ + y˚)/2; and **(b)** averaged rotation distortion defined as (x˚ + y˚)/2 for *tetrakis*-(oxinato)metal complexes exhibiting a small distortion towards dodecahedral geometry.

(a) The average ***bending*** decreases from ca. 15° for the unmodified Ox ligand, to around ca. 4-6° for the 'smaller' chloro substituents, to only ca. 0-5° for the larger methyl substituents;

(b) Similarly, although less prominent, the average ***rotation*** decreases from ca. 47-51° for the highly electron with-drawing di-halido Ox ligands, to around ca. 45-46° for the single halido(Cl) substituents, to only ca. 43° for the more steric and electron donating methyl substituents.

This suggests an approximate relationship between substituents on the outer periphery and the relative distortion of the polyhedron.

In respect to the overarching comparisons of the data presented above, the average M—O and M—N bond lengths are 2.099(5) Å and 2.413(5) Å, respectively, with an average O—M—N bite angle of 70.37(15)˚ (M = Hf and Zr). Moreover, a comparison between the M—O bond lengths in the hafnium(IV) and zirconium(IV) complexes shows that these are generally similar. However, the Hf—N bond tends to be *ca*. 0.05 Å shorter than the corresponding Zr—N bonds within the complexes. Apart from these differences, most other structural properties compared, all the metal-oxine complexes are in general similar.

With regard to the solvent molecules and the effective packing of the metal-oxine molecules, one may conclude that hydrogen bonding between solvates and coordinated oxine ligands influences the stability of the crystal lattice as a whole. Furthermore, all of the complexes display similar intermolecular interactions to some extent, with π-π- and halogen-π staking being most frequent within the crystal lattices and, therefore, dictating the overall arrangement and stability in the crystal lattice as a whole.

9.3. Inter-Structural Evaluation of Hafnium(IV)– and Zirconium(IV) O,O'–Bidentate (acac type) Ligand Complexes

It was indicated in **Chapter 1** that an integral part of this project focused on utilizing different readily available acetylacetone (acacH) type ligands with various electron-withdrawing (CF_3-groups) and/or electron-donating (phenyl groups) substituents on the 1 and 5 position of the ligand (acacH) back-bone, as illustrated in **Figure 9.5**. These ligands form six-membered metallacycles.

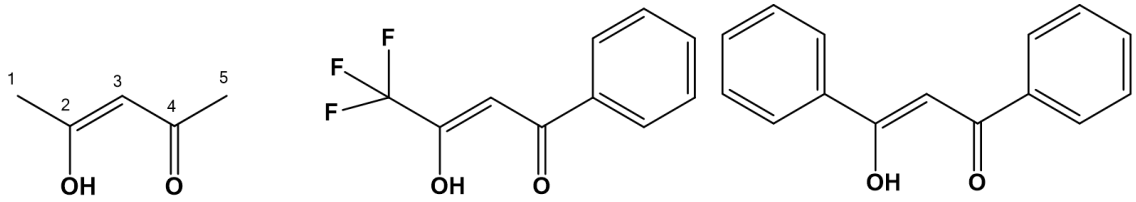

(a) **(b)** **(c)**

Figure 9.5: Schematic structure of acac-type ligands containing different substituents: **(a)** acetylacetone (acacH); **(b)** - 4,4,4-trifluoro-1-phenyl-1,3 butanedione (tfbaH, electron withdrawing) and **(c)** – 1,3-diphenyl-1,3-propandione (dbmH, electron donating).

The electronic and steric modifications on the ligand back-bone may influence the coordination mode(s) around the hafnium and zirconium metal centres so that it might be exploited as a novel extractive compound for the separation of hafnium and zirconium from solution.

Therefore, this section contains a detailed evaluation of presented hafnium(IV) complexes containing various acetylacetone-type (acac) ligands, as well as the correlation of these structures with similar hafnium(IV) and zirconium(IV) structures from literature. In general, with the more significant group of structurally characterized complexes available at this stage, an expanded set of descriptors can now be formulated, relevant to the extended series of zirconium(IV) and hafnium(IV) complexes containing acac-type ligands.

With these factors in mind, a comparative evaluation of the available zirconium(IV) and hafnium(IV) solid-state characteristics, typical of the coordination mode(s) and carefully selected distortion descriptors are summarised **Table 9.2.**

A number of general observations are again possible when considering the data as summarised in **Table 9.2**:

(i) All hafnium(IV) and zirconium(IV) *β*-diketonato complexes seemingly prefer lower symmetry monoclinic crystal systems with relative low symmetry in the solid-state.

(ii) The coordination environment around the metal centre in all the hafnium(IV) and zirconium(IV) *β*-diketonato complexes favour a square-antiprismatic geometry (***D_2-corner-clipped isomer,*** **Figure 9.6(a)**), with a slight distortion towards dodecahedral geometry, except for [Zr/Hf(hfaa)$_4$], which favours the ***C_2-mixed bonding square antiprismatic isomer*** **(Figure 9.6(b)**. As mentioned previously, contrary to this observation, it has been suggested in literature that hafnium(IV) and zirconium(IV) *β*-diketonate complexes, particularly the *tetrakis*(*β*-diketonato) complexes, prefer the square-antiprismatic coordination mode.[7]

(a) **(b)**

Figure 9.6: Graphical illustration of coordination **(a) D_2-isomer** and **(b) C_2-isomer** as defined for (*β*-diketonato)-metal complexes exhibiting a square antiprismatic coordination polyhedron.

[7] J. L. Hoard & J. V. Silverton; *Inorg.Chem.,* ***2***, 235, 1963

Table 9.2: Selected crystallographic characteristics, bond lengths and angles of hafnium(IV) and zirconium(IV) - acetylacetonato complexes.

Compound	$[Zr(dbm)_4]$	$[Hf(dbm)_4]$	$[Zr(acac)]_4$	$[Hf(acac)]_4$	$[Hf(hfaa)_4]$	$[Zr(hfaa)_4]$	$[Hf(tfaa)]_4$	$[Zr(tfaa)]_4$	$[[Hf(OH)(tfba)_3]_2$	$[Hf(OH)(hfaa)_3]_2$
Reference	1	§6.4	8	8	9	10	11	12	§6.5	13
Crystal system	Monoclinic	Monoclinic	Monoclinic	Monoclinic	Monoclinic	Monoclinic	Monoclinic	Monoclinic	Monoclinic	Monoclinic
Space group	$P2_1/c$	$P2_1/c$	$C2/c$	$C2/c$	$P2_1/c$	$P2_1/c$	$C2/c$	$C2/c$	$P2_1/c$	$C2/c$
Coordination Polyhedra & Isomer	Sq-Anti prismatic D_2-corner	Sq-Anti prismatic D_2-corner	Sq-Anti prismatic D_2-corner	Sq-Anti prismatic D_2-corner	Sq-Anti prismatic C_2-mixed	Sq-Anti prismatic C_2-mixed	Sq-Anti prismatic D_2-corner	Sq-Anti prismatic D_2-corner	Sq-Anti prismatic D_2-corner	Sq-Anti prismatic D_2-corner
Avg. Bending (°) [a]	1.86(3)	2.20 (1)	3.66(4)	3.68(8)	4.15(9)	5.03(13)	7.94(8)	7.95(9)	16.38(8)	18.73(9)
Avg. Rotation (°) [b]	43.99(7)	44.07 (9)	46.12(3)	46.21(8)	45.11(8)	45.30(9)	46.51(5)	45.15 (7)	50.34(7)	47.28(8)
Avg. M–O (Å)	2.178(1)	2.1686(4)	2.1863(9)	2.1730(18)	2.1645(26)	2.1753(45)	2.172(15)	2.1841(20)	2.1943(3)	2.190(21)
Shortest M–O (Å)	2.141(1)	2.1330(3)	2.1738(8)	2.1619(13)	2.1396(26)	2.1434(40)	2.1571(13)	2.1633(15)	2.146(2)	2.136(9)
Longest M–O (Å)	2.213(2)	2.2000 (3)	2.1990(1)	2.1865(16)	2.2022(26)	2.226(41)	2.1933(13)	2.2078(15)	2.244(2)	2.258(9)
Avg. O–M–O (°)	74.53(9)	74.74 (9)	74.86(1)	75.10(5)	76.75 (10)	76.13(11)	75.61(5)	75.52(6)	74.59(9)	75.30(5)

(a) Defined as (x˚+ y˚)/2, see ***Figure 9.7(a)*** ; **(b)** defined as (x˚+ y˚)/2, see ***Figure 9.7(b).***

[8] F. Hentschel, V. V. Vinogradov, A. V. Vinogradov, A. V. Agafonov, V. V. Guliants, I. Persson, G. A. Seisenbaeva & V. G. Kessler, *Polyhedron*, **89**, 297, 2015.

[9] W. F. Schwandt, T. J. Woods & G. S. Girolami, *Acta Cryst.*, **E74**, 1182, 2018.

[10] K. V. Zherikova, N. B. Morozova, N. V.Kurat'eva, I. A. Baidina, P. A. Stabnikov & I. K. Igumenov, *Zh. Strukt. Khim. (Russ.)(J.Struct.Chem.)*, **48**, 555, 2007.

[11] J. A. Viljoen, A. Muller & A. Roodt, *Acta Cryst.*, **E64**, 838, 2008.

[12] M. Steyn, A. Roodt & G. Steyl, *Acta Cryst.,* **E64**, m827, 2008.

[13] J. A. Viljoen, H. G. Visser, A. Roodt & M. Steyn, *Acta Cryst.*,**E65**, 1367, 2009.

(iii) In addition, similar to the oxine-type complexes described earlier, although not completely consistent, there are seemingly a very approximate tendency emerging when considering the ***average bending*** distortions (**Figure 9.7**) for the acac-type ligand containing complexes listed in **Table 9.2**:

(a) The average ***bending*** varies from ca. 8° for the *unsymmetric* tfaa ligands, to only ca. 2-4° for the *symmetric* acac, hfaa and dbm ligands.

(b) The average ***rotation*** stays relatively constant between 44-46° for both *symmetric and unsymmetric ligands,* showing that the substituents on the outer periphery of the ligands in the acac-type complexes have little influence on the rotation distortions within these complexes.

(c) The dinuclear, $[[Hf(OH)(tfba)_3]_2$ and $[[Hf(OH)(hfaa)_3]_2$, complexes are inconsistent with **(a)** and **(b)**, both displaying larger than average bending and rotation distortions of ca. 17° and ca. 47-50°**,** respectively.

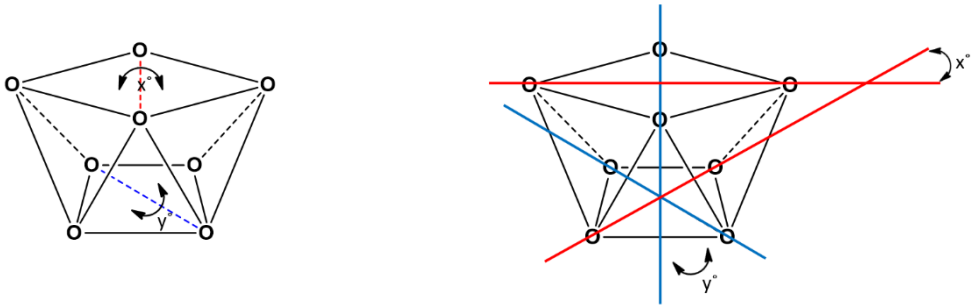

(a) **(b)**

Figure 9.7: Graphical illustration of **(a)** the average bending distortion defined as (x˚+ y˚)/2; and **(b)** averaged rotation distortion defined as (x˚+ y˚)/2 for the *tetrakis*(*β*-diketonato)metal complexes exhibiting a small distortion towards dodecahedral geometry.

It was noticed that, similar to the oxine-type ligand complexes, the substituents on the outer periphery of the ligands in the acac-type complexes show an influence on some of the distortions in the complexes, although different in the sense that there is some indication that the substituents, when equivalent, effects the symmetry potentially different.

In respect to the overarching comparisons of the data presented above, the average M—O bond lengths are 2.179(5) Å with an average O—M—O bite angle of 75.31(35)˚ (M = Hf(IV) and Zr(IV)). Moreover, a comparison between hafnium(IV) and zirconium(IV) bond lengths shows that the Zr—O bonds tend to be ca. 0.01 Å longer than the Hf—O bonds of the corresponding ligand system.

However, with regards other structural properties, it was importantly noted that binuclear hafnium *β*-diketonato complexes $[Hf(OH)(hfaa)_3]_2$ and $[Hf(OH)(tfba)_3]_2$) were isolated, whereas no evidence of any dimer formation could be found in the literature for zirconium *β*-diketonato complexes. The dimer formation, where hafnium(IV) atoms are bridged by two hydroxo groups, cannot be appropriately explained at this stage. It is worth noting that the monomers, $[Zr(hfaa)_4]$ and $[Hf(hfaa)_4]$, and the dimer $[Hf(OH)(hfaa)_3]_2$ and $[Hf(OH)(tfba)_3]_2$ complexes were all obtained under similar aerobic conditions by mixing $Zr/HfCl_4$ with the corresponding ligand in either diether ether and toluene or dimethylformamide (DMF), respectively. The solutions were filtered, and the filtrate was taken to dryness under vacuum. However, monomer crystals were obtained *via* sublimation (15 mTorr and 303 K) of the dry product, whereas the dimeric structure was obtained via recrystallization in acetone ($[Hf(OH)(hfaa)_3]_2$) and DMF ($[Hf(OH)(tfba)_3]_2$) at room temperature. But, neither $[[(Zr(OH)(hfaa)_3]_2$ nor $[Zr(hfaa)_4]$ crystals could be isolated *via* solvent recrystallization. Therefore, at this stage, it can only be speculated that the properties of the solvent used (polarity, Bronsted *pKa* value, etc.), or the lack thereof during synthesis and recrystallization, are contributing factors for the dimer formations observed.

With respect to other physical structural characteristics of the *tetrakis*-(*β*-diketonato)hafnium(IV) complexes are concerned, all aspects are in good comparison to other published structures containing such ligands (**Table 9.2**).

Finally, the influence of solvent molecules in the effective packing of these organometallic molecules shows that hydrogen bonding between these solvent molecules, coordinated acac-ligands and bridging hydroxo-groups influences the lattice stability as a whole. Therefore, the extent of coordination and even the intimate geometry around the metal centre is governed directly by solvent interactions and the hafnium(IV) tending towards a maximum state of coordination, as a preference, or as lowest energy crystallization state.

9.4. Conclusion

The essential parameters of the Hf(IV) and Zr(IV) complexes as described in **Par. 9.2** and **Par 9.3** are all combined in **Table 9.3**.

Table 9.3: Selected crystallographic characteristics, bond lengths and angles of hafnium(IV) and zirconium(IV) complexes containing *N,O* -and *O,O'*-bidentate, and *O,N,N,O*-tetradentate ligands.

Compound	Reference	Crystal system	Space group	Coordination Polyhedra	Polyhedra Isomer	Avg. Bending (°)	Avg. Rotation (°)	Avg. M*–N (Å)	Avg. M*–O (Å)	Avg. Bite angle (°)
[Hf(dilOx)$_4$]	§5.6	Triclinic	$P\bar{1}$	Sq-Antiprism	D_2-corner	1.62(4)	41.97(10)	2.397(3)	2.099(1)	70.33(4)
[Hf(diMeOx)$_4$]	§4.6	Monoclinic	$P2_1/c$	Sq-Antiprism	D_2-corner	0	44.42(9)	2.398(2)	2.098(2)	70.19(9)
Zr(dbm)$_4$]	1	Monoclinic	$P2_1/c$	Sq-Antiprism	D_2-corner	1.86(3)	43.99(7)	-	2.178(1)	74.53(9)
[Hf(dbm)$_4$]	§6.4	Monoclinic	$P2_1/c$	Sq-Antiprism	D_2-corner	2.20 (1)	44.07 (9)	-	2.169(1)	74.74(9)
[Zr(diMeOx)$_4$]	4	Orthorhombic	$Pca2_1$	Sq-Antiprism	D_2-corner	4.66(9)	43.39(6)	2.418(3)	2.104(2)	70.16(8)
[Zr(5ClOx)]$_4$	1	Monoclinic	$P2_1/c$	Sq-Antiprism	D_2-corner	3.54(10)	45.27(13)	2.427(4)	2.100(3)	70.65(9)
[Hf(hfaa)$_4$]	9	Monoclinic	$P2_1/c$	Sq-Antiprism	C_2-comb.	4.15(9)	45.11(8)	-	2.165(3)	76.75(10)
[Zr(acac)]$_4$	8	Monoclinic	$C2/c$	Sq-Antiprism	D_2-corner	3.66(4)	46.12(3)	-	2.186(9)	74.86(1)
[Zr(hfaa)$_4$]	10	Monoclinic	$P2_1/c$	Sq-Antiprism	C_2-comb.	5.03(13)	45.30(9)	-	2.175(5)	76.13(11)
[Hf(5ClOx)]$_4$	§4.5	Monoclinic	$C2/c$	Sq-Antiprism	D_2-corner	6.11(7)	45.20(11)	2.404(1)	2.097(2)	69.97(14)
[Hf(acac)]$_4$	8	Monoclinic	C2/c	Sq-Antiprism	D_2-corner	3.68(8)	46.21(8)	-	2.173(2)	75.10(5)
[Zr(tfaa)]$_4$	12	Monoclinic	$C2/c$	Sq-Antiprism	D_2-corner	7.95(9)	45.15 (7)	-	2.184(2)	75.52(6)
[Hf(diClOx)$_4$]	§5.4	Monoclinic	$P2_1/c$	Sq-Antiprism	D_2-corner	4.38(8)	47.34(9)	2.386(2)	2.099(2)	69.77(7)
[Hf(tfaa)]$_4$	11	Monoclinic	$C2/c$	Sq-Antiprism	D_2-corner	7.94(8)	46.51(5)	-	2.172(2)	75.61(5)
[Hf(diBrOx)$_4$]	§5.5	Monoclinic	$P2_1/c$	Sq-Antiprism	D_2-corner	5.10(9)	48.15(7)	2.399(3)	2.088(3)	70.85(8)
[Zr(diClOx)$_4$]	5	Monoclinic	$C2/c$	Sq-Antiprism	D_2-corner	11.90(8)	47.44(7)	2.452(2)	2.095(2)	70.95(9)
[Zr(Ox)]$_4$	6	Triclinic	$P\bar{1}$	Sq-Antiprism	D_2-corner	12.83 (1)	48.15(8)	2.420(2)	2.106(2)	70.70(10)
[Hf(Ox)]$_4$	§4.4	Triclinic	$P\bar{1}$	Sq-Antiprism	D_2-corner	15.17(6)	49.15(8)	2.398(2)	2.095(1)	70.43(7)
[[Hf(OH)(tfba)$_3$]$_2$	§6.5	Monoclinic	$P2_1/c$	Sq-Antiprism	D_2-corner	16.38(8)	50.34(7)	-	2.194(3)	74.59(9)
[Hf(OH)(hfaa)$_3$]$_2$	13	Monoclinic	$C2/c$	Sq-Antiprism	D_2-corner	18.73(9)	47.28(8)	-	2.190(2)	75.30(5)
[Hf(salophen)$_2$]	§7.4	Triclinic	$P\bar{1}$	Sq-Antiprism	C_2-comb.	22.72(8)	49.56(7)	2.403(2)	2.074(2)	74.22(2)

***M = Hf(IV) or Zr(IV)**

By considering all of the single x-ray structural data discussed in this chapter, some conclusions are possible with regard to all these endeavours of identifying the solid-state properties of hafnium(IV) complexes containing various *N,O* -and *O,O'*-bidentate, and *O,N,N,O*-tetradentate ligands.

Some general trends, or tendencies of trends, are noted.

Firstly, it is worth noting that there is a clear general trend between the ***average* rotation** and the ***average bending*** within the coordination polyhedron. This trend is highlighted in **Figure 9.8** below. The significant outlying exceptions comes from the dinuclear species and tetradentate ligand system, $[Hf(OH)(hfaa)_3]_2$ and $[Hf(salophen)_2]$, and are illustrated to the far right in **Figure 9.8** below. However, since no polymorphic, isostructural nor similar zirconium type complexes are found in literature[2] for $[Hf(salophen)_2]$, no assumptions can be made with regards to the ***average* rotation** or ***average bending*** distortions observed.

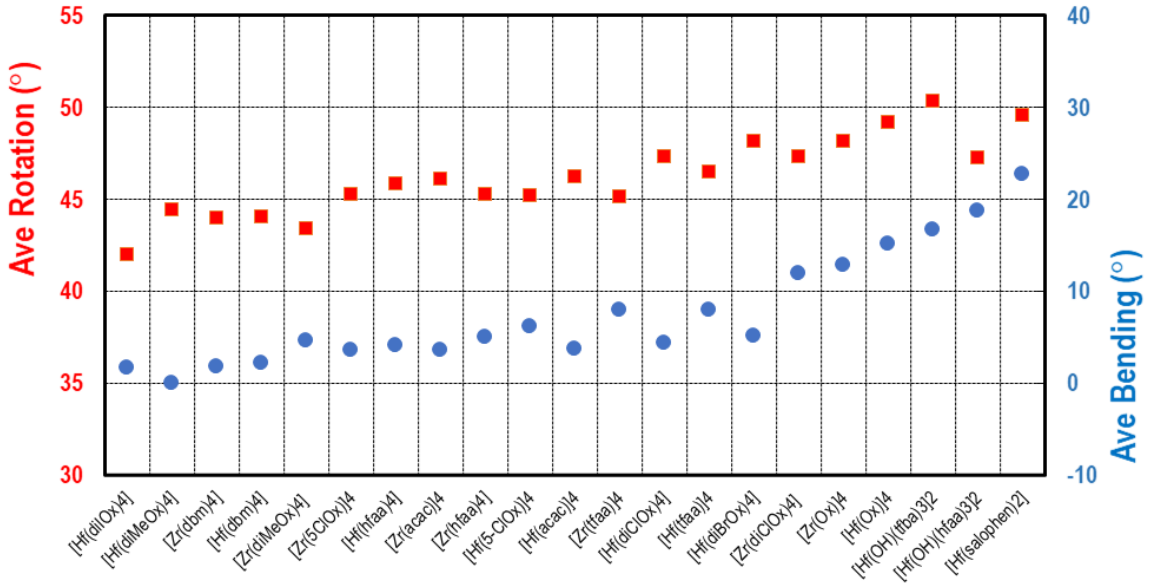

Figure 9.8. Correlation between the *average rotation* (red) and *average bending* (blue) within the coordination polyhedral within the compounds listed in **Table 9.3**.

Secondly, it is observed that eight coordinated hafnium metal complexes show a particular preference towards low symmetry crystal systems, e.g. triclinic and monoclinic systems, except for [Zr(diMeOx)$_4$] which crystallized in a orthorhombic ($Pca2_1$) crystal system. With regard to the expected lattice/crystalline network stabilization, it has become apparent in these systems to expect a certain degree of π-π- and/or halogen-π staking to be present.

Thirdly, it has been elaborately illustrated in **Chapters 4-7,** that *N,O-, O,O'-* and O,*N,N,O*-donating ligands (oxine, acac and salophen type ligands) chelate around hafnium metal centres in a square antiprismatic polyhedral fashion, with slight distortions towards dodecahedral geometries in all cases studied. This suggests that the chelation geometry is mainly governed by intermolecular forces rather than that of the ligands internal geometries and properties.

Fourthly, even though square antiprismatic coordination geometries are always observed, with very comparable physical properties (bond lengths and bite angles), there are some aspects of these structures' geometries that display different tendencies:

(a) The range of coordination isomers (***D$_2$, C$_2$ & D$_4$, see*** **Par. 2.5**) defined for each structure indicates that there are aspects of hafnium(IV) and zirconium(IV) ligand chelation that allows for manipulation to obtain chemically different metal complexes.

(b) It was noted that by modifying recrystallization techniques (solvent *vs* sublimation), especially for the hafnium *β*-diketonato complexes, it is possible to produce either monomeric or dinuclear complexes.

(c) Moreover, by modifying the recrystallization technique, it is possible to produce a *D$_2$-corner-clipped isomer* (*via* solvent recrystallization) or a *C$_2$-mixed bonding isomer* (*via sublimation recrystallization*).

(d) The range of coordination isomers (D_2 *and* C_2) described for each structure, as well as dinuclear species isolated indicate that there are some aspects of Hf (IV) and Zr(IV) ligand chelations that allow for manipulation to yield chemically different behaviours of these metal complexes.

Fifthly, seemingly the ***steric bulk*** does not influence the trend observed in **Figure 9.8**, when considering the data presented in **Table 9.3**, indicating that the susceptibility of chelation geometry to intermolecular forces is greater than that of ligand internal geometry.

Finally, it is noted that when considering ligands for a study on purification/separation of these metals by means or organometallic chelation, the ligand coordination sites will have to be selected to specifically inhibit this kind of coordination geometry around the metal centres, since bidentate ligands *in general* will almost always yield a singular result. Although not definitively proven, the significance here is that these observations can assist a great deal when designing/choosing ligands for future separation studies.

In the concluding **Chapter 10,** some preliminary liquid-liquid extraction investigations of zirconium(IV)- and hafnium(IV)-oxine complexes and competition extractions will be described and discussed.

Chapter 10

Preliminary Solvent Extraction and Attempted Separation of Tetrakis(oxine-type)hafnium(IV) and -Zirconium(IV) Complexes

---

10.1. Introduction

An integral part of this project and related M.Sc.[1] studies, which preceded it, is focused on studying the solid-state and solution behaviour of hafnium(IV), with various *N*- and *O*-donating ligand systems (oxine systems), in order to obtain valuable new data that could be compared to zirconium(IV) to evaluate if metal separation is feasible for industrial applications.

From the crystallographic characterisation chapters presented and related M.Sc.[1,2] and Ph.D.[3] projects previously concluded, the primary observation has been that only *tetrakis*-coordinated complexes are isolated in the final solid-state. Furthermore, in these afore-mentioned studies, the formation of *tetrakis*-(8-hydroxyquinolinato)hafnium(IV) and *tetrakis*(8-hydroxyquinolinato)-zirconium(IV) complexes were evaluated in N,N-dimethylformamide (DMF) and

---

[1] J. A. Viljoen; *Speciation And Interconversion Mechanism Of Mixed Halo and O,O- and N,O-Bidentate Ligand Complexes of Hafnium*, M.Sc. Dissertation (2009), University of the Free State,South Africa.

[2] M. Steyn; *Speciation And Interconversion Mechanism Of Mixed Halo and O,O- and N,O-Bidentate Ligand Complexes of Zirconium*, M.Sc. Dissertation (2009), University of the Free State,South Africa.

[3] M. Steyn; *A Solid State and Mechanistic Study of Multidentate Ligand Zirconium(IV) Halido Complexes*, Ph.D Thesis, (2014), University of the Free State, South Africa.

preliminary step-wise reaction mechanisms for the coordination of the four oxine ligands to the Hf(IV) and Zr(IV) metal centres were postulated, utilising UV/Vis spectroscopic kinetics.

However, to further evaluate potential extraction possibilities, it was decided not to utilise N,N-dimethylformamide (**DMF**) as a reaction solvent due to its high boiling point and expenses[4] associated therewith, making it not industrially and economically viable, but using the more readily available and cheaper methanol (**MeOH**)[5] instead.

This preliminary extraction investigation reported below includes liquid-liquid extractions of zirconium- and hafnium-oxine complexes from methanol (**MeOH**) into dichloromethane (**DCM**) and competition extractions, as qualitatively evaluated by **(i)** UV-vis spectroscopy (**UV/Vis**) and **(ii)** inductively coupled plasma optical emission spectroscopy (**ICP-OES**).

10.2. General Experimental Considerations

10.2.1. Reagents

All reagents used for reaction solutions were of analytical grade and were purchased from Sigma-Aldrich, South Africa. Reagents were used as received without further purification.

[4] https://www.sigmaaldrich.com/ZA/en/search/dmf?focus=products&page=1&perPage=30&-sort= relevance&term=dmf&type=product (Last accessed 27/06/2021).
[5] https://www.sigmaaldrich.com/ZA/en/search/methanol?focus=products&page=1&perPage=30&sort= relevance &term=methanol&type=product (Last accessed 27/06/2021).

10.2.2. Equipment

All UV/vis spectra were obtained on a Varian Cary 50 Conc UV/Vis-spectrophotometer. Temperature control of the reaction solutions was maintained to within ±0.1 ˚C by means of a circulating water bath system. A Shimadzu ICPS-7510 spectrometer with a radial-sequential plasma source was used for the quantification of zirconium and hafnium in the different compounds.

10.3. Evaluation of Extraction of Hf(IV) and Zr(IV) Complexes

10.3.1. General Procedures

The ligand 5-chloro-8-hydroxyquinoline (5Cl-OxH) showed the best potential to discriminate between the zirconium and hafnium (*vide infra*), and also exhibited reasonable solubility in the different solvents selected (**Table 10.1**), and was therefore chosen to preliminarily evaluate the extraction of the Zr(IV) and Hf(IV). $HfCl_4$ (205 mg, 640 *μ*mol) was dissolved in MeOH (20 mL). While stirring this solution, at room temperature, another solution of the coordinating 5-chloro-8-hydroxyquinoline ligand ((5Cl-OxH), 472 mg, 2.628 mmol), also dissolved in MeOH (20 mL), was slowly added, resulting in the formation of intense yellowish solutions as illustrated in **Figure 10.1(a).**

This reaction mixture was combined with a two-fold excess of cold distilled water (80 mL), to which DCM (40mL) was added. After the water addition, a white precipitate formed due to the insolubility of the final product ($[Hf(5Cl\text{-}Ox)_4]$) in water. The DCM in turn dissolves the precipitate and therefore extracts the final product from **MeOH** into **DCM**; *see* **Figure 10.1(b).**

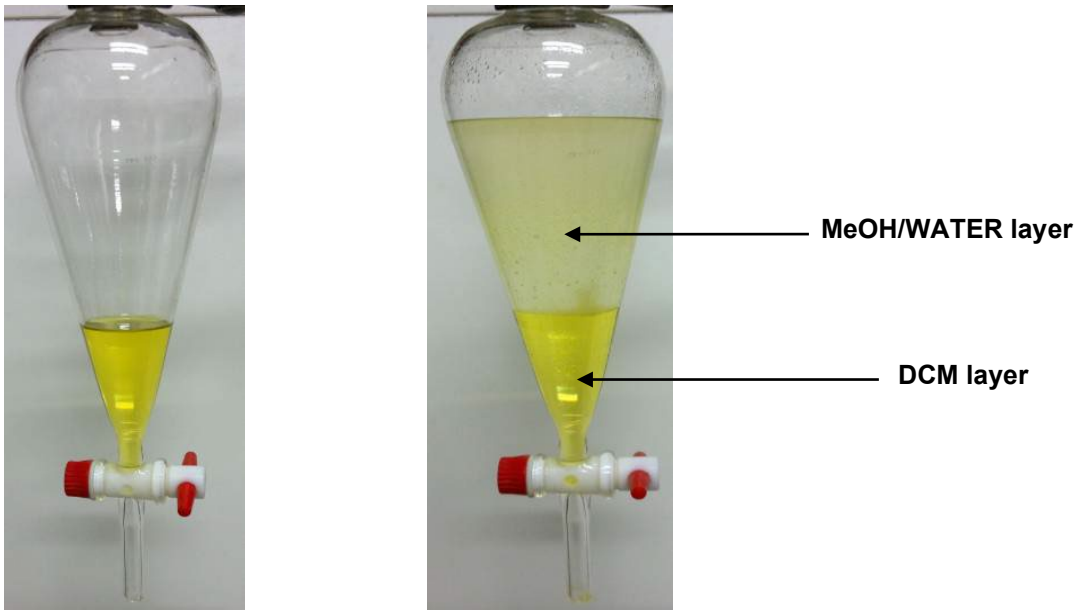

Figure 10.1. Solvent extraction process for $HfCl_4$ + OxH; where **(a)** Initial reaction solution in MeOH after mixing $HfCl_4$ and 5Cl-OxH **(b)** Two layers formed after addition of water and DCM.

10.3.2. Solubility Evaluation of Compounds

Solubility tests indicated that the three starting reagents, $ZrCl_4$/$HfCl_4$ and OxH, are all soluble in methanol whereas only the final metal complexes ([Zr/Hf(5Cl-Ox)$_4$]) and corresponding ligand (5Cl-OxH) are soluble in DCM. Furthermore, the metal starting reagents ($ZrCl_4$/$HfCl_4$) are insoluble in DCM and hydrolyses (decompose) in water (*see* **Table 10.1** for solubility matrix).

Table 10.1. Solubility matrix of the starting reagents and complexes formed in methanol (MeOH), water (H_2O) and dichloromethane (DCM).

	Solubility					
Compound	**MeOH**	**mg/mL**	**Water**	**mg/mL**	**DCM**	**g/L**
$HfCl_4$	✓	≈ 10	X	Hydrolyse [a]	X	≈ 0.1
$ZrCl_4$	✓	≈ 10	X	Hydrolyse [a]	X	≈ 0.1
5Cl-OxH [b]	✓	≈ 20	X	0.02	✓	≈ 15
$Hf(5Cl\text{-}Ox)_4$	✓	≈ 20	X	No data available	✓	≈ 20
$Zr(5Cl\text{-}Ox)_4$	✓	≈ 20	X	No data available	✓	≈ 20

[a] Hydrolyse to form insoluble halidooxido compounds Ref. 6; [b] Ref. 7.

In an attempt to evaluate the amount of metal complex and free ligand extracted, UV/Vis spectroscopy was firstly utilised. This is theoretically possible due to the fact that the metal complex ($[Zr/Hf(5Cl\text{-}Ox)_4]$) and the free ligand extracted should produce different absorbance maxima, which can be directly correlated to their concentrations according to Beer's Law.

Therefore, before any experiments could be performed it was necessary to establish whether the different solvents used for the extraction procedure may influence the UV/Vis spectra of the starting and final complexes to be extracted. To study this, a UV/Vis absorption spectrum was taken of each solvent utilised in the extraction process (MeOH, water and DCM) to determine where their absorbance maxima are observed.

It was determined that the different solvents used (*DCM, MeOH and Water*) and mixtures thereof should have a minimal or no effect or interference on the absorbance maxima of the complexes extracted since metal complexes concerning this study ($[Zr/Hf(5Cl\text{-}Ox)_4]$) commonly have absorbance maxima larger

[6] R. H Nielsen,*"Hafnium and Hafnium Compounds"*, Kirk-Othmer Encyclopedia of Chemical Technology, John Wiley & Sons, Inc., 2000.
[7] Z. Ma and B. Moulton, *J. Chem. Crystallogr.,* **39**, 913, 2009.

than the solvents used. After establishing that the solvents employed for liquid-liquid extraction are suitable for UV/Vis spectroscopy experiments, it was necessary to evaluate the UV/Vis spectra of only the free ligands before and after extraction. It should then be possible to establish the amount of unreacted/free ligand in the reaction mixture after extraction.

To investigate the extraction behavior of the free quinoline ligands, 5-chloro-8-hydroxyquinoline (5Cl-OxH) (111 mg, 618 *µ*mol) was dissolved in 20 mL MeOH (3.090 x 10^{-2} M), and a UV/Vis spectrum was taken of the solution (**Figure 10.2***, blue line*). However, the reaction mixture had to be diluted 100 times (*3.090 x 10^{-4} M*) in order to obtain a spectrum with an absorbance maximum peak less than 1 to adhere to Beer's Law.

The methanol solution containing the 5-ClOxH (3.09 x 10^{-2} M) was then extracted from methanol into a DCM solution as described earlier and diluted 100 times to also adhere to Beer's Law. The following UV/Vis spectrum was obtained (**Figure 10.2***, brown line*).

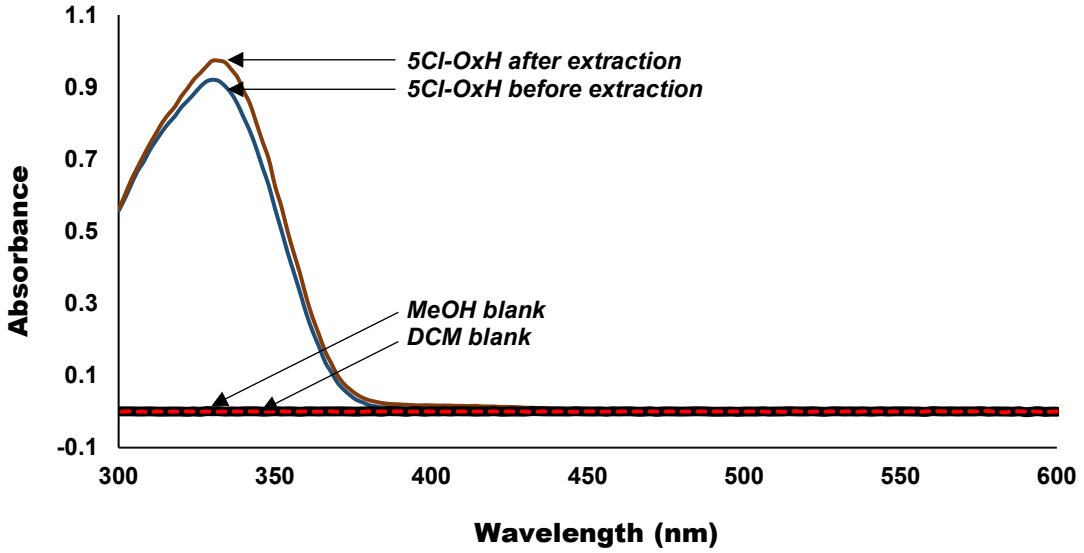

Figure 10.2: Typical UV/Vis spectrum of 5Cl-OxH (3.090 x 10^{-4} M) in MeOH at 25˚C *before extraction* (blue line) and in DCM at 25˚C *after extraction* (brown line). MeOH and DCM blank solution spectra are represented by red dotted and solid black lines, respectively.

Interestingly, after extraction, the absorbance maximum of the 5Cl-OxH shifts by *ca. 2 nm* but even more interesting is the fact that the peak increased by 0.05 (5.4%) absorbance units. The increase of peak height is probably due to solvent effects such as the polarity of the solvents (Polarity index, ε_{MeOH} = 32.7, ε_{DCM} = 8.9).[8] By using the peak height after extraction, as a starting reference, it should be possible to establish the amount of free ligand still in the reaction mixture after extraction. If it is assumed that every four equivalent of free ligands will form one equivalent Hf(5Cl-Ox)$_4$. In that case, if Beer's Law is obeyed, the decrease of the absorbance peak height should be proportional to a quarter of the metal complex formation [metal:ligand=1:4]. This assumption is based on the fact that a high ligand concentration should force the reaction mechanism (equilibrium) to the right and consequently form a fully coordinated metal complex, [Hf(L,L')$_4$], as illustrated in the scheme below:[1]

$$[HfX_4] + (L,L') \rightleftharpoons [HfX_3(L,L')] + X^-$$

$$[HfX_3(L,L')] + (L,L') \rightleftharpoons [HfX_2(L,L')_2] + X^-$$

$$[HfX_2(L,L')_2] + (L,L') \rightleftharpoons [Hf\text{-}X1(L,L')_3] + X^-$$

$$[Hf\text{-}X(L,L')_3] + (L,L') \rightleftharpoons [Hf(L,L')_4] + X^-$$

Scheme 10.1: The generalised step-wise reaction mechanism of hafnium halo complexes reacting with *N,O*-donating bidentate ligands, where (L,L') = *N,O*-bidentate ligand and X = halides (*This is similar to that proposed for the corresponding zirconium(IV) complexes*).[2]

Below is presented a step-wise procedure for the preliminary evaluation of the extraction of the hafnium(IV) and zirconium(IV) complexes.

[8] C. Reichardt and T. Welton, "*Solvents* and *Solvent Effects* in *Organic Chemistry*", WILEY-VCH Verlag GmbH & Co., 2011.

10.4. Extraction of Hafnium

The hafnium extractions were evaluated using the different solution mixtures as given in **Table 10.2**.

(a) Hf Reactant Solutions Before Extraction

Utilising the procedure described above, after *ca*. 10 min. a UV/Vis spectrum was recorded of each individual reaction mixture following a 100 times dilution. Preliminary results are shown in **Figure 10.3**. For clarity and illustration, only the overlaid spectra of **Hf 1** and **Hf 7** are displayed. (**Figure 10.3;** *before extraction*).

Table 10.2: Solution constitution for the extraction of $[Hf(5Cl\text{-}Ox)_4]$, using the following: (a) A stock solution containing 5Cl-OxH (1.107 g, 6.2 x 10^{-3} mol) was prepared in 100mL methanol, [5Cl-OxH] = 6.2 x 10^{-2} M. (b) A stock solution containing $HfCl_4$ (0.245 g, 7.6 x 10^{-4} mol) was prepared in 50mL methanol, $[HfCl_4]$ = 1.5 x 10^{-2} M, and (c) pure Methanol.

Mixture number [a]	Volume stock solutions (mL)			μmol ClOxH	[5Cl-OxH] (M)	μmol Hf	[Hf] (M)	mol Ratio of 5Cl-OxH : Hf [b]
	5Cl-OxH (a)	Metal reactant (b)	MeOH (c)					
Hf 1	10	0	10	310	3.1 x 10^{-2}	0	0	4.1 : 0.0
Hf 2	10	1	9	310	3.1 x 10^{-2}	7.5	7.5 x 10^{-4}	4.1 : 0.1
Hf 3	10	3	7	310	3.1 x 10^{-2}	23	2.3 x 10^{-3}	4.1 : 0.3
Hf 4	10	5	5	310	3.1 x 10^{-2}	38	3.8 x 10^{-3}	4.1 : 0.5
Hf 5	10	7	3	310	3.1 x 10^{-2}	53	5.3 x 10^{-3}	4.1 : 0.7
Hf 6	10	9	1	310	3.1 x 10^{-2}	68	6.8 x 10^{-3}	4.1 : 0.9
Hf 7	10	10	0	310	3.1 x 10^{-2}	75	7.5 x 10^{-3}	4.1 : 1.0[a]

[a] Note: the numbering used is **Hf 1** - **Hf 7** to indicate the solutions before extraction, while **Hf 1E** - **Hf 7E** are used after extraction, [Par 10.4(b)] [b] The mol ratios used were based on having **(a)** a constant (excess) amount of 5Cl-OxH ligand in solution, **(b)** with step-wise increasing amounts of Hf, **(c)** to finally converge to an approximate 4:1 ratio {small excess ligand allowed} to ensure a final equimolar ratio for the formation of the *tetrakis* complex, i.e., $[Hf(5Cl\text{-}Ox)_4]$ (**Scheme 10.1**).

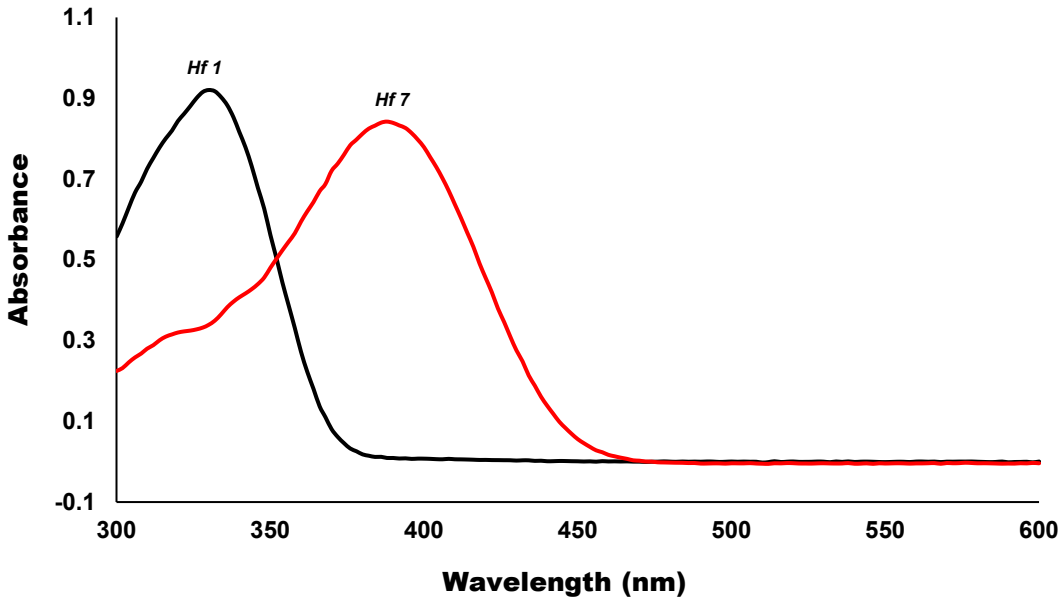

Figure 10.3: UV/Vis spectra of mixture **(a) Hf 1** (*black line,* [5Cl-OxH] = 3.1 x 10^{-4} M and [$HfCl_4$] = 0 M) and **(b) Hf 7** (*red line*, [5Cl-OxH] = 3.1 x 10^{-4} M and [$HfCl_4$] = 7.5 x 10^{-5} M) in MeOH at 25˚C *before extraction*.

It is evident that complex formation did occur as a new absorbance peak (***metal-complex***, [$Hf(5Cl\text{-}Ox)_4$]) forms at *ca*. 390 nm.

Moreover, it is further apparent that the newly formed peak increases as the metal concentration increases, and subsequently, a decrease is observed at the free ligand absorbance peak (ca. 340 nm), confirming that the new peak must the formation of metal-complex. This is best illustrated by overlaying the seven hafnium UV\Vis reaction spectra (**Hf 1** - **Hf 7**) as illustrated in **Figure 10.4**.

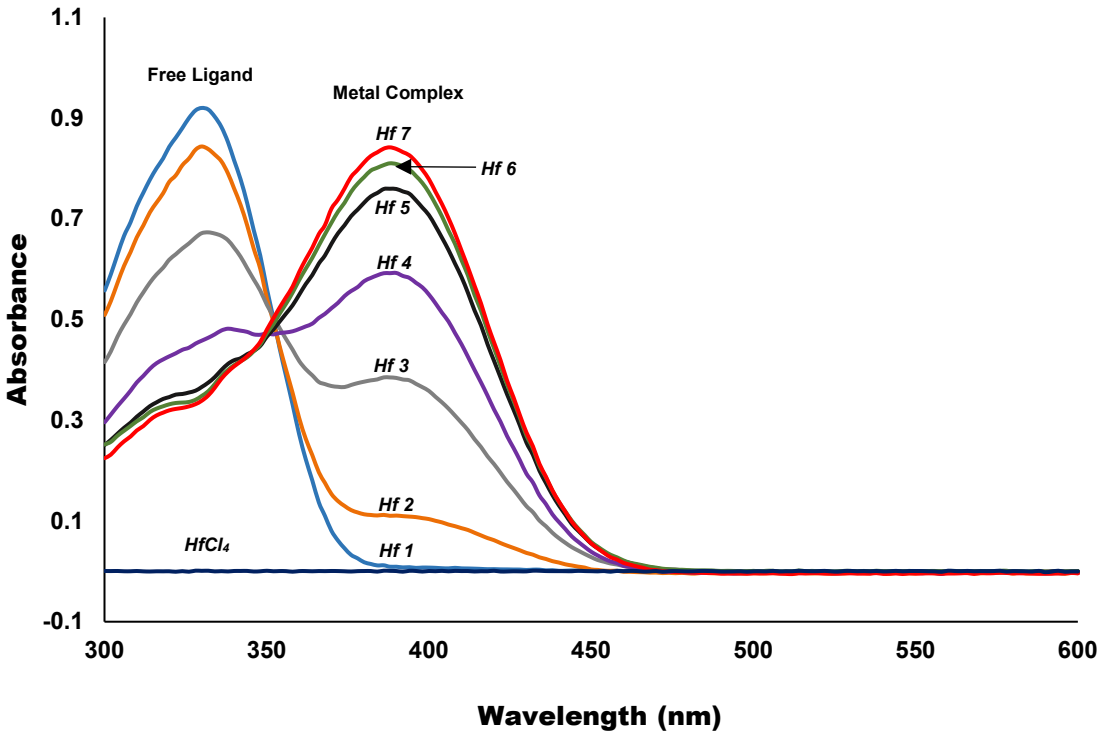

Figure 10.4: UV/Vis spectra of reaction **Hf 1 – Hf 7 (Table 10.2)** and **$HfCl_4$** *before extraction* in MeOH at 25°C overlayed, showing the decrease in free ligand concentration at 329nm and the increase of metal complex formation at 390nm (*100 times diluted*).Dark Blue = [$HfCl_4$]= 7.5 x 10^{-5} M, Light blue = **Hf 1** ([5Cl-OxH] = 3.1 x 10^{-4} M and [$HfCl_4$] = 0 M), Orange = **Hf 2** [5Cl-OxH] = 3.1 x 10^{-4} M and [$HfCl_4$] = 7.5 x 10^{-6} M), Grey = **Hf 3** [5Cl-OxH] = 3.1 x 10^{-4} M and [$HfCl_4$] = 2.3 x 10^{-5} M), Purple = **Hf 4** ([5Cl-OxH] = 3.1 x 10^{-4} M and [$HfCl_4$] = 3.8 x 10^{-5} M), **Black** = **Hf 5** ([5Cl-OxH] = 3.1 x 10^{-4} M and [$HfCl_4$] = 5.3 x 10^{-5} M), Green = **Hf 6** ([5Cl-OxH] = 3.1 x 10^{-4} M and [$HfCl_4$] = 6.8 x 10^{-5} M), Red = **Hf 7** ([5Cl-OxH] = 3.1 x 10^{-4} M and [$HfCl_4$] = 7.5 x 10^{-5} M).

An overarching conclusion from **Figure 10.4** made is that the step-wise formation of increasing amounts of the *tetrakis*-oxinato complexes of [Hf(5Cl-Ox)$_4$] is clearly and effectively observed and monitored by UV/vis spectroscopy.

(b) Hf Reactant Solutions After Extraction

After obtaining the UV/Vis spectra of reaction mixtures **Hf 1 – Hf 7**, each reaction mixture was extracted (**Hf 1E – Hf 7E)** from methanol solution into a dichloromethane (DCM) solution as described earlier. A UV/Vis spectrum was collected of each extracted mixture to evaluate whether extraction did occur, and

if so, how effective it was. For clarity and for illustration, only the overlaid spectra of **Hf 1E** and **Hf 7E** (*E* = *extracted*) are shown in **Figure 10.5.**

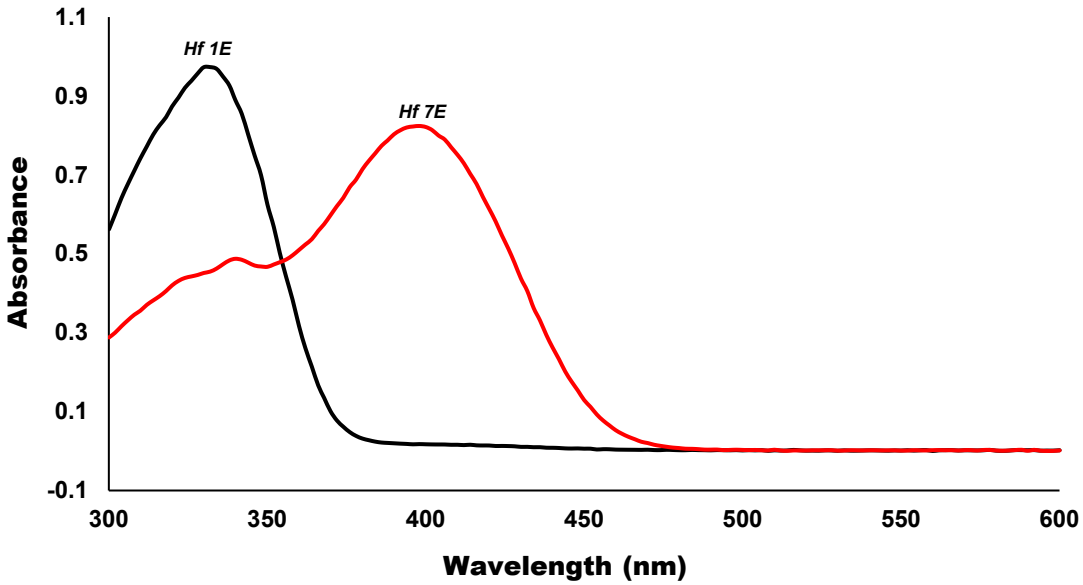

Figure 10.5: UV/Vis spectra of mixture **(a) Hf 1E** (*black line,* [5Cl-OxH] = 3.1 x 10^{-4} M and [$HfCl_4$] = 0 M) and **(b) Hf 7E** (*red line*, [5Cl-OxH] = 3.1 x 10^{-4} M and [$HfCl_4$] = 7.5 x 10^{-5} M) in DCM at 25˚C *after extraction* (*100 times diluted*).

After extraction of **Hf 1** - **Hf 7**, the same trend is observed as *before extraction*. The free ligand absorbance peak decreases while the metal complex formation peak increases (new absorbance peak step-wise forming at *ca*. 400 nm, *see* **Figure 10.6**).

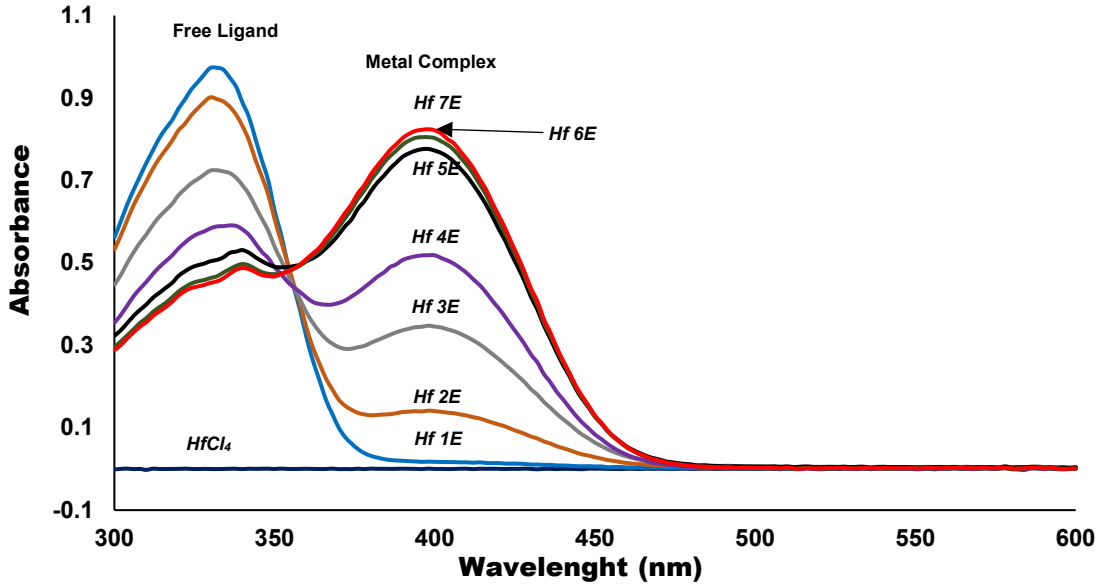

Figure 10.6: UV/Vis spectra of reaction **Hf 1E – Hf 7E (Tabel 10.2)** and **$HfCl_4$** *after extraction* in DCM at 25°C overlayed, showing the decrease in free ligand concentration at 331nm and the increase of metal complex formation at 400nm (*100 times diluted*). Dark Blue = [$HfCl_4$]= 7.5 x 10^{-5} M, Light blue = **Hf 1E** ([5Cl-OxH] = 3.1 x 10^{-4} M and [$HfCl_4$] = 0 M), Orange = **Hf 2E** [5Cl-OxH] = 3.1 x 10^{-4} M and [$HfCl_4$] = 7.5 x 10^{-6} M), Grey = **Hf 3E** [5Cl-OxH] = 3.1 x 10^{-4} M and [$HfCl_4$] = 2.3 x 10^{-5} M), Purple = **Hf 4E** ([5Cl-OxH] = 3.1 x 10^{-4} M and [$HfCl_4$] = 3.8 x 10^{-5} M), **Black** = **Hf 5E** ([5Cl-OxH] = 3.1 x 10^{-4} M and [$HfCl_4$] = 5.3 x 10^{-5} M), Green = **Hf 6E** ([5Cl-OxH] = 3.1 x 10^{-4} M and [$HfCl_4$] = 6.8 x 10^{-5} M), Red = **Hf 7E** ([5Cl-OxH] = 3.1 x 10^{-4} M and [$HfCl_4$] = 7.5 x 10^{-5} M).

Overarching conclusions flowing from **Figure 10.4** and **Figure 10.6** are that the step-wise formation of increasing amounts of the *tetrakis*-oxinato complex of [Hf(5Cl-Ox)$_4$]:

(i) Is clearly and effectively observed and monitored by UV/vis spectroscopy;

(ii) The extracted final complexes correlate excellently with the initial complexes formed;

(iii) Extraction is visually virtually quantitative.

(c) Comparison of Hf Reactant Solutions Before and After Extraction

To further confirm the above conclusions, the excellent agreement between the UV/vis spectra for the formation and extraction of the $[Hf(5Cl\text{-}Ox)_4]$ complex is illustrated by overlaying the spectra of each individual reaction mixture *before* and *after extraction* (**Figure 10.7**).

Figure 10.7 also illustrates that the free ligand-specific absorbance peak in the spectrum stays constant at *ca*. 330 nm. However, the product-specific peak shifts noticeably by about 10 nm (390 nm – 400 nm) following the extraction. This is most likely not due to a difference in product extracted but probably only due to a difference in solvent effects, as mentioned earlier (MeOH and DCM).

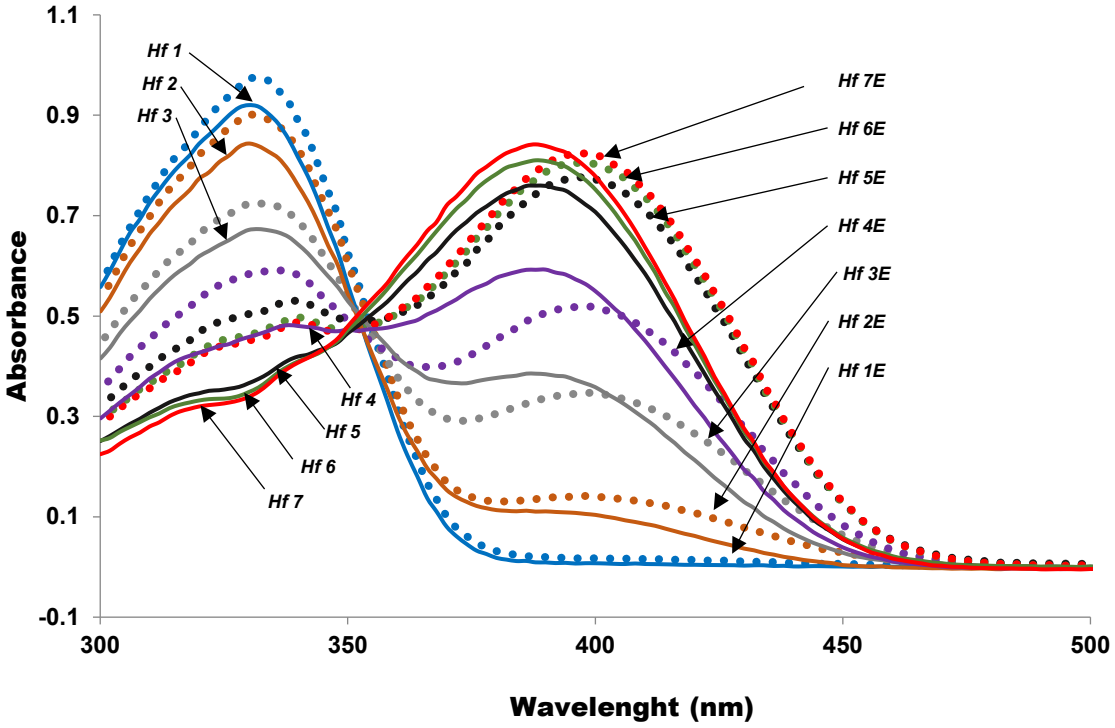

Figure 10.7: UV/Vis spectra of reaction **Hf 1 – Hf 7 (***solid lines***, Tabel 10.2)** *before extraction* in MeOH at 25°C overlayed and **Hf 1E – 7E (***dotted lines*, **Tabel 10.2)** *after extraction* in DCM at 25°C overlayed. Light blue = **Hf 1 & 1E** ([5Cl-OxH] = 3.1 x 10^{-4} M and $[HfCl_4]$ = 0 M), Orange = **Hf 2 & 2E** [5Cl-OxH] = 3.1 x 10^{-4} M and $[HfCl_4]$ = 7.5 x 10^{-6} M), Grey = **Hf 3 & 3E** [5Cl-OxH] = 3.1 x 10^{-4} M and $[HfCl_4]$ = 2.3 x 10^{-5} M), Purple = **Hf 4 & 4E** ([5Cl-OxH] = 3.1 x 10^{-4} M and $[HfCl_4]$ = 3.8 x 10^{-5} M), **Black** = **Hf 5 & 5E** ([5Cl-OxH] = 3.1 x 10^{-4} M and $[HfCl_4]$ = 5.3 x 10^{-5} M), Green = **Hf 6 & 6E** ([5Cl-OxH] = 3.1 x 10^{-4} M and $[HfCl_4]$ = 6.8 x 10^{-5} M), Red = **Hf 7 & 7E** ([5Cl-OxH] = 3.1 x 10^{-4} M and $[HfCl_4]$ = 7.5 x 10^{-5} M).

The overarching conclusions regarding the *tetrakis*-oxinato complex of [Hf(5Cl-Ox)$_4$] made above, i.e., that: it may be effectively observed and monitored by UV/vis spectroscopy, the extracted final complexes correlate excellently with the initial complexes formed and extraction is virtually quantitative, is further confirmed by **Figure 10.7**.

10.5. Extraction of Zirconium

(a) Zr Reactant Solutions Before Extraction

The exact same procedure as was used for the hafnium described above, was followed for zirconium. The zirconium complex extractions were evaluated using the different solution mixtures as given in **Table 10.3**.

Table 10.3: Solution constitution for the extraction of [Zr(5Cl-Ox)$_4$], using the following: (a) A stock solution containing 5Cl-OxH (1.107 g, 6.2 x 10^{-3} mol) was prepared in 100mL methanol, [5Cl-OxH] = 6.2 x 10^{-2} M. (b) A stock solution containing $ZrCl_4$ (0.2181 g, 7.6 x 10^{-4} mol) was prepared in 50mL methanol, [$ZrCl_4$] = 1.5 x 10^{-2} M, and (c) pure Methanol.

Mixture number [a]	Volume stock solutions (mL)			μmol 5Cl-OxH	[5Cl-OxH] (M)	μmol Zr	[Zr] (M)	mol Ratio of 5Cl-OxH : Zr [b]
	5Cl-OxH (a)	Metal reactant (b)	MeOH (c)					
Zr 1	10	0	10	310	3.1 x 10^{-2}	0	0	4.1 : 0.0
Zr 2	10	1	9	310	3.1 x 10^{-2}	7.5	7.5 x 10^{-4}	4.1 : 0.1
Zr 3	10	3	7	310	3.1 x 10^{-2}	23	2.3 x 10^{-3}	4.1 : 0.3
Zr 4	10	5	5	310	3.1 x 10^{-2}	38	3.8 x 10^{-3}	4.1 : 0.5
Zr 5	10	7	3	310	3.1 x 10^{-2}	53	5.3 x 10^{-3}	4.1 : 0.7
Zr 6	10	9	1	310	3.1 x 10^{-2}	68	6.8 x 10^{-3}	4.1 : 0.9
Zr 7	10	10	0	310	3.1 x 10^{-2}	75	7.5 x 10^{-3}	4.1 : 1.0[a]

[a] Note: Similar to the hafnium described above, the numbering used is **Zr 1** - **Zr 7** to indicate the solutions before extraction, while **Zr 1E** to **Zr 7E** are used after extraction, [Par. 10.5(b)]. [b] The mol ratios used were based on having **(a)** a constant amount of 5Cl-OxH ligand in solution, **(b)** with step-wise increasing amounts of Zr, **(c)** to finally converge to an approximate 4:1 ratio {small excess ligand allowed} to ensure a final equimolar ratio for the formation of the *tetrakis* complex, i.e., [Zr(5Cl-Ox)$_4$] (**Scheme 10.1**).

After *ca*. 10 min. a UV/Vis spectrum was recorded of each individual reaction mixture *before extraction* after 100 times dilution (**Figure 10.8**).

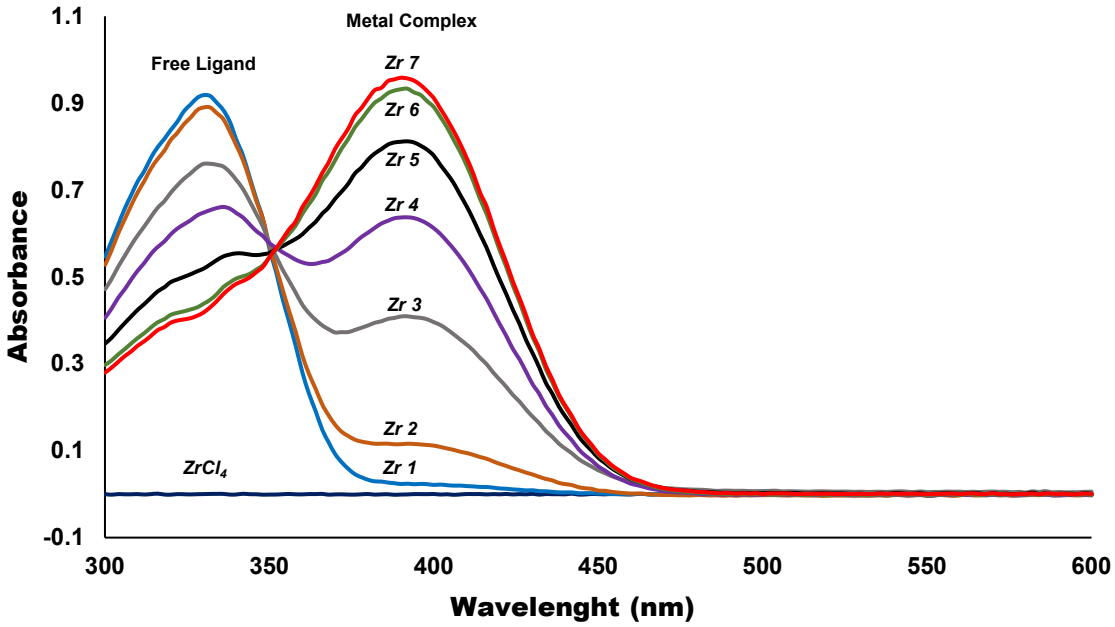

Figure 10.8: UV/Vis spectra of reactions **Zr 1 – Zr 7 (Table 10.3)** and **$ZrCl_4$** *before extraction* in MeOH at 25°C overlayed, showing the decrease in free ligand concentration at 329nm and the increase of metal complex formation at 390nm (*100 times diluted*). Dark Blue = $[ZrCl_4]$= 7.5 x 10^{-5} M, Light blue = **Zr 1** ([5Cl-OxH] = 3.1 x 10^{-4} M and $[ZrCl_4]$ = 0 M), Orange = **Zr 2** [5Cl-OxH] = 3.1 x 10^{-4} M and $[ZrCl_4]$ = 7.5 x 10^{-6} M), Grey = **Zr 3** [5Cl-OxH] = 3.1 x 10^{-4} M and $[ZrCl_4]$ = 2.3 x 10^{-5} M), Purple = **Zr 4** ([5Cl-OxH] = 3.1 x 10^{-4} M and $[ZrCl_4]$ = 3.8 x 10^{-5} M), **Black** = **Zr 5** ([5Cl-OxH] = 3.1 x 10^{-4} M and $[ZrCl_4]$ = 5.3 x 10^{-5} M), Green = **Zr 6** ([5Cl-OxH] = 3.1 x 10^{-4} M and $[ZrCl_4]$ = 6.8 x 10^{-5} M), Red = **Zr 7** ([5Cl-OxH] = 3.1 x 10^{-4} M and $[ZrCl_4]$ = 7.5 x 10^{-5} M).

As in the case of the hafnium extractions described above, an overarching conclusion flowing from **Figure 10.8** is that the step-wise formation of increasing amounts of the *tetrakis*-oxinato complex of $[Zr(5Cl\text{-}Ox)_4]$ is clearly and effectively observed and monitored by UV/vis spectroscopy.

(b) Zr Reactant Solutions After Extraction

After obtaining the UV/Vis spectra of reaction mixtures **Zr 1 – Zr 7**, each reaction mixture was extracted **(Zr 1E – Zr 7E)** from methanol into dichloromethane (DCM) as described earlier. A UV/Vis spectrum was collected of each extracted mixture to evaluate if extraction did occur (**Figure 10.9**).

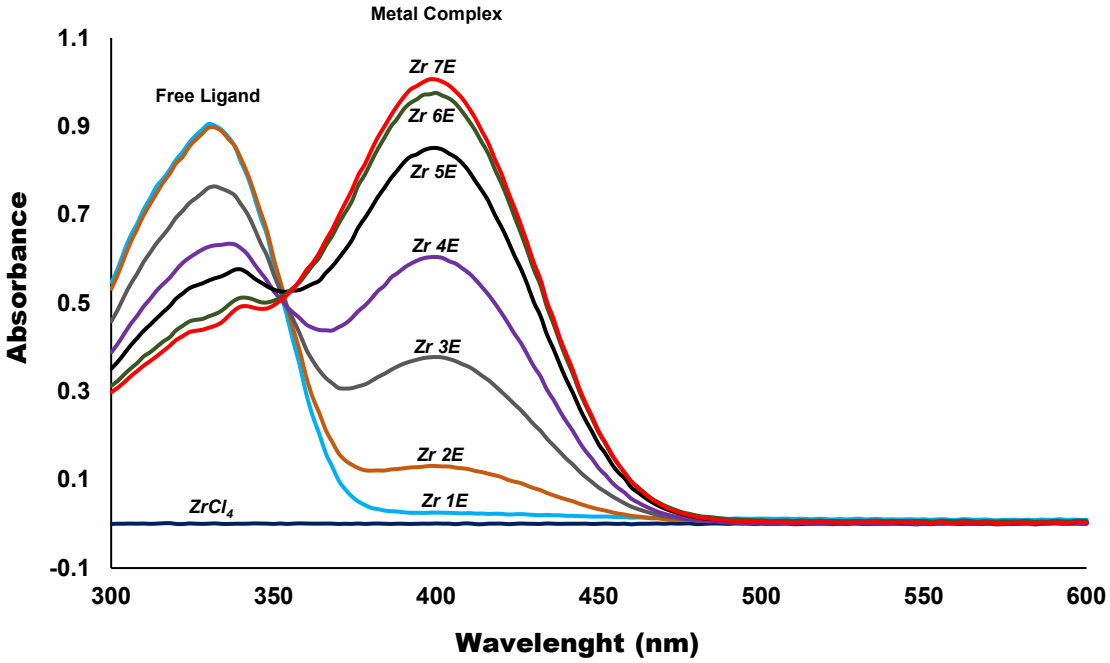

Figure 10.9: UV/Vis spectra of reaction **Zr 1E – Zr 7E (Tabel 10.3)** and **$ZrCl_4$** *after extraction* in DCM at 25°C overlayed, showing the decrease in free ligand concentration at 331nm and the increase of metal complex formation at 400nm (*100 times diluted*). Dark Blue = [$ZrCl_4$]= 7.5 x 10^{-5} M, Light blue = **Zr 1E** ([5Cl-OxH] = 3.1 x 10^{-4} M and [$ZrCl_4$] = 0 M), Orange = **Zr 2E** [5Cl-OxH] = 3.1 x 10^{-4} M and [$ZrCl_4$] = 7.5 x 10^{-6} M), Grey = **Zr 3E** [5Cl-OxH] = 3.1 x 10^{-4} M and [$ZrCl_4$] = 2.3 x 10^{-5} M), Purple = **Zr 4E** ([5Cl-OxH] = 3.1 x 10^{-4} M and [$ZrCl_4$] = 3.8 x 10^{-5} M), **Black** = **Zr 5E** ([5Cl-OxH] = 3.1 x 10^{-4} M and [$ZrCl_4$] = 5.3 x 10^{-5} M), Green = **Zr 6E** ([5Cl-OxH] = 3.1 x 10^{-4} M and [$ZrCl_4$] = 6.8 x 10^{-5} M), Red = **Zr 7E** ([5Cl-OxH] = 3.1 x 10^{-4} M and [$ZrCl_4$] = 7.5 x 10^{-5} M).

Again, overarching conclusions flowing from **Figure 10.8** and **10.9** are that the step-wise formation of increasing amounts of the *tetrakis*-oxinato complex of [Zr(5Cl-Ox)$_4$]:

(i) Is clearly and effectively observed and monitored by UV/vis spectroscopy;

(ii) The extracted final complexes correlate excellently with the initial complexes formed;

(iii) Extraction is again visually virtually quantitative.

(c) Comparison of Zr Reactant Solutions Before and After Extraction

As presented above for the hafnium examples, a complete overlay of these two sets of spectra (*before and after extraction*) is shown in **Figure 10.10** below to allow direct visual comparison. In this case, again as observed before, a ca. 10 nm shift in the absorbance peak (ca. 390 to 400 nm) of the metal complex product (most likely due to solvent effects) is observed.

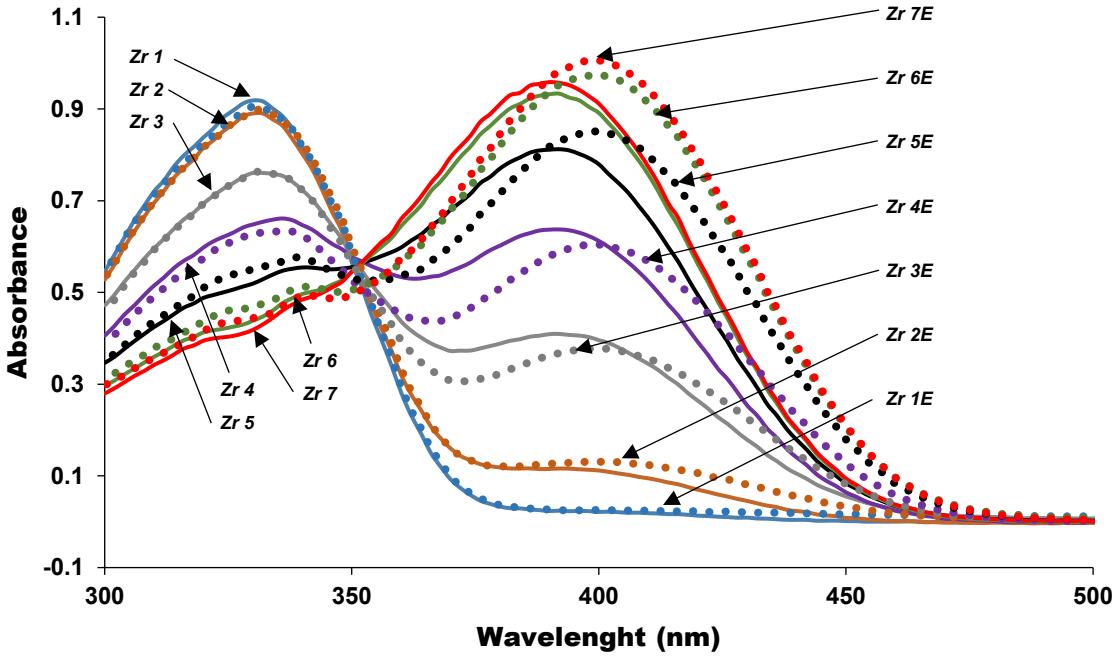

Figure 10.10: UV/Vis spectra of reaction **Zr 1 – 7** (*solid lines*, **Tabel 10.3**) *before extraction* in MeOH at 25°C overlayed and **Zr 1E – 7E** (*dotted lines*, **Tabel 10.3**) *after extraction* in DCM at 25°C overlayed. Light blue = **Zr 1 &1E** ([5Cl-OxH] = 3.1 x 10^{-4} M and [$ZrCl_4$] = 0 M), Orange = **Zr 2 & 2E** [5Cl-OxH] = 3.1 x 10^{-4} M and [$ZrCl_4$] = 7.5 x 10^{-6} M), Grey = **Zr 3 & 3E** [5Cl-OxH] = 3.1 x 10^{-4} M and [$ZrCl_4$] = 2.3 x 10^{-5} M), Purple = **Zr 4 &4E** ([5Cl-OxH] = 3.1 x 10^{-4} M and [$ZrCl_4$] = 3.8 x 10^{-5} M), **Black** = **Zr 5 & 5E** ([5Cl-OxH] = 3.1 x 10^{-4} M and [$ZrCl_4$] = 5.3 x 10^{-5} M), Green = **Zr 6 & 6E** ([5Cl-OxH] = 3.1 x 10^{-4} M and [$ZrCl_4$] = 6.8 x 10^{-5} M), Red = **Zr 7 & 7E** ([5Cl-OxH] = 3.1 x 10^{-4} M and [$ZrCl_4$] = 7.5 x 10^{-5} M).

The overarching conclusions regarding the *tetrakis*-oxinato complex of [Zr(5Cl-Ox)$_4$] made above, i.e., that: it may be effectively observed and monitored by UV/vis spectroscopy, the extracted final complexes correlate excellently with the initial complexes formed and extraction is virtually quantitative, is further supported by **Figure 10.10**.

10.6. Overarching Comparison of Hf/Zr Extractions

Finally, an attempt is made to critically compare the results obtained for both the hafnium and zirconium extractions, as described above.

The spectra shown in **Figure 10.7** and **Figure 10.10** clearly confirm very similar behaviour for both the two metals, and it is visually evident that these types of extraction experiments can be very successfully performed and monitored by UV/vis spectroscopy for each step and concentration of certain extraction parameters. In each case, the chelating ligand and metal complex solutions are clearly definable and identifiable, with varying degrees of validity regarding quantitative weight of absorbance change measured.

It appears as if for each metal centre extraction, a similar degree of absorbance **(i)** decrease is observed for the free ligand solutions, **(ii)** concurrent with the corresponding related complex solution absorbance increase.

This leads to some overarching conclusions:

(a) The degree of UV/vis spectroscopic change/ difference within the Zr/Hf-oxine system is not a measurable valid **metal-specific** entity for a relative final product concentration **quantification**. This yet again manifested in the (classically known) similar influence which the hafnium/zirconium metal centres have on the four oxin- ligand-array, and how much of an effect the primarily ligand-based electron transitions, responsible for the absorbance

spectra following lanthanide contraction in the hafnium (relative to zirconium), surfaces as a relatively measurable entity.

(b) The broad absorbance peaks (due to these electron transitions) and changes observed between 350 – 450 nm do suggest external (solvent) influences at the outer periphery of the complexes, especially when considering the previously discussed anomalies with regard to solvent effect/interaction on product peak shifts (MeOH to DCM, described above).

(c) Thus, from the comparative spectra shown in **Figure 10.11** below, where the combination of the individual hafnium and zirconium experimental data is shown (*after extraction*), it becomes apparent that for both these metals, the product peak in each case is **indistinguishable** from the other (comparing the hafnium product peaks to the zirconium peaks – after extraction). The UV/Vis methodology discussed here, although very valuable to evaluate a single zirconium of hafnium complex, can therefore unfortunately **not be quantitatively, nor qualitatively, used** in a mixture extraction (of both metals) to determine whether complete extraction of only one metal has been achieved. In this case, other analytical methods of qualitative analysis, such as ICP-OES clearly needs to be employed.

(d) However, the results from this UV/vis study is not all negative: Both of these metal centres' 5Cl-OxH complexes are extremely similar, including their observed complex formation and -stabilities, extraction ability and then finally, their UV/vis spectroscopy. Thus, this study allows a fair **qualitative** (but also within some 10% accuracy, thus reasonably **quantitative**) analytical technique to estimate the **total** Zr/Hf within a specific sample. Thus, although the **relative** amounts of Zr and Hf cannot be determined, the **total amount** may be estimated. This might be exploited further in future.

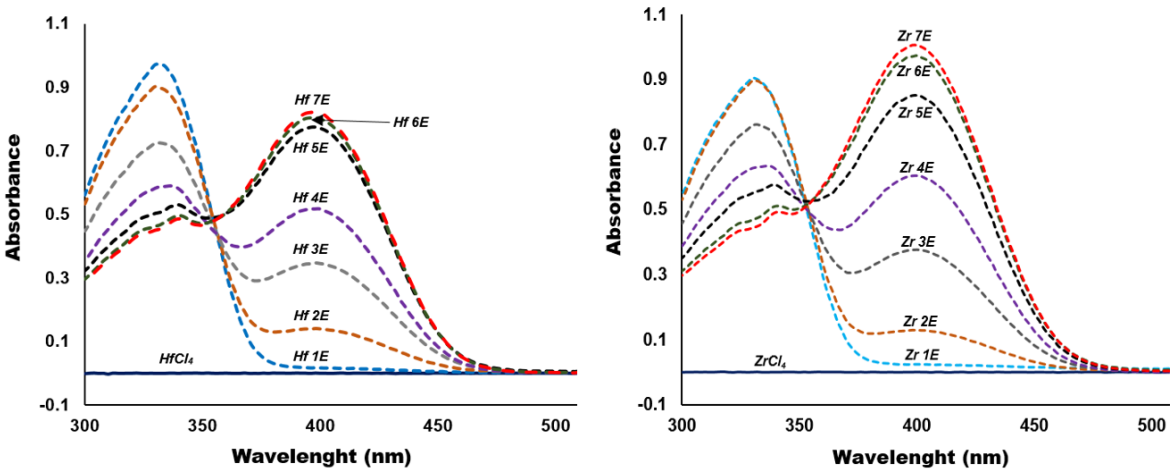

Figure 10.11: UV/Vis spectra of reaction mixture **(a)** Hf 1E – Hf 7E (**Table 10.2**) and **(b)** Zr 1E – Zr 7E (**Table 10.3**) overlaid *after extraction* in DCM at 25°C.). Dark Blue = $[MCl_4]$= 7.5 x 10^{-5} M, Light blue = **M 1E** ([5Cl-OxH] = 3.1 x 10^{-4} M and $[MCl_4]$ = 0 M), Orange = **M 2E** [5Cl-OxH] = 3.1 x 10^{-4} M and $[MCl_4]$ = 7.5 x 10^{-6} M), Grey = **M 3E** [5Cl-OxH] = 3.1 x 10^{-4} M and $[MCl_4]$ = 2.3 x 10^{-5} M), Purple = **M 4E** ([5Cl-OxH] = 3.1 x 10^{-4} M and $[MCl_4]$ = 3.8 x 10^{-5} M), **Black** = **M 5E** ([5Cl-OxH] = 3.1 x 10^{-4} M and $[MCl_4]$ = 5.3 x 10^{-5} M), Green = **M 6E** ([5Cl-OxH] = 3.1 x 10^{-4} M and $[MCl_4]$ = 6.8 x 10^{-5} M), Red = **M 7E** ([5Cl-OxH] = 3.1 x 10^{-4} M and $[MCl_4]$ = 7.5 x 10^{-5} M) (**M** = **Hf** or **Zr**).

10.7. Preliminary Liquid-liquid Extraction of a Mixture of Zirconium and Hafnium

Following the success of extracting the metal complexes using different solvent combinations as described above, any differences or preferences towards extraction occurring when using mixtures of zirconium and hafnium for separation applications were investigated. Hence, mixtures of zirconium and hafnium were therefore considered to evaluate whether there might be **relative preferences** for any of the metals using the above-mentioned extraction procedure.

10.7.1 General Procedure

To investigate potential differences via preliminary competition experiments, a starting mixture consisting of 1:1 ratio ($ZrCl_4$:$HfCl_4$) of **two** molar equivalents [155 *μ*mol each (1 equivalent)] was dissolved in 40 mL methanol (MeOH). To this solution, 8.1 equivalents (1.25 mmol; thus ca. 4 equivalents for each of the Zr and Hf present), of the **six** different oxine ligands (**Table 10.4**) were added to enable formation of the corresponding *tetrakis*-oxine complexes and allowing 'full' coordination to be achieved.

In a typical extraction; a 50:50 molar mixture $HfCl_4$/$ZrCl_4$ (50 mg $HfCl_4$, 155 *μ*mol : 37 mg $ZrCl_4$,155 *μ*mol) was dissolved in MeOH (40 mL). While stirring this solution, at room temperature, another solution of the corresponding oxine ligand (1.24 mmol) also dissolved in MeOH (40 mL) was slowly added, resulting in the formation of intense yellowish solutions. After *ca*. 10 min, cold distilled water (80 mL) and DCM (40 mL) was added to the reaction mixture. The DCM layer (extracted layer) was collected and dried. The samples were then taken for ICP-OES for elemental analysis (**Table 10.4**).

10.7.2. ICP-OES Results

Table 10.4 below summarises the results obtained for the zirconium and hafnium recovered after extraction using the procedure described above, following Shimadzu ICP-7500 analysis.

Table 10.4: Elemental analyses obtained for Zr/Hf obtained from liquid-liquid extraction.

Ligand [a]		Zr (37 mg $ZrCl_4$,155 μmol)		Hf (50 mg $HfCl_4$,155 μmol)		Extracted	
(1.24 mmol)	Mass (mg)	Theoretical %	Determined %	Theoretical %	Determined %	Zr %	Hf %
5Cl-OxH	225	5.37	4.7	10.51	6.87	87.5	65.4
7Br-OxH	324	4.44	3.83	8.69	6.27	86.3	72.2
diCl-OxH	268	4.62	4.30	9.04	7.2	93.1	79.7
diBr-OxH	379	3.40	3.00	6.65	5.23	88.2	78.7
diI-OxH	497	2.65	2.30	5.19	3.38	86.8	65.1
Cl-I-OxH	383	3.37	2.96	6.60	5.37	87.8	81.4

[a] ***5Cl-OxH*** *= 5-Chloro-8-hydroxyquinoline;* ***7Br-OxH*** *= 7-Bromo-8-hydroxy-quinoline;* ***diCl-OxH*** *= 5,7-Dichloro-8-hydroxyquinoline;* ***diBr-OxH*** *= 5,7-Dibromo-8-hydroxyquinoline;* ***diI-OxH*** *= 5,7-Diiodo-8-hydroxyquinoline;* ***Cl-I-OxH*** *= 5-Chloro-7-iodo-8-hydroxyquinoline.*

It is apparent from the above ICP-OES results that both zirconium and hafnium are extracted, albeit with a slightly higher preference towards zirconium. It is unclear at this point what the effect of the kinetic formation of the different complexes are.

Moreover, when considering **Table 10.4**, and in particular the **5Cl-OxH** and **diI-OxH** ligands, more promising results (albeit not ideal!) for potential separation via liquid-liquid extraction experiments emerges which should be investigated further in future utilising for example multiple step-type experiments involving smaller ligand concentrations in a follow-up mode in future.

10.8. Conclusion

Although the extraction experiments described herein are clearly very preliminary, some positives came forth wherein (small) differences in the amounts of Zr:Hf extracted were observed, and could in principle be considered a preliminary proof-of-concept for separation. This, however, will require more extended studies in future.

It is apparent from the results that both hafnium -and zirconium complexes and the free oxine ligands are easily extracted from methanol in relative high yields with no preference towards any oxine ligand. Furthermore, the amount of free oxine ligand in the extracted phase might be reduced by reaction conditions like for instance longer reaction times.

ICP-OES results obtained for Zr/Hf comparative studies pointed out that both zirconium and hafnium are readily extracted in high yields with a somewhat higher preference towards zirconium. From these results, it is concluded that both **5Cl-OxH** and **diI-OxH** show promising results for separation utilising liquid-liquid extraction method.

Chapter 11

Evaluation of Study and Future Aims

11.1. Overview

The high-level aims of this research project, as has been identified in the Introduction (**Chapter 1**) and followed on throughout the preceding chapters, have been the synthesis, subsequent characterisation and critical solid-state evaluation of novel hafnium(IV) coordination compounds. Extending on the solid-state studies, a preliminary investigation of the solution extraction behaviour of some of these complexes was also initiated. In each area of focus, a discussion on novel and comparative findings have been presented.

In this chapter, a summary of the successful research foci and scope for future investigation will be discussed.

11.2. Synthesis of Novel Hafnium(IV) Complexes

One key aspect of this research project has been the establishment of an extended range of novel hafnium(IV) complexes, that have been successfully synthesised and analysed via UV/Vis, IR and NMR spectroscopy, and in addition, via single crystal X-ray crystallography.

Three types of *N*- and *O*-donating ligand systems were identified for this study, as discussed in the aims in **Chapter 1**, based on the known coordination abilities of

these ligands (**Chapter 2**), and primarily focused on the range of *N,O*-, *O,O'*-, *N,O,O,N*- and *N,N',N',N*- coordination modes. A further significance of these types of ligands chosen lies in the fact that so few complex examples of hafnium(IV) were previously known in literature.

As highlighted in **Chapter 2**, the literature indicates that hafnium(IV) complexes could only be synthesised under anhydrous and inert (Schlenk) conditions to avoid hydrolysis of the tetrachloridohafnium (IV) starting reagent ($HfCl_4$) and thus the formation of unreactive oxido-metal species. However, it was illustrated in this study that it is possible to synthesise hafnium(IV) complexes containing these various *N,O*- and *O,O'*-bidentate ligand systems as well as *N,O,O,N*- and *N,N',N',N* tetradentate ligand systems under normal aerobic conditions, and that rather, reasonably dry conditions should be maintained to avoid hydrolysis. This simple bench-top technique utilised in all cases involved synthesis without any special precautions, equipment or laborious crystallisation techniques needed, making it ideal for industrial applications and more economically viable.

Finally, most compounds reported in **Chapter 3** yielded crystalline products with sufficient stability and quality for structural characterisation by means of single crystal X-ray Diffraction (XRD). Unfortunately, some compounds were, due to solvent loss, too unstable to produce measurable X-ray diffraction data.

11.3. Crystallographic Structural Characterisation

The in-depth single crystal X-Ray diffraction characterisation investigations described in **Chapters 4** – **9,** reported the crystal structures of *nine* new Hf(IV) and one Zr(IV) compounds: six new hafnium(IV) compounds with bidentate *N,O'*-donating ligands, two new hafnium(IV) compounds with bidentate *O,O'*-donating ligands and one hafnium(IV) compound with a tetradentate *N,O,O,N*-donating ligand. An additional zirconium(IV) compound with a tetradentate *N,N',N',N*-donating ligand was also successfully obtained and characterised. These solid-state studies enabled to proceed with one of the primary aims of this study, which was to investigate the influence these ligand systems have on the structural

properties of the hafnium(IV) and zirconium(IV) metal centres and to correlate the effect thereof on the different metal coordination polyhedrons.

The single X-ray data of the six oxine-type complexes yielded valuable information and insight into the geometric coordination characteristics around the hafnium(IV) metal centre. Correlation of these six structures with similar zirconium type structures showed that the coordination environment around these metal centres favours the square-antiprismatic geometry (***D_2-corner-clipped isomer)*** for all known *tetrakis*-oxine complexes. It could therefore be postulated that most, if not all, eight-coordinated (*tetrakis*) hafnium(IV) and zirconium(IV) complexes containing oxine-type ligands should yield a square-antiprismatic geometry around the metal centres. Moreover, as discussed in **Chapter 9**, an approximate relationship between the outer periphery of the oxine ligand substituents (*electron-donating vs electron-withdrawing and steric bulk*) and the relative distortion of the square-antiprismatic polyhedron was observed. Moreover, other general structural properties (i.e. bond lengths, ligand bite angles, etc.) were similar for all compounds.

With regard to the solvent molecules and the effective packing of the metal-oxine complexes, it has been shown that hydrogen bonding between solvates and coordinated oxine ligands influences the stability of the crystal lattice as a whole. Furthermore, all of the complexes displayed similar intermolecular interactions to some extent, with π-π- and halogen-π staking being most frequent within the crystal lattices and, therefore, contributing to the overall arrangement and stability in the crystal lattices.

In **Chapter 6** the description of the two Hf(IV)-acetylacetonato complexes also yielded some interesting insight into the intimate geometric coordination characteristics around the hafnium(IV) metal centre. Firstly, the correlation of these structures with similar zirconium type structures showed that the coordination environment around these metal centres favours the ***D_2-corner-clipped*** square-antiprismatic isomer geometry when recrystallised from organic solvents and the ***C_2-mixed bonding*** square antiprismatic isomer geometry when recrystallised *via*

sublimation. Secondly, binuclear hafnium *β*-diketonato complexes ([Hf(OH)(hfaa)$_3$]$_2$ and [Hf(OH)(tfba)$_3$]$_2$) were isolated, whereas *no evidence* of any dimer formation could be found in the literature for zirconium *β*-diketonato complexes. Due to the small pool of available data on these types of complexes, it can thus only be speculated that the properties of the solvent used (polarity, Bronsted *pKa* value, etc.), or the lack thereof during synthesis and recrystallisation, are contributing factors for the dimer formations observed. However, all other Hf(IV) and Zr(IV) compounds' general structural properties (i.e. bond lengths, ligand bite angles, etc.) are very comparable; almost identical. This suggests and indicate that both hafnium(IV) and zirconium(IV) display a certain preference for the chelation sites of the coordinating atoms, regardless of the steric properties of the ligands as such.

Finally, the importance of a detailed and step-wise solid-state crystallographic investigation becomes quite evident. The various solid-state characteristics within each crystal structure, and all the complexes taken as a group, shedded significant light on coordination preferences and ligand influences on the complex structure of both Hf(IV)- and Zr(IV)-type complexes. This enhanced insight contributes to enhancing the knowledge base for Hf(IV)- and Zr(IV)- multidentate complexes.

11.4. Preliminary Solution Extractions

The preliminary liquid-liquid extraction investigation of zirconium- and hafnium-oxinate complexes from methanol (MeOH) into dichloromethane (DCM) and competition extractions, utilising UV-vis spectroscopy (UV/Vis) and inductively coupled plasma optical emission spectroscopy (ICP-OES) was performed and described in **Chapter 10**.

From these preliminary liquid-liquid extraction investigations, it was shown that [Hf(5ClOx)$_4$] and [Zr(5ClOx)$_4$] were both easily extracted from methanol into dichloro-methane and could be spectrophotometrically followed for each step and concentration of certain extraction parameters. However, from the comparative spectral stacked plots, where the combination of the individual hafnium and

zirconium experimental data was overlayed (*after extraction*), it became apparent that for both these metals, the product peak in each case was virtually indistinguishable from the other.

Very preliminary ICP-OES results obtained for Zr/Hf competitive studies suggested that both the zirconium- and hafnium-oxinate complexes are readily extracted in high yields with a *slightly* higher preference towards zirconium. It was concluded that 5ClOxH and diIOxH showed the most promising results for separation utilising liquid-liquid extraction method.

11.5. Future Research

This PhD study has yielded valuable insights and an extended knowledge base into the chelation behaviour of hafnium(IV) with various organic ligands. The lack of crystallographic data available and the reporting of vigorous synthetic procedures for hafnium(IV) and zirconium(IV) compounds in literature, underlines the significant potential future research leading directly from the results obtained in this study. Thus, some key points for future investigations can be summarised, as described below.

1. Synthesis and Crystallisation

The bench-top synthetic route utilised and presented in **Chapter 3** readily yielded crystalline products. However, some of the isolated compounds were of very poor quality and could not be analysed via single crystal XRD. Thus, further investigations, especially using more environmentally friendly solvents with lower boiling points, for synthesis and recrystallisation might yield better quality crystals which could significantly increase the available crystallographic data pool. Furthermore, recrystallisation via sublimation and organic solvent should be compared to investigate the hafnium(IV) dimer type of complexes observed when reacted to some fluorinated *β*-diketonato ligand systems. These differences in chelation behaviour between hafnium(IV) and zirconium(IV) could yield valuable information and could be exploited in future separation

studies. Hence, extended knowledge on the latter will also enable solventless complex formation/ extraction to be explored.

2. Solvent Extraction Studies

The rudimentary findings of the liquid-liquid extraction studies presented in **Chapter 10** indicated that both hafnium(IV) -and zirconium(IV) oxine complexes are readily extracted in high yields with a lesser preference towards hafnium. Capitalisation on these observations could in principle lead to improved extraction in solution upon exploring even better ligand systems. Therefore, different solvents and other ligand systems also need to be investigated in significant depth.

Appendix A.1

Supplementary Crystallographic Data

A.1. $[Hf(Ox)_4]\cdot 2(C_7H_8)$ – (Hf_1a) – § 4.3

Table A.1.1: Atomic coordinates (x 10^4) and equivalent isotropic displacement parameters ($Å^2$ x 10^3) for $[Hf(Ox)_4]\cdot 2(C_7H_8)$.

Atom	*x*	*y*	*z*	*U(eq)*
Hf	1942(1)	2469(1)	6517(1)	11(1)
N(4)	1342(3)	2939(3)	7981(2)	14(1)
N(3)	2993(3)	4043(3)	6239(2)	14(1)
N(2)	2853(3)	823(3)	5933(2)	13(1)
N(1)	504(3)	2037(3)	5909(2)	15(1)
O(2)	2786(3)	3022(2)	5050(2)	13(1)
O(1)	910(3)	1197(2)	7570(2)	14(1)
O(3)	3619(3)	1828(2)	6929(2)	14(1)
C(105)	2150(5)	9418(4)	9396(3)	23(1)
C(42)	1269(5)	2752(4)	9567(3)	20(1)
O(4)	440(3)	3817(2)	6519(2)	14(1)
C(39)	4106(4)	3707(3)	6462(3)	14(1)
C(45)	-1373(5)	4969(4)	8906(3)	22(1)
C(104)	1550(5)	8725(4)	10261(3)	23(1)
C(37)	5553(4)	2116(4)	7076(3)	20(1)
C(205)	3890(7)	6201(5)	8981(4)	46(2)
C(18)	159(4)	675(3)	7407(3)	15(1)
C(204)	4356(6)	5098(5)	8971(4)	39(1)
C(12)	-455(4)	2069(4)	4758(3)	22(1)
C(21)	2922(4)	-275(3)	6404(3)	12(1)
C(29)	3295(4)	1114(3)	4969(3)	12(1)
C(46)	-1805(5)	5423(4)	8124(3)	25(1)
C(203)	3829(5)	4553(4)	8601(3)	28(1)
C(19)	-91(4)	1124(3)	6511(3)	13(1)
C(11)	301(4)	2510(4)	5067(3)	19(1)

C(24)	3809(4)	293(3)	4459(3)	14(1)
C(34)	4924(4)	4487(4)	6312(3)	16(1)
C(32)	3397(5)	5985(4)	5694(3)	19(1)
C(33)	4522(5)	5659(4)	5911(3)	20(1)
C(15)	-1430(5)	-332(4)	6941(4)	24(1)
C(49)	305(4)	3765(3)	8060(3)	14(1)
C(22)	3422(4)	-1154(3)	5959(3)	16(1)
C(206)	2888(6)	6785(4)	8601(3)	39(2)
C(101)	4169(5)	8733(4)	9727(4)	24(1)
C(31)	2648(4)	5148(3)	5866(3)	15(1)
C(107)	5587(5)	8748(5)	9431(4)	41(1)
C(26)	4198(4)	1852(4)	3018(3)	16(1)
C(44)	-297(4)	4116(4)	8891(3)	17(1)
C(102)	3554(5)	8060(4)	10597(3)	29(1)
C(28)	3249(4)	2319(3)	4504(3)	12(1)
C(48)	-158(4)	4235(3)	7253(3)	15(1)
C(41)	1816(4)	2455(3)	8712(3)	16(1)
C(13)	-1014(5)	1134(4)	5345(3)	24(1)
C(36)	6377(5)	2882(4)	6923(3)	22(1)
C(27)	3701(4)	2663(3)	3526(3)	16(1)
C(35)	6077(4)	4046(4)	6546(3)	21(1)
C(17)	-420(4)	-252(4)	8055(3)	20(1)
C(202)	2835(4)	5123(4)	8235(3)	21(1)
C(38)	4435(4)	2497(3)	6844(3)	15(1)
C(14)	-872(4)	617(4)	6263(3)	18(1)
C(106)	3449(5)	9423(4)	9129(3)	20(1)
C(23)	3857(4)	-878(3)	4999(3)	15(1)
C(47)	-1215(4)	5072(3)	7294(3)	18(1)
C(16)	-1200(5)	-747(4)	7813(3)	24(1)
C(25)	4271(4)	700(3)	3460(3)	16(1)
C(201)	2346(5)	6255(4)	8215(3)	23(1)
C(103)	2263(5)	8043(4)	10863(4)	29(1)
C(43)	237(5)	3580(4)	9650(3)	21(1)
C(207)	1292(5)	6861(4)	7794(4)	35(1)

Table A.1.2: Hydrogen coordinates (x 10^4) and isotropic displacement parameters (Å^2 x 10^3) for $[Hf(Ox)_4]\cdot 2(C_7H_8)$.

Atom	*x*	*y*	*z*	*U(eq)*
H(105)	1678	9886	8988	28
H(22)	1611	2386	10072	24
H(25)	-1785	5219	9443	26
H(104)	679	8716	10438	28
H(37)	5773	1336	7340	24
H(205)	4239	6565	9242	55
H(204)	5034	4712	9215	47
H(12)	-570	2415	4159	26
H(41)	2627	-479	7062	15
H(26)	-2515	5984	8140	30
H(203)	4145	3796	8599	34
H(11)	671	3158	4665	22
H(32)	3126	6756	5433	23
H(33)	5025	6207	5796	24
H(15)	-1950	-678	6801	29
H(42)	3453	-1919	6319	20
H(206)	2578	7542	8607	47
H(31)	1885	5379	5712	18
H(10A)	5795	8976	9879	62
H(10B)	5836	9283	8814	62
H(10C)	6029	7996	9411	62
H(46)	4487	2105	2361	20
H(102)	4019	7609	11014	34
H(21)	2533	1901	8658	19
H(13)	-1498	829	5139	28
H(36)	7137	2598	7079	27
H(47)	3674	3441	3202	19
H(35)	6635	4540	6446	25
H(17)	-293	-549	8652	24
H(202)	2480	4740	7994	25
H(106)	3843	9895	8542	24
H(43)	4185	-1453	4698	18
H(27)	-1534	5403	6776	21
H(16)	-1573	-1376	8256	29

H(45)	4624	183	3103	19
H(103)	1871	7571	11449	34
H(23)	-115	3791	10209	25
H(20A)	1627	7132	7117	53
H(20B)	867	7501	8039	53
H(20C)	699	6344	7951	53

Table A.1.3: Anisotropic displacement parameters ($Å^2$ x 10^3) for $[Hf(Ox)_4]\cdot 2(C_7H_8)$.

Atom	U^{11}	U^{22}	U^{33}	U^{23}	U^{13}	U^{12}
Hf	12(1)	12(1)	12(1)	-5(1)	-4(1)	-2(1)
N(4)	15(2)	12(2)	14(2)	-2(1)	-3(2)	-6(1)
N(3)	13(2)	17(2)	13(2)	-8(1)	-1(2)	-4(1)
N(2)	10(2)	13(2)	19(2)	-6(1)	-6(2)	-2(1)
N(1)	11(2)	18(2)	16(2)	-7(1)	-4(2)	1(1)
O(2)	14(2)	12(1)	15(2)	-5(1)	-1(1)	-5(1)
O(1)	16(2)	16(1)	13(1)	-5(1)	-4(1)	-5(1)
O(3)	12(2)	15(1)	18(2)	-7(1)	-4(1)	-2(1)
C(105)	29(3)	18(2)	29(3)	-11(2)	-18(2)	5(2)
C(42)	23(3)	24(2)	15(2)	-4(2)	-7(2)	-7(2)
O(4)	15(2)	14(1)	14(2)	-6(1)	-5(1)	0(1)
C(39)	11(2)	20(2)	13(2)	-10(2)	1(2)	-4(2)
C(45)	22(3)	24(2)	19(2)	-11(2)	1(2)	-5(2)
C(104)	16(2)	23(2)	32(3)	-12(2)	-3(2)	-5(2)
C(37)	19(2)	23(2)	22(2)	-12(2)	-7(2)	-1(2)
C(205)	71(5)	63(4)	20(3)	-9(3)	-5(3)	-52(4)
C(18)	12(2)	17(2)	16(2)	-7(2)	-1(2)	-2(2)
C(204)	34(3)	69(4)	17(3)	-6(3)	-4(2)	-27(3)
C(12)	18(3)	32(2)	17(2)	-8(2)	-9(2)	0(2)
C(21)	9(2)	16(2)	14(2)	-5(2)	-4(2)	-3(2)
C(29)	13(2)	13(2)	12(2)	-4(2)	-4(2)	-6(2)
C(46)	19(3)	24(2)	31(3)	-13(2)	-5(2)	4(2)
C(203)	28(3)	36(3)	18(2)	-6(2)	-3(2)	-9(2)
C(19)	8(2)	13(2)	16(2)	-5(2)	-3(2)	-1(2)
C(11)	16(2)	22(2)	18(2)	-5(2)	-6(2)	-2(2)
C(24)	11(2)	15(2)	19(2)	-7(2)	-6(2)	-3(2)
C(34)	15(2)	21(2)	13(2)	-10(2)	1(2)	-8(2)

C(32)	24(3)	16(2)	16(2)	-5(2)	-4(2)	-3(2)
C(33)	26(3)	21(2)	17(2)	-11(2)	-1(2)	-7(2)
C(15)	17(3)	24(2)	38(3)	-12(2)	-10(2)	-4(2)
C(49)	12(2)	15(2)	16(2)	-5(2)	-1(2)	-6(2)
C(22)	15(2)	14(2)	22(2)	-6(2)	-6(2)	-2(2)
C(206)	68(5)	25(2)	20(3)	-9(2)	8(3)	-26(3)
C(101)	22(3)	24(2)	29(3)	-12(2)	-8(2)	-2(2)
C(31)	15(2)	17(2)	15(2)	-7(2)	-4(2)	-4(2)
C(107)	24(3)	51(3)	45(4)	-14(3)	-5(3)	-5(3)
C(26)	12(2)	26(2)	14(2)	-6(2)	-6(2)	-6(2)
C(44)	16(2)	20(2)	14(2)	-4(2)	0(2)	-9(2)
C(102)	31(3)	28(2)	21(3)	-2(2)	-12(2)	2(2)
C(28)	8(2)	16(2)	16(2)	-5(2)	-3(2)	-5(2)
C(48)	19(2)	14(2)	14(2)	-4(2)	-2(2)	-6(2)
C(41)	15(2)	15(2)	18(2)	-6(2)	-6(2)	0(2)
C(13)	13(2)	31(2)	35(3)	-16(2)	-13(2)	3(2)
C(36)	15(2)	32(2)	29(3)	-18(2)	-8(2)	0(2)
C(27)	16(2)	16(2)	17(2)	-5(2)	-8(2)	0(2)
C(35)	17(2)	29(2)	21(2)	-13(2)	-1(2)	-11(2)
C(17)	18(2)	22(2)	18(2)	-6(2)	-5(2)	-3(2)
C(202)	17(2)	27(2)	19(2)	-11(2)	0(2)	-6(2)
C(38)	17(2)	16(2)	15(2)	-8(2)	-5(2)	-5(2)
C(14)	13(2)	19(2)	27(2)	-9(2)	-8(2)	-2(2)
C(106)	23(3)	17(2)	19(2)	-5(2)	-2(2)	-9(2)
C(23)	7(2)	18(2)	24(2)	-11(2)	-3(2)	-3(2)
C(47)	13(2)	19(2)	18(2)	-4(2)	-1(2)	-5(2)
C(16)	20(3)	23(2)	28(3)	-6(2)	-5(2)	-7(2)
C(25)	14(2)	20(2)	18(2)	-13(2)	-3(2)	-1(2)
C(201)	27(3)	21(2)	13(2)	-3(2)	10(2)	-12(2)
C(103)	32(3)	27(2)	21(2)	-2(2)	-5(2)	-6(2)
C(43)	21(3)	26(2)	14(2)	-10(2)	2(2)	-8(2)
C(207)	29(3)	27(3)	27(3)	1(2)	3(2)	5(2)

Table A.1.4: Bond lengths (Å) for $[Hf(Ox)_4]\cdot 2(C_7H_8)$.

Atoms	*Bond Length (Å)*	*Atoms*	*Bond Length (Å)*
Hf-O(4)	2.085(3)	**C(11)-H(11)**	0.93
Hf-O(2)	2.096(3)	**C(24)-C(25)**	1.417(6)
Hf-O(1)	2.098(3)	**C(24)-C(23)**	1.419(5)
Hf-O(3)	2.103(3)	**C(34)-C(35)**	1.409(6)
Hf-N(3)	2.391(3)	**C(34)-C(33)**	1.414(6)
Hf-N(1)	2.395(3)	**C(32)-C(33)**	1.364(6)
Hf-N(4)	2.400(3)	**C(32)-C(31)**	1.407(6)
Hf-N(2)	2.404(3)	**C(32)-H(32)**	0.93
N(4)-C(41)	1.328(5)	**C(33)-H(33)**	0.93
N(4)-C(49)	1.365(5)	**C(15)-C(16)**	1.380(7)
N(3)-C(31)	1.322(5)	**C(15)-C(14)**	1.407(6)
N(3)-C(39)	1.353(5)	**C(15)-H(15)**	0.93
N(2)-C(21)	1.317(5)	**C(49)-C(44)**	1.413(6)
N(2)-C(29)	1.363(5)	**C(49)-C(48)**	1.422(6)
N(1)-C(11)	1.325(5)	**C(22)-C(23)**	1.357(6)
N(1)-C(19)	1.360(5)	**C(22)-H(42)**	0.93
O(2)-C(28)	1.332(5)	**C(206)-C(201)**	1.389(7)
O(1)-C(18)	1.326(5)	**C(206)-H(206)**	0.93
O(3)-C(38)	1.340(5)	**C(101)-C(102)**	1.377(7)
C(105)-C(104)	1.377(7)	**C(101)-C(106)**	1.386(6)
C(105)-C(106)	1.385(7)	**C(101)-C(107)**	1.513(7)
C(105)-H(105)	0.93	**C(31)-H(31)**	0.93
C(42)-C(43)	1.362(6)	**C(107)-H(10A)**	0.96
C(42)-C(41)	1.409(6)	**C(107)-H(10B)**	0.96
C(42)-H(22)	0.93	**C(107)-H(10C)**	0.96
O(4)-C(48)	1.329(5)	**C(26)-C(25)**	1.366(6)
C(39)-C(34)	1.418(6)	**C(26)-C(27)**	1.400(6)
C(39)-C(38)	1.433(6)	**C(26)-H(46)**	0.93
C(45)-C(46)	1.367(6)	**C(44)-C(43)**	1.411(6)
C(45)-C(44)	1.410(6)	**C(102)-C(103)**	1.378(7)
C(45)-H(25)	0.93	**C(102)-H(102)**	0.93
C(104)-C(103)	1.382(7)	**C(28)-C(27)**	1.383(6)
C(104)-H(104)	0.93	**C(48)-C(47)**	1.385(6)
C(37)-C(38)	1.367(6)	**C(41)-H(21)**	0.93
C(37)-C(36)	1.407(6)	**C(13)-C(14)**	1.411(6)
C(37)-H(37)	0.93	**C(13)-H(13)**	0.93

C(205)-C(204)	1.359(9)	**C(36)-C(35)**	1.377(6)
C(205)-C(206)	1.393(9)	**C(36)-H(36)**	0.93
C(205)-H(205)	0.93	**C(27)-H(47)**	0.93
C(18)-C(17)	1.382(6)	**C(35)-H(35)**	0.93
C(18)-C(19)	1.424(6)	**C(17)-C(16)**	1.407(6)
C(204)-C(203)	1.371(7)	**C(17)-H(17)**	0.93
C(204)-H(204)	0.93	**C(202)-C(201)**	1.386(6)
C(12)-C(13)	1.356(7)	**C(202)-H(202)**	0.93
C(12)-C(11)	1.409(6)	**C(106)-H(106)**	0.93
C(12)-H(12)	0.93	**C(23)-H(43)**	0.93
C(21)-C(22)	1.408(5)	**C(47)-H(27)**	0.93
C(21)-H(41)	0.93	**C(16)-H(16)**	0.93
C(29)-C(24)	1.413(5)	**C(25)-H(45)**	0.93
C(29)-C(28)	1.432(5)	**C(201)-C(207)**	1.482(7)
C(46)-C(47)	1.410(6)	**C(103)-H(103)**	0.93
C(46)-H(26)	0.93	**C(43)-H(23)**	0.93
C(203)-C(202)	1.371(7)	**C(207)-H(20A)**	0.96
C(203)-H(203)	0.93	**C(207)-H(20B)**	0.96
C(19)-C(14)	1.423(6)	**C(207)-H(20C)**	0.96

Table A.1.5: Bond angles (°) for $[Hf(Ox)_4]\cdot 2(C_7H_8)$.

Atoms	*Bond angle (°)*	*Atoms*	*Bond angle (°)*
O(4)-Hf-O(2)	94.50(11)	**C(31)-C(32)-H(32)**	120.2
O(4)-Hf-O(1)	97.00(11)	**C(32)-C(33)-C(34)**	119.9(4)
O(2)-Hf-O(1)	141.84(10)	**C(32)-C(33)-H(33)**	120
O(4)-Hf-O(3)	142.31(11)	**C(34)-C(33)-H(33)**	120
O(2)-Hf-O(3)	97.89(11)	**C(16)-C(15)-C(14)**	119.6(4)
O(1)-Hf-O(3)	94.85(11)	**C(16)-C(15)-H(15)**	120.2
O(4)-Hf-N(3)	78.53(12)	**C(14)-C(15)-H(15)**	120.2
O(2)-Hf-N(3)	73.74(11)	**N(4)-C(49)-C(44)**	122.8(4)
O(1)-Hf-N(3)	144.27(11)	**N(4)-C(49)-C(48)**	115.4(4)
O(3)-Hf-N(3)	71.16(11)	**C(44)-C(49)-C(48)**	121.7(4)
O(4)-Hf-N(1)	73.68(11)	**C(23)-C(22)-C(21)**	119.6(4)
O(2)-Hf-N(1)	77.94(11)	**C(23)-C(22)-H(42)**	120.2
O(1)-Hf-N(1)	70.73(11)	**C(21)-C(22)-H(42)**	120.2
O(3)-Hf-N(1)	143.78(11)	**C(201)-C(206)-C(205)**	121.0(5)

N(3)-Hf-N(1)	138.19(12)	**C(201)-C(206)-H(206)**	119.5
O(4)-Hf-N(4)	71.04(11)	**C(205)-C(206)-H(206)**	119.5
O(2)-Hf-N(4)	145.17(11)	**C(102)-C(101)-C(106)**	118.2(5)
O(1)-Hf-N(4)	72.67(11)	**C(102)-C(101)-C(107)**	121.5(5)
O(3)-Hf-N(4)	78.70(11)	**C(106)-C(101)-C(107)**	120.2(5)
N(3)-Hf-N(4)	72.39(11)	**N(3)-C(31)-C(32)**	122.3(4)
N(1)-Hf-N(4)	124.51(12)	**N(3)-C(31)-H(31)**	118.9
O(4)-Hf-N(2)	142.23(11)	**C(32)-C(31)-H(31)**	118.9
O(2)-Hf-N(2)	70.84(11)	**C(101)-C(107)-H(10A)**	109.5
O(1)-Hf-N(2)	77.98(11)	**C(101)-C(107)-H(10B)**	109.5
O(3)-Hf-N(2)	75.31(11)	**H(10A)-C(107)-H(10B)**	109.5
N(3)-Hf-N(2)	126.37(12)	**C(101)-C(107)-H(10C)**	109.5
N(1)-Hf-N(2)	69.32(11)	**H(10A)-C(107)-H(10C)**	109.5
N(4)-Hf-N(2)	138.57(11)	**H(10B)-C(107)-H(10C)**	109.5
C(41)-N(4)-C(49)	118.5(4)	**C(25)-C(26)-C(27)**	122.0(4)
C(41)-N(4)-Hf	129.1(3)	**C(25)-C(26)-H(46)**	119
C(49)-N(4)-Hf	112.2(3)	**C(27)-C(26)-H(46)**	119
C(31)-N(3)-C(39)	118.9(4)	**C(45)-C(44)-C(43)**	124.7(4)
C(31)-N(3)-Hf	128.1(3)	**C(45)-C(44)-C(49)**	118.6(4)
C(39)-N(3)-Hf	112.9(2)	**C(43)-C(44)-C(49)**	116.7(4)
C(21)-N(2)-C(29)	118.0(3)	**C(101)-C(102)-C(103)**	121.4(5)
C(21)-N(2)-Hf	129.4(3)	**C(101)-C(102)-H(102)**	119.3
C(29)-N(2)-Hf	112.5(2)	**C(103)-C(102)-H(102)**	119.3
C(11)-N(1)-C(19)	118.5(4)	**O(2)-C(28)-C(27)**	125.2(4)
C(11)-N(1)-Hf	128.7(3)	**O(2)-C(28)-C(29)**	117.2(3)
C(19)-N(1)-Hf	112.7(3)	**C(27)-C(28)-C(29)**	117.7(4)
C(28)-O(2)-Hf	123.6(2)	**O(4)-C(48)-C(47)**	124.6(4)
C(18)-O(1)-Hf	123.2(3)	**O(4)-C(48)-C(49)**	117.3(4)
C(38)-O(3)-Hf	123.4(2)	**C(47)-C(48)-C(49)**	118.0(4)
C(104)-C(105)-C(106)	120.6(4)	**N(4)-C(41)-C(42)**	122.1(4)
C(104)-C(105)-H(105)	119.7	**N(4)-C(41)-H(21)**	118.9
C(106)-C(105)-H(105)	119.7	**C(42)-C(41)-H(21)**	118.9
C(43)-C(42)-C(41)	119.7(4)	**C(12)-C(13)-C(14)**	121.0(4)
C(43)-C(42)-H(22)	120.1	**C(12)-C(13)-H(13)**	119.5
C(41)-C(42)-H(22)	120.1	**C(14)-C(13)-H(13)**	119.5
C(48)-O(4)-Hf	123.8(3)	**C(35)-C(36)-C(37)**	121.2(4)
N(3)-C(39)-C(34)	122.9(4)	**C(35)-C(36)-H(36)**	119.4
N(3)-C(39)-C(38)	116.0(4)	**C(37)-C(36)-H(36)**	119.4
C(34)-C(39)-C(38)	121.0(4)	**C(28)-C(27)-C(26)**	120.6(4)

C(46)-C(45)-C(44)	119.3(4)	**C(28)-C(27)-H(47)**	119.7
C(46)-C(45)-H(25)	120.4	**C(26)-C(27)-H(47)**	119.7
C(44)-C(45)-H(25)	120.4	**C(36)-C(35)-C(34)**	119.9(4)
C(105)-C(104)-C(103)	119.0(5)	**C(36)-C(35)-H(35)**	120
C(105)-C(104)-H(104)	120.5	**C(34)-C(35)-H(35)**	120
C(103)-C(104)-H(104)	120.5	**C(18)-C(17)-C(16)**	120.1(4)
C(38)-C(37)-C(36)	121.3(4)	**C(18)-C(17)-H(17)**	119.9
C(38)-C(37)-H(37)	119.4	**C(16)-C(17)-H(17)**	119.9
C(36)-C(37)-H(37)	119.4	**C(203)-C(202)-C(201)**	121.8(4)
C(204)-C(205)-C(206)	120.0(5)	**C(203)-C(202)-H(202)**	119.1
C(204)-C(205)-H(205)	120	**C(201)-C(202)-H(202)**	119.1
C(206)-C(205)-H(205)	120	**O(3)-C(38)-C(37)**	125.4(4)
O(1)-C(18)-C(17)	124.5(4)	**O(3)-C(38)-C(39)**	116.5(4)
O(1)-C(18)-C(19)	117.4(4)	**C(37)-C(38)-C(39)**	118.1(4)
C(17)-C(18)-C(19)	118.1(4)	**C(15)-C(14)-C(13)**	126.1(4)
C(205)-C(204)-C(203)	120.1(6)	**C(15)-C(14)-C(19)**	118.2(4)
C(205)-C(204)-H(204)	120	**C(13)-C(14)-C(19)**	115.7(4)
C(203)-C(204)-H(204)	120	**C(105)-C(106)-C(101)**	120.6(4)
C(13)-C(12)-C(11)	119.2(4)	**C(105)-C(106)-H(106)**	119.7
C(13)-C(12)-H(12)	120.4	**C(101)-C(106)-H(106)**	119.7
C(11)-C(12)-H(12)	120.4	**C(22)-C(23)-C(24)**	119.5(4)
N(2)-C(21)-C(22)	123.1(4)	**C(22)-C(23)-H(43)**	120.2
N(2)-C(21)-H(41)	118.4	**C(24)-C(23)-H(43)**	120.2
C(22)-C(21)-H(41)	118.4	**C(48)-C(47)-C(46)**	119.9(4)
N(2)-C(29)-C(24)	123.0(4)	**C(48)-C(47)-H(27)**	120
N(2)-C(29)-C(28)	115.2(3)	**C(46)-C(47)-H(27)**	120
C(24)-C(29)-C(28)	121.8(4)	**C(15)-C(16)-C(17)**	122.2(4)
C(45)-C(46)-C(47)	122.5(4)	**C(15)-C(16)-H(16)**	118.9
C(45)-C(46)-H(26)	118.7	**C(17)-C(16)-H(16)**	118.9
C(47)-C(46)-H(26)	118.7	**C(26)-C(25)-C(24)**	120.1(4)
C(204)-C(203)-C(202)	120.0(5)	**C(26)-C(25)-H(45)**	119.9
C(204)-C(203)-H(203)	120	**C(24)-C(25)-H(45)**	119.9
C(202)-C(203)-H(203)	120	**C(202)-C(201)-C(206)**	117.1(5)
N(1)-C(19)-C(14)	123.1(4)	**C(202)-C(201)-C(207)**	120.8(4)
N(1)-C(19)-C(18)	115.1(4)	**C(206)-C(201)-C(207)**	122.1(5)
C(14)-C(19)-C(18)	121.7(4)	**C(102)-C(103)-C(104)**	120.2(5)
N(1)-C(11)-C(12)	122.4(4)	**C(102)-C(103)-H(103)**	119.9
N(1)-C(11)-H(11)	118.8	**C(104)-C(103)-H(103)**	119.9
C(12)-C(11)-H(11)	118.8	**C(42)-C(43)-C(44)**	120.0(4)

C(29)-C(24)-C(25)	117.8(4)	**C(42)-C(43)-H(23)**	120
C(29)-C(24)-C(23)	116.8(4)	**C(44)-C(43)-H(23)**	120
C(25)-C(24)-C(23)	125.4(4)	**C(201)-C(207)-H(20A)**	109.5
C(35)-C(34)-C(33)	125.0(4)	**C(201)-C(207)-H(20B)**	109.5
C(35)-C(34)-C(39)	118.5(4)	**H(20A)-C(207)-H(20B)**	109.5
C(33)-C(34)-C(39)	116.4(4)	**C(201)-C(207)-H(20C)**	109.5
C(33)-C(32)-C(31)	119.6(4)	**H(20A)-C(207)-H(20C)**	109.5
C(33)-C(32)-H(32)	120.2	**H(20B)-C(207)-H(20C)**	109.5

Appendix A.2

Supplementary Crystallographic Data

A.2. $[Hf(5\text{-}ClOx)_4]\cdot 2(C_7H_8)$ – (Hf_1b) – § 4.4

Table A.2.1: Atomic coordinates (x 10^4) and equivalent isotropic displacement parameters ($Å^2$ x 10^3) for $[Hf(5\text{-}ClOx)_4]\cdot 2(C_7H_8)$.

Atom	*x*	*y*	*z*	$U_{(eq)}$
C(11)	3467(1)	8816(1)	758(2)	17(1)
C(12)	3553(1)	8170(1)	721(2)	21(1)
C(13)	3333(1)	7747(1)	1007(2)	21(1)
C(14)	3032(1)	7967(1)	1361(2)	17(1)
C(15)	2784(1)	7591(1)	1695(2)	20(1)
C(16)	2506(1)	7858(1)	2019(2)	23(1)
C(17)	2469(1)	8516(1)	2065(2)	20(1)
C(18)	2716(1)	8909(1)	1776(2)	16(1)
C(19)	2980(1)	8625(1)	1393(2)	15(1)
C(21)	1506(1)	9523(1)	-227(2)	25(1)
C(22)	931(1)	9310(2)	-1096(2)	38(1)
C(23)	879(1)	9319(2)	-1874(2)	36(1)
C(24)	1396(1)	9549(1)	-1807(2)	22(1)
C(25)	1403(1)	9613(1)	-2556(2)	22(1)
C(26)	1934(1)	9859(1)	-2405(2)	19(1)
C(27)	2495(1)	10054(1)	-1494(2)	17(1)
C(28)	2521(1)	10003(1)	-731(2)	14(1)
C(29)	1963(1)	9752(1)	-901(2)	16(1)
C(31)	3924(1)	11344(1)	1501(2)	18(1)
C(32)	4077(1)	11977(1)	1533(2)	22(1)
C(33)	3670(1)	12435(1)	1412(2)	24(1)
C(34)	3097(1)	12261(1)	1244(2)	20(1)
C(35)	2625(1)	12676(1)	1098(2)	23(1)
C(36)	2081(1)	12452(1)	921(2)	26(1)
C(37)	1961(1)	11801(1)	875(2)	23(1)

C(38)	2401(1)	11375(1)	1010(2)	19(1)
C(39)	2971(1)	11610(1)	1200(2)	17(1)
C(41)	3319(1)	10885(1)	3121(2)	16(1)
C(42)	3707(1)	11172(1)	4016(2)	20(1)
C(43)	4372(1)	11125(1)	4617(2)	19(1)
C(44)	4668(1)	10787(1)	4334(2)	15(1)
C(45)	5349(1)	10697(1)	4866(2)	18(1)
C(46)	5578(1)	10367(1)	4506(2)	19(1)
C(47)	5149(1)	10103(1)	3593(2)	17(1)
C(48)	4481(1)	10178(1)	3039(2)	14(1)
C(49)	4242(1)	10520(1)	3414(2)	14(1)
N(1)	3189(1)	9039(1)	1082(1)	14(1)
N(2)	2011(1)	9729(1)	-126(1)	17(1)
N(3)	3393(1)	11161(1)	1348(1)	16(1)
N(4)	3576(1)	10571(1)	2821(1)	14(1)
O(1)	2728(1)	9530(1)	1829(1)	16(1)
O(2)	3022(1)	10185(1)	144(1)	14(1)
O(3)	2327(1)	10756(1)	967(1)	19(1)
O(4)	4039(1)	9953(1)	2164(1)	15(1)
Cl(1)	2872(1)	6777(1)	1728(1)	29(1)
Cl(2)	724(1)	9364(1)	-3688(1)	35(1)
Cl(3)	2747(1)	13483(1)	1145(1)	33(1)
Cl(4)	5909(1)	11005(1)	6007(1)	27(1)
Hf(1)	3036(1)	10116(1)	1282(1)	14(1)
C(01A)	9930(4)	7780(3)	8386(4)	37(2)
C(02A)	10079(2)	7753(2)	9308(2)	29(1)
C(03A)	10697(2)	7905(2)	10150(3)	25(2)
C(04A)	10828(2)	7863(2)	11002(2)	36(2)
C(05A)	10340(2)	7669(2)	11013(2)	38(2)
C(06A)	9723(2)	7517(2)	10172(3)	39(2)
C(07A)	9592(2)	7559(2)	9319(2)	33(2)
C(01B)	9909(5)	7488(5)	10710(7)	51(2)
C(02B)	10030(3)	7671(2)	10059(4)	38(2)
C(03B)	10641(2)	7908(3)	10452(2)	35(2)
C(04B)	10781(2)	8051(3)	9873(3)	34(2)
C(05B)	10310(2)	7956(2)	8903(3)	28(2)
C(06B)	9699(2)	7719(2)	8510(2)	29(2)
C(07B)	9559(2)	7576(3)	9089(4)	43(3)
C(1)	5332(4)	4190(4)	4131(5)	51(2)
C(2)	5116(3)	4115(3)	3171(2)	35(2)
C(3)	4455(3)	4088(4)	2375(4)	38(3)
C(4)	4261(3)	4046(4)	1481(3)	43(2)

C(5)	4730(4)	4030(3)	1382(3)	46(2)
C(6)	5391(4)	4057(4)	2178(5)	55(3)
C(7)	5584(3)	4099(4)	3073(3)	46(3)

Table A.2.2: Hydrogen coordinates (x 10^4) and isotropic displacement parameters ($Å^2$ x 10^3) for $[Hf(5\text{-}ClOx)_4]\cdot 2(C_7H_8)$.

Atom	*x*	*y*	*z*	$U_{(eq)}$
H(11)	3612	9097	547	20
H(12)	3760	8031	501	25
H(13)	3379	7319	970	25
H(16)	2336	7602	2216	27
H(17)	2276	8686	2291	24
H(21)	1534	9518	297	30
H(22)	585	9164	-1144	46
H(23)	500	9172	-2450	43
H(26)	1924	9898	-2910	23
H(27)	2851	10219	-1406	20
H(31)	4207	11040	1591	22
H(32)	4453	12087	1637	26
H(33)	3771	12856	1441	28
H(36)	1781	12735	829	31
H(37)	1586	11660	755	28
H(41)	2866	10917	2726	19
H(42)	3509	11395	4198	23
H(43)	4628	11315	5209	23
H(46)	6027	10316	4872	23
H(47)	5315	9878	3364	20
H(01A)	10314	7909	8491	56
H(01B)	9584	8075	7976	56
H(01C)	9797	7372	8097	56
H(03A)	11023	8035	10143	30
H(04A)	11241	7965	11565	43
H(05A)	10428	7641	11584	45
H(06A)	9397	7387	10179	46
H(07A)	9178	7457	8756	40
H(01D)	9832	7045	10664	76
H(01E)	9534	7709	10534	76
H(01F)	10285	7594	11348	76
H(03B)	10956	7972	11101	42
H(04B)	11190	8210	10136	41

H(05B)	10404	8051	8516	33
H(06B)	9384	7655	7861	34
H(07B)	9150	7418	8826	52
H(1A)	5113	4543	4135	76
H(1B)	5796	4257	4582	76
H(1C)	5226	3817	4296	76
H(3)	4141	4099	2441	46
H(4)	3819	4028	948	51
H(5)	4600	4001	784	55
H(6)	5704	4046	2112	66
H(7)	6026	4117	3605	55

Table A.2.3: Anisotropic displacement parameters ($Å^2$ x 10^3) for [Hf(5-ClOx)$_4$] ·2(C_7H_8).

Atom	U^{11}	U^{22}	U^{33}	U^{23}	U^{13}	U^{12}
C(11)	19(1)	17(1)	15(1)	2(1)	12(1)	0(1)
C(12)	24(1)	21(1)	20(1)	2(1)	16(1)	5(1)
C(13)	25(1)	15(1)	19(1)	0(1)	13(1)	1(1)
C(14)	17(1)	16(1)	13(1)	1(1)	7(1)	-2(1)
C(15)	21(1)	17(1)	15(1)	2(1)	9(1)	-3(1)
C(16)	22(1)	27(2)	17(1)	1(1)	12(1)	-9(1)
C(17)	20(1)	27(1)	15(1)	-3(1)	12(1)	-5(1)
C(18)	13(1)	20(1)	11(1)	-2(1)	6(1)	-2(1)
C(19)	11(1)	17(1)	10(1)	-2(1)	5(1)	-2(1)
C(21)	16(1)	41(2)	18(1)	-4(1)	10(1)	-6(1)
C(22)	17(1)	70(2)	24(2)	-9(2)	12(1)	-18(1)
C(23)	15(1)	64(2)	18(1)	-10(1)	6(1)	-15(1)
C(24)	16(1)	26(2)	19(1)	-3(1)	10(1)	-1(1)
C(25)	18(1)	26(1)	13(1)	-5(1)	6(1)	-1(1)
C(26)	22(1)	21(1)	15(1)	0(1)	12(1)	3(1)
C(27)	16(1)	16(1)	18(1)	0(1)	11(1)	2(1)
C(28)	15(1)	9(1)	15(1)	0(1)	8(1)	2(1)
C(29)	14(1)	15(1)	15(1)	0(1)	9(1)	1(1)
C(31)	20(1)	19(1)	16(1)	-1(1)	12(1)	0(1)
C(32)	24(1)	21(1)	20(1)	-1(1)	14(1)	-5(1)
C(33)	35(2)	16(1)	17(1)	0(1)	16(1)	-1(1)
C(34)	28(1)	15(1)	13(1)	1(1)	12(1)	4(1)
C(35)	37(2)	16(1)	15(1)	3(1)	16(1)	10(1)
C(36)	31(2)	26(2)	15(1)	2(1)	13(1)	13(1)
C(37)	21(1)	27(2)	16(1)	-1(1)	9(1)	7(1)

C(38)	16(1)	22(1)	11(1)	-2(1)	6(1)	5(1)
C(39)	21(1)	16(1)	11(1)	-1(1)	9(1)	4(1)
C(41)	17(1)	16(1)	19(1)	1(1)	14(1)	0(1)
C(42)	26(1)	18(1)	21(1)	-1(1)	18(1)	1(1)
C(43)	25(1)	18(1)	15(1)	-3(1)	13(1)	-3(1)
C(44)	17(1)	14(1)	14(1)	0(1)	10(1)	-3(1)
C(45)	17(1)	19(1)	12(1)	0(1)	6(1)	-5(1)
C(46)	13(1)	22(1)	17(1)	4(1)	7(1)	-1(1)
C(47)	15(1)	18(1)	17(1)	2(1)	10(1)	3(1)
C(48)	16(1)	13(1)	15(1)	1(1)	10(1)	-1(1)
C(49)	13(1)	13(1)	14(1)	0(1)	9(1)	-1(1)
N(1)	14(1)	17(1)	12(1)	0(1)	8(1)	-1(1)
N(2)	13(1)	20(1)	15(1)	-2(1)	8(1)	-1(1)
N(3)	17(1)	16(1)	13(1)	-2(1)	8(1)	2(1)
N(4)	14(1)	14(1)	16(1)	0(1)	10(1)	-1(1)
O(1)	16(1)	18(1)	16(1)	-4(1)	11(1)	-2(1)
O(2)	12(1)	15(1)	13(1)	-1(1)	7(1)	-2(1)
O(3)	14(1)	18(1)	20(1)	-3(1)	10(1)	1(1)
O(4)	13(1)	17(1)	14(1)	-3(1)	9(1)	-1(1)
Cl(1)	33(1)	17(1)	31(1)	4(1)	19(1)	-4(1)
Cl(2)	24(1)	55(1)	16(1)	-11(1)	8(1)	-11(1)
Cl(3)	57(1)	16(1)	32(1)	5(1)	32(1)	10(1)
Cl(4)	22(1)	29(1)	14(1)	-4(1)	5(1)	-3(1)
Hf(1)	12(1)	15(1)	14(1)	-2(1)	8(1)	0(1)
C(01A)	38(4)	30(3)	35(4)	2(3)	20(3)	-1(3)
C(02A)	28(3)	18(3)	29(3)	3(2)	13(3)	6(2)
C(03A)	21(3)	24(3)	31(4)	-3(3)	17(3)	-2(2)
C(04A)	16(3)	35(3)	35(3)	-8(3)	7(3)	-3(2)
C(05A)	36(4)	46(4)	27(3)	4(3)	19(3)	12(3)
C(06A)	28(3)	47(4)	37(4)	3(3)	20(3)	5(3)
C(07A)	18(4)	32(5)	30(4)	-7(3)	7(3)	-6(3)
C(01B)	51(6)	47(5)	59(6)	2(5)	38(6)	0(5)
C(02B)	71(6)	19(4)	50(5)	13(3)	51(5)	17(3)
C(03B)	34(5)	37(4)	27(5)	-1(4)	16(4)	8(3)
C(04B)	28(4)	41(5)	32(4)	-2(3)	18(3)	4(3)
C(05B)	29(4)	24(3)	26(3)	-2(3)	17(3)	5(3)
C(06B)	26(4)	23(4)	24(4)	3(3)	11(3)	2(3)
C(07B)	45(6)	28(6)	63(6)	10(4)	38(5)	5(4)
C(1)	62(5)	32(4)	43(4)	10(3)	27(4)	7(4)
C(2)	44(5)	11(3)	32(4)	6(3)	17(4)	4(3)
C(3)	37(4)	28(4)	48(7)	1(4)	27(5)	-3(3)
C(4)	47(5)	26(4)	53(6)	-4(4)	32(5)	-1(4)

C(5)	68(7)	25(4)	41(5)	-9(4)	34(6)	-8(4)
C(6)	55(7)	38(5)	84(9)	-23(6)	50(7)	-16(5)
C(7)	34(5)	31(5)	69(9)	-4(5)	32(6)	5(3)

Table A.2.4: Bond lengths (Å) for $[Hf(5\text{-}ClOx)_4]\cdot 2(C_7H_8)$.

Atoms	*Bond Length (Å)*	*Atoms*	*Bond Length (Å)*
C(11)-N(1)	1.321(3)	**C(45)-C(46)**	1.366(4)
C(11)-C(12)	1.405(4)	**C(45)-Cl(4)**	1.745(2)
C(11)-H(11)	0.93	**C(46)-C(47)**	1.409(3)
C(12)-C(13)	1.367(4)	**C(46)-H(46)**	0.93
C(12)-H(12)	0.93	**C(47)-C(48)**	1.380(3)
C(13)-C(14)	1.418(4)	**C(47)-H(47)**	0.93
C(13)-H(13)	0.93	**C(48)-O(4)**	1.333(3)
C(14)-C(19)	1.415(3)	**C(48)-C(49)**	1.423(3)
C(14)-C(15)	1.421(3)	**C(49)-N(4)**	1.367(3)
C(15)-C(16)	1.360(4)	**N(1)-Hf(1)**	2.402(2)
C(15)-Cl(1)	1.745(3)	**N(2)-Hf(1)**	2.396(2)
C(16)-C(17)	1.412(4)	**N(3)-Hf(1)**	2.396(2)
C(16)-H(16)	0.93	**N(4)-Hf(1)**	2.420(2)
C(17)-C(18)	1.382(3)	**O(1)-Hf(1)**	2.0982(17)
C(17)-H(17)	0.93	**O(2)-Hf(1)**	2.1015(17)
C(18)-O(1)	1.327(3)	**O(3)-Hf(1)**	2.0968(17)
C(18)-C(19)	1.430(3)	**O(4)-Hf(1)**	2.0799(17)
C(19)-N(1)	1.365(3)	**C(01A)-C(02A)**	1.492(7)
C(21)-N(2)	1.322(3)	**C(01A)-H(01A)**	0.96
C(21)-C(22)	1.399(4)	**C(01A)-H(01B)**	0.96
C(21)-H(21)	0.93	**C(01A)-H(01C)**	0.96
C(22)-C(23)	1.364(4)	**C(02A)-C(03A)**	1.39
C(22)-H(22)	0.93	**C(02A)-C(07A)**	1.39
C(23)-C(24)	1.405(4)	**C(03A)-C(04A)**	1.39
C(23)-H(23)	0.93	**C(03A)-H(03A)**	0.93
C(24)-C(25)	1.416(4)	**C(04A)-C(05A)**	1.39
C(24)-C(29)	1.418(3)	**C(04A)-H(04A)**	0.93
C(25)-C(26)	1.370(4)	**C(05A)-C(06A)**	1.39
C(25)-Cl(2)	1.746(2)	**C(05A)-H(05A)**	0.93
C(26)-C(27)	1.413(3)	**C(06A)-C(07A)**	1.39
C(26)-H(26)	0.93	**C(06A)-H(06A)**	0.93
C(27)-C(28)	1.382(3)	**C(07A)-H(07A)**	0.93
C(27)-H(27)	0.93	**C(01B)-C(02B)**	1.499(8)

C(28)-O(2)	1.327(3)	**C(01B)-H(01D)**	0.96
C(28)-C(29)	1.423(3)	**C(01B)-H(01E)**	0.96
C(29)-N(2)	1.367(3)	**C(01B)-H(01F)**	0.96
C(31)-N(3)	1.324(3)	**C(02B)-C(03B)**	1.39
C(31)-C(32)	1.401(4)	**C(02B)-C(07B)**	1.39
C(31)-H(31)	0.93	**C(03B)-C(04B)**	1.39
C(32)-C(33)	1.372(4)	**C(03B)-H(03B)**	0.93
C(32)-H(32)	0.93	**C(04B)-C(05B)**	1.39
C(33)-C(34)	1.409(4)	**C(04B)-H(04B)**	0.93
C(33)-H(33)	0.93	**C(05B)-C(06B)**	1.39
C(34)-C(39)	1.418(4)	**C(05B)-H(05B)**	0.93
C(34)-C(35)	1.422(4)	**C(06B)-C(07B)**	1.39
C(35)-C(36)	1.365(4)	**C(06B)-H(06B)**	0.93
C(35)-Cl(3)	1.742(3)	**C(07B)-H(07B)**	0.93
C(36)-C(37)	1.414(4)	**C(1)-C(2)**	1.487(7)
C(36)-H(36)	0.93	**C(1)-H(1A)**	0.96
C(37)-C(38)	1.382(3)	**C(1)-H(1B)**	0.96
C(37)-H(37)	0.93	**C(1)-H(1C)**	0.96
C(38)-O(3)	1.328(3)	**C(2)-C(3)**	1.39
C(38)-C(39)	1.423(4)	**C(2)-C(7)**	1.39
C(39)-N(3)	1.369(3)	**C(3)-C(4)**	1.39
C(41)-N(4)	1.321(3)	**C(3)-H(3)**	0.93
C(41)-C(42)	1.406(3)	**C(4)-C(5)**	1.39
C(41)-H(41)	0.93	**C(4)-H(4)**	0.93
C(42)-C(43)	1.364(4)	**C(5)-C(6)**	1.39
C(42)-H(42)	0.93	**C(5)-H(5)**	0.93
C(43)-C(44)	1.409(3)	**C(6)-C(7)**	1.39
C(43)-H(43)	0.93	**C(6)-H(6)**	0.93
C(44)-C(45)	1.419(3)	**C(7)-H(7)**	0.93
C(44)-C(49)	1.422(3)		

Table A.2.5: Bond angles (°) for $[Hf(5ClOx)_4]\cdot 2(C_7H_8)$.

Atoms	*Bond angle (°)*	*Atoms*	*Bond angle (°)*
O(4)-Hf-O(2)	94.50(11)	**C(31)-C(32)-H(32)**	120.2
O(4)-Hf-O(1)	97.00(11)	**C(32)-C(33)-C(34)**	119.9(4)
O(2)-Hf-O(1)	141.84(10)	**C(32)-C(33)-H(33)**	120
O(4)-Hf-O(3)	142.31(11)	**C(34)-C(33)-H(33)**	120
O(2)-Hf-O(3)	97.89(11)	**C(16)-C(15)-C(14)**	119.6(4)
O(1)-Hf-O(3)	94.85(11)	**C(16)-C(15)-H(15)**	120.2

O(4)-Hf-N(3)	78.53(12)	**C(14)-C(15)-H(15)**	120.2
O(2)-Hf-N(3)	73.74(11)	**N(4)-C(49)-C(44)**	122.8(4)
O(1)-Hf-N(3)	144.27(11)	**N(4)-C(49)-C(48)**	115.4(4)
O(3)-Hf-N(3)	71.16(11)	**C(44)-C(49)-C(48)**	121.7(4)
O(4)-Hf-N(1)	73.68(11)	**C(23)-C(22)-C(21)**	119.6(4)
O(2)-Hf-N(1)	77.94(11)	**C(23)-C(22)-H(42)**	120.2
O(1)-Hf-N(1)	70.73(11)	**C(21)-C(22)-H(42)**	120.2
O(3)-Hf-N(1)	143.78(11)	**C(201)-C(206)-C(205)**	121.0(5)
N(3)-Hf-N(1)	138.19(12)	**C(201)-C(206)-H(206)**	119.5
O(4)-Hf-N(4)	71.04(11)	**C(205)-C(206)-H(206)**	119.5
O(2)-Hf-N(4)	145.17(11)	**C(102)-C(101)-C(106)**	118.2(5)
O(1)-Hf-N(4)	72.67(11)	**C(102)-C(101)-C(107)**	121.5(5)
O(3)-Hf-N(4)	78.70(11)	**C(106)-C(101)-C(107)**	120.2(5)
N(3)-Hf-N(4)	72.39(11)	**N(3)-C(31)-C(32)**	122.3(4)
N(1)-Hf-N(4)	124.51(12)	**N(3)-C(31)-H(31)**	118.9
O(4)-Hf-N(2)	142.23(11)	**C(32)-C(31)-H(31)**	118.9
O(2)-Hf-N(2)	70.84(11)	**C(101)-C(107)-H(10A)**	109.5
O(1)-Hf-N(2)	77.98(11)	**C(101)-C(107)-H(10B)**	109.5
O(3)-Hf-N(2)	75.31(11)	**H(10A)-C(107)-H(10B)**	109.5
N(3)-Hf-N(2)	126.37(12)	**C(101)-C(107)-H(10C)**	109.5
N(1)-Hf-N(2)	69.32(11)	**H(10A)-C(107)-H(10C)**	109.5
N(4)-Hf-N(2)	138.57(11)	**H(10B)-C(107)-H(10C)**	109.5
C(41)-N(4)-C(49)	118.5(4)	**C(25)-C(26)-C(27)**	122.0(4)
C(41)-N(4)-Hf	129.1(3)	**C(25)-C(26)-H(46)**	119
C(49)-N(4)-Hf	112.2(3)	**C(27)-C(26)-H(46)**	119
C(31)-N(3)-C(39)	118.9(4)	**C(45)-C(44)-C(43)**	124.7(4)
C(31)-N(3)-Hf	128.1(3)	**C(45)-C(44)-C(49)**	118.6(4)
C(39)-N(3)-Hf	112.9(2)	**C(43)-C(44)-C(49)**	116.7(4)
C(21)-N(2)-C(29)	118.0(3)	**C(101)-C(102)-C(103)**	121.4(5)
C(21)-N(2)-Hf	129.4(3)	**C(101)-C(102)-H(102)**	119.3
C(29)-N(2)-Hf	112.5(2)	**C(103)-C(102)-H(102)**	119.3
C(11)-N(1)-C(19)	118.5(4)	**O(2)-C(28)-C(27)**	125.2(4)
C(11)-N(1)-Hf	128.7(3)	**O(2)-C(28)-C(29)**	117.2(3)
C(19)-N(1)-Hf	112.7(3)	**C(27)-C(28)-C(29)**	117.7(4)
C(28)-O(2)-Hf	123.6(2)	**O(4)-C(48)-C(47)**	124.6(4)
C(18)-O(1)-Hf	123.2(3)	**O(4)-C(48)-C(49)**	117.3(4)
C(38)-O(3)-Hf	123.4(2)	**C(47)-C(48)-C(49)**	118.0(4)
C(104)-C(105)-C(106)	120.6(4)	**N(4)-C(41)-C(42)**	122.1(4)
C(104)-C(105)-H(105)	119.7	**N(4)-C(41)-H(21)**	118.9
C(106)-C(105)-H(105)	119.7	**C(42)-C(41)-H(21)**	118.9
C(43)-C(42)-C(41)	119.7(4)	**C(12)-C(13)-C(14)**	121.0(4)
C(43)-C(42)-H(22)	120.1	**C(12)-C(13)-H(13)**	119.5

C(41)-C(42)-H(22)	120.1	**C(14)-C(13)-H(13)**	119.5
C(48)-O(4)-Hf	123.8(3)	**C(35)-C(36)-C(37)**	121.2(4)
N(3)-C(39)-C(34)	122.9(4)	**C(35)-C(36)-H(36)**	119.4
N(3)-C(39)-C(38)	116.0(4)	**C(37)-C(36)-H(36)**	119.4
C(34)-C(39)-C(38)	121.0(4)	**C(28)-C(27)-C(26)**	120.6(4)
C(46)-C(45)-C(44)	119.3(4)	**C(28)-C(27)-H(47)**	119.7
C(46)-C(45)-H(25)	120.4	**C(26)-C(27)-H(47)**	119.7
C(44)-C(45)-H(25)	120.4	**C(36)-C(35)-C(34)**	119.9(4)
C(105)-C(104)-C(103)	119.0(5)	**C(36)-C(35)-H(35)**	120
C(105)-C(104)-H(104)	120.5	**C(34)-C(35)-H(35)**	120
C(103)-C(104)-H(104)	120.5	**C(18)-C(17)-C(16)**	120.1(4)
C(38)-C(37)-C(36)	121.3(4)	**C(18)-C(17)-H(17)**	119.9
C(38)-C(37)-H(37)	119.4	**C(16)-C(17)-H(17)**	119.9
C(36)-C(37)-H(37)	119.4	**C(203)-C(202)-C(201)**	121.8(4)
C(204)-C(205)-C(206)	120.0(5)	**C(203)-C(202)-H(202)**	119.1
C(204)-C(205)-H(205)	120	**C(201)-C(202)-H(202)**	119.1
C(206)-C(205)-H(205)	120	**O(3)-C(38)-C(37)**	125.4(4)
O(1)-C(18)-C(17)	124.5(4)	**O(3)-C(38)-C(39)**	116.5(4)
O(1)-C(18)-C(19)	117.4(4)	**C(37)-C(38)-C(39)**	118.1(4)
C(17)-C(18)-C(19)	118.1(4)	**C(15)-C(14)-C(13)**	126.1(4)
C(205)-C(204)-C(203)	120.1(6)	**C(15)-C(14)-C(19)**	118.2(4)
C(205)-C(204)-H(204)	120	**C(13)-C(14)-C(19)**	115.7(4)
C(203)-C(204)-H(204)	120	**C(105)-C(106)-C(101)**	120.6(4)
C(13)-C(12)-C(11)	119.2(4)	**C(105)-C(106)-H(106)**	119.7
C(13)-C(12)-H(12)	120.4	**C(101)-C(106)-H(106)**	119.7
C(11)-C(12)-H(12)	120.4	**C(22)-C(23)-C(24)**	119.5(4)
N(2)-C(21)-C(22)	123.1(4)	**C(22)-C(23)-H(43)**	120.2
N(2)-C(21)-H(41)	118.4	**C(24)-C(23)-H(43)**	120.2
C(22)-C(21)-H(41)	118.4	**C(48)-C(47)-C(46)**	119.9(4)
N(2)-C(29)-C(24)	123.0(4)	**C(48)-C(47)-H(27)**	120
N(2)-C(29)-C(28)	115.2(3)	**C(46)-C(47)-H(27)**	120
C(24)-C(29)-C(28)	121.8(4)	**C(15)-C(16)-C(17)**	122.2(4)
C(45)-C(46)-C(47)	122.5(4)	**C(15)-C(16)-H(16)**	118.9
C(45)-C(46)-H(26)	118.7	**C(17)-C(16)-H(16)**	118.9
C(47)-C(46)-H(26)	118.7	**C(26)-C(25)-C(24)**	120.1(4)
C(204)-C(203)-C(202)	120.0(5)	**C(26)-C(25)-H(45)**	119.9
C(204)-C(203)-H(203)	120	**C(24)-C(25)-H(45)**	119.9
C(202)-C(203)-H(203)	120	**C(202)-C(201)-C(206)**	117.1(5)
N(1)-C(19)-C(14)	123.1(4)	**C(202)-C(201)-C(207)**	120.8(4)
N(1)-C(19)-C(18)	115.1(4)	**C(206)-C(201)-C(207)**	122.1(5)
C(14)-C(19)-C(18)	121.7(4)	**C(102)-C(103)-C(104)**	120.2(5)
N(1)-C(11)-C(12)	122.4(4)	**C(102)-C(103)-H(103)**	119.9

N(1)-C(11)-H(11)	118.8	**C(104)-C(103)-H(103)**	119.9
C(12)-C(11)-H(11)	118.8	**C(42)-C(43)-C(44)**	120.0(4)
C(29)-C(24)-C(25)	117.8(4)	**C(42)-C(43)-H(23)**	120
C(29)-C(24)-C(23)	116.8(4)	**C(44)-C(43)-H(23)**	120
C(25)-C(24)-C(23)	125.4(4)	**C(201)-C(207)-H(20A)**	109.5
C(35)-C(34)-C(33)	125.0(4)	**C(201)-C(207)-H(20B)**	109.5
C(35)-C(34)-C(39)	118.5(4)	**H(20A)-C(207)-H(20B)**	109.5
C(33)-C(34)-C(39)	116.4(4)	**C(201)-C(207)-H(20C)**	109.5
C(33)-C(32)-C(31)	119.6(4)	**H(20A)-C(207)-H(20C)**	109.5
C(33)-C(32)-H(32)	120.2	**H(20B)-C(207)-H(20C)**	109.5

Appendix A.3

Supplementary Crystallographic Data

A.3. $[Hf(diMeOx)_4]\cdot 2DMF$ – (Hf_1h) – § 4.5

Table A.3.1: Atomic coordinates (x 10^4) and equivalent isotropic displacement parameters ($Å^2$ x 10^3) for $[Hf(diMeOx)_4]\cdot 2DMF$.

Atom	*x*	*y*	*z*	$U_{(eq)}$
Hf(1)	3881(1)	3079(1)	6664(1)	13(1)
C(01)	1539(4)	2498(2)	4203(2)	45(1)
C(02)	3731(4)	1983(3)	4067(2)	61(1)
C(03)	1559(5)	1477(3)	3577(2)	51(1)
C(04)	7126(3)	2436(2)	4419(1)	33(1)
C(05)	7017(4)	957(2)	4278(1)	37(1)
C(06)	7343(4)	1912(2)	3637(1)	42(1)
C(11)	3746(3)	4269(2)	7640(1)	21(1)
C(12)	4259(4)	4820(2)	8017(1)	27(1)
C(13)	5599(4)	5067(2)	8098(1)	27(1)
C(14)	6479(3)	4760(2)	7807(1)	20(1)
C(15)	7893(3)	4938(2)	7862(1)	24(1)
C(015)	8620(4)	5485(2)	8269(1)	31(1)
C(16)	8590(3)	4597(2)	7537(1)	25(1)
C(017)	8763(3)	3767(2)	6786(1)	22(1)
C(17)	7972(3)	4098(2)	7143(1)	18(1)
C(18)	6598(3)	3925(2)	7083(1)	16(1)
C(19)	5860(3)	4232(2)	7422(1)	17(1)
C(21)	6353(3)	1976(2)	7365(1)	15(1)
C(22)	6915(3)	1422(2)	7732(1)	18(1)
C(23)	6120(3)	1142(2)	8041(1)	18(1)
C(24)	4751(3)	1403(2)	7985(1)	15(1)
C(25)	3821(3)	1141(2)	8277(1)	17(1)
C(025)	4293(3)	575(2)	8704(1)	20(1)
C(26)	2499(3)	1412(2)	8153(1)	19(1)

C(027)	485(3)	2153(2)	7627(1)	28(1)
C(27)	1978(3)	1931(2)	7754(1)	18(1)
C(28)	2880(3)	2205(2)	7474(1)	15(1)
C(29)	4263(3)	1943(2)	7596(1)	12(1)
C(31)	712(3)	2645(2)	6025(1)	18(1)
C(32)	-253(3)	2284(2)	5652(1)	24(1)
C(33)	175(3)	1745(2)	5344(1)	22(1)
C(34)	1571(3)	1522(2)	5410(1)	19(1)
C(35)	2163(3)	980(2)	5108(1)	22(1)
C(035)	1280(3)	559(2)	4672(1)	23(1)
C(36)	3541(3)	839(2)	5229(1)	22(1)
C(037)	5934(3)	978(2)	5745(1)	25(1)
C(37)	4428(3)	1172(2)	5638(1)	19(1)
C(38)	3866(3)	1692(2)	5936(1)	16(1)
C(39)	2449(3)	1888(2)	5808(1)	15(1)
C(41)	4751(3)	3376(2)	5593(1)	16(1)
C(42)	4644(3)	3715(2)	5134(1)	19(1)
C(43)	3705(3)	4330(2)	4984(1)	18(1)
C(44)	2867(3)	4632(2)	5291(1)	14(1)
C(45)	1898(3)	5291(2)	5181(1)	17(1)
C(045)	1656(3)	5710(2)	4694(1)	22(1)
C(46)	1203(3)	5528(2)	5529(1)	17(1)
C(47)	1387(3)	5157(2)	5990(1)	14(1)
C(047)	584(3)	5476(2)	6348(1)	17(1)
C(48)	2301(3)	4501(2)	6098(1)	13(1)
C(49)	3039(3)	4245(2)	5745(1)	12(1)
N(1)	4521(3)	3986(1)	7347(1)	16(1)
N(2)	5067(2)	2229(1)	7296(1)	13(1)
N(3)	2023(2)	2461(1)	6101(1)	15(1)
N(4)	3956(2)	3620(1)	5887(1)	13(1)
N(5)	7160(3)	1801(2)	4122(1)	30(1)
N(6)	2248(3)	2010(2)	3961(1)	38(1)
O(1)	5899(2)	3487(1)	6718(1)	14(1)
O(2)	2508(2)	2679(1)	7086(1)	16(1)
O(3)	4573(2)	2039(1)	6331(1)	15(1)
O(4)	2578(2)	4111(1)	6519(1)	14(1)
O(5)	6915(3)	2392(2)	4828(1)	42(1)
O(6)	297(3)	2546(2)	4133(1)	56(1)

Table A.3.2: Hydrogen coordinates (x 10^4) and isotropic displacement parameters (Å^2 x 10^3) for [Hf(diMeOx)$_4$]·2DMF.

Atom	*x*	*y*	*z*	$U_{(eq)}$
H(01)	2035	2827	4445	54
H(02A)	4073	2345	4332	92
H(02B)	4070	2163	3791	92
H(02C)	4030	1424	4147	92
H(03A)	589	1564	3529	76
H(03B)	1764	905	3661	76
H(03C)	1868	1607	3288	76
H(04)	7275	2964	4306	39
H(05A)	6851	961	4598	55
H(05B)	7843	654	4272	55
H(05C)	6263	695	4068	55
H(06A)	7601	2478	3592	62
H(06B)	6502	1787	3419	62
H(06C)	8049	1544	3577	62
H(11)	2839	4098	7595	25
H(12)	3685	5017	8212	33
H(13)	5929	5437	8346	32
H(1A)	9574	5521	8258	47
H(1B)	8522	5248	8570	47
H(1C)	8225	6033	8237	47
H(16)	9524	4700	7579	30
H(1D)	9718	3886	6895	33
H(1E)	8443	4027	6481	33
H(1F)	8633	3175	6755	33
H(21)	6905	2173	7162	18
H(22)	7817	1246	7766	22
H(23)	6488	780	8287	21
H(2A)	3524	426	8841	31
H(2B)	4960	860	8938	31
H(2C)	4694	81	8601	31
H(26)	1894	1243	8343	23
H(2D)	48	1831	7355	42
H(2E)	390	2735	7551	42
H(2F)	64	2035	7894	42
H(31)	411	3028	6226	21
H(32)	-1177	2413	5616	29
H(33)	-452	1523	5089	27

H(3D)	1859	297	4484	35
H(3E)	718	970	4481	35
H(3F)	707	147	4776	35
H(36)	3927	499	5028	26
H(3A)	6361	1247	6037	37
H(3B)	6338	1176	5487	37
H(3C)	6063	386	5777	37
H(41)	5404	2966	5694	20
H(42)	5205	3524	4933	23
H(43)	3619	4551	4678	22
H(4D)	860	6059	4657	33
H(4E)	1516	5292	4447	33
H(4F)	2437	6042	4668	33
H(46)	571	5958	5459	21
H(4A)	941	5236	6656	26
H(4B)	-360	5323	6247	26
H(4C)	661	6071	6368	26

Table A.3.3: Anisotropic displacement parameters ($Å^2$ x 10^3) for $[Hf(diMeOx)_4]$ ·2DMF.

Atom	U^{11}	U^{22}	U^{33}	U^{23}	*U13*	U^{12}
Hf(1)	16(1)	13(1)	11(1)	2(1)	5(1)	3(1)
C(01)	41(2)	30(2)	61(3)	5(2)	6(2)	2(2)
C(02)	33(2)	57(3)	92(4)	17(3)	10(2)	1(2)
C(03)	54(3)	58(3)	41(2)	4(2)	13(2)	0(2)
C(04)	21(2)	26(2)	46(2)	-9(2)	-6(2)	1(1)
C(05)	45(2)	27(2)	36(2)	-1(2)	4(2)	1(2)
C(06)	54(3)	32(2)	36(2)	3(2)	2(2)	-6(2)
C(11)	25(2)	22(2)	16(1)	3(1)	6(1)	8(1)
C(12)	46(2)	23(2)	14(2)	1(1)	9(1)	15(2)
C(13)	49(2)	17(2)	13(2)	-1(1)	2(1)	9(2)
C(14)	35(2)	11(1)	13(1)	1(1)	-1(1)	3(1)
C(15)	36(2)	13(1)	18(2)	3(1)	-4(1)	-4(1)
C(015)	47(2)	21(2)	22(2)	-3(1)	-2(2)	-6(2)
C(16)	28(2)	20(2)	22(2)	4(1)	-4(1)	-4(1)
C(017)	18(2)	26(2)	21(2)	2(1)	2(1)	-3(1)
C(17)	20(2)	14(1)	19(2)	4(1)	1(1)	-2(1)
C(18)	24(2)	10(1)	13(1)	4(1)	3(1)	2(1)
C(19)	26(2)	11(1)	14(1)	1(1)	2(1)	2(1)

C(21)	14(1)	16(1)	17(1)	0(1)	5(1)	-1(1)
C(22)	17(2)	17(1)	20(2)	3(1)	5(1)	4(1)
C(23)	24(2)	14(1)	13(1)	3(1)	0(1)	2(1)
C(24)	20(2)	12(1)	12(1)	-1(1)	2(1)	-1(1)
C(25)	26(2)	14(1)	12(1)	0(1)	5(1)	-4(1)
C(025)	26(2)	20(2)	15(1)	4(1)	5(1)	-3(1)
C(26)	21(2)	24(2)	14(1)	2(1)	7(1)	-4(1)
C(027)	18(2)	44(2)	26(2)	12(2)	10(1)	1(1)
C(27)	18(2)	21(1)	16(1)	1(1)	5(1)	-1(1)
C(28)	17(2)	14(1)	13(1)	0(1)	4(1)	0(1)
C(29)	16(1)	12(1)	10(1)	-1(1)	4(1)	1(1)
C(31)	19(2)	17(1)	17(2)	1(1)	5(1)	3(1)
C(32)	20(2)	19(2)	32(2)	4(1)	3(1)	2(1)
C(33)	22(2)	18(2)	24(2)	-2(1)	-2(1)	-2(1)
C(34)	26(2)	13(1)	17(1)	2(1)	4(1)	-1(1)
C(35)	29(2)	18(2)	19(2)	-4(1)	5(1)	-2(1)
C(035)	26(2)	23(2)	20(2)	-7(1)	4(1)	-1(1)
C(36)	32(2)	14(1)	20(2)	-4(1)	9(1)	4(1)
C(037)	28(2)	26(2)	21(2)	-4(1)	7(1)	8(1)
C(37)	23(2)	16(1)	18(2)	2(1)	7(1)	3(1)
C(38)	20(2)	12(1)	16(1)	4(1)	6(1)	1(1)
C(39)	20(2)	12(1)	14(1)	2(1)	6(1)	-1(1)
C(41)	17(2)	14(1)	18(1)	0(1)	5(1)	1(1)
C(42)	23(2)	20(1)	17(2)	-2(1)	11(1)	-2(1)
C(43)	27(2)	17(1)	10(1)	1(1)	4(1)	-9(1)
C(44)	14(1)	14(1)	12(1)	0(1)	-1(1)	-5(1)
C(45)	17(2)	15(1)	16(1)	4(1)	-4(1)	-6(1)
C(045)	20(2)	21(2)	22(2)	10(1)	-5(1)	-2(1)
C(46)	12(1)	13(1)	23(2)	5(1)	-4(1)	0(1)
C(47)	13(1)	13(1)	17(1)	-2(1)	1(1)	-1(1)
C(047)	16(2)	16(1)	19(2)	-4(1)	1(1)	3(1)
C(48)	13(1)	12(1)	12(1)	0(1)	1(1)	-1(1)
C(49)	13(1)	12(1)	12(1)	-1(1)	2(1)	-3(1)
N(1)	22(1)	14(1)	12(1)	3(1)	5(1)	5(1)
N(2)	18(1)	12(1)	11(1)	1(1)	4(1)	2(1)
N(3)	20(1)	11(1)	14(1)	3(1)	5(1)	2(1)
N(4)	16(1)	10(1)	15(1)	1(1)	5(1)	0(1)
N(5)	38(2)	22(1)	28(2)	-1(1)	-1(1)	-3(1)
N(6)	30(2)	37(2)	49(2)	7(2)	9(2)	2(1)
O(1)	17(1)	14(1)	10(1)	-1(1)	3(1)	1(1)
O(2)	15(1)	20(1)	14(1)	5(1)	4(1)	4(1)
O(3)	19(1)	13(1)	13(1)	1(1)	3(1)	2(1)

O(4)	19(1)	15(1)	10(1)	2(1)	4(1)	5(1)
O(5)	35(2)	45(2)	45(2)	-21(1)	0(1)	2(1)
O(6)	42(2)	47(2)	79(2)	5(2)	12(2)	11(1)

Table A.3.4: Bond lengths (Å) for [Hf(diMeOx)$_4$]·2DMF.

Atoms	*Bond Length (Å)*	*Atoms*	*Bond Length (Å)*
C(01)-O(6)	1.218(5)	**C(027)-H(2D)**	0.96
C(01)-N(6)	1.337(5)	**C(027)-H(2E)**	0.96
C(01)-H(01)	0.93	**C(027)-H(2F)**	0.96
C(02)-N(6)	1.450(5)	**C(27)-C(28)**	1.389(4)
C(02)-H(02A)	0.96	**C(28)-O(2)**	1.332(3)
C(02)-H(02B)	0.96	**C(28)-C(29)**	1.417(4)
C(02)-H(02C)	0.96	**C(29)-N(2)**	1.365(3)
C(03)-N(6)	1.449(5)	**C(31)-N(3)**	1.316(4)
C(03)-H(03A)	0.96	**C(31)-C(32)**	1.409(4)
C(03)-H(03B)	0.96	**C(31)-H(31)**	0.93
C(03)-H(03C)	0.96	**C(32)-C(33)**	1.362(4)
C(04)-O(5)	1.226(4)	**C(32)-H(32)**	0.93
C(04)-N(5)	1.330(4)	**C(33)-C(34)**	1.413(4)
C(04)-H(04)	0.93	**C(33)-H(33)**	0.93
C(05)-N(5)	1.442(4)	**C(34)-C(39)**	1.414(4)
C(05)-H(05A)	0.96	**C(34)-C(35)**	1.432(4)
C(05)-H(05B)	0.96	**C(35)-C(36)**	1.367(4)
C(05)-H(05C)	0.96	**C(35)-C(035)**	1.530(4)
C(06)-N(5)	1.443(5)	**C(035)-H(3D)**	0.96
C(06)-H(06A)	0.96	**C(035)-H(3E)**	0.96
C(06)-H(06B)	0.96	**C(035)-H(3F)**	0.96
C(06)-H(06C)	0.96	**C(36)-C(37)**	1.419(4)
C(11)-N(1)	1.328(4)	**C(36)-H(36)**	0.93
C(11)-C(12)	1.407(4)	**C(037)-C(37)**	1.504(4)
C(11)-H(11)	0.93	**C(037)-H(3A)**	0.96
C(12)-C(13)	1.368(5)	**C(037)-H(3B)**	0.96
C(12)-H(12)	0.93	**C(037)-H(3C)**	0.96
C(13)-C(14)	1.414(4)	**C(37)-C(38)**	1.387(4)
C(13)-H(13)	0.93	**C(38)-O(3)**	1.325(3)
C(14)-C(15)	1.417(5)	**C(38)-C(39)**	1.423(4)
C(14)-C(19)	1.426(4)	**C(39)-N(3)**	1.366(3)
C(15)-C(16)	1.381(4)	**C(41)-N(4)**	1.324(3)
C(15)-C(015)	1.518(4)	**C(41)-C(42)**	1.401(4)

C(015)-H(1A)	0.96	**C(41)-H(41)**	0.93
C(015)-H(1B)	0.96	**C(42)-C(43)**	1.369(4)
C(015)-H(1C)	0.96	**C(42)-H(42)**	0.93
C(16)-C(17)	1.416(4)	**C(43)-C(44)**	1.412(4)
C(16)-H(16)	0.93	**C(43)-H(43)**	0.93
C(017)-C(17)	1.504(4)	**C(44)-C(49)**	1.415(4)
C(017)-H(1D)	0.96	**C(44)-C(45)**	1.425(4)
C(017)-H(1E)	0.96	**C(45)-C(46)**	1.373(4)
C(017)-H(1F)	0.96	**C(45)-C(045)**	1.519(4)
C(17)-C(18)	1.375(4)	**C(045)-H(4D)**	0.96
C(18)-O(1)	1.332(3)	**C(045)-H(4E)**	0.96
C(18)-C(19)	1.417(4)	**C(045)-H(4F)**	0.96
C(19)-N(1)	1.367(4)	**C(46)-C(47)**	1.420(4)
C(21)-N(2)	1.322(4)	**C(46)-H(46)**	0.93
C(21)-C(22)	1.403(4)	**C(47)-C(48)**	1.387(4)
C(21)-H(21)	0.93	**C(47)-C(047)**	1.507(4)
C(22)-C(23)	1.373(4)	**C(047)-H(4A)**	0.96
C(22)-H(22)	0.93	**C(047)-H(4B)**	0.96
C(23)-C(24)	1.407(4)	**C(047)-H(4C)**	0.96
C(23)-H(23)	0.93	**C(48)-O(4)**	1.332(3)
C(24)-C(29)	1.416(4)	**C(48)-C(49)**	1.423(4)
C(24)-C(25)	1.428(4)	**C(49)-N(4)**	1.364(3)
C(25)-C(26)	1.367(4)	**N(1)-Hf(1)**	2.413(2)
C(25)-C(025)	1.515(4)	**N(2)-Hf(1)**	2.377(2)
C(025)-H(2A)	0.96	**N(3)-Hf(1)**	2.409(2)
C(025)-H(2B)	0.96	**N(4)-Hf(1)**	2.393(2)
C(025)-H(2C)	0.96	**O(1)-Hf(1)**	2.094(2)
C(26)-C(27)	1.423(4)	**O(2)-Hf(1)**	2.0981(19)
C(26)-H(26)	0.93	**O(3)-Hf(1)**	2.1036(19)
C(027)-C(27)	1.503(4)	**O(4)-Hf(1)**	2.0964(19)

Table A.3.5: Bond angles (°) for for [Hf(diMeOx)$_4$]·2DMF.

Atoms	*Bond angle (°)*	*Atoms*	*Bond angle (°)*
O(6)-C(01)-N(6)	125.3(4)	**C(33)-C(34)-C(39)**	115.9(3)
O(6)-C(01)-H(01)	117.3	**C(33)-C(34)-C(35)**	126.0(3)
N(6)-C(01)-H(01)	117.3	**C(39)-C(34)-C(35)**	118.1(3)
N(6)-C(02)-H(02A)	109.5	**C(36)-C(35)-C(34)**	117.7(3)
N(6)-C(02)-H(02B)	109.5	**C(36)-C(35)-C(035)**	121.2(3)
H(02A)-C(02)-H(02B)	109.5	**C(34)-C(35)-C(035)**	121.1(3)

N(6)-C(02)-H(02C)	109.5	**C(35)-C(035)-H(3D)**	109.5
H(02A)-C(02)-H(02C)	109.5	**C(35)-C(035)-H(3E)**	109.5
H(02B)-C(02)-H(02C)	109.5	**H(3D)-C(035)-H(3E)**	109.5
N(6)-C(03)-H(03A)	109.5	**C(35)-C(035)-H(3F)**	109.5
N(6)-C(03)-H(03B)	109.5	**H(3D)-C(035)-H(3F)**	109.5
H(03A)-C(03)-H(03B)	109.5	**H(3E)-C(035)-H(3F)**	109.5
N(6)-C(03)-H(03C)	109.5	**C(35)-C(36)-C(37)**	125.1(3)
H(03A)-C(03)-H(03C)	109.5	**C(35)-C(36)-H(36)**	117.5
H(03B)-C(03)-H(03C)	109.5	**C(37)-C(36)-H(36)**	117.5
O(5)-C(04)-N(5)	126.3(3)	**C(37)-C(037)-H(3A)**	109.5
O(5)-C(04)-H(04)	116.9	**C(37)-C(037)-H(3B)**	109.5
N(5)-C(04)-H(04)	116.9	**H(3A)-C(037)-H(3B)**	109.5
N(5)-C(05)-H(05A)	109.5	**C(37)-C(037)-H(3C)**	109.5
N(5)-C(05)-H(05B)	109.5	**H(3A)-C(037)-H(3C)**	109.5
H(05A)-C(05)-H(05B)	109.5	**H(3B)-C(037)-H(3C)**	109.5
N(5)-C(05)-H(05C)	109.5	**C(38)-C(37)-C(36)**	117.9(3)
H(05A)-C(05)-H(05C)	109.5	**C(38)-C(37)-C(037)**	120.7(3)
H(05B)-C(05)-H(05C)	109.5	**C(36)-C(37)-C(037)**	121.4(3)
N(5)-C(06)-H(06A)	109.5	**O(3)-C(38)-C(37)**	124.2(3)
N(5)-C(06)-H(06B)	109.5	**O(3)-C(38)-C(39)**	117.2(2)
H(06A)-C(06)-H(06B)	109.5	**C(37)-C(38)-C(39)**	118.6(3)
N(5)-C(06)-H(06C)	109.5	**N(3)-C(39)-C(34)**	123.5(3)
H(06A)-C(06)-H(06C)	109.5	**N(3)-C(39)-C(38)**	114.0(2)
H(06B)-C(06)-H(06C)	109.5	**C(34)-C(39)-C(38)**	122.5(3)
N(1)-C(11)-C(12)	121.8(3)	**N(4)-C(41)-C(42)**	122.2(3)
N(1)-C(11)-H(11)	119.1	**N(4)-C(41)-H(41)**	118.9
C(12)-C(11)-H(11)	119.1	**C(42)-C(41)-H(41)**	118.9
C(13)-C(12)-C(11)	120.4(3)	**C(43)-C(42)-C(41)**	119.4(3)
C(13)-C(12)-H(12)	119.8	**C(43)-C(42)-H(42)**	120.3
C(11)-C(12)-H(12)	119.8	**C(41)-C(42)-H(42)**	120.3
C(12)-C(13)-C(14)	120.0(3)	**C(42)-C(43)-C(44)**	120.6(3)
C(12)-C(13)-H(13)	120	**C(42)-C(43)-H(43)**	119.7
C(14)-C(13)-H(13)	120	**C(44)-C(43)-H(43)**	119.7
C(13)-C(14)-C(15)	125.9(3)	**C(43)-C(44)-C(49)**	115.9(3)
C(13)-C(14)-C(19)	115.8(3)	**C(43)-C(44)-C(45)**	125.4(3)
C(15)-C(14)-C(19)	118.3(3)	**C(49)-C(44)-C(45)**	118.7(3)
C(16)-C(15)-C(14)	118.0(3)	**C(46)-C(45)-C(44)**	117.7(3)
C(16)-C(15)-C(015)	121.0(3)	**C(46)-C(45)-C(045)**	121.9(3)
C(14)-C(15)-C(015)	120.9(3)	**C(44)-C(45)-C(045)**	120.4(3)
C(15)-C(015)-H(1A)	109.5	**C(45)-C(045)-H(4D)**	109.5
C(15)-C(015)-H(1B)	109.5	**C(45)-C(045)-H(4E)**	109.5
H(1A)-C(015)-H(1B)	109.5	**H(4D)-C(045)-H(4E)**	109.5

C(15)-C(015)-H(1C)	109.5	**C(45)-C(045)-H(4F)**	109.5
H(1A)-C(015)-H(1C)	109.5	**H(4D)-C(045)-H(4F)**	109.5
H(1B)-C(015)-H(1C)	109.5	**H(4E)-C(045)-H(4F)**	109.5
C(15)-C(16)-C(17)	124.1(3)	**C(45)-C(46)-C(47)**	124.2(3)
C(15)-C(16)-H(16)	118	**C(45)-C(46)-H(46)**	117.9
C(17)-C(16)-H(16)	118	**C(47)-C(46)-H(46)**	117.9
C(17)-C(017)-H(1D)	109.5	**C(48)-C(47)-C(46)**	118.8(3)
C(17)-C(017)-H(1E)	109.5	**C(48)-C(47)-C(047)**	121.5(2)
H(1D)-C(017)-H(1E)	109.5	**C(46)-C(47)-C(047)**	119.7(2)
C(17)-C(017)-H(1F)	109.5	**C(47)-C(047)-H(4A)**	109.5
H(1D)-C(017)-H(1F)	109.5	**C(47)-C(047)-H(4B)**	109.5
H(1E)-C(017)-H(1F)	109.5	**H(4A)-C(047)-H(4B)**	109.5
C(18)-C(17)-C(16)	118.5(3)	**C(47)-C(047)-H(4C)**	109.5
C(18)-C(17)-C(017)	119.4(3)	**H(4A)-C(047)-H(4C)**	109.5
C(16)-C(17)-C(017)	122.1(3)	**H(4B)-C(047)-H(4C)**	109.5
O(1)-C(18)-C(17)	123.8(3)	**O(4)-C(48)-C(47)**	124.4(2)
O(1)-C(18)-C(19)	117.1(3)	**O(4)-C(48)-C(49)**	117.3(2)
C(17)-C(18)-C(19)	119.2(3)	**C(47)-C(48)-C(49)**	118.2(2)
N(1)-C(19)-C(18)	114.7(2)	**N(4)-C(49)-C(44)**	123.2(2)
N(1)-C(19)-C(14)	123.5(3)	**N(4)-C(49)-C(48)**	114.5(2)
C(18)-C(19)-C(14)	121.8(3)	**C(44)-C(49)-C(48)**	122.3(2)
N(2)-C(21)-C(22)	122.5(3)	**C(11)-N(1)-C(19)**	118.4(3)
N(2)-C(21)-H(21)	118.7	**C(11)-N(1)-Hf(1)**	128.4(2)
C(22)-C(21)-H(21)	118.7	**C(19)-N(1)-Hf(1)**	113.17(17)
C(23)-C(22)-C(21)	119.3(3)	**C(21)-N(2)-C(29)**	118.5(2)
C(23)-C(22)-H(22)	120.3	**C(21)-N(2)-Hf(1)**	127.59(18)
C(21)-C(22)-H(22)	120.3	**C(29)-N(2)-Hf(1)**	113.74(17)
C(22)-C(23)-C(24)	120.2(3)	**C(31)-N(3)-C(39)**	118.2(2)
C(22)-C(23)-H(23)	119.9	**C(31)-N(3)-Hf(1)**	128.55(19)
C(24)-C(23)-H(23)	119.9	**C(39)-N(3)-Hf(1)**	113.09(18)
C(23)-C(24)-C(29)	116.3(2)	**C(41)-N(4)-C(49)**	118.7(2)
C(23)-C(24)-C(25)	125.2(3)	**C(41)-N(4)-Hf(1)**	127.79(19)
C(29)-C(24)-C(25)	118.4(3)	**C(49)-N(4)-Hf(1)**	113.50(17)
C(26)-C(25)-C(24)	117.5(3)	**C(04)-N(5)-C(05)**	120.5(3)
C(26)-C(25)-C(025)	121.8(3)	**C(04)-N(5)-C(06)**	122.7(3)
C(24)-C(25)-C(025)	120.7(3)	**C(05)-N(5)-C(06)**	116.8(3)
C(25)-C(025)-H(2A)	109.5	**C(01)-N(6)-C(03)**	121.1(3)
C(25)-C(025)-H(2B)	109.5	**C(01)-N(6)-C(02)**	122.2(4)
H(2A)-C(025)-H(2B)	109.5	**C(03)-N(6)-C(02)**	116.7(4)
C(25)-C(025)-H(2C)	109.5	**C(18)-O(1)-Hf(1)**	124.59(17)
H(2A)-C(025)-H(2C)	109.5	**C(28)-O(2)-Hf(1)**	123.09(17)
H(2B)-C(025)-H(2C)	109.5	**C(38)-O(3)-Hf(1)**	123.35(17)

C(25)-C(26)-C(27)	124.9(3)	**C(48)-O(4)-Hf(1)**	123.83(16)
C(25)-C(26)-H(26)	117.5	**O(1)-Hf(1)-O(4)**	108.44(8)
C(27)-C(26)-H(26)	117.5	**O(1)-Hf(1)-O(2)**	141.52(7)
C(27)-C(027)-H(2D)	109.5	**O(4)-Hf(1)-O(2)**	84.51(8)
C(27)-C(027)-H(2E)	109.5	**O(1)-Hf(1)-O(3)**	83.35(8)
H(2D)-C(027)-H(2E)	109.5	**O(4)-Hf(1)-O(3)**	141.82(7)
C(27)-C(027)-H(2F)	109.5	**O(2)-Hf(1)-O(3)**	109.03(8)
H(2D)-C(027)-H(2F)	109.5	**O(1)-Hf(1)-N(2)**	78.40(8)
H(2E)-C(027)-H(2F)	109.5	**O(4)-Hf(1)-N(2)**	142.90(7)
C(28)-C(27)-C(26)	118.0(3)	**O(2)-Hf(1)-N(2)**	70.87(8)
C(28)-C(27)-C(027)	120.8(3)	**O(3)-Hf(1)-N(2)**	74.17(7)
C(26)-C(27)-C(027)	121.1(3)	**O(1)-Hf(1)-N(4)**	75.30(7)
O(2)-C(28)-C(27)	123.5(3)	**O(4)-Hf(1)-N(4)**	70.39(7)
O(2)-C(28)-C(29)	117.9(2)	**O(2)-Hf(1)-N(4)**	141.93(8)
C(27)-C(28)-C(29)	118.5(3)	**O(3)-Hf(1)-N(4)**	78.33(7)
N(2)-C(29)-C(24)	123.0(2)	**N(2)-Hf(1)-N(4)**	143.72(8)
N(2)-C(29)-C(28)	114.3(2)	**O(1)-Hf(1)-N(3)**	141.10(7)
C(24)-C(29)-C(28)	122.6(2)	**O(4)-Hf(1)-N(3)**	80.26(8)
N(3)-C(31)-C(32)	122.5(3)	**O(2)-Hf(1)-N(3)**	75.64(8)
N(3)-C(31)-H(31)	118.7	**O(3)-Hf(1)-N(3)**	69.58(8)
C(32)-C(31)-H(31)	118.7	**N(2)-Hf(1)-N(3)**	117.89(8)
C(33)-C(32)-C(31)	119.5(3)	**N(4)-Hf(1)-N(3)**	72.32(8)
C(33)-C(32)-H(32)	120.2	**O(1)-Hf(1)-N(1)**	69.92(8)
C(31)-C(32)-H(32)	120.2	**O(4)-Hf(1)-N(1)**	74.58(8)
C(32)-C(33)-C(34)	120.2(3)	**O(2)-Hf(1)-N(1)**	79.61(8)
C(32)-C(33)-H(33)	119.9	**O(3)-Hf(1)-N(1)**	141.74(8)
C(34)-C(33)-H(33)	119.9	**N(2)-Hf(1)-N(1)**	74.00(8)
N(3)-Hf(1)-N(1)	146.09(8)	**N(4)-Hf(1)-N(1)**	118.34(8)

Appendix A.4

Supplementary Crystallographic Data

A.4. $[Hf(diClOx)_4]\cdot 3DMF$ – (Hf_1d) – § 5.4

Table A.4.1: Atomic coordinates (x 10^4) and equivalent isotropic displacement parameters ($Å^2$ x 10^3) for $[Hf(diClOx)_4]\cdot 3DMF$.

Atom	*x*	*y*	*z*	$U_{(eq)}$
C(11A)	3038(3)	2633(4)	3071(2)	28(1)
C(12A)	2559(3)	2246(5)	3197(3)	34(2)
C(13A)	2738(3)	1646(4)	3575(3)	32(2)
C(14A)	3388(3)	1402(4)	3812(2)	26(1)
C(15A)	3656(3)	789(4)	4210(2)	32(2)
C(16A)	4293(3)	563(4)	4391(2)	31(1)
C(17A)	4713(3)	936(4)	4197(2)	25(1)
C(18A)	4504(3)	1549(4)	3824(2)	24(1)
C(19A)	3839(3)	1786(4)	3646(2)	23(1)
C(21A)	5054(3)	3224(4)	4424(2)	26(1)
C(22A)	5032(3)	3515(4)	4884(2)	30(1)
C(23A)	4561(3)	4094(4)	4851(2)	29(1)
C(24A)	4132(3)	4416(4)	4373(2)	26(1)
C(25A)	3640(3)	5031(4)	4287(3)	28(1)
C(26A)	3262(3)	5309(4)	3809(3)	32(2)
C(27A)	3357(3)	4980(4)	3381(2)	29(1)
C(28A)	3821(3)	4371(4)	3432(2)	27(1)
C(29A)	4204(3)	4085(4)	3938(2)	25(1)
C(31A)	4453(3)	4166(4)	2147(2)	28(1)
C(32A)	4671(4)	4703(4)	1859(3)	33(2)
C(33A)	5295(3)	4995(4)	2062(2)	30(1)
C(34A)	5726(3)	4728(3)	2556(2)	24(1)
C(35A)	6388(3)	4947(4)	2816(3)	29(1)
C(36A)	6756(3)	4677(4)	3299(3)	32(2)

C(37A)	6478(3)	4150(4)	3553(2)	30(1)
C(38A)	5835(3)	3895(4)	3329(2)	26(1)
C(39A)	5470(3)	4192(4)	2821(2)	24(1)
C(41A)	5739(3)	1872(4)	2997(2)	28(1)
C(42A)	6003(4)	1322(4)	2740(3)	36(2)
C(43A)	5621(4)	1051(4)	2258(3)	33(2)
C(44A)	4974(4)	1326(4)	2020(2)	29(1)
C(45A)	4510(4)	1103(4)	1531(3)	33(2)
C(46A)	3893(4)	1349(4)	1353(3)	37(2)
C(47A)	3665(3)	1862(4)	1653(2)	32(2)
C(48A)	4085(3)	2140(4)	2137(2)	27(1)
C(49A)	4740(3)	1874(4)	2307(2)	26(1)
C(11B)	321(4)	6669(5)	4518(3)	37(2)
C(12B)	322(4)	6299(5)	4964(3)	46(2)
C(1B3)	682(4)	5617(5)	5162(3)	46(2)
C(14B)	1064(4)	5256(5)	4918(3)	38(2)
C(15B)	1455(4)	4516(6)	5080(3)	51(2)
C(16B)	1778(4)	4218(5)	4808(3)	44(2)
C(17B)	1723(3)	4614(4)	4350(3)	31(1)
C(18B)	1362(3)	5331(4)	4174(2)	27(1)
C(19B)	1038(3)	5654(4)	4474(2)	32(2)
C(31B)	-535(3)	7899(4)	2602(2)	28(1)
C(32B)	-841(3)	8396(4)	2165(2)	31(1)
C(33B)	-503(3)	8634(4)	1881(2)	30(1)
C(34B)	157(3)	8387(4)	2038(2)	26(1)
C(35B)	567(3)	8592(4)	1789(2)	30(1)
C(36B)	1195(4)	8329(4)	1979(3)	34(2)
C(37B)	1455(3)	7850(4)	2431(3)	33(2)
C(38B)	1086(3)	7636(4)	2703(2)	26(1)
C(39B)	431(3)	7902(4)	2491(2)	24(1)
C(41B)	706(3)	5615(4)	2528(2)	29(1)
C(42B)	437(4)	5063(4)	2107(3)	35(2)
C(43B)	-206(4)	4838(4)	1933(2)	34(2)
C(44B)	-584(3)	5140(4)	2186(2)	31(1)
C(45B)	-1251(3)	4956(4)	2058(2)	30(1)
C(46B)	-1568(4)	5245(4)	2344(3)	36(2)
C(47B)	-1235(4)	5748(5)	2779(3)	36(2)
C(48B)	-592(3)	5967(4)	2922(2)	27(1)
C(49B)	-268(3)	5662(4)	2617(2)	26(1)
C(21B)	2270(3)	7092(4)	4324(2)	28(1)
C(22B)	2794(4)	7476(4)	4708(3)	34(2)
C(23B)	2695(4)	8198(4)	4939(3)	35(2)

C(24B)	2058(3)	8518(4)	4785(2)	29(1)
C(25B)	1868(4)	9245(4)	4982(3)	38(2)
C(26B)	1240(4)	9495(4)	4812(3)	39(2)
C(27B)	747(3)	9053(4)	4420(3)	31(1)
C(28B)	889(3)	8357(4)	4184(2)	26(1)
C(29B)	1556(3)	8090(4)	4388(2)	25(1)
C(80)	1554(5)	3382(6)	1731(3)	55(2)
C(81)	2471(5)	4061(6)	1649(4)	62(2)
C(82)	1558(5)	3505(7)	889(3)	68(3)
C(90)	1136(6)	2866(7)	-378(5)	84(4)
C(91)	1360(7)	3466(13)	-1033(6)	142(7)
C(92)	240(5)	3319(7)	-1111(5)	77(3)
C(70)	3315(5)	3348(6)	610(3)	52(2)
C(71)	4370(4)	2983(6)	630(4)	59(2)
C(72)	3365(5)	2363(6)	-13(3)	60(2)
C(60)	6420(6)	2973(8)	1040(5)	91(4)
C(62)	6017(6)	2812(9)	1725(7)	134(7)
C(61)	6545(7)	4034(7)	1642(6)	108(5)
C(52)	7673(7)	1994(12)	3697(7)	139(7)
C(50)	8709(8)	2200(11)	4312(6)	107(5)
C(51)	8580(8)	1107(9)	3631(7)	135(6)
N(1A)	3656(3)	2413(3)	3289(2)	24(1)
N(2A)	4647(3)	3483(3)	3971(2)	24(1)
N(3A)	4839(3)	3909(3)	2614(2)	25(1)
N(4A)	5128(3)	2142(3)	2784(2)	25(1)
N(1B)	679(3)	6363(3)	4284(2)	27(1)
N(3B)	82(3)	7659(3)	2766(2)	24(1)
N(4B)	366(3)	5910(3)	2777(2)	25(1)
N(2B)	1665(3)	7373(3)	4164(2)	24(1)
N(8)	1823(4)	3617(4)	1426(3)	49(2)
N(9)	928(4)	3189(4)	-821(3)	51(2)
N(7)	3683(3)	2913(4)	419(3)	44(2)
N(6)	6287(4)	3205(5)	1444(3)	66(2)
N(5)	8333(5)	1766(6)	3894(4)	80(3)
O(1A)	4866(2)	1911(2)	3615(2)	25(1)
O(2A)	3954(2)	4062(3)	3058(2)	28(1)
O(3A)	5536(2)	3419(3)	3545(2)	26(1)
O(4A)	3910(2)	2604(3)	2443(2)	26(1)
O(1B)	1270(2)	5728(2)	3742(2)	25(1)
O(3B)	1308(2)	7215(3)	3137(2)	26(1)
O(4B)	-245(2)	6424(3)	3330(2)	28(1)
O(2B)	469(2)	7948(3)	3789(2)	27(1)

O(8)	1767(3)	3478(4)	2200(2)	48(1)
O(9)	1781(5)	2770(6)	-130(3)	99(3)
O(7)	3545(3)	3839(4)	983(2)	61(2)
O(6)	6235(3)	2271(4)	840(3)	65(2)
O(5)	9372(9)	1915(10)	4561(6)	187(6)
Cl(1A)	3142(1)	320(1)	4458(1)	42(1)
Cl(2A)	5524(1)	608(1)	4433(1)	35(1)
Cl(5A)	6736(1)	5614(1)	2507(1)	38(1)
Cl(6A)	6946(1)	3850(1)	4179(1)	41(1)
Cl(7A)	4773(1)	452(1)	1156(1)	44(1)
Cl(8A)	2854(1)	2102(2)	1425(1)	49(1)
Cl(3A)	3496(1)	5399(1)	4806(1)	36(1)
Cl(4A)	2862(1)	5361(1)	2780(1)	38(1)
Cl(1B)	1504(2)	4017(2)	5635(1)	83(1)
Cl(2B)	2116(1)	4159(1)	4002(1)	38(1)
Cl(5B)	250(1)	9189(1)	1231(1)	41(1)
Cl(6B)	2259(1)	7518(2)	2660(1)	54(1)
Cl(7B)	-1674(1)	4328(1)	1525(1)	39(1)
Cl(8B)	-1647(1)	6123(2)	3133(1)	61(1)
Cl(3B)	2478(1)	9830(1)	5454(1)	51(1)
Cl(4B)	-49(1)	9386(1)	4218(1)	40(1)
HfA	4567(1)	3007(1)	3162(1)	23(1)
HfB	705(1)	6830(1)	3500(1)	23(1)

Table A.4.2: Hydrogen coordinates (x 10^4) and isotropic displacement parameters ($Å^2$ x 10^3) for $[Hf(diClOx)_4]\cdot 3DMF$.

Atom	*x*	*y*	*z*	$U_{(eq)}$
H(11A)	2915	3058	2825	34
H(12A)	2124	2396	3025	41
H(13A)	2428	1405	3673	39
H(16A)	4453	157	4647	37
H(21A)	5372	2830	4444	31
H(22A)	5328	3321	5199	36
H(23A)	4523	4275	5147	35
H(26A)	2942	5714	3761	38
H(31A)	4022	3982	2005	34
H(32A)	4389	4861	1531	40
H(33A)	5438	5367	1877	36
H(36A)	7190	4840	3461	38
H(41A)	6003	2050	3326	34
H(42A)	6434	1146	2898	43
H(43A)	5791	685	2089	39
H(46A)	3606	1184	1027	45
H(11B)	62	7143	4383	44
H(12B)	69	6531	5121	56
H(1B3)	684	5376	5459	56
H(16B)	2042	3743	4924	52
H(31B)	-775	7730	2785	34
H(32B)	-1272	8563	2067	37
H(33B)	-705	8957	1586	36
H(36B)	1457	8466	1808	41
H(41B)	1140	5777	2635	35
H(42B)	695	4854	1947	42
H(43B)	-391	4487	1650	40
H(46B)	-2005	5111	2251	44
H(21B)	2347	6610	4171	34
H(22B)	3211	7250	4809	40
H(23B)	3044	8469	5193	41
H(26B)	1133	9966	4957	47
H(80)	1154	3110	1579	66
H(81A)	2609	4196	1381	93
H(81B)	2430	4574	1814	93
H(81C)	2788	3699	1894	93
H(82A)	1853	3733	754	102

H(82B)	1494	2912	810	102
H(82C)	1147	3794	739	102
H(90)	852	2702	-231	101
H(91A)	1116	3691	-1368	213
H(91B)	1639	3899	-820	213
H(91C)	1620	2997	-1056	213
H(92A)	170	3568	-1435	116
H(92B)	17	2786	-1165	116
H(92C)	74	3692	-926	116
H(70)	2865	3278	456	62
H(71A)	4544	2628	443	89
H(71B)	4491	3561	610	89
H(71C)	4543	2808	981	89
H(72A)	3686	2099	-106	90
H(72B)	3124	1936	76	90
H(72C)	3072	2689	-296	90
H(60)	6647	3336	915	110
H(62A)	6005	3191	1983	201
H(62B)	5582	2640	1509	201
H(62C)	6272	2322	1885	201
H(61A)	6732	4287	1427	162
H(61B)	6200	4387	1648	162
H(61C)	6875	3977	1983	162
H(52A)	7435	1658	3400	208
H(52B)	7502	1897	3951	208
H(52C)	7629	2582	3605	208
H(50)	8551	2657	4432	128
H(51A)	8221	884	3341	202
H(51B)	8888	1363	3520	202
H(51C)	8788	657	3866	202

Table A.4.3: Anisotropic displacement parameters ($Å^2$ x 10^3) for [Hf(diClOx)$_4$] ·3DMF.

Atom	U^{11}	U^{22}	U^{33}	U^{23}	U^{13}	U^{12}
C(11A)	31(4)	30(3)	27(3)	4(3)	16(3)	5(3)
C(12A)	27(4)	46(4)	30(3)	6(3)	11(3)	7(3)
C(13A)	27(4)	43(4)	31(3)	-1(3)	16(3)	-2(3)
C(14A)	30(4)	30(3)	20(3)	-1(2)	11(3)	-3(3)
C(15A)	34(4)	42(4)	22(3)	5(3)	14(3)	-4(3)
C(16A)	35(4)	37(3)	20(3)	9(3)	11(3)	2(3)
C(17A)	26(3)	31(3)	21(3)	2(2)	13(3)	2(3)
C(18A)	32(4)	24(3)	19(3)	-3(2)	12(3)	-2(2)
C(19A)	27(3)	26(3)	19(3)	-4(2)	14(3)	-3(2)
C(21A)	27(3)	29(3)	25(3)	1(2)	13(3)	-1(3)
C(22A)	34(4)	33(3)	22(3)	-5(3)	9(3)	-10(3)
C(23A)	35(4)	34(3)	21(3)	-8(3)	15(3)	-10(3)
C(24A)	32(4)	26(3)	26(3)	-5(2)	17(3)	-9(3)
C(25A)	30(4)	29(3)	35(3)	-8(3)	22(3)	-5(3)
C(26A)	39(4)	23(3)	41(4)	-2(3)	24(3)	-2(3)
C(27A)	35(4)	25(3)	31(3)	0(3)	19(3)	1(3)
C(28A)	36(4)	21(3)	32(3)	-1(2)	21(3)	3(3)
C(29A)	33(4)	21(3)	26(3)	-3(2)	19(3)	-6(2)
C(31A)	32(4)	26(3)	25(3)	5(2)	11(3)	5(3)
C(32A)	41(4)	29(3)	30(3)	4(3)	15(3)	3(3)
C(33A)	46(4)	20(3)	30(3)	2(2)	22(3)	4(3)
C(34A)	37(4)	18(3)	27(3)	-4(2)	22(3)	1(2)
C(35A)	39(4)	24(3)	33(3)	-1(3)	24(3)	1(3)
C(36A)	27(4)	32(3)	42(4)	-4(3)	21(3)	-2(3)
C(37A)	36(4)	30(3)	27(3)	1(3)	17(3)	3(3)
C(38A)	35(4)	21(3)	26(3)	1(2)	18(3)	3(3)
C(39A)	30(4)	20(3)	26(3)	-5(2)	17(3)	0(2)
C(41A)	31(4)	28(3)	28(3)	2(2)	14(3)	2(3)
C(42A)	39(4)	32(3)	41(4)	-1(3)	22(3)	10(3)
C(43A)	53(5)	25(3)	32(4)	1(3)	30(3)	6(3)
C(44A)	52(4)	22(3)	24(3)	2(2)	26(3)	-4(3)
C(45A)	54(5)	26(3)	29(3)	-3(3)	29(3)	-6(3)
C(46A)	57(5)	34(4)	25(3)	-2(3)	21(3)	-15(3)
C(47A)	37(4)	37(4)	23(3)	4(3)	13(3)	-7(3)
C(48A)	40(4)	22(3)	20(3)	1(2)	15(3)	-4(3)
C(49A)	38(4)	20(3)	24(3)	4(2)	17(3)	-3(3)
C(11B)	45(4)	45(4)	28(3)	-2(3)	22(3)	0(3)
C(12B)	52(5)	58(5)	37(4)	1(4)	26(4)	-8(4)

C(1B3)	56(5)	61(5)	26(4)	7(3)	20(4)	-4(4)
C(14B)	36(4)	49(4)	26(3)	9(3)	11(3)	-7(3)
C(15B)	54(5)	61(5)	35(4)	28(4)	17(4)	6(4)
C(16B)	30(4)	46(4)	44(4)	22(3)	5(4)	0(3)
C(17B)	23(3)	33(3)	31(3)	7(3)	4(3)	2(3)
C(18B)	25(3)	27(3)	24(3)	2(2)	5(3)	-6(3)
C(19B)	29(4)	37(4)	24(3)	4(3)	5(3)	-7(3)
C(31B)	35(4)	29(3)	24(3)	3(2)	15(3)	4(3)
C(32B)	30(4)	35(3)	29(3)	5(3)	13(3)	6(3)
C(33B)	30(4)	30(3)	27(3)	8(3)	9(3)	7(3)
C(34B)	34(4)	21(3)	22(3)	5(2)	11(3)	3(2)
C(35B)	34(4)	28(3)	28(3)	8(3)	15(3)	3(3)
C(36B)	43(4)	36(4)	34(4)	9(3)	26(3)	1(3)
C(37B)	31(4)	36(3)	37(4)	11(3)	19(3)	7(3)
C(38B)	30(4)	23(3)	26(3)	2(2)	12(3)	0(2)
C(39B)	29(3)	23(3)	23(3)	1(2)	14(3)	-2(2)
C(41B)	33(4)	29(3)	28(3)	5(3)	14(3)	5(3)
C(42B)	38(4)	41(4)	32(4)	-5(3)	20(3)	4(3)
C(43B)	43(4)	31(3)	24(3)	-4(3)	11(3)	6(3)
C(44B)	41(4)	24(3)	23(3)	1(2)	10(3)	4(3)
C(45B)	36(4)	24(3)	29(3)	-3(2)	11(3)	-4(3)
C(46B)	36(4)	38(4)	37(4)	-5(3)	17(3)	-13(3)
C(47B)	39(4)	44(4)	33(4)	-8(3)	23(3)	-11(3)
C(48B)	37(4)	27(3)	23(3)	-2(2)	17(3)	0(3)
C(49B)	30(4)	21(3)	23(3)	2(2)	8(3)	0(2)
C(21B)	34(4)	27(3)	26(3)	3(2)	15(3)	1(3)
C(22B)	33(4)	38(4)	30(3)	2(3)	14(3)	1(3)
C(23B)	38(4)	38(4)	26(3)	-1(3)	12(3)	-11(3)
C(24B)	39(4)	26(3)	25(3)	1(2)	17(3)	-3(3)
C(25B)	58(5)	26(3)	31(4)	-10(3)	20(4)	-11(3)
C(26B)	51(5)	28(3)	38(4)	-9(3)	19(4)	4(3)
C(27B)	36(4)	29(3)	32(3)	-2(3)	18(3)	3(3)
C(28B)	33(4)	27(3)	22(3)	2(2)	15(3)	6(3)
C(29B)	36(4)	24(3)	19(3)	-2(2)	15(3)	-5(3)
C(80)	57(6)	70(6)	46(5)	17(4)	30(5)	21(5)
C(81)	75(7)	62(6)	63(6)	3(5)	43(5)	-5(5)
C(82)	61(6)	101(8)	48(5)	19(5)	28(5)	20(6)
C(90)	82(9)	63(7)	77(8)	6(6)	-1(7)	3(6)
C(91)	99(12)	220(20)	130(14)	11(14)	73(11)	-20(12)
C(92)	69(7)	64(6)	92(8)	-15(6)	26(6)	5(5)
C(70)	64(6)	52(5)	46(5)	12(4)	31(5)	13(4)
C(71)	56(6)	46(5)	71(6)	-10(4)	20(5)	4(4)

C(72)	82(7)	55(5)	42(5)	6(4)	23(5)	1(5)
C(60)	98(10)	85(9)	104(10)	-15(7)	54(8)	-24(7)
C(62)	49(7)	103(10)	250(20)	90(12)	56(10)	10(7)
C(61)	154(13)	57(7)	177(14)	25(8)	133(12)	25(7)
C(52)	83(11)	200(20)	138(15)	0(13)	45(11)	-17(11)
C(50)	90(10)	123(12)	106(11)	-28(9)	38(9)	-46(10)
C(51)	152(15)	84(10)	178(17)	-49(10)	77(13)	-65(10)
N(1A)	29(3)	25(2)	21(2)	1(2)	14(2)	3(2)
N(2A)	28(3)	24(2)	22(2)	0(2)	13(2)	-2(2)
N(3A)	37(3)	19(2)	23(3)	1(2)	17(2)	1(2)
N(4A)	36(3)	22(2)	22(2)	4(2)	17(2)	3(2)
N(1B)	28(3)	36(3)	18(2)	1(2)	10(2)	-3(2)
N(3B)	27(3)	23(2)	23(3)	2(2)	12(2)	6(2)
N(4B)	34(3)	21(2)	21(2)	3(2)	12(2)	6(2)
N(2B)	29(3)	24(2)	23(3)	-1(2)	13(2)	0(2)
N(8)	66(5)	46(4)	38(4)	7(3)	22(4)	2(3)
N(9)	53(5)	45(4)	53(4)	4(3)	21(4)	5(3)
N(7)	46(4)	41(3)	44(4)	6(3)	17(3)	9(3)
N(6)	72(6)	70(5)	52(5)	-20(4)	20(4)	26(4)
N(5)	79(7)	64(5)	122(8)	-24(5)	65(7)	-29(5)
O(1A)	29(2)	24(2)	24(2)	5(2)	14(2)	4(2)
O(2A)	40(3)	27(2)	22(2)	1(2)	19(2)	4(2)
O(3A)	35(3)	27(2)	21(2)	1(2)	17(2)	-1(2)
O(4A)	30(2)	28(2)	22(2)	1(2)	13(2)	0(2)
O(1B)	32(2)	21(2)	23(2)	4(2)	13(2)	1(2)
O(3B)	28(2)	25(2)	25(2)	6(2)	13(2)	2(2)
O(4B)	35(3)	29(2)	26(2)	-6(2)	18(2)	-6(2)
O(2B)	32(3)	26(2)	23(2)	-4(2)	10(2)	3(2)
O(8)	44(3)	67(4)	41(3)	10(3)	24(3)	2(3)
O(9)	106(7)	100(6)	81(6)	-3(5)	29(5)	7(5)
O(7)	71(4)	59(4)	52(4)	-3(3)	24(3)	2(3)
O(6)	63(4)	60(4)	82(5)	-37(4)	40(4)	-28(3)
O(5)	221(17)	192(15)	164(13)	-3(11)	93(13)	-48(13)
Cl(1A)	36(1)	55(1)	38(1)	15(1)	20(1)	-5(1)
Cl(2A)	31(1)	43(1)	32(1)	17(1)	16(1)	7(1)
Cl(5A)	42(1)	37(1)	47(1)	4(1)	30(1)	-5(1)
Cl(6A)	35(1)	56(1)	31(1)	6(1)	11(1)	1(1)
Cl(7A)	78(1)	36(1)	30(1)	-4(1)	33(1)	-1(1)
Cl(8A)	34(1)	78(1)	32(1)	8(1)	9(1)	-3(1)
Cl(3A)	41(1)	41(1)	35(1)	-15(1)	24(1)	-4(1)
Cl(4A)	47(1)	35(1)	35(1)	6(1)	21(1)	16(1)
Cl(1B)	94(2)	105(2)	51(1)	53(1)	28(1)	19(2)

Cl(2B)	28(1)	31(1)	48(1)	6(1)	8(1)	3(1)
Cl(5B)	47(1)	47(1)	34(1)	19(1)	23(1)	9(1)
Cl(6B)	34(1)	76(1)	59(1)	33(1)	27(1)	16(1)
Cl(7B)	42(1)	38(1)	33(1)	-11(1)	10(1)	-6(1)
Cl(8B)	45(1)	95(2)	57(1)	-38(1)	36(1)	-29(1)
Cl(3B)	57(1)	47(1)	49(1)	-25(1)	19(1)	-13(1)
Cl(4B)	46(1)	39(1)	38(1)	-1(1)	21(1)	14(1)
HfA	31(1)	22(1)	21(1)	2(1)	15(1)	3(1)
HfB	29(1)	23(1)	20(1)	1(1)	13(1)	1(1)

Table A.4.4: Bond lengths (Å) for [Hf(diClOx)$_4$]·3DMF.

Atoms	*Bond Length (Å)*	*Atoms*	*Bond Length (Å)*
C(11A)-N(1A)	1.315(8)	**C(41B)-N(4B)**	1.321(8)
C(11A)-C(12A)	1.404(9)	**C(41B)-C(42B)**	1.409(9)
C(11A)-H(11A)	0.93	**C(41B)-H(41B)**	0.93
C(12A)-C(13A)	1.371(9)	**C(42B)-C(43B)**	1.370(10)
C(12A)-H(12A)	0.93	**C(42B)-H(42B)**	0.93
C(13A)-C(14A)	1.390(9)	**C(43B)-C(44B)**	1.401(9)
C(13A)-H(13A)	0.93	**C(43B)-H(43B)**	0.93
C(14A)-C(19A)	1.416(8)	**C(44B)-C(49B)**	1.412(9)
C(14A)-C(15A)	1.428(9)	**C(44B)-C(45B)**	1.419(10)
C(15A)-C(16A)	1.356(10)	**C(45B)-C(46B)**	1.361(9)
C(15A)-Cl(1A)	1.746(6)	**C(45B)-Cl(7B)**	1.743(6)
C(16A)-C(17A)	1.402(9)	**C(46B)-C(47B)**	1.411(9)
C(16A)-H(16A)	0.93	**C(46B)-H(46B)**	0.93
C(17A)-C(18A)	1.375(8)	**C(47B)-C(48B)**	1.374(9)
C(17A)-Cl(2A)	1.742(6)	**C(47B)-Cl(8B)**	1.728(7)
C(18A)-O(1A)	1.320(7)	**C(48B)-O(4B)**	1.324(7)
C(18A)-C(19A)	1.417(9)	**C(48B)-C(49B)**	1.428(8)
C(19A)-N(1A)	1.362(8)	**C(49B)-N(4B)**	1.363(8)
C(21A)-N(2A)	1.315(8)	**C(21B)-N(2B)**	1.320(8)
C(21A)-C(22A)	1.413(8)	**C(21B)-C(22B)**	1.383(9)
C(21A)-H(21A)	0.93	**C(21B)-H(21B)**	0.93
C(22A)-C(23A)	1.371(10)	**C(22B)-C(23B)**	1.381(10)
C(22A)-H(22A)	0.93	**C(22B)-H(22B)**	0.93
C(23A)-C(24A)	1.410(9)	**C(23B)-C(24B)**	1.406(10)
C(23A)-H(23A)	0.93	**C(23B)-H(23B)**	0.93
C(24A)-C(25A)	1.415(9)	**C(24B)-C(29B)**	1.407(9)
C(24A)-C(29A)	1.419(8)	**C(24B)-C(25B)**	1.418(9)

C(25A)-C(26A)	1.358(10)	**C(25B)-C(26B)**	1.351(11)
C(25A)-Cl(3A)	1.742(6)	**C(25B)-Cl(3B)**	1.747(7)
C(26A)-C(27A)	1.424(9)	**C(26B)-C(27B)**	1.401(10)
C(26A)-H(26A)	0.93	**C(26B)-H(26B)**	0.93
C(27A)-C(28A)	1.380(9)	**C(27B)-C(28B)**	1.392(8)
C(27A)-Cl(4A)	1.733(7)	**C(27B)-Cl(4B)**	1.722(7)
C(28A)-O(2A)	1.315(7)	**C(28B)-O(2B)**	1.312(8)
C(28A)-C(29A)	1.426(9)	**C(28B)-C(29B)**	1.433(9)
C(29A)-N(2A)	1.351(8)	**C(29B)-N(2B)**	1.370(7)
C(31A)-N(3A)	1.328(8)	**C(80)-O(8)**	1.239(10)
C(31A)-C(32A)	1.400(9)	**C(80)-N(8)**	1.299(10)
C(31A)-H(31A)	0.93	**C(80)-H(80)**	0.93
C(32A)-C(33A)	1.362(10)	**C(81)-N(8)**	1.504(12)
C(32A)-H(32A)	0.93	**C(81)-H(81A)**	0.96
C(33A)-C(34A)	1.416(9)	**C(81)-H(81B)**	0.96
C(33A)-H(33A)	0.93	**C(81)-H(81C)**	0.96
C(34A)-C(39A)	1.404(8)	**C(82)-N(8)**	1.417(11)
C(34A)-C(35A)	1.409(9)	**C(82)-H(82A)**	0.96
C(35A)-C(36A)	1.362(10)	**C(82)-H(82B)**	0.96
C(35A)-Cl(5A)	1.748(6)	**C(82)-H(82C)**	0.96
C(36A)-C(37A)	1.407(9)	**C(90)-N(9)**	1.268(13)
C(36A)-H(36A)	0.93	**C(90)-O(9)**	1.338(14)
C(37A)-C(38A)	1.379(9)	**C(90)-H(90)**	0.93
C(37A)-Cl(6A)	1.735(7)	**C(91)-N(9)**	1.406(14)
C(38A)-O(3A)	1.317(7)	**C(91)-H(91A)**	0.96
C(38A)-C(39A)	1.429(9)	**C(91)-H(91B)**	0.96
C(39A)-N(3A)	1.370(8)	**C(91)-H(91C)**	0.96
C(41A)-N(4A)	1.325(8)	**C(92)-N(9)**	1.440(12)
C(41A)-C(42A)	1.412(9)	**C(92)-H(92A)**	0.96
C(41A)-H(41A)	0.93	**C(92)-H(92B)**	0.96
C(42A)-C(43A)	1.364(10)	**C(92)-H(92C)**	0.96
C(42A)-H(42A)	0.93	**C(70)-O(7)**	1.251(10)
C(43A)-C(44A)	1.400(10)	**C(70)-N(7)**	1.347(10)
C(43A)-H(43A)	0.93	**C(70)-H(70)**	0.93
C(44A)-C(45A)	1.411(9)	**C(71)-N(7)**	1.415(11)
C(44A)-C(49A)	1.429(8)	**C(71)-H(71A)**	0.96
C(45A)-C(46A)	1.325(10)	**C(71)-H(71B)**	0.96
C(45A)-Cl(7A)	1.751(6)	**C(71)-H(71C)**	0.96
C(46A)-C(47A)	1.418(10)	**C(72)-N(7)**	1.441(11)
C(46A)-H(46A)	0.93	**C(72)-H(72A)**	0.96
C(47A)-C(48A)	1.392(9)	**C(72)-H(72B)**	0.96
C(47A)-Cl(8A)	1.709(7)	**C(72)-H(72C)**	0.96

C(48A)-O(4A)	1.319(7)	**C(60)-O(6)**	1.240(13)
C(48A)-C(49A)	1.412(9)	**C(60)-N(6)**	1.355(14)
C(49A)-N(4A)	1.356(8)	**C(60)-H(60)**	0.93
C(11B)-N(1B)	1.329(8)	**C(62)-N(6)**	1.339(15)
C(11B)-C(12B)	1.401(10)	**C(62)-H(62A)**	0.96
C(11B)-H(11B)	0.93	**C(62)-H(62B)**	0.96
C(12B)-C(1B3)	1.327(12)	**C(62)-H(62C)**	0.96
C(12B)-H(12B)	0.93	**C(61)-N(6)**	1.451(15)
C(1B3)-C(14B)	1.425(11)	**C(61)-H(61A)**	0.96
C(1B3)-H(1B3)	0.93	**C(61)-H(61B)**	0.96
C(14B)-C(19B)	1.399(9)	**C(61)-H(61C)**	0.96
C(14B)-C(15B)	1.420(11)	**C(52)-N(5)**	1.402(17)
C(15B)-C(16B)	1.345(12)	**C(52)-H(52A)**	0.96
C(15B)-Cl(1B)	1.736(7)	**C(52)-H(52B)**	0.96
C(16B)-C(17B)	1.413(9)	**C(52)-H(52C)**	0.96
C(16B)-H(16B)	0.93	**C(50)-N(5)**	1.339(16)
C(17B)-C(18B)	1.365(9)	**C(50)-O(5)**	1.44(2)
C(17B)-Cl(2B)	1.730(7)	**C(50)-H(50)**	0.93
C(18B)-O(1B)	1.325(7)	**C(51)-N(5)**	1.514(17)
C(18B)-C(19B)	1.425(9)	**C(51)-H(51A)**	0.96
C(19B)-N(1B)	1.357(9)	**C(51)-H(51B)**	0.96
C(31B)-N(3B)	1.325(8)	**C(51)-H(51C)**	0.96
C(31B)-C(32B)	1.399(9)	**N(1A)-HfA**	2.405(5)
C(31B)-H(31B)	0.93	**N(2A)-HfA**	2.370(5)
C(32B)-C(33B)	1.370(9)	**N(3A)-HfA**	2.375(5)
C(32B)-H(32B)	0.93	**N(4A)-HfA**	2.391(5)
C(33B)-C(34B)	1.415(9)	**N(1B)-HfB**	2.385(5)
C(33B)-H(33B)	0.93	**N(3B)-HfB**	2.389(5)
C(34B)-C(35B)	1.413(9)	**N(4B)-HfB**	2.388(5)
C(34B)-C(39B)	1.414(8)	**N(2B)-HfB**	2.384(5)
C(35B)-C(36B)	1.352(10)	**O(1A)-HfA**	2.103(4)
C(35B)-Cl(5B)	1.738(6)	**O(2A)-HfA**	2.103(4)
C(36B)-C(37B)	1.407(9)	**O(3A)-HfA**	2.102(4)
C(36B)-H(36B)	0.93	**O(4A)-HfA**	2.088(4)
C(37B)-C(38B)	1.387(9)	**O(1B)-HfB**	2.099(4)
C(37B)-Cl(6B)	1.730(7)	**O(3B)-HfB**	2.101(4)
C(38B)-O(3B)	1.317(7)	**O(4B)-HfB**	2.086(4)
C(38B)-C(39B)	1.407(9)	**O(2B)-HfB**	2.106(4)
C(39B)-N(3B)	1.370(7)		

Table A.4.5: Bond angles (°) for for [Hf(diClOx)$_4$]·3DMF.

Atoms	*Bond angle (°)*	*Atoms*	*Bond angle (°)*
N(1A)-C(11A)-C(12A)	122.1(6)	**C(24B)-C(23B)-H(23B)**	120.4
N(1A)-C(11A)-H(11A)	118.9	**C(23B)-C(24B)-C(29B)**	117.3(6)
C(12A)-C(11A)-H(11A)	118.9	**C(23B)-C(24B)-C(25B)**	126.6(6)
C(13A)-C(12A)-C(11A)	119.6(6)	**C(29B)-C(24B)-C(25B)**	116.0(6)
C(13A)-C(12A)-H(12A)	120.2	**C(26B)-C(25B)-C(24B)**	122.1(6)
C(11A)-C(12A)-H(12A)	120.2	**C(26B)-C(25B)-Cl(3B)**	120.0(5)
C(12A)-C(13A)-C(14A)	119.4(6)	**C(24B)-C(25B)-Cl(3B)**	117.9(6)
C(12A)-C(13A)-H(13A)	120.3	**C(25B)-C(26B)-C(27B)**	120.9(6)
C(14A)-C(13A)-H(13A)	120.3	**C(25B)-C(26B)-H(26B)**	119.6
C(13A)-C(14A)-C(19A)	117.9(6)	**C(27B)-C(26B)-H(26B)**	119.6
C(13A)-C(14A)-C(15A)	126.6(6)	**C(28B)-C(27B)-C(26B)**	121.3(6)
C(19A)-C(14A)-C(15A)	115.5(6)	**C(28B)-C(27B)-Cl(4B)**	119.2(5)
C(16A)-C(15A)-C(14A)	121.5(6)	**C(26B)-C(27B)-Cl(4B)**	119.5(5)
C(16A)-C(15A)-Cl(1A)	120.0(5)	**O(2B)-C(28B)-C(27B)**	125.6(6)
C(14A)-C(15A)-Cl(1A)	118.6(5)	**O(2B)-C(28B)-C(29B)**	118.2(5)
C(15A)-C(16A)-C(17A)	120.7(6)	**C(27B)-C(28B)-C(29B)**	116.2(6)
C(15A)-C(16A)-H(16A)	119.6	**N(2B)-C(29B)-C(24B)**	122.6(6)
C(17A)-C(16A)-H(16A)	119.6	**N(2B)-C(29B)-C(28B)**	114.1(5)
C(18A)-C(17A)-C(16A)	122.0(6)	**C(24B)-C(29B)-C(28B)**	123.3(6)
C(18A)-C(17A)-Cl(2A)	119.0(5)	**O(8)-C(80)-N(8)**	127.8(10)
C(16A)-C(17A)-Cl(2A)	119.0(5)	**O(8)-C(80)-H(80)**	116.1
O(1A)-C(18A)-C(17A)	125.3(6)	**N(8)-C(80)-H(80)**	116.1
O(1A)-C(18A)-C(19A)	118.3(5)	**N(8)-C(81)-H(81A)**	109.5
C(17A)-C(18A)-C(19A)	116.4(5)	**N(8)-C(81)-H(81B)**	109.5
N(1A)-C(19A)-C(14A)	121.6(6)	**H(81A)-C(81)-H(81B)**	109.5
N(1A)-C(19A)-C(18A)	114.6(5)	**N(8)-C(81)-H(81C)**	109.5
C(14A)-C(19A)-C(18A)	123.8(6)	**H(81A)-C(81)-H(81C)**	109.5
N(2A)-C(21A)-C(22A)	123.0(6)	**H(81B)-C(81)-H(81C)**	109.5
N(2A)-C(21A)-H(21A)	118.5	**N(8)-C(82)-H(82A)**	109.5
C(22A)-C(21A)-H(21A)	118.5	**N(8)-C(82)-H(82B)**	109.5
C(23A)-C(22A)-C(21A)	118.0(6)	**H(82A)-C(82)-H(82B)**	109.5
C(23A)-C(22A)-H(22A)	121	**N(8)-C(82)-H(82C)**	109.5
C(21A)-C(22A)-H(22A)	121	**H(82A)-C(82)-H(82C)**	109.5
C(22A)-C(23A)-C(24A)	120.8(6)	**H(82B)-C(82)-H(82C)**	109.5
C(22A)-C(23A)-H(23A)	119.6	**N(9)-C(90)-O(9)**	117.2(13)
C(24A)-C(23A)-H(23A)	119.6	**N(9)-C(90)-H(90)**	121.4
C(23A)-C(24A)-C(25A)	126.5(6)	**O(9)-C(90)-H(90)**	121.4
C(23A)-C(24A)-C(29A)	116.3(6)	**N(9)-C(91)-H(91A)**	109.5
C(25A)-C(24A)-C(29A)	117.2(6)	**N(9)-C(91)-H(91B)**	109.5

C(26A)-C(25A)-C(24A)	121.5(6)	**H(91A)-C(91)-H(91B)**	109.5
C(26A)-C(25A)-Cl(3A)	119.7(5)	**N(9)-C(91)-H(91C)**	109.5
C(24A)-C(25A)-Cl(3A)	118.7(5)	**H(91A)-C(91)-H(91C)**	109.5
C(25A)-C(26A)-C(27A)	119.9(6)	**H(91B)-C(91)-H(91C)**	109.5
C(25A)-C(26A)-H(26A)	120	**N(9)-C(92)-H(92A)**	109.5
C(27A)-C(26A)-H(26A)	120	**N(9)-C(92)-H(92B)**	109.5
C(28A)-C(27A)-C(26A)	122.1(6)	**H(92A)-C(92)-H(92B)**	109.5
C(28A)-C(27A)-Cl(4A)	120.0(5)	**N(9)-C(92)-H(92C)**	109.5
C(26A)-C(27A)-Cl(4A)	117.9(5)	**H(92A)-C(92)-H(92C)**	109.5
O(2A)-C(28A)-C(27A)	125.5(6)	**H(92B)-C(92)-H(92C)**	109.5
O(2A)-C(28A)-C(29A)	117.9(5)	**O(7)-C(70)-N(7)**	123.6(9)
C(27A)-C(28A)-C(29A)	116.5(5)	**O(7)-C(70)-H(70)**	118.2
N(2A)-C(29A)-C(24A)	122.7(6)	**N(7)-C(70)-H(70)**	118.2
N(2A)-C(29A)-C(28A)	114.6(5)	**N(7)-C(71)-H(71A)**	109.5
C(24A)-C(29A)-C(28A)	122.7(6)	**N(7)-C(71)-H(71B)**	109.5
N(3A)-C(31A)-C(32A)	122.4(6)	**H(71A)-C(71)-H(71B)**	109.5
N(3A)-C(31A)-H(31A)	118.8	**N(7)-C(71)-H(71C)**	109.5
C(32A)-C(31A)-H(31A)	118.8	**H(71A)-C(71)-H(71C)**	109.5
C(33A)-C(32A)-C(31A)	119.9(6)	**H(71B)-C(71)-H(71C)**	109.5
C(33A)-C(32A)-H(32A)	120.1	**N(7)-C(72)-H(72A)**	109.5
C(31A)-C(32A)-H(32A)	120.1	**N(7)-C(72)-H(72B)**	109.5
C(32A)-C(33A)-C(34A)	119.5(6)	**H(72A)-C(72)-H(72B)**	109.5
C(32A)-C(33A)-H(33A)	120.3	**N(7)-C(72)-H(72C)**	109.5
C(34A)-C(33A)-H(33A)	120.3	**H(72A)-C(72)-H(72C)**	109.5
C(39A)-C(34A)-C(35A)	115.9(6)	**H(72B)-C(72)-H(72C)**	109.5
C(39A)-C(34A)-C(33A)	117.2(6)	**O(6)-C(60)-N(6)**	119.3(11)
C(35A)-C(34A)-C(33A)	126.9(6)	**O(6)-C(60)-H(60)**	120.4
C(36A)-C(35A)-C(34A)	122.4(6)	**N(6)-C(60)-H(60)**	120.4
C(36A)-C(35A)-Cl(5A)	119.4(5)	**N(6)-C(62)-H(62A)**	109.5
C(34A)-C(35A)-Cl(5A)	118.2(5)	**N(6)-C(62)-H(62B)**	109.5
C(35A)-C(36A)-C(37A)	119.8(6)	**H(62A)-C(62)-H(62B)**	109.5
C(35A)-C(36A)-H(36A)	120.1	**N(6)-C(62)-H(62C)**	109.5
C(37A)-C(36A)-H(36A)	120.1	**H(62A)-C(62)-H(62C)**	109.5
C(38A)-C(37A)-C(36A)	122.0(6)	**H(62B)-C(62)-H(62C)**	109.5
C(38A)-C(37A)-Cl(6A)	118.9(5)	**N(6)-C(61)-H(61A)**	109.5
C(36A)-C(37A)-Cl(6A)	119.0(5)	**N(6)-C(61)-H(61B)**	109.5
O(3A)-C(38A)-C(37A)	125.7(6)	**H(61A)-C(61)-H(61B)**	109.5
O(3A)-C(38A)-C(39A)	118.3(6)	**N(6)-C(61)-H(61C)**	109.5
C(37A)-C(38A)-C(39A)	116.0(5)	**H(61A)-C(61)-H(61C)**	109.5
N(3A)-C(39A)-C(34A)	122.6(6)	**H(61B)-C(61)-H(61C)**	109.5
N(3A)-C(39A)-C(38A)	113.6(5)	**N(5)-C(52)-H(52A)**	109.5
C(34A)-C(39A)-C(38A)	123.8(6)	**N(5)-C(52)-H(52B)**	109.5

N(4A)-C(41A)-C(42A)	122.2(6)	**H(52A)-C(52)-H(52B)**	109.5
N(4A)-C(41A)-H(41A)	118.9	**N(5)-C(52)-H(52C)**	109.5
C(42A)-C(41A)-H(41A)	118.9	**H(52A)-C(52)-H(52C)**	109.5
C(43A)-C(42A)-C(41A)	119.7(7)	**H(52B)-C(52)-H(52C)**	109.5
C(43A)-C(42A)-H(42A)	120.2	**N(5)-C(50)-O(5)**	115.8(16)
C(41A)-C(42A)-H(42A)	120.2	**N(5)-C(50)-H(50)**	122.1
C(42A)-C(43A)-C(44A)	119.8(6)	**O(5)-C(50)-H(50)**	122.1
C(42A)-C(43A)-H(43A)	120.1	**N(5)-C(51)-H(51A)**	109.5
C(44A)-C(43A)-H(43A)	120.1	**N(5)-C(51)-H(51B)**	109.5
C(43A)-C(44A)-C(45A)	127.5(6)	**H(51A)-C(51)-H(51B)**	109.5
C(43A)-C(44A)-C(49A)	117.2(6)	**N(5)-C(51)-H(51C)**	109.5
C(45A)-C(44A)-C(49A)	115.3(6)	**H(51A)-C(51)-H(51C)**	109.5
C(46A)-C(45A)-C(44A)	123.0(6)	**H(51B)-C(51)-H(51C)**	109.5
C(46A)-C(45A)-Cl(7A)	119.7(5)	**C(11A)-N(1A)-C(19A)**	119.2(5)
C(44A)-C(45A)-Cl(7A)	117.3(6)	**C(11A)-N(1A)-HfA**	128.5(4)
C(45A)-C(46A)-C(47A)	120.7(7)	**C(19A)-N(1A)-HfA**	112.3(4)
C(45A)-C(46A)-H(46A)	119.6	**C(21A)-N(2A)-C(29A)**	119.1(5)
C(47A)-C(46A)-H(46A)	119.6	**C(21A)-N(2A)-HfA**	127.8(4)
C(48A)-C(47A)-C(46A)	121.1(7)	**C(29A)-N(2A)-HfA**	113.1(4)
C(48A)-C(47A)-Cl(8A)	119.9(5)	**C(31A)-N(3A)-C(39A)**	118.3(5)
C(46A)-C(47A)-Cl(8A)	118.9(5)	**C(31A)-N(3A)-HfA**	127.7(4)
O(4A)-C(48A)-C(47A)	124.8(6)	**C(39A)-N(3A)-HfA**	114.0(4)
O(4A)-C(48A)-C(49A)	118.9(6)	**C(41A)-N(4A)-C(49A)**	119.0(5)
C(47A)-C(48A)-C(49A)	116.2(6)	**C(41A)-N(4A)-HfA**	127.8(4)
N(4A)-C(49A)-C(48A)	114.2(5)	**C(49A)-N(4A)-HfA**	113.2(4)
N(4A)-C(49A)-C(44A)	122.2(6)	**C(11B)-N(1B)-C(19B)**	118.7(6)
C(48A)-C(49A)-C(44A)	123.5(6)	**C(11B)-N(1B)-HfB**	127.7(5)
N(1B)-C(11B)-C(12B)	121.9(7)	**C(19B)-N(1B)-HfB**	113.3(4)
N(1B)-C(11B)-H(11B)	119	**C(31B)-N(3B)-C(39B)**	118.4(5)
C(12B)-C(11B)-H(11B)	119	**C(31B)-N(3B)-HfB**	128.5(4)
C(1B3)-C(12B)-C(11B)	120.3(8)	**C(39B)-N(3B)-HfB**	113.1(4)
C(1B3)-C(12B)-H(12B)	119.9	**C(41B)-N(4B)-C(49B)**	118.0(5)
C(11B)-C(12B)-H(12B)	119.9	**C(41B)-N(4B)-HfB**	129.1(5)
C(12B)-C(1B3)-C(14B)	119.8(7)	**C(49B)-N(4B)-HfB**	112.9(4)
C(12B)-C(1B3)-H(1B3)	120.1	**C(21B)-N(2B)-C(29B)**	117.9(5)
C(14B)-C(1B3)-H(1B3)	120.1	**C(21B)-N(2B)-HfB**	128.8(4)
C(19B)-C(14B)-C(15B)	117.3(7)	**C(29B)-N(2B)-HfB**	113.3(4)
C(19B)-C(14B)-C(1B3)	116.9(7)	**C(80)-N(8)-C(82)**	126.0(9)
C(15B)-C(14B)-C(1B3)	125.7(7)	**C(80)-N(8)-C(81)**	118.7(8)
C(16B)-C(15B)-C(14B)	120.4(6)	**C(82)-N(8)-C(81)**	115.3(7)
C(16B)-C(15B)-Cl(1B)	121.3(6)	**C(90)-N(9)-C(91)**	121.2(11)
C(14B)-C(15B)-Cl(1B)	118.3(6)	**C(90)-N(9)-C(92)**	120.6(10)

C(15B)-C(16B)-C(17B)	121.1(7)	**C(91)-N(9)-C(92)**	118.1(10)
C(15B)-C(16B)-H(16B)	119.4	**C(70)-N(7)-C(71)**	121.9(8)
C(17B)-C(16B)-H(16B)	119.4	**C(70)-N(7)-C(72)**	118.8(8)
C(18B)-C(17B)-C(16B)	121.7(7)	**C(71)-N(7)-C(72)**	119.3(7)
C(18B)-C(17B)-Cl(2B)	119.8(5)	**C(62)-N(6)-C(60)**	134.0(12)
C(16B)-C(17B)-Cl(2B)	118.6(5)	**C(62)-N(6)-C(61)**	112.9(11)
O(1B)-C(18B)-C(17B)	125.6(6)	**C(60)-N(6)-C(61)**	112.8(10)
O(1B)-C(18B)-C(19B)	117.9(6)	**C(50)-N(5)-C(52)**	114.2(13)
C(17B)-C(18B)-C(19B)	116.5(6)	**C(50)-N(5)-C(51)**	124.7(13)
N(1B)-C(19B)-C(14B)	122.3(7)	**C(52)-N(5)-C(51)**	121.0(12)
N(1B)-C(19B)-C(18B)	114.7(5)	**C(18A)-O(1A)-HfA**	122.3(4)
C(14B)-C(19B)-C(18B)	122.9(6)	**C(28A)-O(2A)-HfA**	121.9(4)
N(3B)-C(31B)-C(32B)	122.7(6)	**C(38A)-O(3A)-HfA**	123.2(4)
N(3B)-C(31B)-H(31B)	118.6	**C(48A)-O(4A)-HfA**	122.9(4)
C(32B)-C(31B)-H(31B)	118.6	**C(18B)-O(1B)-HfB**	123.1(4)
C(33B)-C(32B)-C(31B)	119.8(6)	**C(38B)-O(3B)-HfB**	122.6(4)
C(33B)-C(32B)-H(32B)	120.1	**C(48B)-O(4B)-HfB**	123.6(4)
C(31B)-C(32B)-H(32B)	120.1	**C(28B)-O(2B)-HfB**	123.0(4)
C(32B)-C(33B)-C(34B)	119.5(6)	**O(4A)-HfA-O(3A)**	141.00(15)
C(32B)-C(33B)-H(33B)	120.2	**O(4A)-HfA-O(1A)**	106.24(16)
C(34B)-C(33B)-H(33B)	120.2	**O(3A)-HfA-O(1A)**	85.90(16)
C(35B)-C(34B)-C(39B)	117.1(6)	**O(4A)-HfA-O(2A)**	86.57(17)
C(35B)-C(34B)-C(33B)	126.0(6)	**O(3A)-HfA-O(2A)**	107.88(17)
C(39B)-C(34B)-C(33B)	116.9(6)	**O(1A)-HfA-O(2A)**	140.10(15)
C(36B)-C(35B)-C(34B)	120.8(6)	**O(4A)-HfA-N(2A)**	143.47(17)
C(36B)-C(35B)-Cl(5B)	120.6(5)	**O(3A)-HfA-N(2A)**	74.83(16)
C(34B)-C(35B)-Cl(5B)	118.6(5)	**O(1A)-HfA-N(2A)**	77.31(16)
C(35B)-C(36B)-C(37B)	120.9(6)	**O(2A)-HfA-N(2A)**	70.99(16)
C(35B)-C(36B)-H(36B)	119.6	**O(4A)-HfA-N(3A)**	78.38(17)
C(37B)-C(36B)-H(36B)	119.6	**O(3A)-HfA-N(3A)**	70.82(17)
C(38B)-C(37B)-C(36B)	121.7(6)	**O(1A)-HfA-N(3A)**	142.93(17)
C(38B)-C(37B)-Cl(6B)	118.7(5)	**O(2A)-HfA-N(3A)**	76.01(16)
C(36B)-C(37B)-Cl(6B)	119.6(5)	**N(2A)-HfA-N(3A)**	121.09(17)
O(3B)-C(38B)-C(37B)	124.6(6)	**O(4A)-HfA-N(4A)**	70.82(17)
O(3B)-C(38B)-C(39B)	119.2(5)	**O(3A)-HfA-N(4A)**	77.92(17)
C(37B)-C(38B)-C(39B)	116.2(6)	**O(1A)-HfA-N(4A)**	73.36(16)
N(3B)-C(39B)-C(38B)	114.1(5)	**O(2A)-HfA-N(4A)**	145.21(16)
N(3B)-C(39B)-C(34B)	122.6(6)	**N(2A)-HfA-N(4A)**	140.99(18)
C(38B)-C(39B)-C(34B)	123.3(5)	**N(3A)-HfA-N(4A)**	73.80(16)
N(4B)-C(41B)-C(42B)	122.5(6)	**O(4A)-HfA-N(1A)**	74.08(16)
N(4B)-C(41B)-H(41B)	118.7	**O(3A)-HfA-N(1A)**	143.53(16)
C(42B)-C(41B)-H(41B)	118.7	**O(1A)-HfA-N(1A)**	70.48(17)

C(43B)-C(42B)-C(41B)	119.6(6)	**O(2A)-HfA-N(1A)**	77.49(17)
C(43B)-C(42B)-H(42B)	120.2	**N(2A)-HfA-N(1A)**	73.15(17)
C(41B)-C(42B)-H(42B)	120.2	**N(3A)-HfA-N(1A)**	142.56(18)
C(42B)-C(43B)-C(44B)	119.5(6)	**N(4A)-HfA-N(1A)**	118.72(17)
C(42B)-C(43B)-H(43B)	120.2	**O(4B)-HfB-O(1B)**	104.20(17)
C(44B)-C(43B)-H(43B)	120.2	**O(4B)-HfB-O(3B)**	140.80(16)
C(43B)-C(44B)-C(49B)	117.1(6)	**O(1B)-HfB-O(3B)**	88.85(16)
C(43B)-C(44B)-C(45B)	126.2(6)	**O(4B)-HfB-O(2B)**	87.38(17)
C(49B)-C(44B)-C(45B)	116.7(6)	**O(1B)-HfB-O(2B)**	141.18(16)
C(46B)-C(45B)-C(44B)	121.9(6)	**O(3B)-HfB-O(2B)**	105.44(17)
C(46B)-C(45B)-Cl(7B)	118.9(5)	**O(4B)-HfB-N(2B)**	143.63(16)
C(44B)-C(45B)-Cl(7B)	119.2(5)	**O(1B)-HfB-N(2B)**	78.72(17)
C(45B)-C(46B)-C(47B)	120.1(7)	**O(3B)-HfB-N(2B)**	74.68(17)
C(45B)-C(46B)-H(46B)	120	**O(2B)-HfB-N(2B)**	70.99(17)
C(47B)-C(46B)-H(46B)	120	**O(4B)-HfB-N(1B)**	73.32(17)
C(48B)-C(47B)-C(46B)	121.4(6)	**O(1B)-HfB-N(1B)**	70.94(17)
C(48B)-C(47B)-Cl(8B)	119.0(5)	**O(3B)-HfB-N(1B)**	145.09(18)
C(46B)-C(47B)-Cl(8B)	119.5(5)	**O(2B)-HfB-N(1B)**	77.53(18)
O(4B)-C(48B)-C(47B)	124.9(6)	**N(2B)-HfB-N(1B)**	73.64(17)
O(4B)-C(48B)-C(49B)	117.4(6)	**O(4B)-HfB-N(4B)**	70.96(17)
C(47B)-C(48B)-C(49B)	117.7(6)	**O(1B)-HfB-N(4B)**	73.73(16)
N(4B)-C(49B)-C(44B)	123.1(6)	**O(3B)-HfB-N(4B)**	77.88(17)
N(4B)-C(49B)-C(48B)	114.7(5)	**O(2B)-HfB-N(4B)**	143.95(17)
C(44B)-C(49B)-C(48B)	122.1(6)	**N(2B)-HfB-N(4B)**	141.15(17)
N(2B)-C(21B)-C(22B)	123.5(6)	**N(1B)-HfB-N(4B)**	120.46(17)
N(2B)-C(21B)-H(21B)	118.2	**O(4B)-HfB-N(3B)**	77.58(17)
C(22B)-C(21B)-H(21B)	118.2	**O(1B)-HfB-N(3B)**	143.63(16)
C(23B)-C(22B)-C(21B)	119.5(7)	**O(3B)-HfB-N(3B)**	70.78(17)
C(23B)-C(22B)-H(22B)	120.3	**O(2B)-HfB-N(3B)**	74.70(16)
C(21B)-C(22B)-H(22B)	120.3	**N(2B)-HfB-N(3B)**	121.55(17)
C(22B)-C(23B)-C(24B)	119.1(6)	**N(1B)-HfB-N(3B)**	140.30(18)
C(22B)-C(23B)-H(23B)	120.4	**N(4B)-HfB-N(3B)**	72.73(16)

Appendix A.5

Supplementary Crystallographic Data

A.5. $[Hf(diBrOx)_4]\cdot 3DMF$ – (Hf_1e) – § 5.5

Table A.5.1: Atomic coordinates (x 10^4) and equivalent isotropic displacement parameters ($Å^2$ x 10^3) for $[Hf(diBrOx)_4]\cdot 3DMF$.

Atom	*x*	*y*	*z*	$U_{(eq)}$
C(11)	7237(4)	1593(1)	10158(3)	12(1)
C(12)	7055(4)	1779(1)	11017(3)	16(1)
C(13)	8119(4)	1982(1)	11477(3)	14(1)
C(14)	9394(4)	2007(1)	11089(3)	10(1)
C(15)	10587(4)	2207(1)	11471(3)	13(1)
C(16)	11751(4)	2222(1)	11005(3)	15(1)
C(17)	11794(4)	2030(1)	10128(3)	12(1)
C(18)	10673(4)	1829(1)	9700(3)	9(1)
C(19)	9480(4)	1817(1)	10211(3)	9(1)
C(31)	6411(4)	1077(1)	6394(3)	12(1)
C(32)	5889(4)	913(1)	5498(3)	16(1)
C(33)	6786(4)	736(1)	4994(3)	15(1)
C(34)	8236(4)	718(1)	5385(3)	14(1)
C(35)	9310(4)	555(1)	4940(3)	15(1)
C(36)	10689(5)	565(1)	5371(3)	16(1)
C(37)	11066(4)	727(1)	6303(3)	13(1)
C(38)	10084(4)	876(1)	6807(3)	11(1)
C(39)	8664(4)	882(1)	6306(3)	10(1)
C(41)	10686(4)	1664(1)	6512(3)	12(1)
C(42)	10850(4)	1856(1)	5665(3)	15(1)
C(43)	9756(4)	2050(1)	5208(3)	13(1)

C(44)	8471(4)	2060(1)	5600(3)	9(1)
C(45)	7241(4)	2249(1)	5213(3)	11(1)
C(46)	6065(4)	2240(1)	5665(3)	12(1)
C(47)	6061(4)	2051(1)	6545(3)	12(1)
C(48)	7217(4)	1864(1)	6982(3)	9(1)
C(49)	8413(4)	1866(1)	6470(3)	10(1)
C(21)	11429(4)	976(1)	9995(3)	14(1)
C(22)	11986(4)	725(1)	10697(3)	14(1)
C(23)	11122(4)	476(1)	10995(3)	14(1)
C(24)	9680(4)	475(1)	10599(3)	13(1)
C(25)	8657(4)	234(1)	10826(3)	14(1)
C(26)	7268(4)	270(1)	10433(3)	15(1)
C(27)	6826(4)	542(1)	9768(3)	13(1)
C(28)	7770(4)	767(1)	9447(3)	10(1)
C(29)	9202(4)	740(1)	9913(3)	10(1)
C(50)	7264(6)	3955(1)	7293(4)	34(1)
C(51)	7478(7)	3545(1)	8652(4)	47(2)
C(52)	9599(7)	3770(2)	8046(6)	62(2)
C(60)	3372(5)	3528(1)	9078(4)	33(1)
C(62)	2918(6)	3568(1)	7276(4)	38(1)
C(61)	4134(6)	3056(1)	8138(4)	40(1)
C(70)	3658(5)	4445(1)	8237(3)	26(1)
C(71)	3250(7)	5067(2)	8207(6)	62(2)
C(72)	4918(6)	4803(1)	7206(4)	35(1)
N(1)	8416(3)	1608(1)	9763(2)	10(1)
N(3)	7760(3)	1064(1)	6790(2)	10(1)
N(4)	9501(3)	1665(1)	6905(2)	9(1)
N(2)	10081(3)	984(1)	9614(2)	10(1)
N(5)	8100(5)	3770(1)	7974(3)	30(1)
N(6)	3464(4)	3388(1)	8195(3)	31(1)
N(7)	3925(4)	4760(1)	7901(3)	28(1)
O(1)	10625(3)	1656(1)	8871(2)	10(1)
O(3)	10347(3)	1018(1)	7699(2)	10(1)
O(4)	7305(3)	1686(1)	7814(2)	9(1)
O(2)	7455(3)	1003(1)	8748(2)	11(1)
O(5)	5986(4)	3960(1)	7168(3)	39(1)
O(6)	3813(4)	3395(1)	9880(3)	46(1)
O(7)	2843(5)	4383(1)	8813(3)	48(1)
Br(1)	10587(1)	2470(1)	12652(1)	18(1)

Br(2)	13441(1)	2041(1)	9527(1)	17(1)
Br(5)	8850(1)	313(1)	3724(1)	23(1)
Br(6)	12975(1)	736(1)	6886(1)	19(1)
Br(7)	7215(1)	2522(1)	4051(1)	15(1)
Br(8)	4417(1)	2047(1)	7155(1)	14(1)
Br(3)	9199(1)	-157(1)	11634(1)	18(1)
Br(4)	4892(1)	598(1)	9274(1)	18(1)
Hf	8932(1)	1340(1)	8278(1)	9(1)

Table A.5.2: Hydrogen coordinates (x 10^4) and isotropic displacement parameters ($Å^2$ x 10^3) for $[Hf(diBrOx)_4]\cdot 3DMF$.

Atom	*x*	*y*	*z*	$U_{(eq)}$
H(11)	6504	1454	9855	15
H(12)	6211	1763	11271	19
H(13)	8001	2105	12046	17
H(16)	12516	2358	11267	18
H(31)	5789	1199	6725	15
H(32)	4934	926	5247	19
H(33)	6446	627	4396	18
H(36)	11380	465	5051	20
H(41)	11437	1530	6811	14
H(42)	11700	1851	5416	18
H(43)	9852	2176	4640	16
H(46)	5262	2360	5388	15
H(21)	12031	1141	9793	16
H(22)	12939	728	10958	17
H(23)	11486	309	11455	16
H(26)	6609	114	10605	19
H(50)	7706	4094	6875	40
H(51A)	6474	3575	8551	70
H(51B)	7855	3603	9325	70
H(51C)	7696	3308	8526	70
H(52A)	9876	3927	7565	93
H(52B)	9917	3541	7920	93
H(52C)	10011	3842	8700	93

H(60)	2939	3743	9086	40
H(62A)	2212	3428	6890	57
H(62B)	3673	3611	6903	57
H(62C)	2510	3785	7430	57
H(61A)	4787	3017	8734	61
H(61B)	4629	3052	7576	61
H(61C)	3431	2877	8066	61
H(70)	4136	4259	8011	32
H(71A)	2441	5002	8501	92
H(71B)	2961	5212	7639	92
H(71C)	3901	5192	8684	92
H(72A)	5317	4582	7082	53
H(72B)	5655	4958	7483	53
H(72C)	4439	4896	6594	53

Table A.5.3: Anisotropic displacement parameters ($Å^2$ x 10^3) for [Hf(diBrOx)$_4$] ·3DMF.

Atom	U^{11}	U^{22}	U^{33}	U^{23}	U^{13}	U^{12}
C(11)	12(2)	14(2)	11(2)	0(2)	2(2)	0(2)
C(12)	14(2)	19(2)	15(2)	4(2)	9(2)	2(2)
C(13)	21(2)	12(2)	10(2)	1(2)	5(2)	2(2)
C(14)	15(2)	10(2)	6(2)	2(1)	2(2)	4(1)
C(15)	21(2)	11(2)	7(2)	-2(2)	1(2)	-2(2)
C(16)	16(2)	15(2)	12(2)	-2(2)	2(2)	-3(2)
C(17)	12(2)	15(2)	10(2)	2(2)	2(2)	-2(2)
C(18)	13(2)	9(2)	6(2)	3(1)	3(1)	1(1)
C(19)	13(2)	9(2)	5(2)	2(1)	0(1)	1(1)
C(31)	11(2)	14(2)	13(2)	3(2)	2(2)	1(2)
C(32)	14(2)	16(2)	15(2)	1(2)	-2(2)	-4(2)
C(33)	21(2)	13(2)	11(2)	0(2)	-1(2)	-2(2)
C(34)	22(2)	10(2)	9(2)	1(2)	5(2)	1(2)
C(35)	25(2)	14(2)	6(2)	-1(2)	2(2)	3(2)
C(36)	27(2)	14(2)	10(2)	3(2)	7(2)	7(2)
C(37)	10(2)	13(2)	14(2)	5(2)	4(2)	4(1)
C(38)	16(2)	5(2)	12(2)	4(2)	5(2)	2(1)
C(39)	13(2)	7(2)	10(2)	2(2)	4(2)	2(1)
C(41)	11(2)	12(2)	11(2)	-1(2)	1(2)	1(1)
C(42)	13(2)	21(2)	13(2)	0(2)	6(2)	-2(2)
C(43)	18(2)	13(2)	10(2)	4(2)	6(2)	-3(2)

C(44)	11(2)	10(2)	7(2)	0(1)	0(1)	0(1)
C(45)	17(2)	8(2)	7(2)	2(1)	-1(2)	0(1)
C(46)	16(2)	8(2)	12(2)	1(2)	0(2)	4(2)
C(47)	8(2)	13(2)	14(2)	-2(2)	4(2)	-1(1)
C(48)	12(2)	6(2)	9(2)	-2(1)	0(1)	-3(1)
C(49)	9(2)	8(2)	12(2)	-1(2)	2(1)	-2(1)
C(21)	15(2)	17(2)	10(2)	2(2)	3(2)	2(2)
C(22)	12(2)	18(2)	13(2)	-2(2)	0(2)	5(2)
C(23)	21(2)	14(2)	7(2)	2(2)	2(2)	5(2)
C(24)	19(2)	13(2)	7(2)	-1(2)	5(2)	4(2)
C(25)	26(2)	8(2)	10(2)	1(2)	9(2)	0(2)
C(26)	23(2)	14(2)	10(2)	-1(2)	8(2)	-5(2)
C(27)	11(2)	16(2)	13(2)	-3(2)	1(2)	-3(2)
C(28)	14(2)	11(2)	6(2)	-2(1)	3(1)	2(1)
C(29)	14(2)	9(2)	8(2)	-1(1)	4(2)	0(1)
C(50)	48(3)	21(3)	34(3)	-1(2)	15(3)	0(2)
C(51)	83(5)	25(3)	36(3)	0(2)	17(3)	8(3)
C(52)	43(4)	47(4)	91(6)	-20(4)	-8(4)	10(3)
C(60)	28(3)	39(3)	32(3)	5(2)	4(2)	-4(2)
C(62)	48(3)	33(3)	31(3)	4(2)	-4(3)	-4(2)
C(61)	39(3)	38(3)	42(3)	5(3)	-3(3)	4(2)
C(70)	31(3)	27(3)	22(2)	-1(2)	4(2)	1(2)
C(71)	68(5)	32(3)	89(6)	-27(4)	25(4)	-3(3)
C(72)	34(3)	31(3)	41(3)	5(2)	4(2)	-4(2)
N(1)	11(2)	9(2)	10(2)	4(1)	4(1)	3(1)
N(3)	12(2)	8(2)	10(2)	1(1)	3(1)	-1(1)
N(4)	11(2)	7(2)	8(2)	-1(1)	2(1)	-2(1)
N(2)	11(2)	10(2)	8(2)	-2(1)	3(1)	3(1)
N(5)	39(2)	20(2)	28(2)	-4(2)	3(2)	4(2)
N(6)	30(2)	32(2)	31(2)	6(2)	-1(2)	-1(2)
N(7)	31(2)	24(2)	30(2)	-7(2)	5(2)	-2(2)
O(1)	10(1)	11(1)	7(1)	-3(1)	2(1)	-1(1)
O(3)	12(1)	10(1)	9(1)	1(1)	2(1)	5(1)
O(4)	10(1)	10(1)	7(1)	4(1)	2(1)	1(1)
O(2)	12(1)	11(1)	10(1)	3(1)	1(1)	-1(1)
O(5)	34(2)	32(2)	50(2)	-5(2)	8(2)	5(2)
O(6)	40(2)	62(3)	37(2)	14(2)	5(2)	-5(2)
O(7)	60(3)	49(3)	43(2)	8(2)	34(2)	5(2)
Br(1)	27(1)	17(1)	11(1)	-6(1)	6(1)	-2(1)
Br(2)	12(1)	24(1)	16(1)	-5(1)	6(1)	-7(1)
Br(5)	38(1)	20(1)	12(1)	-6(1)	2(1)	5(1)
Br(6)	11(1)	27(1)	20(1)	2(1)	5(1)	5(1)

Br(7)	21(1)	14(1)	10(1)	5(1)	1(1)	0(1)
Br(8)	10(1)	21(1)	12(1)	1(1)	4(1)	4(1)
Br(3)	35(1)	10(1)	10(1)	3(1)	6(1)	3(1)
Br(4)	13(1)	19(1)	22(1)	2(1)	4(1)	-5(1)
Hf	9(1)	10(1)	8(1)	1(1)	2(1)	0(1)

Table A.5.4: Bond lengths (Å) for [Hf(diBrOx)$_4$]·3DMF.

Atoms	*Bond Length (Å)*	*Atoms*	*Bond Length (Å)*
C(11)-N(1)	1.325(5)	**C(22)-C(23)**	1.370(6)
C(11)-C(12)	1.407(5)	**C(22)-H(22)**	0.93
C(11)-H(11)	0.93	**C(23)-C(24)**	1.408(6)
C(12)-C(13)	1.364(6)	**C(23)-H(23)**	0.93
C(12)-H(12)	0.93	**C(24)-C(29)**	1.413(5)
C(13)-C(14)	1.407(5)	**C(24)-C(25)**	1.421(5)
C(13)-H(13)	0.93	**C(25)-C(26)**	1.367(6)
C(14)-C(15)	1.414(5)	**C(25)-Br(3)**	1.891(4)
C(14)-C(19)	1.417(5)	**C(26)-C(27)**	1.410(6)
C(15)-C(16)	1.367(5)	**C(26)-H(26)**	0.93
C(15)-Br(1)	1.901(4)	**C(27)-C(28)**	1.372(5)
C(16)-C(17)	1.412(5)	**C(27)-Br(4)**	1.890(4)
C(16)-H(16)	0.93	**C(28)-O(2)**	1.318(4)
C(17)-C(18)	1.381(5)	**C(28)-C(29)**	1.429(5)
C(17)-Br(2)	1.888(4)	**C(29)-N(2)**	1.368(5)
C(18)-O(1)	1.306(4)	**C(50)-O(5)**	1.213(6)
C(18)-C(19)	1.427(5)	**C(50)-N(5)**	1.338(7)
C(19)-N(1)	1.370(5)	**C(50)-H(50)**	0.93
C(31)-N(3)	1.326(5)	**C(51)-N(5)**	1.461(7)
C(31)-C(32)	1.397(6)	**C(51)-H(51A)**	0.96
C(31)-H(31)	0.93	**C(51)-H(51B)**	0.96
C(32)-C(33)	1.364(6)	**C(51)-H(51C)**	0.96
C(32)-H(32)	0.93	**C(52)-N(5)**	1.427(7)
C(33)-C(34)	1.416(6)	**C(52)-H(52A)**	0.96
C(33)-H(33)	0.93	**C(52)-H(52B)**	0.96
C(34)-C(39)	1.410(5)	**C(52)-H(52C)**	0.96
C(34)-C(35)	1.419(5)	**C(60)-O(6)**	1.223(6)
C(35)-C(36)	1.366(6)	**C(60)-N(6)**	1.333(7)
C(35)-Br(5)	1.895(4)	**C(60)-H(60)**	0.93
C(36)-C(37)	1.413(6)	**C(62)-N(6)**	1.459(6)
C(36)-H(36)	0.93	**C(62)-H(62A)**	0.96

C(37)-C(38)	1.373(5)	**C(62)-H(62B)**	0.96
C(37)-Br(6)	1.885(4)	**C(62)-H(62C)**	0.96
C(38)-O(3)	1.321(5)	**C(61)-N(6)**	1.442(7)
C(38)-C(39)	1.429(5)	**C(61)-H(61A)**	0.96
C(39)-N(3)	1.362(5)	**C(61)-H(61B)**	0.96
C(41)-N(4)	1.328(5)	**C(61)-H(61C)**	0.96
C(41)-C(42)	1.399(5)	**C(70)-O(7)**	1.213(6)
C(41)-H(41)	0.93	**C(70)-N(7)**	1.337(6)
C(42)-C(43)	1.361(6)	**C(70)-H(70)**	0.93
C(42)-H(42)	0.93	**C(71)-N(7)**	1.441(7)
C(43)-C(44)	1.417(5)	**C(71)-H(71A)**	0.96
C(43)-H(43)	0.93	**C(71)-H(71B)**	0.96
C(44)-C(49)	1.410(5)	**C(71)-H(71C)**	0.96
C(44)-C(45)	1.420(5)	**C(72)-N(7)**	1.450(6)
C(45)-C(46)	1.365(5)	**C(72)-H(72A)**	0.96
C(45)-Br(7)	1.899(4)	**C(72)-H(72B)**	0.96
C(46)-C(47)	1.405(5)	**C(72)-H(72C)**	0.96
C(46)-H(46)	0.93	**N(1)-Hf**	2.389(3)
C(47)-C(48)	1.380(5)	**N(3)-Hf**	2.413(3)
C(47)-Br(8)	1.890(4)	**N(4)-Hf**	2.383(3)
C(48)-O(4)	1.317(4)	**N(2)-Hf**	2.410(3)
C(48)-C(49)	1.430(5)	**O(1)-Hf**	2.095(3)
C(49)-N(4)	1.363(5)	**O(3)-Hf**	2.083(2)
C(21)-N(2)	1.320(5)	**O(4)-Hf**	2.080(2)
C(21)-C(22)	1.409(5)	**O(2)-Hf**	2.095(3)
C(21)-H(21)	0.93		

Table A.5.5: Bond angles (°) for for [Hf(diBrOx)$_4$]·3DMF.

Atoms	*Bond angle (°)*	*Atoms*	*Bond angle (°)*
N(1)-C(11)-C(12)	122.4(4)	**O(2)-C(28)-C(29)**	118.2(3)
N(1)-C(11)-H(11)	118.8	**C(27)-C(28)-C(29)**	116.7(3)
C(12)-C(11)-H(11)	118.8	**N(2)-C(29)-C(24)**	122.8(4)
C(13)-C(12)-C(11)	119.8(4)	**N(2)-C(29)-C(28)**	114.4(3)
C(13)-C(12)-H(12)	120.1	**C(24)-C(29)-C(28)**	122.8(3)
C(11)-C(12)-H(12)	120.1	**O(5)-C(50)-N(5)**	126.5(5)
C(12)-C(13)-C(14)	120.0(4)	**O(5)-C(50)-H(50)**	116.8
C(12)-C(13)-H(13)	120	**N(5)-C(50)-H(50)**	116.8
C(14)-C(13)-H(13)	120	**N(5)-C(51)-H(51A)**	109.5
C(13)-C(14)-C(15)	126.9(4)	**N(5)-C(51)-H(51B)**	109.5
C(13)-C(14)-C(19)	116.6(4)	**H(51A)-C(51)-H(51B)**	109.5
C(15)-C(14)-C(19)	116.5(3)	**N(5)-C(51)-H(51C)**	109.5
C(16)-C(15)-C(14)	121.7(4)	**H(51A)-C(51)-H(51C)**	109.5
C(16)-C(15)-Br(1)	118.3(3)	**H(51B)-C(51)-H(51C)**	109.5
C(14)-C(15)-Br(1)	120.0(3)	**N(5)-C(52)-H(52A)**	109.5
C(15)-C(16)-C(17)	120.1(4)	**N(5)-C(52)-H(52B)**	109.5
C(15)-C(16)-H(16)	120	**H(52A)-C(52)-H(52B)**	109.5
C(17)-C(16)-H(16)	120	**N(5)-C(52)-H(52C)**	109.5
C(18)-C(17)-C(16)	122.1(4)	**H(52A)-C(52)-H(52C)**	109.5
C(18)-C(17)-Br(2)	118.7(3)	**H(52B)-C(52)-H(52C)**	109.5
C(16)-C(17)-Br(2)	119.2(3)	**O(6)-C(60)-N(6)**	125.1(5)
O(1)-C(18)-C(17)	125.1(3)	**O(6)-C(60)-H(60)**	117.5
O(1)-C(18)-C(19)	118.5(3)	**N(6)-C(60)-H(60)**	117.5
C(17)-C(18)-C(19)	116.4(3)	**N(6)-C(62)-H(62A)**	109.5
N(1)-C(19)-C(14)	123.1(3)	**N(6)-C(62)-H(62B)**	109.5
N(1)-C(19)-C(18)	113.7(3)	**H(62A)-C(62)-H(62B)**	109.5
C(14)-C(19)-C(18)	123.2(3)	**N(6)-C(62)-H(62C)**	109.5
N(3)-C(31)-C(32)	122.6(4)	**H(62A)-C(62)-H(62C)**	109.5
N(3)-C(31)-H(31)	118.7	**H(62B)-C(62)-H(62C)**	109.5
C(32)-C(31)-H(31)	118.7	**N(6)-C(61)-H(61A)**	109.5
C(33)-C(32)-C(31)	119.7(4)	**N(6)-C(61)-H(61B)**	109.5
C(33)-C(32)-H(32)	120.1	**H(61A)-C(61)-H(61B)**	109.5
C(31)-C(32)-H(32)	120.1	**N(6)-C(61)-H(61C)**	109.5
C(32)-C(33)-C(34)	119.6(4)	**H(61A)-C(61)-H(61C)**	109.5
C(32)-C(33)-H(33)	120.2	**H(61B)-C(61)-H(61C)**	109.5
C(34)-C(33)-H(33)	120.2	**O(7)-C(70)-N(7)**	125.3(5)

C(39)-C(34)-C(33)	116.8(4)	**O(7)-C(70)-H(70)**	117.3
C(39)-C(34)-C(35)	116.5(4)	**N(7)-C(70)-H(70)**	117.3
C(33)-C(34)-C(35)	126.7(4)	**N(7)-C(71)-H(71A)**	109.5
C(36)-C(35)-C(34)	121.6(4)	**N(7)-C(71)-H(71B)**	109.5
C(36)-C(35)-Br(5)	118.2(3)	**H(71A)-C(71)-H(71B)**	109.5
C(34)-C(35)-Br(5)	120.2(3)	**N(7)-C(71)-H(71C)**	109.5
C(35)-C(36)-C(37)	119.9(4)	**H(71A)-C(71)-H(71C)**	109.5
C(35)-C(36)-H(36)	120	**H(71B)-C(71)-H(71C)**	109.5
C(37)-C(36)-H(36)	120	**N(7)-C(72)-H(72A)**	109.5
C(38)-C(37)-C(36)	122.2(4)	**N(7)-C(72)-H(72B)**	109.5
C(38)-C(37)-Br(6)	118.6(3)	**H(72A)-C(72)-H(72B)**	109.5
C(36)-C(37)-Br(6)	119.2(3)	**N(7)-C(72)-H(72C)**	109.5
O(3)-C(38)-C(37)	125.6(4)	**H(72A)-C(72)-H(72C)**	109.5
O(3)-C(38)-C(39)	118.0(3)	**H(72B)-C(72)-H(72C)**	109.5
C(37)-C(38)-C(39)	116.4(4)	**C(11)-N(1)-C(19)**	118.1(3)
N(3)-C(39)-C(34)	122.7(3)	**C(11)-N(1)-Hf**	128.6(3)
N(3)-C(39)-C(38)	114.1(3)	**C(19)-N(1)-Hf**	113.3(2)
C(34)-C(39)-C(38)	123.1(3)	**C(31)-N(3)-C(39)**	118.5(3)
N(4)-C(41)-C(42)	122.7(4)	**C(31)-N(3)-Hf**	128.9(3)
N(4)-C(41)-H(41)	118.6	**C(39)-N(3)-Hf**	112.6(2)
C(42)-C(41)-H(41)	118.6	**C(41)-N(4)-C(49)**	118.2(3)
C(43)-C(42)-C(41)	119.5(4)	**C(41)-N(4)-Hf**	128.8(3)
C(43)-C(42)-H(42)	120.2	**C(49)-N(4)-Hf**	112.9(2)
C(41)-C(42)-H(42)	120.2	**C(21)-N(2)-C(29)**	118.6(3)
C(42)-C(43)-C(44)	119.9(4)	**C(21)-N(2)-Hf**	128.3(3)
C(42)-C(43)-H(43)	120.1	**C(29)-N(2)-Hf**	112.7(2)
C(44)-C(43)-H(43)	120.1	**C(50)-N(5)-C(52)**	122.8(5)
C(49)-C(44)-C(43)	116.7(3)	**C(50)-N(5)-C(51)**	119.8(5)
C(49)-C(44)-C(45)	116.6(3)	**C(52)-N(5)-C(51)**	117.4(5)
C(43)-C(44)-C(45)	126.7(4)	**C(60)-N(6)-C(61)**	119.9(4)
C(46)-C(45)-C(44)	121.2(3)	**C(60)-N(6)-C(62)**	121.2(5)
C(46)-C(45)-Br(7)	118.8(3)	**C(61)-N(6)-C(62)**	118.9(4)
C(44)-C(45)-Br(7)	120.0(3)	**C(70)-N(7)-C(71)**	122.0(5)
C(45)-C(46)-C(47)	120.5(4)	**C(70)-N(7)-C(72)**	120.4(4)
C(45)-C(46)-H(46)	119.8	**C(71)-N(7)-C(72)**	117.6(5)
C(47)-C(46)-H(46)	119.8	**C(18)-O(1)-Hf**	123.7(2)
C(48)-C(47)-C(46)	122.2(3)	**C(38)-O(3)-Hf**	123.4(2)
C(48)-C(47)-Br(8)	118.5(3)	**C(48)-O(4)-Hf**	122.9(2)
C(46)-C(47)-Br(8)	119.3(3)	**C(28)-O(2)-Hf**	123.9(2)

O(4)-C(48)-C(47)	125.8(3)	**O(4)-Hf-O(3)**	140.45(10)
O(4)-C(48)-C(49)	118.1(3)	**O(4)-Hf-O(1)**	104.26(10)
C(47)-C(48)-C(49)	116.1(3)	**O(3)-Hf-O(1)**	88.95(10)
N(4)-C(49)-C(44)	122.9(3)	**O(4)-Hf-O(2)**	88.89(10)
N(4)-C(49)-C(48)	113.8(3)	**O(3)-Hf-O(2)**	104.74(10)
C(44)-C(49)-C(48)	123.3(3)	**O(1)-Hf-O(2)**	139.99(10)
N(2)-C(21)-C(22)	122.2(4)	**O(4)-Hf-N(4)**	70.97(10)
N(2)-C(21)-H(21)	118.9	**O(3)-Hf-N(4)**	77.11(10)
C(22)-C(21)-H(21)	118.9	**O(1)-Hf-N(4)**	74.89(10)
C(23)-C(22)-C(21)	119.9(4)	**O(2)-Hf-N(4)**	144.38(10)
C(23)-C(22)-H(22)	120	**O(4)-Hf-N(1)**	74.75(10)
C(21)-C(22)-H(22)	120	**O(3)-Hf-N(1)**	144.07(10)
C(22)-C(23)-C(24)	119.5(4)	**O(1)-Hf-N(1)**	70.69(10)
C(22)-C(23)-H(23)	120.3	**O(2)-Hf-N(1)**	76.95(10)
C(24)-C(23)-H(23)	120.3	**N(4)-Hf-N(1)**	122.54(10)
C(23)-C(24)-C(29)	117.0(4)	**O(4)-Hf-N(2)**	146.39(10)
C(23)-C(24)-C(25)	126.1(4)	**O(3)-Hf-N(2)**	72.25(10)
C(29)-C(24)-C(25)	116.8(4)	**O(1)-Hf-N(2)**	78.53(10)
C(26)-C(25)-C(24)	120.8(4)	**O(2)-Hf-N(2)**	70.65(10)
C(26)-C(25)-Br(3)	118.4(3)	**N(4)-Hf-N(2)**	139.41(10)
C(24)-C(25)-Br(3)	120.7(3)	**N(1)-Hf-N(2)**	74.80(10)
C(25)-C(26)-C(27)	120.6(4)	**O(4)-Hf-N(3)**	78.17(10)
C(25)-C(26)-H(26)	119.7	**O(3)-Hf-N(3)**	70.48(10)
C(27)-C(26)-H(26)	119.7	**O(1)-Hf-N(3)**	144.84(10)
C(28)-C(27)-C(26)	121.8(4)	**O(2)-Hf-N(3)**	74.39(10)
C(28)-C(27)-Br(4)	118.3(3)	**N(4)-Hf-N(3)**	72.91(10)
C(26)-C(27)-Br(4)	119.9(3)	**N(1)-Hf-N(3)**	140.57(11)
O(2)-C(28)-C(27)	125.2(4)	**N(2)-Hf-N(3)**	118.98(10)

Appendix A.6

Supplementary Crystallographic Data

A.6. $[Hf(dilOx)_4]\cdot DMF$ – (Hf_1f) – § 5.6

Table A.6.1: Atomic coordinates (x 10^4) and equivalent isotropic displacement parameters ($Å^2$ x 10^3) for $[Hf(dilOx)_4]\cdot DMF$.

Atom	*x*	*y*	*z*	$U_{(eq)}$
HfA	10040(1)	3402(1)	2931(1)	25(1)
HfB	15027(1)	6627(1)	2068(1)	25(1)
I(4B)	14223(1)	5974(1)	-218(1)	31(1)
I(6A)	9214(1)	4045(1)	5220(1)	31(1)
I(7A)	12303(1)	7186(1)	667(1)	34(1)
I(1B)	17314(1)	2835(1)	4313(1)	35(1)
I(06)	12725(1)	7449(1)	3671(1)	37(1)
I(8A)	10926(1)	4154(1)	275(1)	36(1)
I(4A)	7743(1)	2563(1)	1351(1)	37(1)
I(2B)	15905(1)	5858(1)	4722(1)	36(1)
I(8B)	17403(1)	7502(1)	70(1)	36(1)
I(2A)	12426(1)	2520(1)	4918(1)	36(1)
I(5A)	7745(1)	7113(1)	3202(1)	39(1)
I(3B)	12773(1)	2910(1)	1805(1)	41(1)
I(7B)	18079(1)	10230(1)	1191(1)	60(1)
I(1A)	13069(1)	-233(1)	3814(1)	64(1)
I(3)	6790(3)	-113(2)	3909(1)	70(2)
O(1A)	11127(9)	2981(8)	3599(6)	44(1)
O(4B)	16104(7)	7043(6)	1390(5)	25(1)
O(1B)	15499(7)	6203(6)	3095(5)	25(1)
O(3A)	9571(9)	3761(8)	3756(6)	44(1)

O(3B)	13977(7)	7016(6)	2541(5)	25(1)
N(4A)	10915(9)	4596(8)	2755(7)	31(1)
N(1B)	15903(9)	5433(8)	2232(7)	31(1)
N(4B)	15657(9)	7776(8)	2269(7)	31(1)
O(2B)	14558(7)	6259(6)	1238(5)	25(1)
N(1A)	10677(9)	2257(8)	2733(7)	31(1)
N(2B)	14118(9)	5463(8)	2520(7)	31(1)
C(41A)	11137(10)	4946(9)	3218(8)	24(1)
N(3A)	9107(9)	4564(8)	2475(7)	31(1)
C(27B)	13933(10)	5270(9)	814(7)	25(3)
C(11B)	16135(10)	5088(10)	1764(7)	28(3)
C(19B)	16142(10)	5055(9)	2914(7)	23(3)
C(13B)	16796(10)	3949(10)	2642(9)	30(3)
C(44B)	16722(12)	8862(10)	1799(8)	32(1)
C(47B)	17137(12)	8058(10)	821(8)	32(1)
C(31A)	8840(10)	4931(9)	1830(7)	25(1)
C(46A)	11541(10)	5609(9)	669(8)	24(1)
C(44A)	11569(10)	5714(9)	1833(7)	24(1)
C(17A)	12154(14)	1953(12)	4179(10)	48(1)
C(48B)	16510(12)	7718(10)	1317(8)	32(1)
C(12B)	16582(11)	4349(11)	1944(9)	36(4)
C(22B)	13358(10)	4393(9)	3350(7)	26(3)
C(18A)	11527(14)	2298(12)	3671(10)	48(1)
C(21B)	13850(11)	5106(10)	3163(8)	30(3)
C(14A)	11727(14)	1167(12)	3203(10)	48(1)
C(28A)	8587(16)	2313(11)	2743(9)	49(2)
C(41B)	15461(12)	8110(10)	2754(8)	32(1)
C(43A)	11794(10)	6072(9)	2344(7)	24(1)
C(35A)	8298(10)	5953(9)	3393(7)	25(1)
C(16B)	16539(11)	4413(10)	4318(8)	32(4)
C(37A)	8926(10)	4761(9)	4185(7)	25(1)
C(15B)	16742(10)	3991(10)	3883(8)	28(3)
C(49B)	16293(12)	8136(10)	1791(8)	32(1)
C(25B)	13304(11)	4078(10)	1625(9)	33(4)
N(3B)	14391(9)	7826(8)	1251(7)	31(1)
C(48A)	10908(10)	4516(9)	1624(7)	24(1)
C(42A)	11584(10)	5682(9)	3028(7)	24(1)
C(17B)	16137(10)	5188(9)	4061(7)	24(3)
C(28B)	14140(9)	5578(9)	1331(7)	20(3)

C(34A)	8441(10)	5670(9)	2815(7)	25(1)
C(24B)	13465(10)	4369(10)	2184(8)	26(3)
C(32A)	8369(10)	5642(9)	1644(7)	25(1)
C(29B)	13897(10)	5116(10)	2036(7)	24(3)
C(11A)	10456(14)	1928(12)	2235(10)	48(1)
C(46B)	17558(12)	8762(10)	787(8)	32(1)
C(39A)	8889(10)	4918(9)	2968(7)	25(1)
C(45A)	11754(10)	6028(9)	1107(7)	24(1)
C(39B)	13758(15)	8162(11)	1545(9)	45(2)
C(38A)	9146(10)	4459(9)	3672(7)	25(1)
C(38B)	13554(15)	7709(11)	2269(9)	45(2)
C(45B)	17370(12)	9172(10)	1262(8)	32(1)
C(29A)	8810(16)	1865(11)	3450(9)	49(2)
C(37B)	12961(15)	8026(11)	2613(9)	45(2)
N(5)	10038(9)	1909(8)	-365(7)	31(1)
C(18B)	15904(10)	5508(9)	3370(7)	25(3)
C(15A)	12392(14)	839(12)	3731(10)	48(1)
C(47A)	11149(10)	4837(9)	939(7)	24(1)
C(25A)	7728(16)	860(11)	3431(9)	49(2)
C(27A)	7984(16)	1980(11)	2402(9)	49(2)
C(43B)	16450(12)	9195(10)	2312(8)	32(1)
C(12A)	10837(14)	1225(12)	2199(10)	48(1)
C(21A)	9629(16)	1862(11)	4419(9)	49(2)
C(24A)	8358(16)	1124(11)	3822(9)	49(2)
C(52)	9814(14)	1165(12)	-525(10)	48(1)
O(2A)	8988(7)	3002(7)	2471(5)	30(2)
O(4A)	10505(9)	3824(8)	1898(6)	44(1)
N(2A)	9429(10)	2198(8)	3750(6)	34(3)
C(49A)	11138(10)	4978(9)	2073(7)	24(1)
C(26B)	13531(10)	4509(9)	957(7)	26(3)
C(19A)	11310(14)	1896(12)	3199(10)	48(1)
C(16A)	12574(14)	1243(12)	4201(10)	48(1)
C(13A)	11464(14)	831(13)	2696(10)	48(1)
C(14B)	16564(10)	4315(10)	3151(7)	26(3)
C(33A)	8174(10)	6018(9)	2114(7)	25(1)
C(31B)	14592(15)	8164(11)	595(9)	45(2)
C(36A)	8524(10)	5505(9)	4055(7)	25(1)
C(33B)	13525(14)	9229(11)	485(9)	45(2)
C(22A)	9227(15)	1125(11)	4819(9)	49(2)

C(35B)	12604(15)	9130(11)	1586(9)	45(2)
C(34B)	13290(15)	8879(11)	1191(9)	45(2)
C(32C)	14158(14)	8880(11)	198(9)	45(2)
C(23A)	8610(15)	777(11)	4523(9)	49(2)
C(42B)	15849(12)	8792(10)	2803(8)	32(1)
C(26A)	7562(16)	1244(11)	2751(9)	49(2)
O(5)	9897(9)	1310(8)	775(6)	44(1)
C(36B)	12479(15)	8737(11)	2273(9)	45(2)
C(53)	10248(14)	2632(12)	-965(10)	48(1)
I(5B)	11733(2)	10109(1)	1098(1)	54(1)
C(23B)	13182(10)	4007(10)	2895(7)	26(3)
N(6)	4975(9)	1876(8)	4602(7)	31(1)
C(63)	5235(14)	1160(12)	4448(10)	48(1)
C(62)	4776(14)	2617(12)	3996(10)	48(1)
O(6)	5123(9)	1315(8)	5753(6)	44(1)
C(61)	5009(14)	1920(13)	5244(10)	48(1)
C(51)	9989(14)	1924(13)	259(10)	48(1)
I(3A)	7570(4)	-431(2)	3893(2)	62(2)
I(5C)	12537(6)	10426(4)	1116(3)	87(4)

Table A.6.2: Hydrogen coordinates (x 10^4) and isotropic displacement parameters(Å^2 x 10^3) for [Hf(dilOx)$_4$]·DMF.

Atom	*x*	*y*	*z*	$U_{(eq)}$
H(21)	10987	4690	3694	29
H(011)	15992	5353	1288	33
H(013)	17091	3442	2773	36
H(31)	8979	4695	1481	30
H(26)	11654	5835	183	29
H(012)	16740	4120	1594	43
H(042)	13143	4177	3814	31
H(041)	13994	5340	3512	36
H(021)	15023	7858	3088	39
H(23)	12088	6577	2214	29
H(016)	16667	4188	4801	38
H(22)	11743	5913	3375	29

H(32)	8178	5874	1176	30
H(11)	10025	2191	1899	57
H(026)	17986	8976	434	39
H(023)	16683	9696	2317	39
H(12)	10675	1012	1840	57
H(41)	10042	2115	4632	59
H(52A)	9263	1248	-788	71
H(52B)	9746	715	-89	71
H(52C)	10286	1038	-804	71
H(046)	13418	4297	589	31
H(16)	13004	1024	4551	57
H(13)	11712	333	2691	57
H(33)	7858	6514	1973	30
H(031)	15030	7929	385	54
H(36)	8404	5705	4430	30
H(033)	13242	9711	208	54
H(42)	9389	875	5293	59
H(032)	14310	9123	-279	54
H(43)	8342	287	4798	59
H(022)	15701	8986	3176	39
H(46)	7159	1018	2508	59
H(036)	12066	8939	2528	54
H(53A)	10638	2480	-1287	71
H(53B)	10540	3033	-798	71
H(53C)	9703	2864	-1207	71
H(043)	12877	3506	3037	32
H(63A)	4748	980	4220	71
H(63B)	5386	733	4882	71
H(63C)	5747	1280	4137	71
H(62A)	5070	3085	4063	71
H(62B)	4140	2711	3964	71
H(62C)	4989	2541	3564	71
H(61)	4943	2431	5311	57
H(51)	10026	2432	333	57

Table A.6.3: Anisotropic displacement parameters (Å^2 x 10^3) for [Hf(dilOx)$_4$]·DMF.

Atom	U^{11}	U^{22}	U^{33}	U^{23}	U^{13}	U^{12}
HfA	31(1)	27(1)	14(1)	-5(1)	3(1)	3(1)
HfB	31(1)	28(1)	14(1)	-5(1)	-3(1)	-2(1)
I(4B)	46(1)	35(1)	11(1)	-4(1)	-3(1)	-3(1)
I(6A)	46(1)	34(1)	11(1)	-4(1)	2(1)	3(1)
I(7A)	43(1)	33(1)	26(1)	-8(1)	5(1)	-7(1)
I(1B)	44(1)	34(1)	27(1)	-9(1)	-6(1)	8(1)
I(06)	55(1)	23(1)	29(1)	-4(1)	5(1)	5(1)
I(8A)	65(1)	31(1)	15(1)	-12(1)	6(1)	0(1)
I(4A)	56(1)	23(1)	29(1)	-4(1)	-6(1)	-6(1)
I(2B)	64(1)	32(1)	16(1)	-13(1)	-6(1)	-1(1)
I(8B)	53(1)	27(1)	26(1)	-9(1)	12(1)	-6(1)
I(2A)	55(1)	26(1)	26(1)	-8(1)	-13(1)	8(1)
I(5A)	49(1)	37(1)	31(1)	-12(1)	-6(1)	12(1)
I(3B)	54(1)	37(1)	32(1)	-13(1)	7(1)	-12(1)
I(7B)	95(1)	42(1)	45(1)	-16(1)	8(1)	-36(1)
I(1A)	103(1)	45(1)	48(1)	-19(1)	-13(1)	39(1)
I(3)	124(4)	53(2)	26(1)	-2(1)	5(1)	-49(2)
O(1A)	54(4)	44(3)	30(3)	-5(2)	2(2)	5(3)
O(4B)	33(3)	27(3)	14(2)	-5(2)	-6(2)	1(2)
O(1B)	33(3)	27(3)	14(2)	-5(2)	-6(2)	1(2)
O(3A)	54(4)	44(3)	30(3)	-5(2)	2(2)	5(3)
O(3B)	33(3)	27(3)	14(2)	-5(2)	-6(2)	1(2)
N(4A)	31(2)	34(2)	26(2)	-7(2)	-2(2)	1(2)
N(1B)	31(2)	34(2)	26(2)	-7(2)	-2(2)	1(2)
N(4B)	31(2)	34(2)	26(2)	-7(2)	-2(2)	1(2)
O(2B)	33(3)	27(3)	14(2)	-5(2)	-6(2)	1(2)
N(1A)	31(2)	34(2)	26(2)	-7(2)	-2(2)	1(2)
N(2B)	31(2)	34(2)	26(2)	-7(2)	-2(2)	1(2)
C(41A)	30(3)	26(3)	18(2)	-8(2)	1(2)	2(2)
N(3A)	31(2)	34(2)	26(2)	-7(2)	-2(2)	1(2)
C(27B)	28(8)	33(8)	8(6)	0(6)	-4(5)	3(6)
C(11B)	25(8)	43(9)	15(7)	-9(6)	-3(6)	2(7)
C(19B)	26(8)	28(8)	18(7)	-10(6)	-5(6)	4(6)
C(13B)	31(9)	24(8)	37(9)	-13(7)	-2(7)	13(6)
C(44B)	47(3)	30(3)	22(3)	-10(2)	-1(2)	-5(2)
C(47B)	47(3)	30(3)	22(3)	-10(2)	-1(2)	-5(2)

C(31A)	28(3)	28(3)	15(2)	-3(2)	4(2)	1(2)
C(46A)	30(3)	26(3)	18(2)	-8(2)	1(2)	2(2)
C(44A)	30(3)	26(3)	18(2)	-8(2)	1(2)	2(2)
C(17A)	61(3)	44(2)	35(2)	-10(2)	-3(2)	5(2)
C(48B)	47(3)	30(3)	22(3)	-10(2)	-1(2)	-5(2)
C(12B)	35(10)	48(11)	26(8)	-14(8)	-13(7)	13(8)
C(22B)	34(9)	27(8)	13(6)	-3(6)	1(6)	-3(6)
C(18A)	61(3)	44(2)	35(2)	-10(2)	-3(2)	5(2)
C(21B)	34(9)	37(9)	16(7)	-5(6)	-1(6)	7(7)
C(14A)	61(3)	44(2)	35(2)	-10(2)	-3(2)	5(2)
C(28A)	93(5)	29(3)	23(3)	-2(2)	9(3)	-12(3)
C(41B)	47(3)	30(3)	22(3)	-10(2)	-1(2)	-5(2)
C(43A)	30(3)	26(3)	18(2)	-8(2)	1(2)	2(2)
C(35A)	28(3)	28(3)	15(2)	-3(2)	4(2)	1(2)
C(16B)	41(10)	35(9)	18(7)	-8(7)	-12(6)	-7(7)
C(37A)	28(3)	28(3)	15(2)	-3(2)	4(2)	1(2)
C(15B)	30(9)	30(8)	22(7)	-5(6)	-3(6)	12(7)
C(49B)	47(3)	30(3)	22(3)	-10(2)	-1(2)	-5(2)
C(25B)	27(9)	31(9)	35(9)	-4(7)	-6(7)	-4(7)
N(3B)	31(2)	34(2)	26(2)	-7(2)	-2(2)	1(2)
C(48A)	30(3)	26(3)	18(2)	-8(2)	1(2)	2(2)
C(42A)	30(3)	26(3)	18(2)	-8(2)	1(2)	2(2)
C(17B)	40(9)	21(7)	12(6)	-8(5)	2(6)	2(6)
C(28B)	24(7)	27(7)	10(6)	-7(5)	-1(5)	-3(6)
C(34A)	28(3)	28(3)	15(2)	-3(2)	4(2)	1(2)
C(24B)	20(8)	35(9)	25(8)	-12(7)	-8(6)	3(6)
C(32A)	28(3)	28(3)	15(2)	-3(2)	4(2)	1(2)
C(29B)	24(8)	36(9)	11(6)	-5(6)	-9(5)	5(6)
C(11A)	61(3)	44(2)	35(2)	-10(2)	-3(2)	5(2)
C(46B)	47(3)	30(3)	22(3)	-10(2)	-1(2)	-5(2)
C(39A)	28(3)	28(3)	15(2)	-3(2)	4(2)	1(2)
C(45A)	30(3)	26(3)	18(2)	-8(2)	1(2)	2(2)
C(39B)	78(5)	28(3)	25(3)	-4(2)	-9(3)	7(3)
C(38A)	28(3)	28(3)	15(2)	-3(2)	4(2)	1(2)
C(38B)	78(5)	28(3)	25(3)	-4(2)	-9(3)	7(3)
C(45B)	47(3)	30(3)	22(3)	-10(2)	-1(2)	-5(2)
C(29A)	93(5)	29(3)	23(3)	-2(2)	9(3)	-12(3)
C(37B)	78(5)	28(3)	25(3)	-4(2)	-9(3)	7(3)
N(5)	31(2)	34(2)	26(2)	-7(2)	-2(2)	1(2)

C(18B)	30(8)	32(8)	18(7)	-13(6)	-2(6)	-4(6)
C(15A)	61(3)	44(2)	35(2)	-10(2)	-3(2)	5(2)
C(47A)	30(3)	26(3)	18(2)	-8(2)	1(2)	2(2)
C(25A)	93(5)	29(3)	23(3)	-2(2)	9(3)	-12(3)
C(27A)	93(5)	29(3)	23(3)	-2(2)	9(3)	-12(3)
C(43B)	47(3)	30(3)	22(3)	-10(2)	-1(2)	-5(2)
C(12A)	61(3)	44(2)	35(2)	-10(2)	-3(2)	5(2)
C(21A)	93(5)	29(3)	23(3)	-2(2)	9(3)	-12(3)
C(24A)	93(5)	29(3)	23(3)	-2(2)	9(3)	-12(3)
C(52)	61(3)	44(2)	35(2)	-10(2)	-3(2)	5(2)
O(2A)	35(6)	29(6)	19(5)	2(4)	6(4)	-8(5)
O(4A)	54(4)	44(3)	30(3)	-5(2)	2(2)	5(3)
N(2A)	61(10)	20(7)	12(6)	5(5)	4(6)	7(6)
C(49A)	30(3)	26(3)	18(2)	-8(2)	1(2)	2(2)
C(26B)	38(9)	31(8)	11(6)	-9(6)	-4(6)	-8(7)
C(19A)	61(3)	44(2)	35(2)	-10(2)	-3(2)	5(2)
C(16A)	61(3)	44(2)	35(2)	-10(2)	-3(2)	5(2)
C(13A)	61(3)	44(2)	35(2)	-10(2)	-3(2)	5(2)
C(14B)	29(8)	33(8)	19(7)	-13(6)	-7(6)	-8(6)
C(33A)	28(3)	28(3)	15(2)	-3(2)	4(2)	1(2)
C(31B)	78(5)	28(3)	25(3)	-4(2)	-9(3)	7(3)
C(36A)	28(3)	28(3)	15(2)	-3(2)	4(2)	1(2)
C(33B)	78(5)	28(3)	25(3)	-4(2)	-9(3)	7(3)
C(22A)	93(5)	29(3)	23(3)	-2(2)	9(3)	-12(3)
C(35B)	78(5)	28(3)	25(3)	-4(2)	-9(3)	7(3)
C(34B)	78(5)	28(3)	25(3)	-4(2)	-9(3)	7(3)
C(32C)	78(5)	28(3)	25(3)	-4(2)	-9(3)	7(3)
C(23A)	93(5)	29(3)	23(3)	-2(2)	9(3)	-12(3)
C(42B)	47(3)	30(3)	22(3)	-10(2)	-1(2)	-5(2)
C(26A)	93(5)	29(3)	23(3)	-2(2)	9(3)	-12(3)
O(5)	54(4)	44(3)	30(3)	-5(2)	2(2)	5(3)
C(36B)	78(5)	28(3)	25(3)	-4(2)	-9(3)	7(3)
C(53)	61(3)	44(2)	35(2)	-10(2)	-3(2)	5(2)
I(5B)	92(2)	41(1)	24(1)	-2(1)	-2(1)	35(1)
C(23B)	29(8)	32(8)	11(6)	4(6)	-6(6)	1(6)
N(6)	31(2)	34(2)	26(2)	-7(2)	-2(2)	1(2)
C(63)	61(3)	44(2)	35(2)	-10(2)	-3(2)	5(2)
C(62)	61(3)	44(2)	35(2)	-10(2)	-3(2)	5(2)
O(6)	54(4)	44(3)	30(3)	-5(2)	2(2)	5(3)

C(61)	61(3)	44(2)	35(2)	-10(2)	-3(2)	5(2)
C(51)	61(3)	44(2)	35(2)	-10(2)	-3(2)	5(2)
I(3A)	103(5)	35(2)	35(2)	6(1)	-13(2)	-37(2)
I(5C)	144(9)	56(3)	44(3)	8(2)	21(3)	52(4)

Table A.6.4: Bond lengths (Å) for [Hf(dilOx)$_4$]·DMF.

Atoms	*Bond Length (Å)*	*Atoms*	*Bond Length (Å)*
HfA-O(2A)	2.088(11)	**C(35A)-C(36A)**	1.36(2)
HfA-O(3A)	2.089(13)	**C(35A)-C(34A)**	1.43(2)
HfA-O(4A)	2.103(12)	**C(16B)-C(15B)**	1.35(2)
HfA-O(1A)	2.112(13)	**C(16B)-C(17B)**	1.42(2)
HfA-N(1A)	2.370(14)	**C(16B)-H(016)**	0.95
HfA-N(3A)	2.401(14)	**C(37A)-C(38A)**	1.35(2)
HfA-N(2A)	2.407(13)	**C(37A)-C(36A)**	1.38(2)
HfA-N(4A)	2.408(14)	**C(15B)-C(14B)**	1.43(2)
HfB-O(3B)	2.084(11)	**C(25B)-C(26B)**	1.36(2)
HfB-O(1B)	2.099(9)	**C(25B)-C(24B)**	1.41(2)
HfB-O(4B)	2.109(10)	**N(3B)-C(31B)**	1.30(2)
HfB-O(2B)	2.110(10)	**N(3B)-C(39B)**	1.36(2)
HfB-N(4B)	2.382(14)	**C(48A)-O(4A)**	1.311(19)
HfB-N(2B)	2.389(14)	**C(48A)-C(47A)**	1.37(2)
HfB-N(1B)	2.403(14)	**C(48A)-C(49A)**	1.44(2)
HfB-N(3B)	2.412(14)	**C(42A)-H(22)**	0.95
I(4B)-C(27B)	2.101(13)	**C(17B)-C(18B)**	1.38(2)
I(6A)-C(37A)	2.111(14)	**C(28B)-C(29B)**	1.443(19)
I(7A)-C(45A)	2.106(15)	**C(34A)-C(33A)**	1.41(2)
I(1B)-C(15B)	2.110(15)	**C(34A)-C(39A)**	1.42(2)
I(06)-C(37B)	2.083(18)	**C(24B)-C(29B)**	1.41(2)
I(8A)-C(47A)	2.098(15)	**C(24B)-C(23B)**	1.44(2)
I(4A)-C(27A)	2.076(18)	**C(32A)-C(33A)**	1.35(2)
I(2B)-C(17B)	2.073(13)	**C(32A)-H(32)**	0.95
I(8B)-C(47B)	2.093(16)	**C(11A)-C(12A)**	1.38(3)
I(2A)-C(17A)	2.09(2)	**C(11A)-H(11)**	0.95
I(5A)-C(35A)	2.111(15)	**C(46B)-C(45B)**	1.40(2)
I(3B)-C(25B)	2.119(16)	**C(46B)-H(026)**	0.95
I(7B)-C(45B)	2.109(16)	**C(39A)-C(38A)**	1.45(2)

I(1A)-C(15A)	2.09(2)	**C(39B)-C(34B)**	1.42(3)
I(3)-C(25A)	2.194(19)	**C(39B)-C(38B)**	1.46(2)
O(1A)-C(18A)	1.30(2)	**C(38B)-C(37B)**	1.36(3)
O(4B)-C(48B)	1.300(19)	**C(29A)-N(2A)**	1.35(3)
O(1B)-C(18B)	1.314(19)	**C(29A)-C(24A)**	1.45(2)
O(3A)-C(38A)	1.34(2)	**C(37B)-C(36B)**	1.41(3)
O(3B)-C(38B)	1.32(2)	**N(5)-C(51)**	1.28(2)
N(4A)-C(41A)	1.321(19)	**N(5)-C(53)**	1.48(2)
N(4A)-C(49A)	1.368(19)	**N(5)-C(52)**	1.48(2)
N(1B)-C(11B)	1.33(2)	**C(15A)-C(16A)**	1.39(3)
N(1B)-C(19B)	1.374(19)	**C(25A)-C(26A)**	1.35(2)
N(4B)-C(41B)	1.33(2)	**C(25A)-C(24A)**	1.42(3)
N(4B)-C(49B)	1.37(2)	**C(25A)-I(3A)**	2.160(18)
O(2B)-C(28B)	1.311(17)	**C(27A)-C(26A)**	1.41(2)
N(1A)-C(19A)	1.35(2)	**C(43B)-C(42B)**	1.37(2)
N(1A)-C(11A)	1.36(2)	**C(43B)-H(023)**	0.95
N(2B)-C(21B)	1.315(19)	**C(12A)-C(13A)**	1.40(3)
N(2B)-C(29B)	1.351(19)	**C(12A)-H(12)**	0.95
C(41A)-C(42A)	1.40(2)	**C(21A)-N(2A)**	1.33(2)
C(41A)-H(21)	0.95	**C(21A)-C(22A)**	1.42(2)
N(3A)-C(31A)	1.320(19)	**C(21A)-H(41)**	0.95
N(3A)-C(39A)	1.37(2)	**C(24A)-C(23A)**	1.41(3)
C(27B)-C(28B)	1.362(19)	**C(52)-H(52A)**	0.98
C(27B)-C(26B)	1.41(2)	**C(52)-H(52B)**	0.98
C(11B)-C(12B)	1.40(2)	**C(52)-H(52C)**	0.98
C(11B)-H(011)	0.95	**C(26B)-H(046)**	0.95
C(19B)-C(14B)	1.38(2)	**C(16A)-H(16)**	0.95
C(19B)-C(18B)	1.44(2)	**C(13A)-H(13)**	0.95
C(13B)-C(12B)	1.40(2)	**C(33A)-H(33)**	0.95
C(13B)-C(14B)	1.42(2)	**C(31B)-C(32C)**	1.41(2)
C(13B)-H(013)	0.95	**C(31B)-H(031)**	0.95
C(44B)-C(43B)	1.41(2)	**C(36A)-H(36)**	0.95
C(44B)-C(49B)	1.44(2)	**C(33B)-C(32C)**	1.36(3)
C(44B)-C(45B)	1.44(2)	**C(33B)-C(34B)**	1.41(2)
C(47B)-C(46B)	1.37(2)	**C(33B)-H(033)**	0.95
C(47B)-C(48B)	1.37(2)	**C(22A)-C(23A)**	1.36(3)
C(31A)-C(32A)	1.38(2)	**C(22A)-H(42)**	0.95
C(31A)-H(31)	0.95	**C(35B)-C(36B)**	1.35(2)
C(46A)-C(45A)	1.36(2)	**C(35B)-C(34B)**	1.46(3)

C(46A)-C(47A)	1.42(2)	**C(35B)-I(5B)**	2.135(19)
C(46A)-H(26)	0.95	**C(35B)-I(5C)**	2.158(19)
C(44A)-C(49A)	1.39(2)	**C(32C)-H(032)**	0.95
C(44A)-C(43A)	1.41(2)	**C(23A)-H(43)**	0.95
C(44A)-C(45A)	1.42(2)	**C(42B)-H(022)**	0.95
C(17A)-C(16A)	1.38(3)	**C(26A)-H(46)**	0.95
C(17A)-C(18A)	1.39(3)	**O(5)-C(51)**	1.24(2)
C(48B)-C(49B)	1.42(2)	**C(36B)-H(036)**	0.95
C(12B)-H(012)	0.95	**C(53)-H(53A)**	0.98
C(22B)-C(23B)	1.34(2)	**C(53)-H(53B)**	0.98
C(22B)-C(21B)	1.40(2)	**C(53)-H(53C)**	0.98
C(22B)-H(042)	0.95	**C(23B)-H(043)**	0.95
C(18A)-C(19A)	1.40(3)	**N(6)-C(61)**	1.33(2)
C(21B)-H(041)	0.95	**N(6)-C(63)**	1.44(2)
C(14A)-C(13A)	1.40(3)	**N(6)-C(62)**	1.50(2)
C(14A)-C(19A)	1.42(3)	**C(63)-H(63A)**	0.98
C(14A)-C(15A)	1.45(3)	**C(63)-H(63B)**	0.98
C(28A)-O(2A)	1.30(2)	**C(63)-H(63C)**	0.98
C(28A)-C(27A)	1.39(3)	**C(62)-H(62A)**	0.98
C(28A)-C(29A)	1.43(3)	**C(62)-H(62B)**	0.98
C(41B)-C(42B)	1.37(2)	**C(62)-H(62C)**	0.98
C(41B)-H(021)	0.95	**O(6)-C(61)**	1.23(2)
C(43A)-C(42A)	1.37(2)	**C(61)-H(61)**	0.95
C(43A)-H(23)	0.95	**C(51)-H(51)**	0.95

Table A.6.5: Bond angles (°) for [Hf(dilOx)$_4$]·DMF.

Atoms	*Bond angle (°)*	*Atoms*	*Bond angle (°)*
O(2A)-HfA-O(3A)	109.2(5)	**C(27B)-C(28B)-C(29B)**	117.9(13)
O(2A)-HfA-O(4A)	82.7(5)	**C(33A)-C(34A)-C(39A)**	115.0(13)
O(3A)-HfA-O(4A)	144.1(5)	**C(33A)-C(34A)-C(35A)**	129.2(14)
O(2A)-HfA-O(1A)	142.2(5)	**C(39A)-C(34A)-C(35A)**	115.7(13)
O(3A)-HfA-O(1A)	83.4(5)	**C(25B)-C(24B)-C(29B)**	117.7(14)
O(4A)-HfA-O(1A)	108.2(5)	**C(25B)-C(24B)-C(23B)**	126.6(15)
O(2A)-HfA-N(1A)	79.1(5)	**C(29B)-C(24B)-C(23B)**	115.5(13)
O(3A)-HfA-N(1A)	139.6(5)	**C(33A)-C(32A)-C(31A)**	121.4(14)
O(4A)-HfA-N(1A)	74.9(5)	**C(33A)-C(32A)-H(32)**	119.3
O(1A)-HfA-N(1A)	69.7(5)	**C(31A)-C(32A)-H(32)**	119.3
O(2A)-HfA-N(3A)	74.9(4)	**N(2B)-C(29B)-C(24B)**	124.6(13)
O(3A)-HfA-N(3A)	70.9(5)	**N(2B)-C(29B)-C(28B)**	114.5(14)
O(4A)-HfA-N(3A)	80.4(5)	**C(24B)-C(29B)-C(28B)**	121.0(13)
O(1A)-HfA-N(3A)	141.6(5)	**N(1A)-C(11A)-C(12A)**	122.3(19)
N(1A)-HfA-N(3A)	146.0(5)	**N(1A)-C(11A)-H(11)**	118.8
O(2A)-HfA-N(2A)	70.4(4)	**C(12A)-C(11A)-H(11)**	118.8
O(3A)-HfA-N(2A)	74.9(5)	**C(47B)-C(46B)-C(45B)**	121.5(16)
O(4A)-HfA-N(2A)	139.7(5)	**C(47B)-C(46B)-H(026)**	119.3
O(1A)-HfA-N(2A)	79.4(5)	**C(45B)-C(46B)-H(026)**	119.3
N(1A)-HfA-N(2A)	71.0(5)	**N(3A)-C(39A)-C(34A)**	123.9(13)
N(3A)-HfA-N(2A)	118.7(5)	**N(3A)-C(39A)-C(38A)**	114.5(13)
O(2A)-HfA-N(4A)	139.6(4)	**C(34A)-C(39A)-C(38A)**	121.6(13)
O(3A)-HfA-N(4A)	80.6(5)	**C(46A)-C(45A)-C(44A)**	121.2(14)
O(4A)-HfA-N(4A)	70.0(5)	**C(46A)-C(45A)-I(7A)**	117.8(11)
O(1A)-HfA-N(4A)	76.5(5)	**C(44A)-C(45A)-I(7A)**	120.8(11)
N(1A)-HfA-N(4A)	119.3(5)	**N(3B)-C(39B)-C(34B)**	124.7(17)
N(3A)-HfA-N(4A)	71.6(5)	**N(3B)-C(39B)-C(38B)**	114.8(16)
N(2A)-HfA-N(4A)	147.3(5)	**C(34B)-C(39B)-C(38B)**	120.4(18)
O(3B)-HfB-O(1B)	82.4(4)	**O(3A)-C(38A)-C(37A)**	125.9(14)
O(3B)-HfB-O(4B)	142.8(4)	**O(3A)-C(38A)-C(39A)**	116.6(13)
O(1B)-HfB-O(4B)	108.4(4)	**C(37A)-C(38A)-C(39A)**	117.5(14)
O(3B)-HfB-O(2B)	109.5(4)	**O(3B)-C(38B)-C(37B)**	125.3(16)
O(1B)-HfB-O(2B)	143.8(4)	**O(3B)-C(38B)-C(39B)**	116.2(17)
O(4B)-HfB-O(2B)	82.9(4)	**C(37B)-C(38B)-C(39B)**	118.5(17)
O(3B)-HfB-N(4B)	79.1(4)	**C(46B)-C(45B)-C(44B)**	120.3(15)
O(1B)-HfB-N(4B)	74.8(4)	**C(46B)-C(45B)-I(7B)**	118.9(12)

O(4B)-HfB-N(4B)	70.3(4)	**C(44B)-C(45B)-I(7B)**	120.7(11)
O(2B)-HfB-N(4B)	140.0(4)	**N(2A)-C(29A)-C(28A)**	116.0(16)
O(3B)-HfB-N(2B)	75.2(4)	**N(2A)-C(29A)-C(24A)**	122.8(16)
O(1B)-HfB-N(2B)	80.5(4)	**C(28A)-C(29A)-C(24A)**	121.0(19)
O(4B)-HfB-N(2B)	140.6(4)	**C(38B)-C(37B)-C(36B)**	122.1(17)
O(2B)-HfB-N(2B)	70.4(4)	**C(38B)-C(37B)-I(06)**	119.8(13)
N(4B)-HfB-N(2B)	146.3(5)	**C(36B)-C(37B)-I(06)**	118.0(14)
O(3B)-HfB-N(1B)	139.1(4)	**C(51)-N(5)-C(53)**	122.6(16)
O(1B)-HfB-N(1B)	70.2(4)	**C(51)-N(5)-C(52)**	120.4(16)
O(4B)-HfB-N(1B)	76.4(4)	**C(53)-N(5)-C(52)**	116.8(14)
O(2B)-HfB-N(1B)	79.9(4)	**O(1B)-C(18B)-C(17B)**	124.6(13)
N(4B)-HfB-N(1B)	119.7(5)	**O(1B)-C(18B)-C(19B)**	118.0(13)
N(2B)-HfB-N(1B)	70.9(5)	**C(17B)-C(18B)-C(19B)**	117.4(14)
O(3B)-HfB-N(3B)	70.7(4)	**C(16A)-C(15A)-C(14A)**	118.8(19)
O(1B)-HfB-N(3B)	140.1(4)	**C(16A)-C(15A)-I(1A)**	119.2(15)
O(4B)-HfB-N(3B)	79.8(4)	**C(14A)-C(15A)-I(1A)**	122.0(15)
O(2B)-HfB-N(3B)	74.8(4)	**C(48A)-C(47A)-C(46A)**	122.1(14)
N(4B)-HfB-N(3B)	71.7(5)	**C(48A)-C(47A)-I(8A)**	118.4(11)
N(2B)-HfB-N(3B)	118.3(5)	**C(46A)-C(47A)-I(8A)**	119.5(10)
N(1B)-HfB-N(3B)	147.0(4)	**C(26A)-C(25A)-C(24A)**	123.9(18)
C(18A)-O(1A)-HfA	123.4(13)	**C(26A)-C(25A)-I(3A)**	121.8(14)
C(48B)-O(4B)-HfB	123.7(10)	**C(24A)-C(25A)-I(3A)**	108.6(13)
C(18B)-O(1B)-HfB	124.1(9)	**C(26A)-C(25A)-I(3)**	112.8(16)
C(38A)-O(3A)-HfA	123.8(10)	**C(24A)-C(25A)-I(3)**	122.8(12)
C(38B)-O(3B)-HfB	124.8(11)	**C(28A)-C(27A)-C(26A)**	121.1(17)
C(41A)-N(4A)-C(49A)	117.9(14)	**C(28A)-C(27A)-I(4A)**	118.9(13)
C(41A)-N(4A)-HfA	128.1(10)	**C(26A)-C(27A)-I(4A)**	120.0(15)
C(49A)-N(4A)-HfA	113.8(10)	**C(42B)-C(43B)-C(44B)**	119.6(15)
C(11B)-N(1B)-C(19B)	118.0(14)	**C(42B)-C(43B)-H(023)**	120.2
C(11B)-N(1B)-HfB	128.4(11)	**C(44B)-C(43B)-H(023)**	120.2
C(19B)-N(1B)-HfB	113.6(10)	**C(11A)-C(12A)-C(13A)**	119.0(19)
C(41B)-N(4B)-C(49B)	117.9(14)	**C(11A)-C(12A)-H(12)**	120.5
C(41B)-N(4B)-HfB	129.4(11)	**C(13A)-C(12A)-H(12)**	120.5
C(49B)-N(4B)-HfB	112.7(10)	**N(2A)-C(21A)-C(22A)**	120.2(19)
C(28B)-O(2B)-HfB	123.3(8)	**N(2A)-C(21A)-H(41)**	119.9
C(19A)-N(1A)-C(11A)	118.9(16)	**C(22A)-C(21A)-H(41)**	119.9
C(19A)-N(1A)-HfA	113.4(12)	**C(23A)-C(24A)-C(25A)**	129.8(17)
C(11A)-N(1A)-HfA	127.6(12)	**C(23A)-C(24A)-C(29A)**	114.7(19)
C(21B)-N(2B)-C(29B)	117.5(14)	**C(25A)-C(24A)-C(29A)**	115.5(16)

C(21B)-N(2B)-HfB	129.2(11)	**N(5)-C(52)-H(52A)**	109.5
C(29B)-N(2B)-HfB	113.3(10)	**N(5)-C(52)-H(52B)**	109.5
N(4A)-C(41A)-C(42A)	121.8(14)	**H(52A)-C(52)-H(52B)**	109.5
N(4A)-C(41A)-H(21)	119.1	**N(5)-C(52)-H(52C)**	109.5
C(42A)-C(41A)-H(21)	119.1	**H(52A)-C(52)-H(52C)**	109.5
C(31A)-N(3A)-C(39A)	117.2(14)	**H(52B)-C(52)-H(52C)**	109.5
C(31A)-N(3A)-HfA	129.9(11)	**C(28A)-O(2A)-HfA**	124.7(12)
C(39A)-N(3A)-HfA	112.6(10)	**C(48A)-O(4A)-HfA**	123.9(10)
C(28B)-C(27B)-C(26B)	121.8(13)	**C(21A)-N(2A)-C(29A)**	120.5(15)
C(28B)-C(27B)-I(4B)	117.9(11)	**C(21A)-N(2A)-HfA**	127.9(13)
C(26B)-C(27B)-I(4B)	120.4(10)	**C(29A)-N(2A)-HfA**	111.6(10)
N(1B)-C(11B)-C(12B)	122.4(14)	**N(4A)-C(49A)-C(44A)**	124.3(14)
N(1B)-C(11B)-H(011)	118.8	**N(4A)-C(49A)-C(48A)**	112.8(13)
C(12B)-C(11B)-H(011)	118.8	**C(44A)-C(49A)-C(48A)**	122.9(13)
N(1B)-C(19B)-C(14B)	124.3(13)	**C(25B)-C(26B)-C(27B)**	119.7(13)
N(1B)-C(19B)-C(18B)	113.1(13)	**C(25B)-C(26B)-H(046)**	120.1
C(14B)-C(19B)-C(18B)	122.5(13)	**C(27B)-C(26B)-H(046)**	120.1
C(12B)-C(13B)-C(14B)	118.8(14)	**N(1A)-C(19A)-C(18A)**	115.1(18)
C(12B)-C(13B)-H(013)	120.6	**N(1A)-C(19A)-C(14A)**	122.3(18)
C(14B)-C(13B)-H(013)	120.6	**C(18A)-C(19A)-C(14A)**	122.6(19)
C(43B)-C(44B)-C(49B)	117.0(15)	**C(17A)-C(16A)-C(15A)**	123(2)
C(43B)-C(44B)-C(45B)	127.9(15)	**C(17A)-C(16A)-H(16)**	118.7
C(49B)-C(44B)-C(45B)	115.1(14)	**C(15A)-C(16A)-H(16)**	118.7
C(46B)-C(47B)-C(48B)	122.1(15)	**C(12A)-C(13A)-C(14A)**	120.1(19)
C(46B)-C(47B)-I(8B)	119.7(12)	**C(12A)-C(13A)-H(13)**	119.9
C(48B)-C(47B)-I(8B)	118.1(12)	**C(14A)-C(13A)-H(13)**	119.9
N(3A)-C(31A)-C(32A)	122.5(14)	**C(19B)-C(14B)-C(13B)**	116.8(13)
N(3A)-C(31A)-H(31)	118.8	**C(19B)-C(14B)-C(15B)**	117.4(13)
C(32A)-C(31A)-H(31)	118.8	**C(13B)-C(14B)-C(15B)**	125.8(15)
C(45A)-C(46A)-C(47A)	119.8(13)	**C(32A)-C(33A)-C(34A)**	119.8(14)
C(45A)-C(46A)-H(26)	120.1	**C(32A)-C(33A)-H(33)**	120.1
C(47A)-C(46A)-H(26)	120.1	**C(34A)-C(33A)-H(33)**	120.1
C(49A)-C(44A)-C(43A)	116.2(13)	**N(3B)-C(31B)-C(32C)**	119.8(19)
C(49A)-C(44A)-C(45A)	117.3(13)	**N(3B)-C(31B)-H(031)**	120.1
C(43A)-C(44A)-C(45A)	126.5(14)	**C(32C)-C(31B)-H(031)**	120.1
C(16A)-C(17A)-C(18A)	120.5(19)	**C(35A)-C(36A)-C(37A)**	120.3(14)
C(16A)-C(17A)-I(2A)	121.0(15)	**C(35A)-C(36A)-H(36)**	119.8
C(18A)-C(17A)-I(2A)	118.5(15)	**C(37A)-C(36A)-H(36)**	119.8
O(4B)-C(48B)-C(47B)	125.3(15)	**C(32C)-C(33B)-C(34B)**	120.2(17)

O(4B)-C(48B)-C(49B)	117.5(15)	**C(32C)-C(33B)-H(033)**	119.9
C(47B)-C(48B)-C(49B)	117.3(15)	**C(34B)-C(33B)-H(033)**	119.9
C(11B)-C(12B)-C(13B)	119.6(15)	**C(23A)-C(22A)-C(21A)**	120.0(18)
C(11B)-C(12B)-H(012)	120.2	**C(23A)-C(22A)-H(42)**	120
C(13B)-C(12B)-H(012)	120.2	**C(21A)-C(22A)-H(42)**	120
C(23B)-C(22B)-C(21B)	121.9(14)	**C(36B)-C(35B)-C(34B)**	121.3(17)
C(23B)-C(22B)-H(042)	119.1	**C(36B)-C(35B)-I(5B)**	117.1(15)
C(21B)-C(22B)-H(042)	119.1	**C(34B)-C(35B)-I(5B)**	121.6(12)
O(1A)-C(18A)-C(17A)	124.1(19)	**C(36B)-C(35B)-I(5C)**	124.0(14)
O(1A)-C(18A)-C(19A)	117.3(18)	**C(34B)-C(35B)-I(5C)**	104.4(13)
C(17A)-C(18A)-C(19A)	118.6(19)	**C(33B)-C(34B)-C(39B)**	114.3(18)
N(2B)-C(21B)-C(22B)	122.0(15)	**C(33B)-C(34B)-C(35B)**	128.8(17)
N(2B)-C(21B)-H(041)	119	**C(39B)-C(34B)-C(35B)**	116.9(16)
C(22B)-C(21B)-H(041)	119	**C(33B)-C(32C)-C(31B)**	121.4(18)
C(13A)-C(14A)-C(19A)	117.2(19)	**C(33B)-C(32C)-H(032)**	119.3
C(13A)-C(14A)-C(15A)	125.8(19)	**C(31B)-C(32C)-H(032)**	119.3
C(19A)-C(14A)-C(15A)	117.0(18)	**C(22A)-C(23A)-C(24A)**	121.8(17)
O(2A)-C(28A)-C(27A)	125.5(16)	**C(22A)-C(23A)-H(43)**	119.1
O(2A)-C(28A)-C(29A)	116.2(18)	**C(24A)-C(23A)-H(43)**	119.1
C(27A)-C(28A)-C(29A)	118.3(17)	**C(41B)-C(42B)-C(43B)**	119.6(15)
N(4B)-C(41B)-C(42B)	124.2(16)	**C(41B)-C(42B)-H(022)**	120.2
N(4B)-C(41B)-H(021)	117.9	**C(43B)-C(42B)-H(022)**	120.2
C(42B)-C(41B)-H(021)	117.9	**C(25A)-C(26A)-C(27A)**	120(2)
C(42A)-C(43A)-C(44A)	119.3(14)	**C(25A)-C(26A)-H(46)**	120
C(42A)-C(43A)-H(23)	120.3	**C(27A)-C(26A)-H(46)**	120
C(44A)-C(43A)-H(23)	120.3	**C(35B)-C(36B)-C(37B)**	120.3(19)
C(36A)-C(35A)-C(34A)	122.0(14)	**C(35B)-C(36B)-H(036)**	119.9
C(36A)-C(35A)-I(5A)	119.5(11)	**C(37B)-C(36B)-H(036)**	119.9
C(34A)-C(35A)-I(5A)	118.4(10)	**N(5)-C(53)-H(53A)**	109.5
C(15B)-C(16B)-C(17B)	120.9(14)	**N(5)-C(53)-H(53B)**	109.5
C(15B)-C(16B)-H(016)	119.5	**H(53A)-C(53)-H(53B)**	109.5
C(17B)-C(16B)-H(016)	119.5	**N(5)-C(53)-H(53C)**	109.5
C(38A)-C(37A)-C(36A)	122.7(14)	**H(53A)-C(53)-H(53C)**	109.5
C(38A)-C(37A)-I(6A)	117.3(11)	**H(53B)-C(53)-H(53C)**	109.5
C(36A)-C(37A)-I(6A)	120.0(10)	**C(22B)-C(23B)-C(24B)**	118.2(14)
C(16B)-C(15B)-C(14B)	121.0(14)	**C(22B)-C(23B)-H(043)**	120.9
C(16B)-C(15B)-I(1B)	118.3(11)	**C(24B)-C(23B)-H(043)**	120.9
C(14B)-C(15B)-I(1B)	120.7(11)	**C(61)-N(6)-C(63)**	122.1(16)
N(4B)-C(49B)-C(48B)	114.9(14)	**C(61)-N(6)-C(62)**	120.0(16)

N(4B)-C(49B)-C(44B)	121.5(14)	**C(63)-N(6)-C(62)**	117.4(14)
C(48B)-C(49B)-C(44B)	123.6(15)	**N(6)-C(63)-H(63A)**	109.5
C(26B)-C(25B)-C(24B)	121.8(15)	**N(6)-C(63)-H(63B)**	109.5
C(26B)-C(25B)-I(3B)	117.4(12)	**H(63A)-C(63)-H(63B)**	109.5
C(24B)-C(25B)-I(3B)	120.7(12)	**N(6)-C(63)-H(63C)**	109.5
C(31B)-N(3B)-C(39B)	119.6(15)	**H(63A)-C(63)-H(63C)**	109.5
C(31B)-N(3B)-HfB	127.8(12)	**H(63B)-C(63)-H(63C)**	109.5
C(39B)-N(3B)-HfB	112.6(10)	**N(6)-C(62)-H(62A)**	109.5
O(4A)-C(48A)-C(47A)	125.0(14)	**N(6)-C(62)-H(62B)**	109.5
O(4A)-C(48A)-C(49A)	118.5(13)	**H(62A)-C(62)-H(62B)**	109.5
C(47A)-C(48A)-C(49A)	116.4(14)	**N(6)-C(62)-H(62C)**	109.5
C(43A)-C(42A)-C(41A)	120.4(14)	**H(62A)-C(62)-H(62C)**	109.5
C(43A)-C(42A)-H(22)	119.8	**H(62B)-C(62)-H(62C)**	109.5
C(41A)-C(42A)-H(22)	119.8	**O(6)-C(61)-N(6)**	121.3(19)
C(18B)-C(17B)-C(16B)	120.5(13)	**O(6)-C(61)-H(61)**	119.3
C(18B)-C(17B)-I(2B)	119.0(11)	**N(6)-C(61)-H(61)**	119.3
C(16B)-C(17B)-I(2B)	120.4(10)	**O(5)-C(51)-N(5)**	123.4(19)
O(2B)-C(28B)-C(27B)	124.8(13)	**O(5)-C(51)-H(51)**	118.3
O(2B)-C(28B)-C(29B)	117.3(12)	**N(5)-C(51)-H(51)**	118.3

Appendix B.1

Supplementary Crystallographic Data

B.1. [Hf(dbm)$_4$] – (Hf_2c) – § 6.4

Table B.1.1: Atomic coordinates (x 10^4) and equivalent isotropic displacement parameters (Å^2 x 10^3) for [Hf(dbm)$_4$].

Atom	*x*	*y*	*z*	$U_{(eq)}$
C(1)	2471(2)	4566(4)	824(2)	16(1)
C(1A)	3045(2)	4590(4)	913(2)	21(1)
C(2)	3380(2)	5007(3)	1542(2)	20(1)
C(2A)	2082(2)	8200(4)	2921(2)	19(1)
C(3)	1718(2)	7475(3)	2424(2)	16(1)
C(3A)	2857(2)	5107(4)	4365(2)	21(1)
C(4)	2632(2)	7829(4)	3128(2)	14(1)
C(4A)	1923(2)	1980(4)	1584(2)	23(1)
C(5)	2304(2)	5291(4)	4056(2)	20(1)
C(6)	3222(2)	4545(4)	3986(2)	20(1)
C(7)	2490(2)	2030(4)	1849(2)	20(1)
C(8)	1565(2)	2868(4)	1806(2)	21(1)
C(11)	2111(2)	4190(4)	131(2)	19(1)
C(12)	1560(2)	4562(4)	-13(2)	24(1)
C(13)	1218(2)	4252(4)	-650(2)	30(1)
C(14)	1427(2)	3532(4)	-1150(2)	27(1)
C(15)	1967(2)	3128(4)	-1011(2)	28(1)
C(16)	2312(2)	3456(4)	-375(2)	24(1)
C(21)	3982(2)	5154(4)	1617(2)	20(1)
C(22)	4274(2)	4504(5)	1174(2)	30(1)
C(23)	4837(2)	4676(5)	1259(2)	39(1)
C(24)	5115(2)	5506(6)	1772(2)	40(1)
C(25)	4827(2)	6137(5)	2215(2)	33(1)
C(26)	4267(2)	5953(4)	2148(2)	26(1)

C(31)	1139(2)	7921(4)	2151(2)	17(1)
C(32)	744(2)	6976(4)	1882(2)	24(1)
C(33)	207(2)	7337(4)	1600(2)	30(1)
C(34)	59(2)	8638(5)	1573(2)	29(1)
C(35)	445(2)	9597(4)	1835(2)	26(1)
C(36)	982(2)	9229(4)	2132(2)	21(1)
C(41)	3041(2)	8754(4)	3539(2)	17(1)
C(42)	2989(2)	10095(4)	3414(2)	20(1)
C(43)	3388(2)	10947(4)	3756(2)	24(1)
C(44)	3825(2)	10485(4)	4251(2)	23(1)
C(45)	3870(2)	9157(4)	4397(2)	24(1)
C(46)	3486(2)	8288(4)	4026(2)	21(1)
C(51)	1908(2)	5727(4)	4499(2)	21(1)
C(52)	1397(2)	5118(4)	4416(2)	24(1)
C(53)	1039(2)	5455(4)	4850(2)	28(1)
C(54)	1181(2)	6423(4)	5350(2)	28(1)
C(55)	1676(2)	7061(4)	5423(2)	29(1)
C(56)	2045(2)	6720(4)	5000(2)	26(1)
C(61)	3797(2)	4165(4)	4335(2)	22(1)
C(62)	3950(2)	3968(4)	5053(2)	31(1)
C(63)	4487(2)	3583(4)	5339(2)	35(1)
C(64)	4870(2)	3402(4)	4925(2)	35(1)
C(65)	4710(2)	3596(4)	4190(3)	34(1)
C(66)	4171(2)	3980(4)	3904(2)	25(1)
C(71)	2861(2)	940(4)	1717(2)	22(1)
C(72)	3418(2)	1171(4)	1818(2)	27(1)
C(73)	3775(2)	184(5)	1735(2)	33(1)
C(74)	3580(2)	-1065(5)	1563(2)	34(1)
C(75)	3029(2)	-1320(4)	1475(2)	31(1)
C(76)	2665(2)	-328(4)	1544(2)	29(1)
C(81)	962(2)	2845(4)	1502(2)	20(1)
C(82)	757(2)	2409(4)	814(2)	26(1)
C(83)	202(2)	2449(4)	537(2)	29(1)
C(84)	-154(2)	2907(4)	934(2)	27(1)
C(85)	36(2)	3330(4)	1619(2)	27(1)
C(86)	594(2)	3319(4)	1901(2)	24(1)
O(1)	2217(1)	4883(2)	1313(1)	16(1)
O(3)	1845(1)	6395(2)	2160(1)	14(1)
O(4)	2824(1)	6747(2)	2972(1)	15(1)
O(5)	2099(1)	5050(2)	3410(1)	18(1)
O(6)	3093(1)	4271(3)	3330(1)	18(1)
O(7)	2728(1)	2980(2)	2224(1)	16(1)

O(8)	1725(1)	3757(3)	2278(1)	18(1)
O(2)	3195(1)	5335(3)	2090(1)	17(1)
Hf	2459(1)	4934(1)	2471(1)	14(1)

Table B.1.2: Hydrogen coordinates (x 10^4) and isotropic displacement parameters (Å^2 x 10^3) for [Hf(dbm)$_4$].

Atom	*x*	*y*	*z*	$U_{(eq)}$
H(1A)	3209	4314	534	25
H(2A)	1954	8959	3121	22
H(3A)	2987	5368	4841	25
H(4A)	1779	1330	1246	27
H(12)	1417	5037	333	29
H(13)	845	4526	-746	36
H(14)	1195	3318	-1589	32
H(15)	2104	2625	-1351	34
H(16)	2685	3182	-283	29
H(22)	4086	3942	813	36
H(23)	5034	4218	961	46
H(24)	5499	5642	1819	47
H(25)	5017	6706	2572	39
H(26)	4077	6374	2467	31
H(32)	845	6079	1893	29
H(33)	-59	6687	1425	35
H(34)	-308	8883	1373	35
H(35)	343	10494	1812	31
H(36)	1244	9878	2323	25
H(42)	2678	10425	3093	24
H(43)	3361	11854	3649	29
H(44)	4095	11074	4492	27
H(45)	4163	8840	4750	29
H(46)	3530	7374	4108	25
H(52)	1295	4470	4062	29
H(53)	696	5020	4803	33
H(54)	933	6651	5646	33
H(55)	1766	7737	5764	34
H(56)	2388	7158	5052	31
H(62)	3693	4094	5349	37

H(63)	4590	3441	5834	41
H(64)	5236	3151	5130	41
H(65)	4967	3467	3891	40
H(66)	4062	4115	3409	30
H(72)	3556	2022	1946	32
H(73)	4157	360	1796	39
H(74)	3828	-1747	1507	40
H(75)	2896	-2182	1365	38
H(76)	2283	-506	1475	34
H(82)	1003	2083	536	31
H(83)	66	2158	67	35
H(84)	-536	2934	738	33
H(85)	-215	3628	1895	32
H(86)	727	3634	2367	29

Table B.1.3: Anisotropic displacement parameters ($Å^2$ x 10^3) for $[Hf(dbm)_4]$.

Atom	U^{11}	U^{22}	U^{33}	U^{23}	U^{13}	U^{12}
C(1)	21(2)	10(2)	17(2)	2(2)	4(2)	2(2)
C(1A)	18(2)	25(2)	19(2)	-2(2)	4(2)	0(2)
C(2)	18(2)	16(2)	24(2)	2(2)	4(2)	3(2)
C(2A)	17(2)	15(2)	24(2)	-5(2)	2(2)	1(2)
C(3)	18(2)	12(2)	17(2)	3(1)	5(1)	0(1)
C(3A)	22(2)	22(2)	17(2)	-2(2)	2(2)	-4(2)
C(4)	16(2)	11(2)	16(2)	1(1)	6(1)	-2(1)
C(4A)	21(2)	21(2)	26(2)	-7(2)	4(2)	-5(2)
C(5)	26(2)	12(2)	21(2)	1(2)	6(2)	-4(2)
C(6)	21(2)	16(2)	21(2)	2(2)	-1(2)	-5(2)
C(7)	25(2)	15(2)	20(2)	3(2)	6(2)	-4(2)
C(8)	24(2)	18(2)	23(2)	0(2)	7(2)	-6(2)
C(11)	22(2)	14(2)	20(2)	2(2)	3(2)	-3(2)
C(12)	25(2)	23(2)	24(2)	-7(2)	4(2)	-1(2)
C(13)	25(2)	26(2)	35(2)	0(2)	-6(2)	1(2)
C(14)	38(3)	22(2)	17(2)	-2(2)	-1(2)	-10(2)
C(15)	39(3)	25(2)	22(2)	-5(2)	10(2)	-8(2)
C(16)	26(2)	23(2)	25(2)	-2(2)	5(2)	-1(2)
C(21)	16(2)	22(2)	22(2)	1(2)	4(2)	0(2)
C(22)	21(2)	43(3)	25(2)	-7(2)	4(2)	3(2)
C(23)	20(2)	67(3)	31(2)	-12(2)	12(2)	6(2)
C(24)	14(2)	73(4)	32(2)	-3(2)	4(2)	-6(2)

C(25)	25(2)	45(3)	27(2)	-6(2)	3(2)	-8(2)
C(26)	21(2)	32(2)	24(2)	-1(2)	3(2)	0(2)
C(31)	16(2)	22(2)	14(2)	3(2)	4(1)	2(2)
C(32)	22(2)	25(2)	25(2)	0(2)	1(2)	-2(2)
C(33)	21(2)	33(3)	31(2)	-2(2)	-3(2)	-6(2)
C(34)	15(2)	43(3)	28(2)	12(2)	2(2)	6(2)
C(35)	26(2)	24(2)	30(2)	9(2)	9(2)	7(2)
C(36)	18(2)	22(2)	23(2)	4(2)	6(2)	-1(2)
C(41)	13(2)	19(2)	19(2)	-4(2)	6(1)	-4(2)
C(42)	20(2)	17(2)	21(2)	1(2)	2(2)	-1(2)
C(43)	27(2)	14(2)	32(2)	-4(2)	7(2)	-4(2)
C(44)	20(2)	20(2)	29(2)	-7(2)	5(2)	-9(2)
C(45)	18(2)	24(2)	29(2)	-1(2)	0(2)	-1(2)
C(46)	22(2)	11(2)	30(2)	-1(2)	5(2)	-3(2)
C(51)	26(2)	21(2)	17(2)	1(2)	4(2)	1(2)
C(52)	26(2)	19(2)	25(2)	-3(2)	-1(2)	1(2)
C(53)	23(2)	27(2)	33(2)	6(2)	6(2)	1(2)
C(54)	30(2)	37(3)	17(2)	4(2)	5(2)	13(2)
C(55)	37(3)	27(2)	19(2)	-6(2)	-3(2)	10(2)
C(56)	25(2)	29(2)	23(2)	1(2)	3(2)	-3(2)
C(61)	23(2)	14(2)	26(2)	-4(2)	1(2)	-5(2)
C(62)	33(3)	24(2)	32(2)	-1(2)	-3(2)	-1(2)
C(63)	32(3)	27(3)	37(2)	1(2)	-10(2)	-5(2)
C(64)	23(2)	18(2)	57(3)	-3(2)	-7(2)	0(2)
C(65)	30(2)	19(2)	53(3)	-5(2)	10(2)	-5(2)
C(66)	20(2)	22(2)	31(2)	-4(2)	2(2)	-3(2)
C(71)	28(2)	20(2)	17(2)	-2(2)	2(2)	2(2)
C(72)	33(2)	24(2)	22(2)	-1(2)	0(2)	0(2)
C(73)	25(2)	37(3)	32(2)	1(2)	-2(2)	3(2)
C(74)	41(3)	28(3)	29(2)	-4(2)	2(2)	15(2)
C(75)	46(3)	17(2)	27(2)	-3(2)	-1(2)	-1(2)
C(76)	30(2)	28(2)	26(2)	-1(2)	4(2)	-1(2)
C(81)	17(2)	16(2)	27(2)	-2(2)	4(2)	-6(2)
C(82)	25(2)	28(2)	25(2)	-7(2)	8(2)	-7(2)
C(83)	29(2)	28(2)	28(2)	-9(2)	-2(2)	-2(2)
C(84)	19(2)	25(2)	33(2)	-5(2)	-5(2)	2(2)
C(85)	26(2)	20(2)	36(2)	-3(2)	12(2)	0(2)
C(86)	28(2)	23(2)	19(2)	-5(2)	1(2)	-4(2)
O(1)	14(1)	16(1)	18(1)	-2(1)	3(1)	2(1)
O(3)	14(1)	13(1)	15(1)	-2(1)	0(1)	1(1)
O(4)	13(1)	14(1)	19(1)	0(1)	1(1)	1(1)
O(5)	19(1)	18(2)	15(1)	-1(1)	0(1)	-3(1)

O(6)	19(1)	16(1)	18(1)	-4(1)	0(1)	2(1)
O(7)	17(1)	14(1)	18(1)	-4(1)	1(1)	-1(1)
O(8)	19(1)	17(1)	17(1)	-6(1)	4(1)	-5(1)
O(2)	15(1)	18(1)	20(1)	-5(1)	4(1)	0(1)
Hf	14(1)	14(1)	14(1)	-2(1)	1(1)	0(1)

Table B.1.4: Bond lengths (Å) for [Hf(dbm)$_4$].

Atoms	*Bond Length (Å)*	*Atoms*	*Bond Length (Å)*
C(1)-O(1)	1.277(4)	**C(41)-C(42)**	1.393(5)
C(1)-C(1A)	1.402(5)	**C(42)-C(43)**	1.383(5)
C(1)-C(11)	1.503(5)	**C(42)-H(42)**	0.95
C(1A)-C(2)	1.396(5)	**C(43)-C(44)**	1.378(6)
C(1A)-H(1A)	0.95	**C(43)-H(43)**	0.95
C(2)-O(2)	1.281(5)	**C(44)-C(45)**	1.386(6)
C(2)-C(21)	1.482(6)	**C(44)-H(44)**	0.95
C(2A)-C(3)	1.393(5)	**C(45)-C(46)**	1.391(5)
C(2A)-C(4)	1.397(5)	**C(45)-H(45)**	0.95
C(2A)-H(2A)	0.95	**C(46)-H(46)**	0.95
C(3)-O(3)	1.282(4)	**C(51)-C(52)**	1.393(6)
C(3)-C(31)	1.501(5)	**C(51)-C(56)**	1.397(5)
C(3A)-C(5)	1.397(6)	**C(52)-C(53)**	1.382(6)
C(3A)-C(6)	1.399(6)	**C(52)-H(52)**	0.95
C(3A)-H(3A)	0.95	**C(53)-C(54)**	1.378(6)
C(4)-O(4)	1.264(4)	**C(53)-H(53)**	0.95
C(4)-C(41)	1.495(5)	**C(54)-C(55)**	1.375(6)
C(4A)-C(7)	1.398(5)	**C(54)-H(54)**	0.95
C(4A)-C(8)	1.399(5)	**C(55)-C(56)**	1.389(6)
C(4A)-H(4A)	0.95	**C(55)-H(55)**	0.95
C(5)-O(5)	1.273(5)	**C(56)-H(56)**	0.95
C(5)-C(51)	1.496(5)	**C(61)-C(62)**	1.376(5)
C(6)-O(6)	1.274(4)	**C(61)-C(66)**	1.379(5)
C(6)-C(61)	1.503(5)	**C(62)-C(63)**	1.393(6)
C(7)-O(7)	1.284(4)	**C(62)-H(62)**	0.95
C(7)-C(71)	1.500(6)	**C(63)-C(64)**	1.375(6)
C(8)-O(8)	1.291(4)	**C(63)-H(63)**	0.95
C(8)-C(81)	1.496(5)	**C(64)-C(65)**	1.408(6)
C(11)-C(12)	1.392(5)	**C(64)-H(64)**	0.95
C(11)-C(16)	1.402(5)	**C(65)-C(66)**	1.398(6)

C(12)-C(13)	1.385(5)	**C(65)-H(65)**	0.95
C(12)-H(12)	0.95	**C(66)-H(66)**	0.95
C(13)-C(14)	1.394(6)	**C(71)-C(72)**	1.378(6)
C(13)-H(13)	0.95	**C(71)-C(76)**	1.401(6)
C(14)-C(15)	1.377(6)	**C(72)-C(73)**	1.375(6)
C(14)-H(14)	0.95	**C(72)-H(72)**	0.95
C(15)-C(16)	1.389(5)	**C(73)-C(74)**	1.382(6)
C(15)-H(15)	0.95	**C(73)-H(73)**	0.95
C(16)-H(16)	0.95	**C(74)-C(75)**	1.370(6)
C(21)-C(26)	1.389(5)	**C(74)-H(74)**	0.95
C(21)-C(22)	1.397(6)	**C(75)-C(76)**	1.382(6)
C(22)-C(23)	1.386(6)	**C(75)-H(75)**	0.95
C(22)-H(22)	0.95	**C(76)-H(76)**	0.95
C(23)-C(24)	1.380(7)	**C(81)-C(86)**	1.395(5)
C(23)-H(23)	0.95	**C(81)-C(82)**	1.397(5)
C(24)-C(25)	1.380(6)	**C(82)-C(83)**	1.375(6)
C(24)-H(24)	0.95	**C(82)-H(82)**	0.95
C(25)-C(26)	1.385(6)	**C(83)-C(84)**	1.365(6)
C(25)-H(25)	0.95	**C(83)-H(83)**	0.95
C(26)-H(26)	0.95	**C(84)-C(85)**	1.381(6)
C(31)-C(36)	1.391(5)	**C(84)-H(84)**	0.95
C(31)-C(32)	1.400(5)	**C(85)-C(86)**	1.384(6)
C(32)-C(33)	1.386(6)	**C(85)-H(85)**	0.95
C(32)-H(32)	0.95	**C(86)-H(86)**	0.95
C(33)-C(34)	1.379(6)	**O(1)-Hf**	2.197(3)
C(33)-H(33)	0.95	**O(3)-Hf**	2.133(2)
C(34)-C(35)	1.393(6)	**O(4)-Hf**	2.200(2)
C(34)-H(34)	0.95	**O(5)-Hf**	2.180(3)
C(35)-C(36)	1.394(5)	**O(6)-Hf**	2.154(2)
C(35)-H(35)	0.95	**O(7)-Hf**	2.189(2)
C(36)-H(36)	0.95	**O(8)-Hf**	2.154(2)
C(41)-C(46)	1.384(5)	**O(2)-Hf**	2.143(3)

Table B.1.5: Bond angles (°) for [Hf(dbm)$_4$].

Atoms	*Bond angle (°)*	*Atoms*	*Bond angle (°)*
O(1)-C(1)-C(1A)	123.1(3)	**C(52)-C(51)-C(56)**	119.5(4)
O(1)-C(1)-C(11)	115.5(3)	**C(52)-C(51)-C(5)**	119.3(4)
C(1A)-C(1)-C(11)	121.5(3)	**C(56)-C(51)-C(5)**	121.1(4)
C(2)-C(1A)-C(1)	121.8(4)	**C(53)-C(52)-C(51)**	120.1(4)
C(2)-C(1A)-H(1A)	119.1	**C(53)-C(52)-H(52)**	119.9
C(1)-C(1A)-H(1A)	119.1	**C(51)-C(52)-H(52)**	119.9
O(2)-C(2)-C(1A)	123.3(4)	**C(54)-C(53)-C(52)**	120.0(4)
O(2)-C(2)-C(21)	114.6(4)	**C(54)-C(53)-H(53)**	120
C(1A)-C(2)-C(21)	122.0(4)	**C(52)-C(53)-H(53)**	120
C(3)-C(2A)-C(4)	121.0(3)	**C(55)-C(54)-C(53)**	120.6(4)
C(3)-C(2A)-H(2A)	119.5	**C(55)-C(54)-H(54)**	119.7
C(4)-C(2A)-H(2A)	119.5	**C(53)-C(54)-H(54)**	119.7
O(3)-C(3)-C(2A)	123.7(3)	**C(54)-C(55)-C(56)**	120.2(4)
O(3)-C(3)-C(31)	114.7(3)	**C(54)-C(55)-H(55)**	119.9
C(2A)-C(3)-C(31)	121.6(3)	**C(56)-C(55)-H(55)**	119.9
C(5)-C(3A)-C(6)	121.2(4)	**C(55)-C(56)-C(51)**	119.5(4)
C(5)-C(3A)-H(3A)	119.4	**C(55)-C(56)-H(56)**	120.2
C(6)-C(3A)-H(3A)	119.4	**C(51)-C(56)-H(56)**	120.2
O(4)-C(4)-C(2A)	124.3(3)	**C(62)-C(61)-C(66)**	120.3(4)
O(4)-C(4)-C(41)	115.6(3)	**C(62)-C(61)-C(6)**	122.3(4)
C(2A)-C(4)-C(41)	120.1(3)	**C(66)-C(61)-C(6)**	117.4(3)
C(7)-C(4A)-C(8)	121.3(4)	**C(61)-C(62)-C(63)**	119.2(4)
C(7)-C(4A)-H(4A)	119.3	**C(61)-C(62)-H(62)**	120.4
C(8)-C(4A)-H(4A)	119.3	**C(63)-C(62)-H(62)**	120.4
O(5)-C(5)-C(3A)	123.9(4)	**C(64)-C(63)-C(62)**	121.8(4)
O(5)-C(5)-C(51)	116.1(4)	**C(64)-C(63)-H(63)**	119.1
C(3A)-C(5)-C(51)	119.9(4)	**C(62)-C(63)-H(63)**	119.1
O(6)-C(6)-C(3A)	123.4(4)	**C(63)-C(64)-C(65)**	118.6(4)
O(6)-C(6)-C(61)	114.5(3)	**C(63)-C(64)-H(64)**	120.7
C(3A)-C(6)-C(61)	122.0(3)	**C(65)-C(64)-H(64)**	120.7
O(7)-C(7)-C(4A)	123.4(4)	**C(66)-C(65)-C(64)**	119.4(4)
O(7)-C(7)-C(71)	115.4(3)	**C(66)-C(65)-H(65)**	120.3
C(4A)-C(7)-C(71)	121.3(4)	**C(64)-C(65)-H(65)**	120.3
O(8)-C(8)-C(4A)	123.3(4)	**C(61)-C(66)-C(65)**	120.6(4)
O(8)-C(8)-C(81)	115.5(3)	**C(61)-C(66)-H(66)**	119.7
C(4A)-C(8)-C(81)	121.2(3)	**C(65)-C(66)-H(66)**	119.7
C(12)-C(11)-C(16)	118.8(3)	**C(72)-C(71)-C(76)**	118.8(4)
C(12)-C(11)-C(1)	119.5(3)	**C(72)-C(71)-C(7)**	118.9(4)
C(16)-C(11)-C(1)	121.7(3)	**C(76)-C(71)-C(7)**	122.1(4)

C(13)-C(12)-C(11)	121.1(4)	**C(73)-C(72)-C(71)**	120.8(4)
C(13)-C(12)-H(12)	119.5	**C(73)-C(72)-H(72)**	119.6
C(11)-C(12)-H(12)	119.5	**C(71)-C(72)-H(72)**	119.6
C(12)-C(13)-C(14)	119.3(4)	**C(72)-C(73)-C(74)**	120.2(5)
C(12)-C(13)-H(13)	120.3	**C(72)-C(73)-H(73)**	119.9
C(14)-C(13)-H(13)	120.3	**C(74)-C(73)-H(73)**	119.9
C(15)-C(14)-C(13)	120.4(4)	**C(75)-C(74)-C(73)**	119.9(4)
C(15)-C(14)-H(14)	119.8	**C(75)-C(74)-H(74)**	120
C(13)-C(14)-H(14)	119.8	**C(73)-C(74)-H(74)**	120
C(14)-C(15)-C(16)	120.3(4)	**C(74)-C(75)-C(76)**	120.3(4)
C(14)-C(15)-H(15)	119.9	**C(74)-C(75)-H(75)**	119.8
C(16)-C(15)-H(15)	119.9	**C(76)-C(75)-H(75)**	119.8
C(15)-C(16)-C(11)	120.1(4)	**C(75)-C(76)-C(71)**	120.0(4)
C(15)-C(16)-H(16)	120	**C(75)-C(76)-H(76)**	120
C(11)-C(16)-H(16)	120	**C(71)-C(76)-H(76)**	120
C(26)-C(21)-C(22)	118.9(4)	**C(86)-C(81)-C(82)**	118.9(4)
C(26)-C(21)-C(2)	119.0(4)	**C(86)-C(81)-C(8)**	119.5(3)
C(22)-C(21)-C(2)	122.1(4)	**C(82)-C(81)-C(8)**	121.5(4)
C(23)-C(22)-C(21)	120.2(4)	**C(83)-C(82)-C(81)**	120.3(4)
C(23)-C(22)-H(22)	119.9	**C(83)-C(82)-H(82)**	119.9
C(21)-C(22)-H(22)	119.9	**C(81)-C(82)-H(82)**	119.9
C(24)-C(23)-C(22)	120.6(4)	**C(84)-C(83)-C(82)**	120.3(4)
C(24)-C(23)-H(23)	119.7	**C(84)-C(83)-H(83)**	119.9
C(22)-C(23)-H(23)	119.7	**C(82)-C(83)-H(83)**	119.9
C(23)-C(24)-C(25)	119.2(4)	**C(83)-C(84)-C(85)**	120.7(4)
C(23)-C(24)-H(24)	120.4	**C(83)-C(84)-H(84)**	119.7
C(25)-C(24)-H(24)	120.4	**C(85)-C(84)-H(84)**	119.7
C(24)-C(25)-C(26)	120.9(4)	**C(84)-C(85)-C(86)**	119.8(4)
C(24)-C(25)-H(25)	119.5	**C(84)-C(85)-H(85)**	120.1
C(26)-C(25)-H(25)	119.5	**C(86)-C(85)-H(85)**	120.1
C(25)-C(26)-C(21)	120.1(4)	**C(85)-C(86)-C(81)**	120.0(4)
C(25)-C(26)-H(26)	119.9	**C(85)-C(86)-H(86)**	120
C(21)-C(26)-H(26)	119.9	**C(81)-C(86)-H(86)**	120
C(36)-C(31)-C(32)	118.9(4)	**C(1)-O(1)-Hf**	133.2(2)
C(36)-C(31)-C(3)	123.0(3)	**C(3)-O(3)-Hf**	135.3(2)
C(32)-C(31)-C(3)	118.1(3)	**C(4)-O(4)-Hf**	134.4(2)
C(33)-C(32)-C(31)	120.6(4)	**C(5)-O(5)-Hf**	132.5(3)
C(33)-C(32)-H(32)	119.7	**C(6)-O(6)-Hf**	134.0(2)
C(31)-C(32)-H(32)	119.7	**C(7)-O(7)-Hf**	133.4(2)
C(34)-C(33)-C(32)	120.0(4)	**C(8)-O(8)-Hf**	130.2(2)
C(34)-C(33)-H(33)	120	**C(2)-O(2)-Hf**	135.0(2)
C(32)-C(33)-H(33)	120	**O(3)-Hf-O(2)**	112.32(10)

C(33)-C(34)-C(35)	120.5(4)	**O(3)-Hf-O(8)**	79.05(10)
C(33)-C(34)-H(34)	119.8	**O(2)-Hf-O(8)**	142.98(9)
C(35)-C(34)-H(34)	119.8	**O(3)-Hf-O(6)**	143.90(9)
C(34)-C(35)-C(36)	119.5(4)	**O(2)-Hf-O(6)**	77.42(10)
C(34)-C(35)-H(35)	120.3	**O(8)-Hf-O(6)**	114.87(10)
C(36)-C(35)-H(35)	120.3	**O(3)-Hf-O(5)**	78.83(9)
C(31)-C(36)-C(35)	120.6(4)	**O(2)-Hf-O(5)**	142.78(10)
C(31)-C(36)-H(36)	119.7	**O(8)-Hf-O(5)**	72.53(9)
C(35)-C(36)-H(36)	119.7	**O(6)-Hf-O(5)**	74.71(10)
C(46)-C(41)-C(42)	119.3(4)	**O(3)-Hf-O(7)**	144.09(9)
C(46)-C(41)-C(4)	120.5(3)	**O(2)-Hf-O(7)**	77.35(10)
C(42)-C(41)-C(4)	120.1(3)	**O(8)-Hf-O(7)**	74.79(9)
C(43)-C(42)-C(41)	120.3(4)	**O(6)-Hf-O(7)**	70.89(9)
C(43)-C(42)-H(42)	119.9	**O(5)-Hf-O(7)**	115.18(9)
C(41)-C(42)-H(42)	119.9	**O(3)-Hf-O(1)**	72.31(9)
C(44)-C(43)-C(42)	120.3(4)	**O(2)-Hf-O(1)**	74.45(10)
C(44)-C(43)-H(43)	119.9	**O(8)-Hf-O(1)**	76.23(9)
C(42)-C(43)-H(43)	119.9	**O(6)-Hf-O(1)**	141.63(9)
C(43)-C(44)-C(45)	119.8(4)	**O(5)-Hf-O(1)**	140.72(10)
C(43)-C(44)-H(44)	120.1	**O(7)-Hf-O(1)**	77.85(9)
C(45)-C(44)-H(44)	120.1	**O(3)-Hf-O(4)**	75.02(9)
C(44)-C(45)-C(46)	120.2(4)	**O(2)-Hf-O(4)**	71.63(9)
C(44)-C(45)-H(45)	119.9	**O(8)-Hf-O(4)**	143.76(9)
C(46)-C(45)-H(45)	119.9	**O(6)-Hf-O(4)**	75.76(9)
C(41)-C(46)-C(45)	120.0(4)	**O(5)-Hf-O(4)**	77.92(9)
C(41)-C(46)-H(46)	120	**O(7)-Hf-O(4)**	138.39(9)
C(45)-C(46)-H(46)	120	**O(1)-Hf-O(4)**	118.10(9)

Appendix B.2

Supplementary Crystallographic Data

B.2. $[Hf(OH)(tfba)_3]_2 \cdot 2DMF$ – (Hf_2b) – § 6.5

Table B.2.1: Atomic coordinates (x 10^4) and equivalent isotropic displacement parameters ($Å^2$ x 10^3) for $[Hf(OH)(tfba)_3]_2 \cdot 2DMF$

Atom	*x*	*y*	*z*	$U_{(eq)}$
C(1)	5471(4)	7683(2)	4852(2)	30(1)
C(2)	5889(4)	6925(2)	5092(2)	23(1)
C(3)	6788(3)	6756(2)	5996(2)	23(1)
C(4)	7430(3)	6123(2)	6218(2)	24(1)
C(5)	8546(3)	5979(2)	7159(2)	26(1)
C(6)	9359(4)	5422(2)	7303(3)	33(1)
C(7)	10431(4)	5277(2)	8163(3)	40(1)
C(8)	10672(5)	5682(3)	8900(3)	49(1)
C(9)	9859(5)	6229(3)	8769(3)	45(1)
C(10)	8804(4)	6388(2)	7898(3)	34(1)
C(11)	3785(4)	4209(2)	1663(3)	33(1)
C(12)	3762(4)	4747(2)	2301(2)	23(1)
C(13)	2820(3)	5237(2)	1939(2)	23(1)
C(14)	2716(3)	5706(2)	2511(2)	17(1)
C(15)	1616(3)	6190(2)	2168(2)	20(1)
C(16)	1676(4)	6694(2)	2765(3)	27(1)
C(17)	676(4)	7157(2)	2477(3)	38(1)
C(18)	-388(4)	7110(2)	1604(3)	45(1)
C(19)	-453(4)	6628(2)	1004(3)	42(1)
C(20)	543(3)	6165(2)	1283(2)	28(1)
C(21)	6419(4)	6077(2)	2317(3)	33(1)
C(22)	6666(4)	5652(2)	3136(2)	24(1)
C(23)	7556(4)	5129(2)	3462(3)	28(1)
C(24)	7798(3)	4717(2)	4211(2)	20(1)

C(25)	8870(3)	4203(2)	4640(2)	21(1)
C(26)	9601(4)	4044(2)	4279(3)	34(1)
C(27)	10581(4)	3563(2)	4707(3)	40(1)
C(28)	10844(4)	3231(2)	5477(3)	37(1)
C(29)	10127(4)	3387(2)	5849(3)	32(1)
C(30)	9153(4)	3868(2)	5430(3)	26(1)
C(31)	6169(4)	3145(2)	4082(3)	26(1)

Table B.2.2: Hydrogen coordinates (x 10^4) and isotropic displacement parameters (Å^2 x 10^3) for $[Hf(OH)(tfba)_3]_2 \cdot 2DMF$.

Atom	*x*	*y*	*z*	$U_{(eq)}$
H(3)	6964	7074	6465	28
H(6)	9175	5136	6803	40
H(7)	10991	4907	8246	48
H(8)	11393	5584	9493	59
H(9)	10019	6498	9275	54
H(10)	8268	6773	7811	41
H(13)	2233	5263	1298	28
H(16)	2406	6717	3370	32
H(17)	723	7505	2880	45
H(18)	-1089	7418	1413	54
H(19)	-1183	6612	398	50
H(20)	496	5829	868	33
H(23)	8018	5040	3182	33
H(26)	9425	4267	3738	40
H(27)	11081	3462	4459	48
H(28)	11510	2894	5758	44
H(29)	10310	3163	6391	38
H(30)	8666	3973	5686	31
H(31)	5680	3489	3635	32
H(32A)	7446	2166	5057	65
H(32B)	8236	2090	4582	65
H(32C)	6985	1625	4242	65
H(33A)	5781	2931	2543	79
H(33B)	5970	2106	2663	79
H(33C)	7177	2599	2967	79
H(1A)	5710(40)	4125(15)	4920(30)	41(14)

Table B.2.3: Anisotropic displacement parameters ($Å^2$ x 10^3) for $[Hf(OH)(tfba)_3]_2$ ·2DMF.

Atom	U^{11}	U^{22}	U^{33}	U^{23}	U^{13}	U^{12}
C(1)	42(2)	27(2)	21(2)	-8(2)	17(2)	-13(2)
C(2)	26(2)	21(2)	30(2)	-7(2)	21(2)	-10(2)
C(3)	22(2)	31(2)	17(2)	-11(2)	12(2)	-14(2)
C(4)	20(2)	31(2)	22(2)	-5(2)	13(2)	-12(2)
C(5)	18(2)	40(2)	16(2)	-4(2)	6(2)	-12(2)
C(6)	29(2)	39(2)	29(2)	0(2)	14(2)	-11(2)
C(7)	28(2)	44(3)	36(2)	10(2)	9(2)	-5(2)
C(8)	39(3)	54(3)	33(2)	4(2)	6(2)	-14(2)
C(9)	46(3)	50(3)	23(2)	-6(2)	9(2)	-18(2)
C(10)	30(2)	44(2)	23(2)	-8(2)	11(2)	-14(2)
C(11)	31(2)	37(2)	21(2)	-11(2)	7(2)	4(2)
C(12)	26(2)	22(2)	21(2)	-9(1)	13(2)	-5(1)
C(13)	21(2)	28(2)	15(2)	-3(1)	6(1)	2(2)
C(14)	15(2)	16(2)	20(2)	2(1)	8(1)	-2(1)
C(15)	18(2)	21(2)	21(2)	4(1)	11(1)	1(1)
C(16)	28(2)	31(2)	25(2)	9(2)	16(2)	11(2)
C(17)	44(3)	41(2)	39(2)	12(2)	29(2)	20(2)
C(18)	34(3)	52(3)	50(3)	18(2)	24(2)	24(2)
C(19)	20(2)	52(3)	37(2)	13(2)	5(2)	10(2)
C(20)	21(2)	31(2)	25(2)	0(2)	7(2)	-1(2)
C(21)	32(2)	43(3)	30(2)	10(2)	20(2)	5(2)
C(22)	30(2)	27(2)	20(2)	2(2)	16(2)	-7(2)
C(23)	30(2)	35(2)	28(2)	7(2)	21(2)	4(2)
C(24)	18(2)	24(2)	19(2)	-4(1)	10(1)	-6(1)
C(25)	18(2)	19(2)	28(2)	-3(2)	14(2)	-4(1)
C(26)	37(2)	31(2)	49(3)	5(2)	33(2)	2(2)
C(27)	42(3)	30(2)	69(3)	4(2)	43(3)	6(2)
C(28)	26(2)	26(2)	59(3)	4(2)	24(2)	3(2)
C(29)	25(2)	33(2)	37(2)	3(2)	17(2)	2(2)
C(30)	20(2)	28(2)	29(2)	-2(2)	13(2)	-1(2)
C(31)	28(2)	21(2)	33(2)	2(2)	19(2)	6(2)
C(32)	50(3)	32(2)	42(3)	-1(2)	21(2)	17(2)
C(33)	83(4)	47(3)	48(3)	8(2)	49(3)	25(3)
N(1)	35(2)	24(2)	33(2)	1(1)	22(2)	8(1)
O(1)	30(1)	16(1)	20(1)	-4(1)	15(1)	-9(1)
O(2)	16(1)	29(1)	18(1)	-5(1)	7(1)	-7(1)
O(3)	21(1)	20(1)	17(1)	-2(1)	7(1)	2(1)

O(4)	18(1)	20(1)	19(1)	-3(1)	9(1)	1(1)
O(5)	25(1)	23(1)	22(1)	3(1)	16(1)	0(1)
O(6)	19(1)	22(1)	20(1)	2(1)	13(1)	1(1)
O(7)	17(1)	18(1)	19(1)	1(1)	11(1)	0(1)
O(8)	28(2)	24(1)	26(1)	-2(1)	16(1)	-2(1)
F(1)	75(2)	27(1)	29(1)	-8(1)	25(1)	1(1)
F(2)	50(2)	32(1)	56(2)	11(1)	29(1)	-10(1)
F(3)	45(2)	23(1)	31(1)	-2(1)	19(1)	0(1)
F(4)	55(2)	32(1)	64(2)	-23(1)	38(2)	-10(1)
F(5)	42(2)	50(2)	42(1)	-17(1)	29(1)	-1(1)
F(6)	66(2)	72(2)	23(1)	-18(1)	4(1)	30(2)
F(7)	45(2)	69(2)	26(1)	14(1)	14(1)	-5(1)
F(8)	59(2)	38(1)	45(2)	19(1)	33(1)	6(1)
F(9)	60(2)	66(2)	53(2)	31(1)	48(2)	22(1)
Hf(1)	16(1)	18(1)	15(1)	0(1)	8(1)	-2(1)

Table B.2.4: Bond lengths (Å) for $[Hf(OH)(tfba)_3]_2 \cdot 2DMF$.

Atoms	*Bond Length (Å)*	*Atoms*	*Bond Length (Å)*
C(1)-F(3)	1.307(5)	**C(21)-F(7)**	1.331(5)
C(1)-F(1)	1.330(4)	**C(21)-F(9)**	1.335(4)
C(1)-F(2)	1.360(4)	**C(21)-C(22)**	1.529(5)
C(1)-C(2)	1.528(5)	**C(22)-O(5)**	1.274(4)
C(2)-O(1)	1.253(4)	**C(22)-C(23)**	1.369(5)
C(2)-C(3)	1.392(5)	**C(23)-C(24)**	1.417(5)
C(3)-C(4)	1.389(5)	**C(23)-H(23)**	0.95
C(3)-H(3)	0.95	**C(24)-O(6)**	1.254(4)
C(4)-O(2)	1.270(4)	**C(24)-C(25)**	1.492(5)
C(4)-C(5)	1.493(5)	**C(25)-C(30)**	1.387(5)
C(5)-C(10)	1.394(5)	**C(25)-C(26)**	1.392(5)
C(5)-C(6)	1.399(6)	**C(26)-C(27)**	1.381(6)
C(6)-C(7)	1.391(6)	**C(26)-H(26)**	0.95
C(6)-H(6)	0.95	**C(27)-C(28)**	1.363(6)
C(7)-C(8)	1.394(7)	**C(27)-H(27)**	0.95
C(7)-H(7)	0.95	**C(28)-C(29)**	1.392(6)
C(8)-C(9)	1.388(7)	**C(28)-H(28)**	0.95
C(8)-H(8)	0.95	**C(29)-C(30)**	1.376(5)
C(9)-C(10)	1.401(6)	**C(29)-H(29)**	0.95
C(9)-H(9)	0.95	**C(30)-H(30)**	0.95
C(10)-H(10)	0.95	**C(31)-O(8)**	1.229(4)

C(11)-F(4)	1.320(5)	**C(31)-N(1)**	1.331(4)
C(11)-F(5)	1.323(5)	**C(31)-H(31)**	0.95
C(11)-F(6)	1.338(4)	**C(32)-N(1)**	1.440(5)
C(11)-C(12)	1.534(5)	**C(32)-H(32A)**	0.98
C(12)-O(3)	1.279(4)	**C(32)-H(32B)**	0.98
C(12)-C(13)	1.362(5)	**C(32)-H(32C)**	0.98
C(13)-C(14)	1.405(5)	**C(33)-N(1)**	1.452(5)
C(13)-H(13)	0.95	**C(33)-H(33A)**	0.98
C(14)-O(4)	1.266(4)	**C(33)-H(33B)**	0.98
C(14)-C(15)	1.484(5)	**C(33)-H(33C)**	0.98
C(15)-C(20)	1.391(5)	**O(1)-Hf(1)**	2.232(2)
C(15)-C(16)	1.396(5)	**O(2)-Hf(1)**	2.167(2)
C(16)-C(17)	1.382(5)	**O(3)-Hf(1)**	2.244(2)
C(16)-H(16)	0.95	**O(4)-Hf(1)**	2.146(2)
C(17)-C(18)	1.377(6)	**O(5)-Hf(1)**	2.170(2)
C(17)-H(17)	0.95	**O(6)-Hf(1)**	2.208(2)
C(18)-C(19)	1.371(6)	**O(7)-Hf(1)**	2.074(2)
C(18)-H(18)	0.95	**O(7)-Hf(1)#1**	2.135(2)
C(19)-C(20)	1.380(5)	**O(7)-H(1A)**	0.783(19)
C(19)-H(19)	0.95	**Hf(1)-O(7)#1**	2.135(2)
C(20)-H(20)	0.95	**Hf(1)-Hf(1)#1**	3.4958(8)
C(21)-F(8)	1.327(5)		

Table B.2.5: Bond angles (°) for $[Hf(OH)(tfba)_3]_2 \cdot 2DMF$.

Atoms	*Bond angle (°)*	*Atoms*	*Bond angle (°)*
F(3)-C(1)-F(1)	108.7(3)	**C(30)-C(25)-C(26)**	118.5(3)
F(3)-C(1)-F(2)	107.3(3)	**C(30)-C(25)-C(24)**	118.9(3)
F(1)-C(1)-F(2)	106.1(3)	**C(26)-C(25)-C(24)**	122.7(3)
F(3)-C(1)-C(2)	113.6(3)	**C(27)-C(26)-C(25)**	120.0(4)
F(1)-C(1)-C(2)	112.5(3)	**C(27)-C(26)-H(26)**	120
F(2)-C(1)-C(2)	108.2(3)	**C(25)-C(26)-H(26)**	120
O(1)-C(2)-C(3)	127.7(3)	**C(28)-C(27)-C(26)**	121.1(4)
O(1)-C(2)-C(1)	113.4(3)	**C(28)-C(27)-H(27)**	119.4
C(3)-C(2)-C(1)	118.6(3)	**C(26)-C(27)-H(27)**	119.4
C(4)-C(3)-C(2)	120.5(3)	**C(27)-C(28)-C(29)**	119.5(4)
C(4)-C(3)-H(3)	119.8	**C(27)-C(28)-H(28)**	120.3
C(2)-C(3)-H(3)	119.8	**C(29)-C(28)-H(28)**	120.3
O(2)-C(4)-C(3)	123.0(3)	**C(30)-C(29)-C(28)**	119.8(4)

O(2)-C(4)-C(5)	115.6(3)	**C(30)-C(29)-H(29)**	120.1
C(3)-C(4)-C(5)	121.2(3)	**C(28)-C(29)-H(29)**	120.1
C(10)-C(5)-C(6)	119.2(4)	**C(29)-C(30)-C(25)**	121.1(4)
C(10)-C(5)-C(4)	121.7(4)	**C(29)-C(30)-H(30)**	119.4
C(6)-C(5)-C(4)	119.1(3)	**C(25)-C(30)-H(30)**	119.4
C(7)-C(6)-C(5)	121.3(4)	**O(8)-C(31)-N(1)**	125.3(4)
C(7)-C(6)-H(6)	119.3	**O(8)-C(31)-H(31)**	117.3
C(5)-C(6)-H(6)	119.3	**N(1)-C(31)-H(31)**	117.3
C(6)-C(7)-C(8)	119.2(4)	**N(1)-C(32)-H(32A)**	109.5
C(6)-C(7)-H(7)	120.4	**N(1)-C(32)-H(32B)**	109.5
C(8)-C(7)-H(7)	120.4	**H(32A)-C(32)-H(32B)**	109.5
C(9)-C(8)-C(7)	120.0(4)	**N(1)-C(32)-H(32C)**	109.5
C(9)-C(8)-H(8)	120	**H(32A)-C(32)-H(32C)**	109.5
C(7)-C(8)-H(8)	120	**H(32B)-C(32)-H(32C)**	109.5
C(8)-C(9)-C(10)	120.8(4)	**N(1)-C(33)-H(33A)**	109.5
C(8)-C(9)-H(9)	119.6	**N(1)-C(33)-H(33B)**	109.5
C(10)-C(9)-H(9)	119.6	**H(33A)-C(33)-H(33B)**	109.5
C(5)-C(10)-C(9)	119.5(4)	**N(1)-C(33)-H(33C)**	109.5
C(5)-C(10)-H(10)	120.2	**H(33A)-C(33)-H(33C)**	109.5
C(9)-C(10)-H(10)	120.2	**H(33B)-C(33)-H(33C)**	109.5
F(4)-C(11)-F(5)	106.8(3)	**C(31)-N(1)-C(32)**	120.6(3)
F(4)-C(11)-F(6)	107.0(3)	**C(31)-N(1)-C(33)**	122.2(3)
F(5)-C(11)-F(6)	107.1(3)	**C(32)-N(1)-C(33)**	117.1(3)
F(4)-C(11)-C(12)	111.3(3)	**C(2)-O(1)-Hf(1)**	129.9(2)
F(5)-C(11)-C(12)	111.7(3)	**C(4)-O(2)-Hf(1)**	134.3(2)
F(6)-C(11)-C(12)	112.7(3)	**C(12)-O(3)-Hf(1)**	130.1(2)
O(3)-C(12)-C(13)	128.8(3)	**C(14)-O(4)-Hf(1)**	140.4(2)
O(3)-C(12)-C(11)	112.6(3)	**C(22)-O(5)-Hf(1)**	133.1(2)
C(13)-C(12)-C(11)	118.7(3)	**C(24)-O(6)-Hf(1)**	138.4(2)
C(12)-C(13)-C(14)	120.1(3)	**Hf(1)-O(7)-Hf(1)#1**	112.32(11)
C(12)-C(13)-H(13)	120	**Hf(1)-O(7)-H(1A)**	123(3)
C(14)-C(13)-H(13)	120	**Hf(1)#1-O(7)-H(1A)**	123(3)
O(4)-C(14)-C(13)	121.2(3)	**O(7)-Hf(1)-O(7)#1**	67.68(11)
O(4)-C(14)-C(15)	116.4(3)	**O(7)-Hf(1)-O(4)**	107.86(9)
C(13)-C(14)-C(15)	122.4(3)	**O(7)#1-Hf(1)-O(4)**	75.49(9)
C(20)-C(15)-C(16)	119.1(3)	**O(7)-Hf(1)-O(2)**	88.80(9)
C(20)-C(15)-C(14)	122.8(3)	**O(7)#1-Hf(1)-O(2)**	79.46(10)
C(16)-C(15)-C(14)	118.1(3)	**O(4)-Hf(1)-O(2)**	141.33(9)
C(17)-C(16)-C(15)	120.2(4)	**O(7)-Hf(1)-O(5)**	145.61(9)
C(17)-C(16)-H(16)	119.9	**O(7)#1-Hf(1)-O(5)**	146.39(9)
C(15)-C(16)-H(16)	119.9	**O(4)-Hf(1)-O(5)**	85.27(9)
C(18)-C(17)-C(16)	119.4(4)	**O(2)-Hf(1)-O(5)**	100.53(9)

C(18)-C(17)-H(17)	120.3	**O(7)-Hf(1)-O(6)**	76.60(9)
C(16)-C(17)-H(17)	120.3	**O(7)#1-Hf(1)-O(6)**	133.36(9)
C(19)-C(18)-C(17)	121.1(4)	**O(4)-Hf(1)-O(6)**	146.27(9)
C(19)-C(18)-H(18)	119.5	**O(2)-Hf(1)-O(6)**	70.57(9)
C(17)-C(18)-H(18)	119.5	**O(5)-Hf(1)-O(6)**	75.58(9)
C(18)-C(19)-C(20)	119.9(4)	**O(7)-Hf(1)-O(1)**	143.72(9)
C(18)-C(19)-H(19)	120	**O(7)#1-Hf(1)-O(1)**	77.52(8)
C(20)-C(19)-H(19)	120	**O(4)-Hf(1)-O(1)**	71.50(9)
C(19)-C(20)-C(15)	120.2(4)	**O(2)-Hf(1)-O(1)**	74.67(9)
C(19)-C(20)-H(20)	119.9	**O(5)-Hf(1)-O(1)**	70.27(9)
C(15)-C(20)-H(20)	119.9	**O(6)-Hf(1)-O(1)**	124.85(9)
F(8)-C(21)-F(7)	107.0(3)	**O(7)-Hf(1)-O(3)**	78.55(9)
F(8)-C(21)-F(9)	106.6(3)	**O(7)#1-Hf(1)-O(3)**	123.40(9)
F(7)-C(21)-F(9)	107.3(3)	**O(4)-Hf(1)-O(3)**	73.49(9)
F(8)-C(21)-C(22)	112.0(3)	**O(2)-Hf(1)-O(3)**	145.09(9)
F(7)-C(21)-C(22)	110.1(3)	**O(5)-Hf(1)-O(3)**	75.00(9)
F(9)-C(21)-C(22)	113.4(3)	**O(6)-Hf(1)-O(3)**	74.85(9)
O(5)-C(22)-C(23)	128.6(3)	**O(1)-Hf(1)-O(3)**	131.91(8)
O(5)-C(22)-C(21)	112.1(3)	**O(7)-Hf(1)-Hf(1)#1**	34.40(7)
C(23)-C(22)-C(21)	119.3(3)	**O(7)#1-Hf(1)-Hf(1)#1**	33.28(6)
C(22)-C(23)-C(24)	121.0(3)	**O(4)-Hf(1)-Hf(1)#1**	91.65(7)
C(22)-C(23)-H(23)	119.5	**O(2)-Hf(1)-Hf(1)#1**	82.87(7)
C(24)-C(23)-H(23)	119.5	**O(5)-Hf(1)-Hf(1)#1**	176.54(7)
O(6)-C(24)-C(23)	121.8(3)	**O(6)-Hf(1)-Hf(1)#1**	106.37(6)
O(6)-C(24)-C(25)	116.9(3)	**O(1)-Hf(1)-Hf(1)#1**	110.25(6)
C(23)-C(24)-C(25)	121.3(3)	**O(3)-Hf(1)-Hf(1)#1**	102.62(6)

Appendix C.1

Supplementary Crystallographic Data

C.1. $[Hf(salophen)_2]\cdot 2C_7H_8$ – (Hf_3a) – § 7.4

Table C.1.1: Atomic coordinates (x 10^4) and equivalent isotropic displacement parameters ($Å^2$ x 10^3) for $[Hf(salophen)_2]\cdot 2C_7H_8$

Atom	*x*	*y*	*z*	$U_{(eq)}$
C(04)	5473(4)	7683(2)	4853(3)	30(1)
C(03)	5889(4)	6926(2)	5091(3)	23(1)
C(02)	6788(3)	6755(2)	5996(2)	23(1)
C(01)	7431(4)	6123(2)	6218(2)	23(1)
C(11)	8546(4)	5979(2)	7159(2)	26(1)
C(16)	9359(4)	5421(2)	7303(3)	33(1)
C(15)	10431(4)	5276(2)	8162(3)	40(1)
C(14)	10672(5)	5681(3)	8900(3)	49(1)
C(13)	9859(5)	6229(3)	8769(3)	45(1)
C(12)	8803(4)	6388(2)	7897(3)	34(1)
C(08)	3785(4)	4209(2)	1663(3)	34(1)
C(07)	3761(4)	4747(2)	2301(2)	22(1)
C(06)	2821(4)	5238(2)	1940(2)	23(1)
C(05)	2716(3)	5706(2)	2511(2)	18(1)
C(31)	1615(3)	6190(2)	2168(2)	20(1)
C(32)	1675(4)	6693(2)	2764(3)	26(1)
C(33)	675(4)	7157(2)	2477(3)	38(1)
C(34)	-388(4)	7110(3)	1603(3)	45(1)
C(35)	-453(4)	6628(2)	1004(3)	42(1)
C(36)	544(4)	6165(2)	1283(3)	28(1)
C(012)	6419(4)	6077(2)	2317(3)	33(1)
C(011)	6665(4)	5653(2)	3135(2)	24(1)
C(010)	7554(4)	5129(2)	3461(3)	28(1)
C(09)	7799(3)	4717(2)	4212(2)	20(1)

C(51)	8869(3)	4202(2)	4639(2)	21(1)
C(56)	9601(4)	4044(2)	4279(3)	34(1)
C(55)	10581(4)	3562(2)	4707(4)	40(1)
C(54)	10842(4)	3230(2)	5476(3)	36(1)
C(53)	10128(4)	3387(2)	5849(3)	31(1)
C(52)	9152(4)	3868(2)	5431(3)	26(1)
C(013)	6169(4)	3145(2)	4081(3)	26(1)
C(015)	7379(5)	2081(2)	4479(3)	43(1)
C(014)	6362(6)	2557(3)	2929(3)	52(1)
N(1)	6594(3)	2612(2)	3833(2)	28(1)
O(2)	5438(2)	6538(1)	4408(2)	21(1)
O(1)	7170(2)	5652(1)	5634(2)	22(1)
O(4)	4665(2)	4654(1)	3135(2)	21(1)
O(3)	3564(2)	5733(1)	3355(2)	19(1)
O(6)	5958(2)	5847(1)	3416(2)	22(1)
O(5)	7134(2)	4771(1)	4550(2)	19(1)
O(7)	5351(2)	4465(1)	4894(2)	17(1)
O(8)	6358(2)	3229(1)	4841(2)	25(1)
F(1)	5519(3)	8025(1)	5531(2)	46(1)
F(2)	6313(3)	8010(1)	4703(2)	46(1)
F(3)	4325(2)	7758(1)	4117(2)	34(1)
F(4)	3554(3)	3577(1)	1835(2)	47(1)
F(5)	4918(2)	4186(1)	1758(2)	42(1)
F(6)	2911(3)	4338(2)	784(2)	64(1)
F(7)	5246(3)	5946(2)	1599(2)	49(1)
F(8)	6486(3)	6755(1)	2472(2)	45(1)
F(9)	7246(3)	5940(1)	2073(2)	50(1)
Hf(1)	5480(1)	5382(1)	4325(1)	16(1)

Table C.1.2: Hydrogen coordinates (x 10^4) and isotropic displacement parameters (Å^2 x 10^3) for [Hf(salophen)$_2$]·2C$_7$H$_8$

Atom	*x*	*y*	*z*	$U_{(eq)}$
H(02)	6963	7073	6465	28
H(16)	9175	5135	6804	39
H(15)	10991	4906	8245	48
H(14)	11393	5583	9492	58
H(13)	10020	6499	9276	53
H(12)	8266	6772	7810	41

H(06)	2235	5264	1299	28
H(32)	2405	6716	3370	32
H(33)	721	7505	2879	45
H(34)	-1089	7417	1412	54
H(35)	-1182	6612	397	50
H(36)	496	5828	869	33
H(010)	8015	5040	3180	33
H(56)	9426	4267	3739	40
H(55)	11082	3462	4460	48
H(54)	11508	2893	5756	44
H(53)	10313	3163	6391	38
H(52)	8665	3973	5687	31
H(013)	5679	3489	3635	32
H(01A)	8237	2091	4581	64
H(01B)	6987	1625	4241	64
H(01C)	7446	2166	5056	64
H(01D)	5782	2931	2544	78
H(01E)	5969	2106	2664	78
H(01F)	7177	2599	2968	78
H(7)	5720(40)	4130(16)	4920(30)	42(15)

Table C.1.3: Anisotropic displacement parameters ($Å^2$ x 10^3) for $[Hf(salophen)_2] \cdot 2C_7H_8$

Atom	U^{11}	U^{22}	U^{33}	U^{23}	U^{13}	U^{12}
C(04)	42(3)	28(2)	20(2)	-8(2)	16(2)	-14(2)
C(03)	26(2)	21(2)	31(2)	-7(2)	22(2)	-10(2)
C(02)	22(2)	32(2)	17(2)	-11(2)	11(2)	-14(2)
C(01)	20(2)	31(2)	22(2)	-4(2)	13(2)	-11(2)
C(11)	17(2)	39(2)	16(2)	-4(2)	6(2)	-12(2)
C(16)	29(2)	39(2)	29(2)	-1(2)	14(2)	-11(2)
C(15)	28(2)	44(3)	36(2)	9(2)	9(2)	-6(2)
C(14)	39(3)	53(3)	33(3)	4(2)	6(2)	-15(2)
C(13)	46(3)	49(3)	23(2)	-6(2)	9(2)	-18(2)
C(12)	30(2)	44(3)	23(2)	-7(2)	11(2)	-13(2)
C(08)	31(2)	39(3)	21(2)	-11(2)	7(2)	4(2)
C(07)	25(2)	22(2)	20(2)	-9(2)	13(2)	-5(2)
C(06)	20(2)	28(2)	15(2)	-2(2)	6(2)	2(2)
C(05)	15(2)	16(2)	20(2)	2(1)	9(2)	-1(1)
C(31)	18(2)	21(2)	21(2)	4(2)	11(2)	2(2)

C(32)	28(2)	31(2)	24(2)	9(2)	16(2)	11(2)
C(33)	45(3)	41(3)	38(2)	11(2)	29(2)	20(2)
C(34)	33(3)	53(3)	51(3)	18(2)	24(2)	25(2)
C(35)	21(2)	52(3)	36(2)	12(2)	5(2)	10(2)
C(36)	21(2)	30(2)	25(2)	0(2)	8(2)	-1(2)
C(012)	31(2)	43(3)	29(2)	10(2)	19(2)	5(2)
C(011)	30(2)	27(2)	20(2)	1(2)	16(2)	-7(2)
C(010)	29(2)	34(2)	28(2)	6(2)	21(2)	3(2)
C(09)	18(2)	24(2)	19(2)	-4(2)	10(2)	-6(2)
C(51)	18(2)	19(2)	27(2)	-3(2)	13(2)	-4(2)
C(56)	37(3)	31(2)	48(3)	4(2)	33(2)	2(2)
C(55)	41(3)	30(2)	69(3)	3(2)	43(3)	5(2)
C(54)	26(2)	26(2)	59(3)	4(2)	24(2)	4(2)
C(53)	24(2)	32(2)	37(2)	3(2)	16(2)	2(2)
C(52)	20(2)	28(2)	29(2)	-2(2)	13(2)	-2(2)
C(013)	28(2)	21(2)	33(2)	2(2)	19(2)	5(2)
C(015)	50(3)	32(2)	41(3)	-1(2)	21(2)	17(2)
C(014)	82(4)	47(3)	47(3)	8(2)	48(3)	25(3)
N(1)	36(2)	24(2)	32(2)	1(2)	22(2)	8(2)
O(2)	30(2)	15(1)	20(1)	-4(1)	15(1)	-9(1)
O(1)	16(1)	29(1)	18(1)	-4(1)	7(1)	-7(1)
O(4)	21(1)	20(1)	17(1)	-2(1)	7(1)	2(1)
O(3)	18(1)	20(1)	18(1)	-3(1)	9(1)	0(1)
O(6)	24(1)	24(1)	22(1)	3(1)	15(1)	0(1)
O(5)	19(1)	22(1)	20(1)	2(1)	13(1)	1(1)
O(7)	17(1)	18(1)	19(1)	1(1)	12(1)	0(1)
O(8)	28(2)	24(1)	26(1)	-2(1)	16(1)	-1(1)
F(1)	76(2)	26(1)	30(1)	-8(1)	25(1)	0(1)
F(2)	50(2)	32(1)	55(2)	11(1)	28(2)	-10(1)
F(3)	45(2)	23(1)	31(1)	-1(1)	19(1)	-1(1)
F(4)	55(2)	32(1)	63(2)	-23(1)	38(2)	-10(1)
F(5)	42(2)	50(2)	42(2)	-17(1)	28(1)	-1(1)
F(6)	66(2)	72(2)	23(1)	-18(1)	4(1)	30(2)
F(7)	45(2)	69(2)	26(1)	13(1)	14(1)	-5(1)
F(8)	59(2)	38(2)	45(2)	19(1)	33(1)	6(1)
F(9)	59(2)	66(2)	52(2)	31(1)	48(2)	22(1)
Hf(1)	15(1)	18(1)	14(1)	0(1)	8(1)	-2(1)

Table C.1.4: Bond lengths (Å) for [Hf(salophen)$_2$]·2C$_7$H$_8$

Atoms	*Bond Length (Å)*	*Atoms*	*Bond Length (Å)*
C(04)-F(3)	1.309(5)	**C(012)-F(7)**	1.331(5)
C(04)-F(1)	1.330(4)	**C(012)-F(9)**	1.336(5)
C(04)-F(2)	1.360(5)	**C(012)-C(011)**	1.529(5)
C(04)-C(03)	1.527(5)	**C(011)-O(6)**	1.274(4)
C(03)-O(2)	1.254(4)	**C(011)-C(010)**	1.369(6)
C(03)-C(02)	1.392(5)	**C(010)-C(09)**	1.420(5)
C(02)-C(01)	1.389(5)	**C(010)-H(010)**	0.95
C(02)-H(02)	0.95	**C(09)-O(5)**	1.254(4)
C(01)-O(1)	1.269(4)	**C(09)-C(51)**	1.491(5)
C(01)-C(11)	1.493(5)	**C(51)-C(52)**	1.389(5)
C(11)-C(12)	1.394(5)	**C(51)-C(56)**	1.392(5)
C(11)-C(16)	1.399(6)	**C(56)-C(55)**	1.382(6)
C(16)-C(15)	1.390(6)	**C(56)-H(56)**	0.95
C(16)-H(16)	0.95	**C(55)-C(54)**	1.361(6)
C(15)-C(14)	1.394(7)	**C(55)-H(55)**	0.95
C(15)-H(15)	0.95	**C(54)-C(53)**	1.390(6)
C(14)-C(13)	1.390(7)	**C(54)-H(54)**	0.95
C(14)-H(14)	0.95	**C(53)-C(52)**	1.377(5)
C(13)-C(12)	1.402(6)	**C(53)-H(53)**	0.95
C(13)-H(13)	0.95	**C(52)-H(52)**	0.95
C(12)-H(12)	0.95	**C(013)-O(8)**	1.228(4)
C(08)-F(4)	1.321(5)	**C(013)-N(1)**	1.331(5)
C(08)-F(5)	1.324(5)	**C(013)-H(013)**	0.95
C(08)-F(6)	1.338(5)	**C(015)-N(1)**	1.439(5)
C(08)-C(07)	1.534(5)	**C(015)-H(01A)**	0.98
C(07)-O(4)	1.281(4)	**C(015)-H(01B)**	0.98
C(07)-C(06)	1.361(5)	**C(015)-H(01C)**	0.98
C(06)-C(05)	1.403(5)	**C(014)-N(1)**	1.451(5)
C(06)-H(06)	0.95	**C(014)-H(01D)**	0.98
C(05)-O(3)	1.265(4)	**C(014)-H(01E)**	0.98
C(05)-C(31)	1.485(5)	**C(014)-H(01F)**	0.98
C(31)-C(36)	1.389(5)	**O(2)-Hf(1)**	2.232(2)
C(31)-C(32)	1.395(5)	**O(1)-Hf(1)**	2.167(2)
C(32)-C(33)	1.383(5)	**O(4)-Hf(1)**	2.245(2)
C(32)-H(32)	0.95	**O(3)-Hf(1)**	2.146(2)
C(33)-C(34)	1.377(6)	**O(6)-Hf(1)**	2.170(2)
C(33)-H(33)	0.95	**O(5)-Hf(1)**	2.208(2)
C(34)-C(35)	1.369(7)	**O(7)-Hf(1)**	2.074(2)
C(34)-H(34)	0.95	**O(7)-Hf(1)#1**	2.134(2)

C(35)-C(36)	1.380(6)	**O(7)-H(7)**	0.778(19)
C(35)-H(35)	0.95	**Hf(1)-O(7)#1**	2.134(2)
C(36)-H(36)	0.95	**Hf(1)-Hf(1)#1**	3.4958(8)
C(012)-F(8)	1.327(5)		

Table C.1.5: Bond angles (°) for $[Hf(salophen)_2]\cdot 2C_7H_8$

Atoms	*Bond angle (°)*	*Atoms*	*Bond angle (°)*
F(3)-C(04)-F(1)	108.7(4)	**C(010)-C(09)-C(51)**	121.3(3)
F(3)-C(04)-F(2)	107.3(3)	**C(52)-C(51)-C(56)**	118.5(4)
F(1)-C(04)-F(2)	106.2(3)	**C(52)-C(51)-C(09)**	118.8(3)
F(3)-C(04)-C(03)	113.5(3)	**C(56)-C(51)-C(09)**	122.8(3)
F(1)-C(04)-C(03)	112.5(3)	**C(55)-C(56)-C(51)**	120.1(4)
F(2)-C(04)-C(03)	108.2(3)	**C(55)-C(56)-H(56)**	120
O(2)-C(03)-C(02)	127.6(4)	**C(51)-C(56)-H(56)**	120
O(2)-C(03)-C(04)	113.5(3)	**C(54)-C(55)-C(56)**	121.1(4)
C(02)-C(03)-C(04)	118.6(3)	**C(54)-C(55)-H(55)**	119.4
C(01)-C(02)-C(03)	120.6(3)	**C(56)-C(55)-H(55)**	119.4
C(01)-C(02)-H(02)	119.7	**C(55)-C(54)-C(53)**	119.5(4)
C(03)-C(02)-H(02)	119.7	**C(55)-C(54)-H(54)**	120.2
O(1)-C(01)-C(02)	122.9(3)	**C(53)-C(54)-H(54)**	120.2
O(1)-C(01)-C(11)	115.7(3)	**C(52)-C(53)-C(54)**	119.8(4)
C(02)-C(01)-C(11)	121.3(3)	**C(52)-C(53)-H(53)**	120.1
C(12)-C(11)-C(16)	119.2(4)	**C(54)-C(53)-H(53)**	120.1
C(12)-C(11)-C(01)	121.6(4)	**C(53)-C(52)-C(51)**	120.9(4)
C(16)-C(11)-C(01)	119.1(3)	**C(53)-C(52)-H(52)**	119.5
C(15)-C(16)-C(11)	121.4(4)	**C(51)-C(52)-H(52)**	119.5
C(15)-C(16)-H(16)	119.3	**O(8)-C(013)-N(1)**	125.4(4)
C(11)-C(16)-H(16)	119.3	**O(8)-C(013)-H(013)**	117.3
C(16)-C(15)-C(14)	119.2(5)	**N(1)-C(013)-H(013)**	117.3
C(16)-C(15)-H(15)	120.4	**N(1)-C(015)-H(01A)**	109.5
C(14)-C(15)-H(15)	120.4	**N(1)-C(015)-H(01B)**	109.5
C(13)-C(14)-C(15)	120.0(4)	**H(01A)-C(015)-H(01B)**	109.5
C(13)-C(14)-H(14)	120	**N(1)-C(015)-H(01C)**	109.5
C(15)-C(14)-H(14)	120	**H(01A)-C(015)-H(01C)**	109.5
C(14)-C(13)-C(12)	120.7(4)	**H(01B)-C(015)-H(01C)**	109.5
C(14)-C(13)-H(13)	119.7	**N(1)-C(014)-H(01D)**	109.5
C(12)-C(13)-H(13)	119.7	**N(1)-C(014)-H(01E)**	109.5
C(11)-C(12)-C(13)	119.5(4)	**H(01D)-C(014)-H(01E)**	109.5
C(11)-C(12)-H(12)	120.3	**N(1)-C(014)-H(01F)**	109.5

C(13)-C(12)-H(12)	120.3	**H(01D)-C(014)-H(01F)**	109.5
F(4)-C(08)-F(5)	106.8(3)	**H(01E)-C(014)-H(01F)**	109.5
F(4)-C(08)-F(6)	107.0(4)	**C(013)-N(1)-C(015)**	120.6(3)
F(5)-C(08)-F(6)	107.0(4)	**C(013)-N(1)-C(014)**	122.2(3)
F(4)-C(08)-C(07)	111.3(3)	**C(015)-N(1)-C(014)**	117.0(3)
F(5)-C(08)-C(07)	111.7(3)	**C(03)-O(2)-Hf(1)**	129.9(2)
F(6)-C(08)-C(07)	112.7(3)	**C(01)-O(1)-Hf(1)**	134.4(2)
O(4)-C(07)-C(06)	128.7(3)	**C(07)-O(4)-Hf(1)**	130.1(2)
O(4)-C(07)-C(08)	112.5(3)	**C(05)-O(3)-Hf(1)**	140.5(2)
C(06)-C(07)-C(08)	118.8(3)	**C(011)-O(6)-Hf(1)**	133.0(2)
C(07)-C(06)-C(05)	120.2(3)	**C(09)-O(5)-Hf(1)**	138.4(2)
C(07)-C(06)-H(06)	119.9	**Hf(1)-O(7)-Hf(1)#1**	112.36(11)
C(05)-C(06)-H(06)	119.9	**Hf(1)-O(7)-H(7)**	123(3)
O(3)-C(05)-C(06)	121.2(3)	**Hf(1)#1-O(7)-H(7)**	123(3)
O(3)-C(05)-C(31)	116.4(3)	**O(7)-Hf(1)-O(7)#1**	67.64(11)
C(06)-C(05)-C(31)	122.4(3)	**O(7)-Hf(1)-O(3)**	107.81(10)
C(36)-C(31)-C(32)	119.1(3)	**O(7)#1-Hf(1)-O(3)**	75.52(10)
C(36)-C(31)-C(05)	122.8(3)	**O(7)-Hf(1)-O(1)**	88.82(10)
C(32)-C(31)-C(05)	118.0(3)	**O(7)#1-Hf(1)-O(1)**	79.43(10)
C(33)-C(32)-C(31)	120.3(4)	**O(3)-Hf(1)-O(1)**	141.34(9)
C(33)-C(32)-H(32)	119.9	**O(7)-Hf(1)-O(6)**	145.66(9)
C(31)-C(32)-H(32)	119.9	**O(7)#1-Hf(1)-O(6)**	146.39(9)
C(34)-C(33)-C(32)	119.3(4)	**O(3)-Hf(1)-O(6)**	85.25(10)
C(34)-C(33)-H(33)	120.3	**O(1)-Hf(1)-O(6)**	100.54(10)
C(32)-C(33)-H(33)	120.3	**O(7)-Hf(1)-O(5)**	76.64(9)
C(35)-C(34)-C(33)	121.2(4)	**O(7)#1-Hf(1)-O(5)**	133.33(9)
C(35)-C(34)-H(34)	119.4	**O(3)-Hf(1)-O(5)**	146.28(9)
C(33)-C(34)-H(34)	119.4	**O(1)-Hf(1)-O(5)**	70.57(9)
C(34)-C(35)-C(36)	119.9(4)	**O(6)-Hf(1)-O(5)**	75.61(9)
C(34)-C(35)-H(35)	120.1	**O(7)-Hf(1)-O(2)**	143.71(9)
C(36)-C(35)-H(35)	120.1	**O(7)#1-Hf(1)-O(2)**	77.54(9)
C(35)-C(36)-C(31)	120.2(4)	**O(3)-Hf(1)-O(2)**	71.51(9)
C(35)-C(36)-H(36)	119.9	**O(1)-Hf(1)-O(2)**	74.67(9)
C(31)-C(36)-H(36)	119.9	**O(6)-Hf(1)-O(2)**	70.25(9)
F(8)-C(012)-F(7)	107.1(3)	**O(5)-Hf(1)-O(2)**	124.84(9)
F(8)-C(012)-F(9)	106.6(3)	**O(7)-Hf(1)-O(4)**	78.52(9)
F(7)-C(012)-F(9)	107.4(3)	**O(7)#1-Hf(1)-O(4)**	123.40(9)
F(8)-C(012)-C(011)	112.0(3)	**O(3)-Hf(1)-O(4)**	73.49(9)
F(7)-C(012)-C(011)	110.0(3)	**O(1)-Hf(1)-O(4)**	145.08(9)
F(9)-C(012)-C(011)	113.4(3)	**O(6)-Hf(1)-O(4)**	75.02(9)
O(6)-C(011)-C(010)	128.6(3)	**O(5)-Hf(1)-O(4)**	74.85(9)
O(6)-C(011)-C(012)	112.1(3)	**O(2)-Hf(1)-O(4)**	131.93(9)

C(010)-C(011)-C(012)	119.2(3)	**O(7)-Hf(1)-Hf(1)#1**	34.37(7)
C(011)-C(010)-C(09)	121.0(3)	**O(7)#1-Hf(1)-Hf(1)#1**	33.27(7)
C(011)-C(010)-H(010)	119.5	**O(3)-Hf(1)-Hf(1)#1**	91.65(7)
C(09)-C(010)-H(010)	119.5	**O(1)-Hf(1)-Hf(1)#1**	82.87(7)
O(5)-C(09)-C(010)	121.7(3)	**O(6)-Hf(1)-Hf(1)#1**	176.52(7)
O(5)-C(09)-C(51)	117.0(3)	**O(5)-Hf(1)-Hf(1)#1**	106.36(6)
O(4)-Hf(1)-Hf(1)#1	102.59(7)	**O(2)-Hf(1)-Hf(1)#1**	110.27(6)

Appendix C.2

Supplementary Crystallographic Data

C.2. $[Zr(bpb)(H_2O)_2]NO_3 \cdot CH_3OH$ – (Zr_1a) – § 7.5

Table C.2.1: Atomic coordinates (x 10^4) and equivalent isotropic displacement parameters ($Å^2$ x 10^3) for $[Zr(bpb)(H_2O)_2]NO_3 \cdot CH_3OH$.

Atom	*x*	*y*	*z*	$U_{(eq)}$
Zr	8105(1)	3644(1)	3703(1)	19(1)
O(1)	8280(1)	4352(1)	2803(1)	25(1)
O(2)	8350(1)	2927(1)	4592(1)	26(1)
O(3)	6800(1)	1352(1)	2833(1)	28(1)
O(4)	6878(1)	5961(1)	4607(1)	31(1)
N(1)	8795(1)	2481(1)	3310(1)	22(1)
N(2)	7135(1)	2831(1)	3380(1)	22(1)
N(3)	7169(1)	4461(1)	4078(1)	23(1)
N(4)	8837(1)	4803(1)	4069(1)	23(1)
C(1)	9649(1)	2313(1)	3334(1)	26(1)
C(2)	10013(1)	1455(1)	3072(1)	29(1)
C(3)	9485(1)	763(1)	2764(1)	29(1)
C(4)	8605(1)	936(1)	2734(1)	27(1)
C(5)	8274(1)	1797(1)	3024(1)	21(1)
C(6)	7310(1)	1982(1)	3066(1)	21(1)
C(7)	6315(1)	3214(1)	3548(1)	22(1)
C(8)	5529(1)	2809(1)	3361(1)	28(1)
C(9)	4765(1)	3231(1)	3590(1)	33(1)
C(10)	4785(1)	4048(1)	4016(1)	34(1)
C(11)	5565(1)	4483(1)	4197(1)	30(1)
C(12)	6334(1)	4085(1)	3957(1)	22(1)
C(13)	7370(1)	5320(1)	4368(1)	23(1)
C(14)	8338(1)	5487(1)	4386(1)	24(1)
C(15)	8693(1)	6312(1)	4696(1)	29(1)

C(16)	9578(1)	6458(1)	4662(1)	34(1)
C(17)	10080(1)	5785(1)	4311(1)	32(1)
C(18)	9690(1)	4961(1)	4023(1)	27(1)
O(5)	7849(1)	3511(1)	5802(1)	42(1)
C(19)	7267(2)	4294(2)	5937(1)	53(1)
O(6)	6403(1)	4036(1)	1895(1)	54(1)
O(7)	7633(1)	3307(1)	1747(1)	38(1)
O(8)	6524(1)	2863(1)	1169(1)	43(1)
N(5)	6846(1)	3410(1)	1606(1)	27(1)

Table C.2.2: Hydrogen coordinates (x 10^4) and isotropic displacement parameters ($Å^2$ x 10^3) for $[Zr(bpb)(H_2O)_2]NO_3 \cdot CH_3OH$.

Atom	*x*	*y*	*z*	$U_{(eq)}$
H(1A)	8218	4982	2788	38
H(1B)	8031	4140	2449	38
H(2A)	8131	3138	4957	39
H(2B)	8240	2304	4590	39
H(1)	10013	2798	3538	31
H(2)	10618	1343	3103	34
H(3)	9723	173	2575	35
H(4)	8232	471	2518	32
H(8)	5512	2240	3075	33
H(9)	4226	2958	3454	40
H(10)	4259	4314	4186	41
H(11)	5573	5051	4484	36
H(15)	8336	6774	4930	35
H(16)	9837	7016	4878	41
H(17)	10685	5886	4268	39
H(18)	10036	4492	3786	32
H(19A)	6723	4172	5698	79
H(19B)	7516	4928	5786	79
H(19C)	7156	4326	6422	79
H(5)	7620(30)	3000(30)	5921(18)	109(13)

Table C.2.3: Anisotropic displacement parameters ($Å^2$ x 10^3) $[Zr(bpb)(H_2O)_2]NO_3 \cdot CH_3OH$.

Atom	U^{11}	U^{22}	U^{33}	U^{23}	U^{13}	U^{12}
Zr	17(1)	14(1)	27(1)	-3(1)	0(1)	0(1)
O(1)	29(1)	18(1)	29(1)	-1(1)	-1(1)	0(1)
O(2)	32(1)	16(1)	29(1)	-1(1)	0(1)	-2(1)
O(3)	26(1)	18(1)	39(1)	-5(1)	-6(1)	-2(1)
O(4)	35(1)	17(1)	41(1)	-5(1)	7(1)	4(1)
N(1)	21(1)	17(1)	27(1)	0(1)	1(1)	0(1)
N(2)	19(1)	17(1)	31(1)	-2(1)	0(1)	-1(1)
N(3)	21(1)	16(1)	31(1)	-3(1)	2(1)	1(1)
N(4)	24(1)	18(1)	26(1)	1(1)	-2(1)	-2(1)
C(1)	21(1)	24(1)	33(1)	-1(1)	2(1)	-1(1)
C(2)	23(1)	27(1)	36(1)	2(1)	5(1)	5(1)
C(3)	32(1)	22(1)	34(1)	-4(1)	6(1)	7(1)
C(4)	30(1)	19(1)	31(1)	-5(1)	1(1)	1(1)
C(5)	23(1)	16(1)	24(1)	0(1)	0(1)	1(1)
C(6)	22(1)	16(1)	25(1)	0(1)	-1(1)	0(1)
C(7)	20(1)	18(1)	28(1)	3(1)	1(1)	1(1)
C(8)	24(1)	23(1)	36(1)	0(1)	-2(1)	-2(1)
C(9)	19(1)	34(1)	47(1)	5(1)	-3(1)	-1(1)
C(10)	21(1)	34(1)	48(1)	4(1)	6(1)	7(1)
C(11)	28(1)	23(1)	40(1)	0(1)	6(1)	5(1)
C(12)	21(1)	18(1)	28(1)	2(1)	2(1)	1(1)
C(13)	28(1)	16(1)	26(1)	1(1)	2(1)	0(1)
C(14)	30(1)	18(1)	23(1)	1(1)	0(1)	-2(1)
C(15)	40(1)	19(1)	28(1)	-2(1)	-1(1)	-4(1)
C(16)	43(1)	24(1)	35(1)	0(1)	-9(1)	-12(1)
C(17)	30(1)	27(1)	40(1)	5(1)	-7(1)	-10(1)
C(18)	25(1)	24(1)	31(1)	3(1)	-2(1)	-3(1)
O(5)	47(1)	33(1)	45(1)	-1(1)	18(1)	-4(1)
C(19)	63(2)	47(1)	48(1)	-3(1)	13(1)	12(1)
O(6)	43(1)	45(1)	75(1)	-28(1)	-3(1)	13(1)
O(7)	25(1)	49(1)	40(1)	-4(1)	-2(1)	4(1)
O(8)	42(1)	48(1)	39(1)	-16(1)	0(1)	-9(1)
N(5)	28(1)	25(1)	28(1)	-1(1)	2(1)	0(1)

Table C.2.4: Bond lengths (Å) for $[Zr(bpb)(H_2O)_2]NO_3 \cdot CH_3OH$.

Atoms	*Bond Length (Å)*	*Atoms*	*Bond Length (Å)*
Zr-N(2)	1.9620(13)	**C(3)-H(3)**	0.95
Zr-N(3)	1.9631(13)	**C(4)-C(5)**	1.386(2)
Zr-O(1)	2.0418	**C(4)-H(4)**	0.95
Zr-N(1)	2.0420(13)	**C(5)-C(6)**	1.514(2)
Zr-O(2)	2.0474	**C(7)-C(8)**	1.383(2)
Zr-N(4)	2.0538(13)	**C(7)-C(12)**	1.422(2)
Zr-C(5)	2.8287(16)	**C(8)-C(9)**	1.388(2)
Zr-C(14)	2.8395(16)	**C(8)-H(8)**	0.95
Zr-C(6)	2.8396(16)	**C(9)-C(10)**	1.382(3)
Zr-C(13)	2.8415(16)	**C(9)-H(9)**	0.95
Zr-C(7)	2.8469(16)	**C(10)-C(11)**	1.388(3)
Zr-C(12)	2.8490(16)	**C(10)-H(10)**	0.95
O(1)-H(1A)	0.85	**C(11)-C(12)**	1.389(2)
O(1)-H(1B)	0.8508	**C(11)-H(11)**	0.95
O(2)-H(2A)	0.8489	**C(13)-C(14)**	1.515(2)
O(2)-H(2B)	0.8505	**C(14)-C(15)**	1.379(2)
O(3)-C(6)	1.2445(19)	**C(15)-C(16)**	1.385(3)
O(4)-C(13)	1.243(2)	**C(15)-H(15)**	0.95
N(1)-C(1)	1.342(2)	**C(16)-C(17)**	1.379(3)
N(1)-C(5)	1.347(2)	**C(16)-H(16)**	0.95
N(2)-C(6)	1.324(2)	**C(17)-C(18)**	1.381(2)
N(2)-C(7)	1.410(2)	**C(17)-H(17)**	0.95
N(3)-C(13)	1.323(2)	**C(18)-H(18)**	0.95
N(3)-C(12)	1.407(2)	**O(5)-C(19)**	1.408(3)
N(4)-C(18)	1.340(2)	**O(5)-H(5)**	0.80(4)
N(4)-C(14)	1.353(2)	**C(19)-H(19A)**	0.98
C(1)-C(2)	1.382(2)	**C(19)-H(19B)**	0.98
C(1)-H(1)	0.95	**C(19)-H(19C)**	0.98
C(2)-C(3)	1.379(3)	**O(6)-N(5)**	1.226(2)
C(2)-H(2)	0.95	**O(7)-N(5)**	1.2571(19)
C(3)-C(4)	1.383(2)	**O(8)-N(5)**	1.240(2)

Table C.2.5: Bond angles (°) for $[Zr(bpb)(H_2O)_2]NO_3 \cdot CH_3OH$.

Atoms	*Bond angle (°)*	*Atoms*	*Bond angle (°)*
N(2)-Zr-N(3)	82.46(6)	**C(14)-N(4)-Zr**	111.23(11)
N(2)-Zr-O(1)	94.15(5)	**N(1)-C(1)-C(2)**	121.82(16)
N(3)-Zr-O(1)	99.94(5)	**N(1)-C(1)-H(1)**	119.1

N(2)-Zr-N(1)	81.48(5)	**C(2)-C(1)-H(1)**	119.1
N(3)-Zr-N(1)	162.89(5)	**C(3)-C(2)-C(1)**	118.97(16)
O(1)-Zr-N(1)	87.11(5)	**C(3)-C(2)-H(2)**	120.5
N(2)-Zr-O(2)	99.45(5)	**C(1)-C(2)-H(2)**	120.5
N(3)-Zr-O(2)	93.99(5)	**C(2)-C(3)-C(4)**	119.40(15)
O(1)-Zr-O(2)	161.7	**C(2)-C(3)-H(3)**	120.3
N(1)-Zr-O(2)	82.86(5)	**C(4)-C(3)-H(3)**	120.3
N(2)-Zr-N(4)	163.08(5)	**C(3)-C(4)-C(5)**	119.02(16)
N(3)-Zr-N(4)	81.46(6)	**C(3)-C(4)-H(4)**	120.5
O(1)-Zr-N(4)	83.48(5)	**C(5)-C(4)-H(4)**	120.5
N(1)-Zr-N(4)	115.02(6)	**N(1)-C(5)-C(4)**	121.31(15)
O(2)-Zr-N(4)	86.91(5)	**N(1)-C(5)-C(6)**	117.07(13)
N(2)-Zr-C(5)	55.21(5)	**C(4)-C(5)-C(6)**	121.55(14)
N(3)-Zr-C(5)	137.42(5)	**N(1)-C(5)-Zr**	42.18(7)
O(1)-Zr-C(5)	88.61(5)	**C(4)-C(5)-Zr**	163.47(12)
N(1)-Zr-C(5)	26.28(5)	**C(6)-C(5)-Zr**	74.91(8)
O(2)-Zr-C(5)	89.13(5)	**O(3)-C(6)-N(2)**	128.82(15)
N(4)-Zr-C(5)	141.12(5)	**O(3)-C(6)-C(5)**	119.56(14)
N(2)-Zr-C(14)	137.38(5)	**N(2)-C(6)-C(5)**	111.59(13)
N(3)-Zr-C(14)	55.10(5)	**O(3)-C(6)-Zr**	166.27(12)
O(1)-Zr-C(14)	89.93(5)	**N(2)-C(6)-Zr**	37.48(7)
N(1)-Zr-C(14)	141.14(5)	**C(5)-C(6)-Zr**	74.11(8)
O(2)-Zr-C(14)	88.33(5)	**C(8)-C(7)-N(2)**	125.86(15)
N(4)-Zr-C(14)	26.38(5)	**C(8)-C(7)-C(12)**	119.61(15)
C(5)-Zr-C(14)	167.41(5)	**N(2)-C(7)-C(12)**	114.52(13)
N(2)-Zr-C(6)	24.24(5)	**C(8)-C(7)-Zr**	164.70(12)
N(3)-Zr-C(6)	106.62(5)	**N(2)-C(7)-Zr**	38.96(7)
O(1)-Zr-C(6)	91.77(5)	**C(12)-C(7)-Zr**	75.63(9)
N(1)-Zr-C(6)	57.25(5)	**C(7)-C(8)-C(9)**	120.11(16)
O(2)-Zr-C(6)	95.60(5)	**C(7)-C(8)-H(8)**	119.9
N(4)-Zr-C(6)	171.29(5)	**C(9)-C(8)-H(8)**	119.9
C(5)-Zr-C(6)	30.98(4)	**C(10)-C(9)-C(8)**	120.29(16)
C(14)-Zr-C(6)	161.61(5)	**C(10)-C(9)-H(9)**	119.9
N(2)-Zr-C(13)	106.51(5)	**C(8)-C(9)-H(9)**	119.9
N(3)-Zr-C(13)	24.18(5)	**C(9)-C(10)-C(11)**	120.61(16)
O(1)-Zr-C(13)	95.41(5)	**C(9)-C(10)-H(10)**	119.7
N(1)-Zr-C(13)	171.37(5)	**C(11)-C(10)-H(10)**	119.7
O(2)-Zr-C(13)	92.44(5)	**C(10)-C(11)-C(12)**	119.78(17)
N(4)-Zr-C(13)	57.28(5)	**C(10)-C(11)-H(11)**	120.1
C(5)-Zr-C(13)	161.60(5)	**C(12)-C(11)-H(11)**	120.1
C(14)-Zr-C(13)	30.94(5)	**C(11)-C(12)-N(3)**	126.27(15)
C(6)-Zr-C(13)	130.73(5)	**C(11)-C(12)-C(7)**	119.48(15)

N(2)-Zr-C(7)	26.87(5)	**N(3)-C(12)-C(7)**	114.25(13)
N(3)-Zr-C(7)	55.60(5)	**C(11)-C(12)-Zr**	164.89(13)
O(1)-Zr-C(7)	97.39(5)	**N(3)-C(12)-Zr**	38.86(7)
N(1)-Zr-C(7)	108.27(5)	**C(7)-C(12)-Zr**	75.46(9)
O(2)-Zr-C(7)	100.29(5)	**O(4)-C(13)-N(3)**	128.48(16)
N(4)-Zr-C(7)	136.68(5)	**O(4)-C(13)-C(14)**	119.68(14)
C(5)-Zr-C(7)	82.05(5)	**N(3)-C(13)-C(14)**	111.84(14)
C(14)-Zr-C(7)	110.54(5)	**O(4)-C(13)-Zr**	165.70(12)
C(6)-Zr-C(7)	51.09(5)	**N(3)-C(13)-Zr**	37.43(8)
C(13)-Zr-C(7)	79.64(5)	**C(14)-C(13)-Zr**	74.46(9)
N(2)-Zr-C(12)	55.75(5)	**N(4)-C(14)-C(15)**	121.55(16)
N(3)-Zr-C(12)	26.72(5)	**N(4)-C(14)-C(13)**	116.89(14)
O(1)-Zr-C(12)	100.78(5)	**C(15)-C(14)-C(13)**	121.53(16)
N(1)-Zr-C(12)	136.77(5)	**N(4)-C(14)-Zr**	42.39(7)
O(2)-Zr-C(12)	97.02(5)	**C(15)-C(14)-Zr**	163.81(13)
N(4)-Zr-C(12)	108.11(5)	**C(13)-C(14)-Zr**	74.60(9)
C(5)-Zr-C(12)	110.77(5)	**C(14)-C(15)-C(16)**	118.97(17)
C(14)-Zr-C(12)	81.79(5)	**C(14)-C(15)-H(15)**	120.5
C(6)-Zr-C(12)	79.91(5)	**C(16)-C(15)-H(15)**	120.5
C(13)-Zr-C(12)	50.85(5)	**C(17)-C(16)-C(15)**	119.38(16)
C(7)-Zr-C(12)	28.91(5)	**C(17)-C(16)-H(16)**	120.3
Zr-O(1)-H(1A)	118.5	**C(15)-C(16)-H(16)**	120.3
Zr-O(1)-H(1B)	120.6	**C(16)-C(17)-C(18)**	118.97(17)
H(1A)-O(1)-H(1B)	104.5	**C(16)-C(17)-H(17)**	120.5
Zr-O(2)-H(2A)	120.4	**C(18)-C(17)-H(17)**	120.5
Zr-O(2)-H(2B)	114.7	**N(4)-C(18)-C(17)**	121.94(17)
H(2A)-O(2)-H(2B)	104.5	**N(4)-C(18)-H(18)**	119
C(1)-N(1)-C(5)	119.43(14)	**C(17)-C(18)-H(18)**	119
C(1)-N(1)-Zr	128.95(11)	**C(19)-O(5)-H(5)**	107(3)
C(5)-N(1)-Zr	111.53(10)	**O(5)-C(19)-H(19A)**	109.5
C(6)-N(2)-C(7)	127.45(14)	**O(5)-C(19)-H(19B)**	109.5
C(6)-N(2)-Zr	118.29(11)	**H(19A)-C(19)-H(19B)**	109.5
C(7)-N(2)-Zr	114.17(10)	**O(5)-C(19)-H(19C)**	109.5
C(13)-N(3)-C(12)	126.98(14)	**H(19A)-C(19)-H(19C)**	109.5
C(13)-N(3)-Zr	118.39(11)	**H(19B)-C(19)-H(19C)**	109.5
C(12)-N(3)-Zr	114.43(10)	**O(6)-N(5)-O(8)**	120.44(16)
C(18)-N(4)-C(14)	119.08(14)	**O(6)-N(5)-O(7)**	120.75(16)
C(18)-N(4)-Zr	129.67(12)	**O(8)-N(5)-O(7)**	118.81(15)